AD NUMBER
AD221594
CLASSIFICATION CHANGES
TO: **UNCLASSIFIED**
FROM: **CONFIDENTIAL**
LIMITATION CHANGES
TO: **Approved for public release; distribution is unlimited.**
FROM: **Distribution authorized to U.S. Gov't. agencies and their contractors; Administrative/Operational Use; 1946. Other requests shall be referred to Defense Office Of Scientific Research And Development, National Defense Research Committee, Washington, DC 22301.**
AUTHORITY
2 Aug 1960 per secdef memo; dod, 10 may 1966

SUMMARY TECHNICAL REPORT
OF THE
NATIONAL DEFENSE RESEARCH COMMITTEE

Manuscript and illustrations for this volume were prepared for publication by the Summary Reports Group of the Columbia University Division of War Research under contract OEMsr-1131 with the Office of Scientific Research and Development. This volume was printed and bound by the Columbia University Press.

Distribution of the Summary Technical Report of NDRC has been made by the War and Navy Departments. Inquiries concerning the availability and distribution of the Summary Technical Report volumes and microfilmed and other reference material should be addressed to the War Department Library, Room 1A–522, The Pentagon, Washington 25, D. C., or to the Office of Naval Research, Navy Department, Attention: Reports and Documents Section, Washington 25, D. C.

Copy No.

29

This volume, like the seventy others of the Summary Technical Report of NDRC, has been written, edited, and printed under great pressure. Inevitably there are errors which have slipped past Division readers and proofreaders. There may be errors of fact not known at time of printing. The author has not been able to follow through his writing to the final page proof.

Please report errors to:

JOINT RESEARCH AND DEVELOPMENT BOARD
PROGRAMS DIVISION (STR ERRATA)
WASHINGTON 25, D. C.

A master errata sheet will be compiled from these reports and sent to recipients of the volume. Your help will make this book more useful to other readers and will be of great value in preparing any revisions.

SUMMARY TECHNICAL REPORT OF DIVISION 6, NDRC

VOLUME 18

Underwater Sound Equipment V

INSTRUMENTS, ATTACK AIDS AND MISCELLANEOUS ORDNANCE

OFFICE OF SCIENTIFIC RESEARCH AND DEVELOPMENT
VANNEVAR BUSH, DIRECTOR

NATIONAL DEFENSE RESEARCH COMMITTEE
JAMES B. CONANT, CHAIRMAN

DIVISION 6
JOHN T. TATE, CHIEF

WASHINGTON, D. C., 1946

NATIONAL DEFENSE RESEARCH COMMITTEE

James B. Conant, *Chairman*

Richard C. Tolman, *Vice Chairman*

Roger Adams	Army Representative[1]
Frank B. Jewett	Navy Representative[2]
Karl T. Compton	Commissioner of Patents[3]

Irvin Stewart, *Executive Secretary*

[1]*Army representatives in order of service:*

Maj. Gen. G. V. Strong — Col. L. A. Denson
Maj. Gen. R. C. Moore — Col. P. R. Faymonville
Maj. Gen. C. C. Williams — Brig. Gen. E. A. Regnier
Brig. Gen. W. A. Wood, Jr. — Col. M. M. Irvine
Col. E. A. Routheau

[2]*Navy representatives in order of service:*

Rear Adm. H. G. Bowen — Rear Adm. J. A. Furer
Capt. Lybrand P. Smith — Rear Adm. A. H. Van Keuren
Commodore H. A. Schade

[3]*Commissioners of Patents in order of service:*

Conway P. Coe — Casper W. Ooms

NOTES ON THE ORGANIZATION OF NDRC

The duties of the National Defense Research Committee were (1) to recommend to the Director of OSRD suitable projects and research programs on the instrumentalities of warfare, together with contract facilities for carrying out these projects and programs, and (2) to administer the technical and scientific work of the contracts. More specifically, NDRC functioned by initiating research projects on requests from the Army or the Navy, or on requests from an allied government transmitted through the Liaison Office of OSRD, or on its own considered initiative as a result of the experience of its members. Proposals prepared by the Division, Panel, or Committee for research contracts for performance of the work involved in such projects were first reviewed by NDRC, and if approved, recommended to the Director of OSRD. Upon approval of a proposal by the Director, a contract permitting maximum flexibility of scientific effort was arranged. The business aspects of the contract, including such matters as materials, clearances, vouchers, patents, priorities, legal matters, and administration of patent matters were handled by the Executive Secretary of OSRD.

Originally NDRC administered its work through five divisions, each headed by one of the NDRC members. These were:

Division A — Armor and Ordnance
Division B — Bombs, Fuels, Gases, & Chemical Problems
Division C — Communication and Transportation
Division D — Detection, Controls, and Instruments
Division E — Patents and Inventions

In a reorganization in the fall of 1942, twenty-three administrative divisions, panels, or committees were created, each with a chief selected on the basis of his outstanding work in the particular field. The NDRC members then became a reviewing and advisory group to the Director of OSRD. The final organization was as follows:

Division 1 — Ballistic Research
Division 2 — Effects of Impact and Explosion
Division 3 — Rocket Ordnance
Division 4 — Ordnance Accessories
Division 5 — New Missiles
Division 6 — Sub-Surface Warfare
Division 7 — Fire Control
Division 8 — Explosives
Division 9 — Chemistry
Division 10 — Absorbents and Aerosols
Division 11 — Chemical Engineering
Division 12 — Transportation
Division 13 — Electrical Communication
Division 14 — Radar
Division 15 — Radio Coordination
Division 16 — Optics and Camouflage
Division 17 — Physics
Division 18 — War Metallurgy
Division 19 — Miscellaneous
Applied Mathematics Panel
Applied Psychology Panel
Committee on Propagation
Tropical Deterioration Administrative Committee

NDRC FOREWORD

As events of the years preceding 1940 revealed more and more clearly the seriousness of the world situation, many scientists in this country came to realize the need of organizing scientific research for service in a national emergency. Recommendations which they made to the White House were given careful and sympathetic attention, and as a result the National Defense Research Committee [NDRC] was formed by Executive Order of the President in the summer of 1940. The members of NDRC, appointed by the President, were instructed to supplement the work of the Army and the Navy in the development of the instrumentalities of war. A year later, upon the establishment of the Office of Scientific Research and Development [OSRD], NDRC became one of its units.

The Summary Technical Report of NDRC is a conscientious effort on the part of NDRC to summarize and evaluate its work and to present it in a useful and permanent form. It comprises some seventy volumes broken into groups corresponding to the NDRC Divisions, Panels, and Committees.

The Summary Technical Report of each Division, Panel, or Committee is an integral survey of the work of that group. The first volume of each group's report contains a summary of the report, stating the problems presented and the philosophy of attacking them and summarizing the results of the research, development, and training activities undertaken. Some volumes may be "state of the art" treatises covering subjects to which various research groups have contributed information. Others may contain descriptions of devices developed in the laboratories. A master index of all these divisional, panel, and committee reports which together constitute the Summary Technical Report of NDRC is contained in a separate volume, which also includes the index of a microfilm record of pertinent technical laboratory reports and reference material.

Some of the NDRC-sponsored researches which had been declassified by the end of 1945 were of sufficient popular interest that it was found desirable to report them in the form of monographs, such as the series on radar by Division 14 and the monograph on sampling inspection by the Applied Mathematics Panel. Since the material treated in them is not duplicated in the Summary Technical Report of NDRC, the monographs are an important part of the story of these aspects of NDRC research.

In contrast to the information on radar, which is of widespread interest and much of which is released to the public, the research on subsurface warfare is largely classified and is of general interest to a more restricted group. As a consequence, the report of Division 6 is found almost entirely in its Summary Technical Report, which runs to over twenty volumes. The extent of the work of a Division cannot therefore be judged solely by the number of volumes devoted to it in the Summary Technical Report of NDRC: account must be taken of the monographs and available reports published elsewhere.

Any great cooperative endeavor must stand or fall with the will and integrity of the men engaged in it. This fact held true for NDRC from its inception, and for Division 6 under the leadership of Dr. John T. Tate. To Dr. Tate and the men who worked with him —some as members of Division 6, some as representatives of the Division's contractors—belongs the sincere gratitude of the nation for a difficult and often dangerous job well done. Their efforts contributed significantly to the outcome of our naval operations during the war and richly deserved the warm response they received from the Navy. In addition, their contributions to the knowledge of the ocean and to the art of oceanographic research will assuredly speed peacetime investigations in this field and bring rich benefits to all mankind.

The Summary Technical Report of Division 6, prepared under the direction of the Division Chief and authorized by him for publication, not only presents the methods and results of widely varied research and development programs but is essentially a record of the unstinted loyal cooperation of able men linked in a common effort to contribute to the defense of their nation. To them all we extend our deep appreciation.

VANNEVAR BUSH, Director
Office of Scientific Research and Development

J. B. CONANT, Chairman
National Defense Research Committee

FOREWORD

As will be noted from the table of contents, this report assembles in one volume information regarding a number of developments which were undertaken by the Division. Although some of the work described did not result in equipment for Service use, it is felt the record of what was undertaken may be of assistance to those responsible for conducting future development programs. The report will make clear the stage to which the various developments were brought. Particular attention may be called to the story of the sound monitors contained in the first three chapters. These monitors, developed by the Harvard Underwater Sound Laboratory, were a most important aid in assuring that sonar gear installed on a ship was in effective operating condition. The shipboard instruments developed by the New London Laboratory and described in Chapter 4 proved to be important aids to our own submarines in their operations. Echo-repeating devices, discussed in Chapter 6, served as a most useful tool, and the general principle underlying their operation is finding continued applications. The work on attack directors and attack plotters, described in Chapters 7 and 8, although not completely successful, did produce one instrument adopted for Service use—the antisubmarine attack plotter. Another important phase of the work is described in Chapter 12, "Sea-Water Batteries." This development provides one method of securing a more adequate running range for electrically propelled torpedoes.

This report has been assembled by J. S. Coleman, and the staff of the Summary Reports Group of Columbia University; the Division appreciates their willingness to undertake the task.

The work described in this report was undertaken under various Navy projects, and in all cases received most cordial support from that Service. In many cases, as work proceeded, it was necessary to solicit from the Navy special facilities for performance tests, and in every instance that Service made a serious effort to supply these.

The report itself indicates which of the Division's contractors were the most concerned with the individual projects.

John T. Tate
Chief, Division 6

PREFACE

THE MATERIAL in this volume, as in other volumes describing equipment developments undertaken by the contractors and laboratories of Division 6, was derived from numerous reports and memoranda prepared by the several laboratory groups concerned. Consequently, the following chapters are more in the nature of a series of edited reports than an integrated, balanced text.

It is believed that the presentation is sufficiently complete to serve as a reference volume to those who may be interested in the efforts of the Division in this field. A complete bibliography has been provided at the end of the volume for the convenience of those who may wish details and data necessary to extend further any of the experimental developments described.

Principal credit for the compilation and preparation of the material in this report should be given to W. J. Meringer and H. J. Sullivan of the Columbia University Summary Reports Group staff. Acknowledgment should also be made for the helpful cooperation of the Bell Telephone Laboratories and the U. S. Navy Underwater Sound Laboratory at New London, Connecticut, in supplying reports, drawings, and photographs not previously available.

JOHN S. COLEMAN

CONTENTS

Chapter 1

THE SOUND GEAR MONITOR

OAX, OCP, and Installed Monitors

The sound gear monitor [SGM] developed by HUSL is an instrument which utilizes a steady nonpinging signal to obtain information concerning the transmitting and receiving characteristics of echo-ranging equipments. By means of such a monitor, sonar gear may be tuned and adjusted for optimum performance, checked for operational deterioration, and compared with other sonar systems. Portable and installed types of the sound gear monitor were developed. The two portable models, known as Model OAX and Model OCP, each comprise an oscillator-amplifier unit and a hydrophone. The OAX operates in the range 17 to 27 kc; the OCP, in the range 7 to 70 kc. Experimental work on a permanently installed type, called the installed sound gear monitor [ISGM], was carried on. The model tested utilized an OAX electronic unit and a special strut-transducer combination.

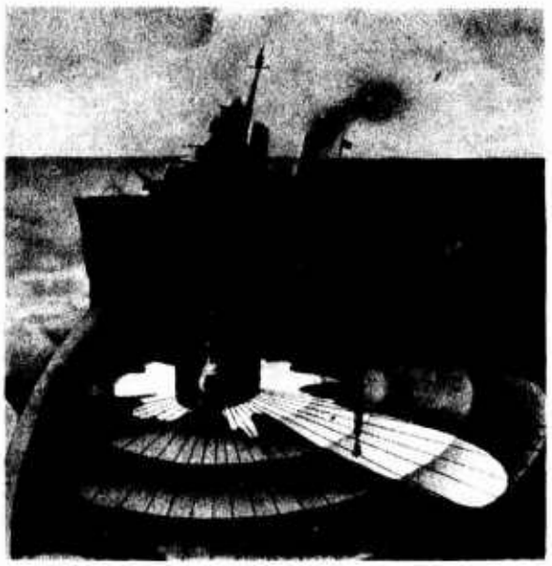

FIGURE 1. Sound gear monitor.

1.1 INTRODUCTION

THE SOUND GEAR MONITOR [SGM] is a device which is used to measure the characteristics of echo-ranging equipment and other sonar devices. Measurements which can be made include (1) transmitting and receiving frequency-response characteristics, (2) transmitting and receiving directivity characteristics, and (3) approximate transmitting power and receiving sensitivity.

These measurements find application in tuning and adjusting sonar equipment for optimum performance, in checking sonar equipment for performance deterioration, and in comparing the performance characteristics of different sonar systems. In each application the monitor makes a direct measurement of the overall response of the sonar system. Thus, the transmitting function of a sonar system is tested by measuring the sound pressure which the sonar projector produces in the water, and the receiving function is tested by evaluating the response of the system to an underwater sound signal of known properties. In both applications the monitor utilizes continuous signals, rather than pulses or "pings."

DESCRIPTION OF SGM

Two types of sound gear monitor were developed. One, called the *portable sound gear monitor* [OAX and OCP], employs a transducer suspended over side; the other, using a transducer mounted on a retractable strut, is known as the *installed sound gear monitor* [ISGM]. Each type consists of two parts, namely, a transducer and an oscillator-amplifier unit. Though the mechanical arrangement of the units differs widely in the two types of monitor, their functions are identical.

The oscillator-amplifier unit is provided with a selector switch which may be set on "receive," "beat," or "send." With the switch in the "receive" position the unit may be used to measure the sound field intensity and the transmitted directivity pattern of the sonar system under test. In the "beat" position, a local signal of the oscillator-amplifier unit is mixed with the signal picked up by the transducer. By heterodyning the two signals and adjusting the calibrated frequency of the local oscillator until "zero beat" is obtained from the unit's loudspeaker, the transmitted frequency can be measured.

When the selector switch is on "send," the calibrated signal of the monitor is transmitted via the transducer to the sonar equipment being checked. This makes it possible to tune the sonar receiver and to determine its receiving sensitivity and directivity patterns.

Advantages of SGM Over Early Procedures

Before the development of sound gear monitors, four methods of tuning QC drivers were in use. These were:[1]

1. The "sing," "hiss," or "sizzle" method.
2. The r-f current method.
3. The driver plate current method.[2]
4. The OL (Navy designation) equipment method.

The first three are inferential methods, i.e., it is inferred that the projector sound output is a maximum though the tuning operation is accomplished by observing something other than the sound intensity in the water. The methods are both convenient and rapid and require no other apparatus than what is already a part of the standard echo-ranging installation. They are reasonably accurate and the probable error should not result in more than a 3-db decrease in echo-to-noise ratio. However, since the observed quantities are small (depending upon hearing acuity or the observation of slight meter deflections), a certain amount of understanding and judgment is required of the operator. The dependability of the methods is not great since slight changes in the equipment because of aging and service wear may seriously affect their accuracy, or possibly prevent their use at all.

In contrast to the inferential methods, the OL equipment permits the direct measurement of the quantity of interest, namely, the intensity of the sound radiated into the water. There are, however, several disadvantages to the OL equipment: (1) it cannot be used when the ship is under way; (2) it is available only on tenders or at bases; (3) its size and weight and the length of time required to put it in operation tend to discourage its frequent use. For these reasons the OL equipment is usually restricted to making acceptance tests on new equipment, determining directivity patterns, and trouble-shooting.

After the sonar driver was tuned to the frequency of projector resonance according to one of the above methods, the receiver-amplifier was tuned for maximum sensitivity at that frequency. The OL equipment does not provide for the generation of a test signal in the water, and therefore it offers no advantage in receiver-amplifier tuning.

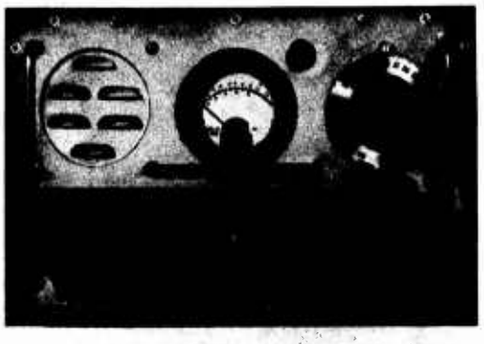

Figure 2. OAX sound gear monitor (production prototype). Model 5-E oscillator-amplifier panel.

With the development of the sound gear monitor it is now possible to perform the necessary tests accurately and conveniently. The portable monitor may be used on ships tied to a dock; in the case of ships under way, the installed monitor may be utilized. The dynamic monitor (see Chapter 2) is an improved device which furnishes an index of the overall acoustical efficacy of sonar echo-ranging gear. It differs from the SGM in the utilization of pulses or pings, instead of continuous signals.

Final Design

OAX Monitor. Figure 2 is a photograph of the oscillator-amplifier panel of a prototype model for commercial manufacture. The final design of the portable OAX monitor (also known as underwater sound portable testing equipment) consists of this unit together with the B-19B transducer (see Section 1.3.2). The frequency range is from 17 to 26 kc.

OCP Monitor. The complete portable X-OCP monitor is shown in Figure 3, including the B-19H transducer. The frequency range is from 7 to 70 kc. The commercially manufactured counterpart is designated as Portable Testing Equipment—Sonar—Model OCP.

ISGM. The original intention in the design of the installed sound gear monitor was to have a bulkhead-mounted oscillator-amplifier unit operating in conjunction with an installed transducer. However, such an electronic unit was never developed. In its place, use was made of the electronic unit of the

FIGURE 3. X-OCP sound gear monitor (production prototype), with B-19H transducer.

portable OAX monitor. The ISGM development was concentrated on the design of a strut for retracting the transducer. Several versions were installed on various ships for experimental purposes. A successful model is shown in Figure 4.

FUTURE IMPROVEMENTS

Portable Monitor. Since the electronic unit has reached a satisfactory stage of development, no recommendations are made for its improvement. Modification of the monitor for use as auxiliary equipment, such as a vacuum-tube voltmeter, or in code communication has been carried out to some extent, and further development along those lines seems desirable. Although the transducers used compare favorably with the latest magnetostrictive designs, there is room for improvement in uniformity of pattern and smoothness of frequency response.

Installed Monitor. It is recommended that a bulkhead-mounted electronic unit be developed for use with the installed transducer. Permanent installation relaxes the weight and portability restrictions applicable to the portable monitor, thereby permitting more rugged mechanical construction, more elaborate circuits, and consequent increased stability of operation. A desirable feature which should be considered for future development of the retractable strut is a remote-control hoist mechanism.

1.2 REQUIREMENTS

Five proposals were made for a measuring device to be used in conjunction with echo-ranging gear. These were:

1. A vibration pickup (contact microphone) to be permanently fastened to the projector mounting shaft. The electrical output of the microphone (by means of an amplifier-indicator) would indicate the mechanical resonance point of the projector as the driver amplifier was tuned through the resonant frequency. This system was considered inadequate because:

   a. It would provide means only for tuning the transmitting system; pattern measurements, power output, and receiving characteristics could not be measured.
   b. It might give fallacious indications of projector resonance because of the acoustic transmission characteristics of the projector mounting shaft, e.g., mechanical resonances of the shaft at frequencies near the projector's resonant point.

2. A vibration pickup (contact microphone) to be mounted on the inner surface of the ship's hull and connected to an amplifier-indicator. This system would not be applicable to measurement of receiving characteristics, but it might possibly permit crude transmitting pattern measurements in addition to the driver tuning operation.[a]

3. A transducer mounted inside the projector dome. When connected to suitable electronic equipment, the transducer could be used both to transmit and receive. It could not, however, be used for pattern measurements. An additional disadvantage would be that the transducer's output would not be a reliable indication of the overall acoustic output of the system, since marine growths on the outer surface of the dome and precipitated solids on its inner surface may seriously attenuate the radiated energy.[b]

4. A transducer to be suspended overside. It could be used for both sending and receiving, for tuning both the driver and the receiver-amplifier, and for measuring transmitting and receiving directivity patterns. Assuming stable characteristics for the transducer and associated electronic equipment, the device would permit measurement of the overall acoustic power output of the sonar transmitter and the

[a] Two slight variations of this proposal were (1) a transducer to be located in a small water tank attached to the inner surface of the ship's hull, and (2) a transducer to be mounted in a water-filled blister, attached to the outer surface of the ship's hull.

[b] This proposal, though rejected by HUSL, was subsequently developed by NRL. Two models of the resulting equipment are known as the OBY[3] and the OCH.[4]

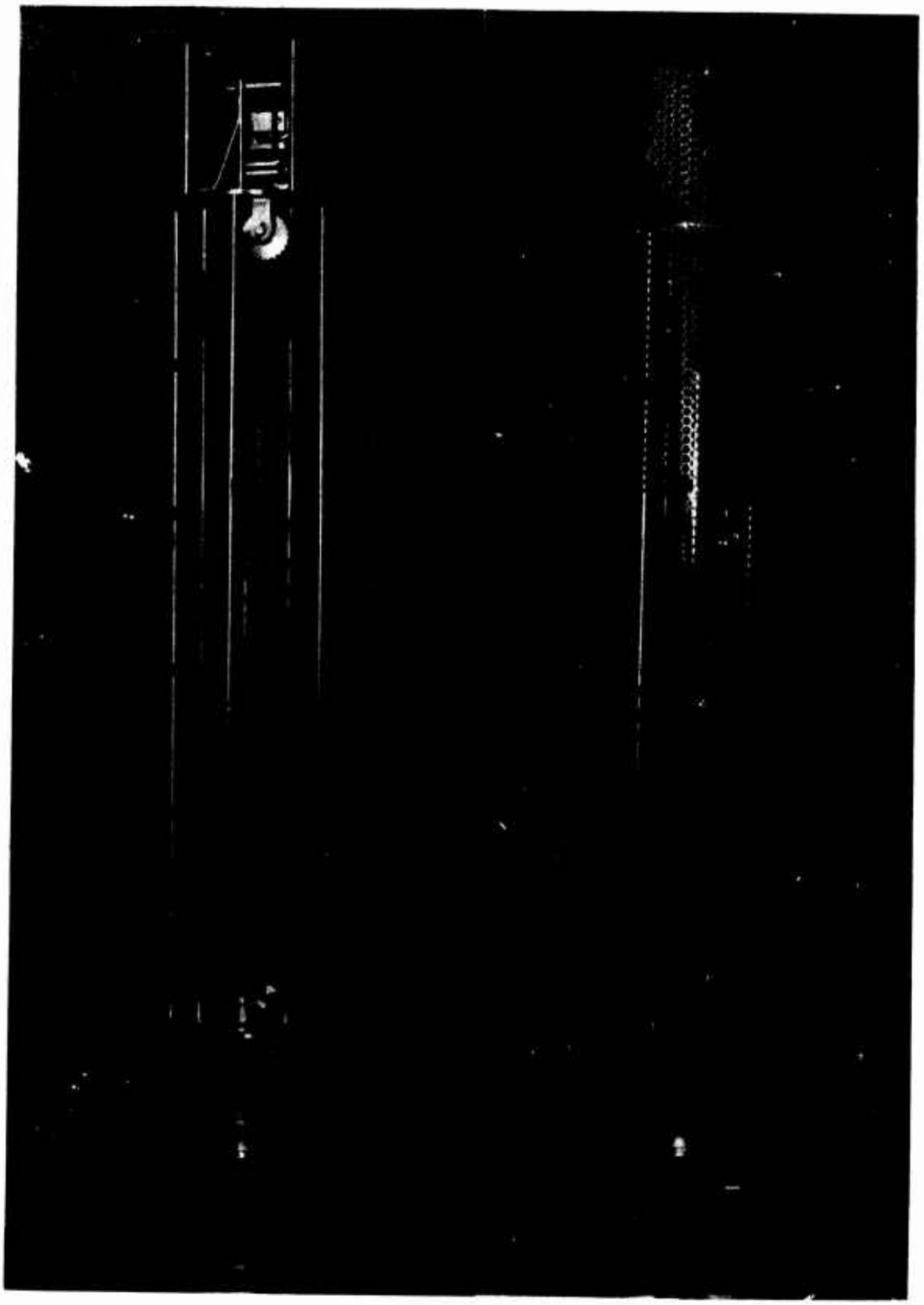

FIGURE 4. Hoist mechanism of installed sound gear monitor.

overall sensitivity of the sonar receiver. If the transducer could be made nondirectional in at least one plane, it could be suspended by a line from the ship's rail, thus eliminating much of the bulk and inconvenience associated with the OL equipment.

5. A transducer mounted on a retractable streamlined strut, to permit lowering to the level of the ship's projector at a known bearing with respect to the projector. The transducer would be used for both sending and receiving. It could be used to make all the measurements possible with the overside transducer suspension described in (4). It would have an advantage over the overside suspension in that it could be used with the ship under way. The strut could be withdrawn through a gate valve when not in use and, with the gate valve closed, could be removed, adjusted, or repaired.

The first three proposals were too limited in potential application. None of them would serve to make reliable pattern measurements; they would not guarantee reliable measurements of transmitted power or receiving sensitivity; even their application to the tuning of the sonar seemed doubtful. As a result no extensive investigations were made. The last two proposals were believed to merit investigation and development, and the respective units were designated portable sound gear monitor and installed sound gear monitor.

The nature of the sonar testing problem imposes certain design considerations which have served as a basis for the development of the monitor. The following discusses separately the considerations for the portable model and the installed model.

1.2.1 Portable Monitor

Overall Electrical Design. The sound gear monitor is designed (1) to make measurements of the acoustic field from sonar gear, and (2) to produce an acoustic test signal in the water at the sonar projector. Hence, the monitor consists of a hydrophone, an oscillator-amplifier unit, suitable indicating devices, and interconnecting cables. The system must be stable over long intervals to allow comparison of the performance of the sonar gear at different times. In order to be applicable to all sonar gear, the frequency response of the unit should be flat and should include all working frequencies.

Electronic Design. The electronic chassis consists of amplifiers and an oscillator which are arranged to satisfy three functions: send, beat, and receive. In the receive position, the amplifier is connected to the transducer and the amplifier output is indicated on a meter. The amplifier must be capable of receiving maximum signal (120 db above 1 bar at 1 meter) without overloading and must also respond to signals as low as 40 db above 1 bar while maintaining a large signal-to-noise ratio. Sensitivity adjustment should be provided to allow indication of these signals at zero on the output meter.

In the beat position, the amplifier output is mixed with the oscillator output to give an audible signal from the loudspeaker. By tuning the oscillator until the beat frequency is brought to zero, the oscillator is set to the frequency of the sonar gear. The oscillator should be stable so that the frequency of the sonar gear may be accurately read from the calibrated dial.

In the send position, the amplifier is disconnected from the transducer, and the oscillator is connected to the power stage in the amplifier, whose output is connected to the transducer. Thus, the system serves as a source for an acoustic test signal. Sufficient power output must be available to provide a field at the sonar projector of the order of 40 db above 1 bar. This should be adjustable so as to avoid overload of the sonar gear.

The oscillator and amplifiers are thus interconnected in three different ways and the design must be such as to avoid any disturbance of the oscillator frequency in any of these three positions. Moreover, the oscillator should be isolated from the amplifier to avoid accidental insertion of oscillator voltage.

Transducer Design. For ease of handling, the transducer should be suspended from the ship's rail by a rope. However, the transducer cable should be provided with strain relief or be otherwise supported at the water seal. To minimize any sidewise motion, an external weight is hung below the transducer. This arrangement does not prevent rotation of the transducer by twisting of the suspension cable. For use in testing sound gear, which radiates primarily in the horizontal plane, the transducer should be nondirectional in this plane to prevent the twisting motion from influencing the measurements. It should have maximum sensitivity in this plane and greatly diminished sensitivity in other planes, since measurements in any plane other than the horizontal are not required. If the transducer has appreciable sensitivity in the vertical direction, sound waves reflected from the harbor bottom or from the ship's hull could produce misleading results. It should have

reasonable sensitivity to avoid need for excessive gain in the amplifier unit, and to produce a desirable value of signal-to-noise ratio. The frequency response should be flat, or nearly so, to avoid complicated compensating networks or frequency calibration charts. The transmitting efficiency should permit the necessary field to be generated with a modest power amplifier in the electronic chassis.

The requirements discussed above are best met by a tubular magnetostriction transducer of the radially vibrating type.[c] Its sensitivity is uniform in a plane perpendicular to the axis of the tube but falls off rapidly with inclination to this plane. The Q of the transducer and the frequency of mechanical resonance are, within limits, independently controllable.

1.2.2 Installed Monitor

Overall Electrical Design. The section on overall electrical design of the portable monitor is applicable to the installed monitor.

Electronic Design. The electronic chassis is the same as that used in the portable monitor, with the exception that in the case of the installed monitor, permanent bulkhead mounting should be provided. Thus it is not subject to such severe restrictions on size and weight as the portable unit.

Transducer Design. Like its portable counterpart, the installed transducer should be of the radially vibrating, tubular, magnetostrictive type.[d] In a horizontal plane the response need not necessarily be uniform through 360 degrees, for the angular orientation of the transducer is held constant by the supporting strut. The response should be uniform, however, over an angle which subtends the ship's projector (or projectors).

The size of the transducer is not of critical importance, but it should be small enough to permit withdrawal through a reasonably sized port in the ship's hull. The transducer should have a streamlined cross section, both to minimize the frictional forces resulting from motion through the water and to minimize the noise generated by water turbulence.

Strut and Hoist Design. Considerations of vulnerability require that the transducer and its strut be retractable. They should be withdrawn through the hull of the ship when the monitor is not in use to minimize the danger to the transducer from collisions with floating debris and to cut down unnecessary water drag. Considerations of serviceability require the transducer and strut, when withdrawn, to be easily removable for replacement or repair. For frequent raising and lowering, a motor-driven hoist mechanism should be provided.

On high-speed combat vessels the frictional forces encountered by the strut are quite large. The mechanical design should consider these forces and, in addition, the possibility of impacts with fish and other objects.

Location of the Transducer. The location of the transducer with respect to the sonar projector is important. The extended transducer should be level with the projector so as to lie in the center of the projector's major vertical lobe.

Since the distances traveled by sound in echo-ranging practice are large compared to the diameter of the sonar projector, the sound energy that reaches a target and is returned from the target consists of essentially plane waves. If the distance between the monitor transducer and the sonar projector is decreased to a value commensurate with the projector diameter, the variations in path length as measured to different points on the active surface of the projector become significant fractions of a wavelength. When this occurs, normal directivity patterns and frequency-response curves are not obtained.

Open-water measurements made with a 19-in. diameter QC projector (24.25 kc) and a portable monitor indicated that any decrease in separation below 4 ft caused a noticeable broadening of the projector's major lobe. From these observations it was decided that the minimum permissible separation, a function of frequency and projector aperture, should be 6 ft.[6]

To assign a definite upper limit to the separation distance is difficult because of several variable factors, such as the contour of the ship's hull. An appropriate limit of 12 ft has been accepted, but no direct observations have been made to substantiate this assumption.

1.3 OAX MONITOR

1.3.1 Description

The OAX monitor is the portable model, with a frequency range of from 17 to 26 kc. The block diagram of Figure 5 illustrates the basic functional design. (It applies equally well to the OCP and in-

[c] Described in Division 6, Volume 13.
[d] Division 6, Volume 13.

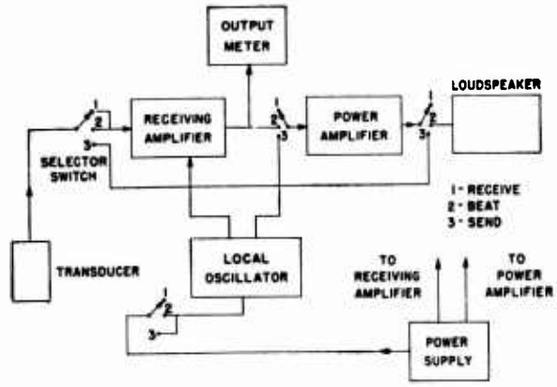

FIGURE 5. Block diagram of sound gear monitors.

stalled monitors.) In this diagram the oscillator-amplifier unit has been divided into five sections as follows:

1. A receiving amplifier with its associated output meter.
2. A power amplifier.
3. A loudspeaker.
4. An oscillator, the frequency of which can be varied by means of a calibrated frequency dial.
5. A power supply which provides plate and filament power for the other circuits.

These five sections can be interconnected for three different functions by means of a selector switch marked receive, beat, and send.

1.3.2 The Final Design

After four early models had been tested, prototype models for commercial manufacture were developed. These were designated Models 5D, 5C, and 5E, which is the chronological order in which the respective designs became fairly well standardized. All three models are known as Model OAX portable monitor. Model 5C is different from Model 5D in that an additional stage of amplification is used. Model 5E differs from Model 5C in the use of four variable resistors of the screwdriver-adjustment type in place of the fixed resistors used in Model 5C.

Since the same transducer was used with each of these models, it is discussed first, the sections following being devoted to a description of the three electronic units.

TRANSDUCER

The B-19B transducer, shown in Figure 6, is a tubular magnetostriction hydrophone of the radially vibrating type. The magnetostrictive element is an oxide-annealed nickel tube 6 in. long, with an outside diameter of 1.5 in. and a wall thickness of 0.035 in. The Alnico polarizing magnets and the transducer windings are contained within the waterproof enclosure formed by the tube and the top and bottom end caps. The arrangement of these parts is shown in Figures 7 and 8. The transducer winding consists of 130 turns of No. 26 SCE wire wound in two layers on wooden coil forms.

The d-c resistance of the transducer is about 6 ohms, and the impedance at 26 kc is $31 + j52$ ohms. The horizontal sensitivity in the useful frequency

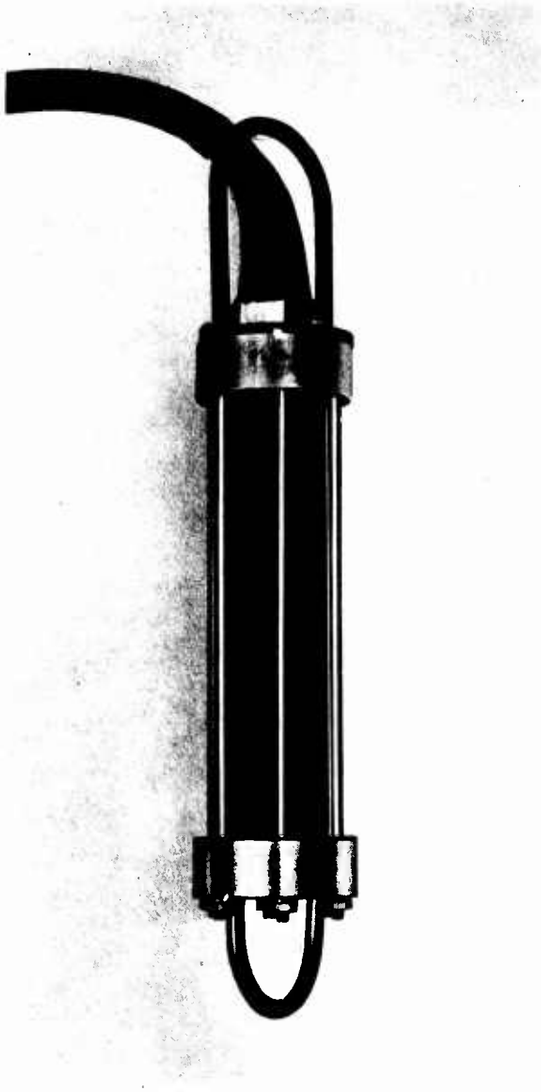

FIGURE 6. B-19B transducer.

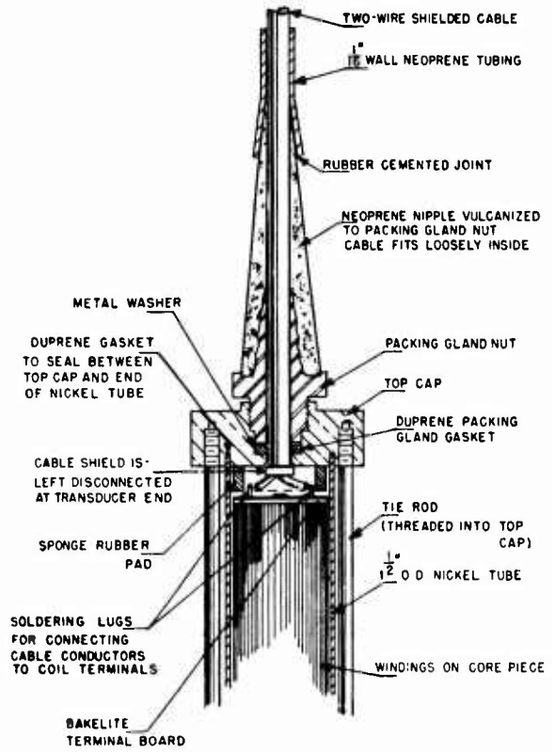

FIGURE 7. Upper section of B-19B transducer.

range (17 to 26 kc) is 115 db below 1 v per bar when the transducer is connected to a 100-ohm resistive load. In this frequency range the horizontal sensitivity may vary ±1.5 db. In a horizontal plane the directivity pattern varies less than ±1.5 db from circular symmetry. In any vertical plane the sensitivity is maximum in a horizontal direction and drops about 10 db for a 30-degree inclination to the horizontal.

A typical curve showing the frequency response of a B-19B transducer is given in Figure 9.

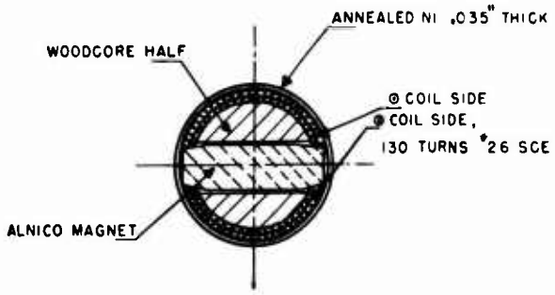

FIGURE 8. Cross section of B-19B transducer.

MODEL 5D

Figure 10 is a block diagram of the Model 5D oscillator-amplifier unit, and Figure 11 is a complete circuit diagram.

The block diagram of Figure 10 shows the circuit divided into sections and illustrates the action of the five-position selector switch. Two receiving positions are provided: full gain, and 30-db fixed attenuation. In either receiving position a variable attenuator permits manual adjustment of the attenuation in 3-db steps over a range of 57 db, providing a total dynamic range of 87 db. The gain of the receiving amplifier is sufficient to produce a 0-db reading of the output meter with an input level of 1.8 mv when no attenuation is used.

The receiving amplifier is a conventional two-stage resistance-coupled amplifier. Un-by-passed cathode resistors provide a small amount of degenerative current feedback, which increases the stability of the amplifier and flattens its frequency response. The output meter is a Weston Type VU meter. A copper oxide rectifier is contained within the meter case.

In either receive position the output of the receiving amplifier is applied to the power amplifier as well as to the output meter. The resistance-capacitance network at the input to V-3A and the capacitance C-14, which shunts the power amplifier output, make the power amplifier effectively inoperative at signal frequencies. In both receive positions plate voltage is not applied to the local oscillator.

In the beat position plate voltage is applied to the local oscillator and the oscillator signal is injected into the receiving amplifier (at the suppressor grid of V-2). Heterodyning between the oscillator signal and the signal from the hydrophone causes

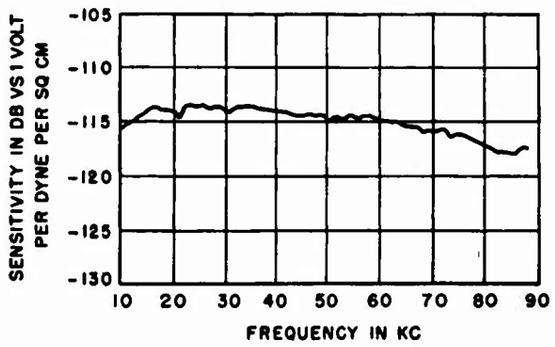

FIGURE 9. Sensitivity calibration of B-19B transducer.

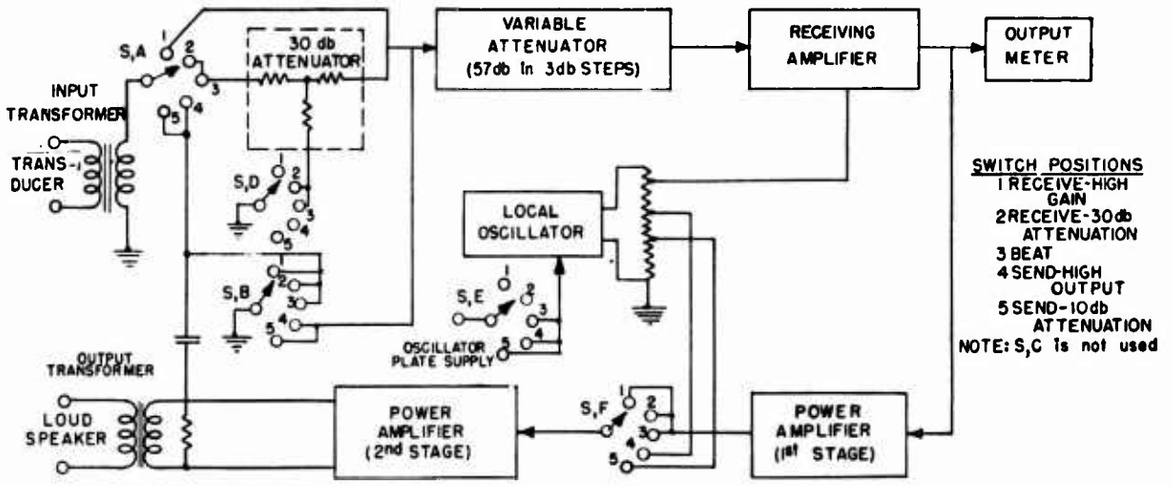

FIGURE 10. Block diagram of portable monitors, Models 5C, 5D, and 5E.

a difference-frequency signal to be applied to the power amplifier and speaker. The resistance-capacitance network at the input of V-3A and the capacitance C-14, which shunts the power amplifier output, cause little attenuation at audible difference frequencies; consequently, the beat note is heard in the loudspeaker.

The local oscillator consists of the tube V-3B in a series-fed Hartley circuit. The stabilizing resistor R-28 in the cathode circuit of the oscillator tube

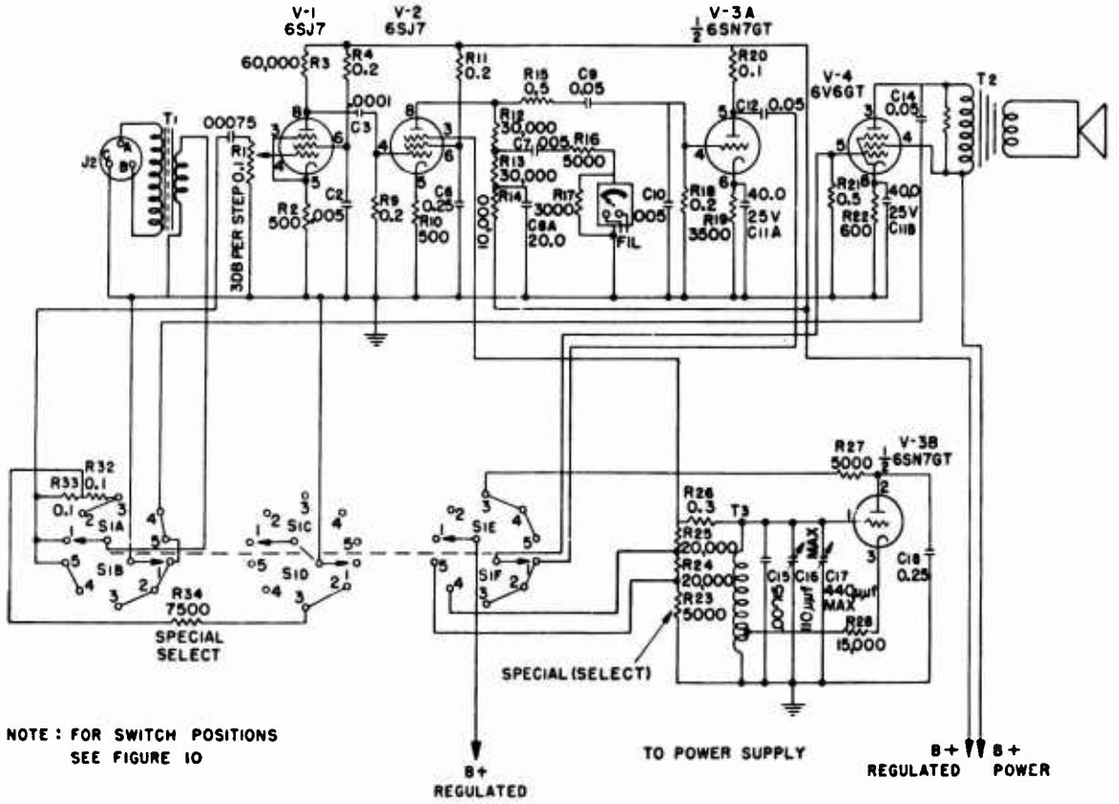

FIGURE 11. Schematic diagram of portable monitor, Model 5D.

improves the waveform of the oscillator output and makes the frequency of oscillation independent of tube characteristics. The trimmer condenser C-16, because of its negative temperature coefficient, stabilizes the frequency with respect to temperature changes. Voltage regulation of the oscillator plate supply voltage is used to overcome the effects of line voltage variations.

In the two send positions of the selector switch the input to the receiving amplifier is grounded. The local oscillator signal is applied to the second stage of the power amplifier, and the output of this amplifier is connected to the transducer. The local oscillator signal is also injected into the second stage of the receiving amplifier in the same manner as described above. This causes the output meter to give a visible indication that the oscillator is functioning. The additional circuits in the send positions are conventional, with the possible exception of the plate circuit of V-4. The plate load impedance of V-4 consists of the input transformer and the speaker transformer in parallel. The fact that the loudspeaker transformer has reasonably high impedance at ultrasonic frequencies makes this arrangement possible.

The output voltages applied to the transducer are approximately 6.0 v in the full gain output position, and 2 v in the 10-db attenuation position.

The Model 5D monitor when used with a B-19B transducer has the following performance characteristics.

1. Frequency response: flat ±3 db from 17 to 26 kc for random rotation of transducer.
2. Receiving sound field: from 60 to 147 db above 1 bar.
3. Sending sound field, two fixed values: 30 db and 40 db above 1 bar at 5 ft.

Model 5C

A block diagram is given in Figure 10 and a schematic circuit diagram is shown in Figure 12.

The receiving amplifier is similar to that of Model 5D except that an additional stage of voltage amplification is used. The gain of the receiving amplifier is 109 db (about 30 db greater than in the Model 5D). The additional gain was incorporated in this unit for two reasons: (1) a modification was made in the B-19B transducer, thereby reducing its sensitivity; and (2) experience in the use of the 5D monitor had indicated that higher gain would be useful.

The power amplifier, oscillator, and meter circuits are identical with those of Model 5D.

The performance characteristics are as follows.

1. Frequency response: flat ±3 db from 17 to 26 kc for random rotation of the transducer.
2. Receiving sound field: from 30 to 117 db above 1 bar.
3. Sending sound fields, two fixed values: 30 db and 40 db above 1 bar at 5 ft.

In only 2 of the 35 units were there deviations of 3 db per kc.

Model 5E

Figure 10 is a block diagram of the Model 5E oscillator-amplifier unit, and a schematic circuit diagram is given in Figure 13. A photograph of the unit is shown in Figure 2.

The circuits of the Models 5C and 5E differ only in the fact that four variable resistors of the screwdriver-adjustment type are used in Model 5E in place of the fixed resistors used in Model 5C. The quantities made adjustable are (1) gain of the receiving amplifier, (2) attenuation of the 30-db receiving attenuator, (3) oscillator voltage injected into the receiving amplifier, and (4) attenuation in the −10-db send position.

Two advantages resulted from the use of the variable components. In the first place, production of the monitors was speeded up because 10 per cent resistors could be used where hand-picked resistors were formerly required. Secondly, recalibration of the monitors to compensate for aging or replacement parts was made possible. The performance of the Model 5E is identical with that of the Model 5C.

To provide a larger range of transmitting pressure levels, an external sending attenuator[5] was developed for use with all Model 5 monitors.

1.3.3 Recommendations for Future Work

The electronic oscillator-amplifier unit of the portable monitor has reached a satisfactory state of engineering development. No direct recommendations are made, therefore, concerning improvement of its present functions. It is recommended that further engineering development work be devoted to those design features which will allow the monitor to serve in the field as an independent signal generator and vacuum-tube voltmeter, in addition to its present features.

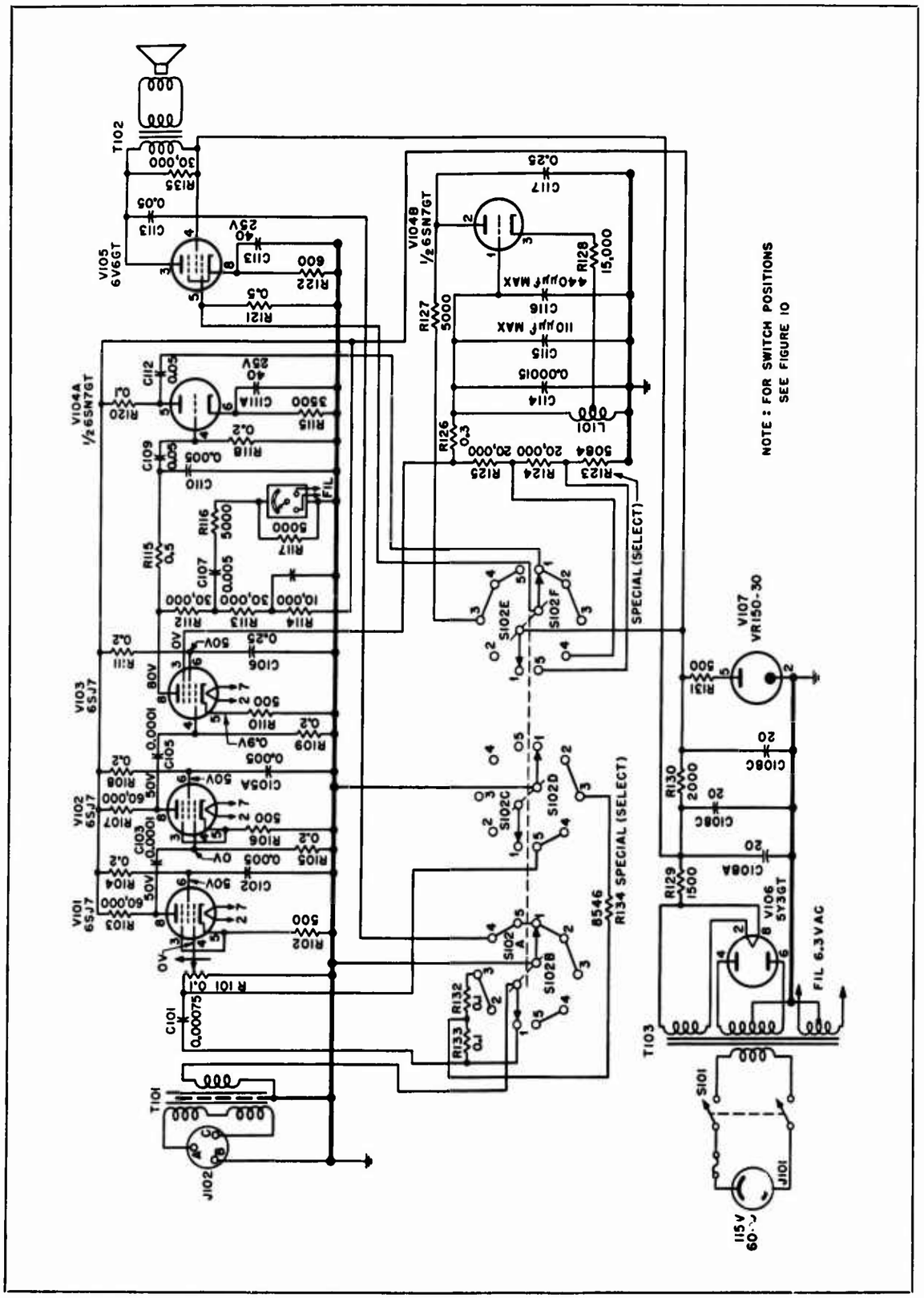

FIGURE 12. Schematic diagram of portable monitor, Model 5C.

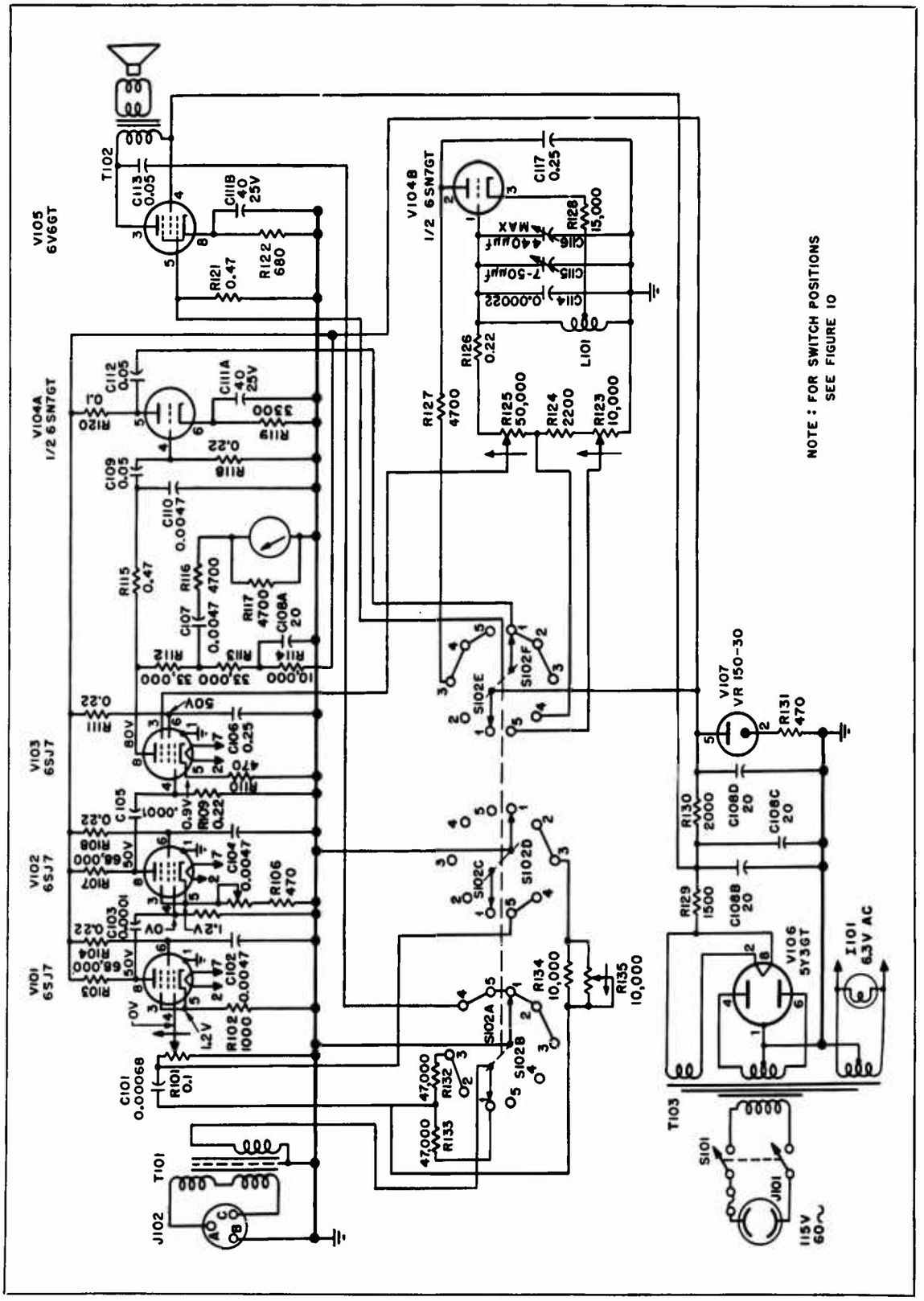

FIGURE 13. Schematic diagram of portable monitor, Model 5E.

Limitations

The principal limitations of the portable monitor are associated with the performance of the transducer. The latter's characteristics with regard to uniformity of pattern and smoothness of frequency response still leave something to be desired, although its present performance appears consistent with the present state of advancement of the magnetostriction transducer art. Further refinements in transducer design should be adapted to the monitor transducer as they become available.

The limitations due to transducer performance appear less significant when compared with errors which are inherent in measurements made with portable equipment. A suspended transducer is never at a precisely known location with respect to the sonar projector, nor can its location be exactly duplicated in consecutive suspensions. During any given set of measurements, the transducer is free to rotate about the suspension cable and is likely to drift when acted on by water currents. The inherent instability of the transducer mounting and the existence of wave interference patterns give rise to fluctuating meter readings which limit the absolute accuracy of any measurements made with portable equipment.

1.4 OCP MONITOR

1.4.1 Development

The OAX portable monitor was designed to operate in the frequency range of from 17 to 26 kc. When the development of sonar equipment tended toward the utilization of frequencies outside this range, the need for portable testing equipment covering a larger frequency range became apparent. Development of three units followed: (1) a modification of the Model 5 series called the extended-range monitor, (2) the Model 7 wide-range monitor, and (3) the Model X-OCP monitor. The latter was designed to be a production prototype model of the OCP portable monitor.

Extended-Range Monitor

The extended-range portable monitor is a standard 5C or 5E model (see Section 1.3.2) which has been converted for broad-band operation. Conversion kits and detailed instructions[6] have been supplied for converting standard models into these wide-range units.

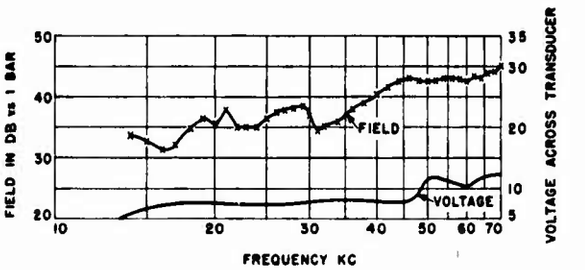

FIGURE 14. Transmitting characteristic of extended range monitor with B-19H transducer.

When used with a B-19H transducer, the monitor operates satisfactorily over the 17- to 71-kc frequency range. Figure 14 shows the transmitter frequency characteristic. The total variation is about 13 db, which is considerably larger than desirable. Only part of this variation results from transducer characteristics. The absolute sound output was about 4 db less than with the standard model monitor, but was otherwise equally satisfactory.

Model 7 Wide-Range Monitor

The Model 7 monitor was the first wide-range unit whose overall design took into consideration the characteristics of the B-19H transducer and the general problems encountered in broad-band ultrasonic equipment. The frequency range of from 7 to 70 kc was selected to coincide with the usable range of the transducer. Electronic circuits were designed to give a flat frequency response in this range and separate equalization networks were employed to compensate for the average variations in the B-19H frequency characteristics. The performance of this unit was in some ways inferior to that of the Model X-OCP monitor described in the next section, due to incomplete investigation of design details.

1.4.2 Final Design

The Model X-OCP portable monitor[7] is the name given to the final design of the wide frequency range unit. The production model is designated as Portable Testing Equipment-Sonar-Model OCP. It uses approximately the same electronic circuits as Model 7 and operates over the same frequency range (7 to 70 kc) and the same range of sound pressure levels. It differs from the previous unit in that primary consideration is given to the problems associated with quantity manufacture of the instrument.

Figure 15 shows the setup used when taking moni-

FIGURE 15. Portable monitor setup.

tor measurements. (This arrangement applies to all portable monitors.) In Figure 3 is shown the Model X-OCP sound gear monitor with a B-19H transducer.

TRANSDUCER

The B-19H transducer used with the OCP monitor is a tubular magnetostriction transducer of the radially vibrating type. (See Figure 16.) It is a miniature reproduction of the Model B-19B. The active element of the B-19H is an oxide-annealed nickel tube 0.75 in. in diameter, 5 in. long, and 0.025 in. in wall thickness. Brass end caps, soldered to the two ends of the tube, form a waterproof enclosure in which are contained the polarizing magnets and the transducer coils. One end of the active element is rigidly fastened to the end of a stainless-steel expanded metal cage, while the other end is kept centered in the cage by a rubber cup. The only function of the cage is to provide protection for the active element.

The diametral polarizing magnet is made from four laminations of 0.014-in. Cunico,[e] and provides a flux density of 4,000 gauss in the nickel. The windings consist of 80 turns of No. 28 SCE wire, wound on two half-round wooden coil forms.

Because the B-19H sensitivity and impedance both rise uniformly with frequency, it is possible to achieve a nearly flat frequency response by correct resistance termination of the transducer. Figure 17 shows the sensitivity of a B-19H unit for various terminations.

The sound field produced by a B-19H, when driven from a constant-voltage source, is shown in Figure 18. Because of the variation in transducer impedance, the electrical power level is not constant through the frequency range. The power level is indicated at several points on the graph.[f]

CIRCUIT PRINCIPLES

A schematic diagram of the X-OCP monitor is shown in Figure 19.

Receiving Amplifier. The receiving amplifier consists of four resistance-coupled pentode amplifier stages. Degenerative voltage feedback is utilized to flatten the frequency response and to stabilize the gain of the amplifier. In order to obtain a large feedback factor, while avoiding oscillation because

[e] A copper-nickel-cobalt alloy manufactured by the General Electric Company.

[f] For further details on this transducer, see Section 6.3.2 of Division 6, Volume 13.

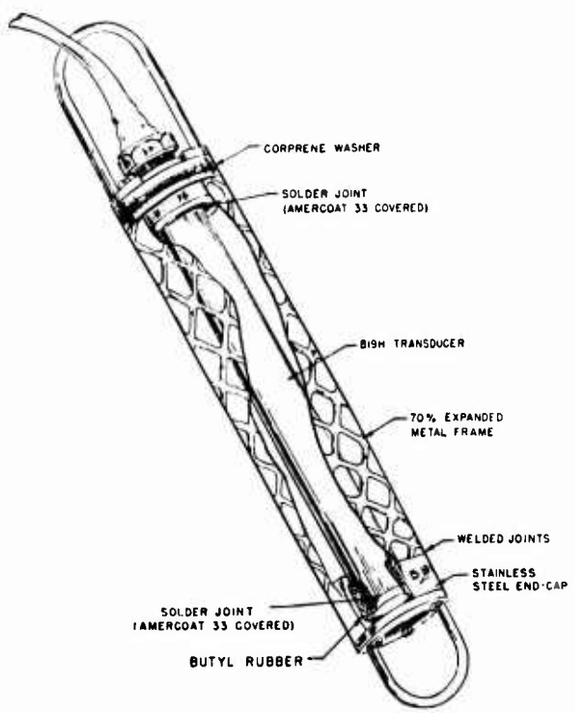

FIGURE 16. Cutaway view of B-19H transducer.

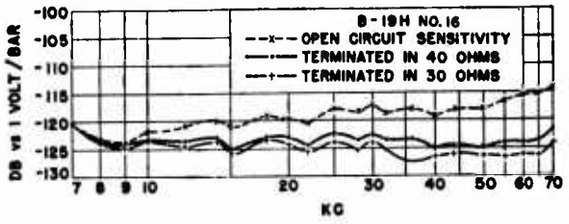

FIGURE 17. Sensitivity of B-19H transducer.

of amplifier phase shift, two feedback loops are used: one involves the first and second stages, the other involves the third and fourth stages. The gain of each pair of stages is flat within 3 db from 5 to 88 kc without the use of feedback. With 15 db of feedback the gain variation is less than 0.3 db. The whole receiving amplifier, i.e., both pairs of stages in tandem, is flat within 0.5 db. This figure includes the frequency-response deviations of the output meter.

Oscillator Circuit. The oscillator uses one triode section of a type 6SN7GT tube (V-108A) in a series-fed Hartley circuit. A single tuning condenser (C-124) and a set of four inductances (L-101, L-102, L-103 and L-104) provide four frequency bands as follows: 5 to 11 kc, 10 to 22 kc, 20 to 44 kc, and 40 to 88 kc.

The resistances R-148 and R-149 provide cathode degeneration which stabilizes the frequency and the amplitude of oscillation and reduces harmonic distortion. The output from the oscillator is applied to a cathode follower (V-108B) which isolates the oscillator from succeeding circuits and provides a low-impedance signal source.

Mixing and Demodulation Circuits. When the selector switch is in the beat position, the output voltage of the local oscillator is applied to the control grid of the third stage (V-103) of the receiving amplifier. Since all stages of the receiving amplifier are adjusted for linear operation, the oscillator signal and the amplified output of the transducer are simply added together at this point in the circuit. No intermodulation frequencies are produced. The resultant output of the receiving amplifier is rectified by V-105 and the rectified signal is applied to the indicating meter M-101. Short time constants are used in the rectifier-meter circuit; thus the meter indication is proportional to the instantaneous sum of the received signal and the local oscillator voltage, not the amplitude of the beat note. This arrangement permits precise adjustment of the local oscillator to the exact frequency of a received signal, for the meter needle responds to the instantaneous phase angle between the signals as the two frequencies are brought together.

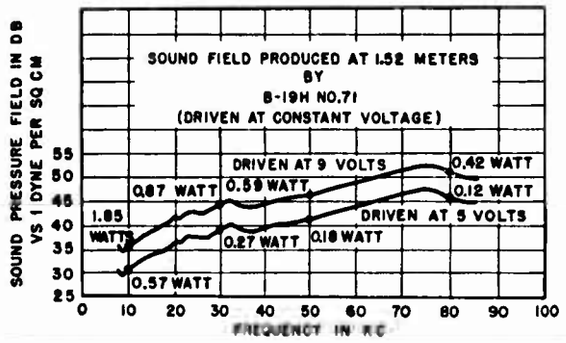

FIGURE 18. Transmitting characteristics of B-19H transducer.

Performance Characteristics. The performance characteristics are as follows:

1. Frequency range: 7 to 70 kc.
2. Receiving level range: 33 to 123 db above 1 bar.
3. Sending level range: In the frequency range of from 13 to 70 kc a maximum sending sound pressure 42 db above 1 bar at 1 m can be produced. At frequencies below 13 kc, the output must be decreased to prevent overload of the B-19H transducer. At 7 kc, the maximum obtainable sound pressure is 33 db above 1 bar at 1 m.
4. Frequency response: The response for either sending or receiving varies by ±4 db.
5. Calibration accuracy: Figure 20 shows the calibration results.
6. Absolute accuracy: For a random measurement the absolute accuracy may be subject to errors totaling 10 db, but the probable error under good conditions should not exceed 4 db. The maximum error of 10 db represents the sum of permissible errors in transducer response, errors due to tube changes not followed by recalibration, and errors due to fluctuation of line voltage and ambient temperature.

1.4.3 Recommendations for Future Work

Section 1.3.3, outlining future work on the OAX monitor, applies equally well to the OCP monitor. The frequency range of the Model X-OCP includes all frequencies currently used by echo-ranging sonar. It does not, however, include the lowest frequencies employed by sonar listening gear, and it would seem desirable to extend the lower frequency limit to 100 c

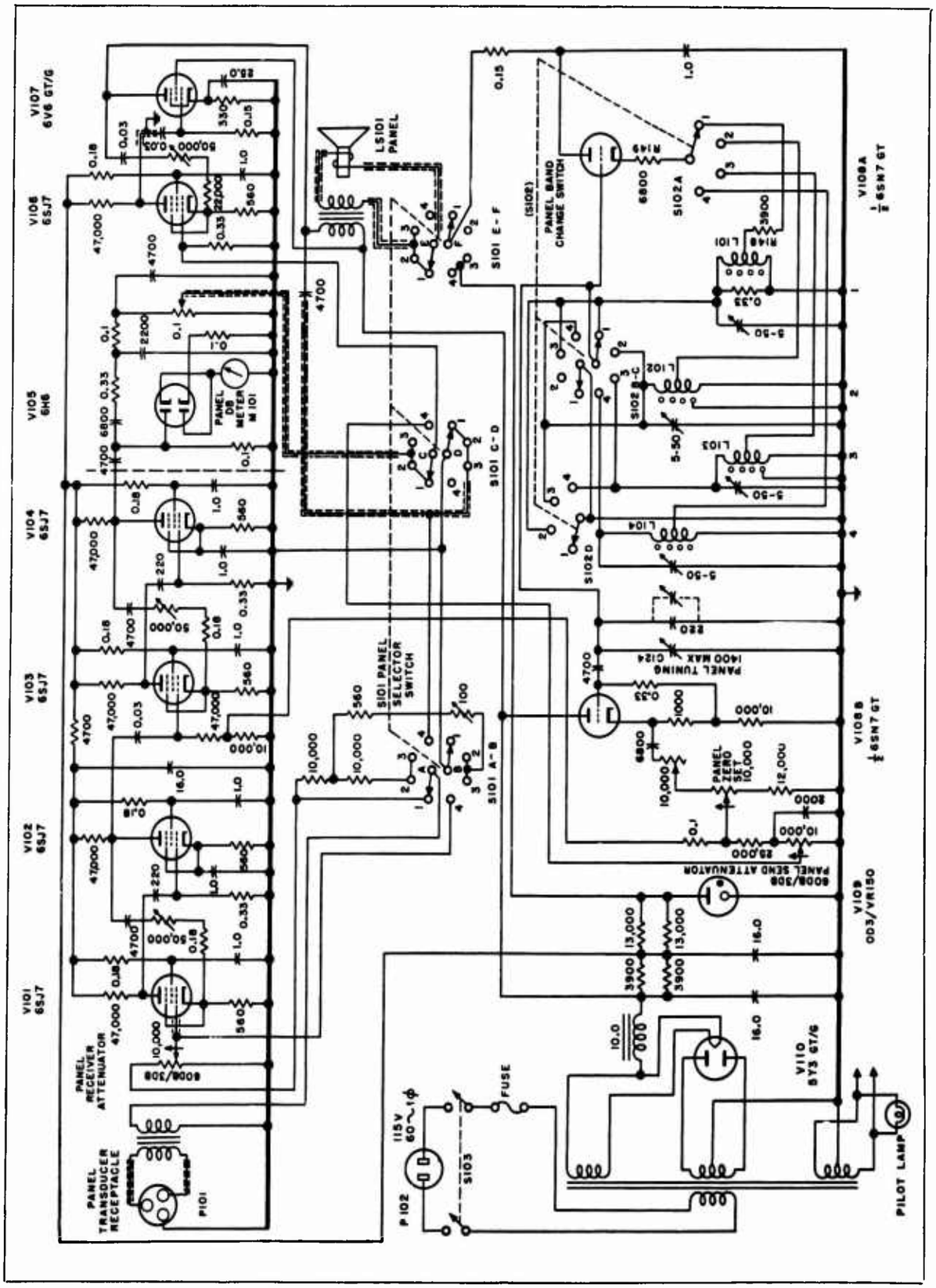

FIGURE 19. Schematic diagram of Model N-OCP portable monitor.

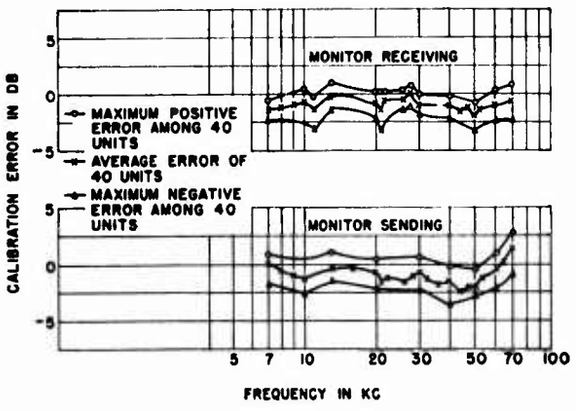

FIGURE 20. Calibration of 10 production units of Model X-OCP.

to make the monitor applicable to this equipment. No direct course of action can be outlined for accomplishing this, for low-frequency response and portability are inversely related in existing transducer designs.

1.5 INSTALLED SOUND GEAR MONITOR

1.5.1 Description

The installed sound gear monitor, like the portable models, consists of an oscillator-amplifier unit and a transducer. Where the portable monitor uses a transducer suspended overside, the ISGM employs a transducer mounted on a retractable strut. It was realized from the beginning of the development of portable models that there are inherent disadvantages in the use of a suspended transducer. Most significant of these disadvantages is the impossibility of using the equipment in rough water or while the ship is under way. If the transducer were permanently installed in a known position with respect to the sonar projector, operation would be possible at all times. An installed transducer would require no time for rigging and removing; consequently the sonar operator could make routine checks and adjustments at regular intervals. Considerations of vulnerability and serviceability require that an installed transducer be retractable.

Since the electrical requirements for an installed oscillator-amplifier unit are substantially the same as those for the portable unit, and because the portable type was expected to be in production and was already available for experimental use, developmental activity was concentrated largely on the transducer, strut mounting, and hoist mechanism.

1.5.2 Strut Design

Experience gained in the development of the first two models of the installed monitor indicated that mechanical design was a major obstacle in the development of a satisfactory prototype model. It was accordingly decided to adapt commercially procurable underwater logs to accommodate the monitor transducer.

The underwater log is a standard device used to measure ship's speed. A part of the log equipment consists of a streamlined strut and a hoist mechanism for retracting the strut through the hull of the ship. By closing a gate valve, it is possible to remove the retracted strut for replacement or repair. To convert the log strut to monitor use it is necessary only to attach a suitable transducer at the lower end and provide cable water seals at the upper end. Major mechanical design problems are eliminated because the log mechanism is designed to withstand

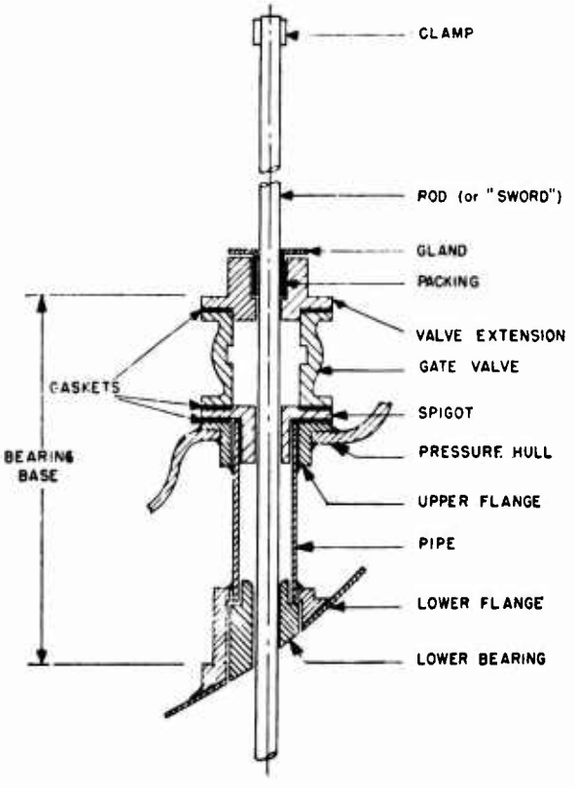

FIGURE 21. General hull arrangement of submarine log installation.

Service usage on combat vessels. The problem of fabricating an installed unit is simplified to the machine work required to attach a transducer to the commercially procured strut.

One of the designs used was called the Pit-Log installed monitor after the trade name of the strut used. The other was called the Bendix Log installed monitor because the log strut used is a product of the Bendix Corporation.

Pit-Log Installed Monitor

Operating Principles. As normally installed on surface vessels, the Pitometer Log (commonly called the Pit-Log) utilizes a strut gate valve, and stuffing box. No provision is made for easy lowering or raising. A handle is attached to the top end of the strut and hoisting is accomplished by the Armstrong method. No guide rails are provided for the top end of the strut. The bearing base at the junction with the hull is sufficiently rugged to withstand any ordinary forces.

For use on submarines several changes are incorporated in the Pit-Log. The double-hull construction of the submarine complicates the gate valve arrangement. Figure 21 shows the mounting employed. The bearing base (upper bearing surface to lower bearing surface) extends over 4 ft. In submarine service the external hydrostatic forces are so large that a nonreversible drive is required for moving the strut. This takes the form of a sprocket chain hoist as shown in Figure 22. The sprocket is driven through a worm wheel and crank. Guide

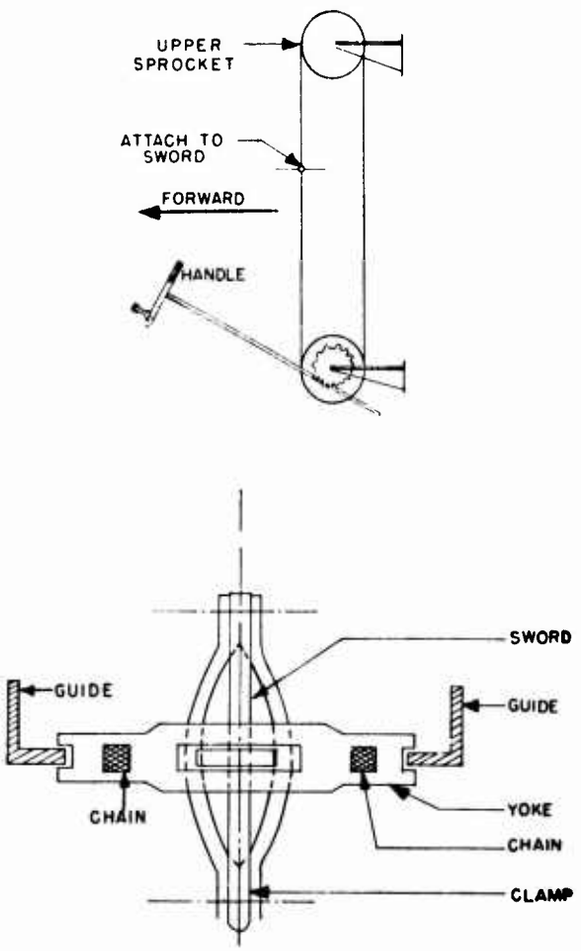

Figure 22. Pit-Log hoisting arrangement.

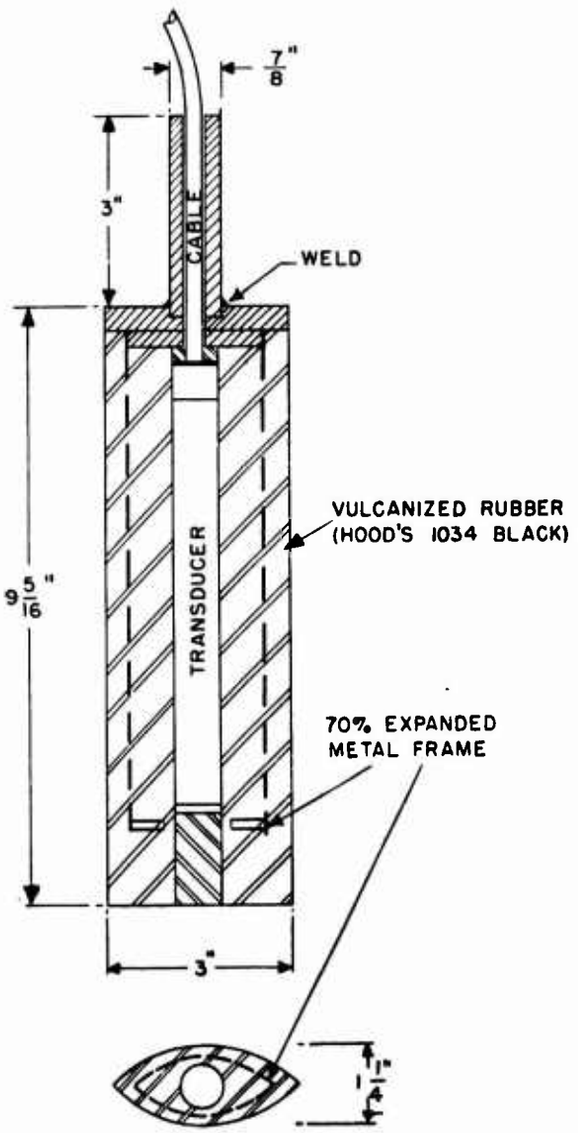

Figure 23. B-19H installed transducer assembly.

rails are provided for supporting the upper end of the strut as illustrated in this figure. The hoist mechanism is so designed that one turn of the hand crank produces a vertical strut motion of about 1 in.

The hoist mechanism and guide rails are not a part of the Pit-Log. They are fabricated by the manufacturer of the submarine and the design may differ slightly among the various boat yards.

Transducer. Several transducers, utilizing the active element of the B-19H unit, were developed for use with the Pit-Log strut. One of these is shown in Figure 23. The magnetostrictive tube is contained within a rubber block of the same cross section as the Pit-Log strut. The rubber is reinforced by a 70 per cent expanded metal frame.

Figure 24 shows an assembly in which a sleeve encloses the upper end of the transducer and the lower end of the strut. The transducer itself is shown in Figure 25. The wires from the transducer pass through a water seal at the upper end of the transducer casing and then through a pair of holes which run vertically up the strut (the two holes are a part of the original strut). The water seal at the top of the transducer is merely a precautionary measure, for the magnetostrictive element itself is hermetically sealed.

The uniform horizontal pattern of the bare B-19H element is distorted when surrounded by a metal and rubber frame. The directivity pattern of the

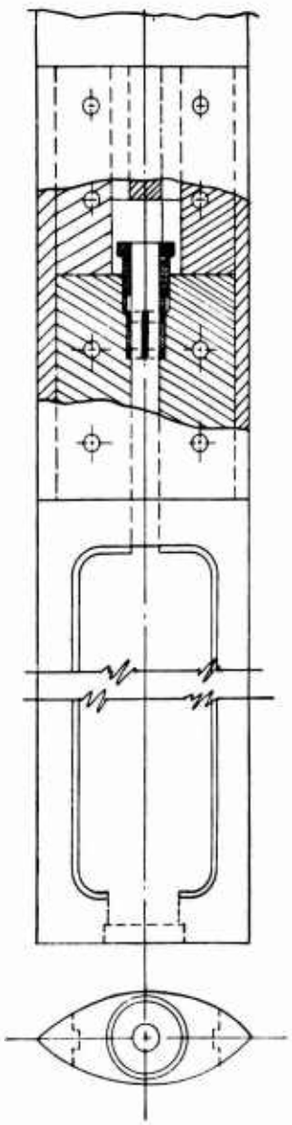

FIGURE 24. Transducer and strut assembly No. 2.

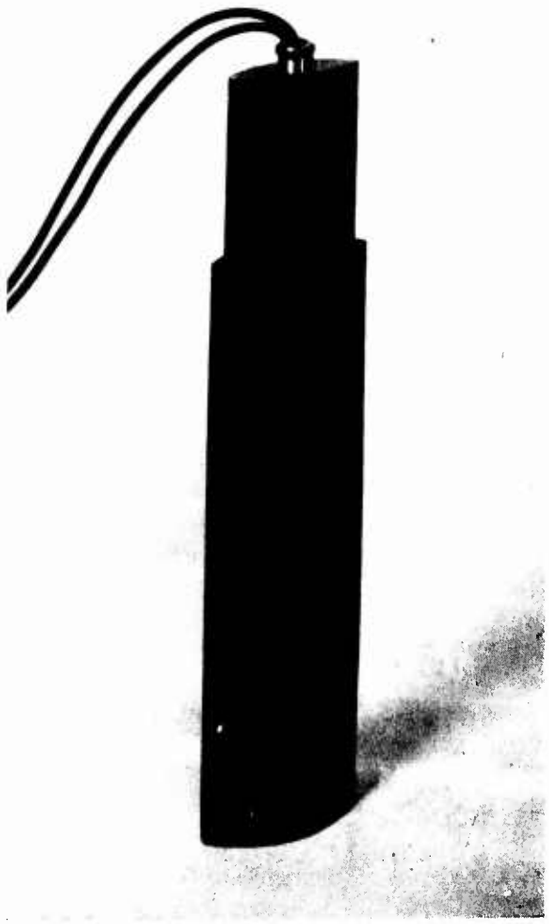

FIGURE 25. B-19H transducer for assembly No. 2.

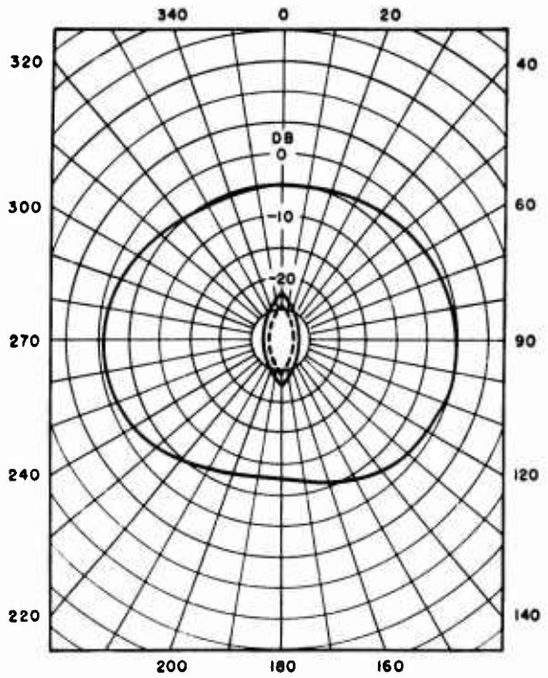

FIGURE 26. Directivity pattern for B-19H transducer (Pit Log assembly No. 2).

transducer shown in Figure 25 is given in Figure 26. This pattern is satisfactory for installed monitor application.

Circuit Principles. The original intention in the design of the installed monitors was that a bulkhead-mounted electronic unit should be developed for use with the installed transducer. The electronic unit was to be a permanent fixture in the ship's sound room. Permanent installation of the equipment relaxes the weight and portability restrictions that apply to the portable monitor, thereby permitting more rugged mechanical construction, more elaborate circuits, and consequent increased stability of operation. Preliminary circuits were worked on from time to time but no operating model was ever completed.

The installed monitors now in service are used in conjunction with the electronic units of the portable monitor. The combination of an installed transducer and a portable electronic unit gives perfectly satisfactory performance but does not represent a finished product suitable for general use.

1.5.3 Recommendations

The development of the installed monitor should be continued to provide a unit suitable for general use on Navy vessels. It is believed that the Pit-Log strut and the transducer already developed are satisfactory for such general use. The remaining components of the complete installed monitor system are yet to be developed. These include a remote-control hoist mechanism for the Pit-Log strut and a permanently installed electronic unit.

The hoist mechanism should be motor driven and should be controlled from the sound room of the ship. Provision should be made for hand-hoisting of the strut in case of motor failure. Guide rails should be used to steady the upper end of the strut during the hoisting process. Attention should be given to the mounting and support of the hoist mechanism itself. If possible the entire unit should be supported at the junction between the Pit-Log and the ship's hull. If bulkhead supports are used, consideration should be given to the elastic bending of the ship's hull structure, which may cause jamming of the strut mechanism.

The electronic unit of the installed monitor should follow the general design used in the portable monitor. Calibration stability should be increased if possible. Consideration should be given to the ambient temperature ranges and the mechanical shocks encountered in this application.

Bendix Log Installed Monitor

The Bendix Log installed monitor was never carried beyond the design stage, largely because the successful development of the Pit-Log type satisfied the existing demand for installed monitors.

1.6 MODIFICATIONS AND AUXILIARIES

The sound gear monitor may be modified for use as a vacuum-tube voltmeter or as a communications device. Moreover, its usefulness is still further increased by auxiliary equipment such as the phase sensitivity test unit, the projector test gear, the artificial projector, and the split projector test unit. For full details, the reader is referred to the completion report on the sound gear monitor[5] and to the other pertinent reports listed in the bibliography.

Chapter 2

THE DYNAMIC MONITOR

Dynamic Monitor

The dynamic monitor is a device designed and calibrated to provide direct measurement and indication of a numerical index, called the figure of merit, of the overall acoustic performance of sonar echo-ranging equipment. The figure of merit is defined as the ratio of transmitted ping intensity 1 meter from the projector to the intensity of the minimum detectable echo at the projector. The instrument consists of an electronic unit and a transducer which receives a ping transmitted by the echo-ranging gear and, after an appropriate time interval, returns an artificial echo of controllable strength, frequency, and duration. The monitor was constructed by the Harvard Underwater Sound Laboratory as an instrumental aid for the scanning sonar program.

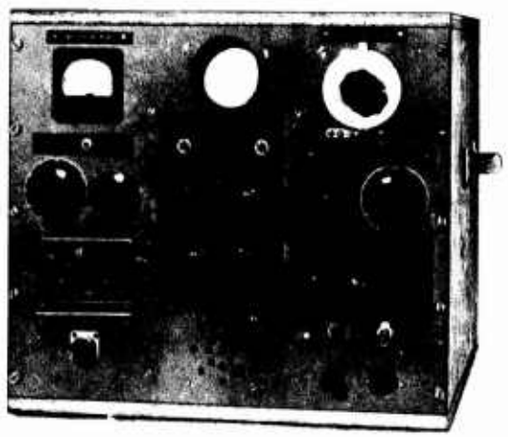

FIGURE 1. Dynamic monitor experimental electronic unit.

2.1 INTRODUCTION

FIGURE-OF-MERIT EVOLUTION

AFTER DEVELOPMENT of the OAX and OCP sound gear monitors[1] it was recognized that an index of the overall acoustic efficacy of sonar echo-ranging gear would be desirable. This resulted in the concept of the figure of merit, which is defined as the ratio of P_o to p_e, where P_o is the transmitted ping intensity 1 m from the projector, and p_e is the intensity of the minimum detectable echo at the projector. An OAX or OCP monitor may be used to determine either P_o or p_e, but not the figure of merit. It was realized that an instrument that would determine the figure of merit in a reasonably direct manner would be of value. For use with the visual channel of scanning sonar equipment, it was furthermore indicated that the transmitted signal of the instrument had to be a pulse rather than continuous. It was to meet these requirements that the dynamic monitor was designed.

PRINCIPLES OF OPERATION

Like the OAX or OCP sound gear monitor, the dynamic monitor consists of a transducer and an electronic unit (see Figure 1), the chief difference being in the electronic unit design, which is so devised as to key an echo when triggered by a ping. Briefly, the dynamic monitor operates as follows:

1. It receives a ping transmitted by the echo-ranging gear being tested.
2. It measures the intensity of that ping.
3. After a suitable delay, corresponding to range, it automatically returns a controllable echo initiated by the ping.
4. It measures the intensity of the echo.
5. It allows the difference frequency between the ping and the echo to be heard.
6. It gives the figure of merit with a minimum of calculation.

SPECIFIC USES OF THE DYNAMIC MONITOR

In terms of the figure of merit, the dynamic monitor is useful for the following specific purposes:

1. To compare the performance of different types of sonar equipment under similar circumstances.
2. To determine the changes in the overall functioning of a particular echo-ranging gear with time.
3. To determine the changes in the overall functioning of a particular sonar gear for varying conditions of target range, ship's speed, etc.
4. To provide a trustworthy numerical index by

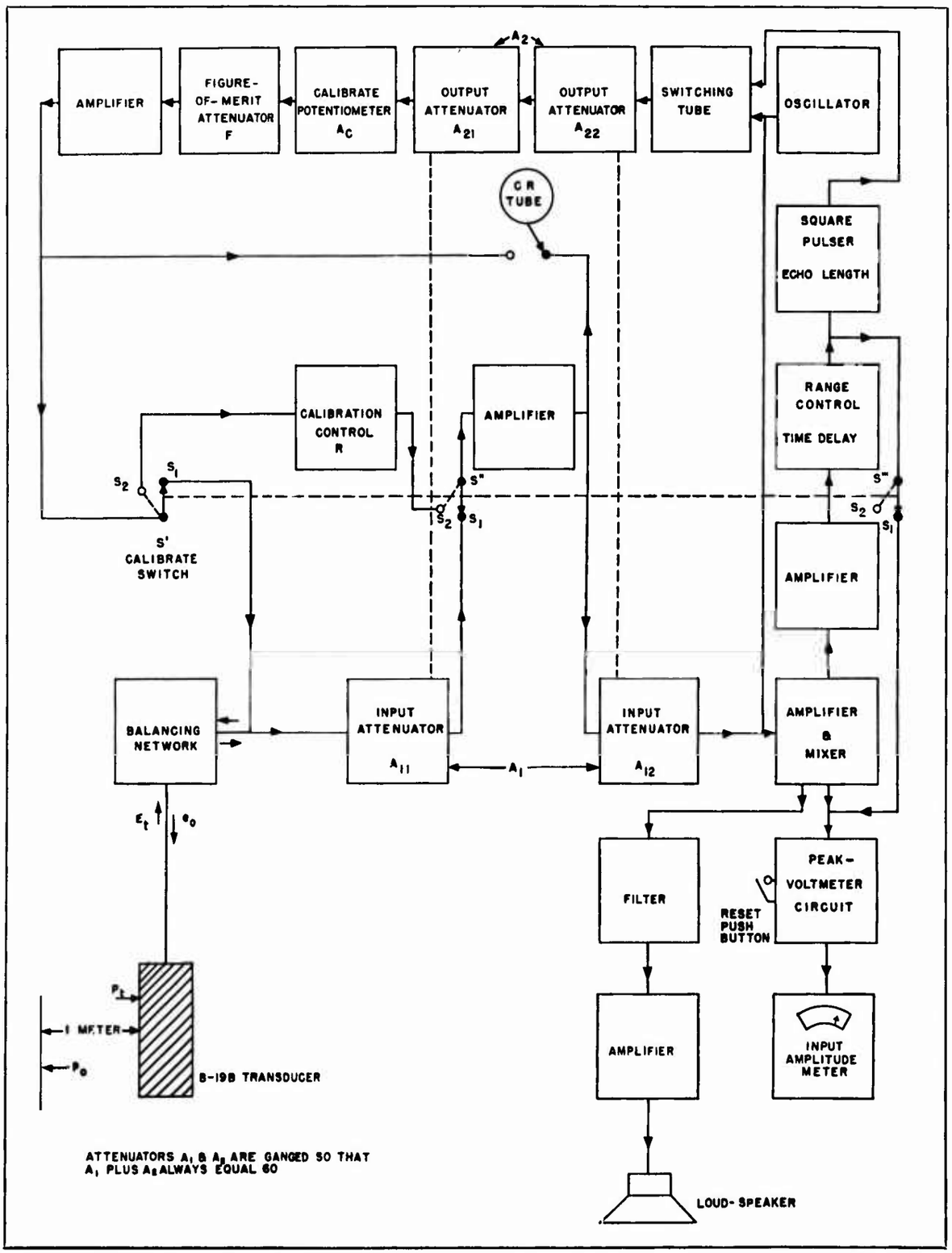

FIGURE 2. Block diagram of dynamic monitor.

which to gauge the improvement in successive models of sonar systems.

A block diagram showing components and circuit sequence is provided in Figure 2.

2.2 DERIVATION OF FIGURE OF MERIT

Because the objective of the dynamic monitor is to provide a means of obtaining directly the figure of merit of echo-ranging sound gear, circuits were designed and a formula evolved in which the calculation is done very simply. The figure of merit [F.M.] of a sonar equipment may be defined as $10 \log_{10} I_o/I_e$ (decibels), where I_o is the sound intensity at 1 m from the projector, and I_e is the minimum detectable echo intensity at the projector.

Since intensity is proportional to the square of pressure,

$$\text{F.M.} = 20 \log_{10} \frac{P_o}{p_e} \text{ db},$$

where P_o is the ping pressure in dynes per square centimeter at a distance of 1 m from the projector (see Figure 3), and p_e is the pressure in dynes per square centimeter of the minimum detectable echo at the projector. Under certain conditions it may be assumed that $P_o = P_t d$, where P_t is the ping pressure in dynes per square centimeter at d meters from the projector. Since $P_t = E_t/A$, where E_t is the voltage developed in the monitor transducer by P_t, and A is the terminated monitor transducer sensitivity in volts per dyne per square centimeter, therefore

$$P_o = \frac{E_t}{A} \cdot d.$$

Similarly, $p_e = p_o/d$, where p_o is the echo pressure in dynes per square centimeter at 1 m from the monitor transducer, and $p_o = e_o S$, where e_o is the voltage input into the monitor transducer of the minimum detectable echo, and S is the pressure in dynes per square centimeter at 1 m from the monitor transducer per volt input into the monitor transducer. Substituting for p_o,

$$p_e = \frac{e_o \cdot S}{d}.$$

Substituting for P_o and p_e,

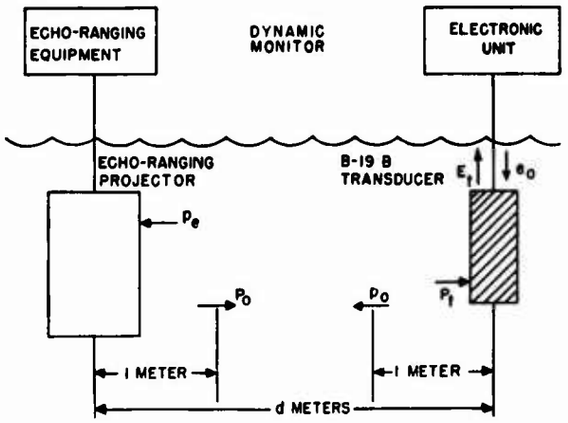

FIGURE 3. Simplified setup for figure-of-merit measurement.

$$\text{F.M.} = 20 \log_{10} \left(\frac{P_o}{p_e}\right) = 20 \log_{10} \frac{\left(\frac{E_t}{A}\right)(d)}{\left(\frac{e_o S}{d}\right)}$$

$$= 20 \log_{10} \left(\frac{E_t}{e_o}\right)\left(\frac{1}{AS}\right)\left(d^2\right).$$

Let [ ] represent $20 \log_{10}$.

Then

$$\text{F.M.} = \left[\frac{E_t}{e_o}\right] - [AS] + [d^2]. \qquad (1)$$

In the section that follows, equation (1) is developed into the form suitable for use with the dynamic monitor. Reference to Figure 4 is an aid in following this development.

The input and output attenuators are ganged in such a way that $A_1 \times A_2$ always equals 10^3 (60 db of attenuation). As defined here, A_1 is the ratio of the voltage appearing at the input terminals to the voltage at the output terminals of the receiving-channel attenuator. The other factors A_2, A_c, F, and R are defined similarly, that is, as ratios of input to output voltages of the respective attenuators. The amplifications G_1, G_2, B_1, and B_2 are defined as ratios of output to input voltages of the respective channels or networks.

It may be shown that[2]

$$E_t = k_1 A_1, \qquad (2)$$

where

$$k_1 = \frac{T_t}{G_1 B_1}.$$

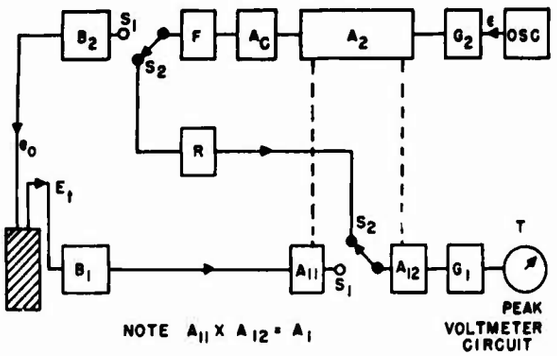

$A_1 = A_{11} \times A_{12}$ attenuation of receiving channel attenuator.
A_2 attenuation of ganged attenuator in transmitting channel.
A_c attenuation of "calibrate" potentiometer.
F attenuation of figure-of-merit attenuator.
B_1, B_2 balancing network constants (or amplifications).
ϵ oscillator voltage output.
e_o minimum detectable voltage output.
E_t ping voltage input.
G_1 amplification of receiving channel.
G_2 amplification of transmitting channel.
R calibration control constant (or attenuation).
S_1, S_2 switch positions of the "calibrate" switch.
T_t standard peak voltmeter reading of ping.
T_c standard peak voltmeter reading of calibrating process.

FIGURE 4. Simplified block diagram of dynamic monitor.

Similarly,

$$e_o = \frac{1}{k_2 A_2 F}, \tag{3}$$

where

$$k_2 = \frac{G_1}{T_c B_2 R \times 10^3}.$$

Equation (2) may be written

$$[E_t] = [k_1] + [A_1], \tag{4}$$

where $[k_1]$ = an electrical constant of the electronic unit,
$[A_1]$ = attenuation in decibels of the receiving-channel attenuator.

Equation (3) may be written:

$$[e_o] = -[k_2] - [A_2] - [F], \tag{5}$$

where $[k_2]$ = an electrical constant of the electronic unit,
$[A_2]$ = attenuation of ganged attenuator in transmitting channel,
$[F]$ = attenuation of figure-of-merit attenuator.

Combining equations (4) and (5):

$$\left[\frac{E_t}{e_o}\right] = [F] + [A_1] + [A_2] + [k_1] + [k_2].$$

Recalling that $[A_1] + [A_2] = 60$ db,

let $$[A_1] + [A_2] + [k_1] + [k_2] = [K_1],$$

where $[K_1]$ is a constant of the electronic unit as a whole.

Then

$$\left[\frac{E_t}{e_o}\right] = [F] + [K_1]. \tag{6}$$

Combining equations (6) and (1):

$$\text{F.M.} = [F] + [K_1] - [AS] + [d^2].$$

Let

$$[K_1] - [AS] = [K], \tag{7}$$

where K is a constant of the electronic unit and the monitor transducer, that is, of the dynamic monitor as a whole.

Then

$$\text{F.M.} = [F] + [K] + [d^2]. \tag{8}$$

The figure of merit may therefore be calculated by the summation of three factors: (1) the setting of the figure-of-merit attenuator, (2) an apparatus constant determined solely by one precise calibration of the monitor transducer and the electronic unit, and (3) a factor which takes into account the distance d separating the monitor transducer and the sonar projector.

It will be shown later that $[K]$ is not a true constant, but is dependent upon the frequency. To make a figure-of-merit determination, it is therefore necessary to select the value of $[K]$ from graph (g) of Figure 19, or from Table 3.

2.3 PRINCIPLES OF OPERATION

The dynamic monitor consists of an electronic unit (see Figure 1) and a magnetostriction transducer similar to that employed with the portable sound gear monitor. In operation the transducer is suspended overside at a distance d meters from the axis of the sonar projector (see Figure 5). The sonar gear is then turned on and executes its normal pinging cycle. The function of the dynamic monitor is to receive the transmitted pulse, to provide a quantitative measure of the strength of this pulse, and to generate, after an appropriate echo-length interval, a small artificial echo. This echo can be adjusted by the dynamic monitor controls until it is just recognizable as such by the operator of the sonar gear. As implied by the definition of the figure of merit, the objective of the dynamic monitor is to provide, as simply as possible, a quantitative comparison of the transmitted intensity and the intensity of the barely recognizable echo. This is accomplished in the dynamic monitor in the following way:

The transmitted pulse (shown in Figure 3 as a pressure P_0 at 1 meter from the projector, or P_t at d meters) is received by the monitor transducer and appears as an electric signal voltage E_t across its terminals. The voltage E_t corresponding to the transmitted pulse is passed through a calibrated attenuator to a vacuum-tube voltmeter capable of reading the peak amplitude of the short pulse. Assuming suitable calibration of the equipment, the attenuator setting required to produce a standard voltmeter reading becomes a measure of the transmitted pulse. At a suitable and adjustable time delay, corresponding to range, after reception of the pulse, a local oscillator in the monitor equipment supplies to the monitor transducer, through another calibrated attenuator, an electric signal e_0 which corresponds to the pressure p_e at the echo-ranging projector. (See Figure 3.)[a] This attenuator is then adjusted so that the artificial echo is just detectable. The frequency and pulse length of the echo pressure can be varied by other controls of the monitor equipment. Again, suitable calibration of the electric circuits would enable the strength of the artificial echo to be known quantitatively.

[a] It is to be understood that the transmitted ping of the echo-ranging system initiates the entire process. The ping produces the voltage E_t; E_t triggers a time-delay circuit; at the end of the time delay the electric signal voltage e_0 appears across the transducer terminals and produces the synthesized echo pressure p_e at the projector.

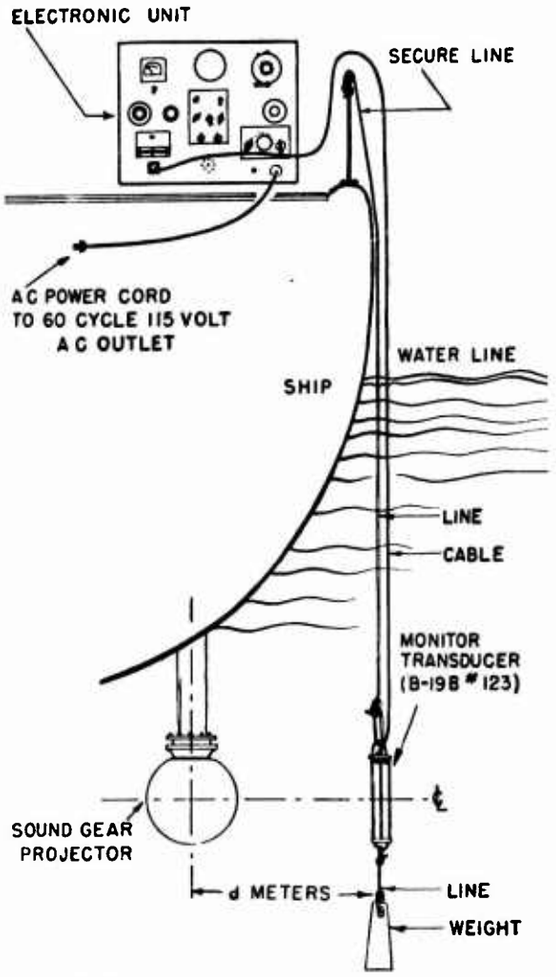

FIGURE 5. Physical setup for figure-of-merit measurement using dynamic monitor.

The equipment as just described would be capable of providing the data necessary to compute the figure of merit, but in measurement equipment of this type it is desirable to provide means which (1) reduce the measurement of the figure of merit to the setting of a single attenuator and (2) make it unnecessary to rely upon the long-term stability of the electronic equipment. The specific design features of the dynamic monitor to achieve these purposes are as follows (see Figure 4):

1. The attenuator in the receiving channel (used to measure the sonar pulse) is ganged with the attenuator in the transmitting channel (which delivers the local oscillator signal to the transducer) so that the transmitting attenuation is decreased when the receiving attenuation is increased.

2. Two auxiliary attenuators are connected elec-

trically in series with the transmitting attenuator, one known as the figure-of-merit attenuator, the other as the calibrate potentiometer.

3. A switch connection is provided to allow the local oscillator signal, generated in the dynamic monitor, to be calibrated by the same vacuum-tube voltmeter (later designated as the input-amplitude meter), which is utilized to measure the intensity of the sonar transmitted pulse.

Before the figure-of-merit ratio of ping intensity to echo intensity is determined, the monitor must be calibrated for this relation.[2]

With the monitor calibrated and the received pings producing standard meter readings, the figure-of-merit attenuator is then adjusted until the artificial echo is just detectable at the sonar gear. The figure-of-merit calculation is made by adding three factors: (1) the setting of the figure-of-merit attenuator, (2) a factor which takes into account the distance d between the monitor transducer and the sonar projector, and (3) an apparatus constant. The apparatus constant is a function of the characteristics of the monitor transducer and of the electronic unit. When the equipment has been calibrated, a standard known value may be assigned to the term contributed to the constant by the electronic unit.

To understand clearly why only the setting of the figure-of-merit attenuator is required, it is helpful to consider an example of a sonar gear for which the figure of merit has been determined. Assume that the intensity of the sonar pulse is increased 10 db, while all other factors, including the sensitivity of the projector in detecting the echo, remain constant. The figure of merit of the sonar gear would thereby be increased by 10 db.

In the process of making the determination after the assumed increase in output power, the attenuation of the receiving channel must be increased by 10 db to obtain the standard meter reading. At the same time that this attenuator setting is increased by 10 db, the attenuation in the transmitting channel is decreased by 10 db through the ganging of the two attenuators. In order to compensate for this reduction of the transmitting attenuation, so that the same echo intensity is transmitted as before, the figure-of-merit attenuation must be increased by the same 10 db. In this manner, the figure-of-merit attenuator setting reflects the improvement in the figure of merit produced by the assumed increase in the intensity of the emitted pulse of the sonar gear.

The second feature specifically designed into the dynamic monitor makes its calibration independent of the long-term stability of the electronic equipment. As described above, a figure-of-merit value is obtained by adding three factors. In the third of these factors certain characteristics of the electronic unit play a part. These characteristics, however, do not involve the amplifier components of the electronic unit in any way. This is shown later by the detailed analysis of the accuracy of the system.

A cathode-ray oscilloscope in the electronic unit enables the operator to compare the pulse length of the ping with the pulse length of the echo. Along a horizontal time axis on the oscilloscope screen the duration and shape of both the received and transmitted pulses may be viewed. In order that the echo frequency may be matched to the ping frequency, a loudspeaker is fed with the difference frequency so that zero beat during ping reception indicates the proper frequency adjustment.

2.3.1 Circuit Analysis

The complete schematic diagram of the electronic unit is shown in Figure 6. The various sections, which will be discussed in turn, are (1) the receiving section, which, with its peak voltmeter circuit, measures the ping intensity; (2) the echo range and echo length section which determines the range of the synthetic echo and the duration of its pulse; (3) the loudspeaker section, which furnishes the beat frequency between the ping and echo; (4) the transmitter section, which furnishes the synthetic echo; (5) the cathode-ray tube circuit, which provides for monitoring of input and output signals; and (6) the anode power supply, which furnishes regulated and unregulated $B+$ voltages.

Receiving Section

In the receiving section (see Figures 6 and 7), the incoming ping passes through attenuators and amplifiers to the input-amplitude meter, where its intensity is measured. This section consists of a resistance-coupled amplifier with a maximum gain of 80 db and a peak voltmeter circuit. The amplifier receives the input signal, a square pulse of radio frequency, from the hydrophone, and amplifies it to 14 v. The output is rectified by tube 6 and appears as a d-c voltage across condenser C and on the grid of tube 5-A. With zero signal, tube 5-A is nonconducting, because of the

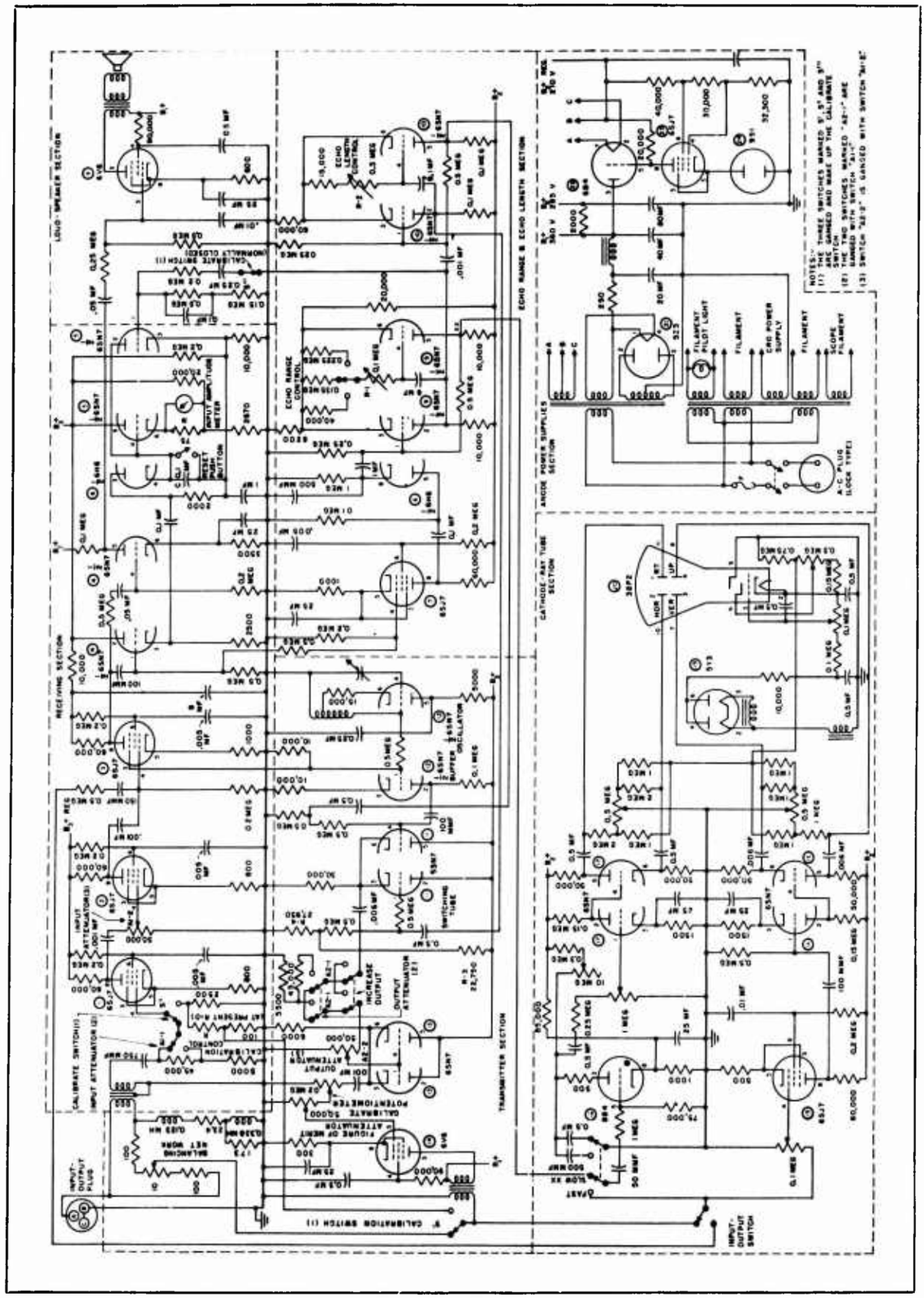

FIGURE 6. Circuit diagram of experimental monitor electronic unit.

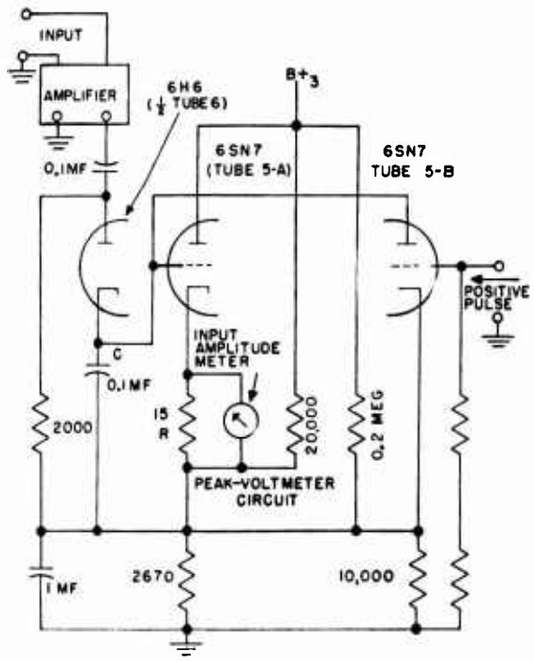

FIGURE 7. Receiving section: amplifier and peak-voltmeter circuit.

positive voltage produced at its cathode by the bleeder resistance connection to B_3+. When the amplified input voltage appears at the grid of tube 5-A, the tube becomes conducting and produces a voltage drop across R. With the input attenuators in the receiver section properly set, the drop across R causes the needle of the input-amplitude meter, connected across R, to deflect to some standard value. This meter reading remains constant for a certain period of time because there is no discharge path for the voltage across C, tube 5-B being cut off by its bleeder-resistance connection to B_3+. At some later time, when the dynamic monitor transmits an echo, a positive pulse is applied to the grid of tube 5-B, so that it conducts and thereby discharges capacitor C. The needle of the input-amplitude meter, therefore, returns to zero 1 to 4 sec after a ping signal deflects it, depending on the setting of R = 1, the echo-range potentiometer. (See Figure 6.)

Figure 8 shows how the amplifier and peak voltmeter circuit responds to different pulse lengths at a frequency of 23 kc. Figure 9 is a graph of the frequency response of the amplifier and peak voltmeter circuit.

Echo Range and Echo Length Section

The input ping signal is brought in parallel from the grid of tube 4 and applied to the grid of tube 7 (see Figure 5). After amplification by tube 7, the input signal is rectified by the second half of tube 6 and used to charge the 0.0005-μf condenser connected between the second cathode of tube 6 and ground. The rectified ping signal gives a positive pulse which is used to trigger tube 9, the echo-range tube.

Prior to this action, triode 9-B (see Figure 10) is conducting, since its grid is at zero potential with respect to its cathode. Triode 9-A is nonconducting, since its grid is at −37 v. When the positive pulse arrives, triode 9-A conducts immediately so that the voltage at point A (Figure 10) drops suddenly. The voltage at point B drops at the same time, through the action of the 6-μf condenser. Thus the current flow in triode 9-B is cut off. The voltage at the plate of 9-B then rises, thereby raising the potential of the grid of triode 9-A.

Triode 9-A is now conducting, while 9-B is cut off.

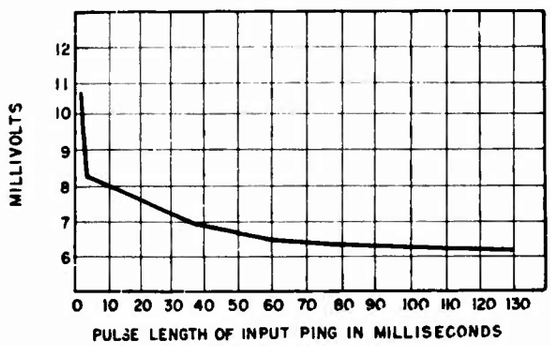

FIGURE 8. Receiver response versus pulse length at 23 kc.

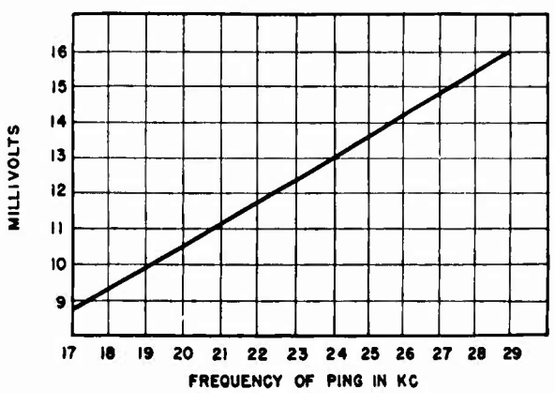

FIGURE 9. Frequency response of receiving section.

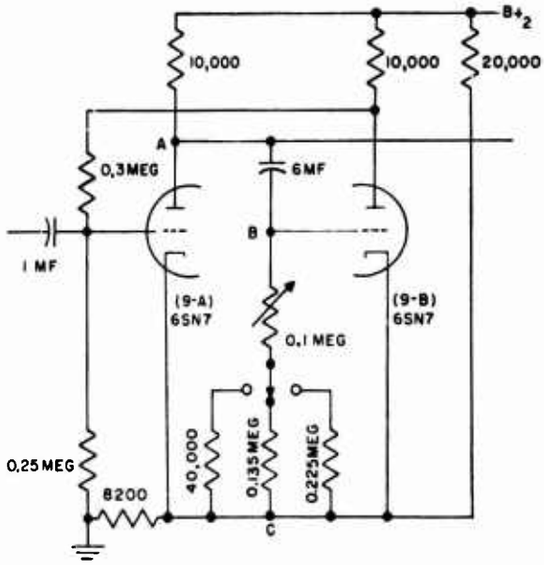

FIGURE 10. Circuit of echo-range tube (tube 9).

Because the potential at point B is well below that at point C, current flows through the grid resistor to charge the 6-μf condenser. As soon, however, as the potential at B has increased sufficiently so that the grid potential is above the cutoff value, triode 9-B again becomes conducting, and the plate voltage of 9-B is lowered. Thereby the potential at the grid of 9-A is decreased to such an extent that this triode is cut off. Hence, the condition of tube 9, which is called a "flip-flop" tube, is now the same as it was before the pulse arrived.

The length of the square voltage pulse at the plate of triode 9-A is varied by changing the resistance between points B and C. The time length of the pulse corresponds to the delay time of the dynamic monitor echo. The square voltage pulse from the plate of triode 9-A is used to supply the positive pulse input for tube 5-B, which acts to discharge the capacitance C in the peak voltmeter circuit. This pulse is also fed to the grid of the echo-length tube 10, through a 0.001-μf condenser with a 0.25-megohm ground return. The action of such a series combination is sometimes described as a *differentiation* process, since E_R (the voltage across a resistor R), is approximately equal to the time derivative of E, or $E_R \cong RC\frac{dE}{dt}$. This is true as the impedance of C is large compared to that of R, over the frequency range involved.

Echo-length tube 10 is another flip-flop tube. Across its grid resistor appear short negative and positive voltage pulses resulting from the differentiated square wave from tube 9-A. The negative pulse has no effect, since the tube is already well beyond cutoff. The positive pulse that comes at the end of the time delay triggers tube 10 so that a short negative square pulse appears at the plate of the first half of the tube (see Figure 6). A positive square pulse of the same time length appears at the plate of the second half of the tube. The length of this pulse, which determines echo length, is controlled by the variable resistor connected to the grid of the second half of the tube. Both the echo-range and the echo-length calibrations are only approximate. The two pulses generated by tube 10 are used to actuate switching tube 11. (See "Transmitter Section.")

Transmitter Section

The transmitter section (see Figure 6) furnishes, after a suitable time delay corresponding to range, the outgoing synthetic echo, the pulse length of which is controllable. The sequence of circuit components is (1) the second half of tube 12, the oscillator tube, (2) the first half of tube 12, which acts as a buffer tube, (3) the switching tube 11 (see below), (4) the output attenuators, which are ganged with the input attenuator as previously described, (5) the cathode-follower tube 13, (6) the calibrate potentiometer, (7) the figure-of-merit attenuator, (8) the amplifier tube 14, (9) the output transformer, (10) the balancing network (see below), and (11) the hydrophone connected to the input-output plug. The frequency response of the transmitter section is given in the graph of Figure 11.

Switching Tube. The switching tube 11 operates as an electronic switch, turning on and off the output of the transmitter oscillator tube 12. This action is

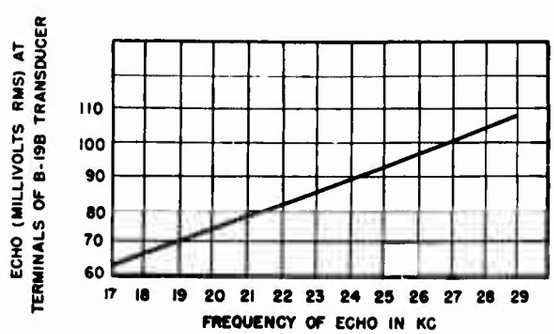

FIGURE 11. Frequency response of transmitter section.

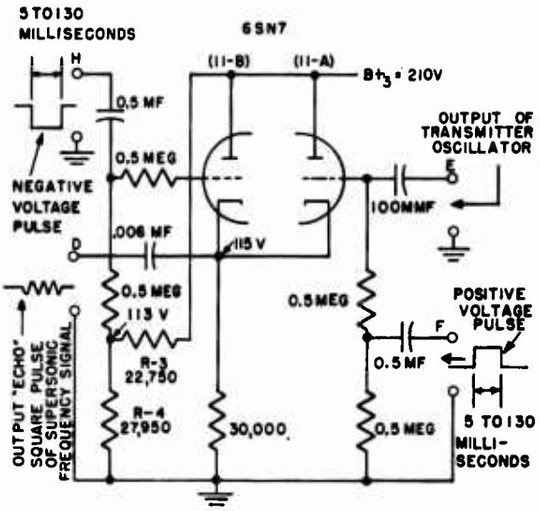

FIGURE 12. Switching tube circuit.

initiated by the positive and negative pulses generated by tube 10 in the echo range and echo length section. In this manner an r-f signal of the desired length and time delay is made to appear at the output terminals of the dynamic monitor.

Before tube 11 switches, no signal output appears at point *D* (see Figure 12), even though the oscillator output is applied to the grid of tube 11-A through point *E*. Tube 11-A, used as a cathode follower, is cut off with a cathode bias of 115 v because of the cathode current of normally conducting tube 11-B.

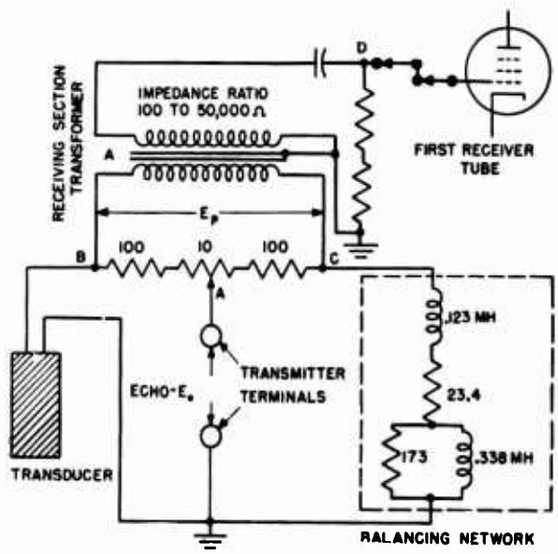

FIGURE 13. Balancing network circuit.

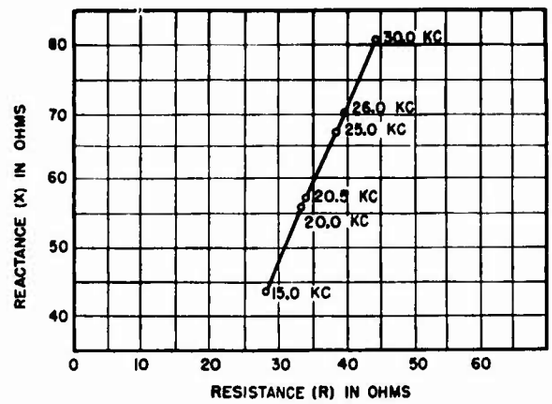

FIGURE 14. Impedance ($R + jX$) of B-19B transducer No. 123 (no polarizing current).

Bleeder resistances R-3 and R-4 put the grid of triode 11-B at 113 v above ground so that 11-B supplies practically all the current through the common cathode resistor. When the positive voltage pulse from tube 10 arrives at point *F*, it is applied to the grid of the cathode follower 11-A. This pulse has sufficient amplitude to overcome the bias and to allow a signal from the oscillator to pass through to the output point *D*. The simultaneous negative pulse at *H* cuts off tube 11-B and the d-c current through the cathode resistor remains unchanged. The bleeder resistances R-3 and R-4 may be adjusted so that no d-c pulse appears at the common cathode point. While tube 11-A is conducting, the signal on its grid appears at *D*. Thus a pulse of signal is produced equal in length to the d-c pulse but without a d-c component.

Balancing Network. The purpose of the balancing network is to prevent the transmitted echo from entering the receiving section in spite of the fact that the transducer terminals are connected to both the receiving section and the transmitting section of the dynamic monitor at all times.

To achieve this, a circuit is so arranged that an echo voltage E_o applied to the transducer has no effect on the receiving circuit. With reference to Figure 13, the impedance between points *A* and ground must be the same via point *B* and the transducer as via point *C* and the balancing network. If this condition holds, the echo pulse E_o will produce a voltage at *B* that is equal in magnitude and phase to the voltage at *C*. The net voltage E_p across the primary of the receiver transformer will therefore be zero when the monitor transmits, and no signal will reach the point *D* in the secondary circuit of the transformer.

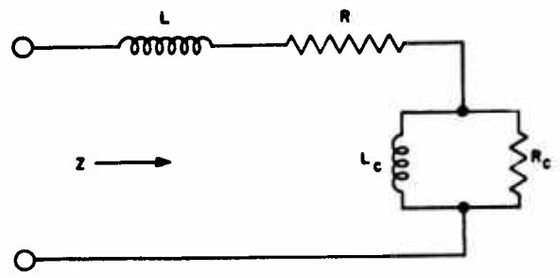

FIGURE 15. Network to balance transducer impedance at two frequencies.

In the ideal case, the impedance of the balancing network would be equal to the transducer impedance at all frequencies of practical interest. Values for the equivalent series resistance and reactance of transducer B-19B No. 123, at different frequencies, are given by the graph of Figure 14. In practice it is not possible to match the impedance of the transducer with a balancing network shown except by using another B-19B unit. It is possible, however, to design a network having an impedance that matches the transducer impedance at two different frequencies. Such a network is shown by Figure 15. The components of this network have values such that its impedance Z is equal to the transducer impedance at two selected frequencies. Since the frequency at which the dynamic monitor transmits may vary from 17.6 to 29.0 kc, the intermediate frequencies of 20.5 and 26.0 kc are chosen as the ones at which the network impedance is to match the transducer impedance.

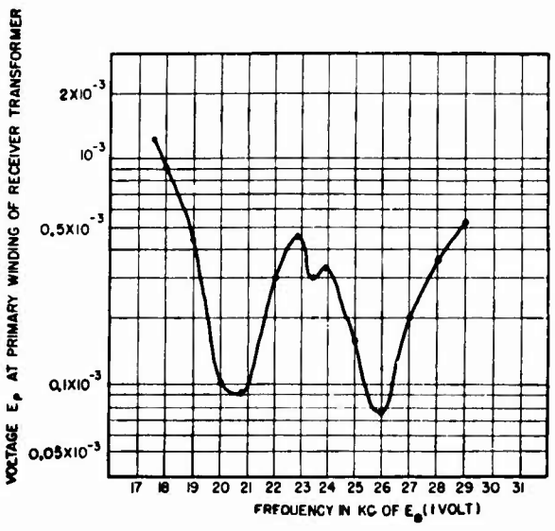

FIGURE 16. Performance of balancing network.

The solution[2] provides the following results: R = 23.4 ohms, R_c = 173.0 ohms, L = 0.123 mh, and L_c = 0.338 mh.

The performance of the balancing network constructed with components having the values listed above is indicated by the graph of Figure 16. At the particular frequencies of 20.5 and 26.0 kc, the ratio of E_p/E_o has the values of −80 and −82 db, respectively.

Loudspeaker Section

The difference frequency of the input ping and the oscillator-output echo is fed to the loudspeaker circuit in the following manner: a 2.5-v signal from the oscillator is applied continuously to the suppressor grid of tube 3, in the receiving section. (See Figure 6.) Tube 3, accordingly, functions as a mixer tube as well as an amplifier. When an input ping signal appears, the output of tube 3 contains four frequency components: (1) a high-level signal of input frequency f_1, (2) a low-level signal of oscillator frequency f_o, (3) a low-level signal of frequency $(f_1 - f_o)$, and (4) a low-level signal frequency $(f_1 + f_o)$. Part of this output is used to produce a reading on the input-amplitude meter via tubes 4-A, 6, and 5-A. Only the signal level of the input frequency is effective in producing this reading, since the levels of the other three frequency components are too low. All four components are also applied to tube 4-B, which is followed by a low-pass filter, a stage of amplification (tube 8), and the loudspeaker. The low-pass filter rejects the three high-frequency components and allows only the signal of frequency $(f_1 - f_o)$ to reach tube 8, a beam-power amplifier. The output of tube 8 is fed to the loudspeaker through an audio-frequency transformer. In adjusting the echo frequency of the dynamic monitor, the oscillator frequency is varied until a zero beat is obtained from the loudspeaker during a ping. In this manner the output frequency is made equal to the input frequency.

Cathode-Ray Tube Section

The cathode-ray tube section (see Figure 6) consists of an amplifier for the vertical deflection plates and sweep and amplifier circuits for the horizontal plates.

Amplifier for Vertical Plates. A signal, either input ping or output echo depending on the position of the input-output switch, is fed to the grid of tube 15, the first amplifier tube (see Figure 17). Triode 16-A forms the second amplifying stage. Triode 16-B is used with a high-impedance output circuit to obtain

two signal voltages of equal magnitude but opposite phase. The equal plate and cathode resistors of 50,000 ohms make the signal voltages at points *A* and *B* equal in magnitude, and the phase inversion puts them 180 degrees out of phase. The triode provides a high gain, functioning as cathode follower and linear amplifier.

Sweep Circuit. The linear sweep for the horizontal deflection plates is obtained from a sawtooth generator of standard type using a condenser and a gas-discharge tube. Tube 18 (see Figure 6), the sweep circuit oscillator, is followed by amplifier tube 17. Two sweep rates are provided: a fast sweep for frequencies ranging from 2 to 10 kc, and a slow sweep for frequencies from about 7 to 125 c. The synchronizing voltage for the fast sweep is obtained either from the grid circuit of tube 3 in the receiver section or from the secondary of the output transformer, depending upon the position of the input-output switch. The synchronizing voltage for the slow sweep comes from a point (marked *XX* in Figure 6) at the plate of the second triode of tube 9, the echo-range tube. In a previous discussion it was shown that a long, square, positive voltage pulse (see Figure 10) is generated at this point when an input ping enters the receiving section of the dynamic monitor. By differentiating this long, positive pulse through a capacitance and resistance in series, a short positive pulse is applied to the grid of the sweep oscillator, tube 18. The tube is thereby discharged and a horizontal sweep of the electron beam is started across the screen of the cathode-ray tube. In this manner the input ping and the horizontal sweep are synchronized. No synchronizing voltage is provided for the output echo when the slow sweep is used.

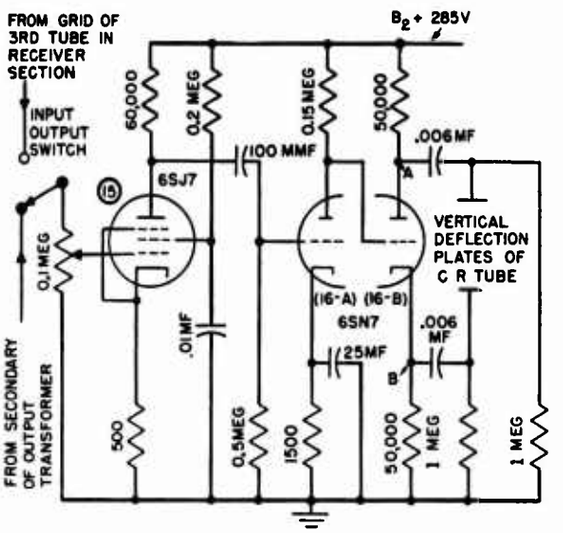

FIGURE 17. Amplifier circuit for vertical plates of CR tube.

ANODE POWER SUPPLIES

The unregulated anode power supply B_1+ (see Figure 6) consists of a full-wave, high-vacuum rectifier with a center-tapped transformer and a condenser-input filter system. The 360 v furnished by this supply provide the power for tube 14, the transmitter output tube, and for tube 8, the power amplifier for the loudspeaker. A high plate voltage is required for tube 14 to produce the necessary power output.

The unregulated B_2+ voltage of 285 v is obtained from a resistance-condenser filter which follows the condenser-input filter. (See Figure 6.) This voltage supplies the d-c power for tubes 15, 16, 17, and 18 in the cathode-ray tube circuit; for tubes 7, 9, and 10 in the pulse-forming circuit; and for the second triode of tube 4, an amplifier in the loudspeaker circuit. None of these tubes requires a regulated power supply.

The regulated B_3+ voltage of 210 v is provided by an electronic voltage-stabilizer circuit which is fed by the unregulated filtered B_1+ supply. The function of the stabilizer circuit is to furnish an output voltage (B_3+) substantially independent of variations either in its load impedance or in the d-c input voltage B_1+, which may fluctuate because of an a-c supply variation. This circuit employs the series-regulating tube 22, the control tube 23, and the glow-discharge tube 24. The regulated B_3+ voltage is used to supply the d-c power for all the tubes in the receiving section, in the peak voltmeter circuit, and in the transmitting section (except tube 14).

The cathode-ray tube has its own anode power supply (see Figure 6) consisting of a half-wave rectifier and a resistance-condenser filter to provide a negative voltage of 940 v.

2.3.2 Figure-of-Merit Determination

When calibrations and adjustments have been made, the dynamic monitor is ready for a figure-of-merit determination. To make such a measurement, the figure-of-merit attenuation is decreased until the operator of the echo-ranging equipment reports that he can just barely detect the echo emitted by the

monitor. When this adjustment has been made, the reading of the figure-of-merit attenuator is noted. The value of the figure of merit for the echo-ranging gear under test is then given by the relation,

$$\text{F.M.} = F + K + 40 \log_{10} d,$$

where F = the reading in db of the figure-of-merit attenuator,
K = 75 to 82 db [see graph (g) of Figure 19],
d = the distance in meters between the center lines of the monitor hydrophone and the projector of the echo-ranging equipment.

24 DISCUSSION OF CONSTANTS

To discuss the constants implicit in the figure-of-merit equation, it is convenient to rearrange some of the relations which have been developed.

From equation (7),

$$[K] = [K_1] - [AS],$$

or

$$K = \frac{K_1}{AS} = \left(\frac{1}{B_1 B_2 R}\right)\left(\frac{1}{AS}\right).$$

Here K_1 is characteristic of the electronic unit,[2] AS characteristic of the monitor transducer, and K characteristic of the dynamic monitor as a whole.

The factor $K_1 = 1/(B_1 B_2 R)$, the electronic unit constant, is fundamentally a function of impedance, and hence of frequency. It therefore has been investigated with respect to frequency and pulse length variations, and also with respect to a-c power supply voltage variations. Since R is a pure resistance control, it is essentially a constant for all variations of frequency, pulse length, and supply voltage for which the dynamic monitor was designed. Values of R yielding a convenient round number for the overall monitor constant K will be possible if a transducer is developed that is considerably less dependent on frequency than the present B-19B type. The B_1 and B_2 terms are functions of the impedances in the balancing network, which has been described.

The variation of K_1 with three parameters is shown by the graphs of Figure 18. From graph (a) it is seen that there is a change of about 1 db in the value of $[K_1]$ over a range of frequency from 17 to 29 kc. This change is a result of the frequency response of the balancing network. The variation of $[K_1]$ with frequency is taken into account by the proper selection of the $K = K_1/AS$ value for a figure-of-merit determination.

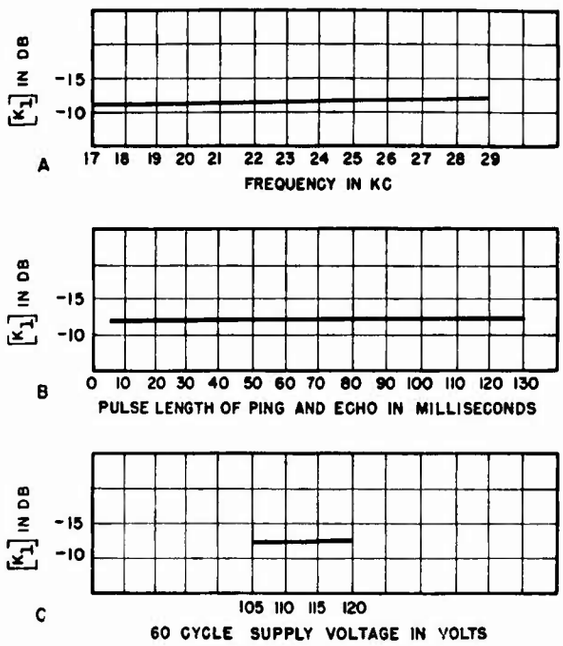

FIGURE 18. $[K_1]$ versus frequency, pulse length, and supply voltage.

Graph (b) of Figure 18 is a plot of $[K_1]$ versus pulse length with the frequency of both ping and echo held constant at 23 kc. The total change in $[K_1]$ over a range of pulse length of from 5 to 130 msec is approximately 1 db. This change is also a result of the frequency response of the balancing network. It is assumed that at frequencies other than 23 kc the change is not greater than 1 db. Since no attempt is made to take into account the variation of $[K_1]$ with pulse length, by the proper selection of the $K = K_1/AS$ value for a figure-of-merit determination, an uncertainty of ± 0.5 db consequently enters the figure-of-merit determination.

Graph (c) of Figure 18 shows the variation of $[K_1]$ with power supply voltage at a frequency of 23 kc and a pulse length of 30 msec. The change in $[K_1]$ over a range of voltage of from 105 to 120 v is approximately 0.5 db and may be slightly greater than the errors involved in measuring $[K_1]$. Since the derivation of the equation $K_1 = 1/(B_1 B_2 R)$ indicates that K_1 is independent of variations in supply voltage, it is assumed that the above change is negligible and K_1 is independent of supply voltage.

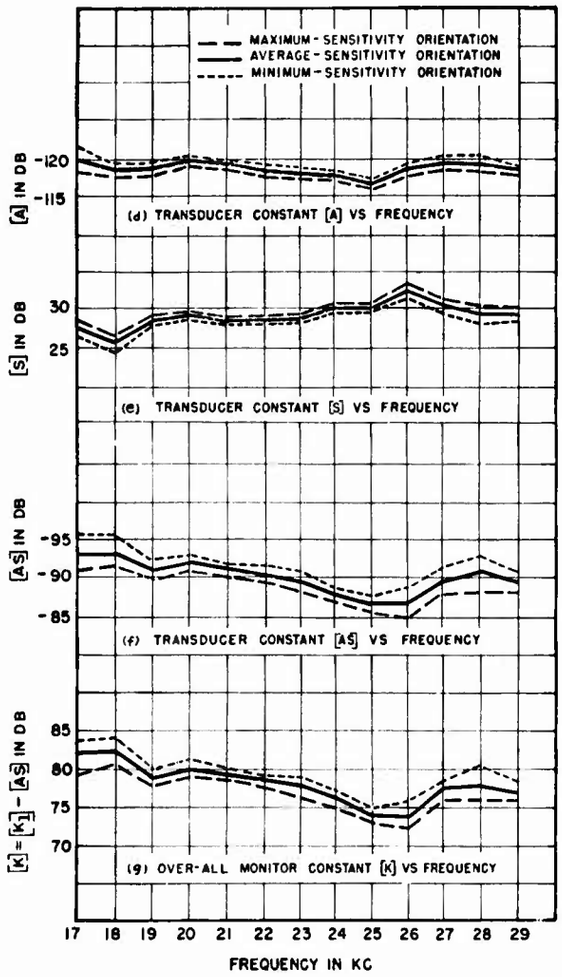

FIGURE 19. [A], [S], [AS], and [K] versus frequency.

The transducer constant AS is composed of the factors A and S, both of which vary considerably with the frequency of the sound waves the transducer receives or transmits. Graphs (d) and (e) of Figure 19 show the frequency relations. The data for these groups are compiled in Tables 1, 2, and 3. In gathering the data, transducer B-19B No. 123 was tested against a calibrated transducer. Factors A and S also depend on the azimuth orientation of the transducer. This is indicated by the graphs where the heavy central line is drawn for an orientation of average sensitivity, the upper and lower lines for maximum and minimum sensitivity. Graph (f) is plotted as the sum of $[A]$ and $[S]$. Because the transducer emits most strongly in the direction for which it is most sensitive, the variations of $[A]$ and $[S]$ with orientation must be added to obtain the variation of $[AS]$. Since no attempt is made to orient the monitor transducer in any particular direction when making a figure-of-merit measurement, these variations introduce an uncertainty into the value of $[AS]$. Graph (f) of Figure 19 shows that the uncertainty ranges from ± 0.3 to ± 2.2 db, depending upon the frequency.

The factor $[K]$, the constant characteristic of the dynamic monitor as a whole, is shown as a function of frequency in graph (g) of Figure 19. Graph (g) is a plot of $[K] = [K_1] - [AS]$, obtained by combining graph (f) with graph (a). The variations associated with the azimuth orientation of the monitor transducer are carried down. The variation in $[K]$ for an orientation of average sensitivity amounts to 7.6 db over a frequency range of from 17 to 29 kc; the uncertainty associated with the azimuth orientation of the transducer ranges from ± 0.3 to ± 2.2 db, depending upon the frequency.

In the final equation for the figure of merit,

$$\text{F.M.} = [F] + [K] + [d^2],$$

or

$$\text{F.M.} = [F] + \left[\left(\frac{1}{AS}\right)\left(\frac{1}{B_1 B_2 R}\right)\right] + [d^2].$$

The development of the above equation shows that a figure-of-merit determination is independent of all factors entering the derivation of the equation except F, A, S, R, d, B_1, and B_2. Fluctuations in the receiving and transmitting channel characteristics, represented by G-1 and G-2 in Figure 4, because of tube aging, frequency response, changes in power supply voltage, etc., cancel out in the calibrating process. Nor do changes in the oscillator voltage e (see Figure 4), resulting from day-to-day inconstancies in power supply voltage or oscillator characteristics, affect the figure-of-merit value. F represents the setting of the figure-of-merit attenuator; A and S, calibrated constants characteristic of the monitor transducer; R, a pure resistance control; d, the distance separating the monitor transducer and the sonar projector; B_1 and B_2, balancing network amplifications. The balancing network consists of several coils, resistors, and a transformer. Only changes with time in any of these factors will affect figure-of-merit measurements, once a precise calibration of the dynamic monitor is made. A precise calibration consists of determining the factor $[K]$ as a function of frequency.

TABLE 1. Characteristics of B-19B No. 123 Magnetostriction Transducer.

Frequency, kc	Open circuit sensitivity, db vs 1 v per dyne/cm²	Terminated sensitivity, db vs 1 v per dyne/cm²	Variation in horizontal pattern, db			Average sensitivity A, db	Sound pressure at 1 m driving at 1 v db vs 1 dyne/cm²	Average sound S, db
			+	−	Total			
17	−117.3	−121.2	2.2	0	2.2	−120.1	26.1	27.2
18	−116.0	−119.9	1.7	0.2	1.9	−119.0	24.9	25.6
19	−115.3	−119.3	0.8	0.1	0.9	−119.0	28.0	28.4
20	−116.6	−120.7	0.7	0	0.7	−120.1	28.7	29.0
21	−115.4	−119.6	0.3	0	0.3	−119.4	28.4	28.6
22	−115.2	−119.4	0.9	0	0.9	−119.0	28.4	28.8
23	−114.7	−118.9	1.3	0	1.3	−118.2	28.1	28.8
24	−113.8	−118.0	0.8	0	0.8	−117.6	29.5	29.9
25	−112.2	−116.4	0.5	0.2	0.7	−116.2	29.7	29.8
26	−115.1	−119.3	1.5	0	1.5	−118.6	31.2	32.0
27	−115.9	−120.1	1.2	0.2	1.4	−119.6	29.6	30.1
28	−116.5	−120.6	2.1	0	2.1	−119.6	28.1	29.2
29	−115.0	−119.1	1.0	0	1.0	−118.6	28.8	29.3

TABLE 2. Characteristics of B-19B No. 123 Magnetostriction Transducer.

Frequency, kc	Average sensitivity A, db	Maximum sensitivity A, db	Minimum sensitivity A, db	Average sound pressure S, db	Maximum sound pressure S, db	Minimum sound pressure S, db	Average AS, db	Maximum AS, db	Minimum AS, db
17	−120.1	−119.0	−121.2	27.2	28.3	26.1	−92.9	−90.7	−95.1
18	−119.0	−118.2	−119.7	25.6	26.6	24.7	−93.1	−91.5	−95.3
19	−119.0	−118.5	−119.4	28.4	28.8	27.9	−90.6	−89.7	−91.5
20	−120.4	−120.0	−120.7	29.0	29.4	28.7	−91.4	−90.7	−92.1
21	−119.4	−119.3	−119.6	28.6	28.7	28.4	−90.8	−90.5	−91.1
22	−119.0	−118.5	−119.4	28.8	29.3	28.4	−90.2	−89.3	−91.1
23	−118.2	−117.6	−118.9	28.8	29.4	28.1	−89.4	−88.1	−90.7
24	−117.6	−117.2	−118.0	29.9	30.3	29.5	−87.7	−86.9	−88.5
25	−116.2	−115.9	−116.6	29.8	30.2	29.5	−86.4	−85.7	−87.1
26	−118.6	−117.8	−119.3	32.0	32.7	31.2	−86.6	−85.1	−88.1
27	−119.6	−118.9	−120.3	30.1	30.8	29.4	−89.5	−88.1	−90.9
28	−119.6	−118.5	−120.6	29.2	30.2	28.1	−90.4	−88.3	−92.5
29	−118.6	−118.1	−119.1	29.3	29.8	28.8	−89.3	−88.3	−90.3

Table 3. Values of Monitor Constant (K).

Frequency, kc	Electronic unit constant K_1, db	Average monitor constant K, db	Minimum monitor constant K, db	Maximum monitor constant K, db	Uncertainty in monitor constant K, db
17	−11.0	81.9	79.7	84.1	2.2
18	−11.0	82.4	80.5	84.3	1.9
19	−11.1	79.5	78.6	80.4	0.9
20	−11.2	80.2	79.5	80.9	0.7
21	−11.2	79.6	79.3	79.9	0.3
22	−11.4	78.8	77.9	79.7	0.9
23	−11.5	77.9	76.6	79.2	1.3
24	−11.4	76.3	75.5	77.1	0.8
25	−11.6	74.8	74.1	75.3	0.7
26	−11.7	74.9	73.4	76.4	1.5
27	−11.7	77.8	76.4	79.2	1.4
28	−12.1	78.3	76.2	80.4	2.1
29	−12.1	77.2	76.0	78.2	1.0

2.5 ACCURACY OF SYSTEM

Accuracy of Figure-of-Merit Determinations

In estimating the accuracy of a given figure of merit, it is necessary to examine the reliability of all the factors that enter into its determination. The equation for the figure of merit is

$$\text{F.M.} = [F] + [K] + [d^2],$$

all factors being expressed in decibels. In the following paragraphs, the uncertainties in each of the factors F, K, and d are discussed in turn.

The adjustment of the calibrate potentiometer is assumed to be sufficiently fine so that any uncertainty on its account may be neglected. Because the smallest step on the receiving-channel attenuator is 2 db, an uncertainty of ±1 db is involved in its setting. Because of the 2-db steps on the figure-of-merit attenuator, a further uncertainty of ±1 db is introduced by its setting. The total uncertainty to be assigned to the factor $[F]$ is therefore ±2 db.

To make a figure-of-merit determination, it is necessary to select the value of $[K]$ from graph (g) of Figure 19, since it is dependent upon the frequency. The adjustment of the calibrate potentiometer is again assumed to be sufficiently fine so that any uncertainty on its account may be neglected. The maximum uncertainty associated with the azimuth orientation of the monitor transducer is ±2.2 db. Since no attempt is made to take into account the variation of the factor $[K_1] = [K] + [\Delta S]$ with pulse length, an uncertainty of ±0.5 db consequently enters the figure-of-merit determination.

There may be an uncertainty of about 5 cm in the value of d, the last item in the figure-of-merit equation. In the worst possible case, that is, when d is as small as 3 m, the uncertainty in $[d^2]$ amounts to about 0.3 db. At 10 m, the uncertainty is about 0.1 db.

The table below summarizes all the significant uncertainties discussed above.

Source	Uncertainty
$[F]$ – attenuator settings	±2.0 db
$[K]$ – transducer orientation	±2.2 db
$[K]$ – pulse length	±0.5 db
$[d^2]$ – distance	±0.3 db
Total	±5 db

A figure-of-merit measurement may therefore be considered correct to within ±5 db in so far as the uncertainties discussed are concerned. The total uncertainty of ±5 db is to be expected under unfavorable conditions. In actual tests, figure-of-merit values of a particular sonar equipment were repeated for different conditions within 2 db.

Accuracy in Determining Ping Pressure

Although the dynamic monitor was designed to measure the figure of merit of sonar equipment, it may also be used to determine approximately the value of P_o, the ping pressure at 1 m from the sonar projector. The possible uncertainties that enter into this determination are listed below.

From the equations developed in the theory, it follows that

$$P_o = \frac{E_t}{A} \cdot d = \frac{T_t A_1 d}{G_1 B_1 A}.$$

The uncertainties associated with the various factors in this equation are as follows:

T_t	input-amplitude meter reading	0.0 db
A_1	receiving-channel attenuator setting	±1.0 db
d	distance	±0.1 db
B_1 and G_1	receiver and balancing network frequency response	±2.5 db
B_1 and G_1	receiver and balancing network pulse length response	±1.0 db
G_1	supply voltage vs receiver-gain response	±0.5 db
A	transducer orientation	±1.1 db
	Total	±6.2 db

The uncertainty in the value of a P_o determination is therefore ±6.2 db. When two sonar equipments of ping pressures P_{o-1} and P_{o-2} respectively are compared under dissimilar conditions of operation, the total uncertainty involved in such a comparison amounts to ±12.4 db.

An uncertainty of ±5.4 db obtains, however, when the ping pressures of two sonar equipments are being compared under like conditions of pulse length and frequency.

Noise Level Limitation

The noise level inherent in the transmitter design limits the transmitter attenuation to approximately 76 db. For example, with the input-amplitude attenuators set at 0 db (the ganged output attenuators being then automatically at 60 db), the transmitter

signal level approaches the transmitter noise level at a figure-of-merit attenuation of 16 db. As the output attenuation is decreased, the figure-of-merit attenuation may, of course, be increased. The following table lists the possible figure-of-merit attenuations for different input-output attenuations.

Input attenuation	Output attenuation	Figure-of-merit attenuation
0 db	60 db	0 – 16 db
2	58	0 – 18
4	56	0 – 20
6	54	0 – 22
8	52	0 – 24
10	50	0 – 26
12	48	0 – 28
14	46	0 – 30
16	44	0 – 32
18	42	0 – 34
20	40	0 – 36
22	38	0 – 38

In practice this limitation of the dynamic monitor is of no serious consequence. By increasing the distance between the hydrophone and the echo-ranging projector, a combination of attenuations may always be found that circumvents the noise level limitation.

2.6 PERFORMANCE FIGURES

In this section several sets of dynamic monitor results are given together with sample conclusions drawn from them with regard to the performance characteristics of the gear under the specific test conditions.

In the table below are listed the results of two tests that illustrate the use of the dynamic monitor in determining changes in the overall functioning of one echo-ranging system, QH Model II.

Echo-ranging gear	Location	Date	Figure-of-merit	
			Visual channel	Audio channel
QH Model II with sea water in the projector	On PY31 at New London dock	11-8-44	131 db	145 db
QH Model II with dry projector	On PY31 at New London dock	11-19-44	142 db	152 db

On November 8, 1944, sea water, which had entered the projector through cracks in the weld around the projector supporting column, was present around a plug located inside the transducer assembly. Between that date and November 19 the projector was removed, dried out, and reassembled so that it was in normal operating condition on the latter date. It is apparent from the table that the change in the figure of merit for both the visual channel and the audio channel indicates an improvement in the operation of the QH Model II after the removal of the sea water from the projector. It is interesting to note that the audio channel of this echo-ranging gear can detect an echo intensity about 10 db lower than the visual channel.

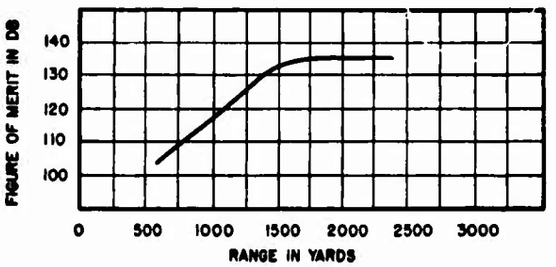

FIGURE 20. Figure of merit versus range for WEA-1 echo-ranging gear aboard the *Aide de Camp* in Boston Harbor.

FIGURE OF MERIT VERSUS RANGE

On June 27, 1944, the echo-ranging equipment WEA-1 on the *Aide de Camp*, a boat of the Harvard Underwater Sound Laboratory, was tested while the *Aide de Camp* was at its Boston dock. Measurements of the figure of merit were made for different echo ranges to determine the effect of reverberation. The graph of Figure 20 shows the figure-of-merit values obtained when the range was varied at which the dynamic monitor injected its synthetic echo.

From the graph it may be deduced that the level of reverberation was appreciably higher at 600 yd than beyond 1,600 yd. Since the ping pressure remained constant throughout the test, it follows that the 28-db difference in the figures of merit for 600 yd and for 1,600 yd is a measure of the difference in the intensities of the minimum detectable echo for the two ranges. It also follows that for ranges of from 1,600 to 2,400 yd some other factor determines the lower limit of the minimum echo and therefore the upper limit of the figure of merit. In most cases, the effect of reverberation at a particular locality may be eliminated by measuring the figure of merit at ranges of from 2,000 to 3,000 yd.

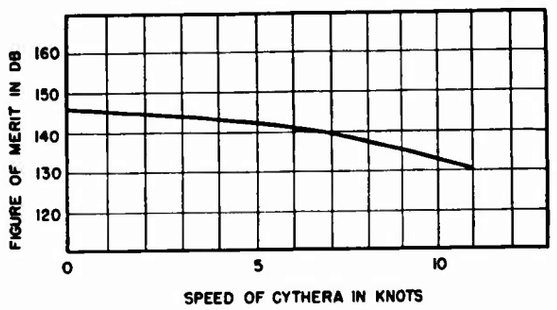

FIGURE 21. Figure of merit (audio channel) versus speed for QH Model II aboard the USS *Cythera* (PY31) in 90 ft of water.

FIGURE OF MERIT VERSUS SHIP'S SPEED

On November 20, 1944, a test was made to determine the effect of ship's speed on the performance of an echo-ranging gear. The figure of merit of QH Model II was measured at five different speeds of the USS *Cythera* (PY31) in 90 ft of water. The dynamic monitor injected its synthetic echo into the ship's installed monitor transducer at a relative ship's bearing of 341 degrees and a range of 2,700 yd. The QH projector was operated without a dome. The results of the test are given by the graph of Figure 21.

At a speed of 11 knots the figure of merit of the echo-ranging gear was 16 db less than at zero speed. Since the ping pressure was not varied during the test, the decrease in the figure-of-merit value signifies that the intensity of the minimum detectable echo had to be increased. This required increase of echo intensity resulted from the heightened ambient noise level produced by the ship's screws and the passage of the ship through the water.

2.7 CONCLUSIONS

In general, a large figure of merit means that the echo-ranging gear is putting a comparatively large amount of sound energy into the water, and is, at the same time, capable of detecting a comparatively weak echo. A small figure of merit, on the other hand, usually indicates that the projector combines the characteristic of a relatively weak ping intensity with that of requiring a somewhat stronger echo in order for it to be detected. Clearly then, a large figure of merit is to be desired since, other things being equal, the larger this ratio is, the greater is the range at which the sonar gear is able to detect the presence of a target.

The figure of merit is a function of all the factors that affect the intensity of the transmitted ping and the intensity of the minimum detectable echo. As far as the minimum echo is concerned, the deciding factors are usually the ambient water noise level, the character of the reverberation, and the electric noise level of the echo-ranging gear.

The electronic unit constant K, one of the factors in the figure-of-merit determination, is not affected by changes in amplification in the local oscillator, tube aging, variations in the a-c power supply voltage, or other circuit deteriorations, since they are taken care of in the calibration process. The characteristics that do enter this factor are electric properties of certain coils, resistors, and the input transformer. The frequency dependence of these is taken into account when the K factor is initially determined. The constancy of this factor, therefore, as far as the electronic unit is concerned, depends only on the constancy of these components. Since the other two factors involved in the figure-of-merit measurement, namely, the setting of the figure-of-merit attenuator and the distance between the projector and transducer, are completely independent of the electronic unit, it is seen that in the operation of the dynamic monitor the reliance on the long-term stability of the electronic equipment is effectively eliminated.

2.8 RECOMMENDATIONS

The experimental model of the dynamic monitor has not received enough engineering development to be utilized as a manufacturing prototype. A few specific factors may be mentioned which should receive attention during reconsideration of the unit. The sound level produced by the built-in loudspeaker is not adequate and should be increased. A low-pass filter should be incorporated in the loudspeaker circuit in order to eliminate spurious signals. The output of the monitor transmitting channel should be increased so that attenuation of 100 db could be employed in this channel instead of the present maximum of 76. Higher transmitter output and wider range of attenuation would eliminate the occasional necessity of moving the monitor transducer during the series of measurements in order to avoid masking of the echo by noise level interference inherent in the monitor transmitting channel. The present mechanical layout of the electronic unit leaves much to be desired from the point of view of accessibility for

repair and maintenance. It appears possible to make changes in the mechanical assemblies which will achieve greater ease of maintenance without sacrificing the compactness of the unit. The location of the ganged input and output attenuators could also be changed with a beneficial reduction in the crosstalk between the transmitting and receiving sections. If the response of the monitor transducer were sufficiently uniform with frequency, it would be possible to construct a dial plate for the figure-of-merit attenuator which could be adjusted for various values of distance d so that the attenuator would read figure of merit directly, but this refinement has not been built into the present model.

Chapter 3

THE OVERSIDE NOISE MONITOR

OAY Sound Measuring Equipment

The portable and rugged Model OAY sound measuring equipment was developed for overside measurements of submarine sound, and for detection of abnormally noisy auxiliaries. The apparatus measures sound pressure level over a dynamic range of 110 db within the frequency range from 100 to 20,000 c. CUDWR-NLL assisted the Navy in OAY development.

FIGURE 1. Model OAY sound measuring equipment.

3.1 INTRODUCTION

THE SUBMARINE NOISE reduction program required sound measurement equipment which could be used to determine acceptable standards of quiet performance and which would express this calibration in absolute terms to permit comparison of the results obtained at different bases with different ships. The OAY gear which was developed for this program comprises a wide-band hydrophone with a flat response and a sound level meter with provision for various types of monitoring and filter channels. It is a flexible measuring system, adaptable to many purposes. The equipment was made portable and sufficiently rugged for use in the conditions to be encountered in the field. A routine for maintaining the equipment and checking the hydrophone calibration was set up to insure the accuracy of the absolute sound level readings.

The OAY gear is chiefly used at submarine bases during the installation of new equipment. A procedure was established for making overside measurements of submarine noise during construction or refitting, so that noisy auxiliary machinery units can be detected and the trouble remedied before the ship leaves the yard. Overside measurements can also be made on submarines in commission, when they are at docks, secured to buoys, anchored, or drifting. The OAY equipment is customarily located aboard the surfaced submarine and the hydrophone is hung overboard at a standardized location, as near as possible to the noisy part of the auxiliary machinery to be measured. Noise level readings thus obtained in absolute units are compared with the standard values for acceptable performance, as previously determined. These results can also be related to the standard Navy 200-yd measurements.

Prior to the development of the OAY gear, the submarine noise reduction program relied upon the Model OR equipment. This apparatus has a sharply falling frequency response above 1,000 c and a broad peak near 500 c, while the OAY has a response that is flat from 100 to 10,000 c and good to 20,000 c. In order to convert OR readings to equivalent OAY readings, it was found that, in general, 9 db could be added to the Model OR readings to give sound pressure levels above 0.0002 dyne per sq cm. In specific cases, however, because the OAY response is so much more uniform than that of the OR, the correlation between new and old readings had to be determined for the particular sounds to be measured.

3.2 DESIGN CONSIDERATIONS

It was initially proposed to develop portable measuring equipment for the submarine noise reduction program by adapting a commercial sound level meter and a commercial hydrophone. When this plan was analyzed, however, it was clear that the work of modification would be extensive, the procurement of sound level meters would be most difficult, and the resulting system would be inconvenient both to transport and to operate. It was accordingly decided to design completely new equipment for the specific requirements of the noise reduction program.

In the selection of a hydrophone, the field of

available hydrophones was investigated, and serious consideration was given to various units developed by Western Electric, the Massachusetts Institute of Technology Underwater Sound Laboratory, and the Brush Company. The nondirectional hydrophone used in the expendable radio sono buoy was also proposed. It was found that none of these hydrophones was altogether satisfactory for the projected measuring equipment because of high self-noise, unsuitable frequency response, or variation of response with temperature. The hydrophone finally adopted was one newly developed by the Brush Company. This hydrophone satisfies the frequency response requirements for the system, is fairly independent of temperature, and has a uniform directivity pattern. The overall response of the hydrophone and the total system is flat from 100 to 10,000 c, and useful to 20,000 c. The hydrophone has sufficiently high sensitivity and low self-noise to permit measurement of submarine noises of the lowest level detectable in the quietest water conditions. Attenuators within the system adjust the range of the meter so that it reads sound levels from 35 to 145 db above 0.0002 dyne per sq cm.

For adaptability to various measuring problems the equipment was designed to include means for self-calibration, as well as output jacks for a monitoring loudspeaker and headphones, for recording equipment, and for commercially available frequency analyzers. An optional 10,000-c high-pass filter was included to facilitate supersonic measurements. An optional 1,000-c low-pass filter was also provided to reduce background noise in certain conditions. The circuit was so designed that the use of these accessories produced no disturbing effect upon the meter reading.

The apparatus was also designed to be portable, rugged, and adaptable to use on shore, on shipboard, or in small boats. It was operable either with a 110-v, 60-c power supply or from storage batteries. The hydrophone was designed for use with as much as 400 ft of cable, and the standard equipment included both a 10-ft and a 400-ft cable, either of which could be fastened to the hydrophone by means of a watertight connector.

The final model of the OAY satisfied the design requirements to a large extent, and approximately 40 units of the measuring equipment were supplied to the Navy for use at submarine bases all over the world. On the basis of the field performance of the OAY, recommendations were made for changes to increase the ruggedness of the equipment and to improve its usefulness. A prototype model incorporating many of the proposed modifications was constructed as a basis for future work.

3.3 CONSTRUCTION OF THE OAY EQUIPMENT

3.3.1 General

The Model OAY sound measuring equipment, as produced for Navy use, is shown in Figure 1 and in the block diagram of Figure 2. It consists of the hydrophone with connecting cable and plug; the sound level meter with its attenuators, four-stage amplifier, balanced vacuum-tube voltmeter, power supply, and internal calibration circuit; and a rotary converter assembly. Accessory equipment which can be used with the meter includes the monitoring headphones, a monitoring amplifier and loudspeaker, and the narrow-band sound frequency analyzer, General Radio Type 760A. In operation, the underwater sound signal is picked up by the hydrophone, amplified, and read on the meter scale. This scale is calibrated in steps of 1 db, and the attenuator adjusts the amplification of the unit so that the reading falls within the meter scale. The internal calibration circuit, which is adjusted initially to correspond to the predetermined sensitivity of the hydrophone, permits a check of the calibration level at the time of measurement. The sound pressure levels are read from the meter in absolute terms, in decibels above 0.0002 dyne per sq cm, by adding the meter reading to the attenuator setting.

3.3.2 Hydrophone

The hydrophone used with the OAY equipment is the Brush RQ-51055 (AX-58) shown in Figure 1. It consists of a Rochelle salt crystal head and a two-stage, built-in amplifier, housed in a cylindrical rubber case. A schematic circuit drawing is given in the upper left-hand corner of Figure 7. A one-stage amplifier that was originally produced with the RQ-51055 was found unsuitable and the two-stage amplifier was substituted. This amplifier, employing negative feedback, provides high input impedance, low output impedance, high gain stability, and high output voltage which is an advantage in combating electrical interference on shipboard. Water ground connection is provided for the system by

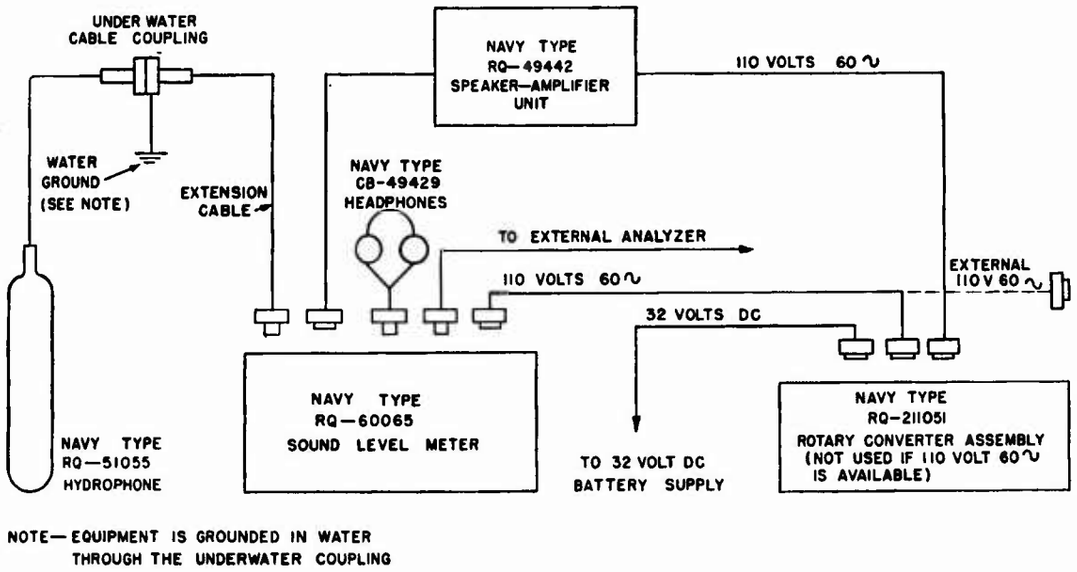

FIGURE 2. Block diagram of OAY sound measuring equipment.

means of the special watertight connector that fastens the hydrophone to its cable extension. The hydrophone is itself equipped with a 17-ft length of cable and both 10-ft and 400-ft cable extensions are provided.

The frequency response of the RQ-51055 hydrophone is shown in Figure 3. The uniformity of frequency response that was desired for the production units was not achieved. The solid line *A* represents the average response for 24 hydrophones of the original production lot, while the dotted line *B* is the average of 18 later units. It was observed that these later units were more nearly uniform.[a]

The temperature dependence of these hydrophones is indicated in Figure 4 which shows the response at low frequencies for temperatures of from 40 to 90 F. The data available indicate that the response is little affected by temperature at frequencies up to 10,000 c. It is also established that the response is not affected by static pressures at depths down to 300 ft.

3.3.3 Sound Level Meter

GENERAL

The sound level meter is the principal part of the OAY equipment. Its mechanical construction can be seen from the photograph in Figure 5. This unit is designed to be both compact and sufficiently rugged for use in the conditions to be encountered in the field. The sound level meter and its power supply are mounted in this single chassis and operate either from batteries or from an a-c supply. Facilities are provided for plugging in headphones, loud-

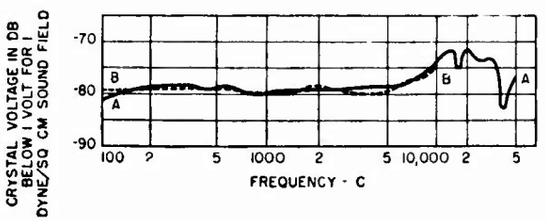

FIGURE 3. Calibration of RQ-51055 hydrophones. *A*. Average of 24 original units. *B*. Average of 18 latest units.

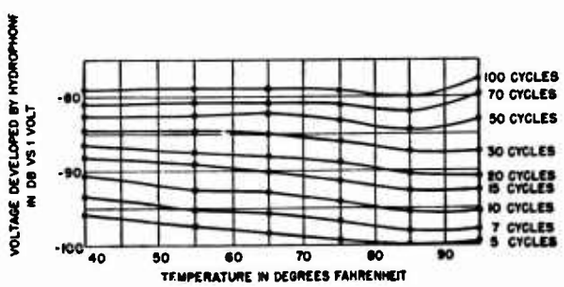

FIGURE 4. Effect of temperature upon sensitivity at low frequencies for RQ-51055 hydrophone No. 32.

[a] The USRL calibration of the hydrophone is given in Division 6, Volume 11, Chapter 7.

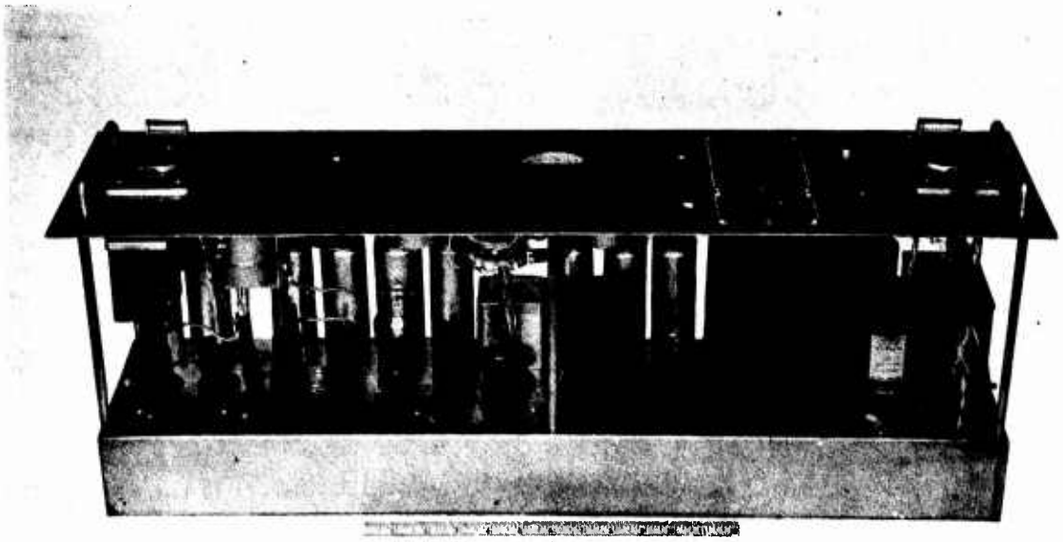

FIGURE 5. Sound level meter chassis.

speaker and amplifier, and a sound analyzer. Any or all of these can be plugged in or out during operation of the equipment without affecting the meter indication. An internal calibration circuit is provided to permit checking of the circuit performance.

The frequency response of the meter circuit, shown in Figure 6, is flat from 100 to 20,000 c, so that the pass band of the system is determined only by the hydrophone response, in Figure 3. The dynamic range of the system, using the RQ-51055 hydrophone, goes from 35 to 145 db above 0.0002 dyne per sq cm. The hum level is about 8 db below thermal noise and the system is able to measure the lowest water noise encountered. The optional 10,000-c high-pass and 1,000-c low-pass filters are controlled by switches on the chassis panel. These filters produce an insertion loss of 18 db per octave in the attenuated frequency range as shown in Figure 6.

METER CIRCUIT

A schematic circuit diagram for the sound level meter is shown at the right of Figure 7. The input circuit of the sound level meter is designed to work from a 200-ohm source, the RQ-51055 hydrophone. The input voltage is stepped up through an input transformer terminated by a high-impedance potentiometer, marked "0.1 meg attenuator" in the drawing. This potentiometer is calibrated in steps of 5 db over a range of 75 db and controls the input to the first amplifier tube. The control is placed in this position to avoid overloading the first stage when high-intensity sounds are measured. Two stages of resistance-coupled amplification follow the potentiometer. Negative feedback is used to reduce the output impedance of the second stage and to stabilize it against line voltage variations. The plate load in the second stage has a split load resistance. Thus short-circuiting the part of the plate load resistance which feeds the monitor amplifier jack does not cause an appreciable change in output voltage. This insures proper operation of the meter, even when a defective plug or amplifier is used.

The 10,000-c high-pass filter and a 1,000-c low-pass filter are located between the second and third amplifier stages. A three-position switch mounted on

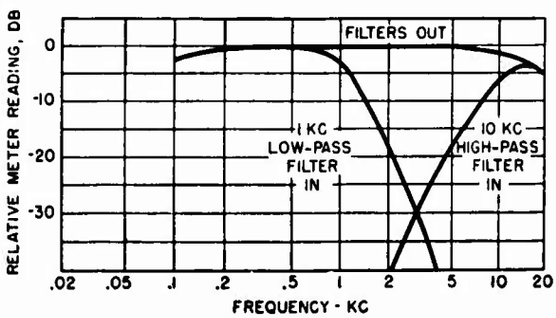

FIGURE 6. Meter reading for constant voltage across calibrating resistor of hydrophone.

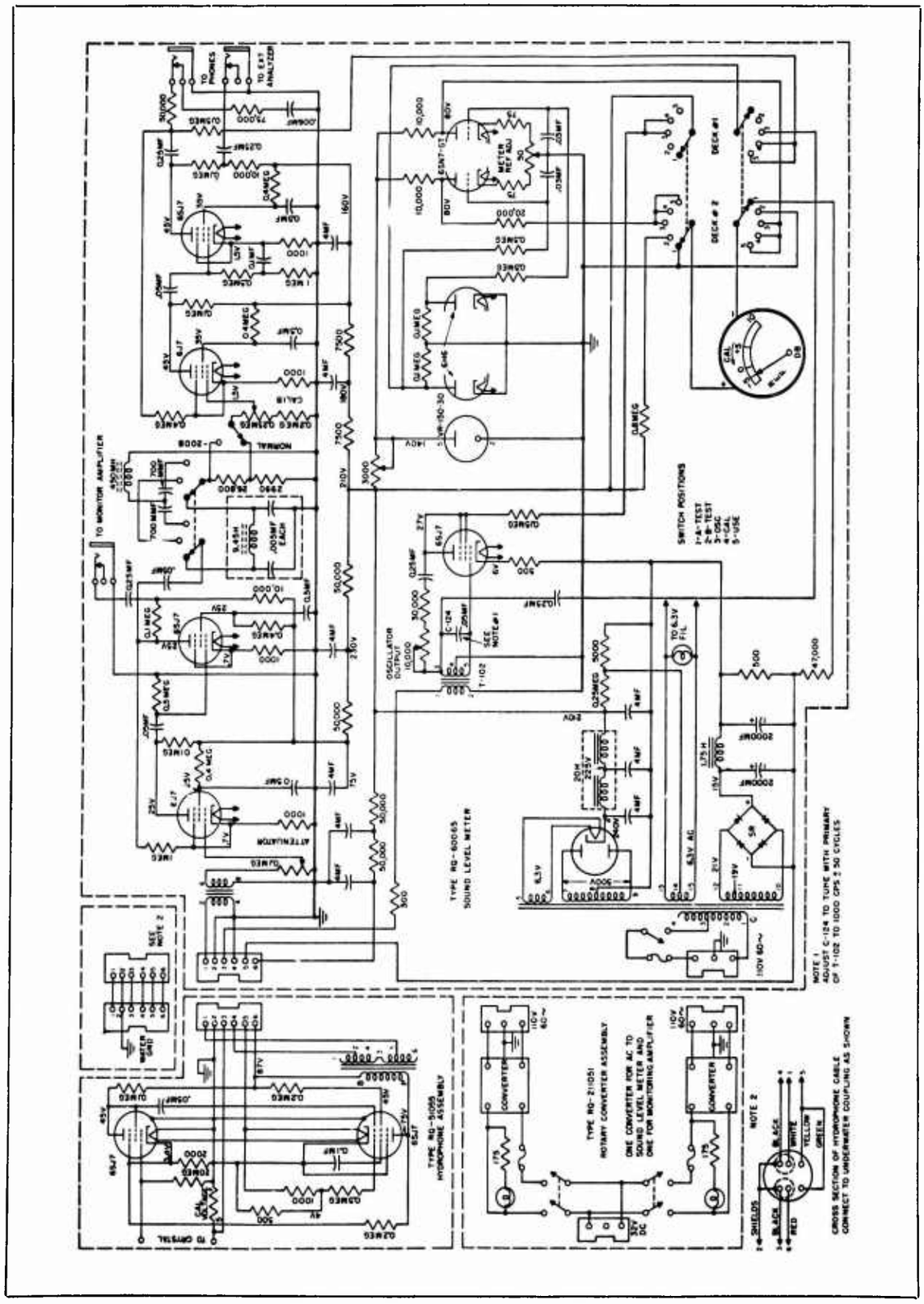

FIGURE 7. Schematic diagram of circuit of Model OAY sound measuring equipment.

the front panel connects these filters into the circuit when desired. The 1,000-c low-pass filter was added to the equipment of the original design shown in Figure 1 to permit reduction of shrimp noise.

The filters are followed by a 20-db range switch and the gain-calibration potentiometer. The first is used to increase the gain when sounds having a level below +50 db are to be measured. The second adjusts the overall gain of hydrophone and sound level meter amplifier to a predetermined value at the start of a given test.

Two additional resistance-coupled amplifier stages, similar to the first two, follow and complete the amplifier. Again the plate load impedance of the output tube is split, one branch feeding the sound analyzer jack, giving the same protection against a defective plug. This output tube also feeds the monitoring phone jack and the vacuum-tube voltmeter. Connected to the auxiliary contacts of the monitoring phone jack is a resistance-capacity network which has impedance characteristics similar to the two headphones in series and which is disconnected when the headset is inserted, thus again insuring that the signal voltage output is not altered.

The balanced vacuum-tube voltmeter reads between rms and peak values. Two tubes (in one envelope) and two resistors act as a bridge circuit. The meter, 0-1 d-c milliammeter with a resistance in series, is connected between the plates of the tubes. The signal voltage is first rectified by a half-wave high-vacuum rectifier and filtered by a resistance-capacitance network and is then applied as a negative voltage to the grid of one of the vacuum tubes, thereby throwing the bridge out of balance. With proper bias and anode potentials applied, the meter reading will be proportional to the signal voltage input. The maximum current through the meter, when one of the tubes is at negative grid-bias cutoff, is only 1.25 ma, thus protecting the meter from damaging overloads. A four-deck, five-position switch makes the indicating meter also available for checking the d-c filament voltage of the hydrophone amplifier tubes and the B supply voltage. The latter check also gives an approximate indication of whether the a-c line voltage is connected to the right tap on the power transformer.

The grounding of the measuring equipment is automatically performed when the cable connector connecting the hydrophone to the cable extension is immersed in water. No other ground should be used as it will form a ground loop and make the measuring equipment inoperative because of severe hum.

The power supply furnishes the necessary direct current for the RQ-51055 hydrophone amplifier as well as for the sound level meter. It supplies 230-v direct current for the anode potential, 12.6-v direct current for the filaments of the hydrophone amplifier tubes, and 6.3-v alternating current for the filaments of the tubes in the sound level meter. The a-c filament winding is held at a slight positive potential to eliminate filament-to-cathode emission. The hydrophone amplifier, the two halves of the four-stage amplifier, and the vacuum-tube voltmeter have separate decoupling filters to reduce common impedances to a minimum. A voltage-regulator tube provides steady B potential to the vacuum-tube voltmeter, within line voltage variations of ±15 percent, thus insuring proper operation.

Total power consumption of the sound level meter and hydrophone assembly is approximately 85 w when operated from a 115-v, 60-c line.

Calibration Circuit

The calibrating circuit shown in Figure 7 provides a constant current at 1,000 c through a 5-ohm resistor in series with the low side of the hydrophone crystal. This current is chosen so that the voltage developed in series with the crystal is the same as that developed by a sound level of +95 db, and during calibration the gain adjustment mentioned above is varied until the meter reads 95 while the calibrating current flows. This then corrects for all circuit variations except changes in crystal sensitivity. The calibration oscillator is of the resistance-stabilized feedback type. The output adjustment is in the feedback path, because its output voltage has to be measured across the tuned circuit. The wave shape is not materially affected by this method since sufficient negative feedback is used to keep the maximum distortion below 4 per cent.

From the discussion of the circuits it is apparent that the overall accuracy of measurement is determined primarily by the hydrophone crystal, since all amplifiers are stabilized by inverse feedback, and any residual variations can be corrected by the calibration circuit. Variations in hydrophones can be expected, as is shown by the curves of Figure 3 which give a plot of frequency against crystal output at the hydrophone amplifier. Figure 6 shows the electrical frequency characteristics for the three settings of the filter switch. These curves show the

meter readings obtained for constant voltage across the calibrating resistor of the hydrophone.

In order to correct for variations in crystal sensitivities, a correction factor is assigned to each hydrophone. This value, of the order of 2 db, is determined at the laboratory before shipment of the OAY equipment. The crystal sensitivity of the average RQ-51055 hydrophone is expressed as −78.5 db in the range from 100 to 5,000 c. (This is crystal voltage below 1 v for a sound pressure level of 1 dyne per sq cm.) The +95 db in decibels above 0.0002 dyne per sq cm calibration level on the OAY sound level meter corresponds to the absolute sound pressure incident upon a hydrophone with this average sensitivity. For each individual hydrophone the assigned correction factor expressing any deviation from the −78.5-db average must be applied to obtain absolute readings.

3.3.4 Accessory Equipment

In the requirements for the OAY it was specified that battery operation be provided. The rotary converter assembly shown at the right in Figure 1 operates from 32-v storage batteries. It supplies power both to the meter and to the monitor amplifier in conditions where 115-v alternating current is not available.

A pair of high-fidelity Rochelle salt headphones is supplied with the equipment. A high-fidelity amplifier and loudspeaker also allow monitoring by ear of the noises picked up by the hydrophone. The amplifier is designed to operate on 115-v 60-c single-phase power, and the unit consumes 105 w. To obtain recordings of characteristic machinery noises and other sounds as a training aid and for detailed study of submarine sounds, recording equipment can be operated from the monitor output.

The sound analyzer normally used with the OAY equipment is the General Radio Type 760A. This can be plugged into the circuit without influencing the meter reading. If the ERPI Type RA-277 analyzer is used, an external coupling circuit is added to provide the proper low-impedance match.

3.4 PERFORMANCE

In general the OAY gear satisfied the requirements of the submarine noise reduction program, as discussed above. Many of these units were put into use at submarine bases throughout the world, and the equipment found application in other types of sound tests where a rugged portable instrument was needed with a wide flat frequency response. On the basis of experience with OAY units in the field, certain improvements were proposed with recommendations for changes in the calibration and standard measurement procedures. A prototype model was constructed incorporating many of these changes.

The desired uniformity of hydrophone frequency response was not achieved with this design, although there was some indication that the latest models had more uniform sensitivity. A rotation scheme for maintaining optimum performance was developed by supplying three hydrophones with each set of OAY equipment. While one of these was in service, the second was on hand in good condition to serve as a spare, and the third was undergoing test and necessary repairs at the New London laboratory.

3.5 RECOMMENDATIONS FOR FUTURE WORK

The proposed changes in the OAY equipment, many of which were incorporated in the prototype model, are summarized in the following paragraphs. This experimental model could be used as a basis for future work.

Sound Level Meter. To increase the usefulness of the meter, certain changes were made in the circuit. The output jack for the frequency analyzer was originally designed for a high-impedance circuit. Since it is often desirable in practice to use the ERPI RA-277 analyzer, which has a low-impedance input, it is recommended that the coupling networks necessary for both high- and low-impedance analyzers be provided. A further simplification in the meter could be made by combining the 20-db range control with the 5-db step attenuator, so that the complete level control would operate from a single switch. For some measurements it is convenient to have a slow characteristic for the meter needle, as well as the normal fast response. In the prototype model the regular speed was made normally available, while the slow response was obtained by holding down a nonlocking push button.

Hydrophone. The chief objection to the Rochelle salt crystals used in the RQ-51055 unit is the damage incurred by this material at temperatures above 120 F. Such temperatures are readily encountered where the unit lies out on deck in the sun. The newly developed ADP crystal is a possible substi-

tute if the 6-db drop in crystal output can be tolerated. Improved methods should insure better uniformity among the production models. A new ADP hydrophone was designed, designated AX-120. It was not found possible, however, to duplicate completely the performance of RQ-51055 hydrophones for which the OAY sound level meter was designed. The necessary changes would impair the performance with the RQ-51055 units. Thus the interchangeability which is so important in the OAY equipment would be lost. The AX-120 hydrophone, which has somewhat lower self-noise than the RQ-51055 and which is independent of temperature, is recommended for a new instrument, and if at some future time it proves desirable to change to the new hydrophone, the present meter could be readily adapted for the purpose.

Hydrophone Cable. Trouble was encountered in breakage of the cable conductors. A type of cable manufactured by the Simplex Wire and Cable Company is recommended for future models. This cable consists of five individually tinned copper conductors each covered with 0.112-in. diameter, 40 per cent rubber insulation in different colors. These strands are cabled with no filling and wound with a cotton separator. Over this is a tinned copper-braid sleeve for shielding, a cotton wind, and a 0.500-in. diameter, 60 per cent rubber jacket.

Filters. Two filters are regular equipment in the sound level meter, and output connections are provided for sound frequency analyzers. In some cases an intermediate degree of frequency analysis would be useful. For this purpose an experimental set of filters was constructed for insertion between the hydrophone and the sound level meter. This set was housed in a small box, approximating an 8-in. cube, and comprised high-pass filters of 100-, 300-, 1,000-, and 3,000-c cutoff, and low-pass filters of 300-, 1,000-, 3,000-, and 10,000-c cutoff. It was constructed so that the hydrophone cable extension was plugged into the box and the filter output cable plugged into the sound level meter. Each filter was controlled by a push button switch. These particular filters were selected as having useful cutoffs, but others would be as easy to provide. The present sound level meter has no space available for a convenient conversion to accommodate the filters inside the chassis. This experimental device could, however, be furnished as an accessory to bases where it would be useful.

Headphones. The headphones furnished with the OAY, using x-cut Rochelle salt for high fidelity, were not designed for the rigors of naval service. Permoflux headphones are sturdier and available, but they have low impedance and therefore require a coupling transformer for the present equipment. In any modification program this transformer could be installed in the meter circuit.

Overside Measurements. The high background encountered at most locations where routine overside measurements are made suggests some modification in the procedure. The present hydrophone calibration level of 95 db is subject to interference from water noise. Although it is possible to calibrate by removing the hydrophone from the water, this is not always convenient. It would be desirable to raise the calibration level to 120 db. In addition, the 23-db average difference between overside measurements of auxiliaries and the corresponding standard Navy sound range measurements at 200 yd recommends use of the overside method for high background conditions. However, the OAY method affords no check on the noise from air leaks or oil leaks which may arise from points on the submarine which are out of water during surface operation when the overside measurements are made. These measurements do not replace range and underway tests but have proved a useful supplement.

Chapter 4

SHIPBOARD INSTRUMENTS: I

Noise Level Monitor and Cavitation Indicator

The noise level monitor [NLM] is used on submarines to detect excessively noisy auxiliaries by indicating changes in their noise outputs. A decibel meter measures noise levels at any of four hydrophones located along the pressure hull. The cavitation indicator [CI] used with the NLM employs a magnetostriction hydrophone mounted aft to receive propellor cavitation noise. The NLM and the CI were developed by CUDWR-NLL.

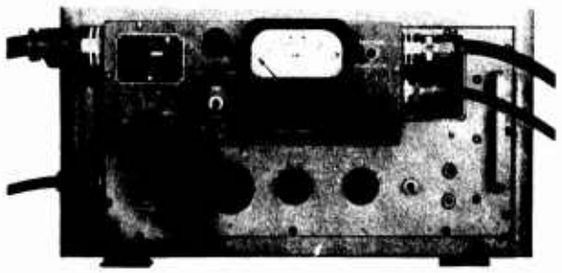

FIGURE 1. Noise level monitor indicator.

4.1 INTRODUCTION

THE SUCCESS of a submarine in escaping from enemy attack depends in large measure on its ability to operate quietly. For this reason a program of submarine noise measurement was instituted early in the war. This program, conducted on sound ranges near the various major submarine bases and later supplemented by overside noise measurements described in Chapter 2, was directed toward locating, measuring, and correcting the noise generated by propellers, gears, pumps, motors, and other sources within the submarine. It also aimed at establishing progressively lower permissible noise limits for slow-speed underway runs. Because the minimum noise level of the various sources may increase as a result of depth-charge shocks, improper adjustments, damaged propellers, etc., while the boat is on patrol, it appeared desirable to provide also a means for making self-noise measurements aboard the submarine while underway.

The *noise level monitor* [NLM] developed for this purpose detects changes in the noise levels of the main propulsion machinery and the auxiliaries of a submarine. Because of the varying distances between the NLM hydrophones and the various machinery noise sources, the equipment cannot indicate the noise intensity in absolute units, as established during the regular Navy sound range tests. The NLM should be calibrated, therefore, in order to give the submarine commander a guide to the significance of any noise level changes which may be detected by the equipment while the boat is on patrol.

The NLM utilizes four permanent-magnet magnetostriction hydrophones spaced at approximately equal intervals from fore to aft on the outside of the pressure hull. The acoustic noise level at any selected hydrophone position is measured by means of a decibel meter.

A method of making noise measurements by the use of artificially introduced masking noise of controlled intensity had previously been suggested as an alternative to direct measurements with a meter. This masking technique was compared directly with the NLM meter method during the development tests and it was found that the two methods gave substantially the same results. The simpler direct measuring arrangement consequently was selected for the production model.

The *cavitation indicator* [CI] employs the spare echo-ranging receiving amplifier and a fifth hydrophone, identical with the NLM units but located as far aft as practicable. The start of propeller cavitation noise is indicated, together with a rough measure of its relative intensity, by a neon lamp indicator panel located in the conning tower or control room. Amplifier gain is adjusted to flash a green lamp on background noise with the submarine running below cavitation speed. As increased speed causes cavitation noise to begin, sufficient additional voltage is generated to flash both the green and an amber light. With severe cavitation the green and amber lights remain on and a red light flashes

4.2 DESIGN CONSIDERATIONS

In the design of equipment to enable submarine personnel to evaluate own-ship's noises while under way, a number of factors should be considered.

1. Equipment for monitoring machinery noise must be capable of accurately indicating noise level changes over a long period of time. This, together with the character of the noises to be measured, imposed a number of requirements on the hydrophone and amplifier.

   a. The hydrophone characteristic and sensitivity must not be appreciably affected by the temperature and pressure variations and severe depth-charge shocks likely to be encountered. It should be adequate to insure a good signal-to-resistance noise ratio in the higher frequency region (14 or 15 kc).

   b. A flat frequency response and high sensitivity over the lower sonic region are also desirable in the hydrophone. However, if this cannot be attained in a unit which meets the other requirements, the response should not be highly peaked and the sensitivity should be adequate to insure a good signal-to-resistance noise ratio at all frequencies between about 100 and 2,000 c.

   c. It is necessary to use at least four hydrophones spaced along the hull in order to insure a good signal-to-ambient-noise ratio for as many machinery units as possible and to minimize the acoustic shielding effects of intervening structures such as the conning tower.

   d. The frequency response of the amplifier used with the NLM should have a response complementing that of the hydrophone in the 100- to 2,000-c range.

   e. The amplifier used with the CI should provide means for discriminating against the lower sonic frequencies, and its gain at the higher frequencies should be sufficient to amplify the lowest expected signal voltages to the extent necessary for actuation of a suitable indicator.

2. The noise of importance to this problem is of two principal types arising from different sources: (a) noise from the main propulsion and auxiliary machinery with frequency components almost wholly confined to the lower sonic region (usually below 1,000 to 1,500 c), and (b) noise arising from propeller cavitation and having a broad continuous spectrum extending high into the supersonic region. Machinery noise, arising from many widely separated sources on the submarine, is present whenever the boat is moving under power, and either remains constant or increases slowly with ship speed. Cavitation noise is normally absent or undetectable at slow speeds, but appears suddenly at a critical speed which depends on the particular submarine and propeller design, the running depth of the boat, and the acceleration.

3. A device for checking cavitation must quickly indicate the occurrence of noise from this source when it first becomes detectable, but accurate comparisons of intensity over a long period of time are not necessary. Since cavitation noise covers a broad frequency spectrum, an indicator can utilize energy in the supersonic region and avoid interference from machinery noises. The requirements imposed on the cavitation noise indicator equipment, in addition to those given above for the hydrophone and the amplifier, are:

   a. The indicator should work automatically when properly adjusted and should preferably give some measure of the intensity of the cavitation noise as well as indicating its occurrence.

   b. The indicator should be located in the conning tower or control room to prevent time delay in the transmission of its information to the proper personnel.

4. The devices for measuring machinery noise and indicating cavitation noise should use existing submarine equipment to the greatest extent possible consistent with the other requirements, and operation of the devices should not be complicated.

4.3 DEVELOPMENT

Selection of Hydrophone System

Three possibilities were considered in selecting an adequate hydrophone system for use with the NLM: (1) the regular JP listening hydrophone,[a] (2) the DCDI hydrophone system, discussed later in this chapter, and (3) a system especially designed for the NLM and employing several hydrophones mounted at intervals along the pressure hull.

The idea of using the JP hydrophone was abandoned after tests indicated a single unit to be inade-

[a] See Division 6, Volume 14.

FIGURE 2. Location of NLM hydrophones.

quate for receiving the sound from the more remote machinery. Also, there was some doubt about the stability of the JP hydrophone over long periods, and it was believed that its depth of submergence during Navy sound range tests usually was insufficient to yield consistently accurate measurements.

Tests were made using seven DCDI hydrophones mounted at intervals between the bow and stern of a submarine. These tests indicated that the use of multiple hydrophones of this type would give the desired results but that units mounted only at the locations of the regular DCDI pickups (clustered near the conning tower) were too far from the forward and aft machinery units for good sound reception. Additional tests with multiple hydrophones indicated that a minimum of four pickups, mounted on the pressure hull and properly spaced with regard to the locations of the major machinery units, would be required to serve the NLM adequately.

The NL-130 permanent-magnet magnetostriction hydrophone,[b] which had just become available, combined the required stability, sensitivity, and frequency characteristic with ruggedness and small size, and was selected for use with the NLM and the CI.

The four NLM units are mounted topside along the pressure hull in the locations indicated in Figure 2. The hydrophone has a sensitivity of approximately −120 db vs 1 v per dyne per sq cm at 1,000 c and a relatively smooth response which rises with frequency at the rate of about 6 db per octave up to 10 kc. It does not require periodic magnetization and its sensitivity and response are known to be very stable over a long period of time. The NL-130 hydrophone thus meets very well the requirements given in Section 4.2.

SELECTION OF AMPLIFIERS

Preliminary studies of the problem of providing suitable equipment for noise level monitoring and cavitation indication led to the conclusion that the JP amplifier and the spare echo-ranging receiving amplifier already in use on submarines would fulfill the requirements shown in Section 4.2.

[b] Division 6, Volume 13.

DEVELOPMENT MODELS AND TESTS

The first development model employed five NL-130 hydrophones (four for the NLM and one for the CI) together with a switching and metering adapter for the JP amplifier and a neon lamp cavitation indicator actuated by the spare echo-ranging receiving amplifier. Two units of this first model, installed on fleet-type submarines, performed satisfactorily during extensive sea tests and six more units were built for installation on other operating submarines. Testing of these first eight units enabled the working out of suitable techniques for operating both the NLM and the CI and led to preparation of a final design for production units.

4.4 PRODUCTION MODEL NLM AND CI

The production model of the NLM and CI is made up in the form of a modification kit for installation at submarine bases and consists of the following main items in addition to the necessary cabling, junction boxes, etc.:

Five NL-130 hydrophones.
NLM adapter unit including decibel meter.
External decibel meter.
Magic eye tube assembly.
Neon lamp cavitation indicator.

The NLM adapter unit, shown installed on a JP amplifier in Figure 1, includes a multideck rotary switch to select any one of the four NLM hydrophones for noise level measurements or to connect the JP hydrophone to the amplifier for normal use as directional listening equipment.

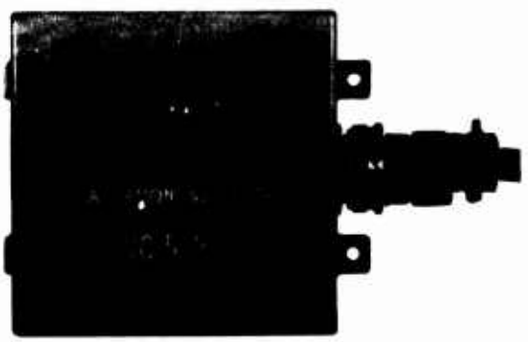

FIGURE 3. Cavitation indicator. The three-lamp indicator mentioned in the text is a more recent development.

The neon lamp cavitation indicator consists of three lamps and a resistor network for adjusting the voltage necessary to flash the lamps. This assembly is contained in a small metal case and is usually installed in the control room or conning tower. The lamps are actuated by the signal from the CI hydrophone after its amplification by the red light indicator circuit of the spare echo-ranging receiving amplifier. The amplifier contains filters which restrict the signal used for actuation of the CI to a frequency band approximately 1,000 c wide. This band can be swept through a considerable range in the supersonic region but is usually centered at about 14 or 15 kc for cavitation noise indication. An earlier model is shown in Figure 3.

Schematic circuit diagrams and a fuller description of NLM and CI equipment are given elsewhere.[1]

Depth-Charge Direction Indicator

The depth-charge direction indicator [DCDI] developed by CUDWR-NLL is a device used on a submarine to indicate the general direction of an enemy attack by detecting the pressure waves from explosions. It consists essentially of three pairs of hydrophones, called blastphones, located to starboard and port, fore and aft, and above, below on the submarine hull. The blastphones, small rugged magnetostriction hydrophones capable of withstanding high pressures, are connected electronically, through three identical split channels in an amplifier-indicator unit, to corresponding pairs of indicator lamps which flash upon explosion of nearby depth charges.

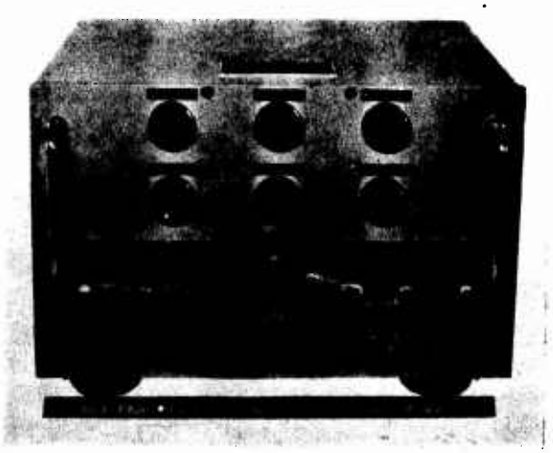

FIGURE 4. Amplifier-indicator panel view of depth-charge direction indicator.

4.5 INTRODUCTION

Battle experience of submarines indicated the importance, as an aid to evasive maneuvers, of accurate information concerning the sector in which the enemy is attacking. Prior to the development of the *depth-charge direction indicator* [DCDI], no equipment was available to provide this information. However, a knowledge of the principles of transmission and detection of shock waves in the earth, gained in connection with geophysical prospecting, was available to be drawn upon in the design of the direction indicator. On the basis of this knowledge, a system was evolved capable of indicating the direction of the explosion by measuring the difference in time of arrival of the shock wave front at two points in the desired plane.

The DCDI employs three pairs of hydrophones, called *blastphones,* which are connected by an electronic circuit to indicator lamps in the submarine. The blastphones are placed to port and starboard, ahead and astern, and above and below the submarine. In general, one blastphone of each pair receives the pressure wave from an explosion a short time before the other. The electronic circuit is so arranged that the first signal received from either blastphone of each pair causes that blastphone's indicator lamp to be lighted and automatically prevents the lighting of the indicator lamp associated with the other blastphone of the pair. Thus, if a charge explodes ahead, to port, and below the position of the submarine, lamps indicating these relationships are lighted, while the astern, starboard, and above lamps remain dark.

The device has performed well in experimental field service. Reliable azimuth indications are consistently obtained at ranges as great as 5,000 to 6,000 yd, but the maximum range of dependable above-below indications is sometimes limited by temperature gradients in the water. Although the DCDI design to be described provides the information originally desired, its usefulness would be enhanced if the bearing accuracy were improved and range information provided. Recommendations for improvement of the particular design discussed include the use of a permanent-magnet type of blastphone to eliminate the necessity for charging circuits, and the elimination of nonstandard electronic tubes.

Development work continued after the DCDI was put in production led to the design and construction

of experimental devices for indicating range as well as more accurate bearings. It is recommended that further development be directed toward extending and completing this work.

4.6 DESIGN REQUIREMENTS

Initial consideration of the problem of providing the desired information led to the following restrictive mechanical and operational specifications.

1. The minimum information given by the indicator system should be sufficient to locate a depth-charge explosion in the correct quadrant in the azimuthal plane and to indicate whether it occurred above or below the submarine's running depth.

2. Directional information should be obtainable for explosions occurring at ranges of up to several thousand yards.

3. The equipment should be capable of operating directly from the d-c supply of a submarine without the use of auxiliary equipment which might limit use of the device during quiet running.

4. The indicator should not only be easily read but also be capable of rapid resetting, preferably automatically, in readiness for succeeding charges.

5. The indicator unit should be as small as possible to permit its installation in the conning tower or control room.

6. The instrument should contain no relays and should otherwise be rugged enough to withstand the severe shocks likely to be encountered.

In addition to the above, the conditions of use impose certain requirements on the design and construction of the blastphone. Since the energy in shock waves, such as those created by depth-charge explosions, is high and covers a broad frequency range, the blastphones need not have high sensitivity or flat frequency-response characteristics. They should, however, be mechanically rugged and their efficiency should be sufficiently high to insure that background water noise, rather than electric circuit noise, limits the signal-to-noise ratio. Further, the response of the units should cover a reasonably broad frequency band to prevent serious distortion in responding to steep pressure fronts.

4.7 EXPERIMENTAL MODELS

Four experimental models of the DCDI were built in the course of the development work. The last of these served as a prototype for production units.

First Model

This experimental laboratory system, designed to operate from portable batteries, consisted of a single, split-channel, amplifier-indicator system supplied by a pair of small, rugged, magnetostriction hydrophones, or blastphones. The circuit was arranged so that a voltage received from one of the blastphones of the pair served, after amplification, to actuate a trigger tube in one side of the split channel, which, in turn, lighted a corresponding indicator lamp. At the same time sufficient additional negative bias was furnished to the grid of the corresponding tube in the other side of the channel to prevent it from "firing" on a signal received a few milliseconds later. Thus, a pressure front from a depth-charge explosion, received first by one blastphone of the pair, would trip the appropriate indicator lamp circuit and automatically prevent the signal, received later by the other blastphone, from tripping the alternate indicator lamp circuit.

This early model was tested in the relatively shallow water of Long Island Sound by suspending its two blastphones about 5 ft apart in the water and exploding 1-lb Nitromon charges at ranges up to 300 yd. The device worked as anticipated, producing reliable indications of the positions of the explosions in relation to the blastphones.

Second Model

The succeeding model, with essentially the same design features as the first but providing three channels and three pairs of blastphones, proved that three-dimensional indications could be obtained.

Third Model

The third model employed the circuit used in the two preceding units, but was designed to operate directly from the 110-v d-c power supply available on submarines and to be small enough for installation in the conning tower or control room. This model was installed on a fleet-type submarine at Pearl Harbor. The ahead-astern and port-starboard blastphones were located around the conning tower superstructure and the above-below blastphones were located in the periscope shears and at the keel (see Figure 5).

This unit did not perform in a satisfactory manner. False flashing of the indicator lamps sometimes occurred, with the result that the directional information was not reliable. A duplicate unit installed

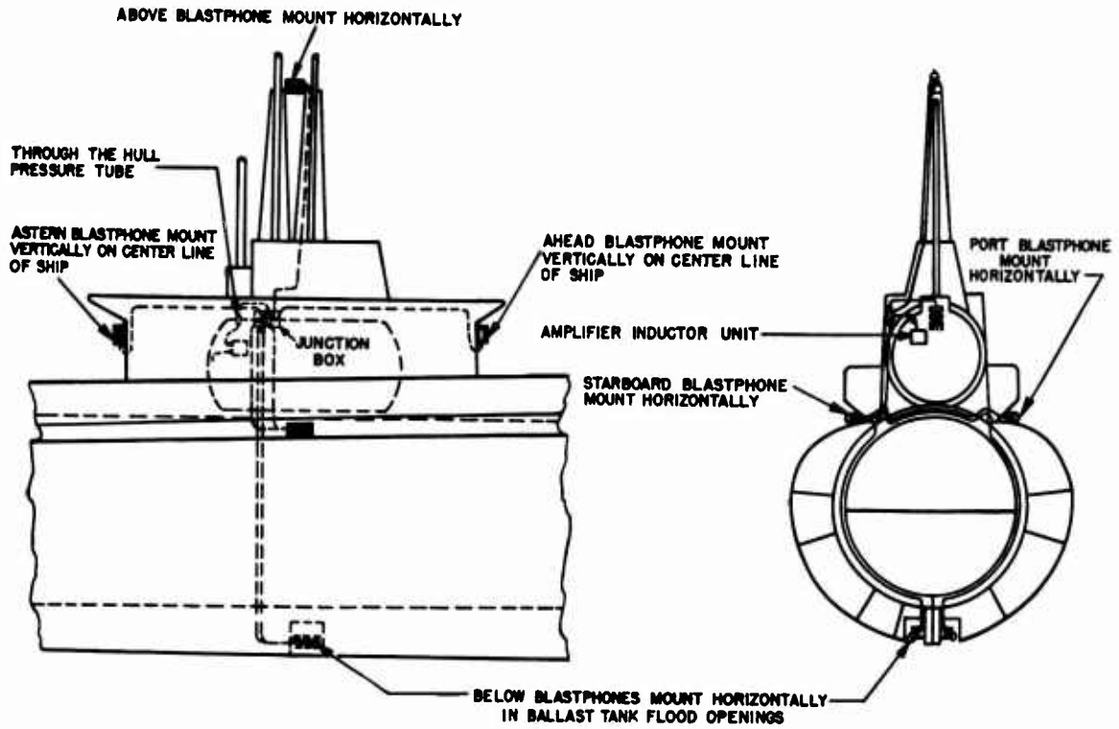

FIGURE 5. Outline diagram of blastphone arrangement on SS313 class submarine.

on a later-type boat at New London did perform satisfactorily, however, and it was subsequently determined that the false flashing of the lamps in the unit installed at Pearl Harbor was due to transients in the power supply of the older boat. To correct this situation a power-supply filter was incorporated in later models of the DCDI.

Tests of a duplicate third model DCDI, installed on a submarine at New London, were carried out with standard 300-lb depth charges. The charges were dropped at various relative bearings, at distances of from 450 to 6,000 yd from the submarine, and were set to explode at depths of from 50 to 500 ft. During the tests the submarine was submerged to keel depths of from 60 to 300 ft in water depths varying from 25 to 125 fathoms. At ranges up to 600 yd all charges gave correct indications. When the range was increased (2,000 to 3,000 yd), the ahead-astern and port-starboard indications were correct, but there was a single case of error in the above-below indications occurring with a charge set to explode at 500 ft. As the range approached 6,000 yd, the DCDI indications became erratic in all channels. Charges exploded at ranges of 6,000 yd or more failed to actuate the indicators.

4.8 PROTOTYPE AND PRODUCTION MODELS

The results of the tests on the third model of the DCDI were judged sufficiently good to justify the construction of a fourth model to be used as a prototype for production units. The original circuit, with the addition of a power supply filter to eliminate the effects of transients, was retained, but the amplifier-indicator components were rearranged to facilitate the use of production methods.

BLASTPHONES

The blastphones used (Model NL-116 described in Division 6, Volume 11) are small, rugged, magnetostriction hydrophones having medium sensitivity[c] and capable of withstanding high static and shock pressures. The units used with the DCDI are 9 in. long and consist of a coil wound on a laminated iron core and sealed inside a nickel tube. The assembly is provided with a rubber mounting and a mesh guard to aid in the reduction of vibration transmission from the hull and to protect the tube. Figure

[c] See Division 6, Volume 13.

6 illustrates the general method of construction and shows the rubber mounting.

External Installation. Figure 5 indicates the location of the blastphones in a typical DCDI installation on a submarine. The use of two units to receive signals from below the boat was found to be necessary in order to permit installation of these units in protected locations without danger of acoustic shielding by the keel. The outputs of the units are paralleled and carried into the hull from junction boxes by means of a 12-conductor cable passing through a packing gland.

FIGURE 6. The Model NL-116 blastphone assembly.

AMPLIFIER-INDICATOR

Figure 4 is a photograph of the amplifier-indicator and Figure 7 is a schematic diagram of one channel of the circuit used in the preproduction and subsequent production models. The three split channels providing for ahead-astern, port-starboard, and above-below indications are identical. For purposes of simplicity in describing the functions of the various circuit elements, attention is confined to the ahead-astern channel shown. Voltages induced in the ahead-astern blastphones by the pressure wave from a depth-charge explosion are impressed across the primaries of the input transformers T-101 and T-102. If the explosion occurs forward of the submarine's beam, then the voltage delivered to the primary of T-101 precedes that arriving at T-102 by a few milliseconds. The voltage induced in the secondary of T-101 is amplified by one section of the dual triode V-101 and is delivered to the control grid of the thyratron tube V-102. If the original signal delivered to T-101 is of sufficient strength,[d] the voltage arriving at the control grid of V-102 fires this tube and allows cathode current to flow, lighting the indicator lamp I-101. The amplified voltage from the other blastphone, arriving a few milliseconds later at the control grid of V-104, is unable to fire this tube for the following reasons. Before V-102 is fired, the grid of V-104 is about 7 v negative with respect to its cathode. As soon as V-102 is fired, current flows through the indicator lamp I-101 and through the resistor R-113. This produces a voltage drop across R-113 which furnishes additional negative bias of about 35 v to the grid of V-104. Since this bias is too great for the signal voltage delivered by the amplifier ahead of V-104 to overcome, this tube is prevented from firing, and its associated indicator lamp I-102 remains dark.

Once V-102 has been fired, current continues to flow through the indicator lamp I-101 for approximately 3 sec. This time interval is controlled by the electronic timing circuit incorporating the gas discharge tube V-103. When V-102 is conducting, the cathode is at a positive potential which charges C-103 at a rate determined by the value of the resistor R-110. At the same time that C-103 is charging, the condenser C-104, with positive side connected to the grid of V-103, is also charging at a lower rate through the larger resistor R-112. When the cathode and grid of V-103 reach triggering voltage, V-103 conducts, momentarily placing the cathode at a positive potential. The voltage across V-102 is thus reduced below that necessary for maintenance of ionization. With the tube no longer capable of conducting, the current flow ceases, the indicator lamp is extinguished, and the operational cycle is completed.

The bank of condensers C-125, C-126, C-127, and C-128 is used as a means of providing current for remagnetizing the blastphones. These condensers are discharged through the coil of each blastphone by closing the switches K-101, K-102, etc., one at a time.

The resistors R-154, R-155, etc., in parallel with the indicator lamps insure that an inoperative indicator lamp does not cause erroneous indications elsewhere in the system. Opening of the manual reset switch K-107 opens the plate circuits of the thyratron tubes and provides a means of extinguishing all the indicator lights before the end of the 3-sec interval.

[d] On the basis of experiment: that induced in the blastphone by a 300-lb depth charge within 6,000 yd.

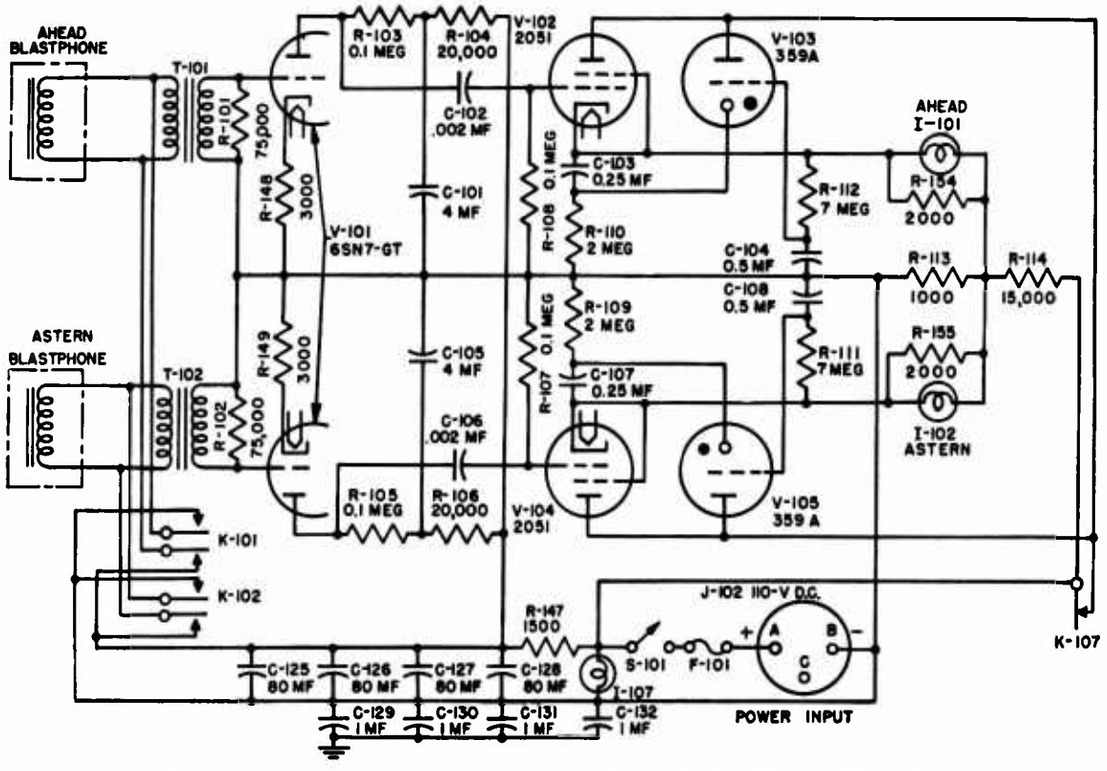

FIGURE 7. Schematic wiring diagram of the ahead-astern channel of the DCDI amplifier-indicator circuit.

Production units of the DCDI were constructed in accordance with the circuit design of the preproduction model.

PERFORMANCE IN SERVICE

In service, the DCDI has given reliable, satisfactory performance. The original experimental model installed on a submarine at New London was found to be operating satisfactorily after more than 18 months of service. Although numerous patrol reports indicate that the device has been of definite aid in the evasion of depth charge attacks, it is believed that performance of the DCDI is less than might be desired in a number of respects.

EFFECT OF TEMPERATURE GRADIENTS

It has been mentioned that errors in the above-below indications were noted during the tests when depth charges were exploded at ranges of from 2,000 to 3,000 yd. Investigation of the causes for these errors led to the conclusion that they were very likely due to the effect of temperature gradients on the transmission of sound. Subsequent analysis[2] of the refraction effects due to this cause has justified this assumption and has shown that when a negative temperature gradient (temperature decrease with increase of depth) exists in the water, with consequent bending downward of the sound waves, *below* indications are always correct, but *above* indications may occasionally be in error. Conversely, when positive gradients exist, *above* indications are reliable, but *below* indications may sometimes be incorrect. Tables[3] have been prepared which determine the reliability of above-below indications if the magnitude of the temperature gradient and the range of the charges are known. Although submarines have bathythermograph equipment for determining the thermal gradient, exact quantitative information from this source is available only when a dive has been made recently. For this reason, and because the DCDI does not provide a means of measuring the range of depth charges, it is questionable how accurately estimates of the reliability of above-below indications can be made in practice.

However, lack of complete reliability of DCDI above-below indications is not necessarily so serious as might at first appear. Very close charges (within about 500 yd) are almost certain to be correctly in-

dicated. If the explosions occur at greater ranges, it is usually of lesser importance to know their depth relative to that of the submarine. In addition, the submarine personnel are very likely to know whether a positive or a negative thermal gradient exists in the water, and, as pointed out above, this information is sufficient to establish the complete reliability in the one case of all *above* and in the other of all *below* indications.

Desirable Improvements

Although the direction indicator has equaled or exceeded the original design objectives in almost all respects, certain features are capable of improvement. Foremost among these are the following:

1. The device should incorporate a means of indicating the range at which depth-charge explosions occur. A direct-reading scale which would indicate the approximate absolute range, or the relative range of successive charges, would be of value.

2. The DCDI indicates the relative bearing of explosions only by quadrants. Provision of a more precise means of indicating azimuth would increase the usefulness of the device. This improvement, together with range indications, would make it possible for the submarine personnel to chart accurately the position of the enemy.

3. The sensitivity of the blastphone, although not extremely critical, is dependent upon the magnetization retained by the nickel tube after subjection to a strong magnetic field produced by a charging current through the coil. Since in normal use the nickel does not retain its magnetization indefinitely and the magnetization may be greatly reduced by the shocks encountered during depth-charge attacks, a means of periodically remagnetizing the tube must be provided. The use of a permanent-magnet type of magnetostriction hydrophone would eliminate this procedure and the charging circuits.

The possibilities noted under several of these items have been explored. Work undertaken after early operational experience was obtained on the DCDI has resulted in the development of a direct-reading meter which indicates the approximate absolute range at which charges are exploding. This development is discussed in detail in the following section of this chapter. Some laboratory work has been done on the problem of indicating azimuth more accurately, with the result that preliminary models of a device to work with the DCDI and yield relative bearing indications in octants have been constructed. This scheme utilizes the signals from the existing ahead-astern and port-starboard blastphone pairs with a secondary pairing of the first unit of each pair receiving the signal. A more complicated method for indicating the azimuth of depth-charge explosions to an accuracy of a few degrees has also been suggested. For this purpose, the difference in time of arrival of the signal at the initially actuated blastphones of the ahead-astern and port-starboard pairs is employed by an electronic timing circuit to actuate a direct reading meter which indicates relative bearing in degrees.

Permanent-magnet magnetostriction hydrophones of a type suitable for use with the DCDI have been developed and are used with the noise level monitor and with the depth-charge range estimator. While development of this permanent-magnet type of blastphone was not sufficiently far advanced to permit its use with the original production model of the DCDI, it was planned that any subsequent production orders for this equipment would incorporate the new blastphone in order to eliminate the charging circuits.

The Depth-Charge Range Estimator

The depth charge range estimator [DCRE] developed by CUDWR-NLL is a device used on submarines in conjunction with the depth charge direction indicator to estimate the range, and to indicate opening and closing range, of enemy depth-charge explosions. It consists essentially of a small permanent-magnet magnetostriction hydrophone, an electronic unit, and a meter calibrated for the intervals 0 to 250, 250 to 500, 500 to 1,000, and over 1,000 yd. Impulses from depth-charge explosions are fed through the hydrophone into a series of four multivibrator-amplifier circuits which are successively sensitive to increasing voltage changes. Through the operation of these circuits, the approximate range of the explosion which is characterized by the amplitude of its initial pressure wave is properly indicated on the meter.

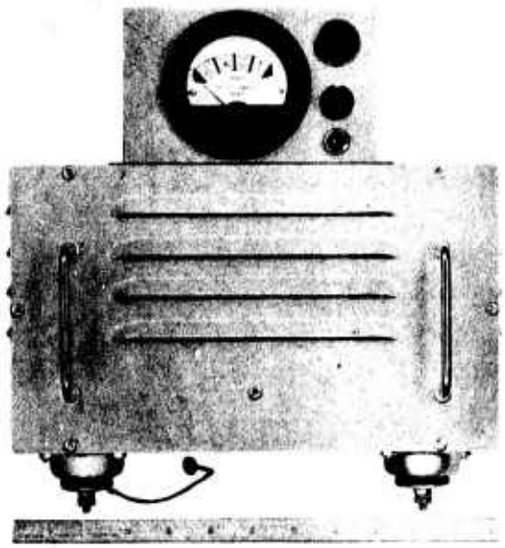

FIGURE 8. DCRE indicator and amplifier units.

4.9 INTRODUCTION

The experience of personnel in submarines subjected to depth-charge attacks during battle and during tests of the depth-charge direction indicator made it evident that virtually no reliable estimate of the range of depth-charge explosions can be made by ear. Tactical use of early models of the DCDI, which provides for determination of the octant in which a depth-charge explosion occurs, showed that this directional information is of considerable assistance during evasive maneuvers, but emphasized the desirability of supplementary information concerning the range of the explosions.

As a consequence, development work was undertaken concurrently with the latter stages of the DCDI development to determine the feasibility of measuring the range of depth-charge explosions by means of the amplitude of the initial pressure wave. This work has established that no theoretical reasons exist which preclude the success of this method of range determination, provided that an approximate rather than a precise range is satisfactory. On this basis the *depth-charge range estimator* [DCRE] was designed and constructed.

The DCRE utilizes a small, permanent-magnet, magnetostriction hydrophone[e] connected, through a series of electronic trigger circuits, to a meter which indicates whether the explosion is in the range interval of 0 to 250, 250 to 500, 500 to 1,000, or over 1,000 yd. Several units of this equipment, installed and tested on fleet-type submarines, have shown reasonably satisfactory performance with 77 per cent of all test charges indicated in the correct range interval and none in error by more than one interval. Opening or closing range, as determined from a series of charges, was always correctly indicated. At ranges of less than 500 yd, good accuracy may be expected.

4.10 DESIGN PROBLEMS

In considering the problem of estimating the range of an underwater explosion by the amplitude of the initial pressure wave reaching a given point, the effect of a number of factors must be evaluated. It is known that the amplitude may be affected by (1) the size of the explosive charge, (2) the effects of acoustic shielding produced by intervening bodies, (3) distortion of the pressure front due to the shape of the charge (Munroe effect), and (4) the transmission properties of the medium which depend largely upon the existing thermal conditions.

EFFECT OF CHARGE SIZE

Studies of the effects of charge size upon the amplitude of the initial pressure wave created by an underwater explosion have shown that the variation in amplitude is proportional to the cube root of the weight of the explosive charge. These studies were

[e] See Division 6, Volume 13.

conducted by the Woods Hole Oceanographic Institution.[f] A very large proportion of the depth charges normally used fall within certain known and not too widely divergent weight limits. Therefore, because a doubling of the charge weight increases the amplitude by only about 2 db, whereas a doubling of the distance away affects the amplitude by 6 or 7 db, the effect of charge size variations may generally be ignored without serious error in estimating the range by the amplitude of the initial wave.

Effect of Shielding

The effect of shielding by the submarine's own hull may be minimized by placing the pickup element in the periscope shears. By thus locating the sensitive element an appreciable distance from the hull, significant self-shielding occurs only when a charge explodes within a very confined region which would place the hull between it and the pickup unit. This is an unlikely occurrence except when the charge is either very close or very deep with respect to the submarine.

Effect of Charge Shape

Since a submarine crew generally does not have information concerning the shape of the depth charges used against it or their orientation when they explode, the possible influence of the Munroe effect upon the amplitude of the pressure front was disregarded.

Effect of Thermal Gradients

Oceanographic studies[4] have shown that the amplitude of the initial pressure wave is not likely to be seriously affected by thermal gradients at ranges of less than 500 yd. At ranges greater than 500 yd the effects of severe thermal gradients may be significant. When the pickup is located at a thermal interface where the thermal gradient undergoes an abrupt change, a region of low intensity (or "shadow zone") may exist and the pressure front from charges exploding within this region reaches the sensitive element with less than normal amplitude. A running-depth change of even a few yards up or down, placing the pickup above or below the interface, can minimize the possibility of incorrect indications due to this cause.

Consideration of these factors indicated that a depth-charge range estimator could be designed to operate on the amplitude of the initial pressure wave, but could not be expected to provide measurement of the ranges to within a few yards; its indications would necessarily be limited to locating the explosion within one or another of several rather coarse range intervals.

4.11 DESIGN REQUIREMENTS

The energy in shock waves from underwater explosions is high and covers a broad frequency range, and the duration of the initial pulse is very short. These characteristics impose several requirements on the hydrophone and circuit of any device designed to utilize the amplitude of such waves as a means of estimating the range at which the explosions occur: (1) the hydrophone, though not necessarily of high sensitivity or flat frequency response, should have a smooth response, free from sharp peaks or dips, over a reasonably broad frequency range; (2) uniformity of sensitivity and response characteristics should be maintained within close limits for all units; and (3) the circuit used must be capable of responding to pulses of very short duration.

Because the equipment is desired for use on submarines and must be operative under extreme evasive and depth-charge shock conditions, its physical size should be small, it should operate from the d-c supply of the ship's batteries without the necessity for converters or generators, and it should be rugged enough to withstand severe shocks.

4.12 EXPERIMENTAL MODELS

The initial DCRE design made use of a system employed in many previous ordnance and explosive studies to determine the amplitude of pressure fronts. Essentially this equipment consisted of a ¼-in. square tourmaline crystal, the output of which, after amplification, was used to actuate a delayed-pointer-return voltmeter. The range measurements obtained in tests of this unit were not accurate but were sufficiently consistent to encourage the development of further models. Some of the undesirable features of this instrument, in addition to the range inaccuracies, were the lack of sufficient delay in the voltmeter pointer return, the high impedance of the input circuit, and the difficulties of installation.

In the second model, the tourmaline crystal was replaced by a magnetostriction hydrophone and an electronic circuit was furnished which utilized a series of thyratron tubes biased to fire at succes-

[f] Described in Division 6, Volumes 6 and 8.

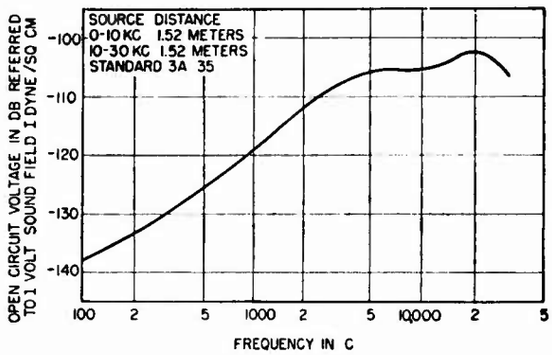

FIGURE 9. Typical NL-130 hydrophone frequency response characteristic.

sively higher input voltages. Range indications were shown in this instrument by a series of lights, the number of lamps lighted being a measure of the total current passed by the thyratron system and thus of the amplitude of the signal generated in the hydrophone by the shock wave. This model was found to generate excessive heat and to be unstable with voltage variations of the ship's power supply.

The unit was redesigned to incorporate increased ventilation and greater stability and was tested at sea from a surface vessel by suspending the hydrophone overside and exploding depth charges at varying ranges. The performance was encouraging in that opening and closing ranges were correctly determined. However, it was evident that the voltages generated by the magnetostriction hydrophone were several times greater than had been anticipated, leading to inaccuracies in magnitudes of the ranges indicated. From these tests it became apparent that the measurement of fine increments of range by this method did not appear to be feasible. Consideration of all the data, however, indicated that estimates of the ranges in the intervals of 0 to 250, 250 to 500, 500 to 1,000, and over 1,000 yd could be accomplished.

4.13 FINAL MODEL

The final model[5] of the depth-charge range estimator was designed with range indications confined to the four intervals listed in the preceding section. This equipment employs a permanent-magnet magnetostriction hydrophone NL-130[g] and has the ranges indicated on a voltmeter. The indicator and amplifier units are shown in Figure 8.

HYDROPHONE

The NL-130 hydrophone has an approximate open circuit sensitivity of −120 db vs 1 v per dyne per sq cm at 1,000 c and its response rises quite smoothly at the rate of about 6 db per octave between 100 and 5,000 c. In its application to the DCRE this hydrophone is mounted in the submarine's periscope shears where it is reasonably free of acoustic shielding from the hull. A typical frequency characteristic is shown in Figure 9.

ELECTRONIC CIRCUIT

In the electronic circuit, a schematic diagram of which is shown in Figure 10, the condensers C-110 and C-111 across the secondary of the input transformer restrict the transmission of frequencies above 5,000 c in order to eliminate the effects of variations which occur in the hydrophone sensitivity above that frequency.

The rectifier circuit including V-101 is loaded with a voltage divider consisting of resistors R-116 to R-121. The four divider steps consisting of resistors R-116, R-117, R-118, and R-119, each providing approximately 6.8 db loss, are connected to a series of four "flip-flop" circuits, based on tubes V-103, V-106, V-107, and V-109. The "flip-flop" circuit is essentially a two-stage amplifier in which one stage normally is conducting while the other stage normally is cut off, and in which the actions of the tubes are temporarily reversed by a small positive voltage on the grid of the nonconducting tube.

Tubes V-103, V-106, V-107, and V-109, have a meter M-101 common to the plate circuits of the normally nonconducting sections. Thus, when a signal of sufficient strength is received from the hydrophone, the voltage developed across the four resistors, R-116 to R-119, causes a reversal of action in the two sections of V-109 and results in a deflection of the meter. The time during which the action of the tube sections is reversed is determined by the values of the resistor R-132 and the condenser C-109, which in this case are adjusted to yield an interval of approximately 2 sec.

Similarly, when the signal from the hydrophone is of greater strength, because of a charge at lesser range, the voltage across the three resistors R-116 to R-118 becomes sufficient to reverse the action of

[g] See Division 6, Volume 11.

V-107 resulting in a greater meter deflection, and so on.

A combination of RC filtering and VR tubes is included in the plate supply to the tubes of the "flip-flop" circuits in order to stabilize these circuits which are sensitive to a sudden decrease of the supply voltage. The heaters are connected in series and take their power from the ship's 115-v d-c supply regulated by means of an Amperite 3-38A tube, V-105.

Calibration

Calibration of the range estimator was found to be difficult and required a considerable number of rather complicated sea tests in order to establish a basis for the circuit sensitivity to be used. The accuracy of calibration depends upon the characteristics of both the hydrophone and the electronic unit. The curves in Figure 11 show the effect on the range estimates of variations in the sensitivity of the hydrophone alone and emphasize the relatively large voltages induced in the pickup unit by the high sound pressures from depth-charge explosions. The manufacturing specifications for NL-130 hydrophones used with the DCRE require that the overall sensitivity be held within ±1 db. These limits are equivalent to a maximum effective range change of ±10

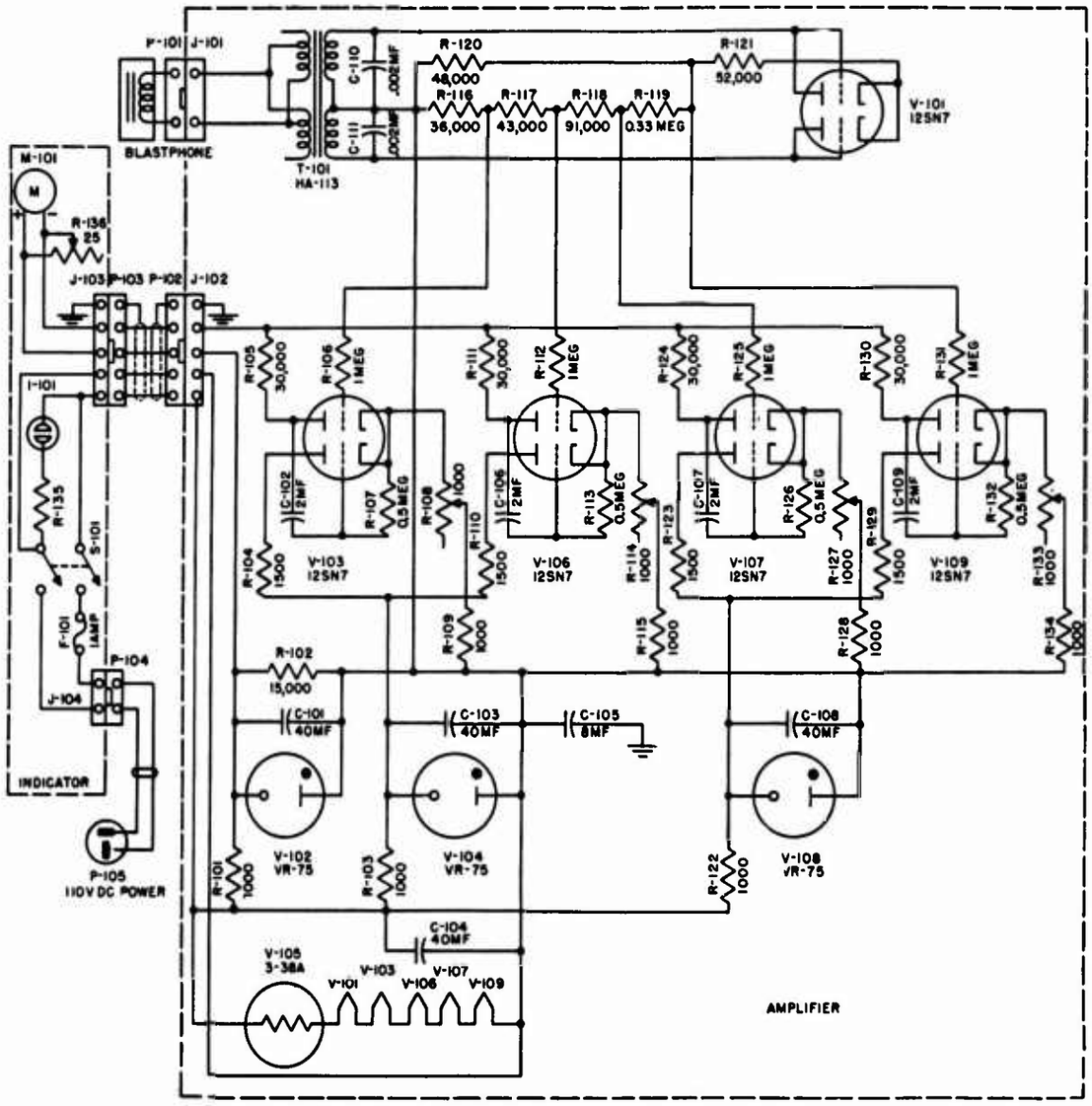

FIGURE 10. Schematic diagram of DCRE circuit.

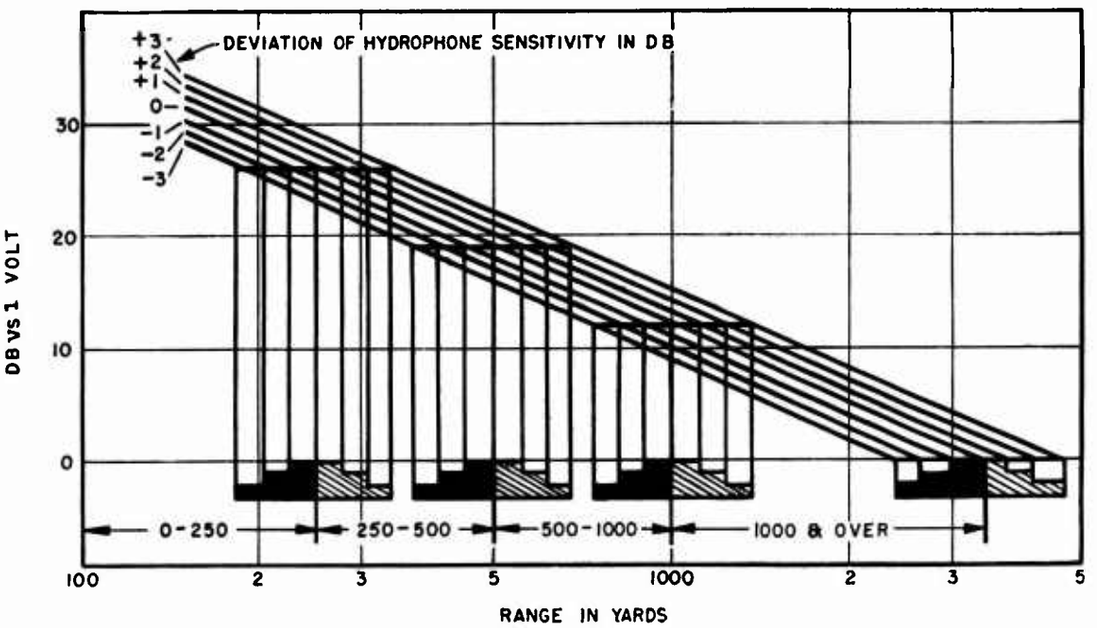

FIGURE 11. Effect of hydrophone sensitivity on DCRE range calibration.

per cent. This is considered satisfactory in view of the other variables in the system.

For preliminary calibration of the electronic equipment, a testing method was developed in which a 12-μf condenser is discharged through a small resistor inserted in series with the hydrophone. To simulate the hydrophone output for the depth-charge range intervals of from 0 to 250, 250 to 500, 500 to 1,000, and over 1,000 yd, the condenser is charged to 20, 9, 4, and 1 v respectively. Although this method does not duplicate the duration and form of the pulse resulting from a depth-charge explosion, it appears satisfactory enough for the purpose. It is recommended, however, that, should further work be undertaken, consideration be given to a built-in method of self-calibration.

PERFORMANCE

Several units of the final model of the range estimator were installed on fleet-type submarines on the Atlantic Coast and at Pearl Harbor. Extensive tests of these units were conducted and indicated that performance was reasonably accurate.[6] Out of a total of 77 charges dropped under controlled conditions, 77 per cent were indicated within the correct range interval. Of the remaining 23 per cent, none were in error by more than one range interval with only 19 per cent indicated short of actual range and only 4 per cent indicated beyond the actual range. During the tests, determinations of whether the range of the "attacking" vessel was opening or closing were correct in every case. The limiting range of the DCRE, as shown by a lack of any indication on the range meter, was found to be about 2,000 yd.

Although some of the submarines equipped with the final model of the DCRE have been on war patrols, no information on the tactical use of this device had been received at the time of writing. On the basis of the tests alone, however, it is believed that the greatest need for improvement of the instrument is the provision of more precise range information. Because of the known factors affecting the amplitude of the initial pressure wave from an underwater explosion, it appears that it probably will be necessary for such an instrument to operate on different principles, perhaps employing multiple hydrophones and a system of triangulation.

Chapter 5

SHIPBOARD INSTRUMENTS: II

Acoustic Marine Speedometer

The three types of acoustic marine speedometer [AMS] *are experimental devices for measuring ship's speed with respect to the water by utilizing some underwater acoustic phenomenon which varies with that speed. Two types developed utilize doppler shift of sound; the third utilizes phase lag. The experimental work was done by HUSL.*

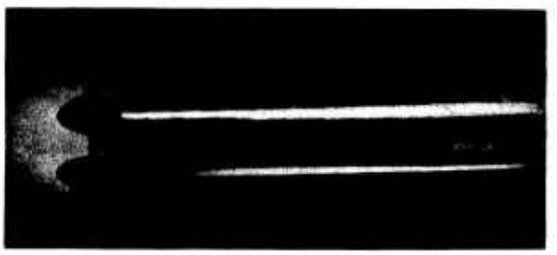

FIGURE 1. Operation of doppler-type speedometer.

5.1 INTRODUCTION

THE FUNCTION of the *acoustic marine speedometer* [AMS] is to measure the speed of a ship with respect to the water by making use of some underwater acoustic phenomenon that varies with speed. The work done on AMS was based on two such phenomena, namely:

1. The difference in frequency (doppler) between the input to a moving projector and the reverberation produced.

2. The variation in phase shift that occurs when a signal travels through water from a transmitting to a receiving transducer, both moving through the water.

These are illustrated in Figures 1 and 2.

In the first case the magnitude of the frequency shift, or doppler, is proportional to the speed of the source with respect to the water. Consequently, a properly calibrated device that measures this doppler can be used to indicate ship's speed.

Likewise, the change in phase introduced by the water path between two transducers located a fixed distance apart is a function of the speed of the transducers, so that a phase-measuring device can serve as a speedometer when calibrated for the purpose.

The possibility of using doppler for speed measurement has been recognized for some time.[a] The use of phase shift as a measure of speed is also a well-known principle. Two other methods of measuring speed involve the principle of pressure change in the water in the direction of ship's motion, and that of change of rotational speed of a free propeller with the speed of the ship.[1] Since these two devices do not utilize any acoustic principle, however, they will not be discussed further.

The work on AMS was stimulated by reports that Pitometer logs currently in service gave inadequate precision for slowly moving vessels, and that their size and weight precluded their use on small craft. Preliminary experimental work revealed that the outstanding problem involved in the development of an acoustic marine speedometer was the construction of suitable transducers.

Three separate models of the acoustic marine speedometer were constructed and tested, two of them based on doppler, the other on phase shift. The first of these, called the *steady-state acoustic marine speedometer* [SAMS], employs separate transducers for transmission and reception, with both of them operating continuously and facing the same direction. The second, known as the *acoustic marine*

FIGURE 2. Operation of phase-shift type speedometer.

[a] The particular application for ship's speed is covered by a patent to Constantin Chilowsky, June 28, 1932, No. 1,864,638.

pinging speedometer [AMPS], makes use of a single transducer which, like a regular echo-ranging projector, first transmits the signal and then receives the scattered sound. The third speedometer is based on the phase-shift principle and is called the *phase acoustic marine speedometer* [PAMS]. This model employs two transducers, one to transmit and the other to receive, each operating continuously. They are arranged to face each other, and only the direct transmitted sound is measured at the receiving transducer.

The priority assigned to this work did not make it possible to produce a satisfactory production model in time to satisfy the operational need for the instrument. By the time the project was terminated, however, it had been established that in all probability further development work would lead to the design of a satisfactory speedometer.

The various methods tested in carrying out the work on the acoustic marine speedometer yielded values of ship's speed that by no means achieved the desired accuracy. A major defect in the SAMS was fluctuation in the frequency meter reading brought about by variations in amplitude and frequency. The AMPS was subject to similar fluctuation phenomena and in addition had a definite inaccuracy inherent in the nature of the system. In any future development, both schemes would benefit considerably by an increased frequency, since such an increase would cause improved acoustic patterns in the unusually small transducers required for the speedometer and a resultant reduction in fluctuation. With such improved directionality patterns, electronic circuits could be devised that would reduce the remaining fluctuations to a considerable degree. Neither the SAMS nor the AMPS was conspicuously sensitive to variation in water temperature or in velocity of sound in water.

The PAMS, on the other hand, was much less susceptible than the other systems to difficulties caused by frequency and amplitude fluctuation, since the steady-state signal was used and the transmitter was pointed directly toward the receiver. This system, however, required a single phase path in the water between the two transducers, and therefore particular care had to be taken to obtain a sharp vertical pattern and thus to prevent reflections from the ship's hull. This again would seem to indicate the desirability of a higher operational frequency to obtain a better pattern. With PAMS, it is not possible to direct the sound beam slightly downward to avoid reflection from the ship's hull, and any improvement in the pattern must take this fact into consideration.

The measurements made with PAMS are extremely sensitive to changes in oscillator frequency and in velocity of sound in water and therefore to changes in water temperature. The proposed PAMS described in Section 5.6 would minimize the difficulty arising from frequency and temperature changes but would introduce additional measuring equipment.

5.2 REQUIREMENTS

The principal requirements set down for the development of the various AMS models were as follows:

1. The complete device should be relatively simple and should occupy a minimum amount of space.
2. Speed values should be indicated on a meter.
3. No operator should be required.
4. Only routine maintenance should be necessary.
5. The unit should be accurate to within 0.1 per cent over a speed range of from 1 to about 40 knots.
6. Any necessary underwater gear should be designed to fit a standard 3-in. gate valve of the sort employed in many marine speedometers now in existence.

These requirements were based on the desire to obtain a simple, foolproof instrument that could be installed on any kind of ship and could operate satisfactorily over a fairly wide range of speeds. The development program was based to a great extent on these requirements, although certain experimental work was carried out from time to time to test the various principles involved, without any attempt to meet the complete set of requirements.

Requirement (6) for underwater gear that would pass through a standard 3-in. gate valve led to the investigation of suitable transducers of small size. Since no satisfactory transducer was available at the beginning of the experiments, it was necessary to design and develop one. Because the development of this part of the equipment and the development of the speedometer systems were carried out simultaneously, some of the experimental transducers were never used in the working models.

5.3 TRANSDUCERS

Because of the importance of the transducer in the development of the acoustic marine speedometer, a detailed description of this aspect of the AMS program precedes discussion of the device itself.

Requirements

Six specific requirements were laid down to insure satisfactory operation of the AMS transducers and to meet the more general requirements set forth in Section 5.2. The first four of the six requirements were intended to apply to all three types of speedometer and the last two to apply only to PAMS. The six specifications were as follows.

1. The transducer should be small enough to pass through a 3-in. gate valve.

2. The horizontal and vertical patterns of the transducer should be sharply directional in order to make the receiver as nearly as possible sensitive to sound from only one direction. It was thought that this requirement could be satisfactorily met by a pattern not over 40 degrees wide, 6 db down from the peak, and with all side and back radiation at least 20 db below the maximum. (A single exception to this requirement is the horizontal pattern of the PAMS transducer, which may be nondirectional without detrimental results save for a slight decrease in the signal-to-noise ratio.)

3. The transducer should receive equally well all frequencies in the band due to doppler, corresponding to the range from zero to maximum speed.

4. The transducers should be properly streamlined to avoid excessive turbulence or cavitation at the maximum speed expected.

5. The electrical phase characteristics of the transducer should not change with frequency. This requirement eliminates the necessity for calibrating the transducer phase characteristics and allows greater latitude in the frequency stability of the transmitter oscillator.[b]

6. The two transducers should have a free water path between them and be fixed with respect to each other.[b]

Models Constructed

Five different transducer designs were investigated, four of them of the magnetostrictive type and one of the crystal type. Of the numerous transducers tested, the three so-called miniature models (cone, QC, and crystal) proved best in actual experiments. The Thuras unit was discarded early in the work and the laminated stacks available at the time proved too insensitive to be useful. The miniature crystal units were found to be best adapted to general experimental work.[c]

In the descriptions that follow it should be noted that the statements concerning the good and bad features of each model are intended to apply only to the specific instruments used in these experiments. Since all these transducers were unusually small, their features and behavior cannot be considered in any way typical of the general transducer groups to which they belong.

Thuras Models. The Thuras-type hydrophone was made of a nickel tube with a nickel sheet passing through the center longitudinally on the diameter. The coil was wound lengthwise around this central lamination. These transducers had serious disadvantages of low sensitivity and nondirectionality, although they did exhibit a flat frequency response. Four variations were made, including one $\frac{3}{8}$ in. in length and $\frac{1}{4}$ in. in diameter that proved useful as a probe hydrophone.[2] (See Figure 3.)

Miniature Cone Models. The miniature cone models consisted of a brass cone 1 in. long with a face area of 1 sq in. A nickel tube with a diameter of $\frac{1}{4}$ in. was attached to the small end. A small magnet was inserted lengthwise in the nickel tube to provide polarization, and a coil was wound on a bobbin placed around the tube. (See Figure 3A.) All five variations of this type that were built were found to have the major shortcoming of sharp resonance. They exhibited high sensitivity, however, which seemed to hold considerable promise.[3] One variation was mounted in a streamline brass strut for actual tests.

A sixth variation was made using polystyrene cones, 16 of which were machined on the back of a piece of polystyrene 2 in. square and $\frac{1}{2}$ in. thick. (See Figure 3B.) The cones were $\frac{3}{8}$ in. long and on the small end of each one was mounted a nickel tube $\frac{1}{8}$ in. in diameter. A magnet was placed on the inside of each tube for polarization and a coil built around each tube. This model had high sensitivity, and did not have the defect of sharp resonance. From

[b] Requirements (5) and (6) pertain only to the PAMS.

[c] In addition to the above transducers, two Brush C-13, 4x4-in. hydrophones were used for experimental work. For purposes of streamlining they were mounted in a large cylindrical strut having a 5/1 length-to-width ratio.

FIGURE 3. Miniature hydrophones used in acoustic marine speedometer experiments.

a mechanical standpoint, however, the unit was unstable and was never actually used.

Miniature QC Models. These models were constructed from a flat brass plate on the back of which were mounted a number of nickel tubes. A polarizing magnet was placed in each tube and a coil was wound around each tube. (See Figure 3C.)

The miniature QC units more nearly approached the six transducer specifications than any of the other types. It was particularly difficult in this instance to meet the size requirement without sacrificing sensitivity. In general, the sensitivity of these models was somewhat less than that of the miniature cone units.

Laminated Stack Models. Four units of this type were constructed, but none was considered satisfactory. (See Figure 3D.) Both low sensitivity and sharp resonance were characteristic of the models tested. It should be noted, however, that since this work was done, progress has been made in combining properties of high sensitivity and broad resonance with small size in transducers of the laminated-stack type. If further work on this project should be carried on in the future, therefore, this type should not be overlooked as a possibility.[3,4]

Miniature Crystal Models. Three of these units were constructed and two of them mounted in streamlined struts. (See Figures 3E and 3F.) Their sensitivities were approximately the same as for the miniature cone models. In general, the six specifications were reasonably well met, although the models had the mechanical shortcomings inherent in crystal transducers.

5.4 STEADY-STATE ACOUSTIC MARINE SPEEDOMETER

Theory

The *steady-state acoustic marine speedometer* [SAMS] employs two transducers, one to transmit and the other to receive. They are mounted beneath the ship, pointing forward, and are in continuous operation. Sound transmitted by the first transducer (projector) is scattered and reflected back from the water and is received by the second transducer (hydrophone). Measurement of ship's speed is based on the doppler shift in the frequency of the received sound.

The received frequency will have the value

$$f' = f \cdot \frac{c + V_o}{c + V_s}, \qquad (1)$$

where f' = received frequency,

f = transmitted frequency,

c = velocity of sound in water (approximately 2,900 knots),

V_o = velocity of the receiver relative to the water, and

V_s = velocity of the transmitter relative to the water.

If the ship is moving at a velocity V with the hydrophone trained dead ahead, then in equation (1), $V_o = V$. The sound from the projector travels forward and is scattered by the water back toward the hydrophone. Thus the hydrophone picks up sound which appears to come from a projector traveling with velocity V toward it, that is, in the direction opposite to that in which the ship is moving. Hence, $V_s = -V$, and equation (1) becomes

$$f' = f \cdot \frac{c + V}{c - V}. \qquad (2)$$

The doppler frequency shift is

$$f' - f = f \cdot \frac{2V}{c - V}. \qquad (3)$$

However, c = 2,900 knots (approximately), which is large in comparison with V. Therefore, $c - V$ is nearly equal to c, and equation (3) may be written

$$f' - f \cong f \cdot \frac{2V}{c} = 6.75 \times 10^{-4} fV \text{ c.} \qquad (4)$$

Thus the doppler is directly proportional to the speed of the ship and can be used as a measure of it. If, for example, a frequency of 20 kc is substituted in the above equation, the magnitude of the doppler comes out to be 13.5 c for a ship's speed of 1 knot.

This discussion involves the approximation that $c - V$ very nearly equals c. At 40 knots the error would be 1.40 per cent; at 10 knots, 0.35 per cent. These compare with the maximum error of 0.1 per cent, specified in Section 5.2. There are two other possibilities of error which are more fundamental in nature. One of these is dependent on the medium, and is due to the change in the velocity of sound in water because of the change in water temperature. The other is caused by variation of the frequency of the oscillator driving the transmitter.

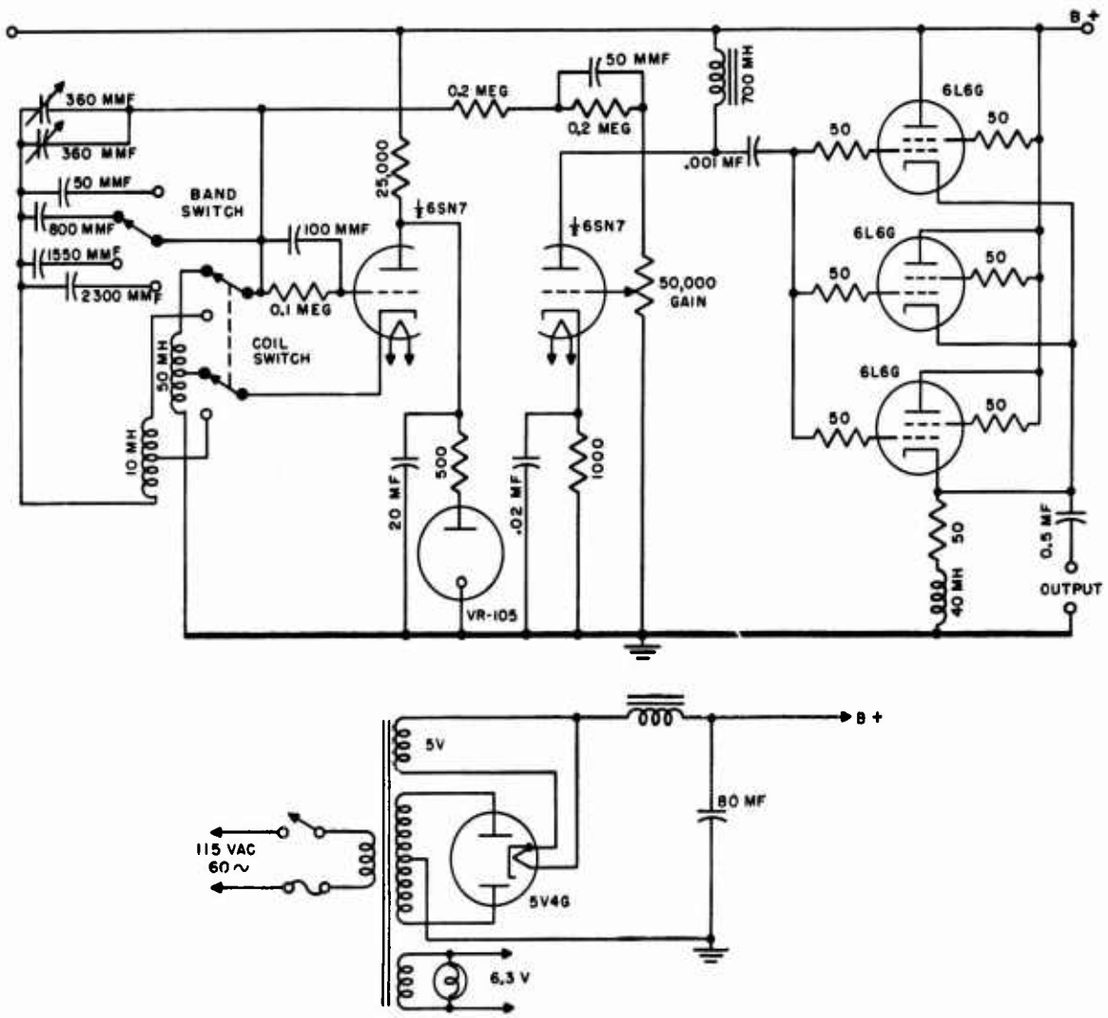

FIGURE 1. Circuit of SAMS oscillator-amplifier.

CIRCUIT DESCRIPTION

The oscillator-amplifier used for transmitting is shown in Figure 4. This unit had an undistorted power output of 115 w for a 1,000-ohm load and a frequency range of from 17 to 140 kc. The receiver (Figure 5) comprised an input transformer, two stages of tuned amplification, a diode detector, and a low-pass filter. Frequency measurements were made with a frequency meter (Figure 6) that operated as a counter. It included three stages of limiting, a differentiator, a diode rectifier, and a d-c meter located at the output and serving as an indicator. The limiters produced square waves from the input signal, which were differentiated to give two pips per cycle. The direct current from the diode rectifier was then proportional to the rate at which pips arrived and therefore proportional to frequency.

OPERATING PRINCIPLES

The oscillator-amplifier output was connected to a transducer (projector) that radiated sound toward the ship's bow. A second transducer (hydrophone) mounted adjacent to the projector received the reflected and scattered sound from the water toward the ship's bow plus some of the directly transmitted sound resulting from direct acoustic coupling between the transducers (see Figure 1). The receiver input therefore contained the original transmitted frequency plus the dopplerized frequency returned from the water. The output of the detector in the

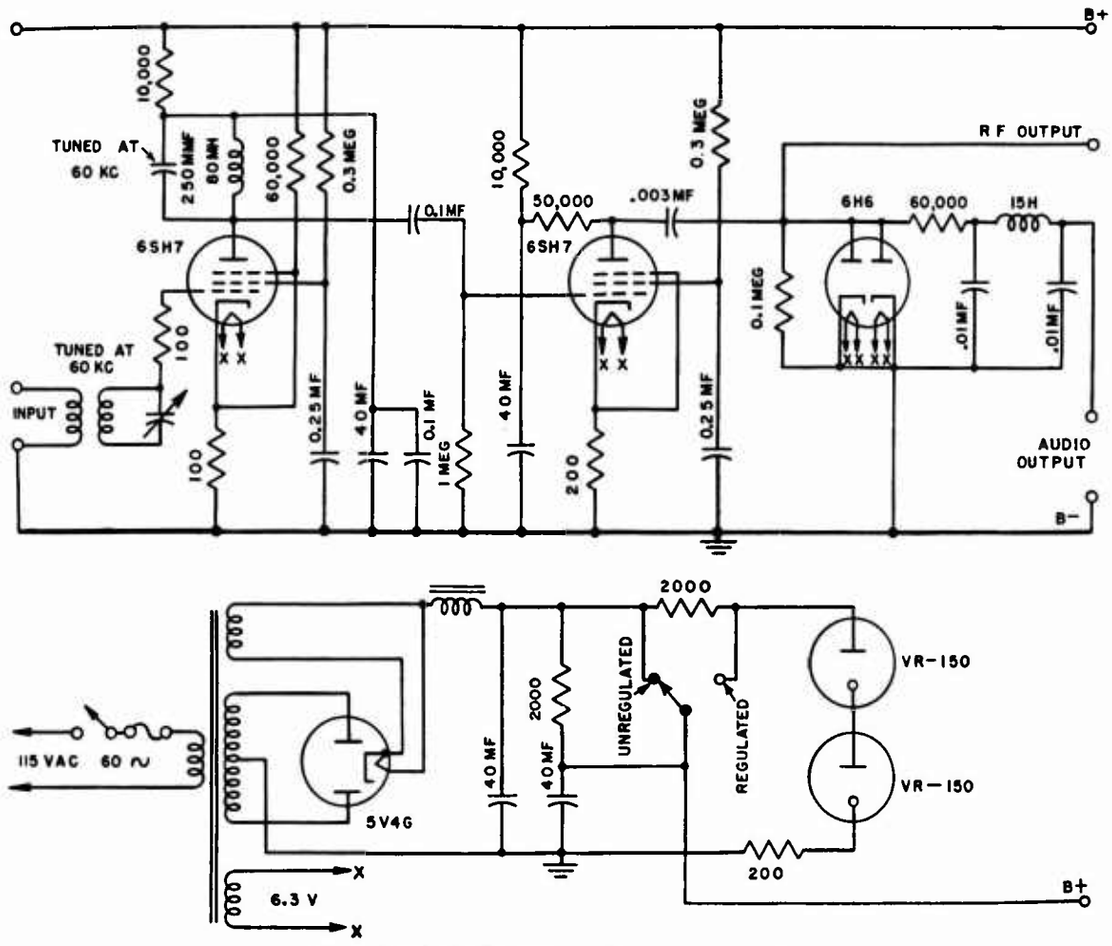

FIGURE 5. Circuit of SAMS receiver and power supply.

receiver then contained only the frequency corresponding to the doppler, the low-pass filter having removed the carrier frequencies. The frequency measured by the frequency meter was then the doppler, which has been shown to be proportional to ship's speed.

EXPERIMENTAL TESTS

The first test of SAMS produced only qualitative results.[5] The main difficulty was due to the miniature cone-type transducers, whose beam patterns failed by a wide margin to meet the pattern specifications. Two miniature QC-type transducers were used in the second set of experiments.[6] The quantitative data are plotted as curve 1 in Figure 7. In further tests,[7] the same transducers were pointed in different directions for the various runs to determine to what extent the results might depend on the direction of the transducer faces relative to the direction of the ship's motion. Data from these tests are plotted in curves 2, 3, and 4 of Figure 7.

Another transducer set used consisted of a similar strut containing two miniature Rochelle salt crystal hydrophones with rubber faces (see Figure 3F). The results obtained were by far the best in any of the SAMS experiments using small transducers.

A third pair of transducers consisted of two Brush C-13 4x4-in. crystal hydrophones, mounted in a cylindrical can. This method of mounting the transducers proved to be unsatisfactory because, at speeds above 6 knots, the equipment exhibited extreme vibration. To overcome this difficulty, a streamline dome was added and better results were obtained. These data are plotted in Figure 8.

EVALUATION OF EXPERIMENTS

The data plotted in Figures 7 and 8 are typical

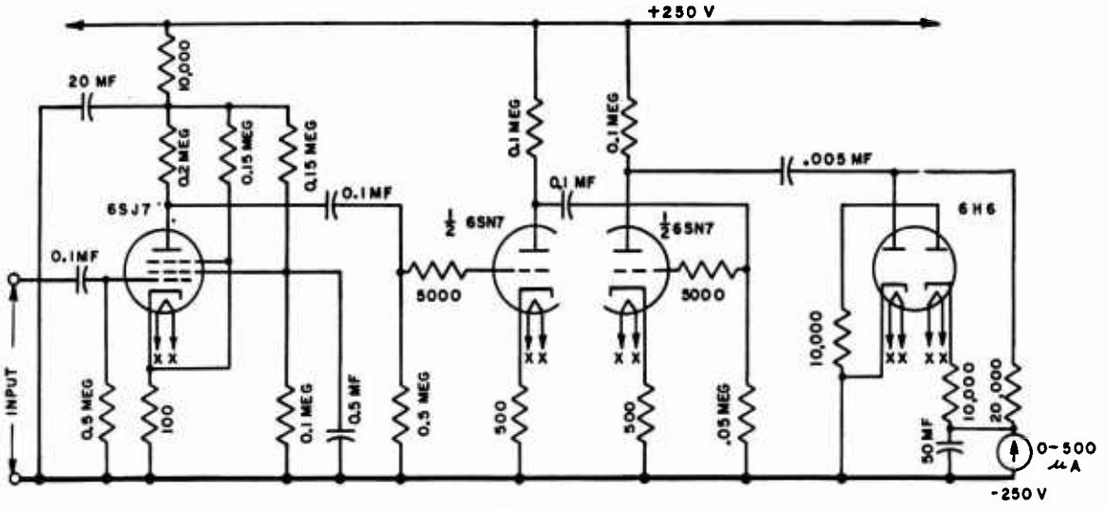

FIGURE 6. Circuit of SAMS frequency meter.

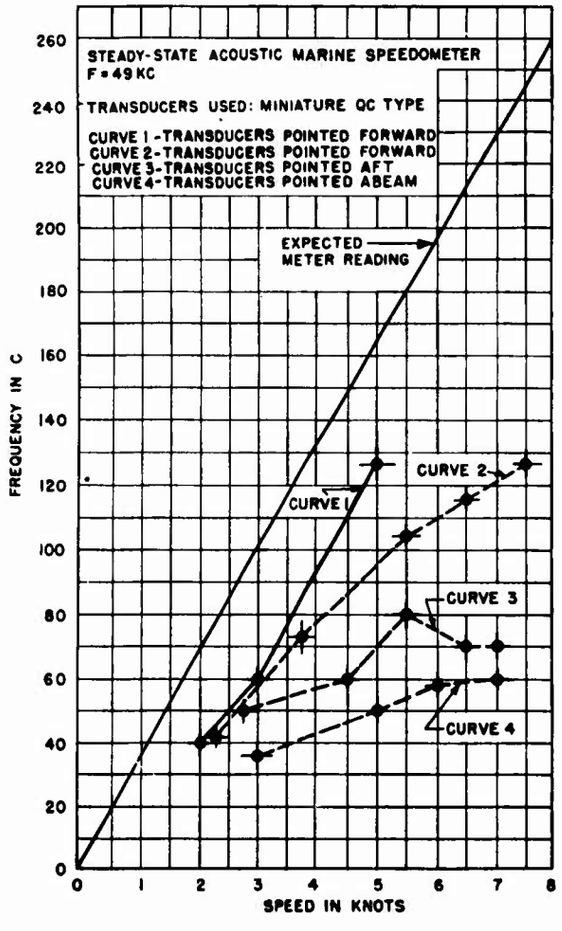

FIGURE 7. Ship's speed versus frequency meter reading—SAMS.

of all the results obtained with SAMS. It is obvious that the error in speed, instead of the specified 0.1 per cent, is 5 to 10 per cent.

The deviation from the computed curve is caused by the fact that the frequency meter must average a number of frequencies. The projector sends sound out through an angle determined by its beam width, and the hydrophone likewise receives sound from different directions because of its beam width. The frequency shift of the received sound is proportional to the cosine of the angle measured between the direction from which the sound approaches and the direction of the ship's motion. Thus the composite signal picked up contains a spectrum of dopplerized frequencies in which the amplitudes of the different components may vary from instant to instant because of the variation in scattering from time to time from any particular direction. The average frequency value of this composite signal is always less than the value computed for the doppler for sound arriving only from the direction of ship's motion.

The frequency meter reading is the average of this composite signal. There are a number of reasons why this average may fluctuate as a function of time and as a function of ship's speed. The amplitudes of the signal components, corresponding to various directions for the received sound, may vary from time to time and cause the frequency meter to exhibit fluctuations. Also, the amplitude variation of a single component corresponding to a single direction may appear as an output from the detector in the receiver, since it rectifies any such variation,

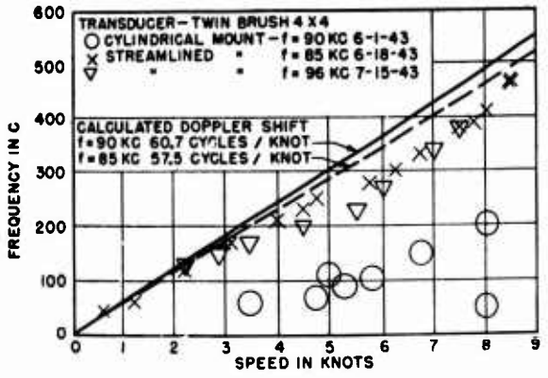

FIGURE 8. Doppler versus speed in knots--SAMS.

as well as forms the difference between the transmitted and received frequencies.

Unfortunately, these two difficulties are related in such a way that the process of correcting for one tends to aggravate the other. The amplitude variation problem can be eliminated to a considerable extent by examining a large volume of water. However, to do this, the transducer beam patterns must be wide, with the result that frequency fluctuations are increased. On the other hand, by using a projector with a narrow beam pattern, a small volume of water is examined, reducing the frequency variation problem but making the amplitude fluctuations more troublesome.

If these effects were constant and independent of ship's speed and the particular waters in which the measurements are being made, then some averaging circuit could be worked out that would reduce the meter fluctuations. Such fluctuations are obviously dependent on the nature of the water, as this determines the nature and variation in the scattered sound. Both the volume of the water and the disturbed surface layer are influential in producing the scattered sound. Also, the fluctuations are dependent on ship's speed, in that the water near the ship is disturbed by the ship's motion, and differently at different speeds; some of the sound is scattered by this disturbed water.

PROPOSALS FOR FUTURE DEVELOPMENT

An improvement on the system described above would be a receiver arranged to have amplification and limiting prior to detection, since limiting does away with most, if not all, of the amplitude variations in the signal. A frequency-sensitive circuit similar to a discriminator would be required in place of the present diode rectifier, and a tuned circuit should be used just ahead of the discriminator to take out the harmonics introduced in the limiting process.[8]

Another scheme for further development of the SAMS eliminates the necessity of using both a transmitting and a receiving transducer.[8] Instead, a single magnetostriction transducer is proposed consisting of a tube ¾ of a wavelength long, mounted on a diaphragm which transmits the sound to the water. The primary advantages of this scheme are the use of a single transducer and of a single electronic circuit for transmission and reception.[9]

Another proposed scheme makes use of a receiving transducer whose output is amplified and shifted in frequency by a known amount and then transmitted on a second transducer.[8] Such a system operates in a steady-state manner if the frequency offset in the electronic part of the circuit is equal to the frequency shift in the water resulting from doppler.[10]

5.5 ACOUSTIC MARINE PINGING SPEEDOMETER

THEORY

The *acoustic marine pinging speedometer* [AMPS] also utilizes the doppler shift in frequency resulting from the relative motion of the ship with respect to the water. The theory developed for the SAMS applies equally well to the AMPS.

EQUIPMENT

The following were built for use in the AMPS system: a one-way combined receiver-transmitter, incorporating a keying oscillator to trigger the transmitter; the transmitter itself; a tuned receiver including a detector and low-pass filter; and suitable power supplies (see Figure 9). Primarily on account of leakage from the transmitter to the receiver, however, another receiver and transmitter were built in separate units. A keying relay was used rather than triggering the transmitter with a pulse and blanking the receiver at the same time. The wiring diagrams of these units are given in Figures 10 and 11. The measurement of frequency was carried out using the SAMS frequency meter. Only one transducer is used.

During the transmitting period the transducer is energized from the transmitter and emits sound toward the ship's bow. During this period the receiver is blanked so that no signal reaches the frequency

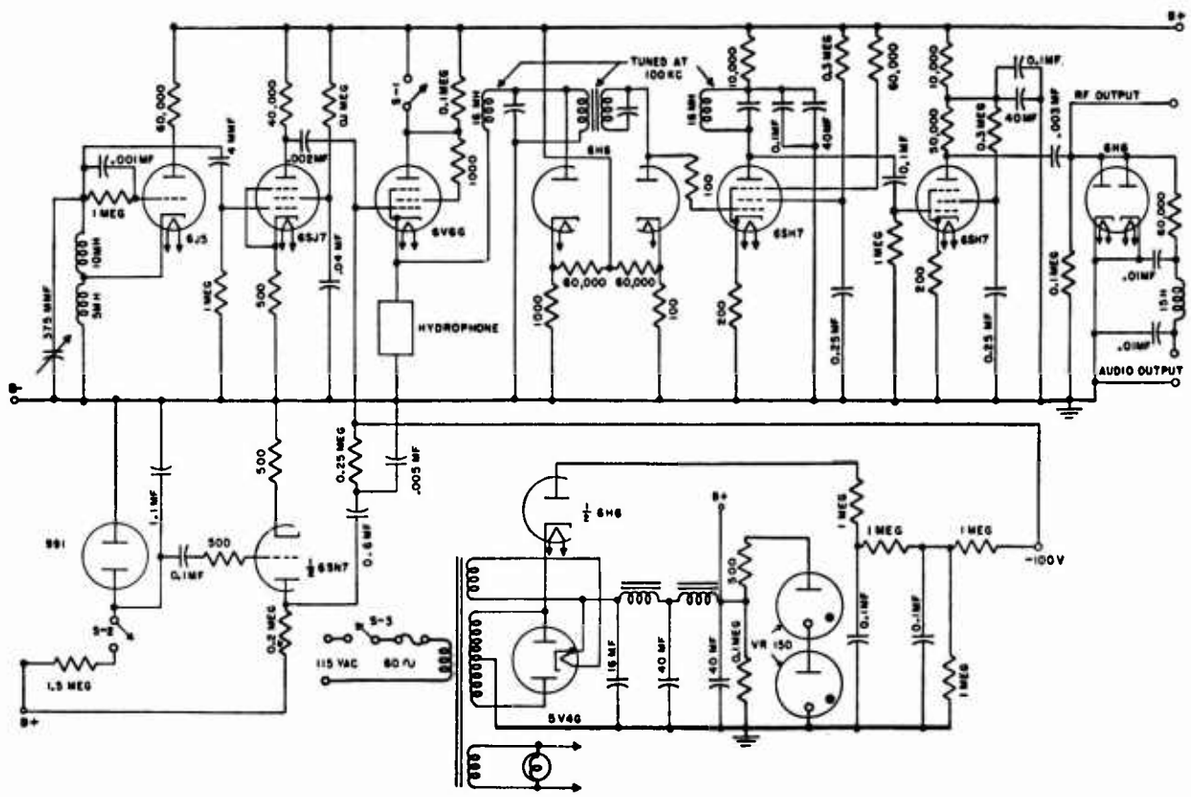

FIGURE 9. Circuit of AMPS oscillator-receiver and power supplies.

meter. On reception the transmitter is turned off, the transducer is connected to the receiver, and the receiver then operates. A small voltage of transmitted frequency is injected into the receiver to beat with the reverberation signal being received. The frequency of the receiver output is then the doppler shift, the two carrier frequencies having been removed by the low-pass filter.

EXPERIMENTAL TESTS

In the first test of AMPS,[11] the ship's QC projector was trained ahead and the reverberation frequency determined by varying the output of a separate oscillator to match it in pitch. Since the transmitted frequency was known, the doppler could be calculated and, from it, the ship's speed.

The values thus obtained agreed within 0.1 knot with those obtained by clocking the ship between buoys which were a known distance apart.

The next test was an unsuccessful one using a miniature cone-type transducer and the combination transmitter-receiver.

A series of tests was run next, using a ship's QC equipment.[12] Some of these experiments were conducted not simply to measure speed, but to investigate the effect on the reverberation frequency reading of the length of time during which sound was being received. In making these tests, a ping of transmitted signal was sent out and, at some specified later instant, the output of the receiver was applied to the frequency meter for a given time interval and then removed. This time interval was called a gate length and, because of the range scale calibration of the QC equipment, could be expressed conveniently in terms of yards of travel of the sound. The results of a series of such measurements taken with the ship at anchor are plotted in Figure 12. The second set, shown in Figure 13, was made with the ship moving at 12 knots. Figure 14 gives a typical curve of speed versus reverberation frequency. The 30-yd gate length was chosen on the basis of the data shown in Figures 12 and 13. The values of speed used in the experimental curve were estimated. The vertical lines through these points indicate an estimate of accuracy in judging speed. The horizontal lines show the frequency meter range of fluctuation.

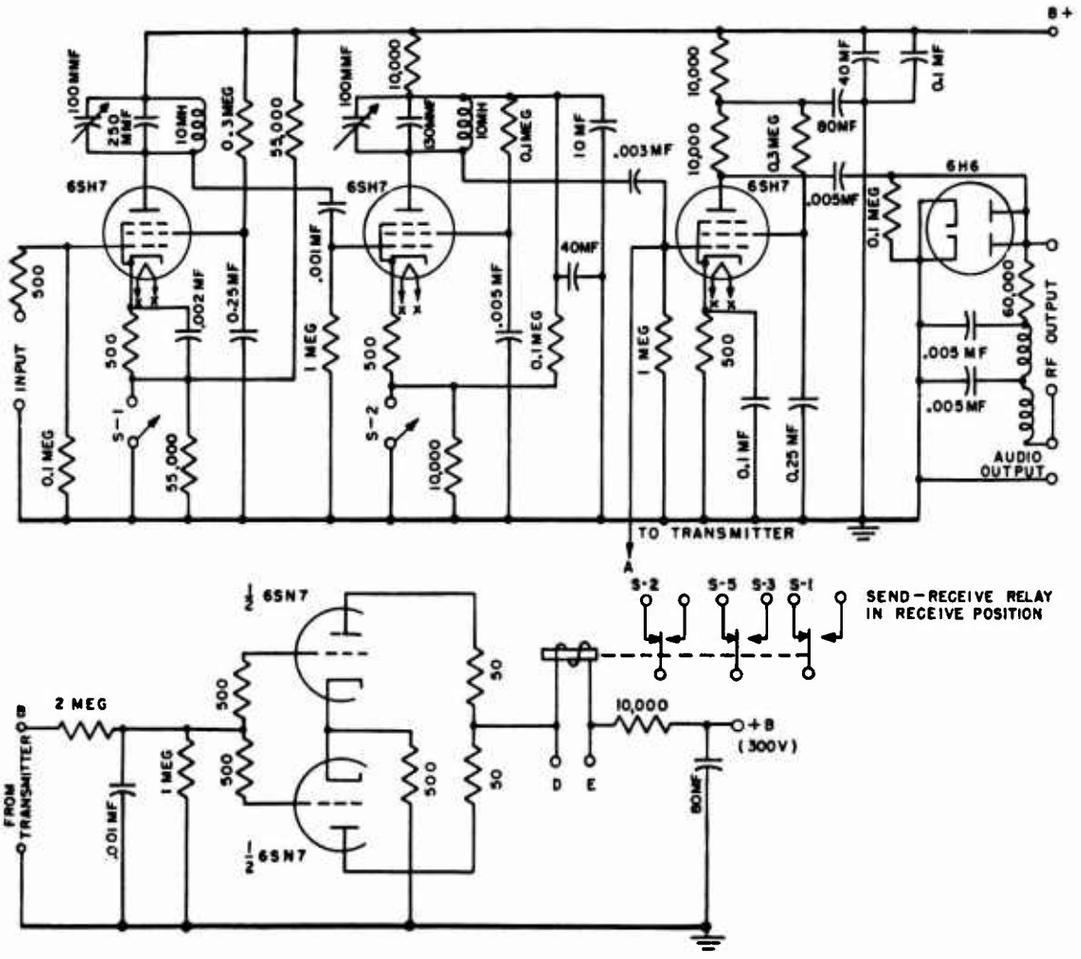

FIGURE 10. Circuit of AMPS separate receiver.

All these measurements were found to be quite erratic, particularly for the shorter gate lengths.

Further tests were made using the separate transmitter and receiver chassis and a Brush C-13 hydrophone mounted in a streamline housing. The data obtained were largely qualitative, with the frequency meter readings fairly steady but not necessarily proportional to speed. Some of these data are plotted in Figure 15.

Observations made using a cathode-ray oscilloscope revealed three facts: (1) only at the very beginning of the receiving period was the reverberation strong enough to actuate the frequency meter; (2) amplifier noise contributed to the meter reading; (3) switching transients affected the meter reading.

Evaluation of Experiments

The very obvious lack of accuracy exhibited by the curves of Figures 12 to 15 indicated the need for careful consideration of the reasons behind these poor results. An analysis of this problem[13] largely resolved itself into a matter of answering the following questions:

1. Exactly what does the frequency meter read?
2. What factors might cause the meter readings to vary while the ship's speed remains constant?
3. What factors might cause the reverberation as received from the water to contain frequency fluctuations?
4. How large an error is introduced into the reading if the meter receives one pip more or less than the normal number per time interval?

Since the reasoning involved in this analysis is pertinent to the entire AMPS problem, it is presented here in some detail, under headings corresponding to the above questions.

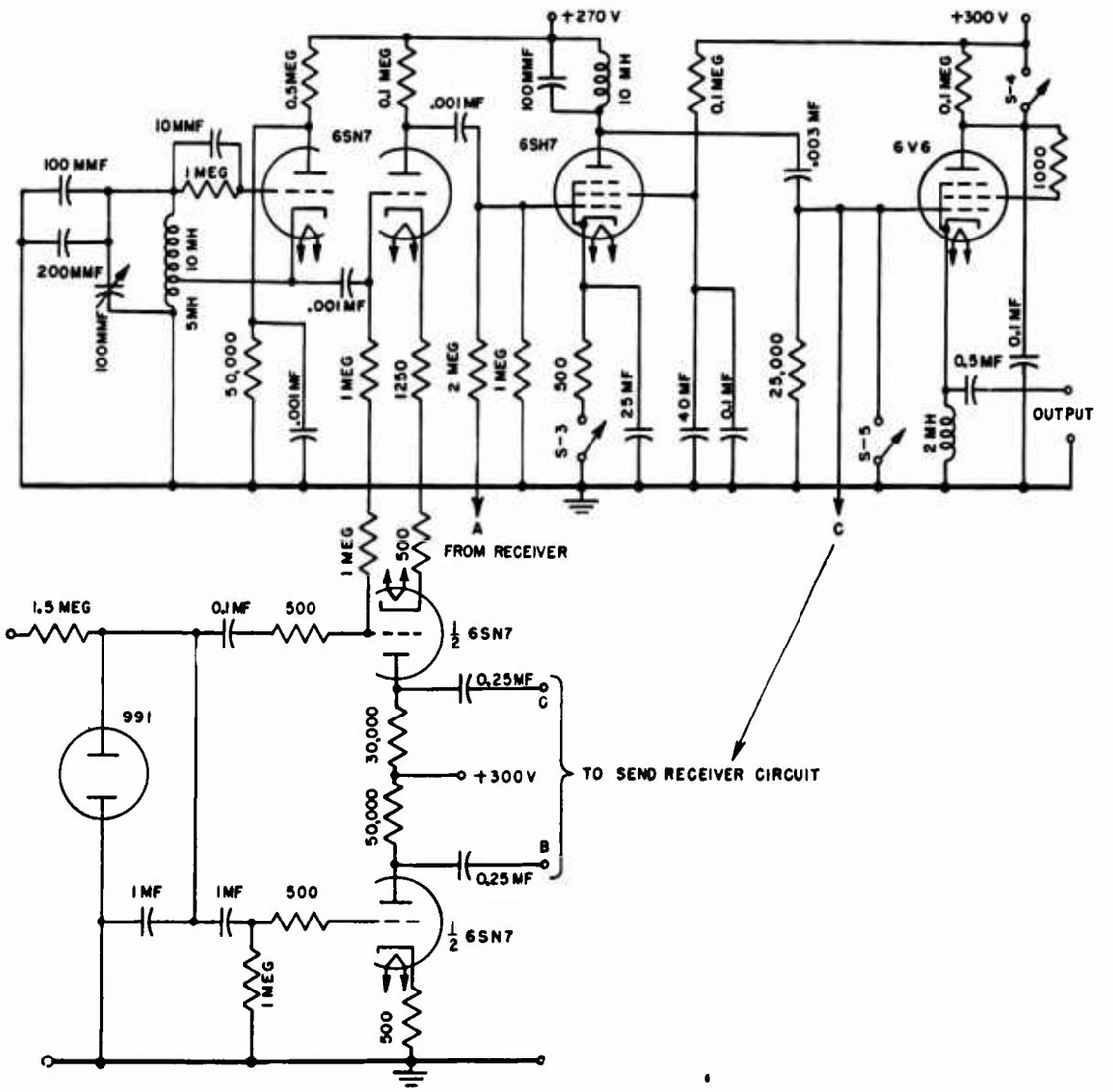

FIGURE 11. Circuit of AMPS separate transmitter.

What the Frequency Meter Reads. The frequency meter was used here as a cycle counter. As explained in Section 5.4, square waves were produced from the input signal by means of limiters in the frequency meter. These waves were limited to a fixed value and then differentiated to give two pips per cycle. Each pip produces a pip of rectified current through the meter. The meter reading depends on the number of pips received. For example, let the minimum integration period of the meter be d. Then if N equally spaced pips are received during d, a definite indication is produced by the frequency meter. This indication is the same for each application of the N pips during the period d. Now if these applications occur periodically at intervals of time c (less than d), then the frequency meter gives a different but still a definite indication. In other words, there is no uncertainty or ambiguity concerning the frequency meter readings in such cases.

Factors That Could Produce Variations in Meter Readings. Any of the following factors could produce fluctuations in the meter reading since, as shown in the preceding paragraph, the reading is proportional to the number of pips received per time interval.

1. Any increase or decrease in the number of pips N, received in time d over the various periodic intervals c.

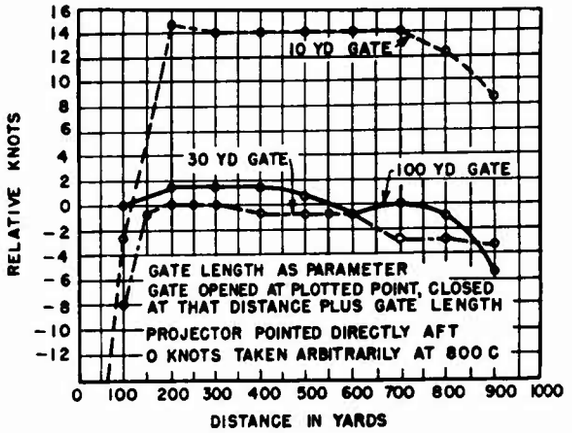

FIGURE 12. Reverberation in relative knots versus distance in yards with ship at rest—AMPS.

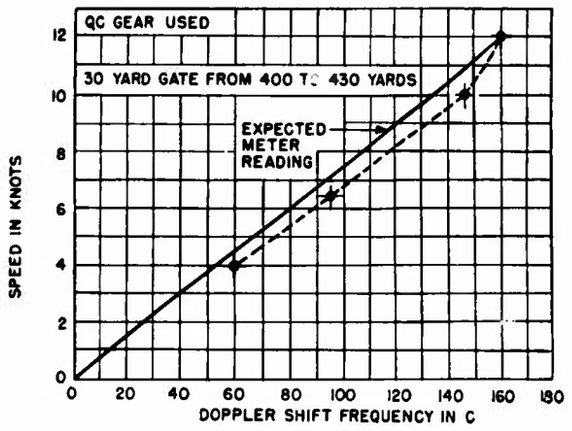

FIGURE 11. Doppler shift versus ship's speed—AMPS.

2. Any variation in the length of d over successive intervals.

3. Any variation from time to time in the length of c.

4. Any variation in the spacing of the N pips such as might occur if the signal applied to the frequency meter is not completely limited to the fixed value.

5. Various electronic difficulties, including improper limiting, lag in the meter, and variation of circuit components with voltage changes or with time.

6. Certain mechanical troubles, such as variations in the distance of gating.

Factors Causing Fluctuation in Reverberation Frequency. The reverberation, as it is received from the water, may fluctuate in frequency for the following reasons:

1. The angular beam pattern by its very nature introduces a continuous spectrum of frequencies due to doppler effect. If, for example, the pattern is X degrees wide 6 db down from maximum response, then the frequencies within that angle, when the hydrophone is trained dead ahead, cover the range from the ping frequency f_o to $f_o \cos X$. (If amplitude fluctuations discussed in the next paragraph are present, the frequency variation may be still further increased.)

2. Variations in amplitude of the received signal can affect the reading of the frequency meter. If the amplitude of a constant frequency signal falls below a certain value, the meter reads incorrectly, whereas for levels above this limiting value, it always reads correctly. Rapid fluctuations in amplitude, above and below this value, distort the waveform applied to the meter and introduce spurious pips, nullify legitimate ones, or produce irregular spacing in the

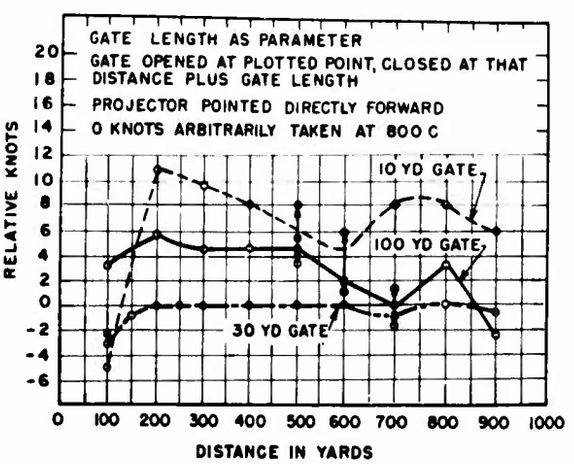

FIGURE 13. Reverberation in relative knots versus distance in yards with ship in motion at 12 knots—AMPS.

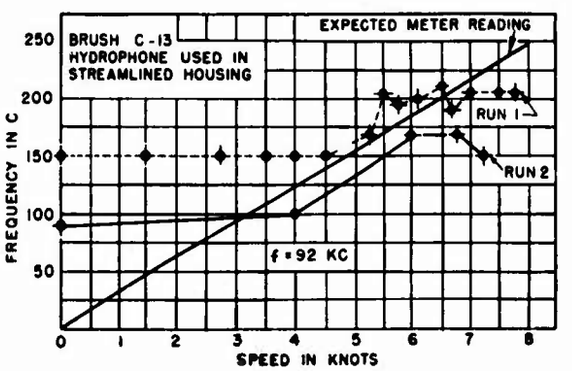

FIGURE 15. Ship's speed versus frequency meter reading—AMPS.

pips received. Relatively slow variations which do not distort the waveform are in most cases limited out.

3. Because of the nature of the medium and its motions, the actual doppler shift may differ from that which was calculated on the assumption that the water would provide a uniform scattering medium. Most important in this respect is refraction of the sound beam due to temperature gradients. The wind moves some of the surface water along, introducing spurious velocity components. Reverberation from the bottom would produce incorrect frequencies because of tide and ocean current effects. These frequency distortions usually cause phase distortion, which is present when the relation between frequency and phase angle is not linear. Since it is the ship's velocity with respect to the water that is desired, the gate must be restricted to include only the region very close to the ship. Otherwise reverberations may enter from surface layers and from the bottom.

Error Introduced by Reception of One Pip Too Many or One Too Few. The principle of uncertainty in acoustics may be interpreted, in the present case, as indicating an unavoidable uncertainty of one in the number of pips (or cycles) that are observed in any finite time interval. The physical basis of this uncertainty may be illustrated by pointing out that the gated interval may not contain an exactly integral number of cycles of the received frequency, and that there is no control over the phase of the received frequency at the initial or final instants of the gated interval. The variable transients associated with the start and finish of the time interval may, therefore, be such as to lead to the reception of one pip more or less, even though the time interval itself remains perfectly constant.

It can be shown[8] that in order to obtain the necessary instrumental accuracy with a 10-yd gate length, the transmitted frequency must be raised to about 1 megacycle, in which case the instrumental error is certainly somewhat less than other errors.

Proposals for Future Development

In line with the preceding discussion of the evaluation of the experiments, an improved system can be proposed for the pinging speedometer, utilizing the same general scheme described for the AMPS. In order to obtain the necessary instrumental accuracy in speed measurement, the frequency should be increased to the order of 1 megacycle. The use of a higher frequency limits the maximum range because of attenuation and therefore also increases ship security. A range gate should be provided to limit reception to a specific value of range some distance ahead of the ship. The transducer should be pointed somewhat downward from the horizontal so that none of the sound rays can impinge on the water surface or the ship's bottom. This avoids erroneous readings caused by distorted layers of water near the surface or by the lack of doppler from the bottom of the ship. Refinement of design of the electronic equipment is indicated to avoid disturbance from switching transients and to provide a steadier reading of the frequency meter for an intermittent input.

5.6 PHASE ACOUSTIC MARINE SPEEDOMETER

Theory

The *phase acoustic marine speedometer* [PAMS] employs two transducers, arranged to face each other along a line parallel to the ship's keel. One of these transmits, the other receives. Unlike the two speedometers previously discussed, measurement of speed is based on the phase shift introduced by the water path between the transducers. This phase shift can be shown to be a function of ship's speed as follows:[14]

Assume the ship to be at rest with the two transducers arranged facing each other and one directly forward of the other. The phase lag due to the water path is

$$\phi = \frac{\omega L}{c}, \tag{5}$$

where ϕ = phase lag in radians,

ω = angular frequency in radians per second,

L = distance between the transducers in centimeters, and

c = speed of sound in water in centimeters per second.

If the ship is moving forward with speed V centimeters per second, the frequency received is the same but the phase lag caused by the water becomes

$$\phi' = \frac{\omega L}{c - V}. \tag{6}$$

The difference in phase caused by the ship's motion is

$$\phi' - \phi = \frac{\omega LV}{c(c - V)}. \qquad (7)$$

But since, for the range of speeds considered, $c - V$ nearly equals c, the phase difference may be written

$$\phi' - \phi = \frac{2\pi fLV}{c^2}, \qquad (8)$$

where f = frequency in cycles per second.

When values of constant quantities and conversions are inserted, this difference becomes

$$\phi' - \phi = 0.435 \times 10^{-6}\, fLV \text{ radians}, \qquad (9)$$

where f is in cycles per second, L is in feet, and V is in knots.

Possibilities of error are:

1. The assumption that $c - V$ nearly equals c.
2. Change in water temperature.
3. Variation of frequency in the oscillator which drives the transmitter.

Equipment

The electronic unit for the PAMS did not go beyond the blueprint stage and experiments carried out used speedometer hydrophones with standard laboratory equipment, as well as a QC echo-ranging gear.

Experimental Work

Two series of experiments were carried out on the PAMS. In the first of these, a crystal 1x1-in. transducer was used as a projector and a miniature cone transducer was used as a hydrophone. The projector was driven from a small power amplifier while the hydrophone output was amplified and led to one pair of plates of a cathode-ray oscilloscope. The oscillator output was applied to the other pair of plates, and the resulting pattern gave a measure of the phase between the transmitted and received signals. The oscillator frequency was not sufficiently stable to allow accurate measurements, and there was too much relative motion between the two transducers because they were not solidly mounted to the ship's hull. As a result, only qualitative observations could be made of the phase shift, but there did appear to be a definite change as the ship's speed was varied.

In the second set of measurements, a QC projector was used as transmitting transducer, and an installed sound gear monitor [ISGM][15] was used to receive. The monitor output was amplified and applied to one pair of plates of the cathode-ray oscilloscope. The driver output of the QC projector was applied to a variable lag line and the output from the line applied to the second pair of plates of the oscilloscope. By adjusting the amount of phase lag in the lag line, a straight-line pattern could be obtained on the cathode-ray tube and the value of phase shift from one ship's speed to another could be obtained.

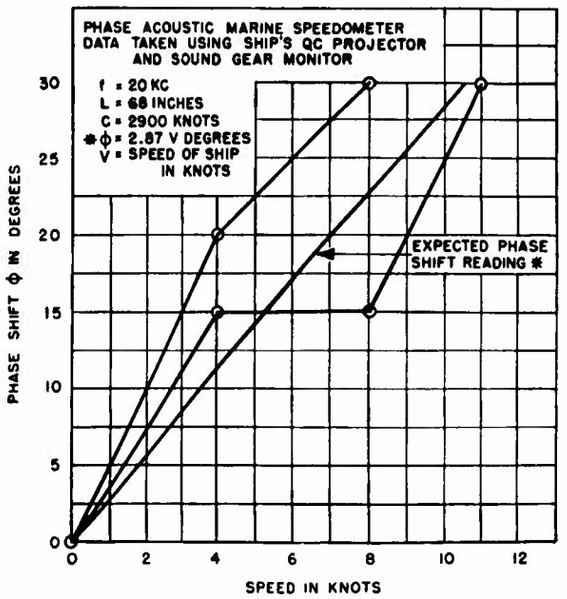

Figure 16. Ship's speed versus phase shift—PAMS.

Evaluation of Experiments

Figure 16 shows the results of the measurements described above. The experimental values obtained are by no means accurate, probably because the waveform was poor at both the QC projector and the ISGM output, so that it was impossible to obtain a straight line on the cathode-ray tube for reference. This waveform was complicated by the presence of spurious pickup due to ground loops. The finest division on the variable lag line was 5 degrees, limiting the potential accuracy. Moreover, the output frequency of the QC projector did not remain constant during the measurement.

Proposals for Future Development

An improved acoustic phase speedometer[16] would use two transducers, one placed ahead of the other,

each having flat phase shift versus frequency characteristics. Readings of phase shift due to the water path would be taken, first using one transducer to transmit and the other to receive, and then with the functions of the two interchanged. The difference between such a pair of readings would be independent of change in the speed of sound in water (and hence of temperature) and of change in the driving frequency. This difference could be obtained automatically and quickly by suitable servomechanisms, which would operate the necessary switch for interchanging the transducers and would balance a phase-indicating device.

The principle of the change in phase due to the water path may be used to cause two other measurable effects. The first[17] proposes measurement of a voltage, obtained from the combination of the transmitted and received signals. Two transducers are placed in the water, one in front of the other, acting respectively as transmitting and receiving units. The received signal is amplified to a definite voltage and is made to beat with an equal voltage from the driver oscillator. The resultant voltage is made zero with the ship at rest by a proper choice of frequency and of distance between transducers. When the ship moves, the phase difference between the signals changes because of the change in phase through the water, and the voltage of the combined signal is approximately proportional to the sine of the phase difference produced by the motion.

The second method[10] also employs separate transmitting and receiving transducers. These are connected in the circuit of a phase-controlled oscillator, whose frequency of oscillation would then be varied with variations in phase due to the water path between the two transducers. Thus a measure of ship's speed would be given by measurement of the oscillator frequency.

As compared with the two speedometers based on doppler shift, the phase speedometer would appear to involve the greatest complexity in apparatus and to offer greater difficulty in development. It is likely that these handicaps would be outweighed by the advantages of the direct transmission path.

Chapter 6

ECHO-REPEATING EQUIPMENT

Echo Repeater

The echo repeater as developed by NRL, UCDWR, and HUSL is an artificial target designed to simulate the reflection properties of an actual vessel. Thus, echo-ranging equipment may be tested economically and with some measure of control over the target. The device consists of a hydrophone and a projector, coupled by an amplifier. In use, the repeater is suspended or towed below the surface of the water at some distance from the ship whose gear is being checked. A ping emitted by the echo-ranging projector is picked up by the hydrophone, amplified and retransmitted to act as an echo for the pinging vessel.

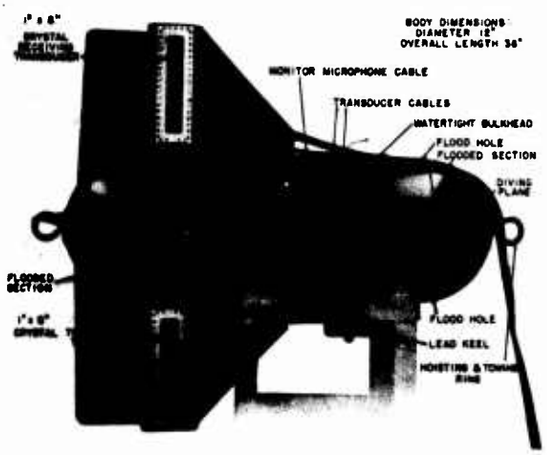

FIGURE 1. An HUSL Echo repeater (Smecho 1).

6.1 INTRODUCTION

THE ULTIMATE MEASURE of performance for both sonar personnel and sonar equipment is efficiency in the detection of neighboring ships. However, during the period of personnel training or equipment development when very frequent use of echo-ranging gear is necessary, it is extremely expensive to employ surface craft or submarines as targets. Moreover it is difficult to maintain adequate control over the movements and the echo-reflecting strength of a target vessel throughout the duration of a training or testing session. For these reasons, various laboratories of the National Defense Research Committee became actively engaged in the development of artificial echo-ranging targets at a very early date. Practice targets for use in the training of sonar personnel became a primary concern of the program initiated by the University of California at its San Diego Laboratory. On the other hand, the main objective of the somewhat later investigation undertaken by Harvard was the development of targets which would be suitable instruments for the testing and calibration of sonar equipment.

Artificial targets comprise two types: (1) the so-called passive targets and (2) the so-called echo repeaters. Passive targets consist of materials having a different acoustic impedance from that of water and a structural form designed to provide surfaces with effective reflection properties. Various plane, spherical, and cylindrical structures of bubble fiber, metal, and other materials have been tried. Of these a hollow steel sphere and a steel triplane arrangement covered with bubble rubber are the only ones with which any satisfactory results were obtained.

Because of their relatively small size, the difficulty of towing them, and, in the case of the triplanes, the stringent accuracy of construction required, passive targets are generally used only in stationary tests and have been largely replaced by echo repeaters when extensive target service is required.

The echo-repeater type of target consists essentially of two transducers coupled by an amplifier (see Figure 2). One of the transducers receives signals which the other transmits or "repeats" after they have been amplified. In the testing procedure, the echo repeater is suspended or towed below the surface of the water at some distance from the ship whose gear is being checked. A ping emitted by the echo-ranging projector is picked up by the receiving transducer of the repeater, amplified, and retransmitted to act as an echo for the sonar gear.

Echo repeaters may be broadly classified as towable or nontowable. With the towable type, an observable doppler shift may be obtained at the proper

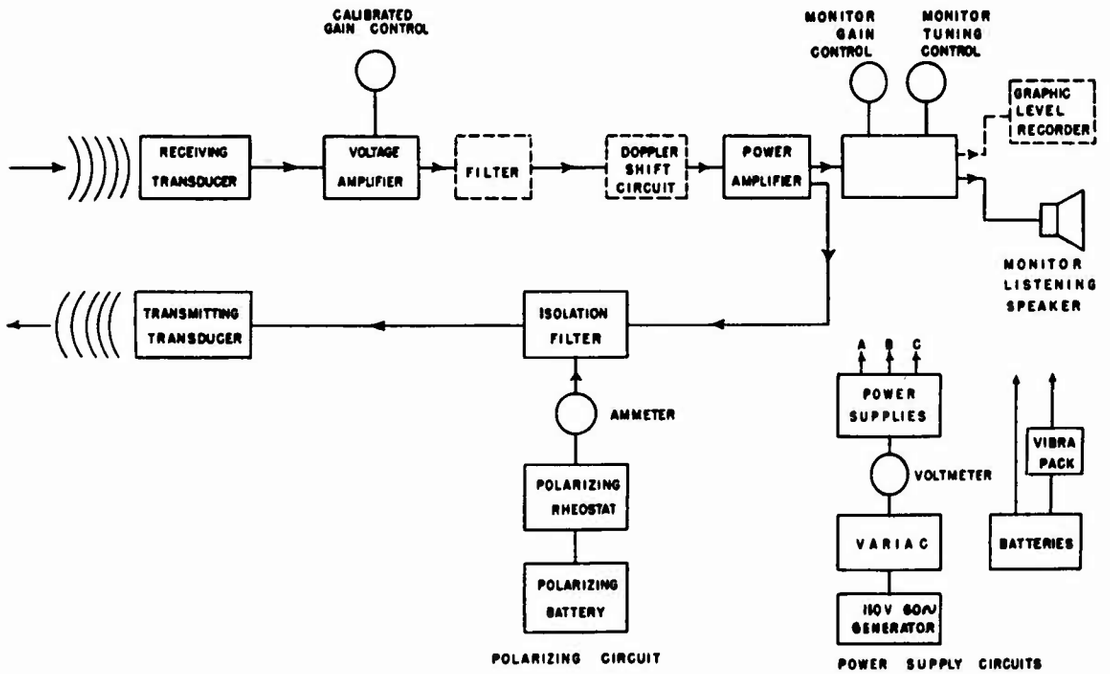

FIGURE 2. Block diagram of typical echo repeater circuits.

speed. For the nontowable type, doppler-shifting circuits have been designed so that the stationary repeater can provide an up or down doppler in its echo as desired. Within these two types, the various models differ from one another in still other respects, such as: the type of transducers used, piezoelectric or magnetostrictive; the operating frequency, ranging from about 13 to 60 kc; and the location of the amplifier unit, whether completely on the deck of the vessel, completely in a self-contained, battery-operated repeater assembly, or partly on deck and partly in the transducer assembly. The design considerations involved in these differences and the detailed description of various models of echo repeater are presented in succeeding sections of this chapter.

The first attempts to devise an electroacoustic artificial sonar target were made by the Naval Research Laboratory. The method employed involved a transducer which, upon receipt of the outgoing sonar pulse, initiated the action of a local oscillator which transmitted an "echo" pulse. This target was unsatisfactory since the echo did not provide a realistic simulation of the frequency, duration, and amplitude of the signal received by the target. Engineers of the San Diego Laboratory of the University of California Division of War Research then improved upon this design by providing sufficient isolation between the receiving and transmitting transducers to permit them to be coupled directly by a suitable amplifier. The development of a group of practice targets which proved satisfactory for personnel training in the Pacific area was the final outcome of the work at San Diego. Late in 1942 the investigation of echo repeaters was established as an individual project in the program at the Harvard Underwater Sound Laboratory [HUSL], and San Diego then made its various models available to HUSL for testing in Atlantic waters and for the assistance of the Harvard group in its development of repeaters for equipment testing and calibration.

The first HUSL echo repeater, known as Fecho, was similar in design to the San Diego Model SR-2. It consisted of a torpedo-like body to which two piezoelectric transducers were attached, and a separate amplifier mounted on the vessel towing the transducer assembly. Depressor vanes on this assembly caused it to be submerged when towed. While some success was achieved in the operation of the Fecho repeater, the difficulties of maneuvering its large size and weight stimulated the design of a less unwieldy model.

Accordingly, the construction of a series of smaller, towable echo repeaters, called Smechoes, was undertaken. The transducer-supporting body of these

models was similar to the torpedo-shaped Fecho, except for size and weight. A number of tests and modifications were made with these repeaters but since fully satisfactory results were never obtained, a fresh start was finally inaugurated with an investigation of repeater assemblies of simplified design. Ring-stack magnetostriction transducers possessing much greater efficiencies than the usual magnetostrictive type became available at this time and were incorporated in these new repeaters. Successful results were obtained in the tests which followed and apparently the transducer improvement was largely responsible. This is borne out by the fact that a Smecho model, after being altered to use the ring-stack transducer, also gave satisfactory performance.

Toward the end of the Harvard development program, the electronic equipment and transducer assembly for a deep-water echo repeater were designed and constructed at the request of the Navy. The self-contained, battery-operated type of unit found necessary for this project was installed in a torpedo-shaped hull furnished by ASDevLant. The completed repeater, known as the Whale, was capable of being towed at depths down to 2,000 ft and gave satisfactory results when echo-ranging was carried on with a tiltable projector.

It is recommended that future work be directed toward the establishment of manufacturing designs and specifications based on the existing types of repeater, and toward the development of a delayed-action type of repeater which apparently would be very valuable in several additional investigations that have been proposed.

6.2 GENERAL DESIGN CONSIDERATIONS

Before a detailed description of various echo repeaters is given, some general problems involved in their design are discussed.

6.2.1 Stationary Repeaters

The stationary repeaters, which have been used in general only for shallow depths up to 30 ft, represent the simplest design. Two transducers separated a short distance vertically are suspended overside a vessel. The transducer leads, relatively short, are connected to a deck amplifier. Gain adjustments and connections to the ship's generator power supply are readily made by the operator, with no complications of voltage regulation or magnetic coupling.

6.2.2 Towable Repeaters

When a transducer assembly is towed through the water, the hydrodynamic forces are such that the depth to which the transducers are submerged is usually only a fraction of the length of the towing cable. The depth of submersion depends mainly on the following factors: the buoyancy (positive or negative) of the transducer assembly, its diving vane design, the length of the towing cable, and the speed of towing.

The advantage of using a body having a positive buoyancy is that it is more easily handled. Other things being equal, less force is required to tow it, and, when the towing stops, it comes to the surface of its own accord. In a shallow harbor this is distinctly useful, since a negatively buoyant body is apt to settle to the bottom at a quick stop and become entangled with the debris. On the other hand, it is difficult to attain depths of over 50 ft with a positively buoyant body, even if the area of the diving vanes is made relatively large.

The length of the conductor cables of a towed repeater involves difficulties of voltage regulation and coupling between the leads if deck-mounted electronic units are used. Careful design has made it possible to develop a deck electronic system using cable lengths of several hundred feet. In some cases it was found advantageous to place a preamplifier within the transducer assembly to reduce the difference in the power levels of the cable conductors. In one of the later HUSL designs of echo repeaters, all amplifier components but one attenuation control and the power supply are included within the transducer body, the deck attenuation allowing a variation of 29 db.

For depths of the order of 1,000 ft, it becomes necessary to make the repeater completely self-contained. It must be sufficiently heavy and equipped with the proper depressing vanes so that enough downward force is developed to neutralize the lift of the cable (about 1 mile in length). The electronic circuit must be operated by batteries and, because of the heavy drain of polarizing current, the use of permanent magnets for polarization or of Permendur transducers, requiring only an initial magnetization, is of great advantage. An automatic switch, operated by hydrostatic pressure at a preset value is also desirable. For such depths it is necessary to use sufficient

wall thickness and proper seals for the chamber containing the electronic equipment so that it can withstand the extreme pressures encountered.

Another factor to be considered in the design of a towable repeater body is its hydrodynamic stability. Because of the limitations of the vertical sensitivity patterns of most transducers, it is desirable to restrict the roll and pitch of the transducer assembly to a few degrees. For investigation of shallow operation stability an extra conductor may be connected between an indicating meter in the deck electronic equipment and a pendulum potentiometer in the towed body. Care must be exercised in choosing a meter of the proper periodicity.

6.2.3 Transducers

The features of transducer design to be considered are (1) type, whether piezoelectric or magnetostrictive, (2) frequency response, (3) horizontal and vertical directional patterns, and (4) efficiency. Piezoelectric transducers were found satisfactory in the San Diego repeaters which were employed in the waters of the Pacific. At HUSL, however, transducers for echo repeaters have been selected almost entirely from the magnetostrictive type on account of the temperature sensitivity of piezoelectric transducers and the relatively wide variations in water temperatures in the Boston area.

Types of Piezoelectric Transducers

The San Diego piezoelectric transducers consisted essentially of 45-degree, x-cut Rochelle salt crystal stacks. The BD-1 model comprised a double bank of 24 crystals, each ¼ in. by 1 ft by 1½ in., insulated by Corprene pads and spacers and immersed in vapor-free castor oil. To reduce acoustic coupling, the stacks of a receiving transducer were connected in series, whereas those of a projecting transducer were connected in parallel, 180 degrees out of phase. The CD-1, CG-1, and CJ-1 models were all similar electrically, each consisting of a single stack of 26 crystals. They exhibited a somewhat more uniform directivity pattern than could be obtained with the BD-1.

Types of Magnetostriction Transducers

A variety of magnetostriction transducers have been used at HUSL for echo repeaters, including hard nickel, annealed nickel, and Permendur types. The method of providing the polarizing magnetic field for these transducers varies. Hard nickel retains sufficient magnetism, when once polarized, for use in a receiving transducer but not in a transmitting transducer in which the values of current are high. Transducers constructed of annealed nickel require a constant flow of direct current or the presence of a permanent magnet in the transducer magnetic circuit to maintain the proper degree of polarization. The polarizing current needed varies from 1 to 6 amp depending on the size of the transducer. With long conductor cables the transmission of the polarizing current presents a considerable problem. The permanent magnets used are either Alnico or sintered iron oxide magnets.

The construction of the more efficient laminated ring stacks does not readily allow the use of permanent magnets, so that a polarizing current is generally used for the nickel ring-stack transmitters. Permendur (50% iron, 48% cobalt, and 2% vanadium) laminations, however, have the advantage that they retain sufficient magnetization even for transmitter transducers. As this alloy is becoming more available, its use in laminated ring stacks is becoming more common, thereby solving the problem of the polarizing current in echo-repeater transducers.

Frequency Response

The ideal echo-repeater transducer has a very broad frequency response. In this respect crystal transducers are better than the magnetostrictive type. Most of the latter have a rather narrow frequency range, and with two such transducers in a repeater the overall response drops twice as rapidly as that of either alone. Because of the nature of this frequency response, any given echo repeater is limited in use to a relatively small range of frequency and its calibration of target strength versus frequency must be accurately determined.

Sensitivity Patterns

The horizontal pattern of most transducers used for echo repeaters usually has a satisfactory circular symmetry. The vertical pattern must be wide enough to intercept the signals of echo-ranging gear at reasonable ranges. For a stationary repeater operating at the depth of the gear on the ranging vessel, a vertical beam angle 3 db down at 10 degrees is adequate. If a towed target is used, the beam should be wider, 3 db down at 30 degrees, because of the roll and pitch of the target and because the target

may not maintain the desired orientation. The width of the vertical pattern is mainly a function of the height of the transducer, a height of about 1 wavelength being commonly used. There are two objections to making the vertical beam width too great: (1) increasing the width increases the maximum power output required in the amplifier; (2) the feedback from the transmitter to the receiver transducer increases as the beam is widened.

With the deep target, the Whale echo repeater, the transducer sections are so arranged and oriented that the direction of maximum radiation is vertical; however, considerable energy is radiated also in a horizontal direction.

Efficiency

Used in its normal sense as the ratio of output to input, the efficiency of the crystal transducers in the early echo repeaters varies from about 20 to 60 per cent depending on the frequency of operation. The first magnetostriction transducers used, of the B-19A, B-19B, and B-19F types, have a much lower efficiency, in general less than 1 per cent. Ring-stack transducers, however, range from 10 to 70 per cent in efficiency. These higher values result mainly from an improved magnetic circuit and a higher mechanical Q.

A low efficiency in a receiving transducer is not a serious handicap since it is relatively easy to provide sufficient amplification of the incoming signal. To compensate for the low efficiency of a transmitting transducer, however, the output of the power amplifier must be correspondingly increased, which is not so easily achieved. Because the efficiency of a transducer is a function of the operating frequency, it is necessary to calibrate an echo repeater over a range of frequencies, if accurate knowledge of its general performance is desired.

6.3 ELECTRONIC DESIGN CONSIDERATIONS

6.3.1 Calibration

An echo repeater may be calibrated in terms of its "equivalent sphere." By definition, the equivalent sphere of any target is a sphere which would reflect as much energy as the target itself. The size of the simulated sphere produced by an echo repeater for a given input signal is directly proportional to its output voltage. The gain or attenuation setting of the repeater amplifier may therefore be used to calculate comparative values of equivalent sphere radii. Since such settings are commonly scaled in decibels, a logarithmic unit of sphere size, the *target strength unit* [TSU] has been agreed upon. A sphere with a 6-ft radius has been arbitrarily assigned a rating of zero TSU; a sphere having a 22-ft radius correspondingly has a target strength of 11.3 TSU. The original specifications of echo repeaters required that they be capable of providing a target strength of 11.3 TSU within ±1 db.

6.3.2 Power Relations

The power incident on a sphere at a relatively large distance from a projector may be expressed by the relation:

$$P_s = \frac{P_p E r^2}{D R^2}$$

where P_s = power incident on the sphere,

P_p = power input into the projector,

E = efficiency of the projector,

r = radius of the sphere,

D = directivity index of the projector pattern, which is defined as the ratio of the average intensity of the pattern to its maximum intensity,

R = distance between the projector and the sphere.

Calculations for a typical QC projector with an electric input of 250 w, an efficiency of 10 per cent and a directivity index of 0.008 show that the power incident on a 22-ft sphere at a distance of 500 yd amounts to 0.672 w.

To simulate a perfectly reflecting sphere, the echo repeater receiving this power must reflect an equal quantity to the projector. The electric input into the repeater transducer necessary to emit a given amount of power is directly proportional to its directivity index and inversely proportional to its efficiency. For a typical ring-stack transducer, 1 wavelength long, with a directivity index of 0.5 and an efficiency of 30 per cent, the electric input for an acoustic output of 0.672 w is 1.12 w. These figures are given primarily to indicate the magnitude of the power requirements. Actual values vary considerably from one projector to another and from one repeater transducer to another.

The minimum power that a repeater can effectively amplify is dependent on its inherent noise level. A received signal must be from 5 to 10 db above the noise level in order to be distinguishable after it is amplified and returned to the echo-ranging equipment.

The maximum power that a repeater can emit is limited by the overloading of the amplifier. If the amplifier is overloaded, the repeater does not maintain the calibrated sphere size. For this reason the power requirement of a repeater amplifier varies inversely with the square of the closest operating range desired. To decrease the closest range from 500 to 100 yd requires that the maximum power of a repeater amplifier be increased by a factor of 25.

6.3.3 Amplifier Gain Requirement

The gain requirement of an echo-repeater amplifier depends mainly on the sensitivity of the receiving transducer and the efficiency of the transmitting transducer. The following example illustrates the order of magnitude of the values involved.

The sensitivity of a 60-kc transducer in a stick assembly enclosed in an oil chamber was found to be −117.5 db (vs 1 v) per dyne per sq cm. When 10 v (20-db level) were applied to the transmitting transducer, similarly mounted, a field of 58 db above 1 dyne per sq cm was obtained at 11 ft[a] from the transducer. To produce a field of 1 dyne per sq cm, the voltage level required would be 20 db − 58 db, or −38 db. The difference between −38 db and −117.5 db is 79.5 db, which is the amplifier gain needed by the repeater to simulate a 22-ft sphere. This value, corresponding to a voltage ratio of about 10,000, was checked by the calibration procedure and found to be correct within ±2 db.

6.3.4 Coupling Limitations

The gain which may be developed by an echo-repeater amplifier without producing oscillation through feedback is limited among other factors by the couplings between the input and the output systems. These couplings may be of three different kinds: acoustic, acoustic-mechanical, and electric.

Pure acoustic coupling is encountered when the sound field generated by the transmitting transducer is impressed on the receiving transducer either directly or by reflection. The pattern of the sound field depends among other things upon the length of the transducers. A ring stack with its axis vertical has a circular pattern in the horizontal plane. If the transducer is 1 wavelength in height, its pattern in the vertical plane is approximately that of a cosine function, the three-dimensional configuration resembling a toroid. If both the receiving and the transmitting transducers are of this type, it is evident that they must be separated the proper vertical distance. In practice, a spacing of 12 in. is adequate for reducing the acoustic feedback to a negligible value. Shorter spacing may be used with longer transducers at the expense, however, of loss of breadth of the horizontal beam.

With a properly mounted array of transducers, for which the direct acoustic coupling is negligible, there may still be coupling because of reflection from air bubbles or other foreign matter in the water, from the surface, the bottom, vessels, animal life, or anything else in the water, including temperature gradients. Whenever a target-towing boat approaches a large vessel, the repeater tends to oscillate. The same result follows when the target is towed through a wake, because of the air bubbles. When a repeater is used for purely tactical purposes, the amplifier gain is usually set just below the howl point, but with a calibrated equipment-testing repeater, there must be sufficient margin between the howl point and the operating point to insure negligible feedback.

Acoustic-mechanical coupling occurs when the vibration of the transmitting transducer is imparted to the receiving transducer through the structural member forming the transducer assembly. The coupling may be established by a too solid mechanical connection, or it may be transmitted from one transducer to the other through a path including the surrounding medium as well as structural supports. Since such coupling may cause oscillation at low volume settings, sections of acoustically insulating material should be placed between parts of the structural assembly of the transducers.

Electric coupling may be classified as electrostatic or magnetic. No definite evidence concerning the presence of electrostatic coupling was obtained during development of the HUSL echo repeaters. Magnetic coupling, however, proved to be a limiting factor in the case of some repeaters using deck elec-

[a] The distance of 11 ft is used because, according to the calibration theory, the comparison calibration value determined at that distance is the gain setting required to produce an equivalent sphere having a radius of 22 ft.

tronic systems. Magnetic coupling occurs whenever the current-carrying conductors of the input and the output circuits are in close proximity. With ring-stack transducers of average efficiency and sensitivity there is a difference in level of approximately 80 db between the receiving and the transmitting pairs of conductors. To reduce the mechanical strain on the electric cables it is necessary to fasten them at intervals to the towing cable, thus bringing them close together. For conductors consisting of simple twisted pairs, the magnetic coupling is almost certain to be excessive. By using four or six wire cables with alternate conductors connected together, the coupling between the conductors is greatly reduced. Even in this case, however, some interaction is encountered unless the conductors are arranged circumferentially around a central nonconducting core. With four wire conductors connected and arranged as described, successful performance may be achieved for cable lengths up to 250 ft. If greater cable lengths are desired, it is advisable to install the amplifier in the transducer housing and use one multiconductor cable to provide power and gain control.

6.3.5 Frequency Response and Stability

Experiments show that when a transducer with a flat frequency response is towed through water, the noise level in the system is relatively high at the normal gain setting of the repeater amplifier. To reduce this noise a filter is usually installed in the amplifier circuit. Because efficient transmitting transducers generally have a rather narrow frequency response, the overall response of the repeater is further limited by the transducer characteristics. If the receiving transducer also has a sharp frequency response, the noise-limiting filter may be dispensed with. The frequency response of the amplifier should be as flat as possible over the operating range of the repeater. In general, the amplifier response is limited near the upper and lower frequency limits by the characteristics of the transformers used, especially those of the output transformer. With a sharply tuned system, the frequency response must be accurately known and the oscillator circuit properly calibrated. The incoming signal, furthermore, should be monitored during operation to make certain that operation is proceeding within the effective frequency range of the repeater.

The amplifier system should also be designed so that its gain is as independent as possible of changes in temperature, line voltage, etc. In most repeater circuits considerable negative feedback is used, and with voltage-regulated power supplies for all stages except the power stage, the effects of reasonable line voltage variations are reduced to a negligible value. On a small target vessel, however, there is often difficulty in keeping the line voltage variation below 20 per cent, and even with battery-operated systems it is necessary to consider the drop in voltage as the batteries begin to run down.

6.3.6 Monitor Service

In the operation of an echo repeater, it is usually desirable to have some means of monitoring the signals. If the system has enough amplification to produce self-oscillation at high gain, the howl-point setting serves as a simple check of performance. If the anticipated howl does not occur, lack of the proper functioning of the transducers or the amplifier is indicated. If the system oscillates at an abnormally low gain setting, undesirable feedback is being introduced at some point in the system.

A monitor is useful not only in indicating whether or not the system is functioning properly but also in serving to measure the relative strength and the frequency of the incoming signals. The monitor circuit includes a monitoring amplifier, a frequency converter, and a loudspeaker. It is connected to the repeater circuit by putting a high-impedance voltage divider across the low-impedance output circuit of the power amplifier. With a fixed gain setting of the monitor amplifier, the repeater operator can judge the intensity of the incoming signals by the sound issuing from the loudspeaker. By feeding in a signal from a local calibrated oscillator, the frequency of the signal may be determined.

Another method of monitoring the repeater system consists of using an oscilloscope. From the size of the vertical deflections on the oscilloscope screen it is possible to estimate the amplitude of the signals. The waveform and the frequency of the signals may also be studied when an oscilloscope is used.

If the power output stage of the repeater amplifier is of class B, AB, or C, the plate current in the output may be used as an indication of signal level. The readings of a meter registering this current also indicate whether self-oscillation is occurring. The relationship between current and signal strength is not linear, however, and the indications for weak signals are not reliable.

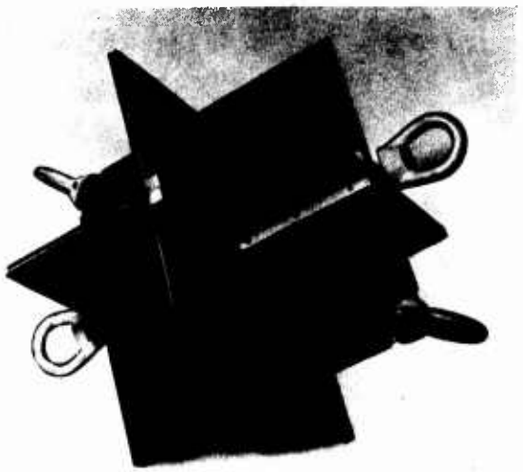

FIGURE 3. Multisection triplane target.

6.3.7 Location of Electronic Units

When a stationary repeater is being used in relatively shallow water, deck electronic units are the simplest solution. In the case of a repeater towed at a depth of 1,000 ft, body electronic units are a necessity. For repeaters towed at depths of from 50 to 100 ft, a choice may be made between deck and body units. In the following paragraphs the relative merits of some of the features of both systems are discussed.

The disadvantage of deck electronic units is that long electric cables are required; about 200 ft of cable are necessary for a towing depth of 100 ft. To make connections to the deck unit two separate cables are generally used since it is not desirable to place the output and the input conductors within the same cable when there is a large difference in level between them. There is sufficient capacity between the cable conductors so that they cannot be used satisfactorily with a high-impedance amplifier; for best operation the amplifier impedance should be matched to the characteristic impedance of the lines. The line losses in long electric cables must be considered, although to date they have not presented any serious limitation. Trouble may also be encountered by the breaking of the cables. This, however, can be avoided if the cables are secured to the towing cable every few feet.

By locating the amplifier and batteries within the transducer assembly, the cable difficulties are completely eliminated. The batteries, however, must be recharged or replaced after every run; and, of course, no control of the repeater-amplifier circuit is available during a run.

An intermediate solution is to place the amplifier unit within the transducer housing and to use a single multiconductor cable to feed power to the various amplifier components. By adding one additional conductor to the cable, some gain control may be made available on the towing vessel by means of a potentiometer circuit.

The chief advantages of deck electronic units are the possibilities of remote gain control and monitoring. Remote gain control is not extremely important in the case of a calibrated repeater operating at a known frequency. The monitoring function is the more important advantage. By means of the monitor it is possible to be certain of the proper operation of the repeater. With sharply resonant transducers and filters, it becomes particularly important for checking operating frequency and amplifier gain.

In the case of a repeater using body electronics and only a power cable, it is still possible to effect some monitoring of the repeater. This can be achieved by inserting chokes in the d-c power line and imposing some of the output voltage of the amplifier on these lines. The a-c voltage reaching the upper end of the cable may then be amplified to operate a loudspeaker or an oscilloscope. Because of the current drawn by the tubes during the peaks of the cycles, the response of the monitor may not be linear with respect to the output of the repeater. This difficulty can be circumvented, however, by calibrating the monitor system. Frequency monitoring is also feasible with this method.

6.4 PASSIVE TARGETS AND ECHO REPEATERS

6.4.1 Passive Targets

MULTISECTION TRIPLANE

The successful triplane model of passive target is illustrated by the photograph of Figure 3. This target consists of steel plates 1/8 in. thick assembled as shown, the overall length of any edge being 12 in. The plates are covered on both sides by a 1/8-in. thickness of bubble rubber. Towing rings are provided so that the target may be towed with either of two orientations of the planes. The reflection sensitivity pattern of the multisection triplane varies

FIGURE 4. Hollow sphere target.

somewhat with direction both horizontally and vertically. The average value of the equivalent sphere diameter is approximately 3 ft.

Figure 4 is a photograph of the hollow steel sphere, 3 ft in diameter, which is also found to function satisfactorily as a small passive target. It is made of two hemispherical shells attached to each other by welded joints at the ends of two perpendicular diameters. Each shell encloses an airtight space, the purpose of which is to provide desirable reflection properties. A space between the two shells allows the inner volume to fill with water on submergence. The reflection pattern of the sphere is, of course, more uniform than that of the triplane, for which reason the former is preferred when accurate data in extended tests are required. A target sphere of 3-ft diameter is of particular interest since it approximates a sea mine in size and reflection properties. Neither the triplane nor the sphere is easily towable so that their use is generally restricted to stationary observations.

FIGURE 5. Towed submerged antisubmarine practice target, Model SR-2.

PERFORMANCE OF PASSIVE TARGETS

Both the triplane and the sphere have served successfully as stationary targets at various testing stations for numerous echo-ranging equipments. Besides their simplicity and ease of maintenance, passive targets also have the advantage of unlimited range of power output. In other words, they do not become overloaded (and therefore less effective in terms of target size at short ranges or high transmitting powers).

6.4.2 San Diego Echo Repeaters

Various echo repeaters designed primarily as practice targets for use in the training of sonar operations and attack teams were successfully developed by the San Diego Laboratory at an early date. Among these are the RR-1, for suspension from a towed raft; the KR-1, for keel mounting; the BR-1, for use in a stationary buoy; and the towed models, SR-2 and SR-5. Each of these uses x-cut Rochelle salt crystal transducers and one of the several 16- to 26-kc amplifiers designed at San Diego. Gains ranging from 90 to 114 db and power outputs as high as 9 w are obtainable with these repeaters.

Figure 5 shows the exterior appearance of the SR-2, and Figure 6 is the circuit diagram of its amplifier. This model is designed for operation at depths between 60 and 90 ft when towed at the end of a 1,200-ft cable. It is of particular interest here because it was the prototype for the first of the Harvard repeaters, the Fecho.

Satisfactory results have been obtained from these repeaters when used in Pacific waters. They are classified as personnel-training devices, however.[b] The remainder of this chapter is devoted almost exclusively to the equipment-testing type of echo repeater which received most of its development at Harvard.

6.4.3 Early Harvard Repeaters

FECHO

First Circuit. Figure 7 is a photograph of the transducer assembly of Fecho, the first echo repeater

[b] For a full description of echo repeaters designed for training application, the reader is referred to Division 6, Volume 4, Chapter 6.

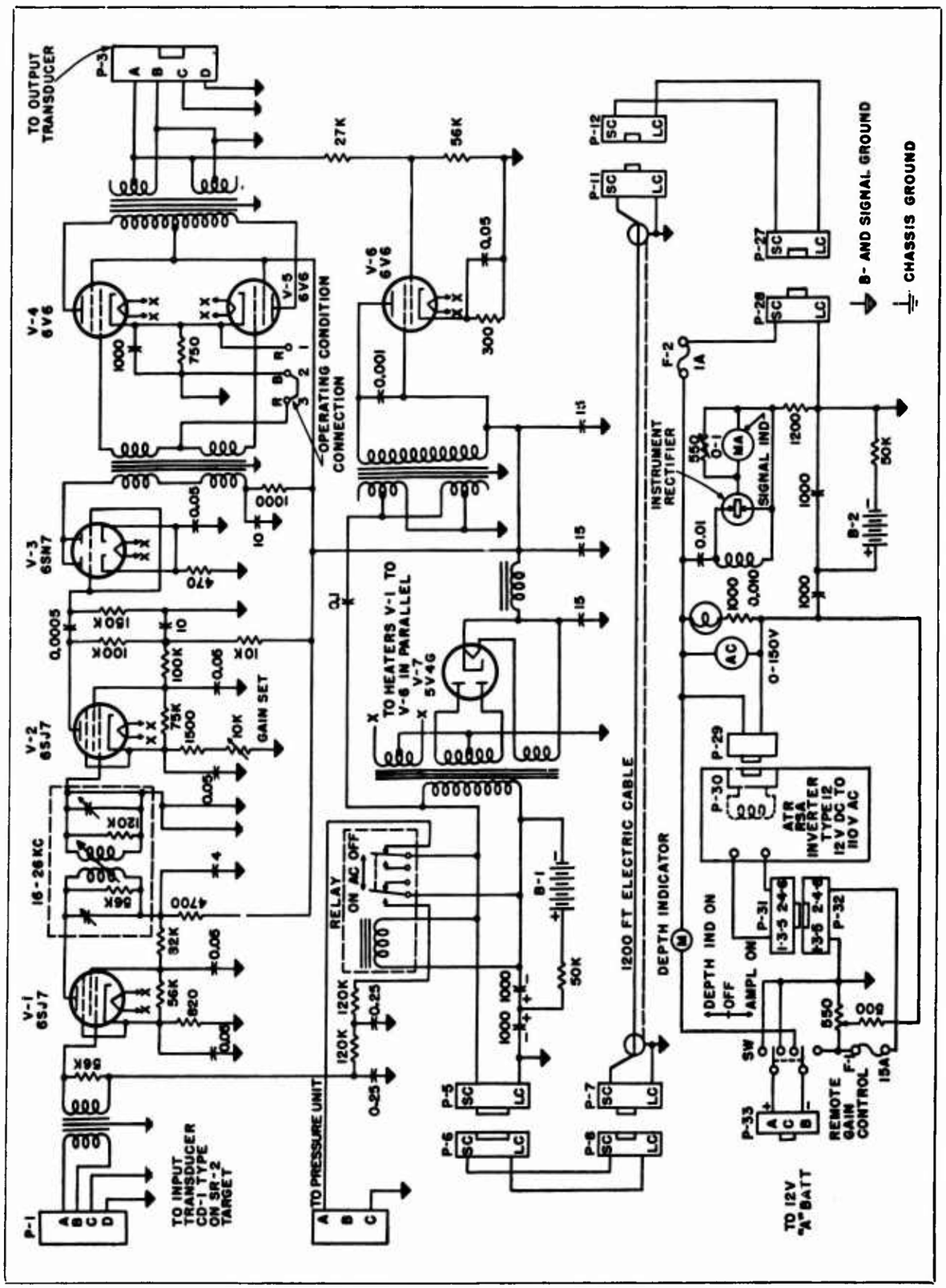

FIGURE 6. Schematic diagram of UAB amplifier for SR-2.

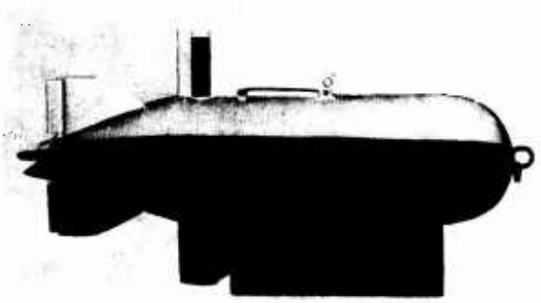

FIGURE 7. Fecho repeater transducer assembly.

assembled at Harvard. The overall length of the torpedo-shaped body is approximately 6 ft, the diameter about 18 in. Sufficient air spaces are provided so that the body is slightly buoyant and preset fins cause it to submerge when towed.

Two x-cut Rochelle salt crystal transducers, each with an area of 1x8 in., are mounted on the top and the bottom respectively, the upper one being used as a receiver, the lower as a transmitter. The former has its crystals connected in series-parallel, the latter all in parallel. The pattern of transducers of this type is broad in a horizontal plane, having circular symmetry within 6 db. Because of the 8-in. length of the crystals the vertical pattern is relatively much sharper.

The connections between the two transducers and the amplifier chassis on board the towing vessel are made by a pair of two-conductor shielded cables. Figure 8 is the schematic diagram of the modified San Diego type S-5 amplifier circuit which was used. The purpose of the modifications was to increase the gain of the amplifier and improve its tuning for operation at 14 kc.

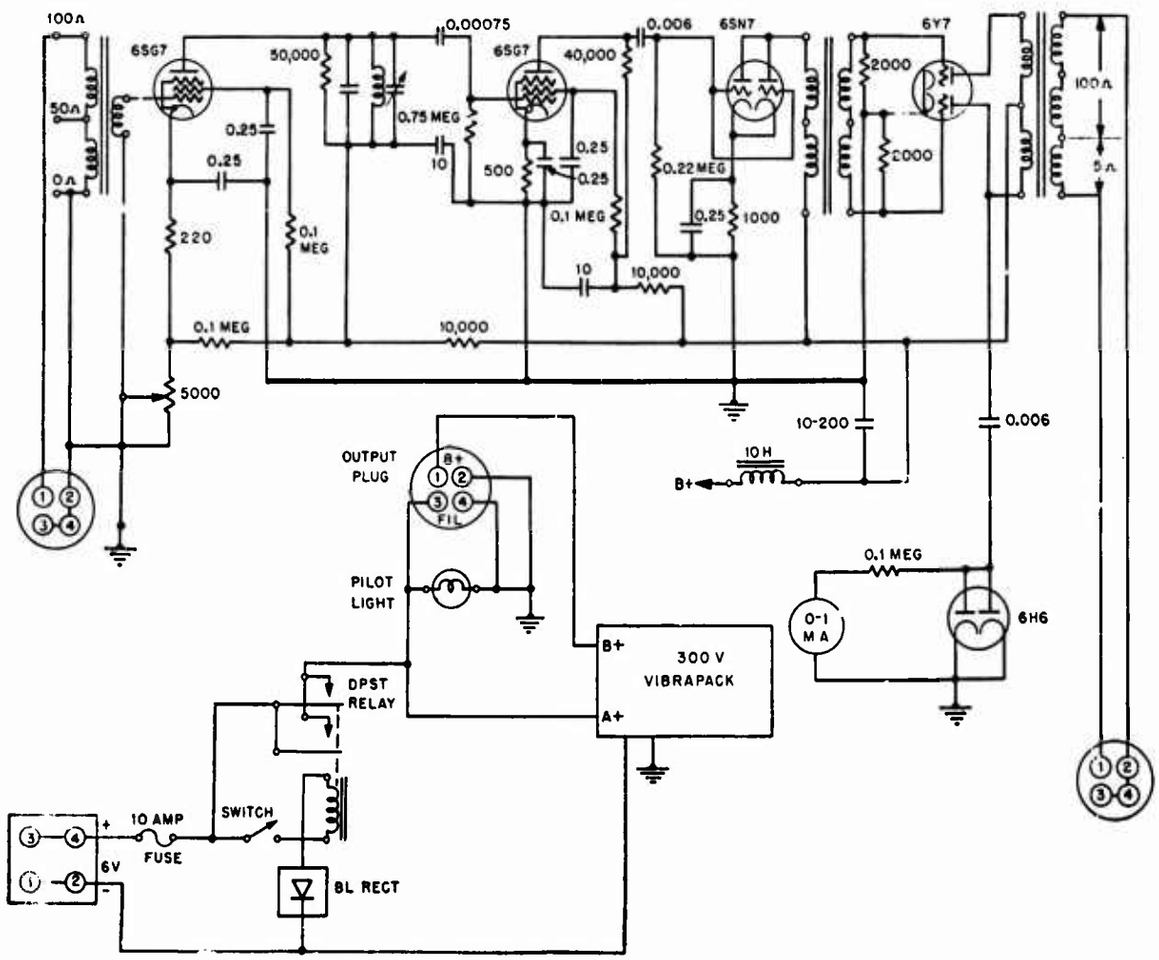

FIGURE 8. Schematic diagram of San Diego amplifier for Fecho repeater.

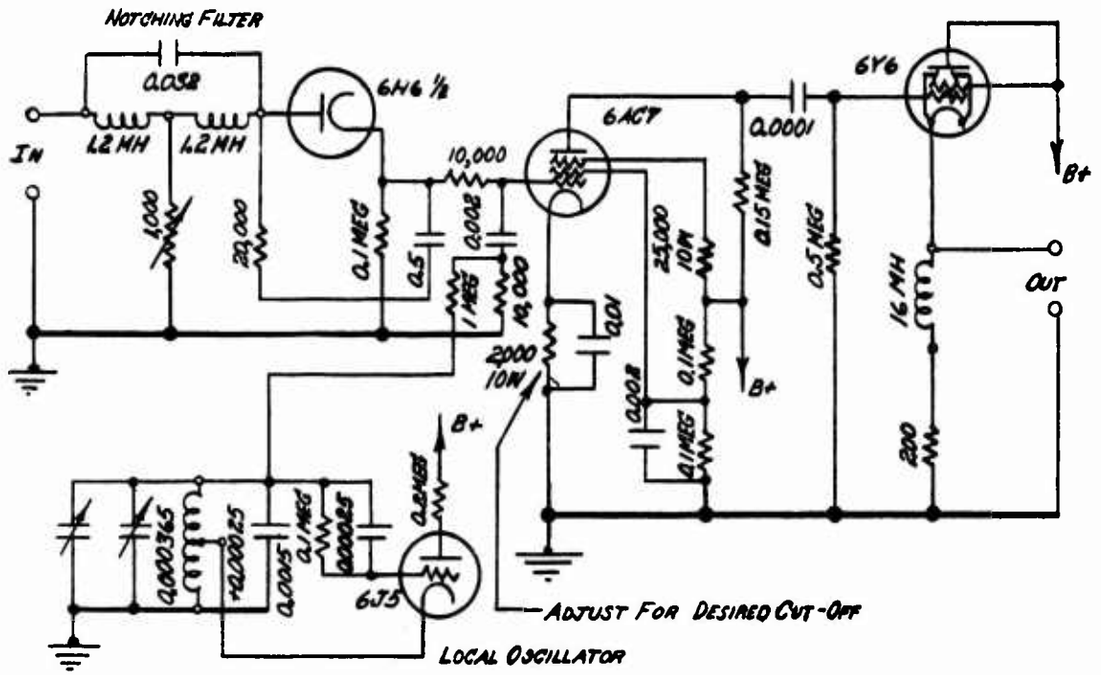

FIGURE 9. Schematic diagram of Fecho doppler circuit.

Fecho Doppler Circuit. The performance of the Fecho repeater with the first HUSL amplifier circuit was not satisfactory. In general, only weak echoes, barely distinguishable amidst the reverberation, were obtained. In order to provide unmistakable signals, separable from reverberation and undesired reflections, a circuit was devised to dopplerize the echo signals. Advantage was taken of the broad resonance of the projector of the equipment under test and the narrow response of the receiving transducer. The projector is adjusted to ping at a frequency 500 c below the peak of the sonar amplifier response. The echo repeater is modified by equipping it with an output oscillator tuned to the amplifier peak frequency. This oscillator is amplitude-modulated in accordance with the strength of the lower frequency signal picked up by the receiving transducer of the echo repeater. A sharply tuned notching filter is located in the input circuit of the repeater to attenuate signals of the low incoming frequency and render both acoustic and electric feedback ineffective, making possible a high level output without howl. Figure 9 is the schematic diagram of the amplifier circuit by means of which the artificial doppler is produced.

Fecho Performance. The chief liability of the Fecho repeater is its large size and weight which make it extremely unwieldy and difficult to handle when being put into the water or taken out. For this reason a smaller, lighter body, known as Smecho (Figure 1) was designed soon after a few tests had indicated the clumsiness of the Fecho model.

Smecho Models

Four different Smecho models were constructed and subjected to testing. Their hydrodynamic performance was relatively poor and their repeater characteristics were unsatisfactory. At the time of the tests on Smecho 4, a reorganization of the research in echo repeater development was effected and a new series of experiments undertaken. During the period of Smecho investigations, however, a separate project of a buoy-supported echo repeater, known as Oscar, had been completed. This model is therefore described first, before the later repeater developments are discussed.

6.4.4 Buoy-Supported Echo Repeater, Oscar

Description of Oscar

The buoy-supported echo repeater, Oscar, was designed specifically for testing echo-ranging systems installed on the *Aide de Camp*, a 110-ft diesel yacht

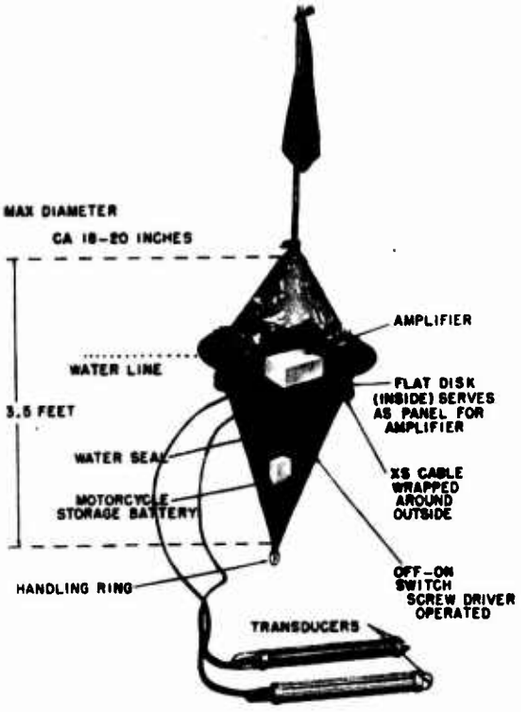

FIGURE 10. Buoy-supported echo repeater, Oscar.

operated by Harvard. The general arrangement of the repeater assembly in its relation to the buoy is shown by the photograph of Figure 10. The flag at the top facilitated locating the buoy, since the buoy structure was visible only a short distance.

The transducers used by the repeater are hung independently from opposite sides of the buoy, separated by a vertical distance of about 15 ft with the upper transducer approximately 30 ft below the surface of the water. The type B-19F tubular magnetostriction hydrophones (see Division 6, Volume 13) are 15 in. long. The transducer cables are fastened permanently to the buoy structure and connected to the amplifier unit by plugs.

The amplifier unit is located in the upper section of the buoy above the water level. The circuit for the amplifier unit, given by Figure 11, is designed to operate over a frequency range of from 21.5 to 24.5 kc. A filter with a frequency response about 3 kc wide lies between the 6SG7 stage and the first half of the 6SL7 tube. The second half of the 6SL7 tube forms a cathode follower feeding into the 6V6GT power tube. The power supply consists of a Vibrapack connected to a motorcycle-type storage battery.

Performance of Oscar

The Oscar echo repeater performed satisfactorily the function for which it was designed. A sufficient number of echoes were usually returned to make possible the desired checks on the operation of sonar equipment. The intensity of the echoes was great

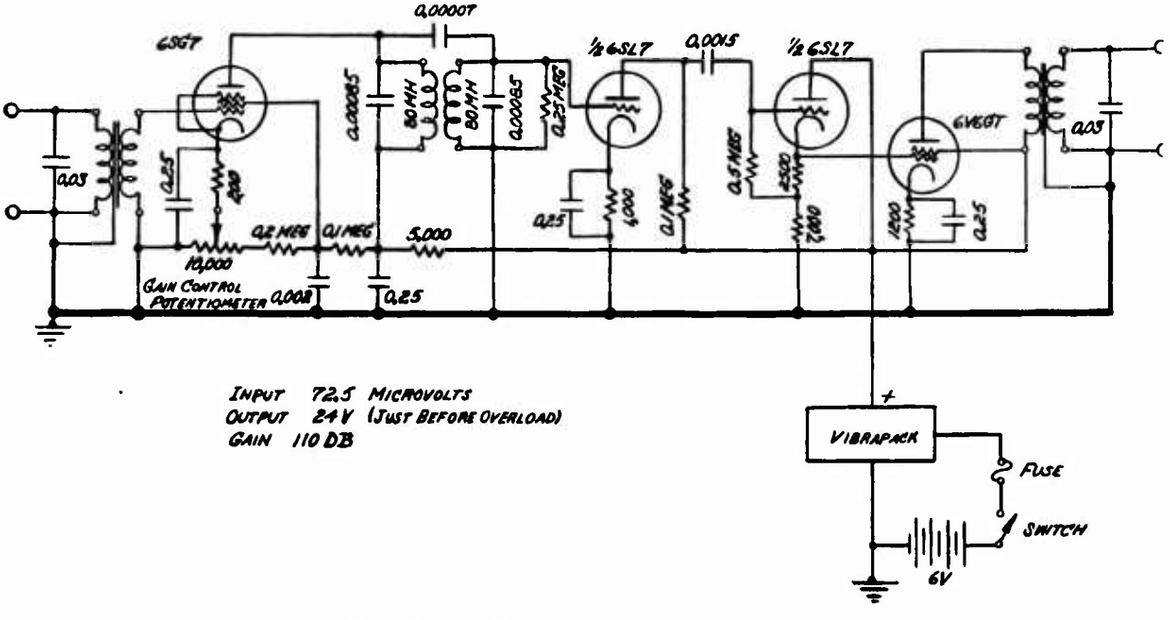

FIGURE 11. Amplifier circuit of Oscar echo repeater.

enough so that lack of control of the gain of the amplifier during operation did not prove a serious handicap.

6.4.5 Stationary Repeaters with Ring-Stack Transducers

DESCRIPTION

Because of the unsatisfactory results obtained with the Smecho models, a fresh attack was made on the repeater project by starting with simpler, nontowable or stationary transducer assemblies. In some cases two transducers were simply suspended in the water overside, separated a few feet vertically. More commonly, however, they were attached to a short length of pipe, one at each end, so that their relative orientation would remain fixed. This manner of mounting the transducers became known as a "pipe" or "stick" assembly, the arrangement of which is indicated by the sketch of Figure 12.

At this time ring-stack transducers became available. These consist of stacks of nickel laminations of a circular form. Mainly because of the improved magnetic circuit inherent in their design, the efficiency of these transducers is approximately 100 times that of the B-19A and B-19B transducers. By using a ring stack for the transmitting transducer, the output of an echo repeater may therefore be considerably increased. The constructional details of a 5-in. 20-kc ring stack are shown in the sketch of Figure 13.

Figure 14 is the schematic diagram of the amplifier unit designed for a repeater using a B-19B hydrophone as receiving transducer and a 5-in. ring-stack hydrophone as transmitting transducer. A filter, slightly overcoupled to provide a band pass in the region of 20 kc, feeds the 6SN7 push-pull driver stage. The maximum gain of the amplifier is about 120 db and the maximum output into 125 ohms about 18 w. The noise output is 15 db above 1 mv with the input terminals shorted and the gain set at its maximum. This considerable random noise is traceable largely to the Vibrapack. The peak values of noise are sufficient to prevent the use of a peak voltmeter at the output terminals.

PERFORMANCE

In order to determine the feedback or coupling limitations of this repeater, tests were made by varying the distance between the receiving and the transmitting transducers. No change in performance was observed as the separation distance was increased beyond 1 ft. Below 1 ft, however, the gain had to be decreased to prevent howling. Neither the insertion of a flexible coupling in the pipe connecting the transducers nor the installation of acoustically insulating baffles affected the maximum possible gain. These observations confirm conclusions reached at the San Diego Laboratory concerning similar hydrophones.

After this checkup the repeater was operated in

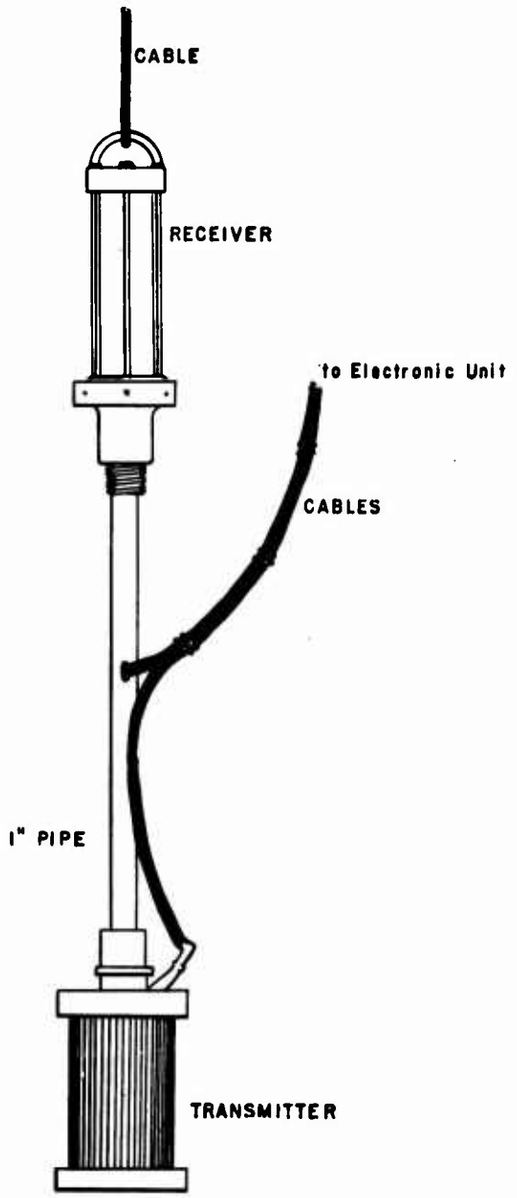

FIGURE 12. Stationary-type transducer assembly (20 kc).

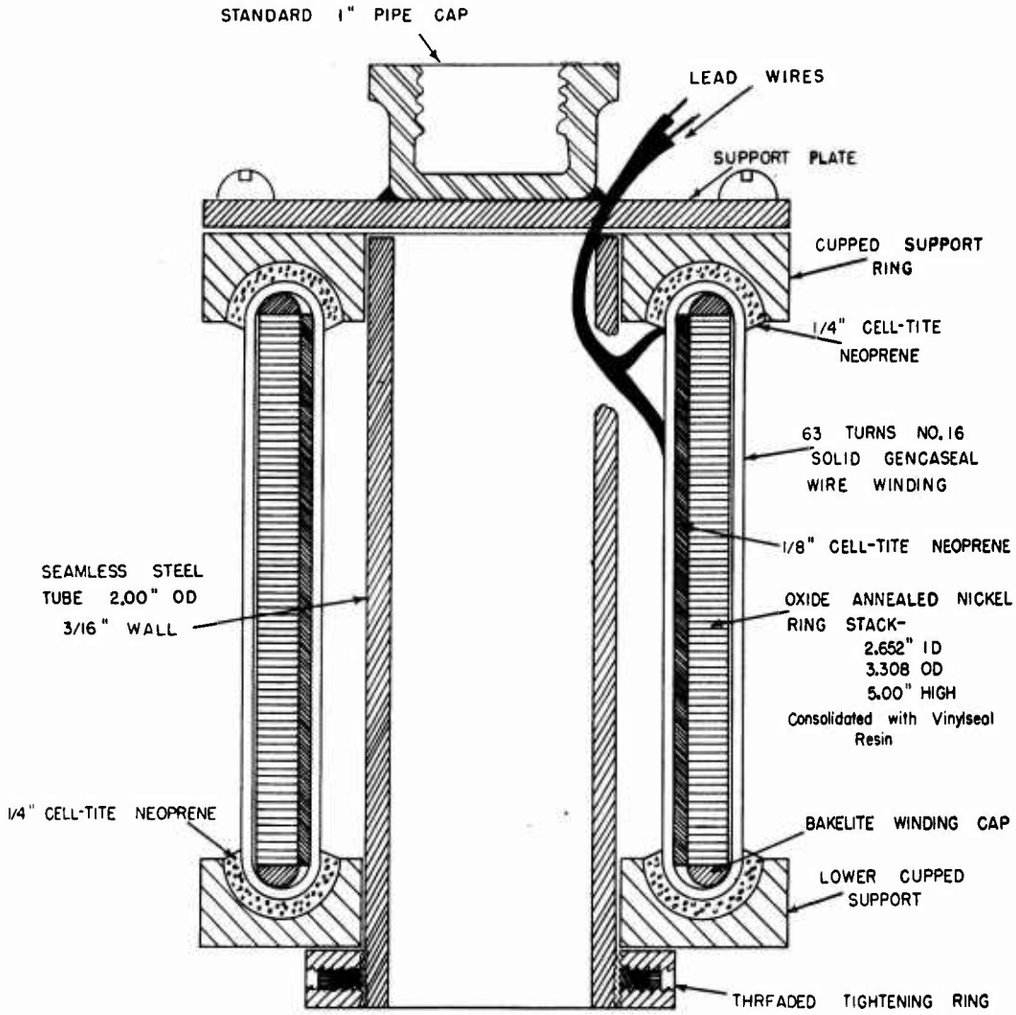

FIGURE 13. Constructional details of 5 m. ring-stack transducer.

tests of QC sonar equipment. During these trials the repeater functioned much more satisfactorily than the Smecho repeaters had. No difficulty was experienced in detecting a large number of intense echoes. Only occasionally did the repeater go into oscillation, and good echoes were returned at the close range of 300 yd. By applying frequency modulation to the ping of the QC gear, distinguishable echoes were obtained even at 75 yd.

6.4.6 Towable Echo Repeaters with Rack Amplifiers

DESCRIPTION

After the successful performance of the combination of the B-19B and the ring-stack transducers as a stationary repeater, they were tried on a Smecho body. To eliminate the noise generated by the passage of the transducers through the water, they were enclosed in streamlined housings of thin sheet steel mounted on a suitable structure. Because of reflections produced by the housing, however, the sensitivity pattern of the hydrophones was seriously distorted. The streamlining was therefore abandoned and Smecho 1 was equipped with a B-19B hydrophone and a 5-in. ring-stack transducer without any housing.

At this time there was also developed a new amplifier unit, consisting of six different sections which are assembled in a rack. The top section contains the monitor loudspeaker and a voltage regulator. On the second panel are mounted the polarizing

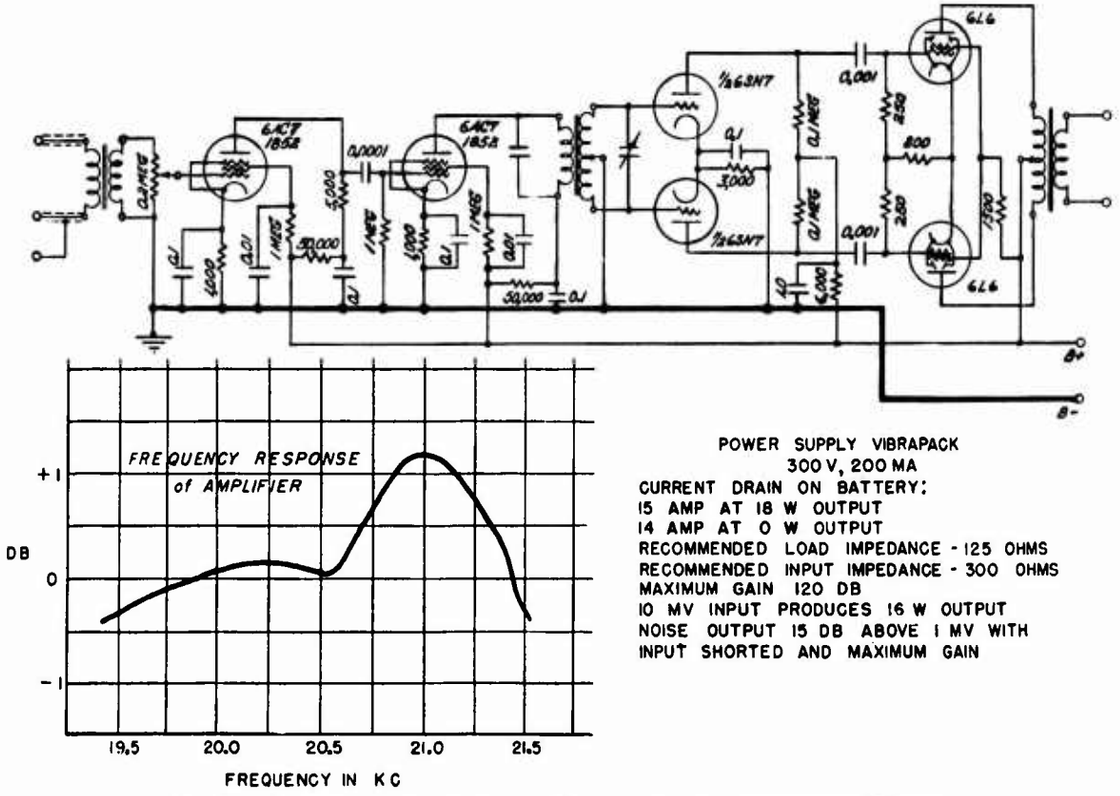

FIGURE 14. Amplifier circuit and frequency response for echo repeater of "stick" type.

current control and ammeter. The third section contains the listening monitor circuit; the fourth, the power amplifier; and the fifth, the voltage amplifier. In the sixth section of the rack, a battery-charging unit is mounted, the batteries themselves being located in the space below the rack. Figure 15 is a view of the rack as installed on the *Juldi-Walla*.

The schematic diagrams of the power amplifier used in the rack are given in Figure 16. The filter shown connected to the input is designed to have a resistance independent of frequency. Negative feedback is utilized to stabilize gain and to reduce distortion, and voltage regulator tubes are included in the power supply for the 6L6 screen voltages. The operating frequency was usually near 20 or 60 kc.

PERFORMANCE

The performance of Smecho[1] (see Figure 1), equipped with a B-19B receiving hydrophone and a 5-in. ring-stack transmitter, was satisfactory in connection with the rack amplifier system just described. For a period of over a year it was successfully used for tests of QC equipment. By means of the echo repeater calibrator a number of calibration tests were made. On the average it was found that the echo repeater could be made to simulate a sphere 44 ft in diameter with the gain set 10 db below the howl point.

6.4.7 High-Frequency Stick Assemblies

DESCRIPTION

The success of the nontowable echo repeaters utilizing the stick assembly of transducers led to the development of a towable 60-kc assembly of similar type. The sketch of Figure 17 shows the essential parts of the internal structure. Two laminated ring stacks are used for the transducers, a 1-in. hard nickel stack as the receiving and a 2-in. soft nickel stack as the transmitting hydrophone. Each has a mean diameter of 1 in. The transducers are contained within two separate chambers filled with castor oil. These chambers are acoustically and electrically insulated from each other to minimize any coupling action between the transducers inside the assembly. A central tube passing through the entire assembly serves as a conduit for the electric cables. The mechanical arrangement is designed to make

FIGURE 15. Rack amplifier on *Juldi-Walla*.

it possible to disassemble the repeater for repairs or replacements without difficulty. In use a steel towing cable is attached to one end of the transducer assembly, the other end of which is fastened to a depressor, designed and constructed by the San Diego Laboratory (see Figure 18).

PERFORMANCE

Several models of the 60-kc echo repeater were constructed before the successful design illustrated by Figure 17 was achieved. In the development of the transducer assembly a series of difficulties extending over a period of several months was encountered. The early calibration measurements, which were made near a pier, sometimes showed variations in equivalent sphere size over a range of 20 to 1. At times this behavior was seemingly correlated with tide effects on the turbulence and the trapped air in the water near docks. It is highly probable also that interference from reflecting surfaces was a contributing factor, since better results were obtained in deep water.

Further difficulties in obtaining consistent calibrations were traced to improper design in the transducer assembly of the echo repeater. In the first models both transducers were located within a single oil chamber. The operation in these cases was found to be seriously limited by magnetic and acoustic coupling within the transducer assembly. Some feedback was also traced to magnetic coupling between the cables leading to the transducers. Investigation of these difficulties was complicated by the multitude of variables involved, such as the length of the cables, the polarity of the connections, and the presence of balancing and filtering sections in the circuits. Eventually, however, the 60-kc repeater was so improved that its variability and erratic behavior were eliminated and consistent calibrations were obtained whenever they were made in undisturbed water. The performance of the repeater at the Florida Field Station has been satisfactory in regard both to consistency in calibration results and to its use as a target for echo-ranging gear. With 90 ft of cable the transducer-depressor combination tows at a depth of about 75 ft.

6.4.8 Artificial Doppler Circuits

As soon as the first echo repeater had been assembled at HUSL, it was realized that it would be advantageous to be able to impart a doppler shift to the repeater signal. In many cases a dopplerized echo is more easily recognized than one without doppler. Moreover, in the development of doppler utilization devices for sonar equipment, a doppler signal is necessary for testing purposes. For these reasons a number of artificial doppler circuits were designed and incorporated into the HUSL echo repeaters of both the towable and nontowable types.

The artificial doppler circuit of the Fecho repeater has already been described (see Figure 9). During the later development of repeaters three other dopplerizing circuits were constructed.[3]

HETERODYNE DOPPLER-SHIFTING CIRCUIT

A block diagram of the first of these, designed for a 60-kc repeater and known as a heterodyne shifting circuit, is given by Figure 19. This circuit contains two local oscillators, one of which operates at a fixed frequency of 80 kc. Part of its output is mixed with

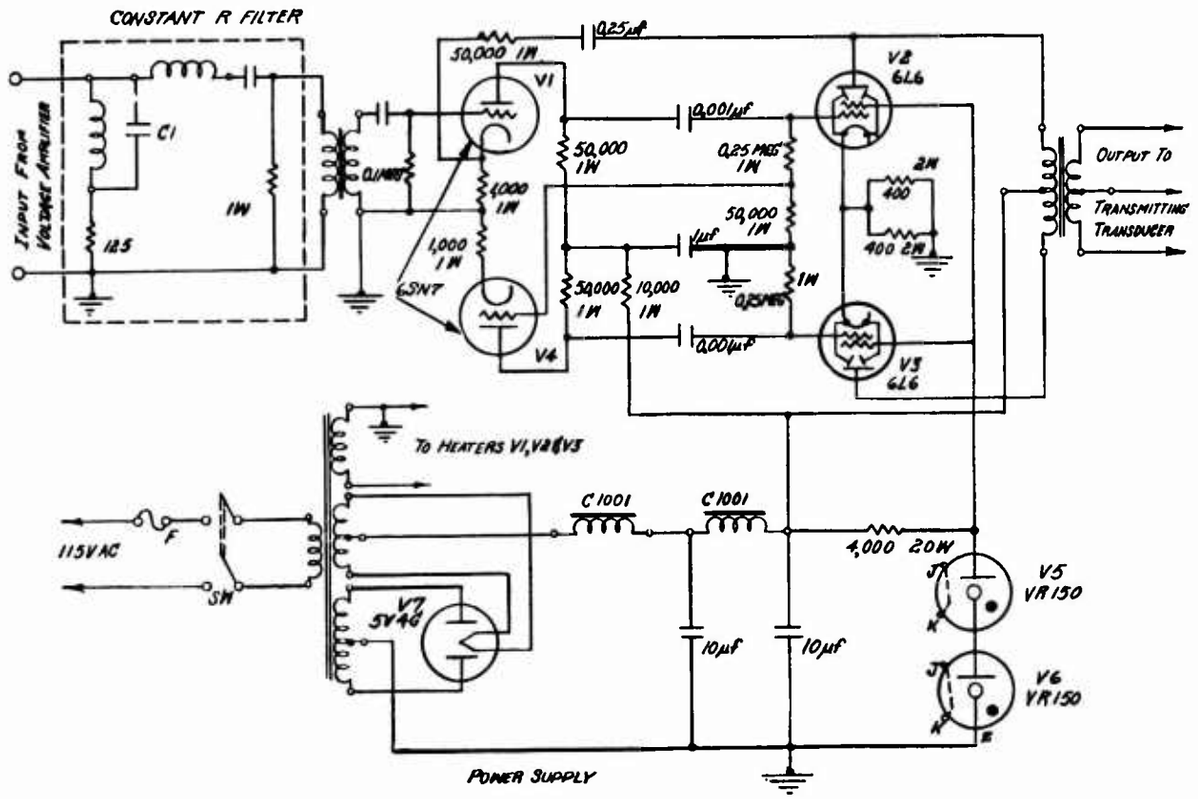

FIGURE 16. Circuit of power amplifier in rack amplifier.

the incoming 60-kc signal to produce an intermediate frequency of 20 kc. The other local oscillator operates at a frequency of 80 kc plus or minus the desired doppler shift to be applied to the outgoing signal. A second mixer tube fed by the two local oscillators is connected to a tuned discriminator circuit which controls the frequency of the doppler-shifting oscillator by means of a reactance tube. The output of this oscillator is also fed to a third mixing tube in which the intermediate frequency is combined with the doppler-shifted frequency. A polarity reversing switch and different discriminator connections make it possible to provide signals with either up or down dopplers ranging from 2 to 5 knots.

Figure 20 is the schematic diagram of a similar circuit developed for the 60-kc echo repeater used at the Florida Field Station. This dopplerizing circuit is connected to the echo repeater between the

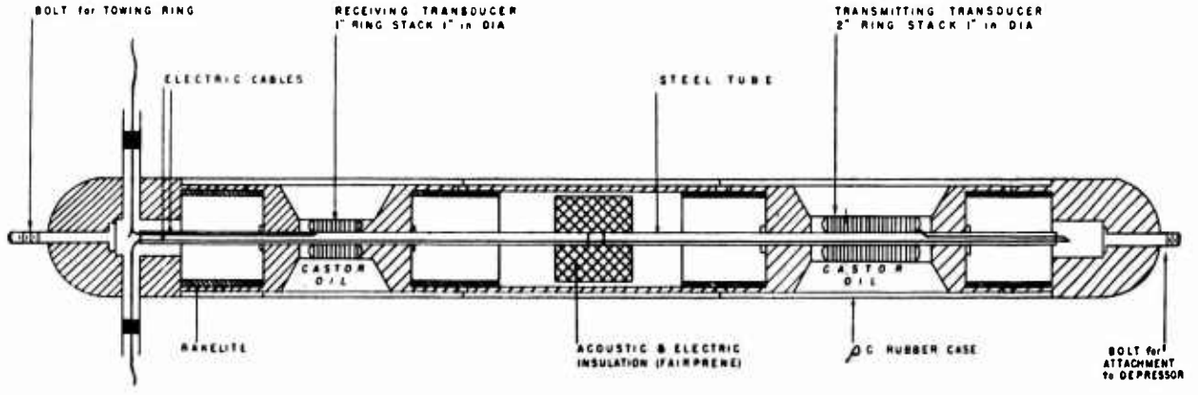

FIGURE 17. Essential parts of 60-kc transducer assembly.

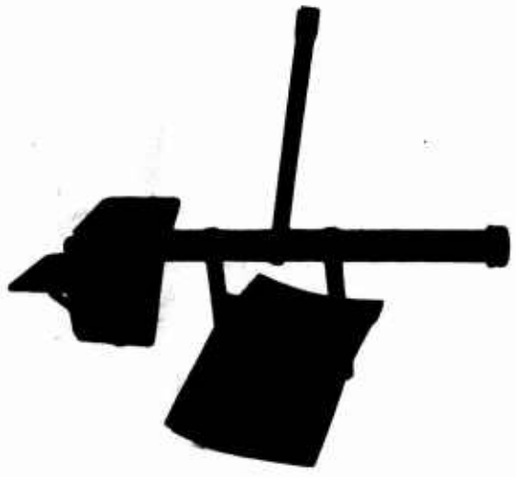

FIGURE 18. Depressor for submerging towed echo repeater.

output of the voltage amplifier and the input of the 60-kc filter. A switch is provided to permit the doppler circuit to be connected in or out of the repeater circuit. An intermediate frequency of 160 kc is used instead of 80 kc as in the block diagram of Figure 19. The local oscillators operate at frequencies of 100 kc and 100 kc $\pm\triangle f$ respectively. The possible doppler shifts, up or down, range from ½ to 10 knots as indicated. A discriminator output meter is connected across the grid of the reactance tube and so provides a measure of the doppler shift developed in the circuit. The zero beat indicator consists of a 6E5 tube by means of which the two local oscillators may be checked against each other. In use the large frequency-shift dial is set to correspond to the position of the discriminator control knob. When the circuit is properly adjusted, the desired doppler shift introduced is maintained within narrow limits without attenuation. Satisfactory operation has been obtained both with the foregoing circuit and with the modifications of it designed for use with 20- and 26-kc echo repeaters.

BALANCED MODULATOR DOPPLER SHIFTER

A second scheme devised to obtain a dopplerized signal from a stationary echo repeater is illustrated by the block diagram of Figure 21. As indicated in the figure, the signal and the output of a local oscillator are applied to phasing circuits which produce four voltages of equal amplitudes but in quadrature relationship for each of the two input voltages. The output voltages of the inverters (see Figure 22) are applied in double push-pull to the grids of four remote cutoff pentodes, the cosine components to one pair, the sine components to the other. The plates of these tubes are connected in parallel to a low-resistance common plate load. The gain of alternate push-pull pairs is equalized by adjustable screen resistors and the common bias point is chosen so that the mutual conductance of the push-pull pairs is a linear function of the grid voltage with the bias voltage as origin, that is, square law operation results. By reversing the leads from the oscillator phase shifter, the output of the circuit is changed from up doppler to down doppler or vice versa. Circuit constants are chosen so that doppler shifts ranging from 10 to 1,000 c may be obtained.

In its final form, a chassis incorporating the above circuit was found to operate fairly satisfactorily after having been allowed to warm up for 10 min before adjustments were made. Because it was found to require frequent checking, however, and because the simpler heterodyne shifter was made available, the balanced modulator circuit has not been used for repeater service.

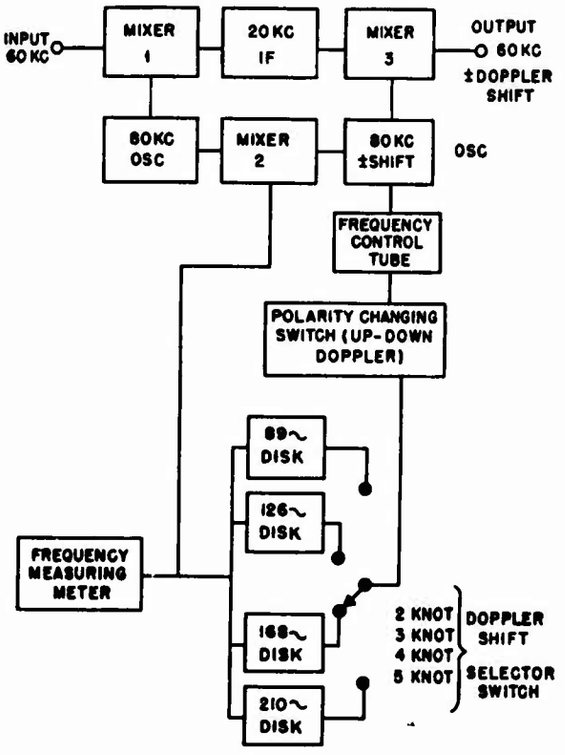

FIGURE 19. Block diagram of heterodyne shifter doppler circuit.

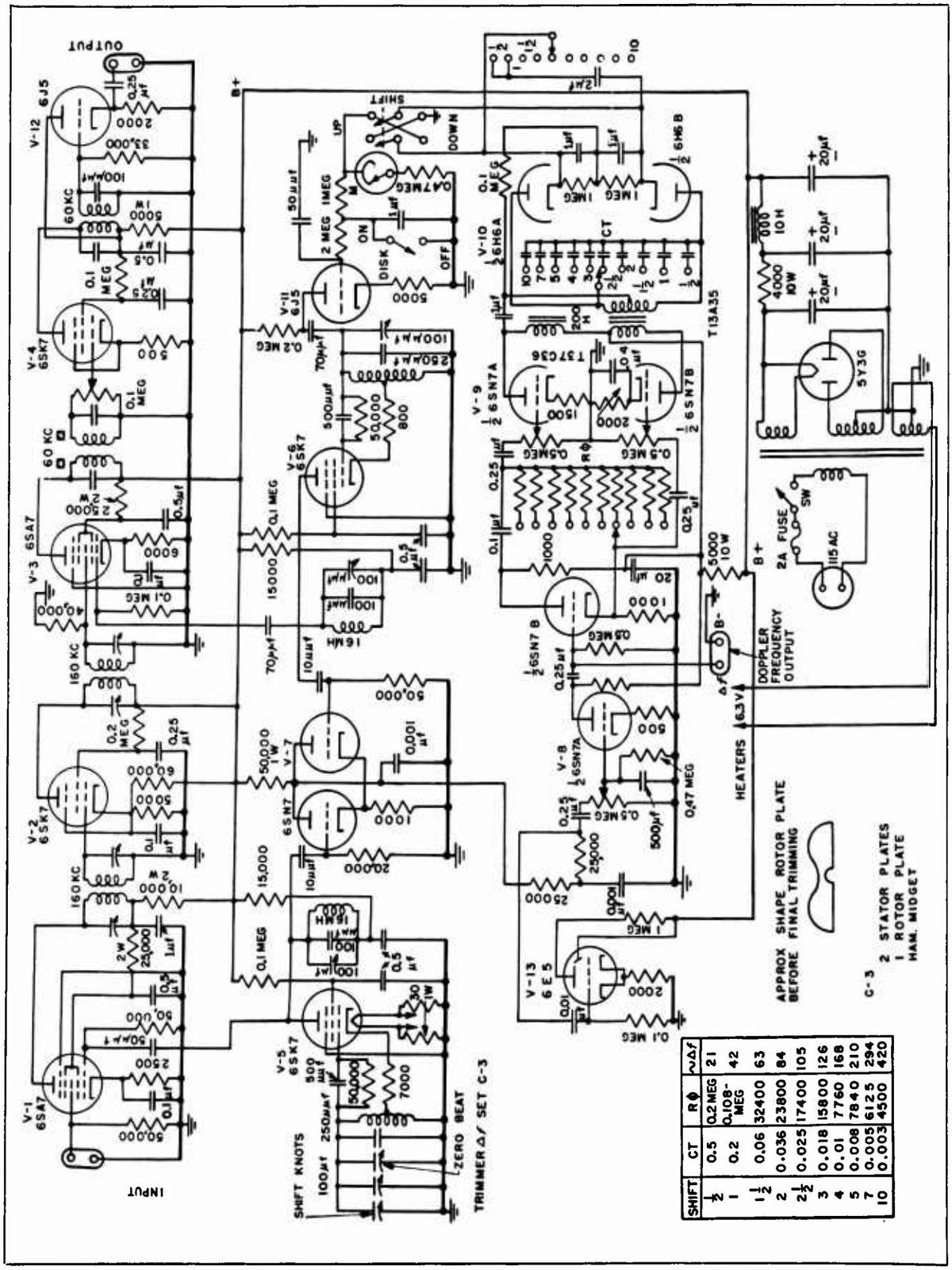

SHIFT	CT	RΦ	~Δf
½	0.5	0.2 MEG	21
1	0.2	0.108-MEG	42
1½	0.06	32400	63
2	0.036	23800	84
2½	0.025	17400	105
3	0.018	15800	126
4	0.01	7760	168
5	0.008	7840	210
7	0.005	6125	294
10	0.003	4500	420

FIGURE 20. Schematic diagram of artificial doppler circuit for 60-kc echo repeater.

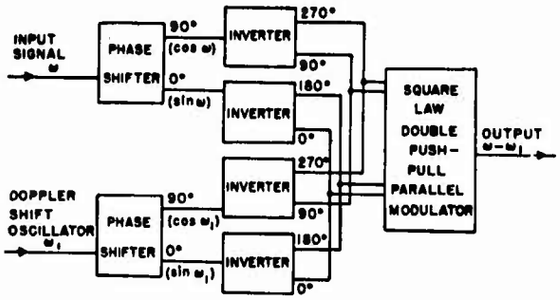

FIGURE 21. Block diagram of balanced modulator doppler-shifting circuit.

6.4.9 Dopplerized Stationary Repeater with Crystal Transducers

A dopplerized echo repeater, which was often used for tests in Boston Harbor, consists of a 20-kc stationary crystal transducer assembly and a deck electronic unit. The latter contains a voltage amplifier, a heterodyne doppler-shifting circuit, a power amplifier, and a listening amplifier, all mounted in one chassis.

The transducer assembly consists of two CD-1 crystal hydrophones suspended over the side of the vessel so that the hydrophones are separated vertically a distance of approximately 10 ft. The block diagram of the electronic unit is given in Figure 23. The heterodyne doppler circuit differs somewhat from that described in connection with Figures 19 and 20 in that no discriminator circuit is included. The frequency meter is therefore operated by a rectifier circuit containing a square-wave oscillator. Figure 24 is the schematic diagram of the entire electronic unit.

While this repeater assembly has not been calibrated, it has been in frequent service and has performed satisfactorily throughout its period of use.

6.4.10 Whale Echo Repeater

General Considerations

The Whale is a self-contained echo-repeater target designed to be towed at 15 knots at a depth of 1,000 ft. The seamanship requirements are thus extraordinarily severe. In order to reach the desired depth, a tow cable some 4,000 ft long is required. Accordingly, the towing vessel, in addition to the requirements for its own propulsion at the assigned speed, must be capable of towing 4,000 ft of heavy cable at this speed. The cable drag is too large to permit the body to be hauled in under way, and the cable winch must be extremely sturdy to retrieve this length of cable when it hangs vertically downward over the fantail. The necessity of reeling in the cable while lying to requires that the body of the Whale must be capable of surviving repeated submergence to 4,000 ft, even though it customarily operates at the more modest depth of 1,000 ft. These problems of seamanship had already been solved by the staff of ASDevLant prior to the initiation of work by HUSL on the echo repeater portion of the Whale.

Description of Mechanical Assembly

The body of the Whale is torpedo-shaped (see Figure 25). One section, which contains the echo-repeater electronic units, is watertight; the others are free flooding. The overall length of the Whale is 16 ft and its hull diameter 15 in. Its weight in air without the repeater assembly is 2,250 lb and in water it has a negative buoyancy of 1,935 lb. A depth recorder constructed by the Woods Hole Oceanographic Institution is installed. A hydrostatic pressure switch actuated at a predetermined pressure (generally 60 ft of water) is used to open and close the electronic circuits.

The pressure chamber of the Whale containing the electronic units is about 5 ft long. It consists of four forged steel cylinders welded together and stress-relieved. The wall thickness of 1⅜ in. is capable of withstanding an external pressure of 4,000 psi. The ends of the pressure section are removable. When attached they are sealed with Bridgman seals which are so designed that an increase in external pressure increases the sealing pressure.

Whale Transducers

Figure 26 is a view of a Whale transducer, one of which was attached to each cover of the pressure section. Windows in the Whale body permit free transmission of sound to or from the transducers. Each unit consists of three stacks of laminations 2 in. high polarized by a permanent magnet. In order to obtain the desired frequency of 24.5 kc, modified Hebbphone-II[c] laminations were used. The modifications consisted of punching a magnet slot in the bottom end of the lamination and shortening the stacks after consolidation.

The stacks are mounted in a heavy aluminum casting with the active faces Cycle-Welded to rubber

[c] See Division 6, Volume 13.

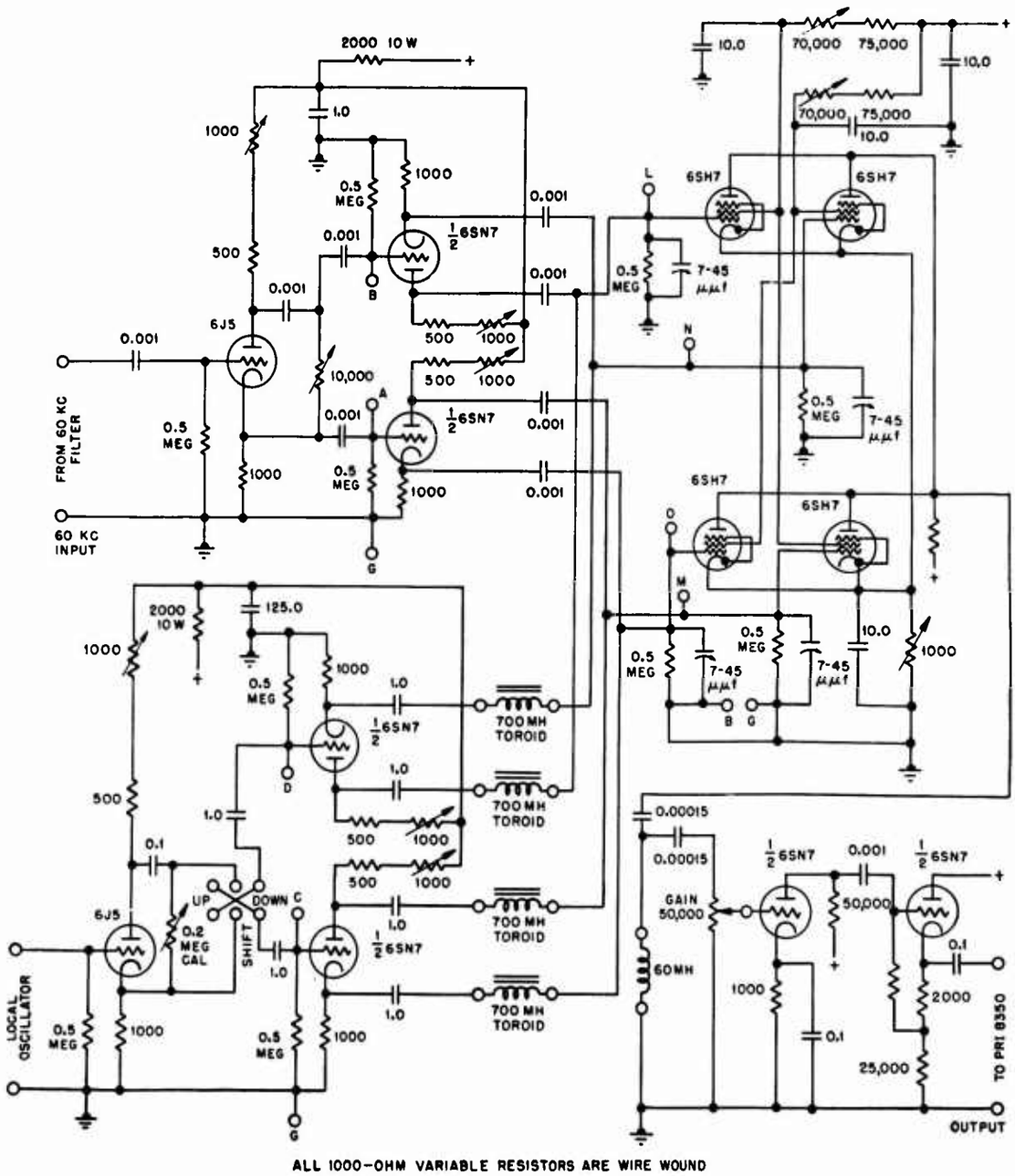

ALL 1000-OHM VARIABLE RESISTORS ARE WIRE WOUND

FIGURE 22. Schematic diagram of balanced modulator doppler-shifting circuit.

diaphragms which are also Cycle-Welded to the aluminum case to make a watertight joint. The space between the sides of the laminated stacks and the aluminum case is filled with pressure release material, Corprene in some places and Cell-Tite neoprene in others. The air spaces within the transducers were vacuum-filled with degassed castor oil. In order to balance the pressure between the inside and the outside of the transducer case, each transducer is equipped with a sylphon bellows. As the transducers are subjected to greater and greater pressure from the outside, the sylphon bellows contract and thereby force more oil into the transducer case to compensate for the contraction of the pressure release mate-

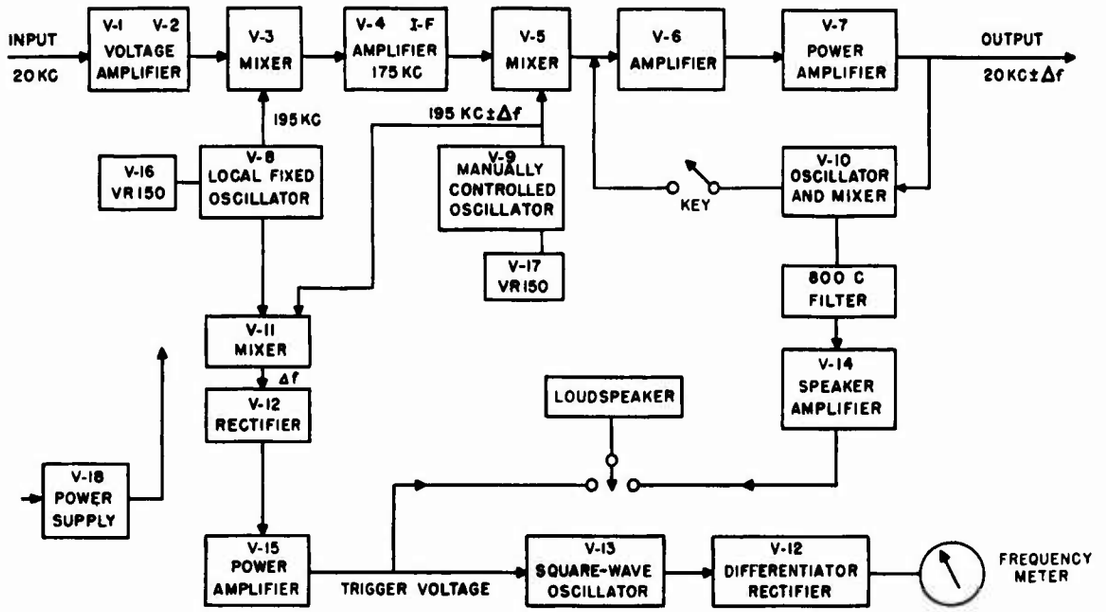

FIGURE 23. Block diagram of 20-kc echo repeater with doppler shifter.

rial. The three stacks of each transducer are connected in series-aiding and two leads are brought out through pressure seals to the neck of the fitting on the pressure chamber. The resonant frequency of the transducers is close to 24.75 kc, the efficiency about 19 per cent.

ELECTRONIC EQUIPMENT OF THE WHALE

The amplifier unit of the Whale is located within the pressure chamber. The power supply for this unit consists of a battery cartridge which contains all batteries required for the various tube voltages. This cartridge is inserted into the pressure chamber at the end opposite that used for the amplifier unit. Battery power was decided upon because of the difficulties attending the feeding of power through a cable 4,000 ft long. Storage batteries are not used because of the danger of explosion.

The schematic diagram of the amplifier unit is given in Figure 27. The input from the receiving transducer is transformer-coupled to the grid of the first amplifier tube through an attenuator calibrated in 2-db steps. The next two amplifier stages are resistance-coupled. To stabilize the gain for varying battery voltages, a negative feedback loop is inserted between the output of the third stage and the input of the second. The third stage is transformer-coupled to a band-pass filter of the constant resistance type. The output of the filter is transformer-coupled to the grids of the driver stage which in turn is also transformer-coupled to the output stage. This stage finally is also transformer-coupled to the transmitting transducer. To improve the linearity of the class B amplifier characteristic, part of its output is fed back to the class A driver stage with the proper phase relation to cause degeneration.

In order to limit the average plate current in the output stage, an RC section is inserted between the dry cell plate supply and the center tap of the primary of the output transformer. In this manner the time during which the output tubes can draw plate currents of more than 75 ma is limited to an interval of 50 to 100 msec. The need for this limitation arises from the possibility that continuous oscillation of the amplifier unit might be caused by surface or other reflections or by the reception of a steady signal. Without this plate current limiter the plate supply cells might quickly become polarized.

The function of the constant resistance filter is to reduce noise at frequencies outside the band over which the Whale is designed to operate. The advantages of this type of filter are that it appears as a resistance at all frequencies and that it permits the use of negative feedback.

PERFORMANCE TESTS OF THE WHALE

Mechanical Tests. A number of tests of the mechanical performance of the Whale were made by

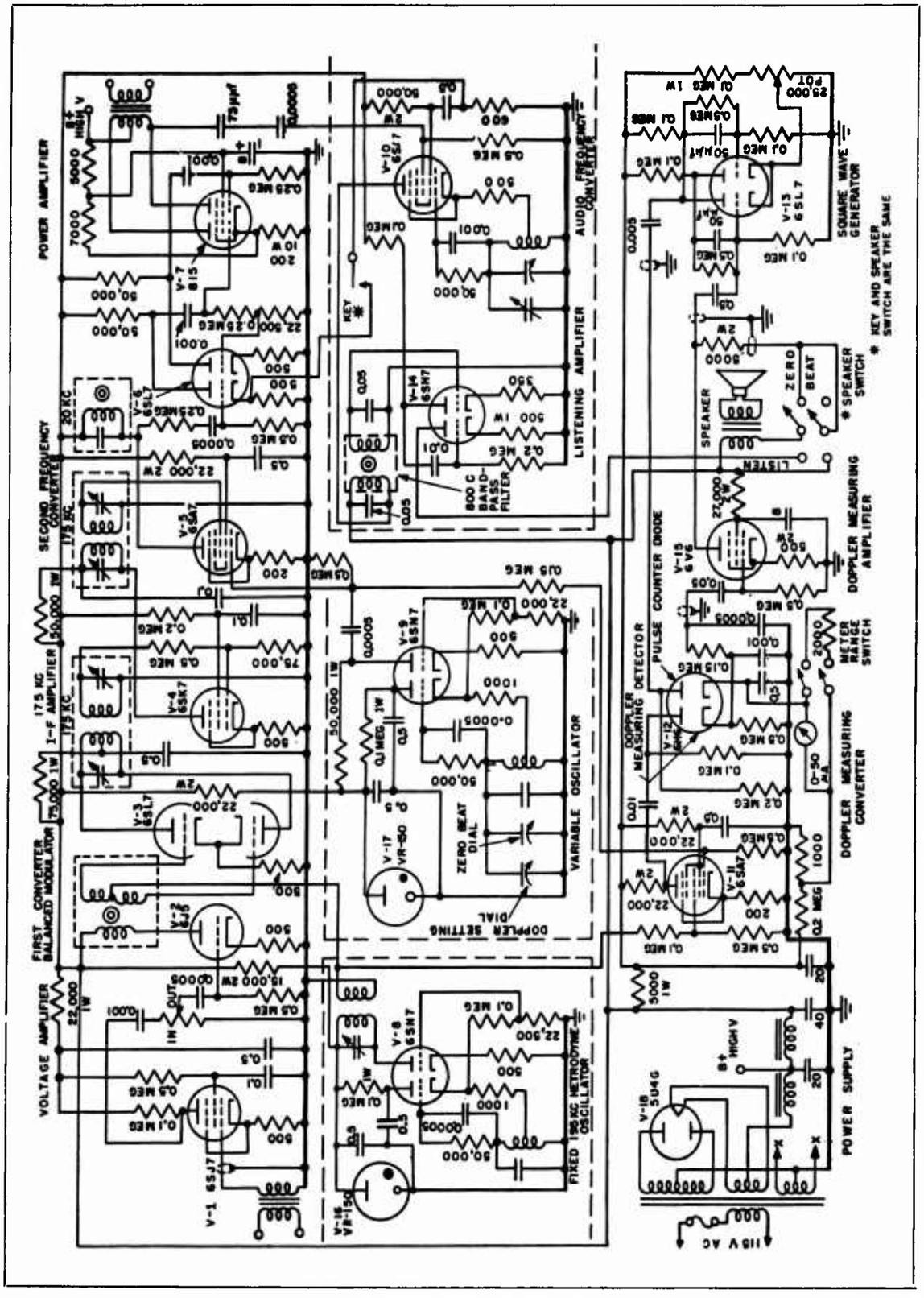

FIGURE 21. Schematic diagram of 20-kc echo repeater with doppler shifter.

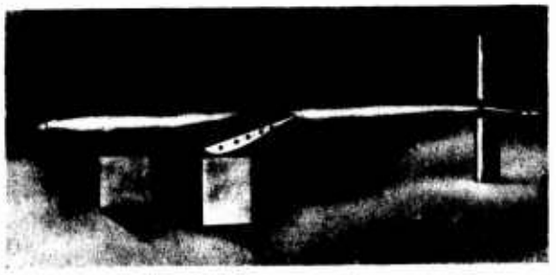

FIGURE 25. Whale body.

FIGURE 26. Transducer of Whale echo repeater.

Navy personnel both before and after the repeater unit had been installed (see Table 1). Of particular interest was the behavior of the pressure seals of the repeater section at great depths. These fortunately proved to be watertight during all the tests including those made at depths of 2,200 ft. The results of a number of towing runs are represented by the graphs of Figure 28. It is apparent from these graphs that there is no difficulty in obtaining desired depths if the proper speed and cable length are used.

Acoustic Test. The sketch of Figure 29 illustrates the method used to check the operation of the Whale echo repeater. As shown in the figure, an external feedback loop is formed by means of two auxiliary Hebbphone transducer sections coupled by an a-c ammeter. To obtain proper mechanical coupling between the auxiliary and the repeater transducers, it is advisable to coat all the transducer faces with castor oil and carefully squeeze out all air bubbles.

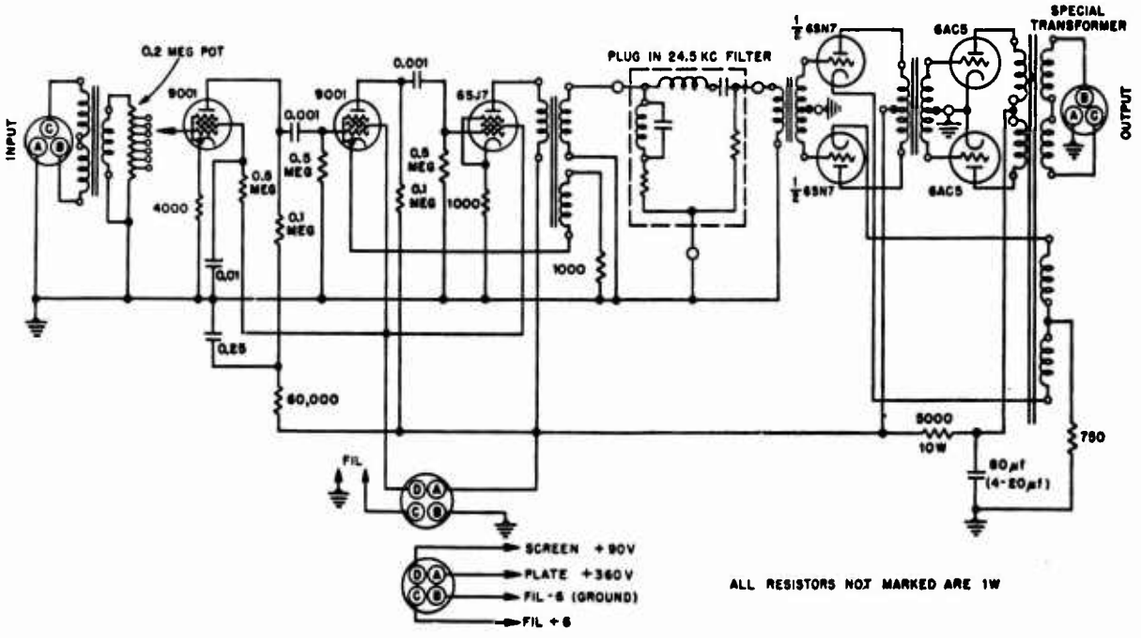

FIGURE 27. Circuit diagram of Whale amplifier unit.

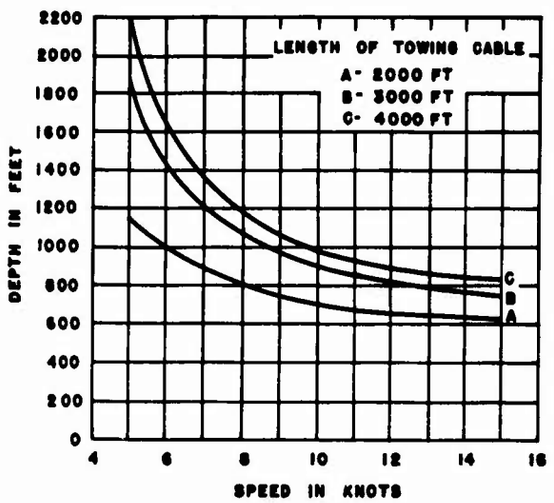

FIGURE 28. Depth versus speed in Whale towing tests.

If the repeater switch is then closed with this arrangement and if the electronic circuits are functioning properly, a state of continuous oscillation of the four transducers is established. With a fixed gain setting the a-c ammeter reading then affords a measure both of amplifier efficiency and of battery regulation.

TABLE 1. Dimensions and characteristics of the Whale.

Dimensions*	
Length	16 ft
Hull diameter	15 in.
Hydrofoil spread	7.5 ft
Hydrofoil width	29 in.
Weight in air	2,250 lb
Weight without ballast	960 lb
Negative buoyancy	1,935 lb
Lift	$51.3V^2$ lb (V = speed in knots)
Drag	1/3 the lift
Center of gravity	48¾ in. abaft the nose
Bridle	⅝-in. steel cable
Fore part	15 ft 6 in.
After part	13 ft 1 in.
Towline	4,000 ft of ⅝-in. steel cable

Towing Characteristics

Speed in knots	Depth in ft Calc.	Depth in ft Obs.	Drag in lb Calc.	Drag in lb Obs.	Shaft horsepower required
8	1,070	1,200	6,300	6,500	280
15	865	.....	17,400	.....	1,450

* These figures were obtained before the echo repeater was placed within the Whale.

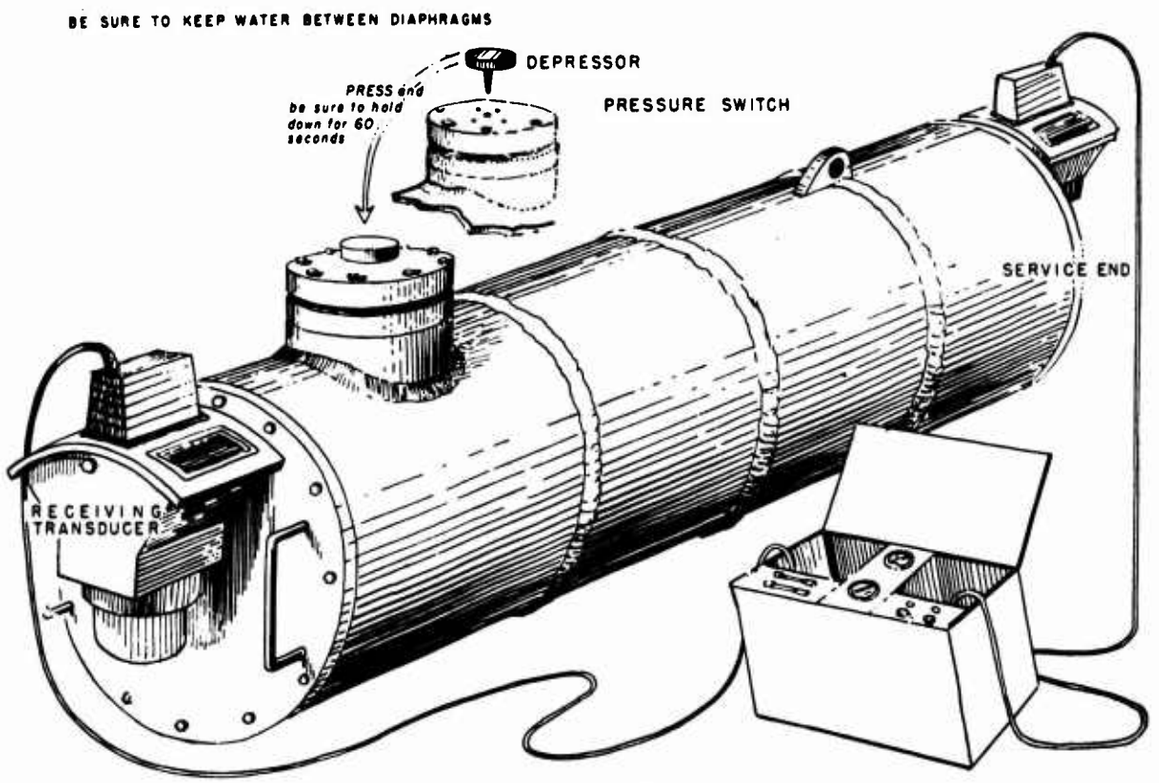

FIGURE 29. Testing arrangement for Whale echo repeater.

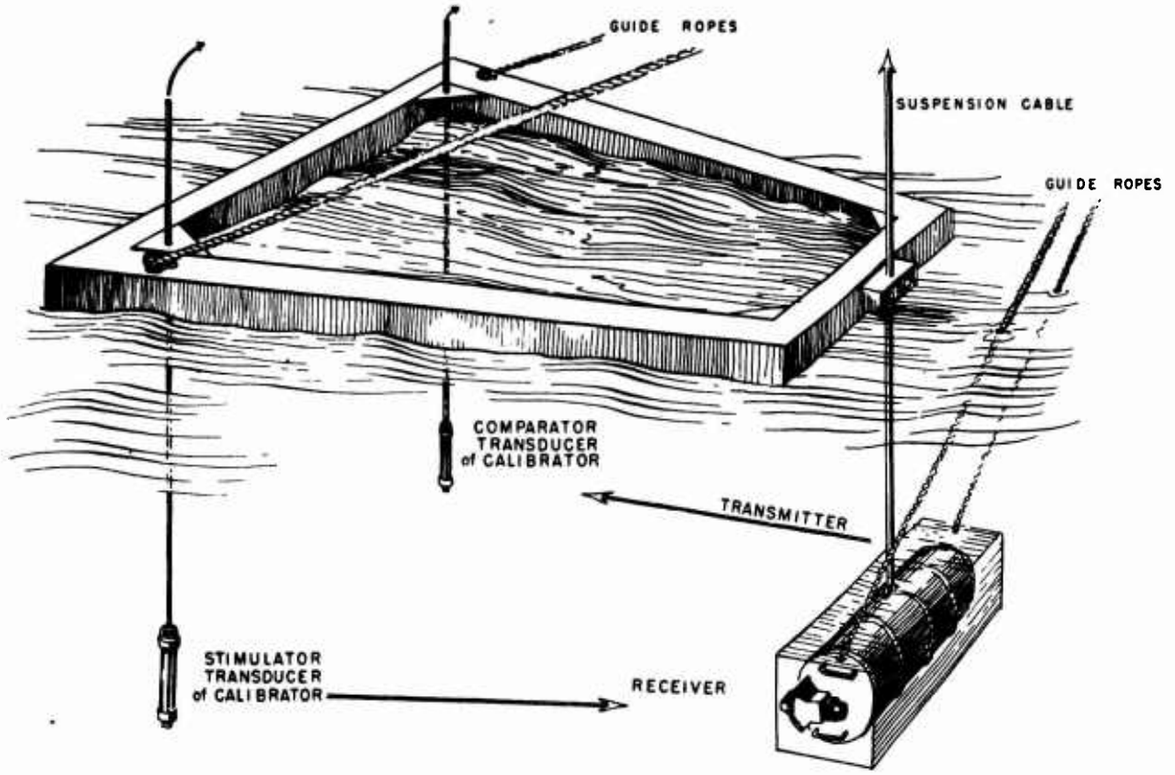

FIGURE 30. Whale calibration arrangement.

CALIBRATION

The calibration of the Whale was carried out by means of the echo repeater calibrator (see Sections 6.6–6.11). Because of its weight and the 5-ft separation of its transducers, it was necessary to provide a special structure to maintain the alignment of all the transducers (see Figure 30). The results of one calibration, which was checked by several later tests, are given by the graph of Figure 45.

TARGET SERVICE TESTS

Sea tests using the Whale for target service tests were made in August 1944. In these trials both QBE equipment and a QCS projector were used for the echo ranging. The depth of the Whale during these tests ranged from about 400 to 2,000 ft. A number of echoes were detected by the QBE gear at ranges from 450 to 1,000 yd. To obtain these echoes it was necessary, however, to tilt the projector downwards at least 25 degrees and on some occasions 45 degrees before the Whale was located. The conclusions to be drawn from these results are that the beam of the Whale is too narrow and that it does not emit sufficient energy in a horizontal direction. This is borne out by the fact that no echoes were detected with the QCS projector, the mounting of which did not permit tilting. With a tiltable projector on the echo ranging vessel, however, the performance of the Whale is satisfactory. On the completion of the tests described above, the Whale was turned over to ASDevLant. It was continuing to give satisfactory target service in the spring of 1945 in connection with tests of sonar equipment for depth determination.

6.4.11 Gas-Pipe Echo Repeater

DESCRIPTION

The final type of HUSL echo repeater consists of a stick assembly of two transducers with an amplifier between them. Cables from the transducer-amplifier assembly lead to a deck electronic unit which includes power controls and a potentiometer providing some control of the amplifier gain. Because of its shape the transducer-amplifier unit became known as the gas-pipe repeater.

The device consists of a cylindrical amplifier assembly enclosed in a steel pipe, ¼ in. thick, 4 in. in outside diameter, and 23 in. long. Transmitting and

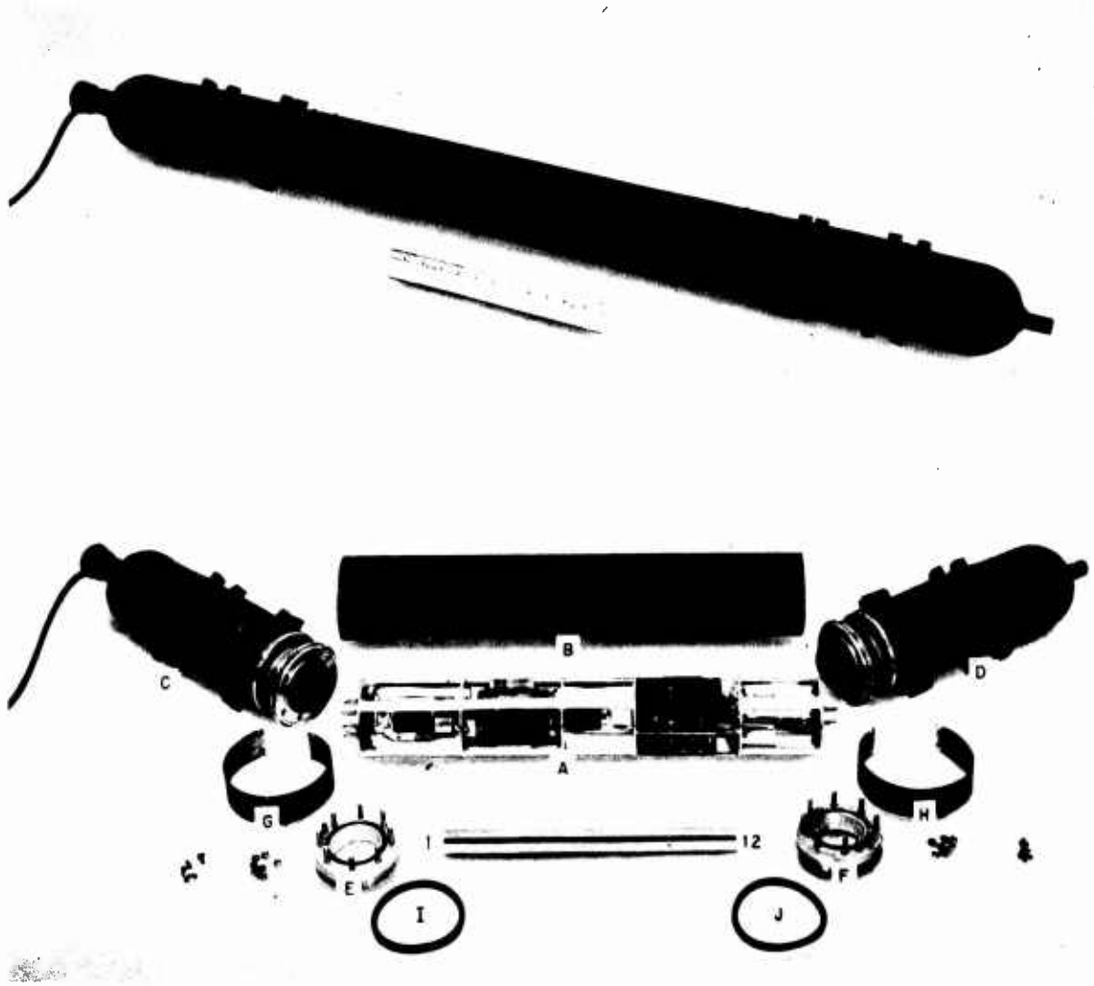

FIGURE 31. Low frequency "gas-pipe" echo repeater assembly.

receiving transducer assemblies are bolted to the ends of the amplifier unit extending the overall length to 41½ ft. The weight of the combination is 87 lb. Figure 31 shows two views of the model. The various parts shown disassembled in the lower photograph are: A, amplifier chassis; B, housing for chassis; C, transmitting transducer; D, receiving transducer; E, F, I, J, water seals; G, H, streamlining bands.

AMPLIFIER UNIT

Figure 32 is the schematic diagram of the amplifier unit. The bias of the first two stages of amplification (9003 tubes) is controlled by a remote attenuator circuit in the deck electronic unit. The 9003 tubes are followed by a phase-inversion, push-pull stage (9002 and 6SN7 tubes). The output of the 6SN7 tubes is transformer-coupled to the driver stage (815 tubes), an auxiliary secondary winding on the transformer supplying negative feedback. The purpose of the potentiometer circuit shown in Figure 32 below the 815 tubes is to provide as stable a screen voltage supply as is possible in the limited space available. A four-conductor shielded cable supplies the two bias voltages, the plate voltage, and current for the tube heaters from the deck electronic unit.

OUTPUT

This repeater operates most efficiently over a frequency range of from 25 to 27 kc. It is possible, however, for the repeater to simulate a 22-ft sphere for any frequency of from 20 to 32 kc by properly adjusting the gain of the amplifier. At 26 kc the

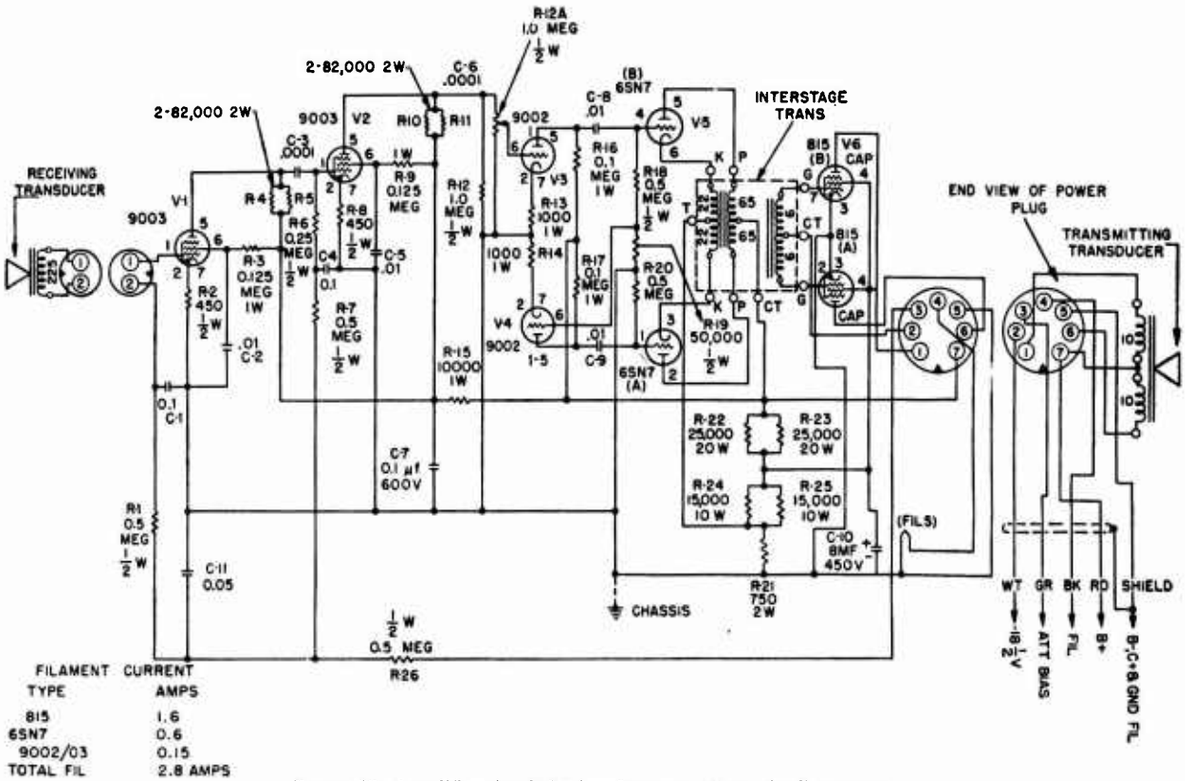

FIGURE 32. Amplifier circuit for low frequency "gas-pipe" repeater.

equivalent sphere radius is about 110 ft with zero attenuation and about 4 ft with maximum attenuation.

6.5 RECOMMENDATIONS FOR FUTURE WORK

The echo repeater derives its primary usefulness from the fact that it provides an artificial target of controllable strength. However, it provides also a "point" target, and in this respect differs from actual targets. Since some of the phenomena involved in the reflection of sonar pulses from actual targets depend upon their extent and geometry, it appears desirable to conduct further investigations of the reflection of sound pulses from extended targets before placing too great reliance upon equipment tests conducted with echo repeaters. A study of the fluctuation of echoes from extended targets as compared with that of echoes from repeaters should also be included.

Although most of the desirable features of echo repeaters, such as audible monitoring, control of calibration, introduction of doppler, and towability, have been included in the design of one or another repeater, no single artificial target has included all of these features in a sufficiently satisfactory form to allow the unit to be used as a manufacturing prototype. Many of the requirements, such as towability at considerable depth and ability to operate over extended periods, are conflicting; but it appears possible to formulate a limited number of specifications covering typical service requirements, and to carry through the engineering design work required to produce manufacturable targets capable of giving trouble-free service. It is recommended that such specifications be established, and that the engineering design work be carried out.

Several investigations have been proposed in which a delayed-action echo repeater is required. For example, such a device would make possible a direct comparison between echoes received from the vessel carrying the repeater and echoes from the repeater itself. At least one such instrument was utilized[1] in connection with an investigation by the West Coast Sound School of the location of the echo point as determined by bearing deviation indicators. It operated, however, on the basis of a locally generated

signal which did not duplicate the amplitude or frequency characteristics of the incident signal. A method has been proposed[2] for obtaining the required echo delay by recording the received signal magnetically on a short loop of wire. The recorded signal would then excite the transmitter by means of a magnetic pickup unit located a suitable distance along the wire from the recording element. In view of the probable utility of some such device it appears that further study should be devoted to the matter. Accordingly the delayed-action echo repeater is recommended as a project for inclusion in any future development program.

The Echo-Repeater Calibrator

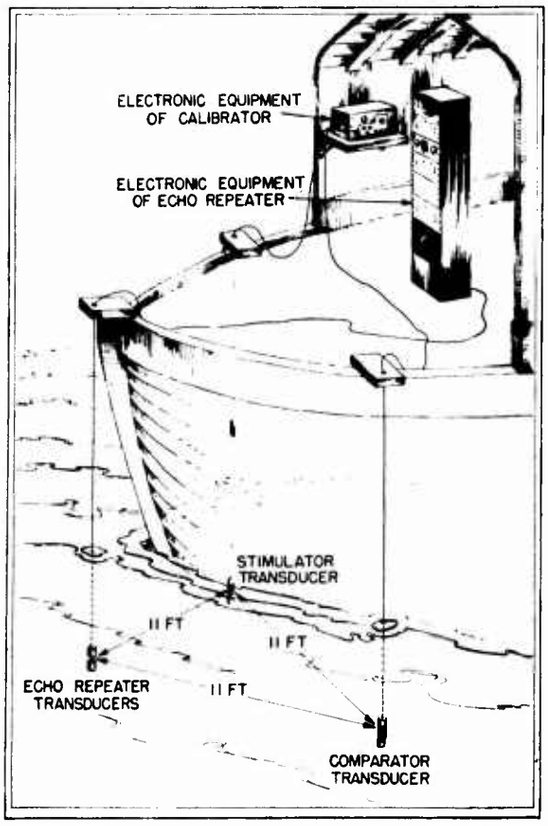

FIGURE 33. Echo repeater calibration.

The echo-repeater calibrator developed by HUSL is used to determine the equivalent target sphere size of an echo repeater. It includes a "stimulator" transducer and a "comparator" transducer, an oscilloscope, and electronic units designed for pulse generation and amplification. In the usual calibration procedure, the transducer combination of an echo repeater and the comparator and stimulator transducers of the echo repeater calibrator are placed at the vertices of an equilateral triangle having sides 11 ft in length. When operation commences, a ping is sent out by the calibrator through the stimulator transducer and picked up by the comparator transducer. The returned ping from the echo repeater being calibrated is likewise picked up by the comparator transducer and the two signals are compared upon the screen of the calibrator's oscilloscope. This permits calibration of the echo repeater at one particular setting of its gain control, and the equivalent sphere size at all other settings can then be determined by computation. Nonportable and portable calibrators have been assembled; the portable unit is the later model.

6.6 INTRODUCTION

For purposes of echo ranging, the size of a target is specified in terms of an equivalent sphere having a perfectly reflecting surface. The target's equivalent sphere would, it is assumed, reflect as much energy to the echo-ranging equipment as the target itself. A class S submarine, for example, is conventionally considered to be replaceable by a sphere with a 22-ft radius. The size of the simulated sphere produced by an echo repeater is directly proportional to the ratio of acoustic output to input. Provided the system as a whole operates linearly, the gain or attenuation settings of the repeater amplifier may be used to calculate comparative values of equivalent sphere radii. To obtain the specific value of the sphere radius corresponding to a particular amplification, however, the echo repeater must be calibrated. It is this function that the *echo-repeater calibrator* [ERC] has been designed to perform; namely, to specify as accurately as possible the actual value of the equivalent sphere radius for a given attenuation setting of the echo-repeater amplifier. With this information the radius for any other setting may easily be computed.

The echo-repeater calibrator consists of a stimulator transducer, a comparator transducer, an oscilloscope, and electronic equipment comprising an oscillator, a pulsing circuit, amplifiers, and a power supply. The calibrator is provided with controls so that frequency, pulse length, keying rate, power output, amplifier gain, and sweep rate may all be varied appropriately.

In calibrating an echo repeater, the repeater, comparator, and stimulator are located so that each is the same distance from the others, i.e., at the vertices of an equilateral triangle. (See Figure 33.) When the stimulator transducer transmits supersonic pulses, the "repeated" pulse from the echo-repeater transmitting transducer arrives at the comparator transducer a few milliseconds later than the direct stimulator pulse, so that both pulses, by virtue of screen persistence, may be seen simultaneously on the oscilloscope of the calibrator. The echo-repeater attenuation is then adjusted until the two images are of equal amplitude. When this condition has been fulfilled, the radius of the equivalent sphere representing the echo repeater is equal to twice the distance between the echo repeater and the comparator hydrophones.

The first ERC model was constructed for checking the Whale, a deep-towed echo repeater. Successful calibration measurements were made with it during July and August 1944. The second model of the calibrator was assembled at the HUSL Florida Station to check the 60-kc echo repeater at that station.

In July 1944, the design of a portable target calibrator with a compact assembly was undertaken. This type of calibrator has electronic equipment not essentially different in operation from that used in the nonportable type. It is, however, contained in a much smaller volume. Model I of the portable target calibrator was completed in November 1944 and operated satisfactorily in calibrating echo repeaters on the HUSL target boat, *Questor,* in Boston Harbor.

In October 1944, construction was begun on Model II, an ultracompact assembly of a portable target calibrator. The electronic circuits, similar to those of Model I, were built around miniature tubes. The laboratory development was completed but it is doubtful whether the increased compactness of Model II outweighs the disadvantages of greater difficulty in construction and servicing.

The results obtained with the various models indicate that the ERC is sound in principle and very useful wherever an echo repeater is required to represent a target sphere of definite strength. It is practically indispensable in the case of deep-towed repeaters or other repeater applications where protracted operation without monitoring is a necessity. Further development to provide a production model of the ERC is recommended. It is suggested, moreover, that special consideration be given to the possibility of developing built-in calibrator equipment for incorporation in future echo-repeater designs.

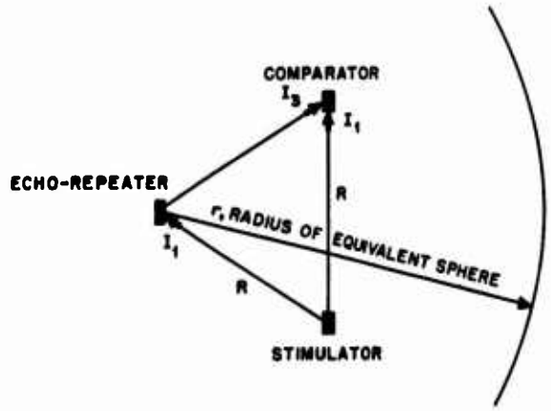

FIGURE 34. Calibration setup.

6.7 THEORY

6.7.1 Equivalent Sphere Concept

Of the various procedures for calibrating an echo repeater, the simplest consists in placing the echo repeater, the comparator, and the stimulator hydrophones at the vertices of an equilateral triangle with sides equal to R (see Figure 34). By adjusting the echo repeater so that the image heights of the stimulator and repeater pulses on the ERC oscilloscope screen are equal, the echo repeater is made to simulate a reflecting sphere whose radius r is equal to $2R$. This means that echo-ranging gear sending energy to the repeater receives energy from the repeater, at its calibrated gain setting, as though the energy were reflected from a sphere of radius $2R$.

In the calibration technique as outlined above, the echo repeater is represented as being at the center of an imaginary sphere, within which are also located the stimulator and the comparator. Now, an elementary analysis of the reflection properties of a sphere discloses that the focal point of radiant energy reflected from a sphere is not at its center but elsewhere within the sphere. Furthermore, as the size of the sphere is varied, the position of the focal point also varies. Since these matters are apparently not taken into account in the calibration process, some justification of the method is necessary. It can be found in the fact that, in echo ranging, the distance between the ranging gear and the target is large compared to the size of the equivalent sphere of the target. As far as the echo-ranging gear is con-

cerned, therefore, the error involved in assuming a fixed focal point of reflection is negligible. In other words, at large distances the equivalent sphere reflects energy as though it came from a point source.

In further justification of the calibration procedure, it should be noted that an echo repeater, not being a real sphere, behaves as a point source even when distances involved are small compared to the size of the equivalent sphere. It is therefore entirely permissible to determine the output of the repeater by examining it at the close range used in calibrating. As far as the incoming signal is concerned, the response of the repeater to a given signal is the same whether that signal has traversed a great distance or merely a short interval. The smallness of the distances employed in the calibration process, therefore, in no way impairs the validity of the results obtained.

6.7.2 Mathematical Relations

The relations between the incident and the reflected intensities for a sphere may be derived from a simple optical analogy. (See Figure 35.)

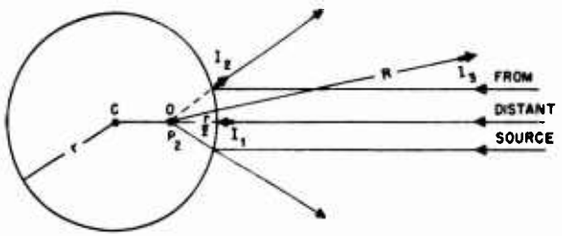

FIGURE 35. Reflection from sphere.

Let I_1 = incident intensity at surface of sphere from distant source,

I_2 = reflected intensity at surface of sphere,

I_3 = reflected intensity at distance R from apparent source,

r = radius of reflecting sphere,

R = distance at which I_3 is measured,

P_2 = power of apparent source of reflected energy.

For a perfectly reflecting sphere, $I_1 = I_2$, and for plane waves coming from a distance, the source of the reflected energy is located midway between the center of the sphere and the surface (focal length $= r/2$).

Then

$$I_2 = \frac{P_2}{\left(\frac{r}{2}\right)^2} = \frac{4P_2}{r^2} I_1.$$

Also

$$I_3 = \frac{P_2}{R^2}.$$

Therefore

$$I_3 = \frac{I_1 r^2}{4R^2}.$$

In the calibration technique, the echo repeater output is adjusted so that $I_3 = I_1$. It follows then that $r = 2R$, which is the relation used in the calibration procedure.

6.8 GENERAL DESCRIPTION OF CALIBRATORS

The echo-repeater calibrators discussed below are of two types, nonportable and portable. Of the nonportable type, the first model was completed at HUSL, the second at the HUSL Florida Station. Of the portable type, Model I was completed; Model II progressed to the breadboard stage but additional engineering development would be required to qualify it for service use. These four calibrators represent the total number developed by HUSL.

The nonportable calibrators have used high-efficiency, ring-stack hydrophones for the stimulator transducer and B-19H hydrophones for the comparator transducers, but the equipment functions equally well with any high-efficiency hydrophones, such as the soft nickel or Permendur type. The electronic equipment of the first model of nonportable type is mounted permanently in a 3-ft relay rack. It includes a Hewlett-Packard oscillator, a pulsing circuit, a power supply, a voltage amplifier, a circuit to supply polarizing current required for certain hydrophones, and a commercial 3-in. oscilloscope. The second nonportable model uses hydrophones of the same type as the first model and the same electronic equipment, with the exceptions that the voltage amplifier is one taken from a 60-kc echo repeater, and that a 60-kc filter has been added to the comparator circuit.

Models I and II of the portable calibrator both

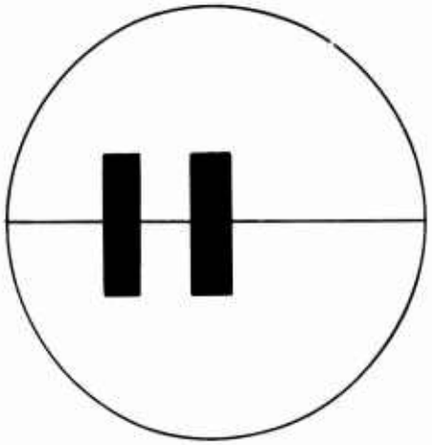

FIGURE 36. Sketch of pulses on oscilloscope screen.

use B-19H/2 (half-length B-19H) hydrophones for comparator and stimulator transducers in 60-kc calibrations. For low-frequency calibrations, thin-walled ring stacks are preferable. The electronic equipment of Model I, mounted on a 10x17-in. chassis and contained in a case 11x14x22 in., forms a compact assembly. The electronic circuits comprise the same units as those of the nonportable type, except that polarizing current is not available. The power output of the two types of calibrator is approximately the same. The Model II portable differs from Model I only in the use of miniature tubes, which reduce the space required for the electronic equipment and consequently make possible an ultracompact assembly.

The voltage amplifier in the portable calibrators is a high-gain untuned amplifier which functions satisfactorily over a range of frequencies of from 18 to 85 kc. Its output is applied to the oscilloscope which, in these models, is a 2-in. tube with its sweep circuit synchronized with the pulsing circuit of the stimulator. For an 11-ft separation of hydrophones, a sweep duration of 10 msec, and a pulse length of 1 msec, the direct signal and the repeated signal have the general appearance suggested by the sketch of Figure 36.

6.9 ELECTRONIC CIRCUITS

Figure 37 is a block diagram of the electronic circuits used for both types of echo-repeater calibrator. In the nonportable type, the oscilloscope sweep circuit makes use of an internally developed voltage. In the portable type, the oscilloscope obtains its sweep voltage from the stimulator pulsing circuit. This is indicated in the figure by the dashed line.

6.9.1 Nonportable Calibrators

Figure 38 is the complete schematic diagram for the present nonportable calibrator. The comparator section consists of a voltage amplifier of standard

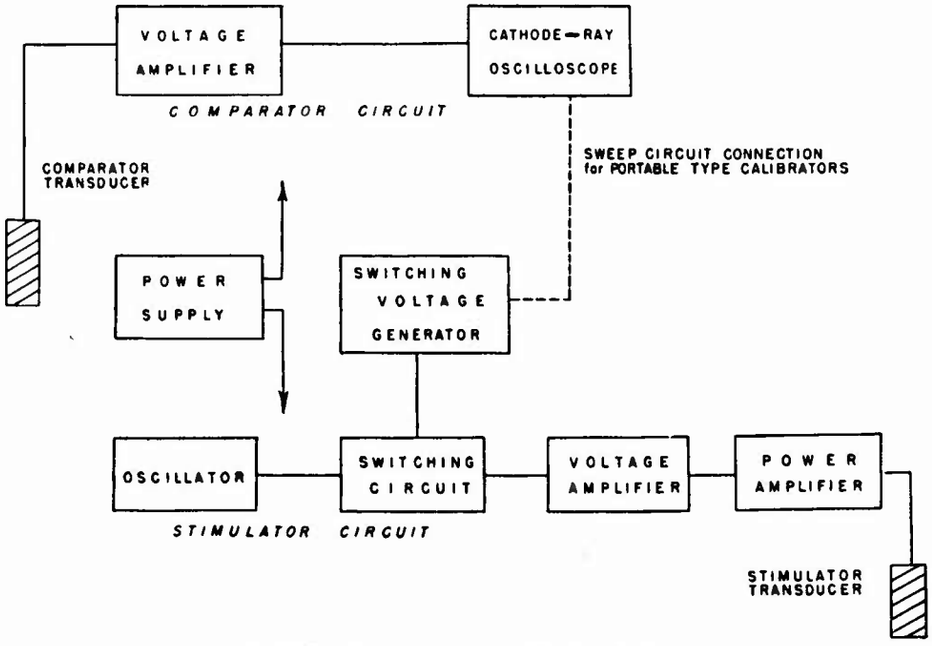

FIGURE 37. Block diagram of calibrator circuits.

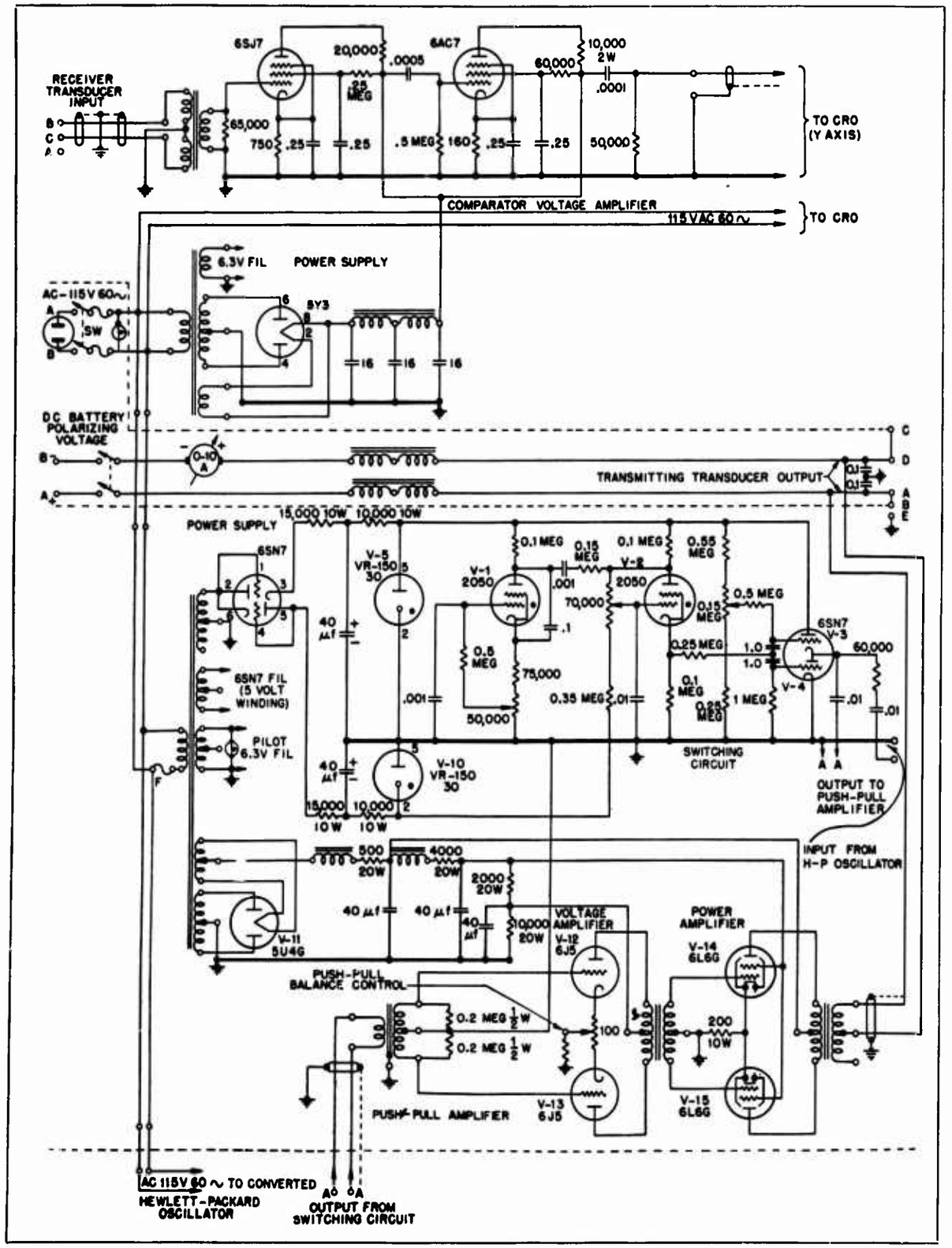

FIGURE 38. Schematic diagram for Whale nonportable calibrator.

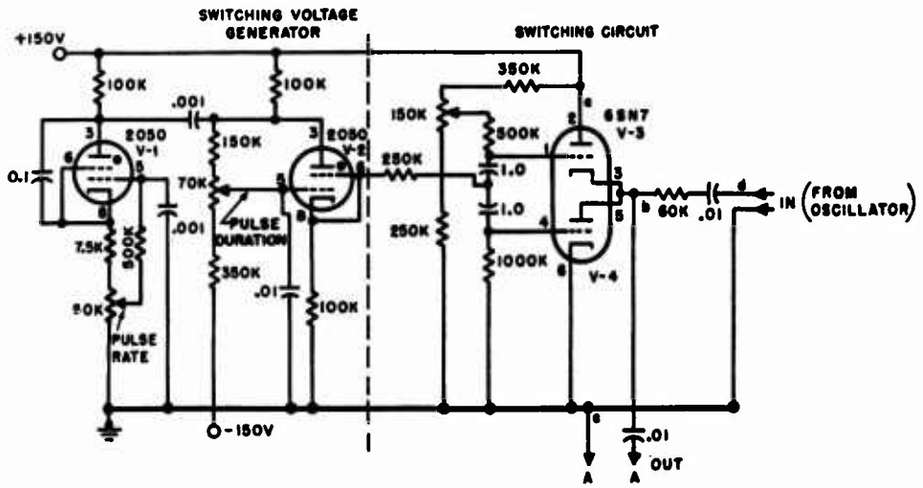

FIGURE 39. Switching circuit of nonportable calibrator.

design and a commercial 3-in. cathode-ray oscilloscope.

The stimulator section comprises a Hewlett-Packard oscillator, a switching voltage generator, a switching circuit, a voltage amplifier, and a power amplifier. A power supply unit is also provided.

Figure 39 is a detailed diagram of the switching voltage generator and switching circuit. Tubes V-1 and V-2 are grid-controlled gas discharge tubes, V-3 and V-4 medium-μ amplifiers. The switching circuit requires the cathode of V-2 to be at ground potential during generation of the pulse, and at some positive potential during the remainder of the pulsing cycle. Tube V-2 (Type 2050) is normally conducting but is "put out" when V-1 fires, since the plate voltage of V-1 drops suddenly, bringing the plate voltage of V-2 momentarily down with it, so that the plate voltage of V-2 is suddenly made less than the extinction voltage. No current can flow under this condition, and the tube goes out. Before the tube goes out, the terminal of the 0.01-μf condenser at the grid becomes sufficiently negative, as it is charged through the 70,000-ohm potentiometer, so that V-2 stays extinguished temporarily. However, the plate voltage of V-2 starts to increase, so that the 0.01-μf grid condenser begins to charge to a new value. After a short delay the grid voltage becomes sufficiently positive to cause plate current to flow in V-2 again. Thus, the setting of the 70,000-ohm potentiometer determines how long V-2 remains out and consequently determines the length of the pulse. Tube V-1, which determines the rate at which the pulses are generated, operates in a simple relaxation oscillator circuit, the fundamental frequency of which is varied by changing the adjustment of the 50,000-ohm potentiometer in the cathode circuit. Tube V-1 is not put out when V-2 fires because the 0.1-μf capacity from plate to cathode prevents the cathode potential from becoming more positive than the plate potential. The filter in the grid circuit helps to minimize unwanted interaction between the two tubes. Since the voltage at the cathode of V-2 falls practically to zero within 0.1 msec, a pulse whose duration is 0.5 msec has a fairly satisfactory envelope. The circuit components which permit these short pulses to be generated under stable conditions are not suitable for pulses much in excess of 6 msec. Changing the components to obtain longer pulses results in the unstable generation of short pulses. Since the pulse length wanted in calibration equipment is in the range of from 0.5 to 4 msec, this circuit is satisfactory. It is not quite ideal, however, for the pulse front is rounded off more than is desirable when the pulses are short.

The switching circuit consists of two dividing networks, *abc* and *dbc*, in which tube V-4 (see Figure 39) comprises the lower leg *bc* of each; tube V-3, the upper leg *ab* of one; and the 60,000-ohm resistor, the upper leg *db* of the other. The 60,000-ohm resistor and V-4 divide the signal voltage from the oscillator, holding the output low as long as the plate resistance of V-4 is low, or as long as the grid of V-4 is at ground potential. When the grid voltage of V-4 is made negative, the a-c plate resistance increases, and the divider causes the output (at *AA*) to increase. Tube V-3 allows the signal to flow

through V-4 without severe distortion, by causing a d-c current to flow in V-4 which exceeds the peak a-c current. By adjusting the circuit components, the d-c plate resistance of V-3 can be made to change proportionately to the change in the d-c plate resistance of V-4. When this situation prevails, the d-c voltage at the junction between the tubes remains constant, and there is no transient. Actually, the transient cannot be entirely eliminated, but it can be made negligible in comparison to the a-c signal output voltage. The circuit does not cut off the output voltage entirely but reduces it about 40 db in the off position. However, it does make possible extremely rapid switching since it is not limited by the inductive response of transformers.

6.9.2 Portable Calibrators

MODEL I

Figure 40 is the complete schematic diagram of Model I of the portable calibrator. The components of its chassis may be classified as follows:

1. Power amplifier.
2. Receiving amplifier.
3. CRO circuit.
4. Power supplies.
5. Pulsing circuit.
6. Synchronized sweep circuit.
7. Switching circuit.

The first four of these components consist of conventional circuits. The power amplifier works on a duty cycle principle in order to reduce the power supply requirement while maintaining high power output. With 300 v at the screens, 400 v at the plates, and 42 v of bias, the quiescent plate current (no excitation) is only about 17 ma. The amplifier provides 35 w of output power before the excitation gets high enough to cause grid current to flow. Feedback is used both to minimize distortion in the amplifier itself, and to match the amplifier to the output transducer so that the energy transmitted to the water varies as little as possible with frequency. This is accomplished by matching the load to the generator for most efficient energy transfer without feedback at some intermediate frequency, and by determining the maximum power output with this matching condition at the frequency extremes. The feedback is then adjusted to reduce the maximum power output at the intermediate frequency to this value, keeping the excitation the same. By properly choosing the frequency and loading conditions used to obtain a match before feedback is applied, the power may be made to vary with frequency so as to compensate approximately for the change in transducer efficiency.

The voltage amplifier has a measured maximum voltage amplification of 157 db referred to the half-length B-19H transducer open circuit voltage and to the plate of V-4. Thus, if the transducer is in a field which generates 1-μv at the transducer terminals on open circuit, the voltage at the plate of V-4 is 37 db above 1 v, or 50 v, when the attenuator is set for maximum gain. This gain is sufficient to amplify the noise due to thermal agitation in the input circuit to about $\frac{1}{3}$ deflection on the CRO. It is greater than necessary and experience seems to indicate that 130 db is sufficient. Figure 40 may be consulted for further details concerning the power amplifier and the voltage amplifier, as well as for information regarding the conventional CRO and power supply circuits.

The remaining components of the portable calibrator chassis, namely, the pulse, sweep, and switching circuits, employ nonconventional circuits. In view of the fact that this version represents a preferred form of calibrator, separate diagrams and descriptions of these circuit arrangements are provided.

Calibrator Pulse Rate and Pulse Length Control System. Figure 41 is an illustration of that part of Figure 40 which has to do with the pulse control. The purpose is to provide a system which will develop control potentials so that pulses of adjustable length may be transmitted at various rates and so that a CRO may be synchronized with them.

With the starting button open and the power turned on, V-6 ignites and remains ignited. The drop across its 1,000-ohm cathode resistor provides a positive bias to the switching tube, thereby preventing the oscillator from functioning. The left side of the 0.05-μf capacitor is at the potential of the plate supply voltage. The right side of the capacitor is at a potential equal to the drop across V-6 and its 1,000-ohm cathode resistor.

If the starting button is closed, the 0.05-μf capacitor discharges to ground through V-5 and its 200-ohm cathode resistor. The right side of the capacitor swings negative with respect to ground, the value of the negative potential being the difference between the original drop across the capacitor and the drop across V-5 with its 200-ohm resistor.

Tube V-6 is quenched because its anode has be-

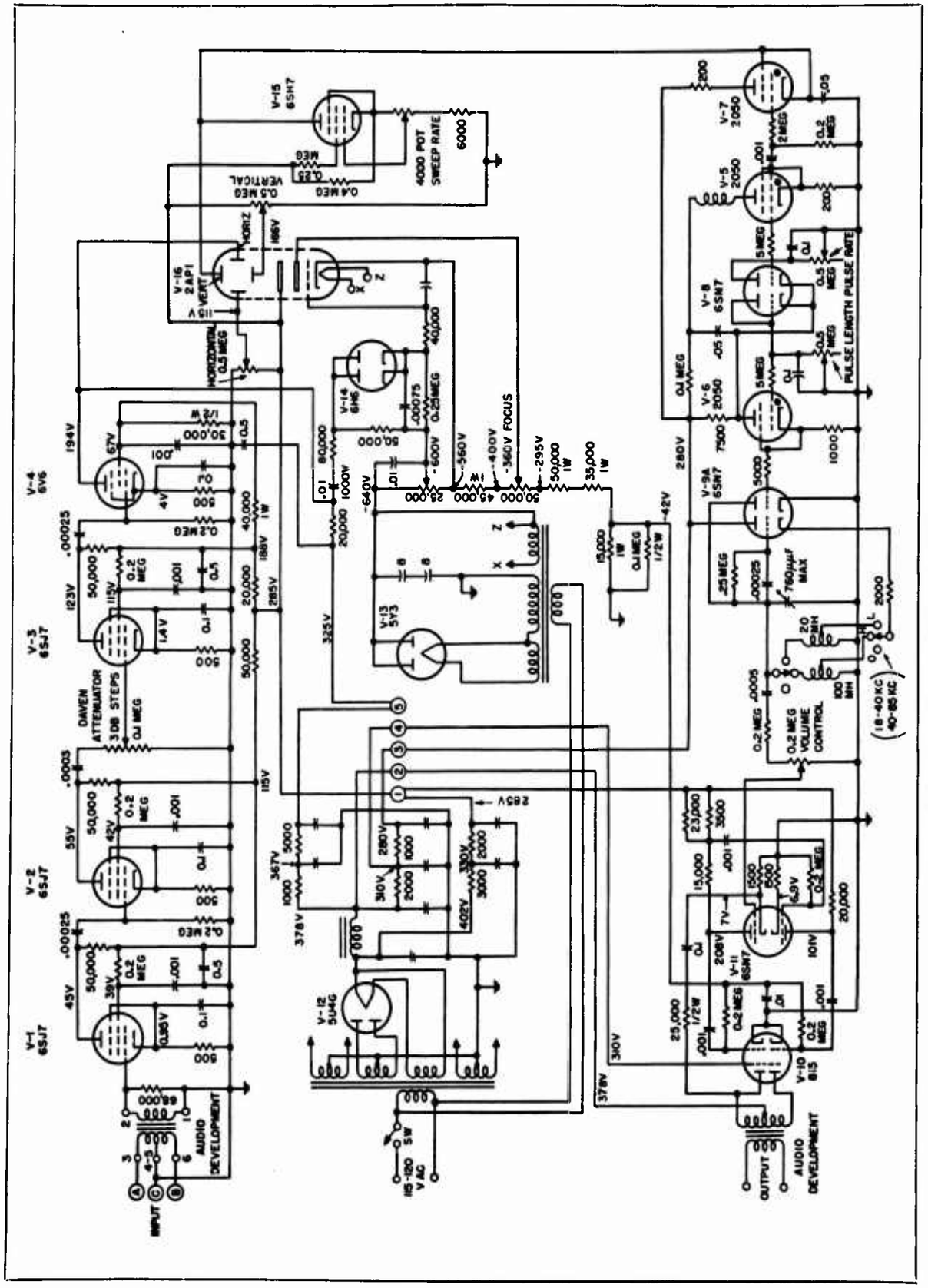

FIGURE 40. Schematic diagram of portable calibrator, Model I.

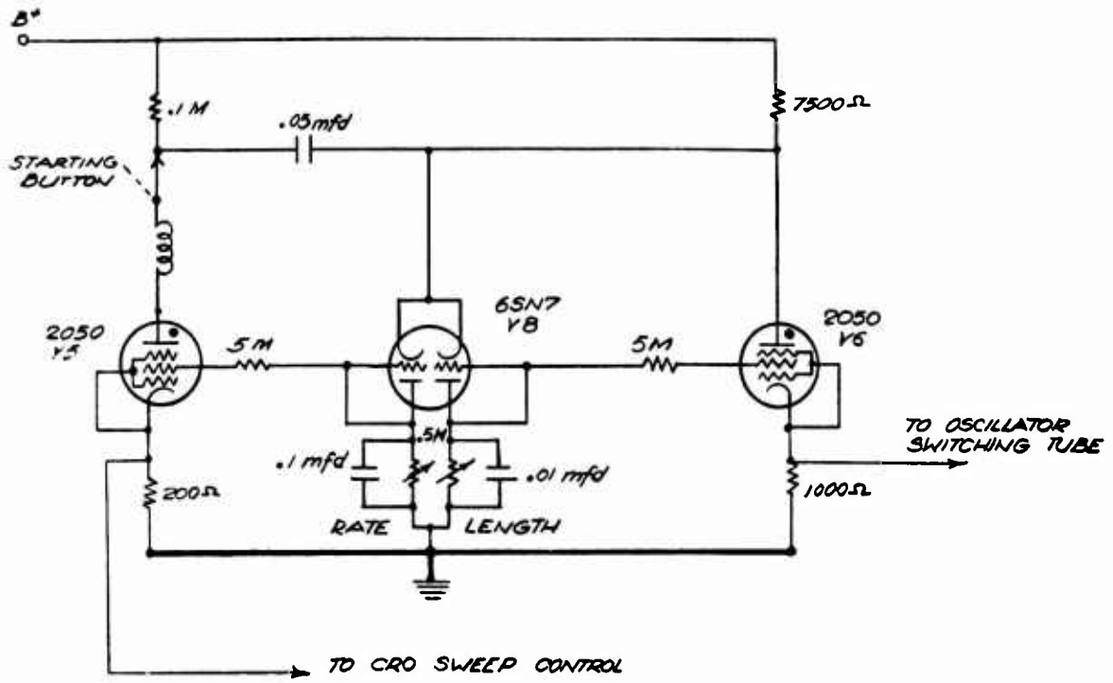

FIGURE 41. Pulse rate and pulse length control system.

come negative, and the 0.1- and 0.01-μf capacitors acquire a negative charge through the rectifier V-8. The potential on the left side of the 0.05-μf capacitor falls below the ionization potential of V-5 because of the flywheel action of the inductor, and consequently V-5 is quenched.

Both thyratrons remain quenched as long as their control grids are held more negative than their firing points by the negative potentials on the 0.1- and 0.01-μf capacitors respectively. They re-ignite when the condenser potentials fall just below the firing point.

During the period when V-6 is quenched, the bias is removed from the oscillator switching tube and the oscillator functions. After an interval dependent on the time constant of the 0.01-μf capacitor and the 0.5-megohm rheostat, V-6 re-ignites stopping the oscillator. The length of the pulse transmitted by the oscillator is determined by this time constant and may therefore be varied by adjustment of the rheostat.

When the negative potential on the 0.1-μf capacitor falls just below the firing point, V-5 re-ignites and the cycle is repeated automatically without use of the starting button. The repetition rate therefore depends on the time constant of the 0.1-μf capacitor and its associated 0.5-megohm rheostat.

When V-5 ignites, a positive potential is developed across its 200-ohm cathode resistor, which potential is utilized to trip the sweep control in the manner shown in the complete circuit diagram (Figure 40).

Since there are no reactances in the cathode circuit of V-6, the d-c pulses are substantially square waves, and because the change in grid current causes a transient in the switching tube, the oscillator is started and stopped with rapidity sufficient to maintain good form in the output pulses.

If for any reason the repetition is interrupted, both thyratrons may remain ignited. Opening the starting button momentarily restores operating conditions.

Synchronized Horizontal Sweep System for Calibrator CRO. The purpose of this system is to provide means whereby (1) the horizontal sweep of the echo-repeater calibrator oscilloscope will be synchronized with the chosen pulse rate, and (2) the speed of the horizontal sweep may be adjusted to present the most desirable image (see Figure 42).

This purpose is achieved by charging a capacitor at a very high rate and then discharging it at a substantially constant rate which may be varied. The voltage developed by the charge on the capacitor is applied to the horizontal deflection plates of the

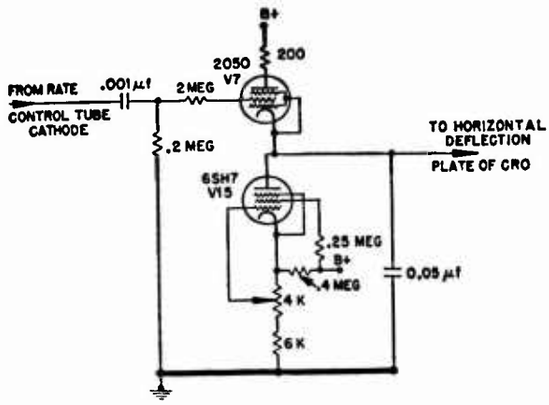

FIGURE 12. Synchronized horizontal sweep system.

CRO. At the initiation of each pulse by the pulsing system, an instantaneous voltage appears at the cathode of the pulse rate tube. This is applied differentially through the 0.001-μf capacitor to the grid of V-7, thereby igniting it. As a result, a surge of current passes into the 0.05-μf capacitor through the 200-ohm protecting resistor and V-7, the time constant of this charging circuit being of the order of 10^{-5} sec. This causes the spot on the CRO to move instantly to its starting position.

The 0.05-μf capacitor immediately starts to discharge through V-15, which is a pentode having its screen and grid voltage adjusted to give a substantially constant plate current independent of plate voltage. As the capacitor discharges, the spot moves across the CRO at a fairly constant speed, depending on the rate of discharge, which may be varied within reasonable limits by adjusting the 4,000-ohm potentiometer, which alters the grid bias. Owing to the slight slope of the plate current versus plate voltage curve of a pentode, the sweep speed is not precisely constant, but the linearity has been found adequate for the present purpose.

A fixed minimum cathode bias is applied to V-15 which must be sufficient to provide also a cathode bias for V-7 to prevent its ignition until its grid is made positive. This bias is obtained from the B voltage through the 0.4-megohm bleeder resistor.

Tube V-14 (see Figure 40) serves to increase the beam intensity when a vertical deflection voltage is present so that the indication is not weakened as a larger area is covered by the beam. This feature was included to overcome the objection of insufficient intensity of indication for use of the equipment in broad daylight, when the intensity control has been adjusted to safeguard the tube during zero signal voltage.

Calibrator Oscillator Switching System. The purpose of this system is to provide means whereby a supersonic oscillator may be switched on and off at a repetition rate of approximately 20 times per second, the on interval being adjustable between 0.0005 and 0.010 sec and the resulting pulse envelope being square in form and free from transients (see Figure 43).

The control for the pulse length and repetition rate is obtained from the pulse control system illustrated in Figure 41. The pulses generated in this circuit are delivered to the switching system in the form of on-and-off positive potentials which are applied to the grid of the switching tube V-9A through the 5,000-ohm resistor which limits the grid current.

During the off period the grid is positive, causing V-9A to conduct, thereby effectively imposing a short circuit on the positive half-cycles developed in the tuned circuit of the oscillator tube V-9B so that it cannot oscillate.

This oscillator is of the conventional Hartley type and is tunable in two ranges over the band of from 14 to 90 kc. The output is taken from the grid side of the tuning coil, at which point the waveform is found to be better than at the cathode.

When the positive bias is removed from the grid of V-9A, the resistance of that tube rises to approximately 5,000 ohms. The slight transient in the tuned circuit caused by the abrupt stoppage of grid current in V-9A "kicks off" the oscillator, which comes to full amplitude within approximately 2 cycles of the tuned frequency.

The change in the plate current of V-9B between the oscillating and nonoscillating condition is slight by virtue of the values chosen for the grid capacitor, the grid leak, and the cathode resistor respectively. Any change that does occur has no appreciable effect on the output, because the drop occurs across the lower third of the tuning coil, which has a resistance of less than 1 ohm. There are therefore no perceptible switching transients in the output circuit.

During the on period the load on the tuned circuit, imposed by the switching tube, causes some deterioration of waveform. For the present purpose this has not been found objectionable. It may be corrected by passing the output through suitable filters or by providing a negative bias for the control grid of the switching tube to raise its effective resistance. This bias may be supplied by a suitable

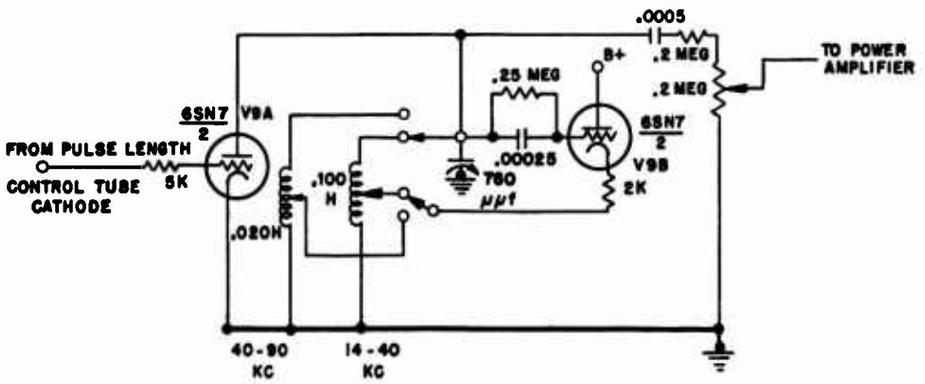

FIGURE 13. Oscillator switching system.

by-passed cathode resistor or by the direct application of a negative potential to the grid of the tube through a high resistance.

The merit of this switching system is that pulses of the desired lengths with a sufficiently square envelope may be transmitted without encountering any objectionable transients. The result is that the CRO shows a symmetrical pulse image with a flat top which is useful in making level comparisons. It has been noted that the form of the pulse envelope is good enough to make it possible to estimate the overall Q of a device being measured by comparing the form of the directly transmitted pulse with that of the pulse received from the device.

This switching system, with minor modifications, was used also in the dual frequency driver.

MODEL II

Figure 44 is the complete schematic diagram of the portable target calibrator Model II. It is a counterpart of Model I using miniature tubes, and the analysis of the operation of Model I can be applied equally well to this circuit. Perhaps the most interesting feature is the power supply, which uses two small thyratrons in a conventional full-wave circuit to obtain the positive voltage, and two small high-vacuum triodes in a voltage-doubling circuit to obtain the high negative voltage for the cathode-ray tube. It was feared that the 6C4 tubes used in the voltage-doubling power rectifier might not stand the voltage, and that the thyratrons might backfire before getting warmed up, causing damage to their cathodes. These troubles have not been observed in the limited laboratory use the calibrator has received.

INCIDENTAL OBSERVATIONS

The ranges of adjustments provided in the calibrator circuits allow selection of sweep duration of between 6 and 24 msec, pulse rates of between 7 and 30 pulses per second, and pulse durations of between 0.5 and 4 msec. These adjustments have been provided in the interest of versatiiity and are not strictly necessary. The pulse rate adjustment is probably of least importance, 20 pulses per second appearing to be a universally acceptable rate. There seems to be little need for increasing the pulse length beyond 2 msec, although it was initially felt that the overall effective Q of the calibration system might prevent short pulses from reaching full amplitude. The adjustability of pulse length was included to permit easy checking of this limitation. Long sweep durations may be found useful in calibrating low-frequency, high Q repeaters, when longer pulse lengths, and consequently greater distances between transducers, are required.

6.10 PERFORMANCE

6.10.1 Calibration Process

The calibration process which, except for the synchronization adjustment, is common to the four calibrators is carried out as follows: The echo-repeater transducers and the calibrator transducers are placed at the vertices of an equilateral triangle in a horizontal plane. Figure 33 illustrates how the transducers may be suspended over the sides and stern of a small boat, at a distance of 11 ft from each other. The usual depth of the transducers is from 6 to 10 feet below the surface of the water. Markers on the hydrophone cables make it easy to insure that the hydrophones are all at the same depth below the water surface.

When the transducers are in place, the calibrator

circuit is turned on. After a sufficient warming-up period, pulses from the stimulator appear on the oscilloscope screen. The frequency and power output of the pulses are adjusted by the oscillator controls. The pulse length and pulse rate are fixed by proper dial settings. The sweep circuit is synchronized with the pulse rate (manually with the nonportable, automatically with the portable type) and the attenua-

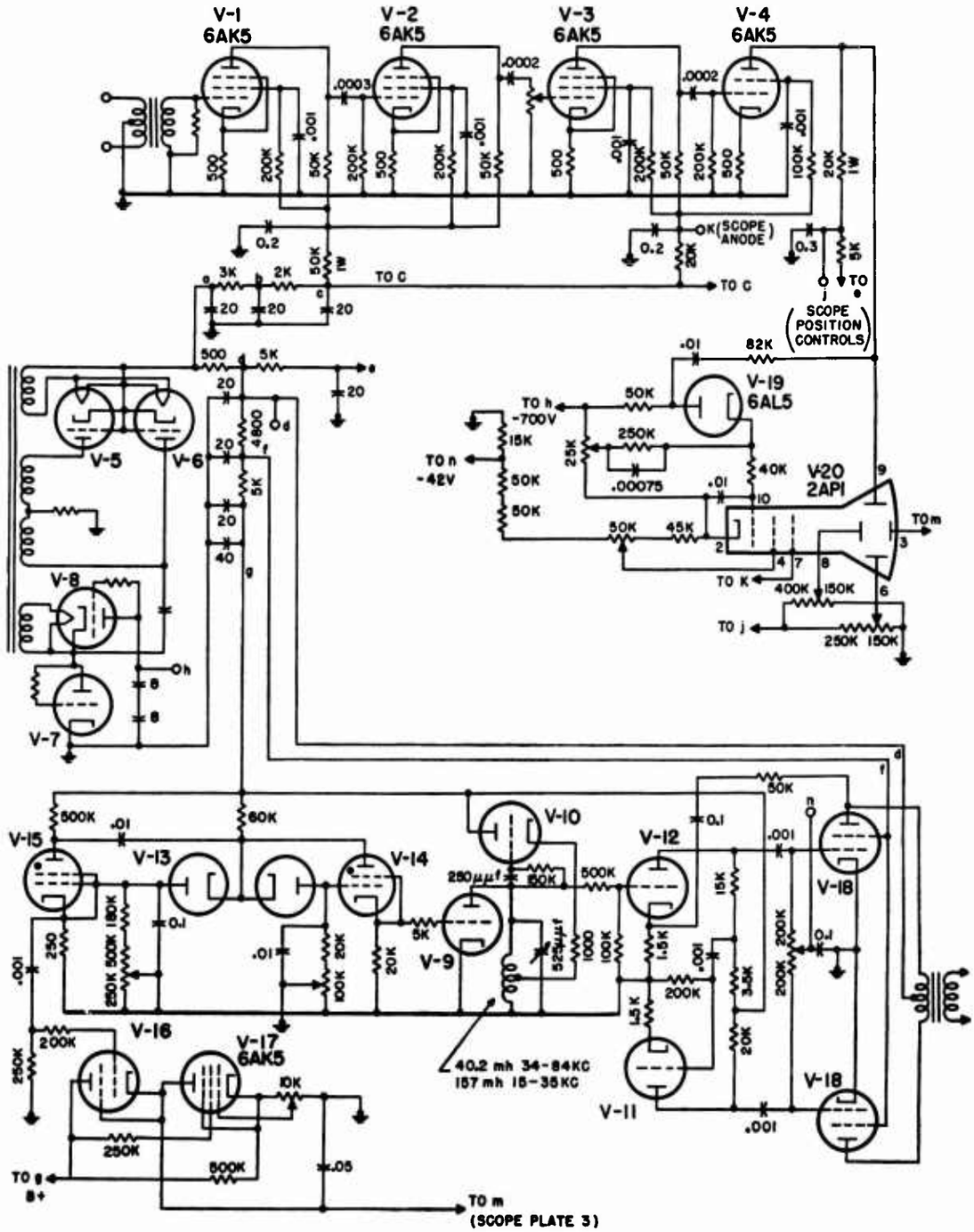

FIGURE 44. Schematic diagram of portable calibrator, Model II.

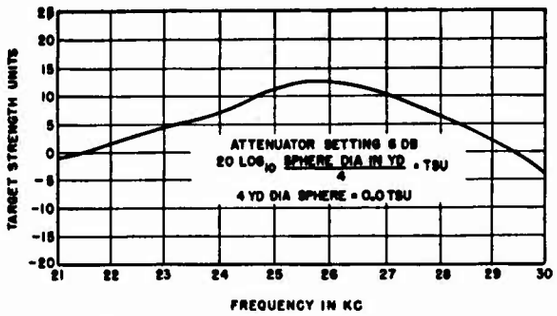

FIGURE 45. Calibration curve for Whale echo repeater.

tion adjusted until a stationary image of convenient height is maintained on the oscilloscope screen, indicating proper reception of the direct stimulator signal.

The echo-repeater circuit is turned on next. When it is functioning properly, the repeated signal also appears on the screen. Since the path difference for the direct and the repeated signals is 11 ft, the separation of the two images on the screen corresponds approximately to 2.2 msec. The pulse length should therefore be about 1 msec if the images are not to overlap. The attenuation of the echo-repeater amplifier is then adjusted until the echo signal has the same height as the direct signal.

Under these conditions the echo repeater simulates a sphere whose radius is twice the distance between the transducers, and a simple calculation gives the radius for any other setting of the gain control. If, for example, the attenuation setting required to obtain equal image heights is 30 db for an 11 ft separation of hydrophones, the radius of the equivalent sphere of the repeater is 22 ft. An attenuation setting of 18 db would then correspond to an equivalent sphere radius of 88 ft. This follows from the fact that decreasing the repeater attenuation by 12 db increases the output voltage, and thereby the equivalent sphere size, by a factor of about 4.

The equivalent sphere concept has led to a further development of calibration standards, in terms of the target strength unit. Target strength units [TSU] are defined by the relation

$$\text{TSU} = 20 \log_{10} \frac{\text{Sphere diameter in yards}}{4}.$$

An equivalent sphere of radius of 2 yd or 6 ft has a TSU of zero; a sphere with a radius of 22 ft has a TSU of 11.3. One may also say that a 22-ft sphere is 11.3 db above a 6-ft sphere in reflecting power.

6.10.2 Typical Results

The first model of the nonportable type of echo-repeater calibrator was constructed for the purpose of checking the performance of the Whale echo repeater (see Section 6.4.10). The results of one calibration run are shown by the graph of Figure 45. The data were obtained in the following manner: The distances between the comparator transducer and the stimulator transducer, between the Whale

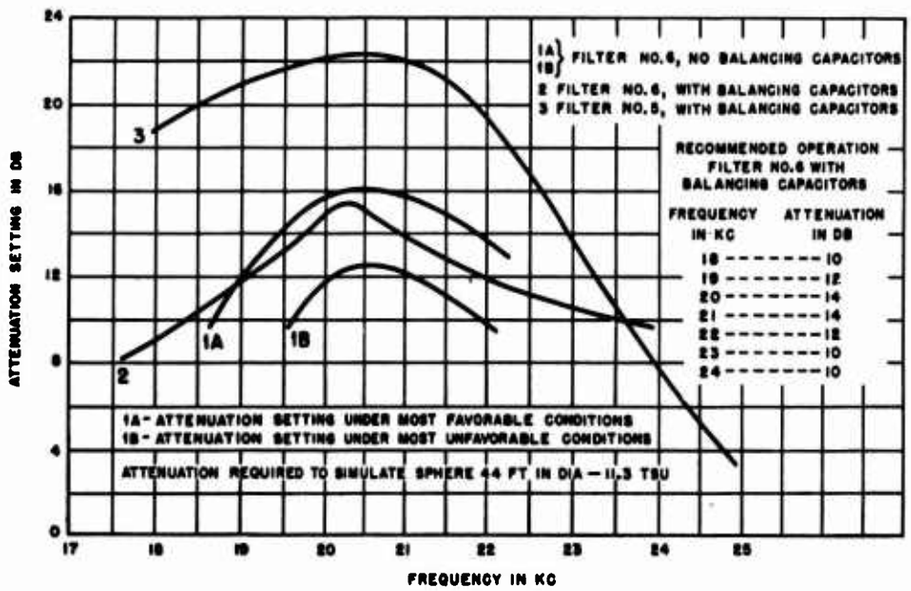

FIGURE 46. Calibration curves for Questor echo repeater.

receiving transducer and the stimulator transducer, and between the Whale transmitting transducer and the comparator transducer were fixed at 11 ft. The attenuation setting of the Whale was kept at 6 db throughout the test. The frequency of the stimulator pulse was varied from 21 to 30 kc. At 25 kc the amplitudes of the direct pulse and the repeater pulse on the oscilloscope screen were equal. It follows that at 25 kc the radius of the equivalent sphere of the Whale is 22 ft when its attenuation setting is 6 db. At other frequencies the gain of the comparator had to be adjusted to obtain the same height of repeated pulse image as at 25 kc. From the observed gains at various frequencies, the corresponding target strength units were then calculated.

The graphs of Figure 46 summarize the calibration data obtained from a series of tests made on the *Questor* echo repeater in President Roads, Boston Harbor, with the Model I portable calibrator. Curves 1A and 1B indicate the attenuations of the echo repeater, to produce a standard target strength of 11.3 units at different frequencies, under the most favorable and the most unfavorable conditions respectively. The difference of about 4 db between the two curves represents the normal uncertainty in making calibrations in water conditions such as those of President Roads. The results for graphs 1A and 1B were obtained with a filter in the amplifier but with no balancing capacitors connected to the transmitting transducer of the echo repeater. Curves 2 and 3 indicate average results when balancing capacitors as well as a filter were used.

6.11 CONCLUSIONS AND RECOMMENDATIONS

Experience with the echo-repeater calibrator has demonstrated the soundness of the acoustic principle employed and the usefulness of the device in in connection with any work involving the employment of echo repeaters to provide a known target strength. The equipment may take a variety of forms to meet specific needs. In many applications of echo repeaters which do not involve towing, it may be convenient to mount the calibrating transducers on a rigid framework attached to the echo repeater itself. In this way calibrations can be made intermittently while the repeater is in use. For deep-towed repeaters or other applications in which the repeater must operate for long periods without monitoring, much time can be saved and uncertainties avoided by making a careful calibration before the repeater is launched.

None of the models of the echo-repeater calibrator received sufficient production engineering development to qualify it as a manufacturing prototype. It is recommended that further development work be devoted to the design of the echo-repeater calibrator, and that the instrument be procured in limited numbers for use by sound schools and other naval groups engaged in the test or evaluation of sonar equipment. It is anticipated that further development work devoted to this subject will also provide design information useful for the construction of echo repeaters having built-in calibration facilities.

Chapter 7

ATTACK PLOTTERS

Automatic Target Positioner

The automatic target positioner is an attachment to the dead reckoning tracer [DRT] which indicates the location of a target at any given instant. It depends upon information received by radar equipment and automatically transmitted by the radar operator as he manipulates the range and bearing cursors of the A scope and the PPI. This information governs the action of small servo motors which control the position of a light spot, representing the target, upon the DRT plotting surface. The light spot may be utilized for the simultaneous tracking of several different targets. This device was developed by the San Diego Laboratory of the University of California Division of War Research [UCDWR].

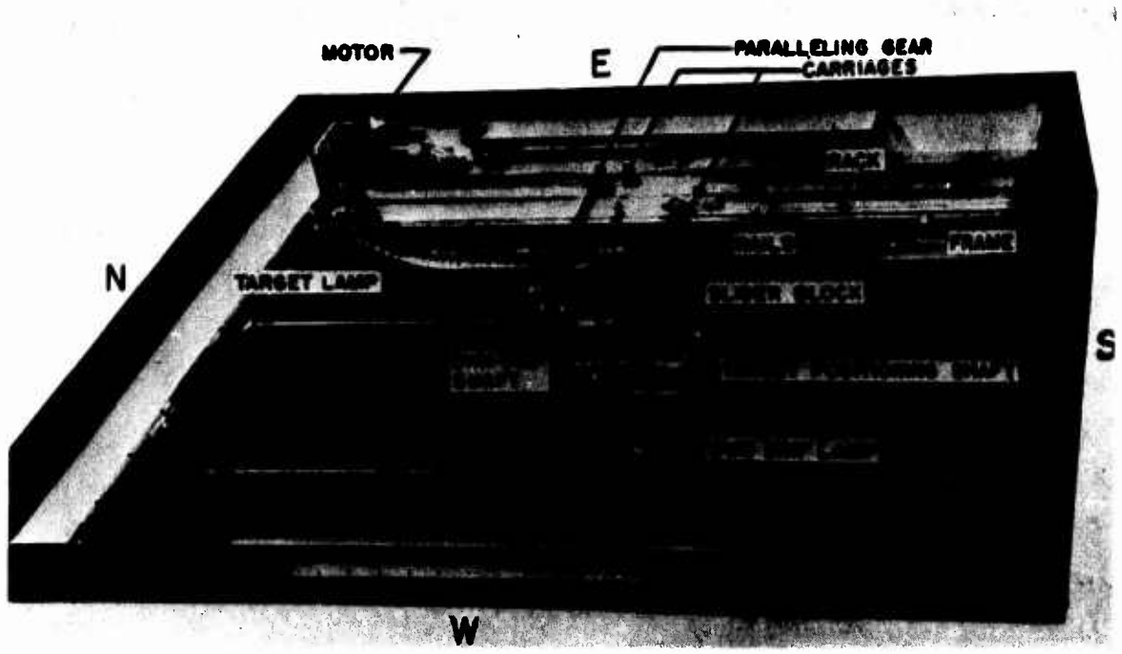

FIGURE 1. Dead reckoning tracer assembly.

7.1 INTRODUCTION

THE AUTOMATIC TARGET POSITIONER [ATP] is an adjunct which may be added to the standard Navy Arma dead reckoning tracer [DRT]. (See Figure 1.) Its purpose is to spot the position of a target on the geographical plot of the DRT automatically and in accordance with input data supplied by the radar operator in the normal course of his operations. At present, ranges and bearings are reported verbally to CIC by the radar operator or from the sonar hut and are then plotted on the DRT by hand with the aid of a drafting machine or by use of the compass-rose projector. This method is slow and its accuracy is dependent on the skill of the plotting personnel. At best, only a very few targets can be plotted simultaneously. The verbal transmission of information may also lead to large errors or blunders.

The automatic target positioner places a target position directly on the plotting surface of the DRT by means of a light spot representing the target. In operation, the following steps are taken. The radar operator locates a target in the usual manner and

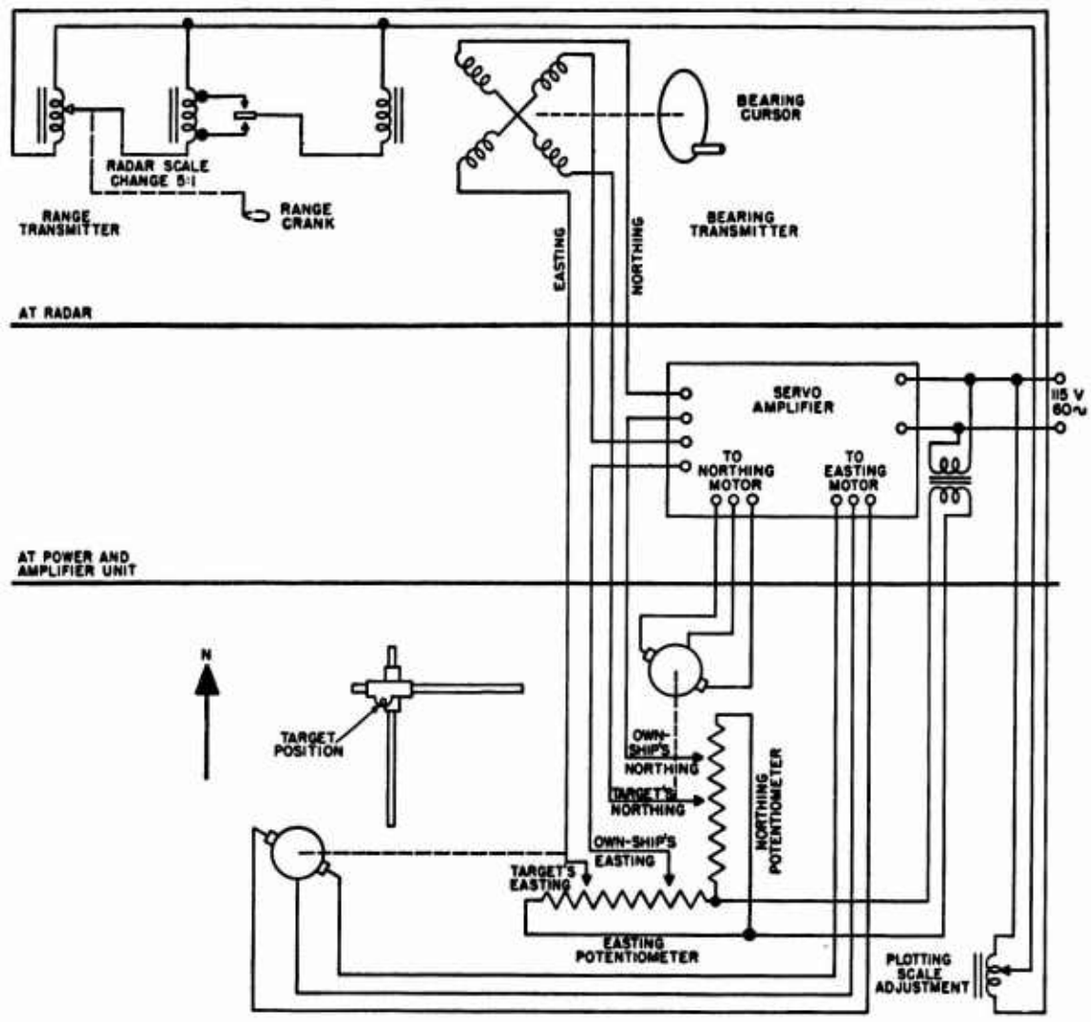

FIGURE 2. Partial electric schematic of the automatic target positioner.

cranks the radar range and bearing cursors into their proper positions on the A and PPI scopes. In so doing, he also transmits the target position data and thus automatically moves the target light spot to the correct position in relation to own-ship's light spot on the DRT.

7.2 GENERAL PRINCIPLES OF OPERATION

The magnitudes of the 60-c a-c voltages in the easting and northing circuits are set in by the manual operation of the range crank and the bearing cursor crank at the radar set. The range crank positions the slider of a precision Variac and affects both the easting and northing voltages uniformly and in proportion to the range (Figure 2). The bearing cursor crank rotates the rotor of a precision two-phase control transformer and thereby determines both the easting and northing voltages in such a way that $V_E = V \cos A$, and $V_N = V \sin A$, where the voltage V varies directly as the range, A is the true bearing of the target, V_E is the generated easting voltage and V_N is the generated northing voltage. That is, the polar coordinates of the target (with own ship as the origin), which are determined by the radar operator as target range and bearing, are converted into corresponding rectangular voltage components V_E and V_N. The next step is the employment of these rectangular target position voltages for the automatic positioning of a target carriage in the DRT with respect to own-ship's position. The basic scheme em-

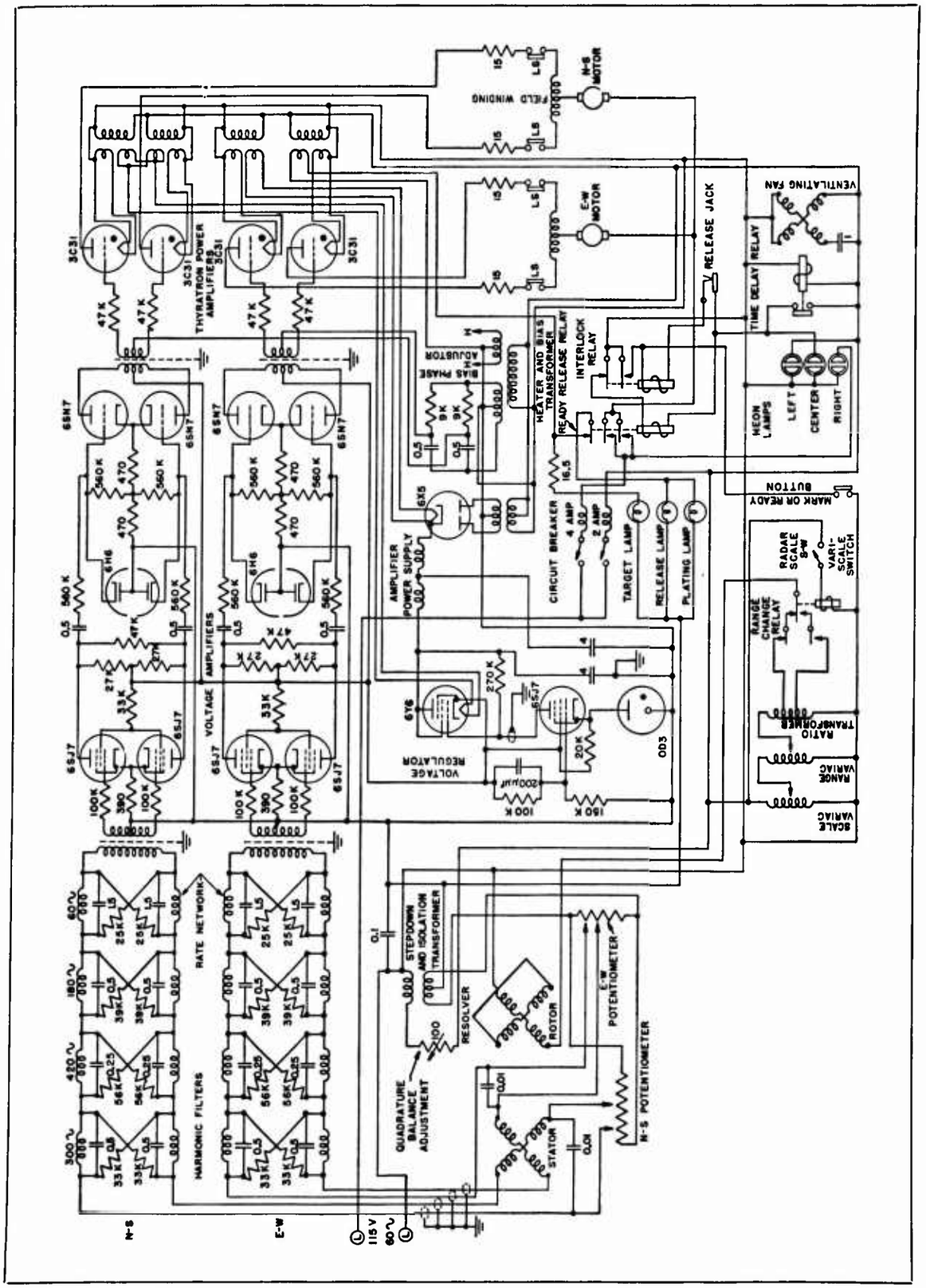

FIGURE 3. Electric schematic of the automatic target positioner circuit.

ployed is to set up easting and northing voltage scales in the DRT by means of linear potentiometers, which extend over the entire travel ranges of the DRT carriages in the east and north directions, and which thereby furnish a coordinate system for locating the target relative to own ship. Suppose for example that a voltage drop of 0.5 v per inch is established on the potentiometers with the positive terminals at the north and east ends respectively. Then for any arbitrary position of own ship on the DRT table (and of the corresponding own-ship electric slider contacts on the potentiometers), voltages $V_E = 1$, $V_N = 2$ would determine a position 2 in. to the right (east) and 4 in. up (north) from own-ship's position.

It remains to explain how the voltages set in by the radar operator cause the target carriage to seek the corresponding voltages on the DRT potentiometer. The method employed (see Figures 2 and 3) is to form circuits which place the E and N control and the DRT potentiometer voltages in series-opposition, and which drive positioning motors with the amplified difference voltage. Thus, to effect east-west positioning, the amplified unbalance voltage drives an east-west positioning motor, which is coupled to the target carriage in such a sense as to drive it in a direction tending to minimize the voltage unbalance and to be satisfied only when this difference is zero. A similar and simultaneous action in the north-south direction produces a resultant rest position of the target carriage, determined by the input coordinates which are set in by the radar operator.

Full details concerning the components and accessories of the ATP may be obtained by consulting the laboratory completion report of the UCDWR on the DRT.

Antisubmarine Attack Plotter

The antisubmarine attack plotter is an instrument which traces upon an oscilloscope screen the courses of own ship and the target during an antisubmarine attack. Speed and bearing information from the ship's log and compass serves to maintain proper position of own-ship's spot upon the screen. The oscilloscope sweep, starting from own-ship's position, as an echo-ranging ping is emitted, moves across the screen in a direction determined by the bearing of the echo-ranging projector. Upon reception of an echo, the sweep terminates in a bright spot which shows the position of the target. Through screen persistence, the position spots remain visible for several minutes and thereby trace out the courses of the two vessels. The instrument also generates a "predictor line" of adjustable direction and length, which appears on the oscilloscope screen as a bright streak, extending forward from own-ship's position. This makes it possible to determine the correct range and bearing to be used by the depth-charge projectors in a forward-throwing attack. The instrument was developed by the General Electric Company under the auspices of the National Defense Research Committee.

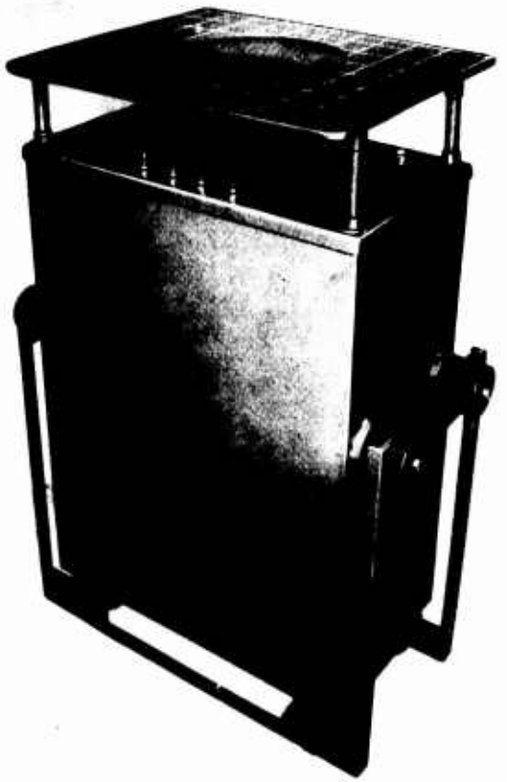

FIGURE 4. The General Electric antisubmarine attack plotter [ASAP].

7.3 INTRODUCTION

In an antisubmarine attack made by a surface vessel on a submerged submarine, the basic problem is to develop from range and bearing information, obtained by use of echo-ranging equipment, the general course and speed of the submarine so that the attacking surface vessel may determine the proper course to steer and proper time to fire. Any one item of information giving momentary range and bearing merely tells the attacking ship where the target is momentarily located relative to the attacking ship. Successive ranges and bearings, and rates of change of these quantities must be interpreted by the conning officer to yield an estimate of the target's course and speed. Changes in these rates must also be examined in order to determine whether the target resorts to some change in course and speed, since such changes may be expected from the submarine when the latter is engaged in evasive maneuvers.

The problem of delivering an accurate attack is complicated by a number of important factors.

1. At best, range and bearing information obtained from echo-ranging equipment under antisubmarine attack approach conditions is neither satisfactorily accurate nor obtained frequently enough. The accuracy and frequency of this range and bearing information depend on the ability of the equipment operator, the capabilities of the equipment itself, the water conditions affecting transmission of sound, and the effective size of the submarine as an acoustic reflector. The last-named factor is in turn dependent on a number of changeable conditions.

2. The maneuverability of the attacking vessel is a major factor in determining not only the accuracy, but especially the rapidity, with which range and bearing information is needed. Unless evasive maneuvers of the submarine can be detected sufficiently early, the lag of the attacking vessel in altering course may lead to inadequate countering of the evasive maneuvers.

3. Depth charges especially, and Hedgehog or Mousetrap projectiles to a lesser extent, require time to sink to the depth at which an explosion is to take place. Accordingly, the charges must be landed on the water in a definite location ahead of the submarine, this ahead-allowance depending on the estimated speed of the submarine and the estimated time required for projectile descent. Because of the necessity of making this allowance, an attacking vessel needs to perform a more difficult operation than would be involved in merely steering a collision course, and the conning officer must continually revalue the allowance which he is to make.

An experienced conning officer, particularly if he is assisted by a sound range recorder in proper operating condition, can ordinarily interpret the range and bearing information received from the echo-ranging equipment so as to conn his ship accurately. There are various qualifications which might be made to this statement, but it is desired to indicate that with the combination of experienced conning officers, good sound operators, and good equipment, an attack director is of much less value than under less favorable conditions. Since the problem is essentially a navigational one, an experienced conning officer may to a large extent perform in his head, perhaps even by inductive judgments, much that an attack director could do for him. However, particularly with the large expansion necessary in the number of antisubmarine vessels, it appeared that difficulties in developing a sufficient number of well-trained conning officers might indicate an important need for attack directors.

Because of the complicated character of the conning problem, as illustrated by the factors listed above, and because of uncertainties as to the best method of presenting attack director information, it was desirable to develop and examine a number of different designs of attack directors. In general, these attack directors were assigned the function of assimilating the echo-ranging data during an attack, and of indicating to the conning officer, either by plotting or computing techniques, the proper attack course to be steered and the proper time for release of depth charges or for firing ahead-thrown missiles.

The *antisubmarine attack plotter* [ASAP],[a] as its name implies, utilizes the plotting rather than the computing technique (see Figure 4). The development of this device grew out of earlier work on a plan position indicator [PPI] for showing on a persistent oscilloscope screen the range and bearing of echoes viewed by the QC sound gear. The PPI presented a relative polar plot of own ship and target, and it was thought that a navigational plot, or map, of ownship's course and target's course would be more useful, particularly to less experienced officers. The present attack plotter automatically draws such a map on the persistent screen of a cathode-ray tube. These courses appear as a series of bright spots on the re-

[a] Originally called the oscilloscope course plotter.

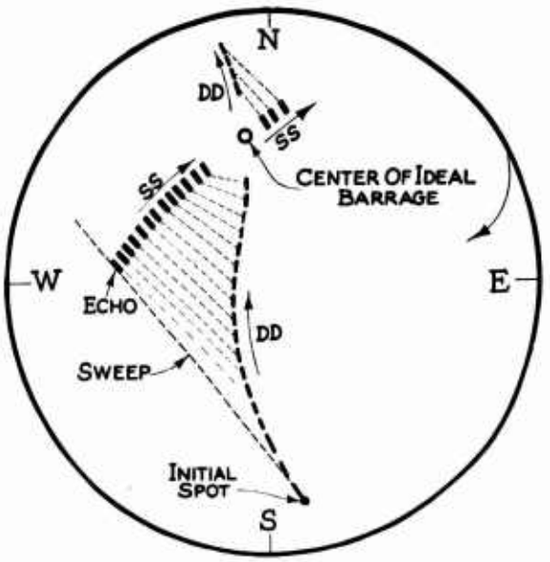

FIGURE 5. A typical attack plot on ASAP screen.

tentive screen and for a typical test attack situation would look somewhat as shown in Figure 5.

In the situation pictured, the attacking ship makes a QC contact with the submarine at a range of 1,500 yd dead ahead while steaming on course 325. Successive QC transmissions and echoes show that the target is drawing to the right, so the conning officer takes lead to the right in order to proceed to the attack. As the courses of both submarine and destroyer develop, he makes adjustments in his helm, so that when contact is lost at 350 yd (the last echo from submarine on left) the conning officer feels certain the ship's stern will cross the target's projected course sufficiently ahead to insure successful attack; that is, he will lead the target by an amount of time equal to the sinking time of the charges to the depth he has decided upon. In the sketch, pinging has been stopped after loss of contact, and so own-ship's course is not plotted. Moreover, we have assumed a friendly submarine and fire has been withheld, so that both ships continue on and contact is resumed. The QC operator scans astern and to starboard, and again finds the target with the echoes as shown, thus completing the traces.

The first tests of an instrument of this kind were made on the USS *Rathburne* at San Diego during April 1942. A more compact and improved instrument was then constructed and tested on the USS *Semmes* at various times during the summer. Statistical tests of a similar instrument were made on the Sangamo trainer at the West Coast Sound School, San Diego, during July 1942. The instrument was modified a little later by the addition of a predictor for use with forward throwers, which indicates on the screen the point to which the charges will be thrown. This modification was tested on the *Semmes* in October. Finally, the General Electric Company performed production design work and produced the ASAP in quantity for the Navy. It was made standard equipment aboard destroyer escorts and was installed extensively in other escort craft such as frigates and mine sweepers. It is difficult to estimate the exact number of equipments put into service but the total probably exceeds 1,000.

7.4 GENERAL DESCRIPTION

The oscilloscope attack plotter indicates on a persistent screen the position and course of the ship on which it is installed, and the position and course of a submarine in its vicinity with which contact has been made by sound echo-ranging apparatus. The course of own ship is supplied to the instrument from the compass repeater system, and from a variable transformer whose voltage output is proportional to ship's speed. The sound beam sent out from the QC gear is shown by sweeping the cathode-ray trace across the screen. The sweep originates at a point on the screen corresponding to own-ship's position, and at the same time as the QC transmission. This point is marked on the screen by momentarily brightening the trace. The direction of motion of the sweep is along the true bearing of the sound beam, and its speed is such as to reproduce correctly the distances of objects from which echoes are obtained. The position of a submarine is marked on the screen by using the echo to brighten the trace at that point. Own-ship's trace and the echo trace form a map on the face of the tube. This map persists for about 2 min if the tube's face is properly shielded from light by a viewing hood, or if the room is reasonably dark.

There is a transparent plotting table mounted directly above the screen on which a more permanent record of the traces can be marked with a grease pencil. In general, own ship and the target both move off screen after an approach. If it is desired to maintain contact with the target for a second approach, a larger transparent sheet can be laid on the plotting table and the traces marked on this. When the traces move off screen, they are brought back by turning own-ship's positioning controls, and the tracing sheet is shifted to match the new position of own-ship's trace. In this way a continuous record of

the motions of own ship and target may be kept over a long period.

The attack plotter sets are designed to be used on the bridge or in the chart room by the control officer who is planning an antisubmarine attack. The courses on the tube, as he views them, are represented on a true bearing scale with south on the side of the tube by the observer. Positioning knobs allow the observer to shift his own-ship's position on the screen at any time, north or south and east or west. The entire instrument can be used as a position plan indicator by turning off the variable autotransformer supplying own-ship's speed.

Once a submarine has been located by standard searching methods, echoes begin to appear on the screen of the tube. If contact is lost, the observer can see where the QC operator should scan to re-establish contact. Conversely, he can see where he has searched unsuccessfully without finding a target. Spurious echoes due to water noise appear on the screen, and also echoes from wakes. Sometimes the former can be diagnosed by their randomness. It is necessary for the QC operator to maintain good contact with the target; otherwise the submarine trace on the screen is not complete enough for the control officer to decide what maneuver the submarine is executing, and to conn the ship accordingly. This requirement is best met when the sound gear includes the right-left bearing indicator [RLI or BDI], which aids the sound operator in keeping the center of the sound beam fixed on the point of the target that gives the strongest echo. If the RLI is not available, a possible alternative is for the sound operator to determine the two cutoffs of the target and then to indicate the center bearing on the oscilloscope by setting the projector on the center bearing and pressing a foot pedal which intensifies the next echo on the screen. This foot pedal is not normally included with the attack plotter but can be added if necessary.

By pressing a predictor knob at the left of the tube, the operator can project a line on the screen, centered about own-ship's position. This line serves two purposes: (1) If the predictor knob is in the central position, the line lies along own-ship's course and is useful in estimating whether this course bears the desired relation to the target. (2) When a forward thrower is being used, the length of the line can be adjusted to match the range of the projectile. Moreover, by turning the predictor knob, the line can be rotated up to 20 degrees on either side of own-ship's course so as to bring its end in a more favorable position with respect to the target on the screen. The final true bearing of this line is read on a synchro repeater, and the operator of the forward thrower should keep his projector trained on this bearing.

7.5 MODE OF OPERATION

Own-Ship's Position Indication

The neck of the cathode-ray tube passes through two yokes fitted with deflection coils and through a focus coil (see Figure 6). When the focus coil has approximately 7 ma flowing through it, a sharply defined bright spot is focused near the center of the screen. By applying a d-c voltage to the north-south pair of coils on the stationary course plotter yoke, the beam can be deflected from the center of the screen to a new position along what is designated as the N-S direction on the screen. A voltage applied to the coils on the other sides of this yoke deflects the beam in the E-W direction. In each case the linear deflection is directly proportional to the voltage applied. The mapping of own-ship's course is effected by applying properly changing voltages to these pairs of deflection coils from two potentiometer units. The movable arms of the potentiometers are driven mechanically at rates proportional to ship's speed along the N-S and the E-W directions. The way in which this is accomplished is as follows.

Scott-connected transformers are supplied from the three field leads of the compass repeater. The two pairs of output leads from the Scott transformers supply a-c voltages proportional to the components of the ship's heading in the N-S direction and in the E-W direction, i.e., to cos a and sin a, where a is the ship's true heading. It is arranged also to obtain from a variable autotransformer an a-c voltage in phase with the Scott transformer voltages and proportional to ship's speed in magnitude.

The a-c voltages from the Scott transformer outputs are applied to the voltage coils of two special watthour meters, while the a-c voltage from the variable autotransformer is applied to the current coils of the two watthour meters, in series with each other and a fixed resistor. The disk of the N-S meter turns at a rate proportional to ship's speed times cos a, and the disk of the E-W meter turns at a rate proportional to ship's speed times sin a. A reversal of direction of rotation of the N-S disk occurs each time the ship's heading shifts through the E-W direction, and of the E-W disk as the heading shifts through the N-S direction.

The rotation of each watthour meter disk is fol-

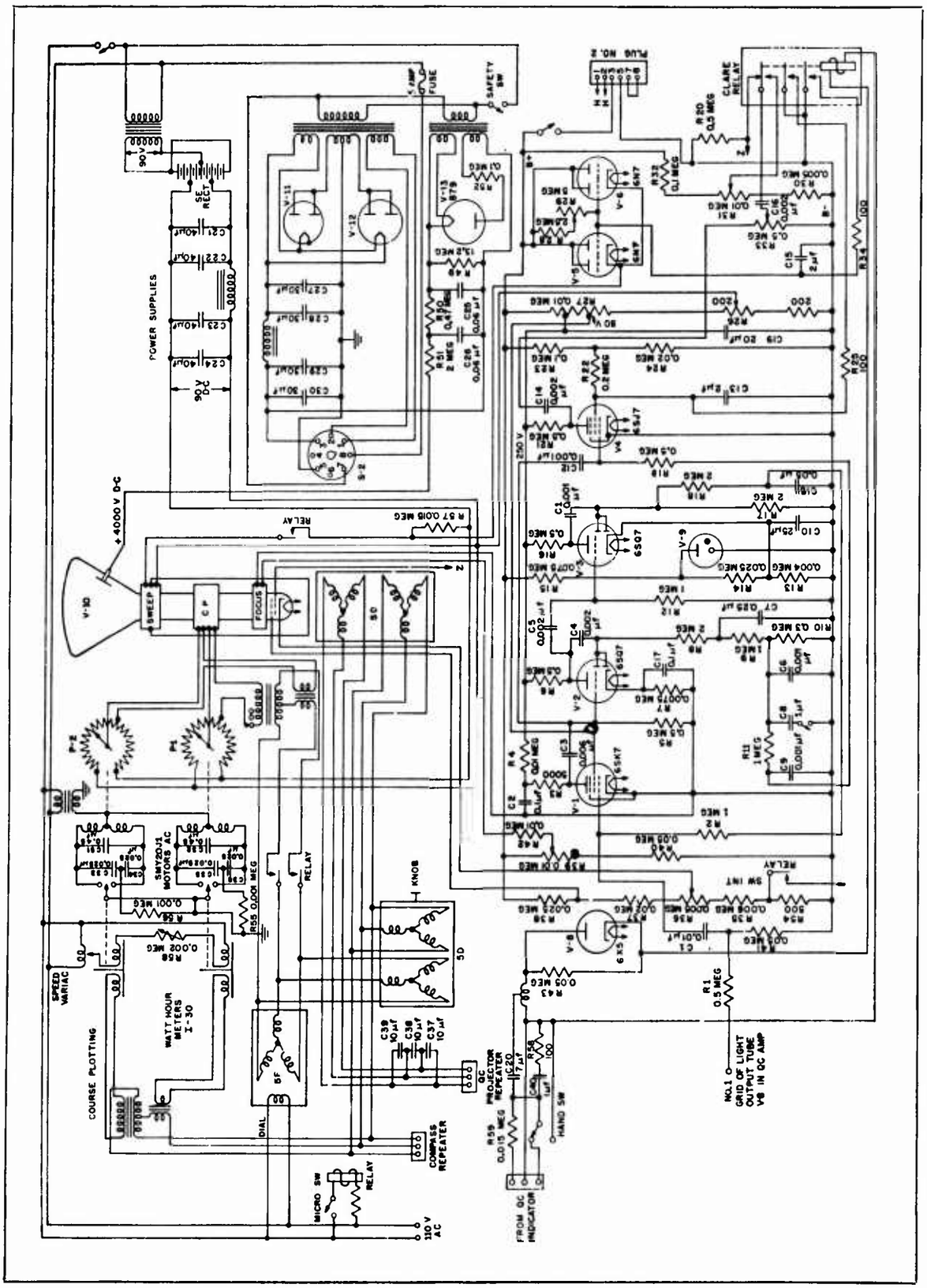

FIGURE 6. Schematic diagram of ASAP circuit.

lowed mechanically by a small synchronous inductor motor which acts as a reversible torque amplifier. Each motor has a gear box whose shaft can turn at 4 rpm. This shaft drives, through gears and a long shaft, the contact arm of the potentiometer with which it is associated; and it drives, directly, a pair of contacts which follow the motion of an arm driven by the associated watthour meter. The motor turns so as to keep the contacts away from the arm which is driven by the watthour meter.

Each potentiometer is mounted on the cabinet so that its winding can be rotated manually with respect to its contact arm. Hence, the moving spot representing own-ship's position can be repositioned at any time. If the potentiometer arm is driven to the end of the winding, it crosses a small gap (⅛ in.) and resumes contact with the winding at its other end. This reverses the polarity of the course plotter coil connected between the arm and the mid-point of the winding. The spot reappears on the opposite side of the screen and travels across the screen once more, or as the watthour meter dictates. The spot disappears before the arm has reached the end of the potentiometer winding, for the electron beam is limited in its traverse by the neck of the tube.

Sweep Direction Control

The yoke on which the sweep coil is wound is mounted on the shaft of a synchro differential generator whose three S leads are wired to the compass repeater system and whose three R leads are wired to the generator which repeats the relative bearing of the QC projector below the ship. Thus the sweep coil is positioned so that a voltage applied to the coil deflects the electron beam across the face of the tube in a direction corresponding to the true bearing of the QC sound transmission.

Keying, Sweep, and Own-Ship's Position

The voltage which deflects the electron beam is of sawtooth wave shape. The beginning of the sweep is synchronized with the transmission of the QC by a keying relay, which has contacts for triple-pole double-throw operation. When the relay coil is pulsed, the armature spring nearest to the frame of the relay grounds the sweep condenser (C-15) and on opening initiates the sweep, i.e., the sloping portion of the sawtooth voltage. Since the keying relay parallels the QC keying relay, the range of the sweep automatically shifts as the QC is shifted from 1,000 to 2,000 yd, 5,000 yd, or hand keying. On a 9-in. oscilloscope tube, ranges beyond 2,000 yd do not appear, the sweep goes off the edge of the screen as the current through V-5 and V-6 (6N7's) continues to increase. Sixty-five milliamperes through the sweep coils gives a deflection of 8½ in. The control of sweep intensity is by R-36, which varies the voltage of the cathode of the oscilloscope with respect to ground.

The middle armature spring of the relay momentarily grounds the screen grid of tube No. 4 (6SJ7) to reduce amplification of the reverberation noise following the QC transmission.

The outer armature spring is used to brighten the spot on the oscilloscope screen at the time when the sweep starts. This is done by momentarily connecting condenser C-16 to a charging circuit, and then discharging it on to the grid of the oscilloscope when the keying relay opens. The brightness of own-ship's spot can be regulated by adjusting the spot intensity potentiometer R-31, which determines the voltage to which C-16 is charged. The brightening of the initiation point of the sweep allows the course of one's own ship to be traced on the screen, as this initiation point moves about under the influence of the course plotter coils.

The keying relay is energized by the discharge of a 7-μf condenser through its coil and rectifier tube V-8 (6X5) whenever the QC keying relay is closed. The pulse from the condenser is stepped up in voltage by a transformer to give faster operation of the relay. The rectifier tube prevents the relay from being energized when the QC keying circuit is opened.

Echo Reception

To place an echo visually on the sweep, an audio signal from the QC receiver-amplifier must reach the grid of the cathode-ray tube. The signals from the QC receiver vary greatly in intensity with the gain setting and include a large amount of local reverberation noise which would cause distracting traces on the screen without contributing any useful information. Moreover, the true echoes from a target have an appreciable length and give short lines (¼ or ⅜ in.) on the screen, instead of points. A more definite trace of the submarine's path is obtained if the circuit is designed so that only the first part of each echo appears on the screen. With these ends in view, the echo-receiving circuit includes three kinds of volume control:

1. A time variation of gain. The purpose of this

is to reduce sensitivity just after transmission of the QC signal in order to avoid cluttering up the screen by reverberation traces. This is accomplished by grounding the screen grid of V-4 by the keying relay at the instant of transmission. The screen grid regains voltage (and sensitivity) at a rate determined by R-22 and C-13. A time constant of 0.2 sec for this circuit has been acceptable in practice.

2. An average control of sensitivity to match the strength of signal received from the QC. Connection is made in the QC amplifier to the resistor on the grid of the power tube which supplies the QC red light output. A part of the signal from this point is fed through C-1 on to the grid of V-1 (6SK7) and is amplified and fed through C-3 and C-12 to the grid of V-4 (6SJ7). From the plate of V-4, the amplified signal goes to the oscilloscope grid via condensers C-14 and C-16. The echo intensity is controlled by potentiometer R-33.

The signal from V-1 is also amplified by V-2 (6SQ7) and V-3 (6SQ7) via C-5. This signal is rectified by the diode half of V-3 and applied as a negative bias to the grid of V-1. The time constant of this control determined by C-18, R-17, and R-18 is approximately 0.2 sec. This slow AVC partially equalizes the intensity of the audio signals being amplified and keeps the general sweep level constant.

3. A control for shortening the duration of a strong echo on the screen. This function is performed by the diode portion of V-2 which rectifies the signal coming through C-4 and so applies momentary negative bias to the grid of the output tube V-4 when a long and strong signal is received. Condensers C-6, C-7, C-9, R-8, R-9, R-10, R-11, and R-19 determine the time constant (approximately 0.05 sec) of this fast AVC and the amount of the suppressing action, and finally filter the audio signal from V-2 to prevent its controlling the grid of V-4.

When the right-hand control switch is positioned on echo, the condenser C-8 is connected between the common point of R-9 and R-10 and B−. The output of V-2 is shorted to ground through C-8 and the short AVC is out of action.

When the switch is on the AVC position, condenser C-8 is opened and the short AVC control comes into operation.

Predictor for Forward Throwers

To place a line on the screen to indicate the position of the center of a forward-thrown charge pattern in relation to the submarine, it is necessary to press the control knob to the left of the screen. This closes a microswitch which energizes a four-pole relay. The relay opens the sweep coil so as to return the sweep to own-ship's position, shorts resistor R-54 in the cathode of the cathode-ray tube to brighten the spot, and energizes the primaries of a pair of Scott-connected transformers from a 5D synchro whose rotor is mechanically connected to the predictor knob. The secondaries of these transformers are connected in series with the course plotter coils and ring potentiometers. The transformers impose a directed 60-c a-c voltage on the spot. This produces a line whose length is proportional to the output voltage of the transformers and whose direction on the screen is changed by turning the rotor of the 5D synchro with the predictor knob. If the knob is set in its central position, the line points along the heading direction of the ship and turns as ship's heading changes. Stops prevent the knob from being turned more than 20 degrees to the left or right, as this represents the maximum train of present forward throwers.

The Scott transformers are tapped so that the output voltage can be changed. This permits the length of the line to be varied with ship's speed. A multiple switch, mounted behind the speed control autotransformer, effects the proper tap changes. On ships having a Pitometer log, this correction is put in manually by a switch mounted directly on the cover. The switch can be set well in advance of the attack if it is to be carried out at some previously decided constant speed.

Power Supplies

The total power requirement of the attack plotter is approximately 2.3 amp at 110 v, 60 c. Power supply chassis are located at the bottom of the cabinet. Transformer T-1, two 5U4G rectifiers, and a filter circuit with 30-μf condensers and a swinging choke supply approximately 400 v for the circuit box; transformer T-2, an 879 rectifier, and filter condensers followed by two 1.0-megohm protective resistors furnish 4,000 v for the screen of the oscilloscope. A safety switch under the large power supply opens when the unit is removed from the cabinet. This breaks the 400- and 4,000-v circuits, but leaves the 110-v a-c line and a 90-v d-c supply in the small chassis box still on. Care should be exercised if the 4,000-v supply to the oscilloscope tube is ever operated with the cabinet open.

The 90-v d-c supply (from transformer T-3, a selenium rectifier, condensers, and choke) powers the 500-ohm potentiometers P-1 and P-2, and provides a

small negative current through the sweep coils and R-57 for centering the spot.

Pitometer Log Follow-Up

On ships having a Pitometer log it is easy to install a small repeater which automatically positions the arm of a variable transformer, to supply voltage proportional to ship's speed. If there is no Pitometer log or similar system to which an automatic follow-up can be applied, the speed transformer must be set manually as the ship's speed changes.

Compass Inverter

On ships which have a synchro generator repeating the gyrocompass, there is no difficulty in supplying ship's heading to the course plotter unit. The primaries of the Scott transformers and the field leads of the synchro differential generators connect directly to the field leads of the synchro generator. The load thus added to the gyrocompass repeater system is less than 25 w. Once an original alignment has been made, the course plotter units position correctly whenever the gyro is turned on, as do all the repeaters on the gyrorepeater system.

Special repeaters for the course plotter must be used on ships which have a d-c gyrocompass repeater system. A d-c repeater, connected to the ship's system, positions a synchro generator which supplies the course plotter unit with the proper voltages for heading indication.

Since the d-c repeater locks in at various positions, the synchro generator must be correctly positioned with respect to the gyrocompass whenever the latter is started. To effect this, the step-by-step motor circuit is opened by the switch button and the synchro generator is then positioned by moving the edge of the disk protruding through the cover. When the gyro indicates the ship's heading is north, the reference mark on the disk should be located in the center of the opening.

Mechanical Geographic Attack Plotter

The mechanical geographic attack plotter [MGAP] is a device for plotting own-ship's course and target's course in an antisubmarine attack. Although the original model (Type R) provided only a ship-centered plot of target's motion, the second and third models (Types F and L) give geographic plots, showing both own-ship's and target's course. Automatically controlled pencils produce the plots on the underside of a sheet of translucent paper lighted from below. The top surface of the paper is thus freed for the operator's use in making measurements and employing templates to plan the course of an attack. The plotter was developed by HUSL.

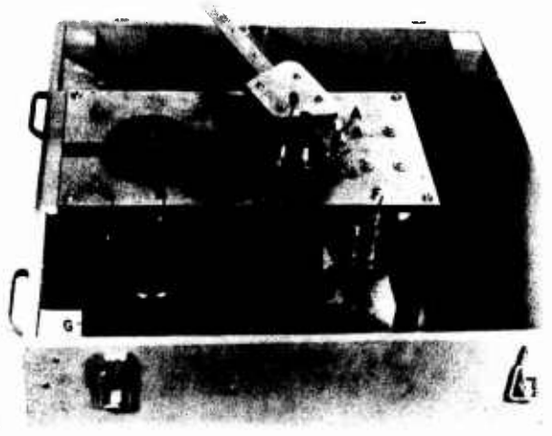

Figure 7. Mechanism of early model mechanical geographic attack plotter, Type R.

7.6 INTRODUCTION

The cathode-ray plotters, attack plotters widely used by the Navy, did not provide permanent traces of ships' courses on the oscilloscope screen. The *mechanical geographic attack plotter* [MGAP] was an attempted improvement, providing permanent traces from a completely mechanical aid for the conning officer.

Instruments of three different types were built and tested. The first was designed to produce a simple relative (ship-centered) plot, and is designated Type R. The submarine's course was traced on a circular plotting board by a pencil attached to an arm of variable length pivoted at the center of the board, at which point own ship was imagined to be. The second, Type F, was a true geographic plotter, providing a trace of the path of own ship as well as that of the target. A carriage corresponding to own ship was driven by a single friction wheel rolling on a plane at a speed proportional to that of the ship and in a direction representing own-ship's true bearing. Mounted on the carriage was an arm which traced

the course of the target as in the first design and also a pencil to trace own-ship's course.

In the final Type L plotter, the motion of the carriage representing own ship is controlled by two lead screws at right angles to each other in the manner of the odograph. The speeds of rotation of these screws are proportional, respectively, to the north-south and east-west components of own-ship's course. On the carriage is the arm whose angular position, governed by the orientation of the ship's projector combined with ship's gyro, represents the true bearing of the target, and whose length, governed by echo time, represents target distance. Pencils, one at the end of the movable arm and the other attached to the carriage, trace out the desired paths on the underside of a translucent sheet of tracing paper illuminated from below to eliminate shadows.

The lead-screw type plotter functioned essentially as planned. However, interest was transferred to the development of computing equipment which would solve the entire attack problem; MGAP merely depicts a history of the maneuvers. The project was therefore terminated.

7.7 RELATIVE PLOTTER—TYPE R

The mechanism of the ship-centered Type R plotter is shown in Figure 7. A circular table rests on support *B*, which in turn supports the translucent plotting chart in such a manner that a pencil in holder *A* can trace the path of a submarine on the underside of the chart.

Three inputs were required to operate this mechanism: (1) ship's heading, (2) target heading, and (3) target range.

Ship's heading was obtained from a specially constructed compass card and soft-iron armature arrangement which provided a small a-c voltage that was a function of compass orientation. This voltage was amplified and used to drive a motor to rotate the plotting table in accordance with ship's heading.

Target range and bearing were introduced by means of two coaxial shafts located inside the hollow shaft of the plotting table. The outer shaft was synchro-driven to rotate with ship's projector. The horizontal arm holding the pencil was keyed to the upper end of this shaft, and thus its angular position corresponded to target bearing. A rack on this arm meshed with a pinion on the inner shaft and thus served to extend or retract the arm as the shaft turned. This shaft was likewise synchro-driven, with motor input taken from a manually operated range follower mounted on the QC range indicator. Thus the distance of the pencil from the shaft at any instant represented submarine range. A range scale of approximately 200 yd to the inch was adopted.

Since suitable targets were not available during the period this plotter was tested at sea, only qualitative performance was observed. As far as could be determined the unit operated according to design.

7.8 FRICTION-DRIVE PLOTTER—TYPE F

The basic component of the friction-drive plotter shown in Figure 8 was a carriage driven by a single friction wheel rolling on a plane at a speed proportional to own-ship's speed and in a direction representing own-ship's bearing. Pivoted on the carriage was a horizontal arm whose angular position at any instant corresponded to target bearing. The length of the arm was varied by a rack and pinion and made proportional to target range. A pencil attached to the carriage and one at the end of the arm produced a continuous record of the course of both own ship and submarine on the underside of a sheet of translucent paper stretched across a frame serving as the lid of the plotter.

Four input quantities were required: (1) own-ship's speed, (2) own-ship's bearing, (3) target bearing, and (4) target range. Each of these drove a specially designed ratchet-type motor — a motor in which a gear-wheel was rotated, tooth by tooth, by the action of a magnet on a ratchet arm. Pulses of current to the magnet were supplied by a thyratron triggered by a transmitting contactor.

On the assumption that completely reliable response could be obtained to electric impulses applied to such motors, the various drives on the carriage were not equipped with follow-up mechanisms. Instead, follow-ups were relegated to the electronic control chassis thereby reducing the weight and volume of equipment moving with the carriage.

One of the ratchet motors turned the carriage to own-ship's true heading in relation to a framework within which the carriage was free to move east-west while the framework itself was free to move north-south. The ship's speed motor drove a friction wheel that moved the carriage over the bottom of the plotter box at a rate proportional to the speed of the ship and in the direction of the ship's true heading. Since the mechanism controlling the target arm rotated with respect to the carriage, slip rings and brushes were provided for the inputs to target range and target bearing motors.

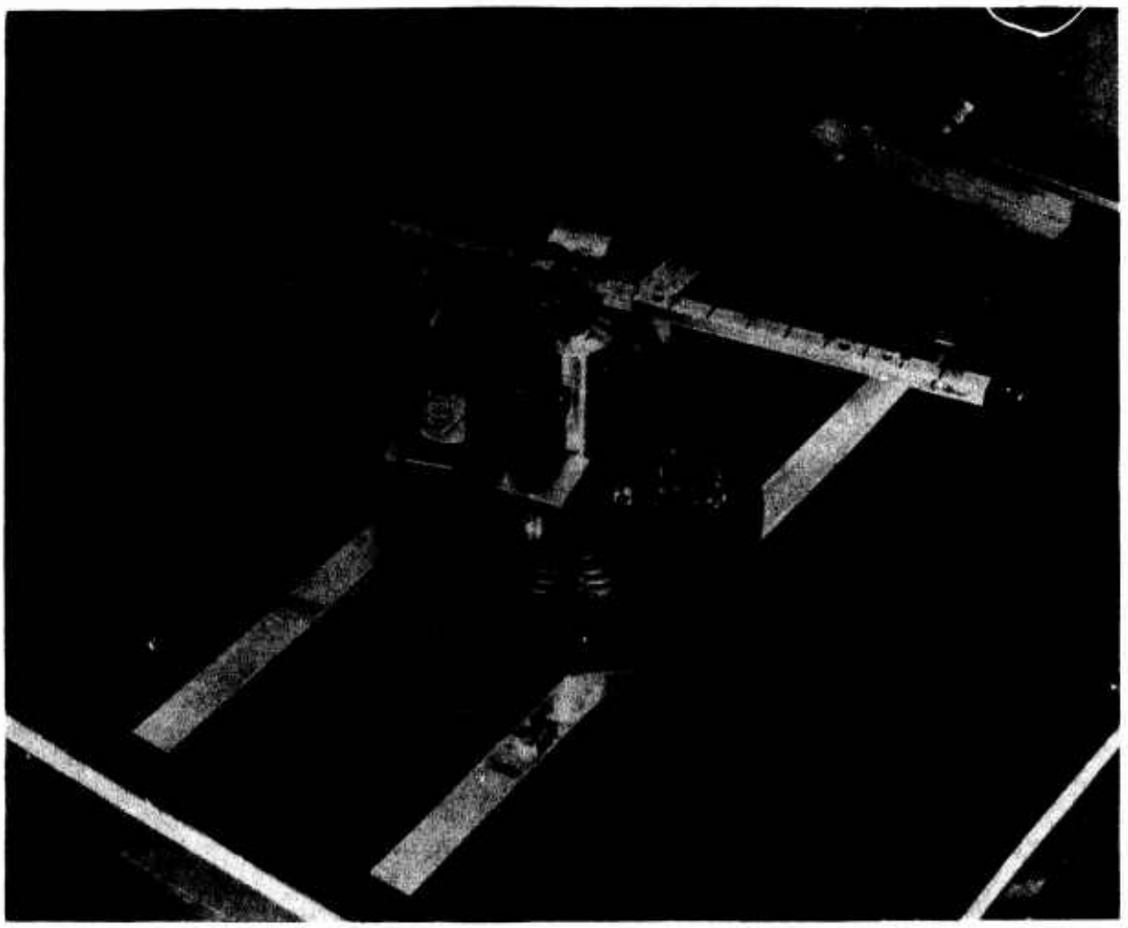

FIGURE 8. Traveling carriage of Type F geographic plotter.

Considerable mechanical backlash showed up in the initial tests. When this was reduced to a reasonable amount, the frictional load was so increased that the ratchet motors were unable to operate the unit, at least with the current pulses then available from the thyratron in the control circuit. Work on this plotter was therefore suspended in favor of the Type L unit.

7.9 LEAD SCREW PLOTTER—TYPE L

The Type L lead screw-driven plotting unit, shown in Figure 9 with its recording surface raised, was produced in cooperation with the Department of Terrestrial Magnetism of the Carnegie Institution of Washington.

7.9.1 General Description

Tautly stretched tracing cloth, treated to prevent absorption of moisture, presents a 24-in. square plotting surface. The true course of own ship and that of the target are both plotted (200 yd to the inch) by automatic pencils on the underside of this surface. Fluorescent lights within the box illuminate the surface in a way that eliminates undesirable shadows.

The auxiliary computing and driving equipment includes a dead reckoning analyzer, servomechanisms, power supplies, and gear boxes for adjusting rotation ratios. To facilitate testing, this auxiliary equipment was assembled on a breadboard chassis.

7.9.2 Sources of Input Information

The four fundamental kinds of information required by the geographic attack plotter are obtained in the following manner:

OWN-SHIP'S SPEED

Own-ship's speed is obtained from an overside im-

FIGURE 9. Geographic plotter, Type L, with plotting surface raised.

peller. However, any device that delivers information in the form of impulses occurring at a rate proportional to ship's speed might be used.

OWN-SHIP'S COURSE

The true course θ_S being followed by own ship is obtained from a compass-controlled servo system which may be either a control transformer servo installed directly on the ship's gyro line or a photoelectric magnetic compass follower such as the one used with the dead reckoning tracer. This information is used directly to indicate own-ship's heading and also to aid in resolving own-ship's speed into N-S and E-W components.

TARGET RANGE

Target range R is supplied by a potentiometer associated with the ship's sonar gear. It controls the length of the target plotting arm.

TARGET BEARING

The true bearing θ_T of the target may be derived by adding relative target bearing, electrically or mechanically, to own-ship's heading, or it may be derived from own-ship's sonar by means of a control-transformer synchro installed in the maintenance of true bearing [MTB] synchro line.[b] This angle determines the direction of instantaneous target vector.

7.9.3 Inputs to the Plotter

The block diagram of Figure 10 shows how the above information is transferred through the auxiliary equipment to the plotter.

Since the course of own ship is to be reproduced by the rotation of two lead screws at right angles to each other, it is necessary to convert own-ship's speed and course into E-W and N-S components of change of position. This is done by means of an integrator in the same manner as in the odograph and yields two rotations which are proportional, respectively, to the two rectangular components.

Target range is also transformed into an angular rotation. It is obtained from a follower added to the chemical range recorder and may be controlled either manually or by an automatic target-training device. This rotation is produced by a servo controlled by the potential difference between the sliding contacts of a pair of potentiometers, one contact attached to the above follower and the other to the shaft of the servo. The angle of rotation of the powered shaft thus becomes proportional to change in target range.

Target bearing and ship bearing are also transferred to the plotter as angular rotations. In each case a control transformer synchro together with a follower mechanism similar to the above determines the angular position of a servo motor.

7.9.4 Operation of Plotting Mechanism

The five rotations representing the five input quantities just described serve to reproduce the motion of own ship and target in the following manner:

X AND Y COMPONENTS OF SHIP'S MOTION

Two lead screws are located along adjacent sides of the plotting box as shown in Figure 11. On each shaft is a nut through which a freely rotating shaft passes. On each end of each shaft is a gear that meshes with a rack in the frame of the plotter housing to assure proper alignment at all times. At the intersection of the two shafts is block A which slides

[b] See Division 6, Volume 15.

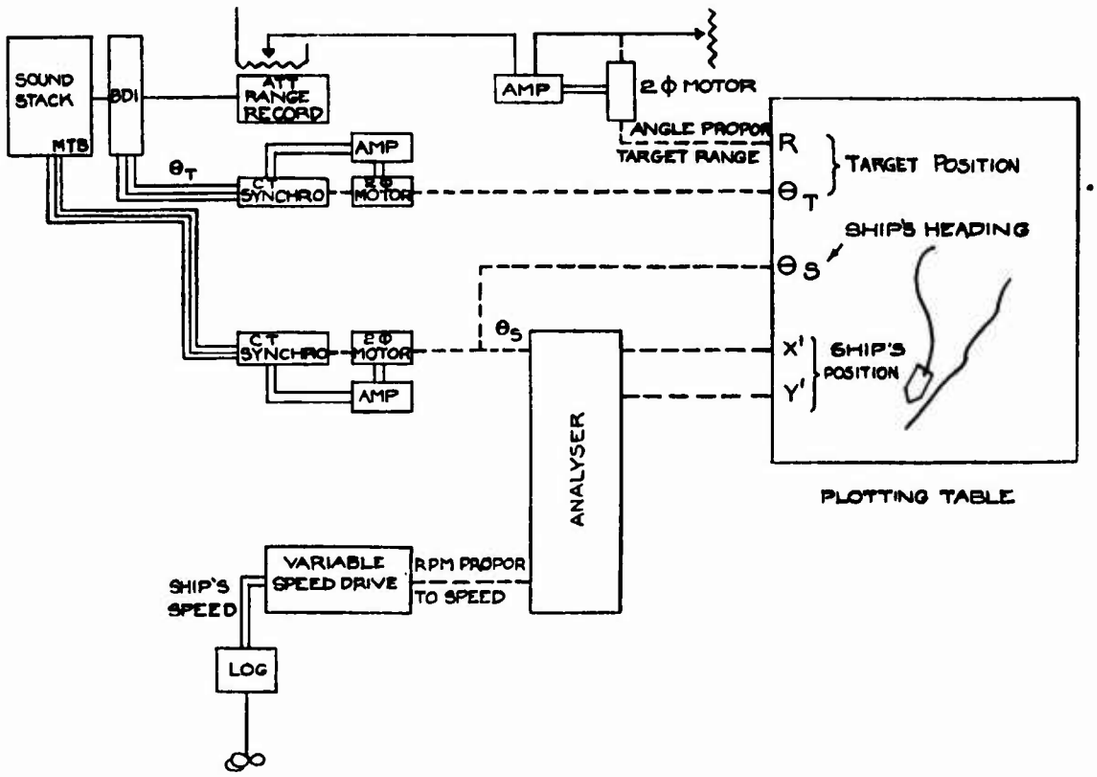

FIGURE 10. Schematic layout of components associated with MGAP, Type L.

freely along them in accordance with the motions of the nuts. The two rotations proportional to the rectangular components of the motion of the ship are applied to the two lead screws and thus, at any instant, the location of the block marks the position of own ship.

OWN-SHIP'S COURSE

The splined-shaft and bevel gear mechanism illustrated in Figure 12 is used to introduce the rotation representing own-ship's course. Because of the spline arrangement on each shaft, gear *D* which is mounted inside block *A* turns through the same angle as gear

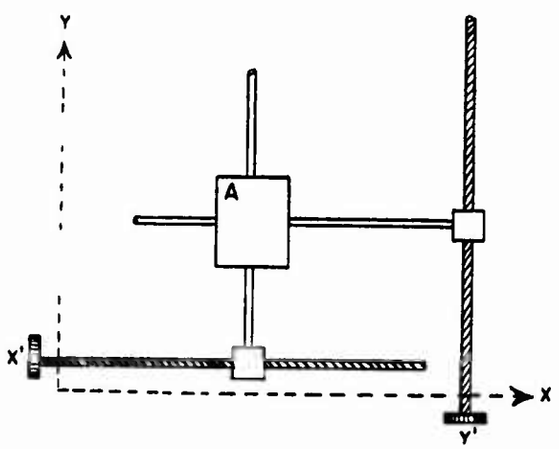

FIGURE 11. Relationship of lead screws to carriage of MGAP, Type L.

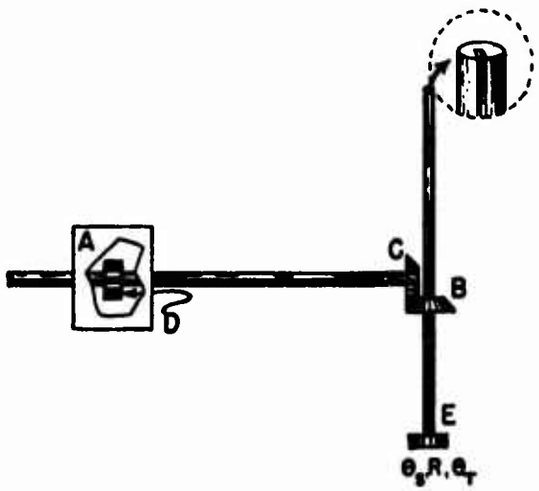

FIGURE 12. Splined shaft and bevel gear mechanism, MGAP, Type L.

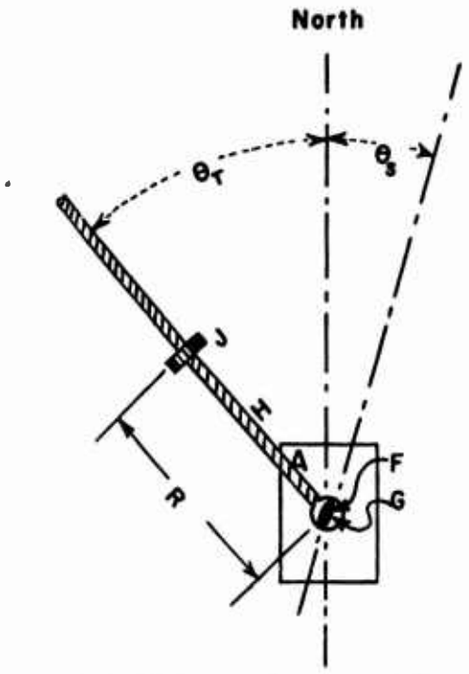

FIGURE 13. Result of rotations θ_S, R, θ_T.

E, independently of the position of the block. A small scale model of the ship is pivoted above the block and can be seen through the tracing cloth. This model is rotated by gear D in such a manner that it always shows own-ship's true heading (θ_S of Figure 13).

TARGET RANGE AND TARGET BEARING

Each of the two rotations which represent target range and target bearing is introduced by a similar splined-shaft and bevel gear mechanism. Above block A is a table (table G of Figure 13) free to rotate about the vertical axis. Its angular setting is determined by target bearing θ_T. Attached to the table is a lead screw H geared to the rotation which represents target range. The lead screw carries a nut J whose position on the screw thus corresponds to the position of the target. (The alternate method shown in Figure 9 accomplishes the same result by a pair of compound screws.)

Pencils mounted on table A and on nut J trace the paths of own ship and target on the underside of the plotting surface. Gear ratios are so chosen that 1 in. is equivalent to 200 yd for both own ship and target.

7.9.5 Tests and Results

Tests on the lead screw plotter were sufficiently extensive to show that the model was performing substantially as designed.

Operating as a dead reckoning tracer, the own-ship tracing of a circular course 6 miles long closed within 100 yd, an error of less than 1 per cent. For tests made in association with sound gear a stationary buoy was used as a target. The position of this buoy was repeatedly indicated within a circle of 50 yd in diameter. Some of the scatter was due to backlash which could have been reduced.

It was concluded that the errors in the device itself were no greater than, and probably less than, those of the information delivered to it. Studies were

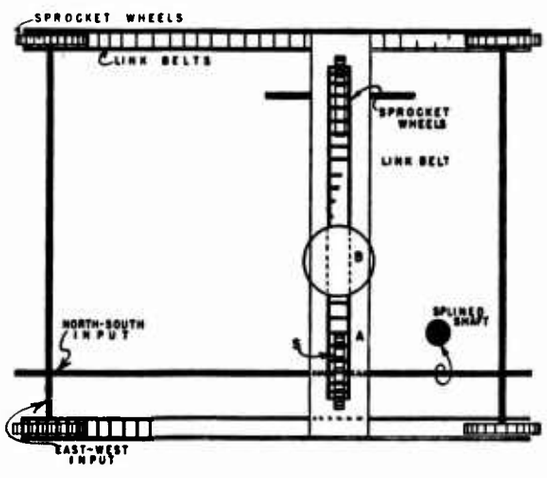

FIGURE 14. Drive for proposed link-belt plotter.

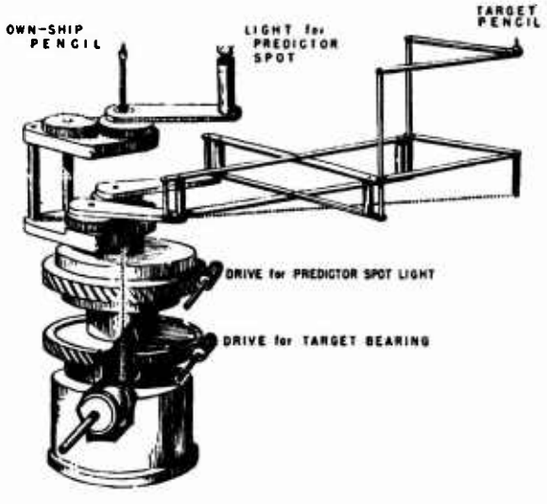

FIGURE 15. Center carriage of proposed link-belt plotter.

made of the errors to be expected in range and bearing input data in the light of records made with an operational bearing recorder. With respect to range, a 50 per cent zone of ±14 yd was characteristic. In the case of bearing, ±2 per cent can be expected with manual BDI operation and slightly greater spread with the automatic target trainer.[c]

7.10 PROPOSED LINK-BELT GEOGRAPHIC PLOTTER

A link-belt type of plotter was being designed at the time this project was terminated. Even though the unit was not constructed its design is significant and is here described.

7.10.1 General Description

The link-belt plotter was designed to be compact and easy to install and maintain aboard ship. All servo units are located in the base and are connected directly to their respective motions to minimize backlash. The major change in the input information is to use the dead reckoning analyzer (standard equipment for operating the DRT aboard many antisubmarine vessels) to supply N-S and E-W components of own-ship's motion.

The design calls for clutches and cranks in the drives to enable the pencil that traces own-ship's course to be moved quickly to any desired position in the plotting area. New waterproof tracing cloth is prescribed as well as an improved clamping arrangement for it.

7.10.2 Operation of Plotting Mechanism

The principal difference between this design and that of the lead screw plotter concerns the manner in which the input motions are employed to obtain the traces of own ship and target.

Own-Ship's Course

In this design, two small link belts are located on opposite sides of the plotting box as shown in Figure 14. These belts pass over sprocket wheels and move carriage *A* in the E-W direction in response to the E-W input. Another link belt moves carriage *B* which represents own ship along carriage *A*, and is powered by the N-S input by way of the sprocket wheel and splined-shaft mechanism shown.

Own-Ship's Bearing, Target Bearing, and Range

Each of these three quantities is transmitted to the center carriage by means of a splined-shaft and miter gear as in the Type L plotter (see Figure 12). Figure 15 shows the design of the center carriage and the pantograph arrangement for tracing the path of the target.

The splined shaft that transmits range information rotates a small drum in the base of the carriage. Around this drum is a beaded chain which controls the extension of the pantograph arm. A second splined shaft carries a worm gear which rotates the plate supporting the pantograph to provide target bearing. Own-ship's bearing is introduced in the same manner and is represented by a model ship which can be seen through the tracing cloth.

The design also calls for a small predictor light. This light may be positioned either fore or aft of the model ship and is intended to aid the conning officer by indicating the explosion point of ahead-thrown or stern-dropped projectiles if fired "now."

It is also suggested that an arrangement could be introduced to have the target pencil record intermittently instead of continuously. This could be accomplished by having the pencil brought into contact with the paper by the action of a solenoid. Thus it would be possible to record the movements of a number of targets on the same plotting sheet.

[c] See Division 6, Volume 15.

Chapter 8

ATTACK DIRECTORS

Attack Director III

Attack director III is a device to provide surface ships with an automatic and continuous solution to the attack problem. With the aid of sonar information, it computes course to steer for either stern-dropped or ahead-thrown charges and predicts time to fire for depth charges. It is designed for use with standard sonar gear, with or without BDI. The equipment consists of a special bearing recorder, a computing unit, a modified range recorder, indicator units for the helmsman and the conning officer, and the conning officer's control unit which permits him to make manual corrections. The principal components of the system are arranged for operation by a three-man team. The development work was carried out jointly by HUSL and the Columbia University Special Studies Group.

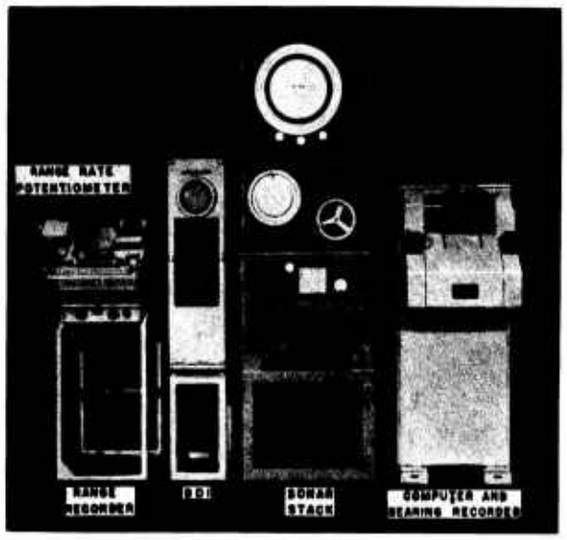

FIGURE 1. AD III and sonar stack arranged for operation by three-man team.

8.1 INTRODUCTION

IN CONDUCTING a surface craft attack on a submarine it is the responsibility of the conning officer to direct the course of the attacking vessel in a way that permits the placement of suitable explosive charges in the immediate vicinity of the target. In the absence of mechanical aids, the conning officer must base his judgments on mental computations involving the sequence of target bearings, ranges, and range rates as called out by the operators of the sonar equipment. From these data he must determine what initial lead angle to assume, when and how much super-lead to take, and the correct time to launch, either forward or astern, the explosive charges.

The development of instruments to aid the conning officer in solving the attack problem has proceeded along three general lines. One of these is represented by the attack plotter which presents visually the maneuvers of both the target and the attacking ship. This presentation of the geometrical situation has been of assistance to the conning officer in making his judgments about the proper course to steer. The other approaches to the attack director problem represent techniques borrowed from the general science of fire control. In one, which may be called the range-keeper solution, the mechanism provides a virtual target whose course and speed are corrected in accordance with the sonar data until the range and bearing of the virtual target coincide suitably with the prevailing sonar indications. Machine solution of the attack problem is then based on the behavior of the virtual target which continues to represent a smoothed average of the sonar data. The third general approach provides for continuous machine solution of the attack problem in terms of sonar data which is introduced directly, rather than by means of matched pointers as in the range-keeper solution. The *Mark III attack director* [AD III] which is described in this section follows this last general method in providing its automatic solution of the attack problem.

The fundamental purpose of the AD III is to function as an automatic conning officer during echo-ranging attacks. Its design, accordingly, was centered around the following objectives: first, to provide an automatic determination of the course and speed

of the target by means of range and bearing recorders, the accuracy of this determination being practically unaffected by own-ship's maneuvers; second, to use this information as the basis for a continuous calculation of course to steer (or train angle for a forward-throwing weapon) and time to fire; third, to permit the conning officer to replace the target's course and speed, as computed from the recorders, by any other values he may wish to substitute. The latter objective is considered important because additional information on target's motion may be available besides that comprised in the ranges and bearings (e.g., doppler, recorder trace characteristics) and because the conning officer may wish to allow for continuation of a turn by the target during the blind time.

In achieving these objectives, certain specific design features were considered desirable. When automatically conning the attack, the director should require no more of its operator than is required of a range recorder operator; it should indicate the correct ship's course independently of present ship's course; it should present to the helmsman a direct indication of course to steer and it should indicate directly the time to fire the barrage. Also, it should be completely flexible, allowing the conning officer to insert whatever information he may wish, allowing for manual correction of apparently erroneous data, and permitting the conning officer to make allowances for changes in the target's course and speed during the blind time. In addition, it should present an attack diagram which facilitates the conning officer's prediction of target maneuver during the blind time. The attempt was made to include all these features in the final form of the AD III.

Tests conducted by ASDevLant indicate that stern-dropping attacks conned automatically by the AD III were considerably better than those conned by average sonar teams but poorer than those conned either by experts using the antisubmarine attack plotter, or by the Mark IV antisubmarine attack director, a device developed by the Librascope Corporation. Numerous deficiencies in the mechanical operation of the AD III were shown up by the tests, but the fundamental methods of obtaining solutions appear sound and it seems that the mechanical shortcomings might easily be corrected in redesign. However, no further development of the AD III has been undertaken, in view of the relatively greater success of the Librascope Mark IV.

Two important questions bearing upon the design and use of attack directors still remain unanswered. The first of these concerns the relative accuracy of recorders and aided followers for the determination of target's course and speed. It is unlikely that this question can be properly answered by merely comparing the number of hits scored in stern-dropping attacks by the AD III, which uses recorders, and the Mark IV, which uses followers. For stern-dropping attacks the overall accuracy is strongly influenced by the method of using data on target's motion and by the evasion of the submarine during the blind time. Attacks with a trainable ahead-throwing weapon, stabilized against roll, would give much more direct information on the relative accuracy in determination of target's motion.

The second unanswered question concerns the usefulness of curved course prediction, i.e., of making at least partial allowance for continuation of a turn by the target during the blind time. Sea tests with the AD III did not use this feature and, for several reasons, the attack teacher tests which indicated its desirability were hardly conclusive.

Although no specific recommendations are being made with reference to further development of the AD III, it is suggested that any future attempt to improve attack directors should combine the best features of the AD III and the Librascope Mark IV.

8.2 MATHEMATICAL ANALYSIS OF ATTACK CONDITIONS

The geometry of an attack guided by sonar information may be formulated in several ways, depending on the approximations and simplifying assumptions which are used. Moreover, it is necessary to distinguish between conditions for stern-dropped and ahead-thrown ordnance. The equations used at various stages of the attack director development differed as improved formulations were worked out, stimulated in some cases by shortcomings in the performance of experimental equipment. The successive states of the analysis are covered by the derivations of equations in the published descriptions of the instruments, to which reference is made later. For purposes of exposition, it seems preferable to proceed directly to the final equations, and then to discuss the earlier incomplete or approximate forms in the light of these final versions.

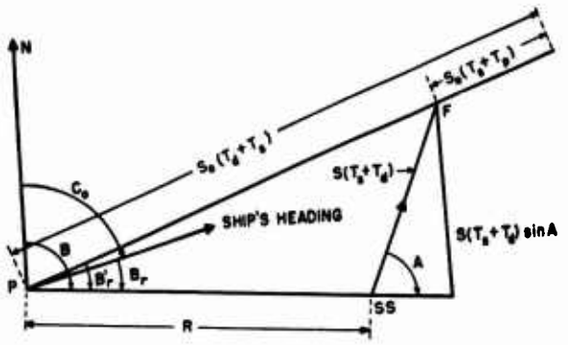

FIGURE 2. Attack triangle, stern-dropped charges.

8.2.1 Stern-Dropped Charges

At some instant after the attacking ship has been brought to a heading approximately toward the target, the situation may be represented by Figure 2, where the symbols have the following meanings:

- P = position of attacking ship's projector.
- SS = position of target.
- R = range of target.
- B = true bearing of target line of sight.
- B_r = present relative bearing of target line of sight.
- B'_r = relative bearing of line of sight if ship were on correct attack course.
- C_o = ship's true heading.
- F = explosion point of charges.
- A = target aspect angle, measured clockwise from the bow of the target to the prolongation of the line of sight. (This differs from the customary Navy definition, which measures the angle to the line of sight rather than its prolongation.)
- S = target speed.
- S_o = speed of ship.
- T_p = time-to-travel distance from sound projector to stern of ship.
- T_d = time interval from the present to dropping of center of barrage.
- T_s = time for charges to sink to target's depth.

ATTACK COURSE

In terms of this notation, the true bearing of the ship's heading is $B - B_r$ and the desired heading is $B - B'_r$. An expression for the desired lead angle, B'_r, is obtained by the following steps. Two relationships existing in Figure 2 may be expressed in the following equations:

$$S_o(T_s + T_d) \sin B'_r - S_o(T_s + T_p) \sin B'_r = S(T_s + T_d) \sin A. \quad (1)$$

$$S_o(T_s + T_d) \cos B'_r - S_o(T_s + T_p) \cos B'_r = R + S(T_s + T_d) \cos A. \quad (2)$$

By considering the contributions to rate of change of bearing due to components of ship's speed and target speed perpendicular to the line of sight we may write

$$R\frac{dB}{dt} = S_o \sin B_r - S \sin A. \quad (3)$$

Similarly, the rate of change of range depends on the components parallel to the line of sight.

$$\frac{dR}{dt} = S \cos A - S_o \cos B_r. \quad (4)$$

By solving equation (1) for $\sin B'_r$, we get the expression

$$\sin B'_r = \frac{(S \sin A)(T_s + T_d)}{S_o(T_d - T_p)}. \quad (5)$$

By solving equation (2) for T_d, we get the following:

$$T_d = \frac{R + ST_s \cos A + S_o T_p \cos B'_r}{S_o \cos B'_r - S \cos A}. \quad (6)$$

Substitution of equation (4) in equation (6) yields

$$T_d = \frac{R + T_s(S_o \cos B_r + dR/dt) + S_o T_p \cos B'r}{S_o \cos B'_r - S_o \cos B_r - dR/dt}. \quad (7)$$

Elimination of T_d in equation (5) by substitution of (7) gives us

$$\sin B'_r = \frac{S \sin A}{S_o} \cdot \frac{R + (T_s + T_p) S_o \cos B'_r}{R + (T_s + T_p)S_o \cos B_r + (T_s + T_p)(dR/dt)}. \quad (8)$$

From equation (3)

$$S \sin A = S_o \sin B_r - R\frac{dB}{dt}.$$

This allows us to eliminate the target aspect angle A from equation (8).

$$\sin B'_r = \frac{S_o \sin B_r - R(dB/dt)}{S_o}.$$

$$\frac{R + (T_s + T_p) S_o \cos B'_r}{R + (T_s + T_p) S_o \cos B_r + (T_s + T_p)(dR/dt)} \quad (9)$$

All the quantities needed for the solution of equation (9) for B'_r, the lead angle (which appears in both sides of the equation), are available from standard equipment, with the exception of dB/dt. This quantity is obtained from the recently developed bearing recorder, but the product $R(dB/dt)$ is obtained explicitly rather than the bearing rate by itself.

If B were plotted on paper moving at a constant speed, i.e., if B were plotted against time, the slope of the resulting trace would be a measure of dB/dt and hence of

$$\frac{S_o \sin B_r - S \sin A}{R}$$

from equation (3). This is not a particularly useful quantity because it varies with range and because an operator would be required to change the slope of his cursor rapidly as the range decreased, which would introduce serious inaccuracies. If B is plotted on paper moving with a speed inversely proportional to range R, as in British Asdic 144, then the slope of the plot is a measure of $S_o \sin B_r - S \sin A$ and is independent of the range value. This quantity is of considerably more interest than the other, for since we know $S_o \sin B_r$, we can easily determine $S \sin A$, which, when combined with $S \cos A$ as obtained from the range recorder [see equation (4)], uniquely determines the target's course and speed.

Unfortunately, changes in $R(dB/dt)$ are not apparent instantly, and as much as 30 sec may elapse after the trace on the bearing recorder starts to change slope before the operator becomes aware of the change and moves the cursor to the new position, thereby putting the new value into the computer. This leads to instability of equation (9) whereby differences between B'_r and B_r are overcorrected.

To illustrate, consider a case in which the ship is momentarily headed directly toward the target and B_r is zero. The bearing rate at that moment is due entirely to the submarine's motion perpendicular to the line of sight, expressed by the term $-S \sin A$ of equation (3). The computer indicates the lead angle B'_r corresponding to this value of $R(dB/dt)$. The ship's course is changed and the lead B'_r is taken. Now the value of $R(dB/dt)$ as shown by equation (3) includes a term due to own-ship's motion perpendicular to the line of sight, which has a sign opposite to that representing target motion, thus reducing the absolute value of $R(dB/dt)$. The earlier, larger value remains in the computer and causes it to call for additional lead until the operator detects the decreased slope on the bearing recorder. By this time an excessive lead has been taken, and when the ship is turned, the same considerations again lead to overshooting, so that a meandering course is followed.

It may be seen that this instability is caused by the effect of own-ship's motion on the rate of change of bearing. This effect may be removed by means of the steps outlined below.

By integration of equation (3) we obtain

$$B = \int \frac{S_o \sin B_r}{R} dt - \int \frac{S \sin A}{R} dt. \quad (10)$$

Now, instead of plotting B on the bearing recorder, we plot B' defined by

$$B' = B - \int \frac{S_o \sin B_r}{R} dt. \quad (11)$$

Differentiation of equation (11) gives

$$R\frac{dB'}{dt} = R\frac{dB}{dt} - S_o \sin B_r. \quad (12)$$

Comparison of equation (12) and equation (3) shows that

$$R\frac{dB'}{dt} = -S \sin A. \quad (13)$$

Thus the value of $R(dB/dt)$ depends only on target aspect and speed and is independent of own-ship's course and speed.

Substitution of equation (12) in equation (9) gives

$$\sin B'_r = -\frac{R(dB'/dt)}{S_o} \cdot \frac{R + (T_s + T_p) S_o \cos B'_r}{R + (T_s + T_p) S_o \cos B_r + (T_s + T_p)(dR/dt)} \quad (14)$$

Equation (14) is stable except for delays in detection of changes in dR/dt which are caused by changes in B_r. However, the range rate is not so critically affected by changes in course (when B_r is small) as is the bearing rate. Also, the range rate has much less effect on the value of B_r than has the bearing rate. In practice, any instability is lost in the inaccuracy of the data supplied to the computer.

An approximate form of equation (14) was used in the Mark I and Mark II NDRC lead angle computers. The simplification consisted in substituting B'_r for sin B'_r, setting cos $B'_r = 1$ in the numerator, and combining T_s and T_p into one value, t. The equation becomes

$$B'_r = -\frac{R(dB'/dt)}{S_o} \cdot \frac{R + tS_o}{R + tS_o \cos B_r + t(dR/dt)} \quad (14a)$$

These approximations are good for lead angles up to 30 degrees, but give a value of B'_r which is too high for leads of 40 degrees or more. The equation was adequate, however, for the first and second models of the computer.

Since the variable-resistance method used for inserting dR/dt in the computer does not provide for negative polarity and since, in practice, range rate is always negative, the coefficients of dR/dt in equations (14) and (14a) are given negative signs before the equations are used as the basis of computer circuit design.

Time to Fire

The expression for time to fire, equation (7), may be developed further as follows: Assuming that the proper course has been taken, then

$$\cos B_r = \cos B'_r,$$

and equation (7) becomes

$$T_d = \frac{R + S_o (T_s + T_p) \cos B'_r + T_s(dR/dt)}{-(dR/dt)}, \quad (7a)$$

or

$$T_d = \frac{R + S_o (T_s + T_p) \cos B'_r - T_s}{-(dR/dt)}. \quad (7b)$$

This is exact only when the proper course is followed, but is not greatly in error unless the course departs considerably from the computed value.

Once again computer circuit design takes into account the negative nature of dR/dt and proceeds as if the denominator of equation (7b) were positive.

8.2.2 Ahead-Thrown Attack

The lead angle required for an ahead-thrown attack is generally much less than that required with stern-dropped charges. In the preliminary stages of the attack the ship is aimed directly toward the target. As the effect of the target's motion becomes apparent, a constant bearing collision course is taken. In this way the range is closed as rapidly as possible. Before the firing range is reached, a lead angle must be assumed to allow for the distance which the target travels while the projectiles are traveling through the air and sinking in the water to the depth of the target. If the charges are fired from a trainable device, the ship's heading at the instant of the firing is not nearly so critical since it need only approximate the correct direction, the difference between the ship's heading and the lead angle being taken up by the training of the weapon.

The geometry at the instant of firing for a successful attack with a trainable forward-throwing weapon such as the Hedgehog is illustrated in Figure 3. The symbols have the following meaning:

- P' = position of attacking ship's projector.
- SS = position of target.
- R = range of target.
- B = true bearing of target line of sight.
- B'_r = relative bearing of line of sight (on a satisfactory attack course).
- B''_r = relative bearing of line of sight measured from azimuth of Hedgehog.
- F = explosion point of charges.
- A = target aspect angle, measured clockwise from the bow of the target to the prolongation of the line of sight. (This differs from the customary Navy definition, which meas-

ures the angle to the line of sight rather than its prolongation.)

S = target speed.

S_o = speed of ship.

R_e = base range of projectile, measured from sound projector to final line of sinking.

T_f = time of flight.

T_s = time for charges to sink to target's depth.

The diagram represents the distance from the projector P to the explosion point F as the sum of two vectors, namely the base range R_e, in the direction of Hedgehog train, and the extra distance traveled as a result of own-ship's motion, S_oT_f, in the direction of ship's heading. Actually, computations are made on a simplified basis, illustrated in Figure 4, in which the two vectors are assumed to be collinear; that is, B''_r and B'_r are assumed equal. In this case, the lead angle B'_r as computed represents the direction in which the ahead-thrown weapon should be trained, whether or not the ship is on precisely that bearing at the instant of firing. The other symbols have the same meaning as in Figure 3. The target travels the distance $S(T_f + T_s)$ during the time of flight T_f and the sinking time T_s of the projectiles.

The computations used are based on the triangle of Figure 4, representing the desired conditions at the instant of firing. We see that

$$(R_e + S_oT_f) \sin B'_r = S(T_f + T_s) \sin A, \quad (15)$$

whence

$$\sin B'_r = \frac{T_f + T_s}{R_e + S_oT_f} \cdot S \sin A. \quad (16)$$

The value of $S \sin A$ may be expressed according to equation (13) as the product of range by the modified bearing rate, dB'/dt. In the definition of B' in equation (11), there is no conflict with the assumptions underlying the present computation, since by hypothesis the ship is on the correct attack course, so that $B_r = B'_r$. Accordingly, we may substitute the value of $S \sin A$ from equation (13) to get

$$\sin B'_r = -\left(\frac{T_f + T_s}{R_e + S_oT_f}\right) R \frac{dB'}{dt}, \quad (17)$$

which is the equation solved by AD III when set for Mousetrap or Hedgehog attacks. The equation for $\sin B'_r$ in terms of the actual bearing rate instead of the modified bearing rate can be obtained by substituting $S \sin A$ from equation (3) in equation (16):

$$\sin B'_r = \frac{T_f + T_s}{R_e + S_oT_f}\left(S_o \sin B_r - R \frac{dB}{dt}\right). \quad (18)$$

This equation was used in the computers which preceded AD III, before equation (17) had been derived, and is subject to the same criticism as equation (9) because it leads to a meandering attack course.

8.3 DESCRIPTION OF MARK II LEAD ANGLE COMPUTER

The immediate precursor of the AD III was the *Mark II lead angle computer* [LAC]. Since the same basic principles of operation are utilized in both cases, a description of the earlier and simpler version forms an appropriate introduction to the dis-

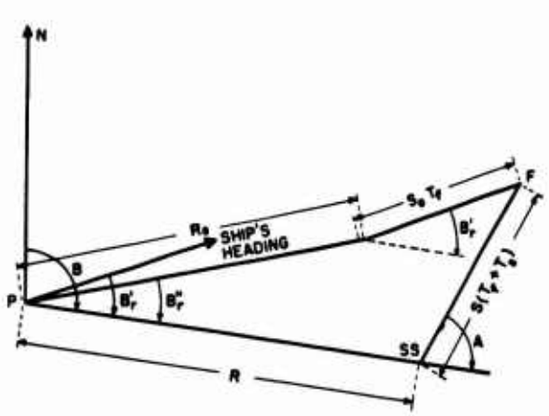

FIGURE 3. Attack geometry for Hedgehog.

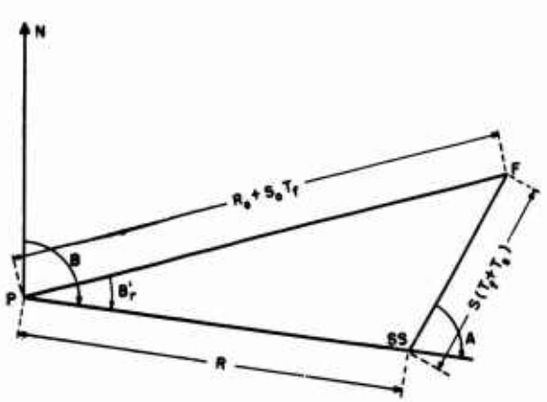

FIGURE 4. Triangle solved for ahead-thrown attack.

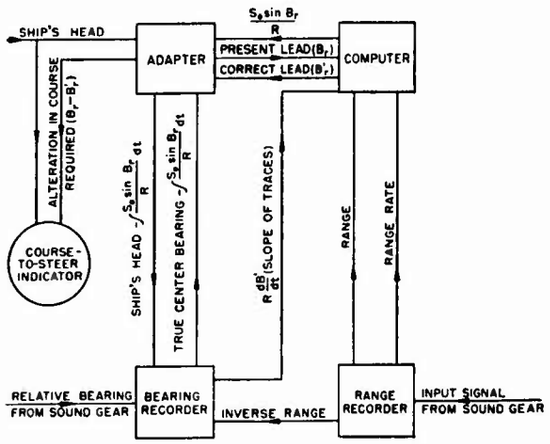

FIGURE 5. Block diagram of lead angle computer.

cussion of the later and more complex design.

The Mark II LAC was built to operate with the British Asdic 144. The purpose of the combination was the obtaining and presentation of the solution of equation (14a). To achieve this the following components are necessary:

1. A range recorder to supply R and dR/dt.
2. A bearing recorder to supply $R(dB'/dt)$ and to split cut-on bearings for providing B_r.
3. An adapter of some sort to take these various outputs and adapt them for use in the computation.
4. A computer to solve the equation.
5. An indicator to present the answer to the conning officer.

The two recorders were supplied by the Asdic 144; the other devices constitute the LAC proper.

Figure 5 is a schematic representation of the various components, with their respective inputs and outputs indicated.

8.3.1 Range Recorder

The range recorder unit of this set (shown in the foreground of Figure 8) has a manual range follower which provides for transmission of range on a Sperry step-motor system. It is provided with a wheel and disk arrangement previously used in the New London bearing recorder. A friction wheel, sliding on a shaft which rotates at constant speed, makes contact with a driven disk at a distance from the axis of the disk which is directly proportional to range; the speed of the disk consequently is inversely proportional to range. This disk is then used to drive the paper of the bearing recorder.

Figure 6 illustrates schematically the method employed to supply an automatic transmission of range rate. *PB* is a light-beam cursor, pivoted at *P*, and *PR* is a contactor arm which moves with an angular displacement δ equal to that of *PB*. The range rate is equal to tan δ, rather than to the angle δ itself, which makes it necessary to obtain a quantity proportional to the tangent of δ. This is accomplished by letting the contactor arm *PR* wipe across a strip resistance. The resistance picked off between leads 2 and 3 is then proportional to tan δ. The strip resistance used is that labeled R-7 in Figure 12.

8.3.2 Bearing Recorder

The bearing recorder unit of the British Asdic 144 is used with slight modification. Figure 7 is a schematic drawing of the recorder showing the resistor strip added for transmitting the slope of the traces.

The input unit to this is designed so that relative sound projector bearing and ship's head are added together in a differential. The output of the differential (true bearing B) is available for plotting.

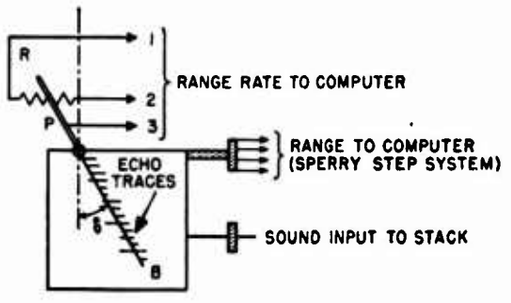

FIGURE 6. Range recorder schematic.

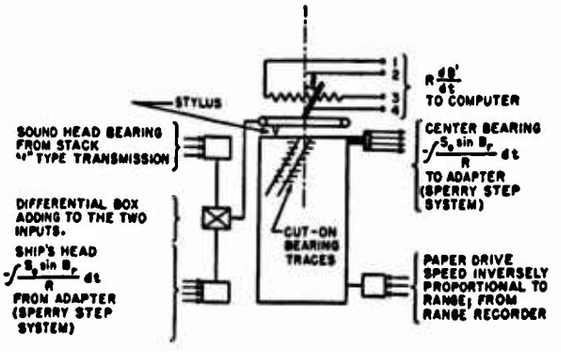

FIGURE 7. Bearing recorder schematic.

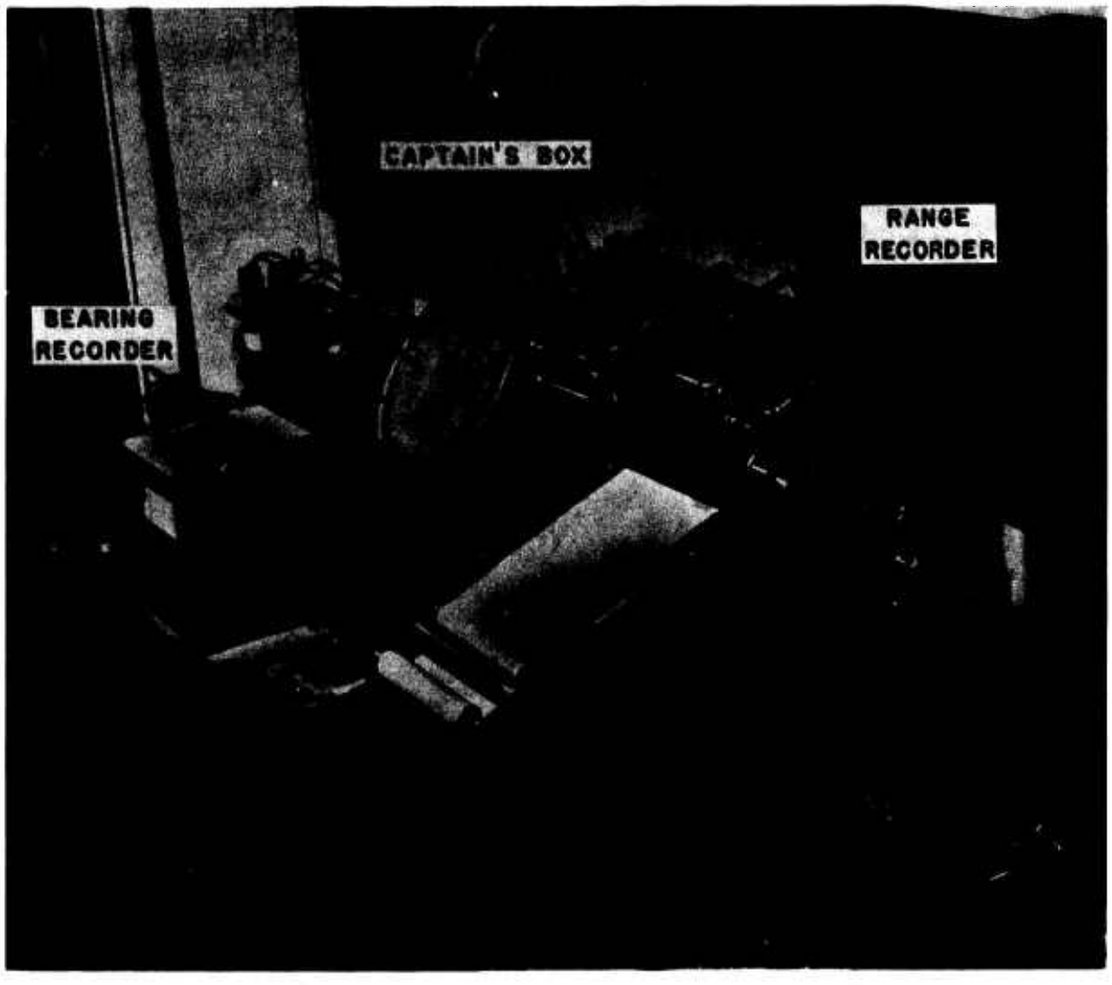

FIGURE 8. Bearing recorder, range recorder, and captain's box of 144 Asdic.

As indicated in equation (14a), however, it is desirable to plot B' rather than B [see equation (11)]. This is accomplished by putting ship's head minus the quantity

$$\int \frac{S_o \sin B_r}{R}\, dt$$

into the recorder instead of ship's head alone. (The method of subtracting these two is explained below.) By plotting B', the slope of the traces becomes proportional to $R(dB'/dt)$, and this quantity is transmitted by a resistance (R-12 in Figure 12) and wiping arm in the manner explained above for the range recorder. The midpoint between the cut-on traces, B', is transmitted to the adapter on a Sperry step system. Figure 8 is a photograph of the recorders and captain's box of the Asdic 144.

8.3.3 Integrator

In order to obtain

$$\int \frac{S_o \sin B_r}{R}\, dt,$$

required to remove the effect of own-ship's motion on the rate of change of bearing, a variable-speed motor is used. Speed of the motor is made proportional to the quantity $S_o \sin B_r/R$, so that the total number of revolutions of the motor in time t is proportional to

$$\int_o^t \frac{S_o \sin B_r}{R}\, dt.$$

Figure 9 is a diagram of the integrator motor and its speed control.

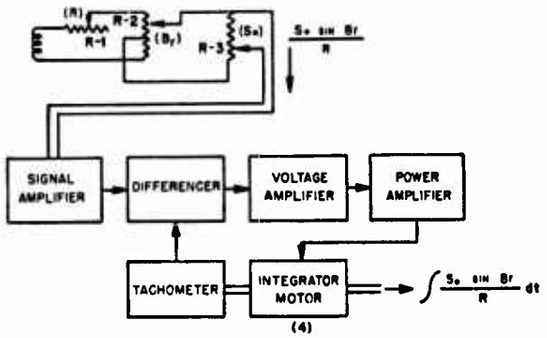

FIGURE 9. LAC II integrator motor.

Range is put in on R-1 so that the voltage drop across R-2 is proportional to $1/R$. B_r is then put in as a linear displacement of the slider from the center tap on R-2. If the output voltage of R-2 were fed into an open circuit, it would be proportional to B_r/R. This output, however, is fed not into an open circuit but into R-3 which is only a few times greater in resistance than R-2. As B_r is increased on R-2, the voltage does not increase linearly but changes according to the relative values of R-2 and R-3. By adjusting this relationship, it is possible to make the output voltage of R-2 very nearly equal to sin B_r/R for values of B_r up to 50 degrees, which is the maximum value needed for computations. S_o is then put in on R-3 so that the output voltage of the entire circuit is S_o sin B_r/R. The remaining part of Figure 9 represents the method of making the speed of the integrator motor proportional to the output voltage of the control circuit.

8.3.4 Adapter

The adapter unit of the Mark II lead angle computer receives and transmits various quantities which are needed in the final computation of equation (14a). Figure 10 illustrates schematically the operation of this device as described in the following text. (Numbers in parenthesis refer to Figure 10).

Ship's heading C_o is fed into the Sperry receiver (1) and servoed by the Brown motor (2). The follow-up method is a simple on-off contactor. The servoed ship's heading is then fed into a differential box (3) where the output of the integrator motor (4) is subtracted from it. The output of the differential box (3) is now ship's head minus the quantity $\int(S_o \sin B_r/R)dt$

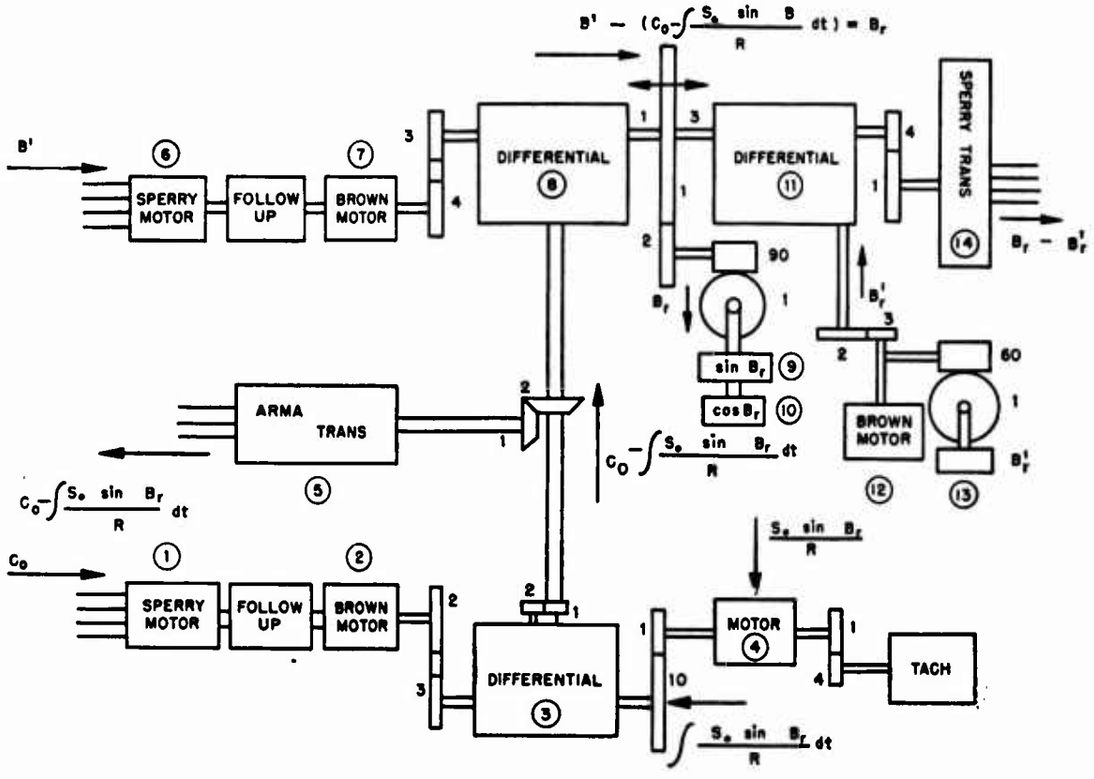

FIGURE 10. Mechanical schematic of LAC II adapter unit.

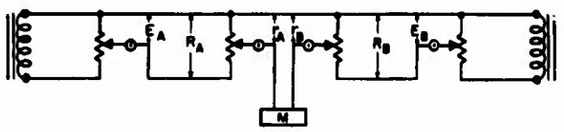

FIGURE 11. Simplified LAC II computer circuit.

which, as explained above, is the value needed as an input to the bearing recorder. This quantity is transmitted by means of an Arma step transmitter (5) which operates the Sperry receiver in the bearing recorder.

From the bearing recorder comes a transmission of the midpoint between the plotted cut-ons as indicated in Figure 7. This is not the true center bearing B, however, because we have subtracted

$$\int \frac{S_o \sin B_r}{R} dt$$

from the input. This transmission is therefore B minus the quantity

$$\int \frac{S_o \sin B_r}{R} dt \text{ or } B'.$$

This quantity is received on the Sperry motor (6), servoed by the Brown motor (7), and fed into the differential box (8). The output of differential box (3) is also fed into box (8), and these two inputs are subtracted so that the output is

$$\left(B - \int \frac{S_o \sin B_r}{R} dt\right)$$

$$-\left(C_o - \int \frac{S_o \sin B_r}{R} dt\right)$$

or the relative center bearing B_r. Since B_r is needed both in the solution of the equation and in the operation of the integrator, the output of box (8) is geared to the potentiometers (9) and (10). It is also fed into the differential box (11). The second input into the differential box (11) is the output of the Brown motor (12) which balances the computer resistor (13) as explained below. The output of (13) is B'_r (the result of the computation as explained in the next section) and thus the two inputs to differential box (11) are B_r and B'_r. These two values are subtracted so that the output of box (11), which is fed to the M-type transmitter (14) is $B_r - B'_r$, or the amount by which the course must be altered to obtain the correct lead over the target.

8.3.5 Computer Circuit

The general method used for solving equation (14a)[a] can be explained with reference to Figure 11. When no current is flowing in the meter M, the following equation holds true:

$$E_A \frac{r_A}{R_A} = E_B \frac{r_B}{R_B},$$

or

$$r_A = \frac{E_B}{E_A} \cdot r_B \frac{R_A}{R_B}.$$

By letting

$$E_B = k_1 \frac{R \frac{dB'}{dt}}{S_o},$$

$$E_A = k_2\left(R + S_o t \cos B_r - t \frac{dR}{dt}\right)^b,$$

$$r_B = k_3(R + S_o t),$$

and balancing r_A until no current flows in the meter, r_A becomes proportional to B'_r. This circuit, then, solves equation (14a) providing r_B, E_B, and E_A can be made proportional to the necessary quantities.

Figure 12 is a diagram of the circuit actually used to solve the equation. Throughout the circuit Ohm's law is used in multiplications and divisions. The three sections A, B, and C are adjusted so that the

[a] With the necessary negative coefficient in the range-rate term.

[b] With the necessary negative coefficient in the range-rate term.

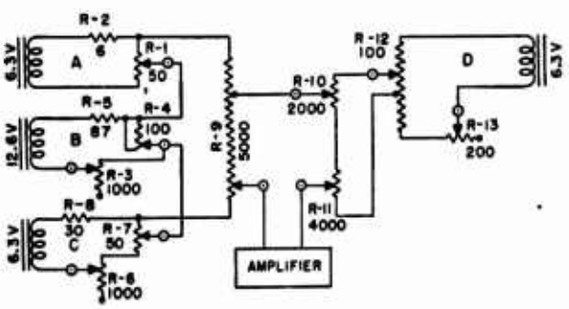

FIGURE 12. Actual LAC II computer circuit.

output voltage from each is proportional to R, to $S_o t \cos B_r$, and to $t\ dR/dt$, respectively. The constant of proportionality must, of course, be the same in each section. A sufficiently close approximation to $\cos B_r$ is obtained by shunting a resistance R-4 as shown in section B. Voltage is maximum when the potentiometer is at the center of its run ($B_r = 0$), and goes to zero at either end ($B_r = \pm 90$ degrees). The voltages of A and B are then added, and the voltage of C is subtracted from the sum. Thus the output voltage of the three circuits taken together is proportional to $(R + S_o t \cos B_r - t\ dR/dt)$ and corresponds to the voltage E_A of Figure 11. These voltages are then fed into a resistance R-9 which corresponds to R_A of Figure 11. Resistance R-9 is center-tapped since B'_r (which corresponds to r_A) can be either positive or negative.

R-11 plus R-10 corresponds to R_B in Figure 11. The slider on R-10 is set to pick off a resistance proportional to $S_o t$, and the slider on R-11 is set to pick off a resistance proportional to R (range). Between the two sliders, then, there appears a resistance proportional to $R + S_o t$, which corresponds to the r_B of Figure 11.

Section D of the actual circuit provides a means of obtaining a voltage proportional to $(R/S_o)\ dB'/dt$ to correspond to E_B of Figure 11. The resistor R-12 on which $R\ dB'/dt$ is obtained is center-tapped since the quantity $(R/S_o)\ dB'/dt$ may be either positive or negative.

Instead of running the leads from r_A and r_B into a meter, as in Figure 11, the corresponding leads of Figure 12 are led into a Brown amplifier. When the circuit is not balanced, the unbalance voltage is amplified and fed into a Brown motor which rotates in such a direction as to restore the balance by changing the slider on R-9. Thus the circuit automatically balances itself.

The relative values of the various resistors and potentiometers used in the circuit are determined by the accuracy needed in the final result (B'_r), and by the constant of proportionality needed in the various sections and in the final answer. For the sake of accuracy, it is essential that R-9 be large in comparison with the sum of the output resistances of sections A, B, and C, and that R-10 plus R-11 be large in comparison with the output resistance of section D. Practical limitations such as the capacity of the resistors available and the range of values of the inputs (R, dR/dt, T, S_o, etc.) are also important considerations. In general, the resistances were chosen to permit the following range of values:

Range	=	0 to 1,200 yd
Range rate	=	0 to 27 knots
$R(dB'/dt)$	=	0 to ± 9 knots
S_o	=	9 to 18 knots
t	=	5 to 50 sec

8.3.6 Course-to-Steer Indicator

Finally, the output of the transmitter (14) of Figure 10, transmits the value $B_r - B'_r$ to the course-to-steer indicator (captain's box) shown in Figure 8. The indicator used was a British A/S 174 bearing plotter which has a ship's heading card with an indicator under it. By moving the indicator an amount $B_r - B'_r$ from relative bearing 0 degree and observing its indication on the ship's heading card, the conning officer can read off the correct course to steer and the amount by which his present course should be altered.

8.3.7 Performance Tests

The performance tests which were carried out on the LAC II gave encouraging results and showed that the basic principles of operation were sound. It appeared that the deficiencies which were found could be readily eliminated and that additional desirable features could be incorporated. Accordingly it was decided to undertake the design and construction of a new model which became known as the attack director Mark III.

8.4 ATTACK DIRECTOR MARK III

The attack director Mark III, basing its computations on sonar information, solves the course-to-steer problem for either stern-dropped or ahead-thrown charges and predicts time to fire for depth charges. The equipment is designed for use in conjunction with standard sonar gear, with or without a bearing deviation indicator [BDI]. It consists of a special bearing recorder and computing unit mounted beside the sonar stack, a modified range recorder, a helmsman's indicator, and two small units for the use of the conning officer designated as the captain's indicator and the captain's box.

In Figure 1 the principal components of AD III are shown in association with a sonar stack and a

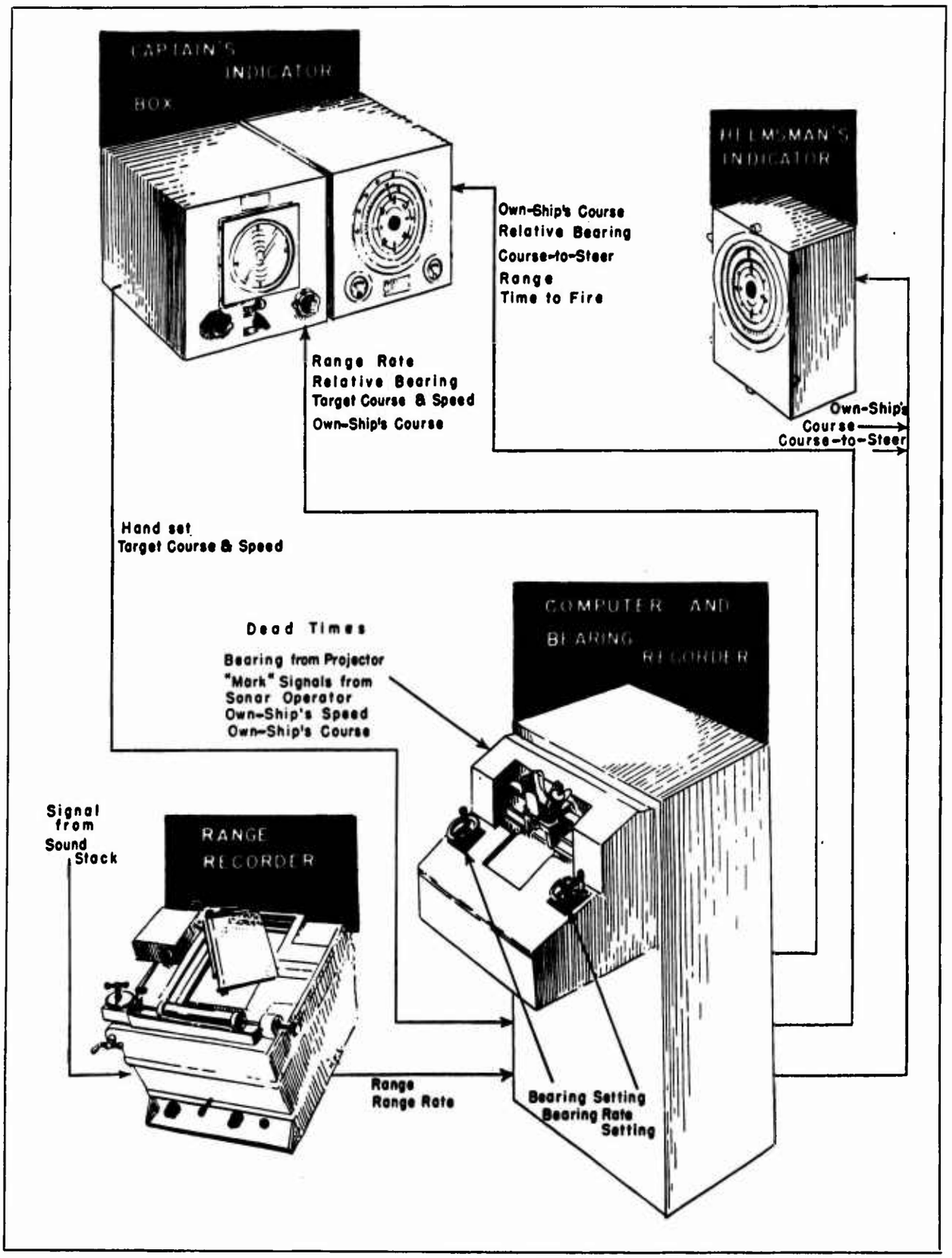

FIGURE 13. Functional schematic of AD III components.

BDI unit, arranged conveniently for operation by a three-man team. One man operates the bearing recorder shown on the right. The stack and BDI are operated by the middle man of the team, who can also either directly observe the trace on the bearing recorder or be coached by its operator to take advantage of the bearing record in maintaining contact. The man on the left operates the range recorder.

The pictorial diagram of Figure 13 shows the complete attack director and the character of the information transmitted between its various parts. The helmsman's indicator is located conveniently for the helmsman, and the captain's indicator and captain's box are mounted side by side at the station occupied by the conning officer during an attack. The two recorders are preferably located as near as possible to the sonar stack (Figure 1) for mutual assistance of the operators.

The purpose of attack director Mark III is to make the most effective use of sonar data in conducting an attack. The input or "raw" data for the device consists of the following:

1. Signals from the sonar receiver, which are applied to the range recorder.
2. Bearing values which are applied to a bearing recorder whenever the sonar operator has the projector correctly trained on the target.
3. Ship's course which comes from the gyrocompass.
4. Ship's speed which is obtained from the Pitometer log.
5. Information concerning dead times which depends on the ordance used and which is put into the director by hand.

The process of lining up the cursors on both recorders serves to "smooth out" the data actually plotted on the recorder paper and thus makes allowance both for errors on the part of the sonar operator and for erratic information due to adverse water conditions.

The output of the director consists essentially of a course-to-steer indication and a time-to-fire signal; however, the components of target motion parallel to and perpendicular to the line of sight appear as a by-product of the computation, and the resultant target course and speed are indicated to the conning officer. Furthermore, provision is made for this officer to insert different values for these quantities manually, if he believes that for some reason the target motion is not being represented correctly. The manual inputs may also be used after loss of contact

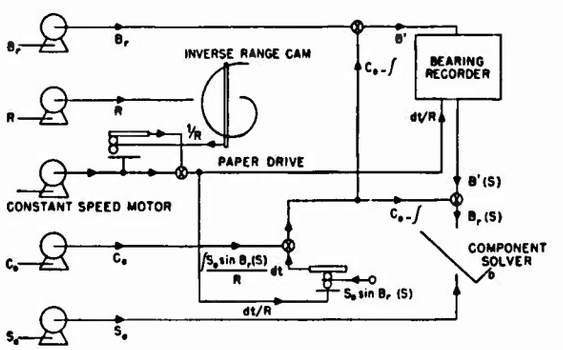

FIGURE 14. Simplified schematic of AD III mechanical computer.

to modify the time-to-fire computation according to last-minute estimates of target maneuvers.

For ahead-thrown charges the time to fire is obtained from the range recorder in the normal way, but for stern-dropped attacks a time-to-fire signal is furnished by an electrical computation.

The detailed description which follows covers first the mechanical computer used for plotting a modified bearing; second, the idealized electrical schematic of the entire equipment; and finally, details of the separate components.

8.4.1 Mechanical Computer

The mechanical computer which is used to plot a modified bearing on the bearing recorder is shown in a simplified form in Figure 14. The operation of this computer is explained in reference to the former figure. The input quantities consist of relative bearing from the sonar stack, range from the range recorder, own-ship's course from the gyrocompass, and own-ship's speed from the Pitometer log. Each of these quantities controls the operation of a servo motor.

The range servo drives an inverse range cam, whose output is proportional to the reciprocal of the range. This output is used to position the balls of an integrator whose disk is driven by a constant speed motor. The output of the integrator, therefore, is proportional to the time increment divided by the range. In order to use the full diameter of the disk instead of only the radius, the integrator output is combined by means of a mechanical differential with the constant speed motor drive at a gear ratio which makes the output proportional to the position of the balls measured from one end

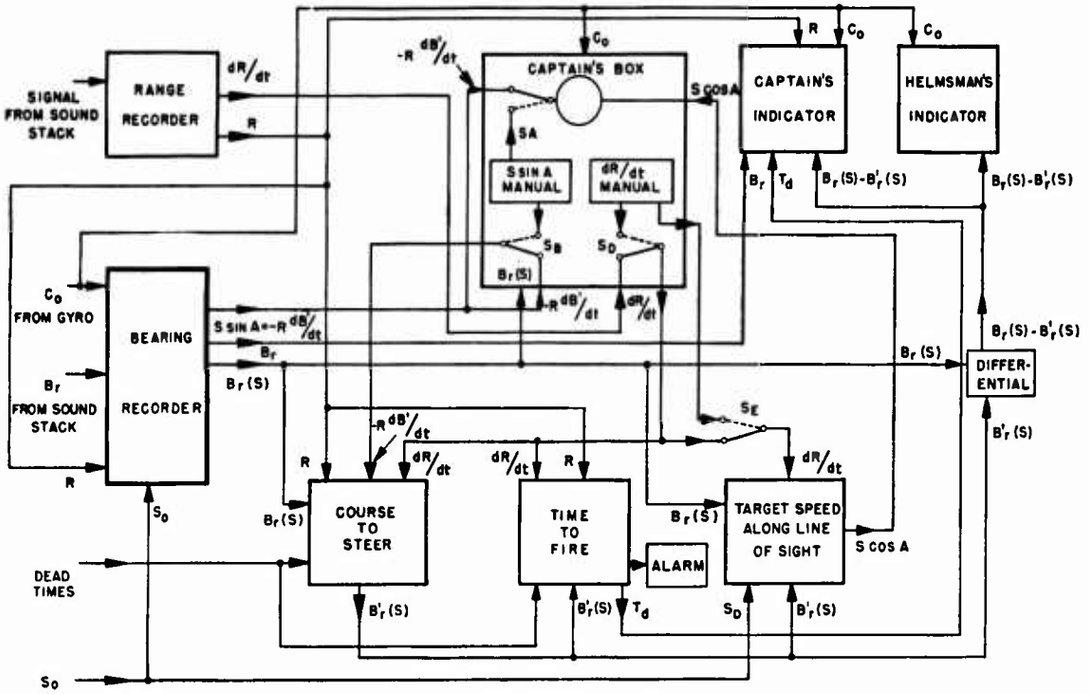

FIGURE 15. AD III simplified electrical schematic.

of the diameter, rather than from the center of the disk.

The output of the servo for own-ship's speed is a shaft position which serves as one of the inputs of a component solver. The other input is the smoothed relative bearing of the sonar projector, obtained as described below. Only one of the two outputs of the solver is used, namely, the component of own-ship's speed normal to the line of sight, $S_o \sin B_r(S)$.[c] This in turn is used to position the balls of an integrator, whose disk is driven at a rate inversely proportional to range. The output represents the contribution of own-ship's motion to the change in target bearing. It is combined by means of a mechanical differential with own-ship's course. The result in turn is combined with relative bearing of the sonar projector to give modified bearing B' for controlling the stylus of the bearing recorder. However, points are recorded only when the sonar operator presses a button, which he does each time he is on the target (with BDI) or at a cut-on (without BDI).

The smoothed value of this modified bearing, obtained from the cursor setting established by the recorder operator, has subtracted from it the difference between ship's course and the integral, to yield a smoothed relative bearing of the target, $B_r(S)$.

It should be noted that the servo motors of the mechanical computer control not only the shaft positions referred to above, but also potentiometers whereby the quantities are made available wherever needed in the electrical portions of the computer.

8.4.2 Electrical Schematic

The simplified electrical schematic (Figure 15) shows the way in which information is carried from one part of the attack director to another. The lines in this schematic do not necessarily represent direct electric connections since, in instances where a given quantity is needed at various points, a separate potentiometer is provided for each of these points, and the potentiometers are ganged and driven by a shaft whose position represents the quantity in question. For instance, the diagram shows range information going from the range recorder to (1) the bearing recorder, (2) the course-to-steer computer, and (3) the captain's indicator. The information is actually transmitted by means of five potentiometers driven by a servo motor located in the mechanical computer. One of these five feeds into the servo

[c] (S) indicates "smoothed."

amplifier where it is balanced against a voltage furnished by a potentiometer in the range recorder which is hand-set to follow the recorded range. By this means, the servo motor drives all five potentiometers to positions representing the smoothed present value of the range. The remaining four potentiometer outputs are applied as follows: one output goes to the captain's indicator, one goes to the time-to-fire circuit, and two feed into the course-to-steer circuit, since range appears on both sides of the equation which is to be electrically balanced [equation (14)]. The servo motor also drives an inverse range cam, as explained in the description of the mechanical computer.

The following discussion of the schematic of Figure 15 is based on the diagram and the logical interrelation of parts rather than on the actual mechanisms and connections used for transmitting the information.

Range, R

The value of range used throughout the computer is based on a pointer, which is moved by the operator of the range recorder to represent the value of present range as estimated by eye from the points on the range recorder. It is used in the bearing recorder to drive the recorder paper at a speed which is inversely proportional to range. It is indicated on the captain's indicator, and used in the computation of course to steer and time to fire.

Range Rate, dR/dt

The range rate is based on the position of a potentiometer geared to the range-rate cursor set by the range recorder operator. It is used to compute course to steer and target speed along the line of sight. In addition, a manual input for range rate is provided in the captain's box together with switches whereby the manually set estimated value can be substituted at the option of the conning officer for the value obtained from the range recorder.

Own-Ship's Course, C_o

This is introduced by a synchro signal from the ship's gyro system which drives a servo motor in the bearing recorder. This quantity is also required in the helmsman's indicator and captain's box.

Projector Bearing, B_r

The relative bearing of the sound projector is transmitted to the mechanical computer for use in obtaining the modified bearing actually plotted on the bearing recorder. The projector bearing is shown only on the captain's indicator.

Dead Time

Quantities involving time of flight, range of ahead-thrown projectiles (actually depending on ship's speed), and sinking time (depending on target depth) are selected according to the nature of the attack and manually set in with constant values. These quantities are required to compute course to steer and time to fire.

Own-Ship's Speed, S_o

This quantity is used in computing target speed along line of sight and operating a component solver in the mechanical computer. Ordinarily, it would be obtained from the Pitometer log, but for attack teacher tests or tests aboard ships lacking a Pitometer log installation, a hand-set input for ship's speed is provided.

Smoothed Relative Bearing, $B_r\,(S)$

This quantity is obtained from the mechanical computer and is used in computing target speed along line of sight and course to steer. The course-to-steer output is the smoothed relative bearing which the target would have if the ship were on the correct attack course $B'_r\,(S)$. A mechanical differential is used to take the difference between $B'_r\,(S)$ and $B_r\,(S)$. This difference, which represents the required change in course, is applied to the captain's indicator and the helmsman's indicator. $B_r\,(S)$ is also used in the captain's box where it is combined with ship's course to indicate true target bearing.

Target Speed Across Line of Sight $S \sin A$ or $-RdB'/dt$

The mechanical computer produces an output equal to the product of range and modified bearing rate, which represents the component of target speed normal to the line of sight. This quantity is used in computing course to steer. It is also applied to an indicator in the captain's box for combination with target speed along the line of sight to produce an indication of target course and speed. Switches in the captain's box make it possible to substitute an estimated value of target speed across the line of sight, first into the indicator in the captain's box by operation of switch S_A, and then into the course-to-steer computer by means of switch S_B, if the dop-

pler effect or other evidence leads the conning officer to doubt the correctness of the computed value.

Course to Steer, $B'_r(S) - B_r(S)$

The course-to-steer computer, as stated above, produces an output which is the smoothed relative bearing the target should have if the ship is on the correct attack course. This quantity is applied to the time-to-fire computer and to the computer of target speed along the line of sight as well as to the differential mentioned previously.

Time to Fire, T_d

The time-to-fire computer operates an alarm which, by means of a sequence cam, sounds a buzzer 5 sec before and 5 sec after firing time, and a bell at the firing time itself. The time remaining before firing is continuously transmitted to the captain's indicator.

Target Speed Along Line of Sight, $S \cos A$

The computer for target speed along line of sight uses own-ship's speed and course for obtaining the contribution of own-ship's motion, and combines this with the observed range rate to obtain the target speed along the line of sight. This is transmitted to the captain's box to contribute to the indication of target course and speed.

8.4.3 Details of Components

The functioning of the attack director has already been described in a general way. In the following paragraphs, each of its component parts is considered in detail.

Bearing Recorder

The bearing recorder (see Figures 1 and 13), which gives the component of target's velocity normal to the bearing line, and smoothed relative bearing, is mounted on a pedestal with the computer. The British bearing recorder used has been rebuilt and modified so that the light-beam cursor can be rotated by means of a knob in front of the unit. Another knob, similarly located, is used to move the light beam translationally in order that the bearing itself may be followed. The paper drive is obtained from the mechanical computer by means of a shaft which rotates at a speed inversely proportional to the range.

The modified true bearing is plotted on the bearing recorder. As was mentioned previously, the sonar stack operator plots the points by closing a switch each time he gets a bearing. Contributions to target's bearing due to own-ship's maneuvers are taken out by means of mechanical integrators and mechanical differentials involving range, relative bearing, own-ship's course, and own-ship's speed. As long as the component of target's velocity normal to the bearing line remains constant, the plot on the bearing recorder is a straight line.

The light-beam cursor is manually rotated to agree with the average slope of the line formed by the series of dots on the bearing recorder paper, and this rotation turns potentiometers that adjust resistances so that they are proportional to the component of target's velocity normal to the bearing line $R\,dB'/dt$ in equations (14) and (16). These resistances are then used by the computer in making the electrical computations.

The modified true bearing as plotted on the bearing recorder is followed by the manually operated cursor to give a smooth, modified true center bearing of the target. The motion of this cursor is transmitted mechanically to the computer, where, by use of a mechanical differential, this motion turns potentiometers to produce resistances in the computer proportional to the cosine of the smoothed relative center bearing of the target, $B_r(S)$. These are also used in the electrical computation.

Range Recorder

The standard range recorder (see Figures 1 and 13) has been modified in three particulars. One of these is the addition of a pointer carried on a lead screw which is manually rotated so as to maintain the pointer on the echo trace. This pointer is attached to the slider of a potentiometer so that its movement causes the potentiometer to produce a voltage proportional to the present range.

The second modification[3] of the range recorder adds a slant-range correction so that the range obtained is the actual horizontal range on the surface of the water rather than the slant range from the projector to the target. In this device target depth is set manually.

The third modification of the range recorder consists of the addition of a tangent potentiometer. The slider of this potentiometer is mechanically coupled to the range-rate cursor in such a manner that the resistance output from the potentiometer is proportional to range rate dR/dt in equations (7b) and (14). This resistance is used directly by the computer.

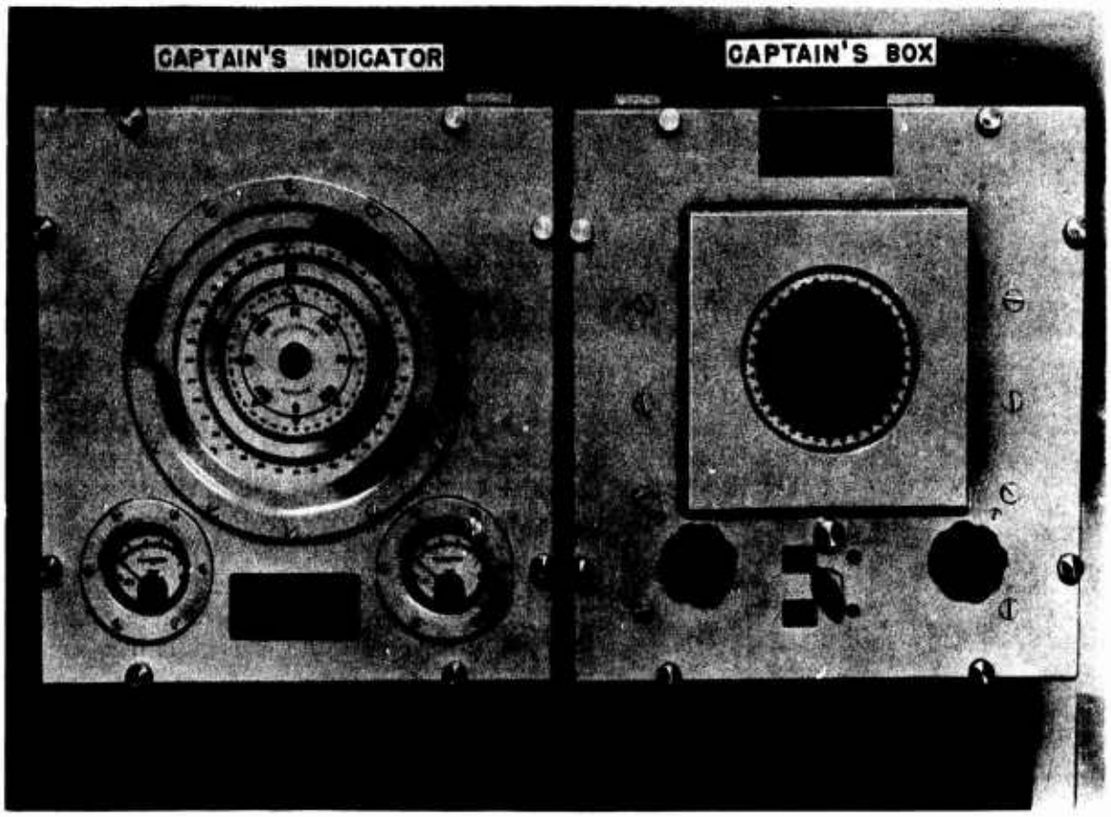

FIGURE 16. AD III captain's indicator and captain's box.

HELMSMAN'S INDICATOR

A standard Submarine Signal Company bearing repeater is used as the helmsman's indicator. In it, course to steer, as obtained from the computer, is given by a movable bug. The helmsman has only to keep zero relative bearing lined up with the bug in order to stay on the proper course. The gyrocompass repeater disk operates in the normal way.

CAPTAIN'S INDICATOR AND BOX

A modified bearing repeater, shown at the left in Figure 16, is used as the captain's indicator. A movable bug shows projector bearing and another bug is added to indicate the course to steer. A gyrocompass card is included also. Meters are used to give range and time to fire.

The captain's box contains a cathode-ray tube with suitable power supplies. The length of the trace on the screen of the tube, measured radially from the center, represents the target's speed, and the direction of the trace shows the target's true bearing. The coils around the cathode-ray tube may be rotated according to smoothed true target bearing by a servo motor which follows the position of a synchro. This is a differential synchro which is supplied with voltages corresponding to own-ship's course C_o and smoothed relative bearing B_r (S). A compass card in front of the cathode-ray tube can also be rotated according to smoothed true target bearing. Thus it is possible to make the plot on the tube screen with respect to either true north or line of sight.

Two knobs on the captain's box may be used to turn potentiometers which give resistances proportional to the rectangular components of estimated target's speed with respect to the line of sight. Microswitches on the shafts of these potentiometers allow the results of these changes to be shown on the cathode-ray tube screen, and the changes may then be inserted into the computer circuit by turning a switch on the captain's box. These knobs and this switch, together with a switch for energizing the time-to-fire balancing circuit in cases where the range

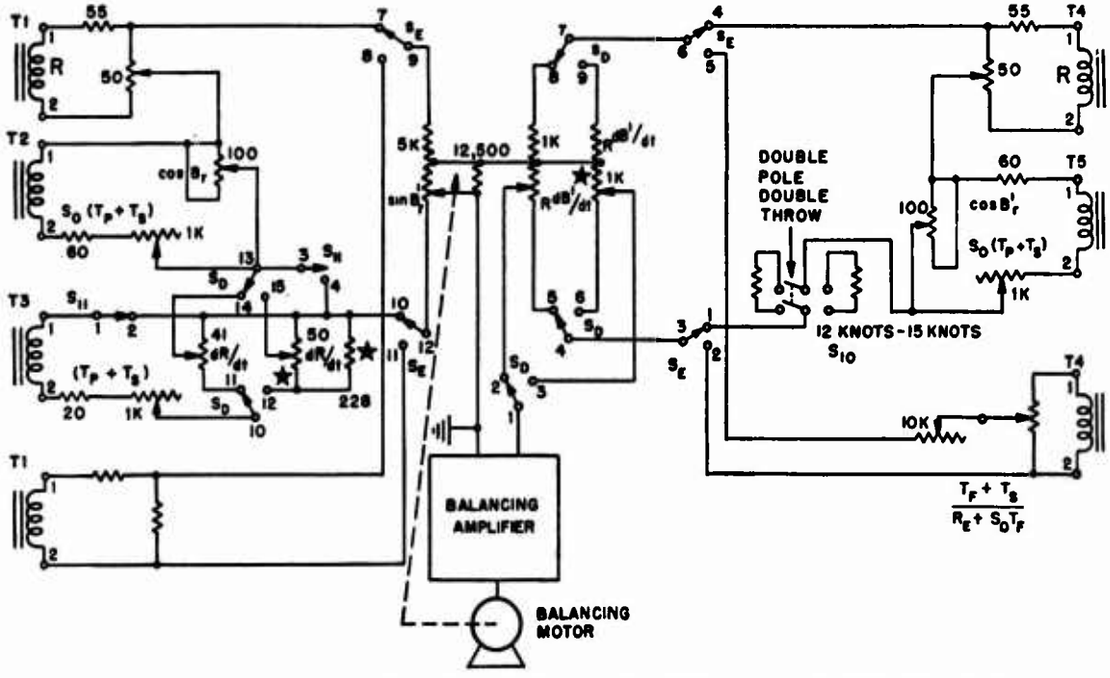

All switches S_E throw together: to lower positions for depth-charge attack; to upper positions for forward-throwing attack.

All switches S_D throw together: to left for normal depth-charge attack; to right for attack utilizing conning officer's estimates of course and speed.

S_{11} (1 and 2) opens when S_{11} (3 and 4) closes. This change produces a collision course computation.

T_1 through T_{10} inclusive have the same primary winding.

All secondaries are electrically shielded from each other.

Primary voltage = 115 v; secondary voltage = 6.3 v.

S_{10} permits adjustment for S_0 of either 12 or 15 knots.

FIGURE 17. AD III wiring schematic for sin B'_r.

is below 200 yd, give the conning officer manual control of the computer whenever he desires it.

COMPUTER

The mechanical portion of the computer (except for the time-to-fire component, which is discussed in the next section) has already been described. In the electrical portions, each circuit utilizes a servo motor, driven by the voltage difference between circuit outputs, which produces a balance by changing certain resistance values in the associated circuit. The difference voltage is thereby reduced to zero and thus the equation represented by the circuit is solved.

Resistances proportional to the range used in the electrical computation are obtained from potentiometers mounted on the shaft of the range-follower motor.

Resistances proportional to range rate are obtained directly from hand-set potentiometers on the range recorder.

Resistances proportional to own-ship's speed are obtained from potentiometers on a shaft which is positioned by a motor controlled by a synchro repeater from the Pitometer log.

Resistances proportional to smoothed relative target bearing B_r (S) are obtained from potentiometers driven by the output of a mechanical differential. Here the smoothed modified bearing, set in from the bearing cursor of the bearing recorder, has subtracted from it the difference between own-ship's course and the integral obtained from the mechanical computer, in order to get a smoothed unmodified bearing.

Resistances proportional to the product of range and modified bearing rate are obtained from potentiometers rotated according to the slope of the cursor lines on the bearing recorder. This quantity represents target speed normal to the line of sight.

A final group of potentiometers, which give resistances proportional to the sine and cosine of the computed relative bearing B'_r, is mechanically con-

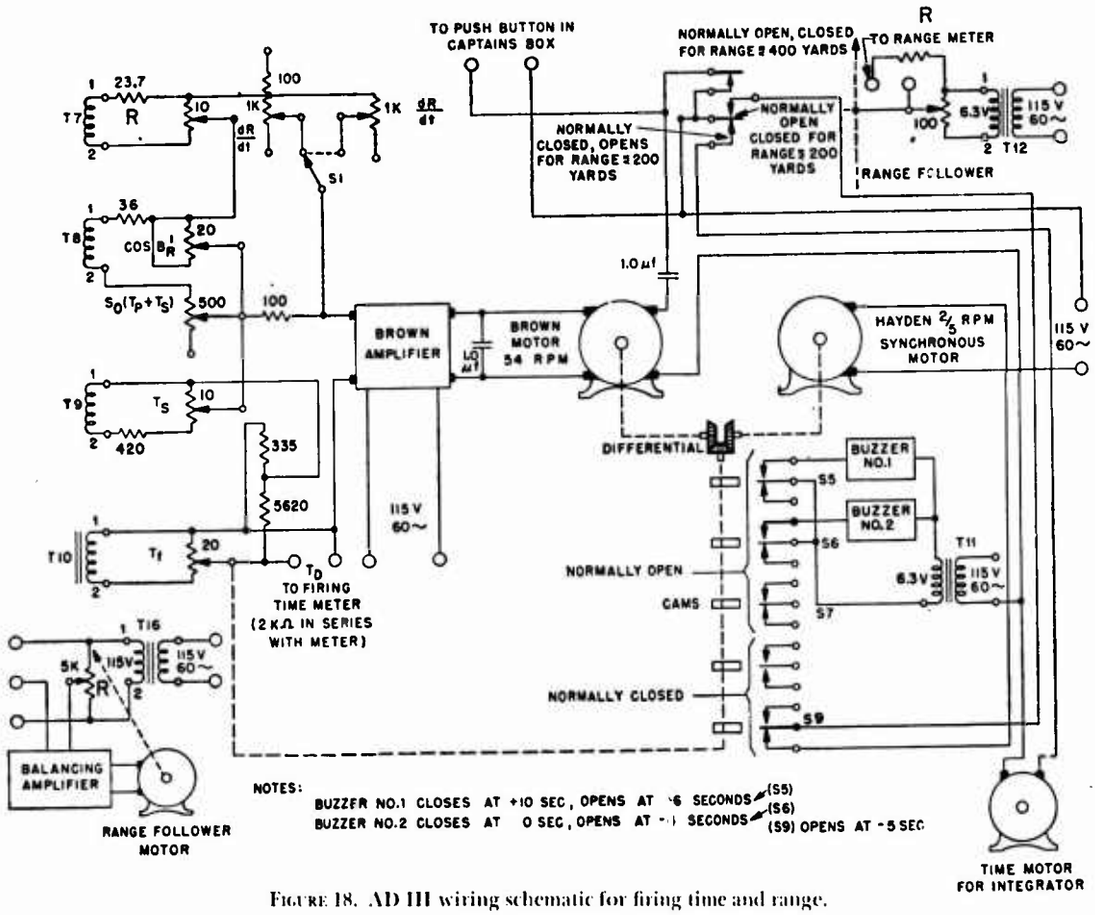

FIGURE 18. AD III wiring schematic for firing time and range.

nected to the balancing motor which produces the solution of equation (14).

After these various resistances are obtained, they are combined in five separate computing circuits. The first circuit (Figure 17) computes the course to steer for depth-charge attack. The second (Figure 18) computes the amount of time remaining before firing for depth-charge attack. The third and fourth circuits compute the two components which are used to plot target's course and speed in the captain's box (Figures 19 and 20). The fifth circuit (also shown in Figure 18) computes course to steer for ahead-thrown attack. All these circuits operate rapidly so that a continuous set of solutions is obtained.

TIME-TO-FIRE MECHANISM

The time-to-fire computing mechanism for depth-charge attack consists of a balancing motor, a balancing potentiometer, a synchronous timing motor, and a set of sequence cams. The balancing motor turns the balancing potentiometer so as to equate two voltages (the difference driving the motor) and hence solves the equation for time to fire [equation (7b)].

When contact with the target is lost, the balancing motor is turned off and the synchronous motor turns the sequence cams at the proper speed to ring a bell, by means of the cams, when the time remaining before firing reaches zero. As mentioned before, the cams also sound a buzzer 5 sec before and 5 sec after the bell rings. The synchronous motor automatically turns itself off by means of the cams after the buzzer has sounded.

8.5 RESULTS OF AD III TRIALS

Numerous tests of the AD III and other directors were made by ASDevLant during the summer and fall of 1944. An extensive summary of the results of these tests has been reported by the Navy.[4] Trials were first made on an attack teacher; then the AD III was installed on the PCE 869 for sea trials

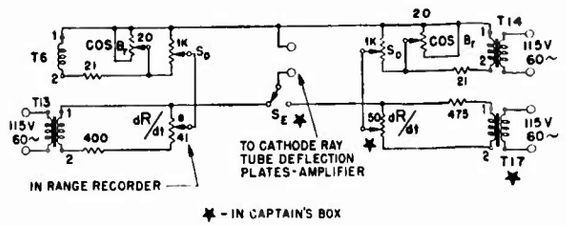

FIGURE 19. AD III wiring schematic for $S \cos A$.

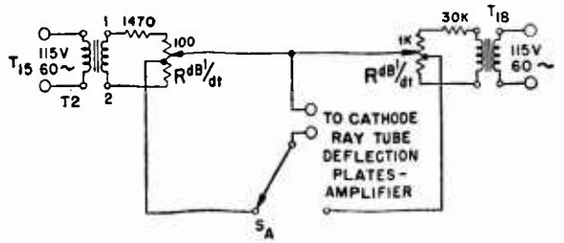

FIGURE 20. AD III wiring schematic for $S \sin A$.

against a submarine of the "R" class. For the purpose of this report, results obtained by ASDevLant may be divided into three categories which are discussed separately below.

Depth-Charge Attacks on Attack Teacher

Table 1 summarizes the results of depth-charge attacks on the attack teacher. Values for the Mark IV antisubmarine attack director, for expert unaided conning and for trained unaided conning are given for comparison. Although the AD III shows superiority over the trained unaided conning, it shows some inferiority to the experts and marked inferiority to the Mark IV director.

TABLE 1. Results of depth-charge attacks on the attack teacher.

Method of attack	% of attacks with total error less than 75 yd	% of attacks with total error less than 125 yd
AD III	24	56
Mark IV	46	74
Expert unaided	30	61
Trained unaided	18	35

While these attack teacher tests were indispensable in pointing out various engineering flaws in the AD III, the results are not fairly indicative of AD III's potentialities because a very poor range recorder was employed. Keying was erratic and the traces ragged, thus causing errors in range rate, which in turn caused errors in lead angle and in firing time. The manner in which errors in range rate affect lead and timing in a depth-charge attack can be seen from equations (2) and (7). At short range, in many cases, a given error in range rate can cause greater error in lead than in timing.

The value of the captain's box was also tested on the attack teacher, but because of the poor range recorder these tests also are not too reliable. It is apparent from Table 2, however, that use of the captain's box did raise the score of the AD III over that obtained without it.

TABLE 2. Effect of captain's box on depth-charge attacks.

Method of use	% of attacks with total error less than 75 yd	% of attacks with total error less than 125 yd
Without captain's box	24	56
With captain's box	30	68

Use of a better range recorder and development of a doctrine for use of the captain's box would probably have increased its superiority over the merely automatic operation of the AD III.

Depth-Charge Tests at Sea

Sea tests of the AD III were much more satisfactory. Numerous small misalignments were corrected before the director was installed on the PCE 869 and a good range recorder was employed. When comparing the success of the AD III at sea with other conning methods as shown in Table 3, certain facts should be borne in mind. In the first place, AD III was tested off Rhode Island, where sound conditions are poor because of thermal gradients and shallow water, whereas the Mark IV was tested off Fort Lauderdale, Florida, where isothermal layers are deep and good sound conditions prevail. Second, in tests of the AD III, as explained in the ASDevLant report, conning was done only by the director, whereas an expert conning officer was used to assist

TABLE 3. Attack results with different conning methods.

Method of conning	% of attacks with total error less than 75 yd	% of attacks with total error less than 125 yd
AD III	53	77
Mark IV	62	87
Expert conning with ASAP	65	81

TABLE 4. Numerical results of ahead-thrown attacks.

	No. of runs	Mousetrap values				Hedgehog values (same base range as Mousetrap)					
		Total error % under		Lead error % under		Time error % under		Lead error % under		Total error % under	
		30 yd	60 yd	30 yd	60 yd	30 yd	60 yd	30 yd	60 yd	30 yd	60 yd
All runs	101	22	60	37	69	66	97	60	93	48	94
Straight runs	29	27	71	44	71	82	100	59	100	51	100
Maneuvering runs	72	20	56	34	65	59	96	60	92	46	91

the Mark IV in its tests by anticipating required leads. Third, the predicting feature in the Mark IV (similar in intent to the captain's box of AD III) was frequently used, whereas the captain's box of AD III was not tested because of a failure in its component parts.

Again the Mark IV and the experts show a superiority over the AD III, although it is less than in the case of the attack teacher trials.

AHEAD-THROWN ATTACKS

Although tests of various other directors did not include the use of forward-throwing weapons, the AD III was given fairly complete tests for this kind of attack, on an attack teacher. No sea tests of this type were made, however.

Table 4 is a summary of the numerical results of the ahead-thrown attacks. It will be noted that they have been scored both for a fixed Mousetrap and for a Hedgehog firing projectile having a base range equal to that of Mousetrap projectiles. In the case of the Hedgehog the train angle used was simply the difference between the actual course and the ordered course of the ship at firing time. Since the tactical characteristics of the attack teacher ship used (tactical diameter = 520 yd) usually prevented it from being on the ordered course at firing time, the scoring for the Hedgehog gives a better estimate of the AD III's accuracy than does that for the Mousetrap.

In a comparison of lead and timing errors with the Hedgehog, it is apparent that lead errors increase very little when the target maneuvers (the change shown is statistically insignificant) but the timing errors increase very noticeably. Apparently the explanation of this is the fact that target changes in course and speed are more quickly observed on the bearing recorder, which gives the lead for an ahead-thrown attack, than on the range recorder, which affects only firing time. Since the slope of the bearing recorder trace, but not the slope of the range recorder trace, is unaffected by own-ship's maneuver, this difference in speed of detection of target's maneuver is as would be expected. These figures may also indicate the desirability of removing the effect of own-ship's motion on the range recorder.

When the values of lead errors for the Hedgehog are averaged, taking account of sign, i.e., whether the error is too much or too little lead, a systematic error of about 10 yd too little lead shows up. This may indicate that the value of the constant in equation (17) $(T_s + T_f)/(R_e + S_o T_f)$ was not properly evaluated for the tests. It is quite possible that the total errors would be made somewhat smaller if the mean value of the lead errors were made zero by changing the constant used.

8.6 CONCLUSIONS

Work on AD III was undertaken on the basis of two suppositions. In the first place, it was supposed that recorders were the best means of smoothing out erratic sonic data and converting them into useful quantities. Second, it was supposed that the predicting features of the captain's box would be advantageous in attacks against maneuvering targets. Unfortunately, neither one of these suppositions has been proven correct or incorrect by tests of the AD III.

Comparative figures for success of the Mark IV (which uses followers or generated values of range and bearing) and the AD III do not settle the question of the accuracy of followers over recorders, or vice versa, for two reasons: (1) engineering defects in the AD III may very well have covered up any advantage of the bearing and range recorder solutions, and (2) the virtual target feature of the Mark IV, rather than its method of setting up the course

and speed of the virtual target, probably contributed a great deal to its success. If comparative tests of the two directors had been made using ahead-thrown weapons, then the engineering difficulties of the AD III and the virtual target of the Mark IV would have had less chance to obscure the results. The captain's box was given tests on the attack teacher and showed some advantage. Because of breakdowns in the box at sea, however, it had no sea trials. It seems probable that if these breakdowns could have been repaired in time for the sea trials, use of the captain's box would have increased the success of the AD III.

In order to determine the validity of the two assumptions upon which the AD III was built, two sets of tests are needed: (1) values of the indicated course and speed of the target as computed by the Mark IV and the AD III should be compared with actual course and speed of the target in order to discover whether bearing and range recorders are more or less accurate in their determinations than are the followers of Mark IV; (2) attacks against maneuvering targets should be made with and without the use of the captain's box with AD III, or the curved course prediction feature of Mark IV, in order to determine the usefulness of such devices.

Attack Director B

Attack director B (AD-B) is an experimental device designed to present attacking surface ships with the collision course to steer. It utilizes the target information presented on the plan position indicator [PPI] of modern scanning sonar systems. The common principle of operation in all models is a time-matching scheme based on the necessity for a coincidence in time and position of the submarine and the exploding antisubmarine ordnance. Allowance is provided for the effect of own-ship's turning circle on the bearing of the fixed attack course. The first two models included mechanically operated time scales and bearing dials. Model III used electromechanical arrangements based on the geometry of the attack. An experimental attack aid, also based on the time-matching principle, was constructed for use with relative-bearing PPI. The work on these devices was carried out by HUSL.

FIGURE 21. Attack director B, Model I.

8.7 INTRODUCTION

The successful development of scanning sonar systems which present submarine target position information on a *plan position indicator* [PPI] raised the question of how an antisubmarine attack should be planned to utilize most effectively the information so presented. The PPI can, of course, be used to deliver range and bearing information for use in accordance with standard doctrine; the line of investigation described below, however, was devoted to the possibilities of devising simple computing linkages or other mechanisms which, in conjunction with the PPI, could be manipulated to indicate directly the proper course to steer.

No complete and convenient solution of the attack problem was obtained, but a graphical time-matching scheme was devised on the basis of the required coincidence in time and position of the submarine and the explosion point of the antisubmarine ordnance. A novel feature of this solution was the inclusion of allowance for the effect of the turning circle of the attacking ship on the bearing of the final attack course. Three experimental models of instruments embodying these principles were constructed and further proposals for improvement were made. To distinguish these devices from other attack aids using fire-control techniques, the name *attack director B* [AD-B] was assigned to them. Their performance demonstrated the soundness of the basic concepts involved, although no sea-going models of the attack director were completed. The concurrent intensive development of other attack directors based on conventional fire-control techniques indicates that

further work on attack director B should be conducted on a low-priority basis.

8.8 PRINCIPLE OF OPERATION

The problem in conducting a successful attack on a submarine is to determine the course of the attacking ship which, for a particular speed, will intersect the submarine's course at the proper time to effect a collision between the submarine and the exploding charges. The explosion point may be in front of the attacking ship or behind it, depending on the type of attack used, and this lead or lag must be included in the calculation, together with whatever other leads or lags are made necessary by such factors as sinking time, "dead time," or distance from sound projector to charge racks. The inclusion of these factors makes the problem somewhat complicated and, even if the correct course should be instantly computed on the basis of true information from the sound gear, the ship's turning circle would necessitate additional computations. Thus a successful attack is usually the result of a converging series of approximations.

All the AD-B solutions are based on the obvious fact that the time after some given instant, t_o, required for a ship to place its charges at the underwater explosion point must be equal to the time after t_o required for the submarine to travel to the explosion point.

Thus, in Figure 22, let

O = own-ship's position at t_o.
T = target's position at t_o.
S_o = own-ship's speed.
S = target's speed.
A = target aspect angle.[d]
r = target range.
E = explosion point.
D_s = distance own ship travels while charges sink.
P = position of own-ship's projector at the instant of explosion.
D_p = distance from own-ship's projector to depth-charge racks.
t = time between t_o and the explosion.

For a stern-dropped attack, it is necessary to steer a collision course between the target and a point trailing $D_s + D_p$ behind the sonar projector. At the instant of explosion, the attacking ship — or more precisely, its projector — must be at P, where $EP = D_s + D_p$. Therefore, in a successful attack course, the time necessary for the ship to travel the distance OP must equal the time required for the submarine to travel the distance TE. (A similar solution is available for an ahead-thrown attack.)

Although it is possible to secure a straightforward mathematical solution for the proper lead angle B to meet these conditions, the resulting expression is rather complicated. It is much easier to determine the solution by indirect cut-and-try (hunting) methods. Thus, in early models of this device, the solution was obtained by a manual matching of time on two scales calibrated in minutes and seconds for the particular speeds of ship and submarine respec-

[d] This usage of "target angle" differs by 180 degrees from the approved definition of the term as "the relative bearing of the ship as seen from the target."

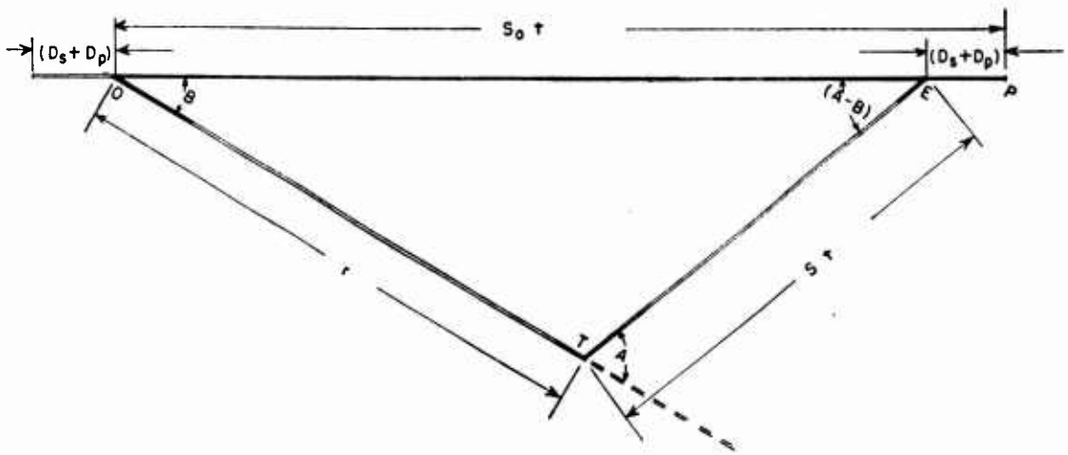

FIGURE 22. Attack triangle for stern-dropped charges.

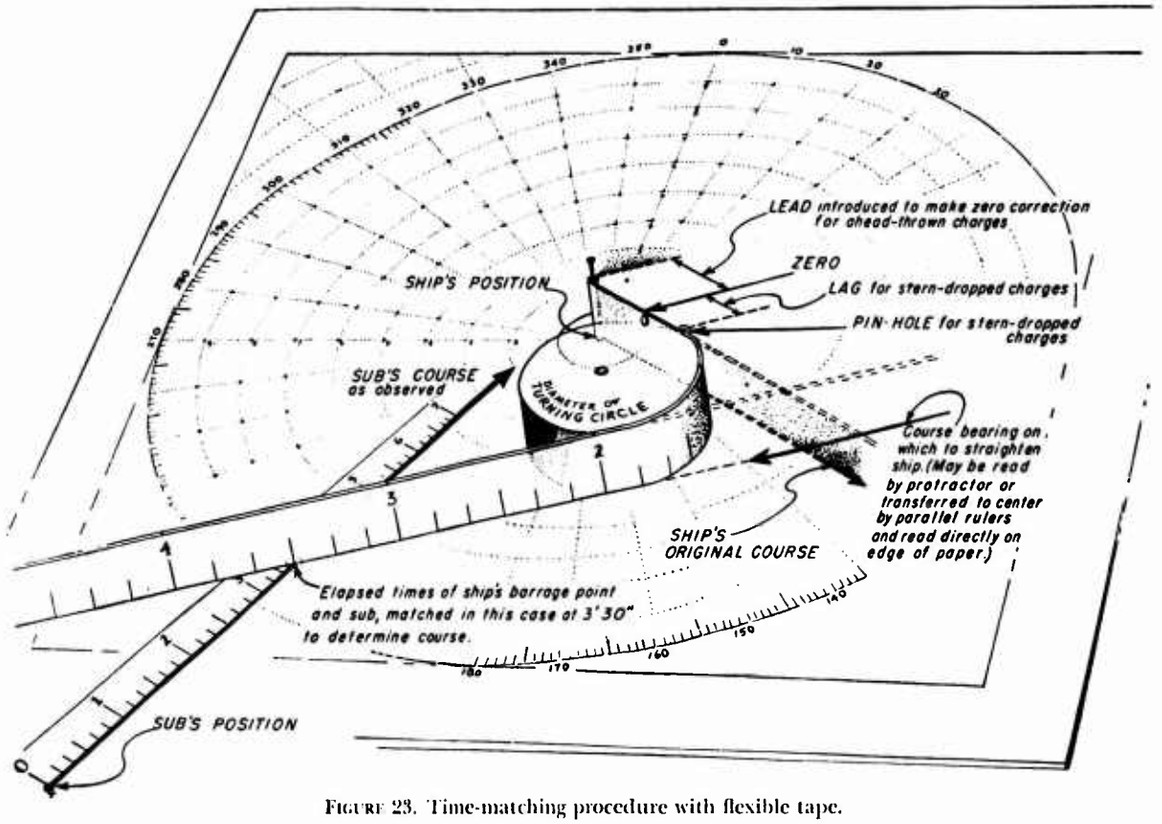

FIGURE 23. Time-matching procedure with flexible tape.

tively. In the final model, the time matching was done by manually adjusting resistance strips to balance opposing voltage drops. A model has been proposed for future development in which the adjusting itself would be automatic through use of a servo link. Regardless of how the adjustment is accomplished, however, the operation is basically a cut-and-try time-matching process.

8.9 ATTACK DIRECTOR B AND MODIFICATIONS

8.9.1 Graphic Aid for Solving Attack Course

The simplest type of graphic aid using manually positioned time scales is illustrated in Figure 23. Assume that a submarine *T* has been located on the screen of a true-bearing PPI, and its echo trace observed long enough to determine its vector. Supported over the screen is a maneuvering board pattern, with own-ship's position at its center. A ruler graduated in minutes and seconds for the target's particular speed is selected and laid with its zero at *T* and its edge along the target's course. The helmsman is given the order to turn toward the target. Meanwhile, a tape, graduated in minutes and seconds for the particular ship's speed, has been selected and is positioned by a pin or other means at the center of the plot. A circular block, with radius proportional to the turning circle of the ship, is placed tangent to the original course line at the point corresponding to the time when the turn actually begins. If the tape is stretched taut around this block, and the time graduations of the two scales are matched at the point of their intersection, the tape direction indicates the course necessary to determine a collision between ship and target. The plot has become, in effect, a geographical map, at a certain instant, of a projected attack. The bearing of the attack-course line may be read by a parallel ruler linkage or other means and provides immediately a unique solution for the course to steer. Additional loops on the tape for the pin can take care of various leads, or, in the case of stern-dropped charges, lags. After the first course change, the use of the turning circle correction can perhaps be ignored for additional computations.

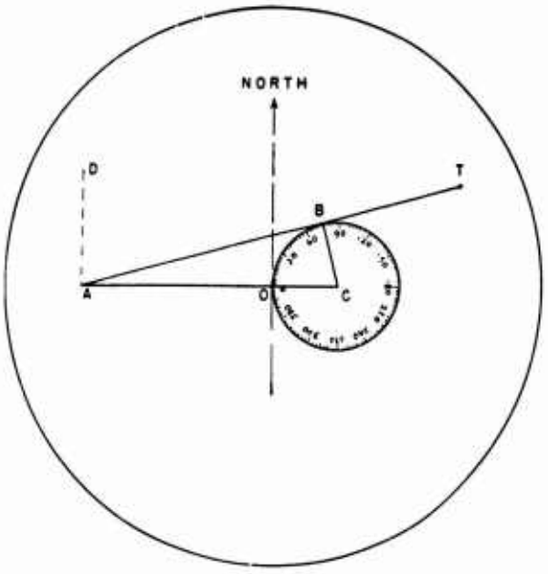

FIGURE 24. Indication of course change to reach point *T*.

AD-B MODEL I

The name, attack director B was first applied to a modification of the model just described which improved the reading of the attack course bearing by use of a gear train, a rotatable "tangent shield" and a bearing dial.

In Figure 24, *O* represents a ship traveling north. Then the arc *OB* stands for the portion of its turning circle required to reach *B*, the point of tangency with the final course toward a target *T* (supposing the target to be at rest). By geometry, the angle *OCB* = *DAB*, the true bearing of the final course. Now, if a dial, graduated in degrees clockwise from point *O* = zero, is centered over *C* as shown in the figure, the desired course is immediately readable at point *B*. If the ship is not traveling true north, however, such a reading is in error, and a correction is needed. This correction may be introduced by an epicyclic train of gears mounted on a bracket so that the line of centers is a straight line, as shown in Figure 25, where gear *O* is fixed. Then, as the bracket is turned around the center of *O* as a pivot, *B* rolls around *O*. As *B* meshes with *C*, *C* still maintains its *directional* orientation even though it is being moved in space around *O*. In other words, when the line of centers *OBC* has been turned clockwise by, say, 75 degrees to *OB'C'*, the rotation of *C relative to the line of centers* is 75 degrees counterclockwise. Thus, an arrow that pointed west at *C* still points west at *C'*, and likewise, in any other position around *O*, and therefore completes one revolution around its axis as that axis makes one revolution around *O*.

Accordingly, if a dial is fastened to *C*, as shown in Figure 26, its graduations always point in the same direction in space. Let its zero be pointing always to the left (west), and let its radius equal *CO*, the length of the line of centers. Then as the assembly is carried around *O*, the circumference of the dial always contains *O*. Furthermore, if a transparent shield whose edge is the line *DPE* is pivoted at *C*, with *CP* equal to *CO* and with its edge therefore always tangent to the dial circle, a means is available for representing the course to steer which takes proper account of the turning circle. Furthermore, this course is directly indicated on the dial (72 degrees in this case in order to intersect a target at *T* from an original course of 25 degrees). This method was used in the Model 1 AD-B.

Time was indicated in the model by another dial instead of by a tape stretched around a template as in the original design. The time dial is the larger and upper of the two shown in Figure 21. It is graduated in seconds of time for the attack speed, and press-fitted to the shaft on which gear *C* rotates, so that this dial always has its zero pointed along the line of centers toward the center of gear *O*. The tangent shield in this case is designed to carry a sliding scale, also graduated in time, in rack-and-pinion engagement with the time dial. Thus, regardless of the amount of rotation of the tangent point from *O*, time may still be read directly from *O* around the arc and along the tangent scale to

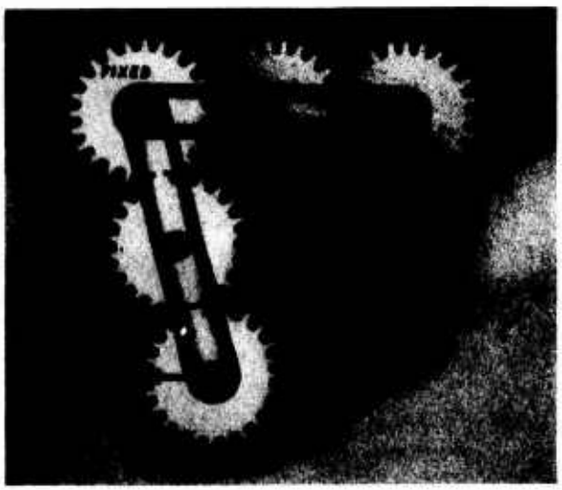

FIGURE 25. Epicyclic gear train, gear at *O* fixed.

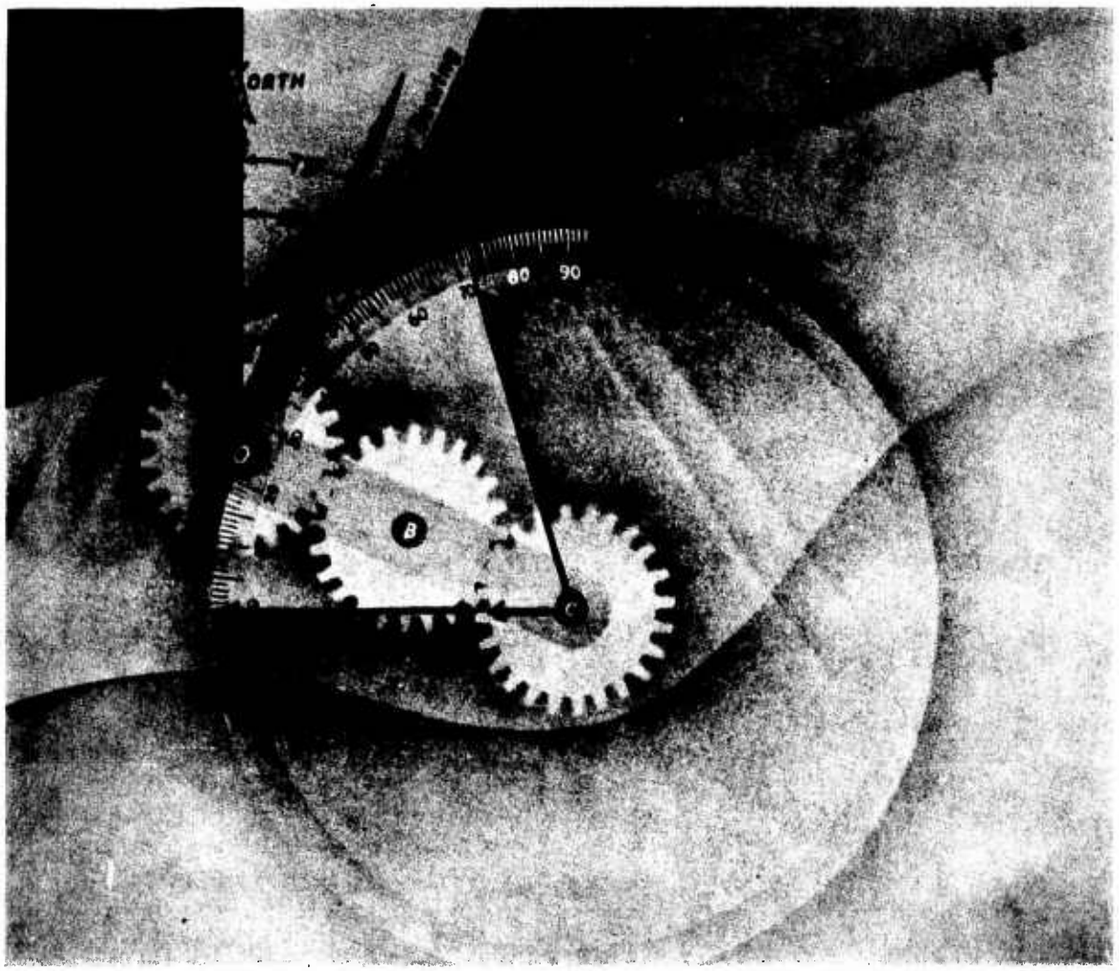

FIGURE 26. Course-to-steer dial.

any given point. The bearing dial, the size of which is no longer significant, is made smaller in this model in order to bring the circular time scale into juxtaposition with its continuation along the straightedge.

In actual antisubmarine warfare, of course, the target is moving, and it is essential to know its speed and course, or at least to estimate them as accurately as possible in the first of a series of approximations. One way of doing this is to maintain ship's course long enough after the initial discovery to determine the target vector. When the latter is known, as in the case already described, a time scale graduated for target speed is laid along its vector. The tangent rule is then adjusted in bearing until a point is found where the two time scales match numerically, determining in this way the unique time and course for collision with the moving target. The plot is then in effect an instantaneous geographical map of a projected attack, and although this map changes continuously (since the CRO is a ship-centered true-bearing PPI), if the time scales are adjusted to maintain their numerical match, the slope of the tangent and the time indicated furnish at every instant a true prediction for a collision course. All that remains to be done, then, is to introduce whatever time corrections are necessary to provide for such factors as sinking time, dead time, distance from sound projector to charge racks, and, in the case of ahead-thrown charges, flight time.

Suppose, for example, that in the case of an ahead-thrown attack, the charges fly a distance of 250 yd, and sink vertically, the entire procedure from firing to explosion consuming 15 sec. The ship must, of course, fire at the instant when it is 250 yd from the explosion point, and it must arrive at the firing

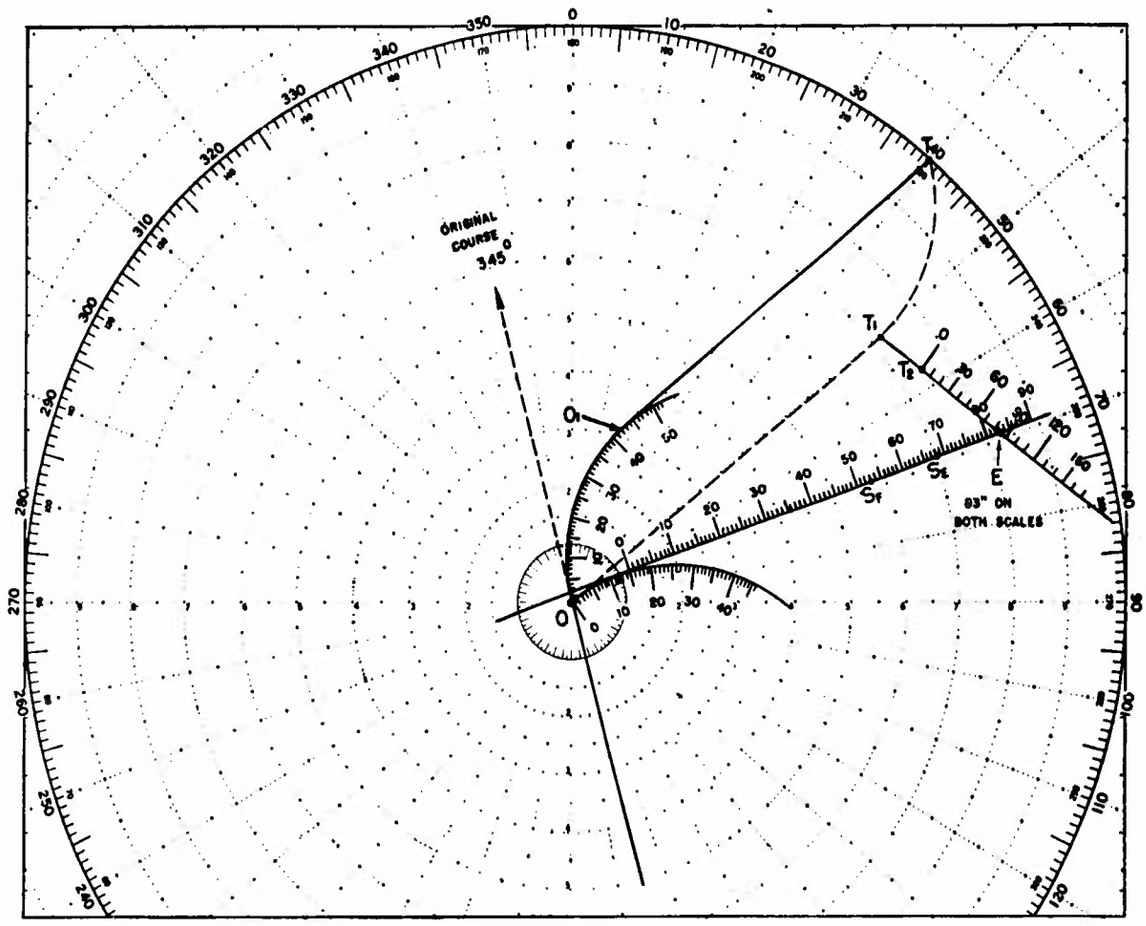

FIGURE 27. Plot of attack on true bearing PPI.

point precisely 15 sec before the submarine is to arrive at the explosion point. During the 15 sec from firing to explosion, the ship travels about 125 yd (at 15 knots), so that if it were to maintain course it would be 125 yd from the explosion point at the instant of explosion. The problem then is to steer a fictitious point 125 yd ahead of the ship for a collision course with the target, but to fire 15 sec before the calculated collision time of this point and the target.

This may be accomplished by the time-scale matching process, if a 125-yd lead is introduced in the scale. Thus, in Figure 27, suppose a ship traveling on a course of 345 degrees locates a target on bearing 40 degrees at 1,000 yd. When the tangent scale is placed on the echo spot, the bearing dial calls for a new course of 50 degrees, and the time to the target's present position is read as approximately 2 min 5 sec, of which the travel around the 65 degrees of the turning circle to O_1 will consume approximately 42 sec. After 42 sec, therefore, the echo spot for a target at rest has traveled along the curved portion of the dotted line from T to T_1, and from there on will travel on the straight line T_1O. Actually, however, the target is moving, and instead of being at T_1 it is observed to be at T_2 at the end of 42 sec. Then T_1T_2 is a vector measure of target's motion. Use of the time-speed-distance scales on the maneuvering board plot shows the target's speed to be 4 knots in this case. A transparent scale is then selected which is graduated in time for a speed of 4 knots, and is laid along the target's course with zero at T_2 or at any other "now" position. Since it is necessary to steer a point 125 yd ahead of the ship, the tangent scale is moved ahead a distance corresponding to the time required to travel 125 yd; i.e., approximately 15 sec. (If the tangent scale were in permanent rack-and-pinion engagement with the time dial, it would have to have its zero point at the time dial's 15-sec point.) Then, by adjusting the

angle of the tangent shield (the rack and pinion maintaining in the meantime the 15-sec lead), a point is found where there is a numerical match between the tangent scale and the target's scale. In Figure 27 this occurs at 83 sec, which is the time remaining until the explosion of the charges. (It is only a coincidence that the 15-sec point on the dial falls in this case close to the point of tangency.) The course indicated by this second approximation includes a short additional arc of the turning circle and a straight run, which the bearing dial (not shown) indicates to be on course 72 degrees. At the expiration of 83 sec (i.e., at the explosion instant), the ship will have arrived at S_E, 123 yd from the explosion. However, the instant of firing must have been 15 sec earlier, while the ship was at S_F, and movement of the ship after this instant, of course, has no effect on the attack. A ship usually shifts course sharply in order not to lose sound contact.

A similar solution is possible for a stern-dropped attack, where a time lag must be introduced instead of a lead. In the case of a target sighted to the left of the ship's course, additional scales (not shown in Figure 21) permit the device to be reversed and used in the same way for attacking a target through a course change to the left.

This attack-predicting device was constructed as a breadboard model without the rack-and-pinion gearing, and worked sufficiently well to demonstrate the soundness of the principles.

AD-B Model II

Model II of attack director B was built with greater precision. In it (see Figure 28) the moving parts were mounted on a base plate of Lucite, so that the whole unit could be attached to the QFH Sangamo conning teacher for testing.

The gears in the gear train are smaller, enabling a larger range scale to be used for a given turning radius than was possible on the previous model.

The sliding time scale *A* is longer and is not in rack-and-pinion engagement with the time dial, but with a separate (transparent) gear *B* above the time dial. This gear is movable by means of the knurled nut *C* to which it is attached. The time dial itself, as in the earlier model, is always positioned with its zero at ship's position, indicated by the small arrowhead at the center of the plot. Any desired lag or lead time may accordingly be introduced into the calculation by turning *C*, which means the sliding rack, until the desired amount of mismatching at the tangent point is obtained. For example, referring to Figure 27, if "0" on the rack is made to coincide with "15" on the fixed dial, a 15-sec lead has been introduced. This mismatch must be introduced when the tangent line is approximately on the target and at the tangent point because the divisions of the time scale around the dial are approximately 20 per cent smaller than those on the straight scale, in order to allow for the speed decay in a tight turn. With the particular turning radius used in this model, this amount of speed decay from 15 knots causes the time scale divisions around the turning circle to be approximately one degree per second, so that the graduations are the same for time and bearing.

The target scale *D* shown in Figure 28 is for a 7½-knot submarine and indicates a time match with the ship's scale at 2 min 20 sec, after a starboard turn by the ship. By selecting the proper scales the device is usable for either port or starboard maneuvers.

An attempt was made to test this model on the QFH conning teacher but, since the model must be operated horizontally, it was necessary to tip the conning teacher in order to place its screen in a horizontal rather than the customary vertical position. Since this procedure introduced errors into the tracking of the conning teacher spot, no significant results were obtained.

AD-B Model III

In the two models already described, the determination of the point of time match was accomplished by a visual and manual hunting procedure. The hunting may also be done electromechanically if the two sides of the attack triangle are linearly wound resistances, insulated from each other and fed by suitable currents.

Referring to Figure 22, if the time for the ship to travel $D_s + D_p + OE$ must be equal to the time for the submarine to travel TE, then

$$\frac{D_s + D_p + OE}{S_o} = \frac{TE}{S},$$

or

$$S(D_s + D_p + OE) = S_o(TE).$$

Thus, if currents are used that are proportional to speeds, and resistances that are proportional to the distances, voltage drops result which, when equalized, indicate a solution.

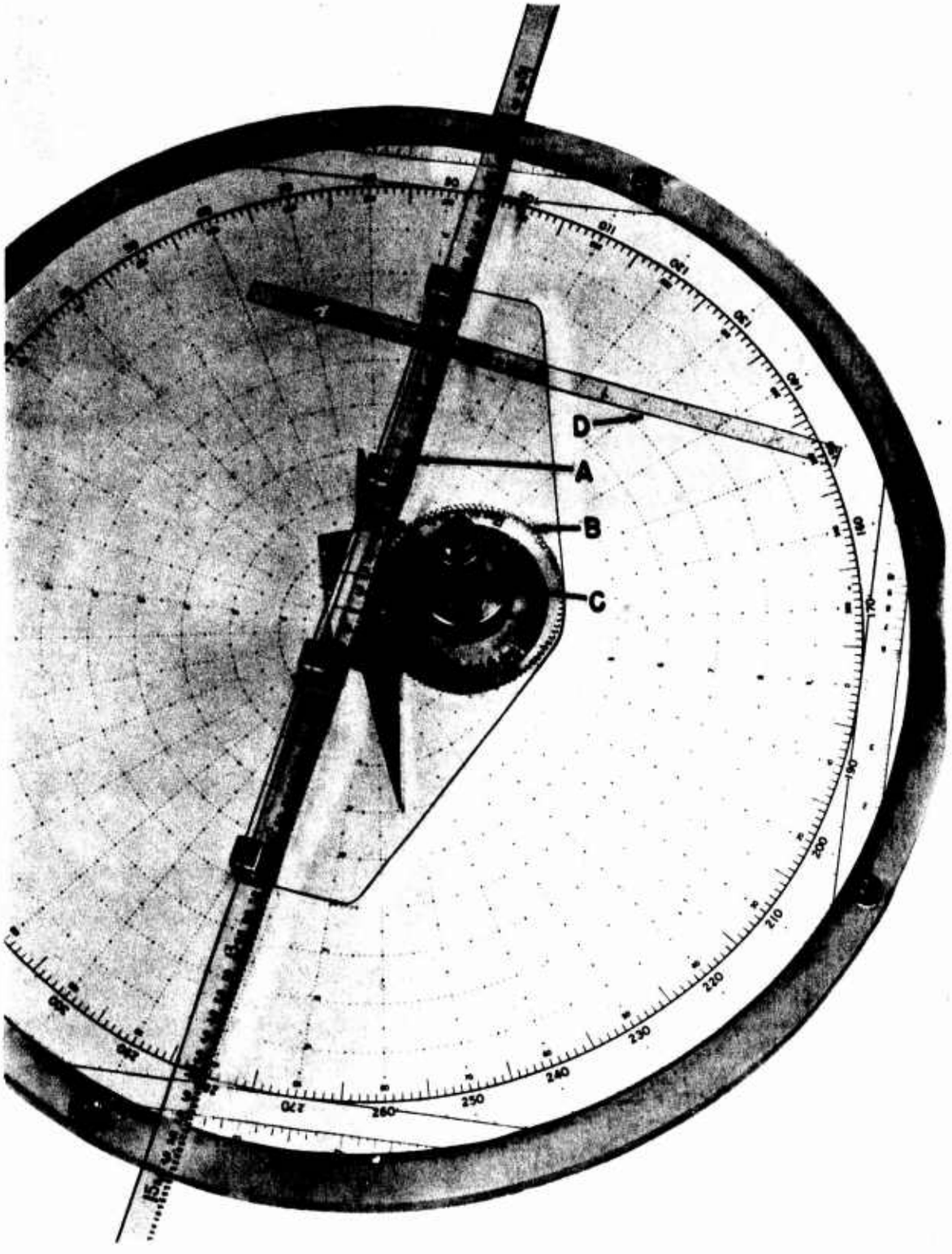

FIGURE 28. Attack director B, Model II.

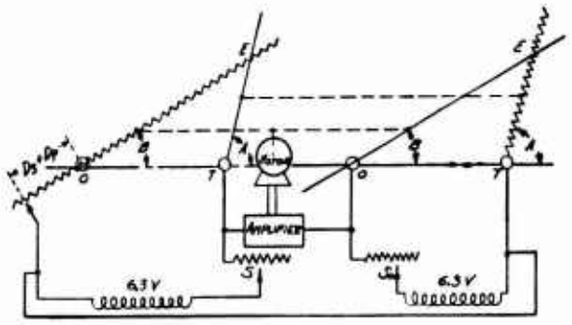

FIGURE 29. Servo-driven, time-matching device.

Figure 29 is a schematic for a device which embodies this principle with the turning circle being neglected for the moment. Two triangles are shown because of the need for insulating OE from TE. The two triangular brackets would in practice be mounted one over the other, rather than side by side, their corresponding arms being positively connected so that the two OE's, for example, would always move together. Thus, the geometrical relationships would be identical at any instant for each triangular bracket. (Mechanical links are shown in dashed lines.) If resistances S_o and S are made large in comparison with the other resistance strips, the currents are only slightly influenced by changes in OE and TE respectively, and close approximations are obtained for the two sides of the equation. If these values are balanced against each other so that their difference operates through an amplifier to drive a correcting motor, the equation is quickly solved in terms of the necessary angular relationship between the arms of the triangle. In other words, if OT is set to represent range (T would have to be movable toward O as range closes), and TE is set so that aspect angle A matches that observed on a scanning sonar screen, then an electrical unbalance is set up which operates to rotate OE around O until a balance is obtained. When this occurs, angle B indicates the proper lead to take.

Figure 30 shows a model which was built to test the principle of an electrical balancing of IR drops in such a solution. The axes of shafts O and T correspond to points O and T in Figure 29 (present positions of own ship and target). The distance from O to T (range) is controlled by the rack-and-pinion setting. The rack assembly, which carries shaft O, is driven back and forth by the pinion, and range is indicated on scale R by a pointer. It will be seen that a resistance strip D and a brass contact rod C are secured in a bracket F and thus may be swung simultaneously around pivot point O, making sliding contact respectively with a brass contact rod B and a resistance strip A. B and A are connected together mechanically in such a way that they move as a unit, rotating around the pivot point T when moved by handle H. The points of contact in this particular setting of the strips are at E_o and E_t. The distance the submarine must travel is thus represented by the distance along the top resistance strip from T to E_t; the distance the ship must travel is represented by the distance along the bottom strip to E_o, plus whatever additional resistance is necessary to simulate $D_s + D_p$. This latter is hand-set on a separate resistance. (Calibrating resistances are also provided to enable proper zero settings to be introduced for each resistance strip, so that the resistance at any point along the strip is proportional to the exact distance of the point from the pivot axis.) Meters were provided so that the currents could be made proportional to the speeds, and an oscilloscope was used to show the balance point by a null indication. The test circuit is shown in Figure 31.

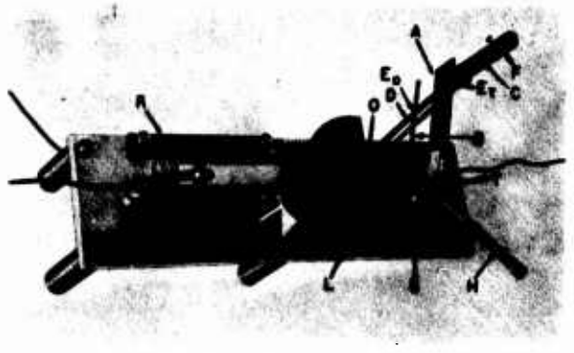

FIGURE 30. Attack director B, Model III.

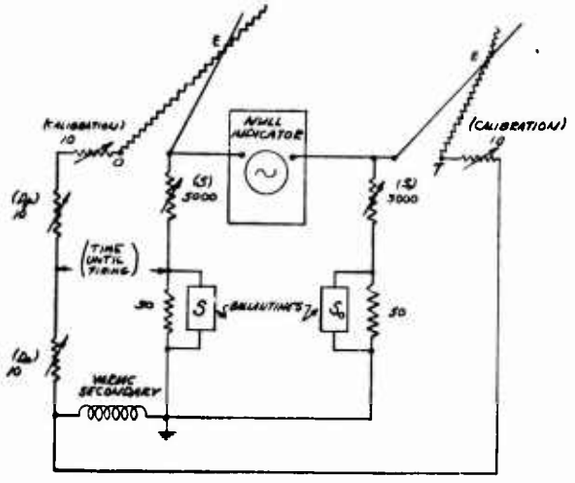

FIGURE 31. Test circuit for Model III.

In operation, then, the upper resistance strip and therefore the integrally connected contact rod underneath it are set by handle *H* (Figure 10), to the target aspect angle as observed on a scanning screen giving a geographic plot of ship and target movement. The dial *G* shows the target aspect angle set to 72 degrees. The range, in this instance 1,400 yd, is also set in. Then bracket *F* is moved back and forth until the null indicator shows the point of balance, the correct lead angle being immediately readable on dial *L*. (Pointer is obscured in this case by the range-set knob.)

8.9.2 Application of Time-Match Principle to Relative Bearing PPI

Since a relative bearing plot is frequently used (with a movable ring to indicate true bearing), the theory was worked out for applying the time-match principle to a relative plot. This was done before the development of the electric model of AD-B (AD-B III). On a relative plot, the appearance of target motion is radically different from what it is on a true plot, if the ship changes direction.

The curve followed on the relative PPI by a target at rest, as an attacking vessel executes a turn, is an arc of a circle which has its center at a point directly to the right or to the left of the center of the PPI by a distance representing the radius of the attacking ship's turning circle. A family of these paths is shown in the upper part of Figure 32. The radii of the successive circles differ by an amount which might conveniently represent the distance traveled in 10 sec by a 15-knot destroyer. An additional set of lines is drawn tangent to the inner circle to represent 10-degree intervals along the arc, with reference to course changes of the attacking ship. If this pattern were engraved on a shield of transparent plastic placed over the CRO of a scanning sonar screen, a target at rest would appear against the background of the pattern to move along one of the arcs, crossing the 10-degree lines at a rate depending on the turning rate of the attacking ship. If, however, the target were moving, the component of its motion along the (final) line of sight would appear as an inward or outward motion with respect to the arcs; that is, it would move from one arc toward the adjacent one. This motion is, of course, combined with the motion of the spot along the arc which is due to the turning of the attacking ship, so that the total motion is diagonally across the spaces

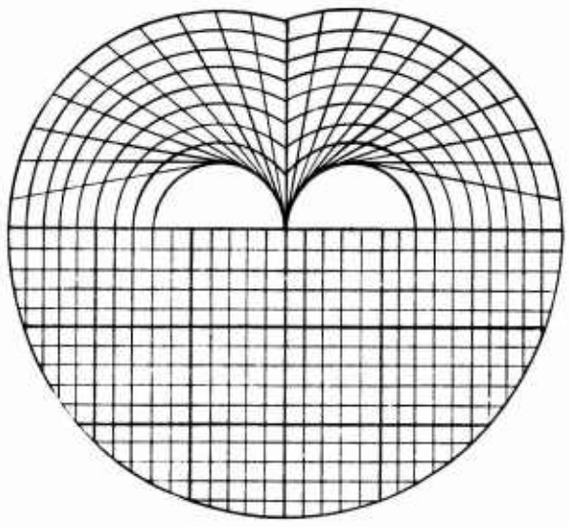

FIGURE 32. Pattern for relative bearing PPI.

bounded by the arcs and the tangent lines. The component transverse to the final line of sight appears as a change of the angular rate, but also produces some inward or outward motion with respect to the arcs. Comparison of the rate at which the target spot appears to move across the tangent lines with own-ship's angular rate obtained from a gyrocompass repeater would permit evaluation of this component. Thus, with the aid of the distorted polar plot shown in Figure 32, it should be possible to estimate target motion in spite of the execution of a turn by the attacking ship. It should be noted that the drawing of this figure is based on perfectly circular motion during a turn; an analogous diagram, however, could be based on the true path of the attacking vessel in question. The lower part of the diagram is a simple Cartesian plot which would be useful in estimating target motion when the ship is traveling in a straight course. For this purpose the pattern would be rotated 180 degrees, assuming that the target is normally discovered in the forward half of the PPI.

Figure 33 shows a breadboard model of an attack aid for use on a relative plot PPI which utilizes the principle of the curved paths of Figure 32, in conjunction with the principle of time matching.

In this case, assume the attacking ship *O* makes a contact *T* on relative bearing 50 degrees and is immediately given full right rudder. Suppose, further, that the range is 1,000 yd at the instant when the ship goes into its turning arc, and also that the turning arc is a part of a true circle. Then the target spot describes the arc *TP* as the ship turns toward

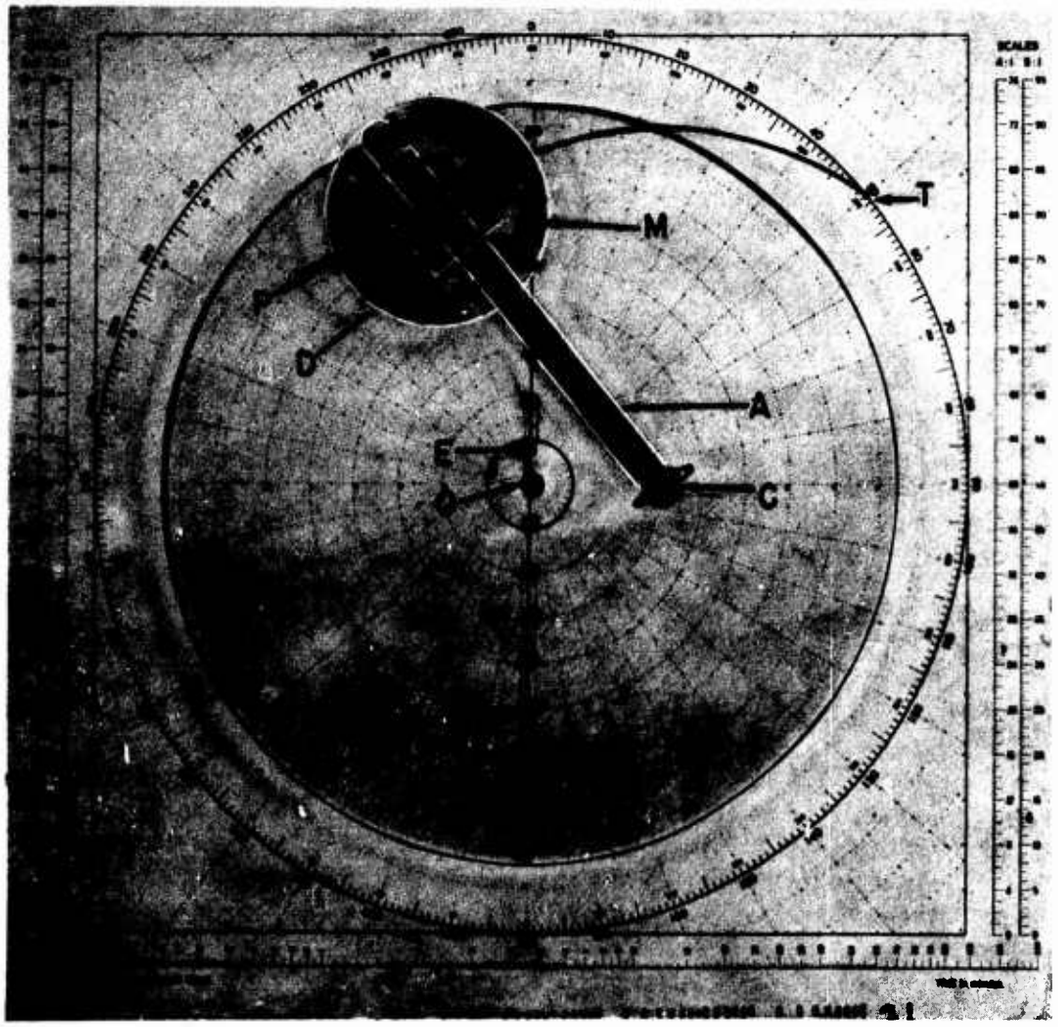

FIGURE 33. Attack aid for relative bearing PPI.

the target, *if the target is not moving in the water.* As before, this arc is a portion of a circle whose center *C* is distant from *O* by an amount equivalent to the radius of the turning circle. This arc may easily be determined by the device shown. Point *P* (the center pin of the disk *D*) is first placed on the target spot *T*, by swinging arm *A* around *C* and sliding the disk bracket along arm *A*. Then if arm *A* is swung back again, point *P* traverses the target spot arc. Furthermore, the known speed and turning radius of own ship determines the position of the target spot at any instant after the initiation of the turn. The target spot is observed as it traverses the arc, and as soon as possible its approximate vector is determined by noting where it actually is located in relation to the point on the arc where, at a certain instant, it would be if the target were not moving in the water. When the target's vector is known, its speed is determined and the particular time scale is selected from the set on the disk which corresponds best to the speed. The disk (with its center at the point where the target spot would be at a certain instant if the target were at rest) is then rotated on pin *P* in order to position the proper scale to point in the direction of the vector. Movement of the arm as a whole then transfers this vector direction along the arc to future positions. It then becomes a problem of matching time on this scale with time

as indicated on ship's scale (dead ahead). In Figure 33, a match *M* is indicated at 165 sec on the 6-knot target scale against a ship scale based on 15 knots. This establishes *PE* as the apparent course along which to bring in the target spot, where *E* is the explosion point.

It is evident that this device is merely a mechanical vector solver. If the ship could come out of its turn to a straight course instantaneously and did so on the true bearing it had at the instant the target spot arrived at *P*, it would be necessary only to maintain the same true bearing and to fire at the proper instant, taking account of time of hight and sinking. Actually, of course, the helmsman must ease the ship out of its turn. Even so, he will have an optical aid if he watches the plot and tries to bring the target spot in along line *PE*. To help in this respect, an elastic spring or other cursor might be stretched between *P* and *E*.

8.10 RECOMMENDATIONS FOR FUTURE WORK

The principal disadvantages of such devices as have been described are to be found not so much in the principle nor in the devices themselves, but in the difficulty of locating accurately the target's successive positions on a CRO screen. On a true-bearing scanning PPI, for example, by the time own-ship's movement is taken out of the total relative movement, the target's vector is but a short line of the same order of length as the individual arcs constituting the echo image on the screen. Since geographic plots are much better, attempts were made to test AD-B Model III by means of a geographic plot on a General Electric antisubmarine attack plotter [ASAP] which had been modified to portray a scanning spiral whose center moved with own-ship's motion. Electronic difficulties, however, prevented an accurate calibration of the movement of the target spot in range and bearing to match that of the Sangamo QFA-5 attack teacher which was generating the problem. Thus, the test was only partially satisfactory although it demonstrated the real value of a geographic plot presentation of the data, where the observed motion of the spot on a long-persistence CRO gives an immediate, visible representation of its vector.

Even in the case of a geographic plot, however, at the present stage of the scanning art the accuracy with which target aspect and course can be determined is none too great, because of the relatively large size of the echo spots and their shifts in position due to refraction effects in the water and electronic instabilities. Optical enlargement of the scanning image would probably not improve the situation sufficiently to justify its use. It would be advisable, therefore, to test the accuracy of AD-B and its modifications by the use of a standard (nonscanning) ASAP, fitted with some kind of cursor to transmit target aspect (angle *A*). In the standard ASAP, there is little ambiguity in the interpretation of target motion once the target has been discovered. It should be emphasized that the attack directors described herein, although developed specifically for scanning procedures, may be used with searchlight systems with equal or even better results, if sufficient information can be provided to the director.

With respect to AD-B Model III, its full electrification would include a method of continuous reception of range and target angle, preferably under servo control, and a resulting continuously servoed correction and indication of course to steer. For greater accuracy, the turning circle correction could also be included. This last would necessitate an initial resistance in the form of an arc (see Figure 34). The arc would need to be rotatable around own-ship's spot (under servoed ship's gyro control) in a manner similar to that in which the dial assembly of AD-B Model I is rotatable, while a straight resistance strip which would always be tangent to the arc would be held against the arc resistance in sliding engagement. The total resistance of the ship's side of the equation would then be that along the arc from a contact made at *O* to the point of tangency *P*, plus the resistance from *P* along the straight strip to the match point, plus whatever lead or lag resistance was needed (supplied as before by a separate rheostat). It is evident that any desired speed decay could be built into the turning arc resistance, and also that it would be possible to use an eccentric arc to copy more closely the actual ship motion.

Referring again to Figure 34A, *OT* would be maintained proportional to range by moving the lead screw automatically by means of range rate transmitted from a chemical recorder or other device. Angle *A* would be maintained equal to the difference between true target course and true target bearing, through the use of some type of cursor protractor over the face of the ASAP together with the appropriate synchro inputs and necessary servo links. The calculating resistances would be continuously fed

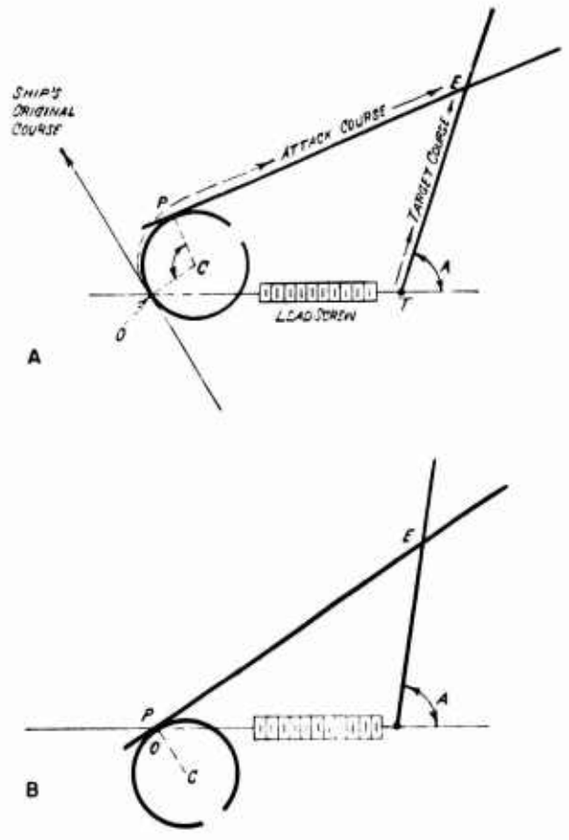

FIGURE 31. Attack course on electromechanical model, before and after traversing turning arc.

with currents proportional to the speeds. When these conditions are met and the electrical unbalance is used to servo *PE* to a balance point, the geometry of the correct course is continuously pictured. To secure a continuous dial indication of the course to steer in true bearing, it is only necessary to combine properly in a DG synchro the angle *OCP* and the ship's gyro. When ship attains the correct course, *O* and *P* correspond, and angle *OCP* becomes zero.

The problem pictured in Figure 34A shows a 99-degree arc of the turning circle to be necessary to attain the attack course. In Figure 34B, the situation is shown at the completion of the turning arc. The diagram is shown relative to the line of sight, which would be the fixed base line of the device. Thus, the orientation of the attack course on the paper has changed, although it is still the same in true bearing.) The course has shortened, the range is slightly less, angle *A* has increased, and angle *OCP* is zero. If the initial conditions do not change, the same true bearing course is indicated as the run is continued, even though angle *A* changes as the bearings swing aft for a depth-charge attack.

8.11 CONCLUSIONS

The simple devices which have been described solve the attack course problem but leave much to be desired. In the case of the earlier models, their use requires a constant manipulation or reading of several scales, the operation of a stop watch, and other adjustments. All the models, including a completely electromechanical one, would be limited by the operator's difficulty in determining target movement on a PPI screen, as has been mentioned.

On the other hand, such devices have at least two definite advantages. First, they are simple but at the same time free from the fault of triangulation schemes which give solutions based on unreliable single observations; for, when a CRO with a persistent screen is used, the original determinations of the target's position are visual averages of several positions. Second, such devices furnish a visual presentation of the geometry of the projected attack. It is suggested that these advantages might make AD-B useful in a training program, where the problem is so often to make clear to students the tactical geometry involved.

Chapter 9

AUTOMATIC CONTROLS

THE SERVOMECHANISM is an accurate, automatic control system, which is extremely valuable wherever close regulation of the position of a device or the state of a process is required. By the end of 1943, this type of system was becoming so widely employed in the projects of the Harvard Underwater Sound Laboratory that it was decided to conduct a general investigation of low-power servo motors and their control amplifiers in order to provide flexible equipment for general usage in the laboratory program.

Accordingly, performance tests were carried out on a group of fractional-horsepower motors and an evaluation was made of their usefulness in servo applications. After a tentative classification of control amplifiers had been drawn up on the basis of their rated characteristics, several preferred types were constructed and tested. Finally, different motor-amplifier combinations were studied to determine their suitability for various types of projects. To facilitate reference and interpretation, the results obtained were presented in tables and graphs wherever possible.

The investigation showed that several specific types of motor (obtainable commercially) are fitted for servo use, and simple, reliable control amplifiers, having widespread applicability in servomechanisms, can be designed and constructed. Moreover, it was found, from the few cases where it was employed, that the quantity known as the complex transfer function provides a very powerful tool for servomechanism analysis.

The results of these studies have proved valuable in the design of automatic control systems for several types of problems. In view of the probable increase in the use of small servomechanisms for fire-control and similar equipment, it is recommended that further studies be undertaken to provide instruments for the experimental determination of complex transfer functions so that the design of high quality servo systems will be facilitated.

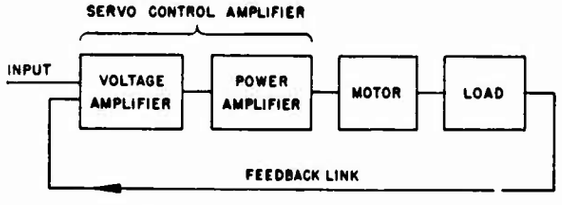

FIGURE 1. Block diagram of servomechanism.

9.1 GENERAL CONSIDERATIONS

A servomechanism consists essentially of a servo motor and its load, a control system for the servo motor, and a feedback link (see Figure 1). The combination is so arranged that deviation from the desired condition of the load activates the motor control system and the resulting operation of the motor immediately tends to remove the deviation. Stability, good transient response (small overshoot), speed, and adequate output power are the fundamental requisites of a good servomechanism. To obtain them in a given case, well-designed components must be carefully matched, both with each other and with the specified load.[a]

The present investigation covered low-power instrument or fire-control servomechanisms of the all-electric, continuous-control type. Such systems contain a fractional-horsepower electric motor, a vacuum-tube amplifier controlling the motor, and a means of obtaining an electrical error signal. They have a very closely regulating corrective action which is initiated by any load deviation, no matter how small, in contrast with the behavior of on-off control systems, which start correction only after finite deviation has occurred.

Since the choice of a motor suited to the specified load is the primary step in assembling a servomechanism, the results of the motor investigation are presented first, in the section immediately following. Subsequent sections deal with control amplifiers, which can be selected in a given case only after specific motor requirements are known.

9.2 SERVO MOTOR PROPERTIES

The motors studied in these tests were wound for 2-phase, 60-c service. All the rotors except two were

[a] For a complete treatment of theory and design, the reader is referred to the reports of work done by Division 7 of NDRC.

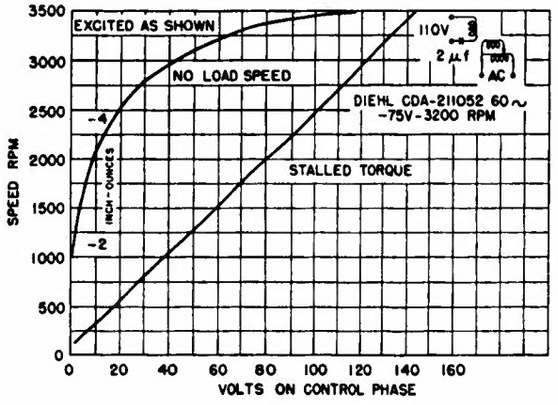

FIGURE 2. Speed-voltage and torque-voltage curves for servo motor.

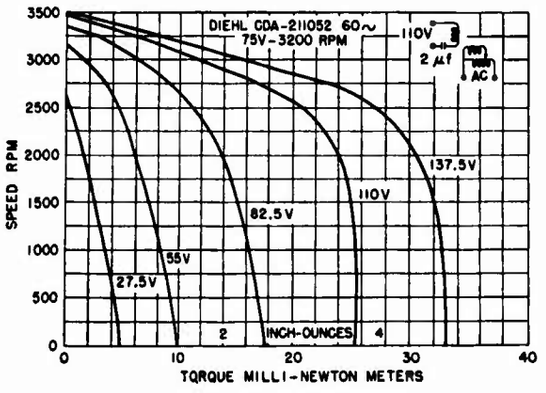

FIGURE 3. Speed-torque curves for servomotor.

of the squirrel cage type. The exceptions were aluminum "drag-cup" or "spinner" rotors. From the available data it appears probable that the squirrel cage construction is preferable at 60 c. In addition to providing high torque, it has the potential advantage that motor inductance can be designed to vary with the slip of the rotor.

Test conditions were chosen to approximate normal servo operation. The exciting phase (No. 1 winding) was connected to the line through capacitors so that the voltage across the motor was in quadrature and so that the current through this phase, with the other phase unexcited, caused the motor temperature to rise almost to rated value. The control phase (No. 2 winding) was connected to a voltage source in phase with the line and of such magnitude that about 80% of the maximum possible torque was produced. A parallel capacitor across the No. 2 winding was given a value such that the current and voltage of the combination were in phase when the motor was stalled. Since motor characteristics vary when the series capacitor of the exciting phase is altered or the regulation of the control voltage source changes, moderate deviations from the test results can be expected in normal operation.

The conventional criterion of merit is the torque inertia ratio T/I. It is a true criterion only when load inertia is zero and total displacement is specified as a fixed number of revolutions of the motor shaft. The torque-squared inertia ratio T^2/I does not suffer from these limitations and is a suitable performance index since speed of response in a well-designed servo is proportional to the fourth root of this quantity. Maximum output watts can be used as a secondary guide to choose between motors of similar torque-squared inertia ratio. Two other important characteristics are the torque volt-amperes ratio T/VA (the motor stiffness) which is useful in deciding on the voltage amplification needed, and the stalled volt-amperes product which determines the size of power amplifier required.

For general low-power applications, it was found that a Diehl motor (CDA 211052) was the best of the group tested with the 54-rpm Brown (M62SAY/X1) a close second. Their characteristics, together with those of two higher powered motors, are listed in Table 1. Figures 2 and 3 show typical performance curves for a good motor. Additional information on small servo motors can be found elsewhere.[1]

9.3 SERVO CONTROL AMPLIFIERS

There are two major sections in a servo control amplifier: the power output stage and the voltage amplifier (Figure 1). The power output stage must be suited to the servo motor which it drives. The voltage amplifier must increase and, in some cases, improve the available error signal until it is adequate for proper excitation of the output stage.

Design of the control amplifiers studied was based on 60-c carrier frequency operation. With this system, the error signals set up by deviations appear as amplitude changes and phase reversals of a 60-c input carrier wave. The resulting amplifier output then drives the servo motor at a rate and in a direction corresponding to input amplitude and phase, respectively.

TABLE 1.

A. *Measurements on servo motors.*

Motor	Rated values: Voltage ph 1/ph 2	Rated values: No load speed (rpm)	Rated values: Stalled torque (Newton meters)	Rotor: Type	Rotor: Inertia kg m²	Test voltage ph 1/ph 2	Phasing capacitors (μf) ph 1/ph 2
Brown 54-rpm M62SAY/XI	225/115	54	.....	Squirrel cage	2.07	225/115 225/165	1S/1P
Diehl CDA-211052	75/75	3,200	0.021	Squirrel cage	1.50	70/82.5 70/110 95/95	2S/2P 2S/2P 2½S/2P
Ford 223085	65/115	3,250	0.085	Squirrel cage	39.70	62/115 75/115	4S/5P 5S/5P
Holtzer-Cabot RBT-4422	50/50	.....	.....	Aluminum cup	36.90	50/50	12S/12P

B. *Measurements on servo motors.*

Motor	Stalled: Amperes ph 1/ph 2	Stalled: Torque (Newton meters)	Stalled: Temp rise (degrees)	Speed: No load (rpm)	Speed: For max output (rpm)
Brown 54 rpm M62SAY XI	0.090/0.022 0.090/0.029	0.590 0.850	35	48 54	32 44
Diehl CDA-211052	0.089/0.088 0.089/0.127 0.115/0.101	0.017 0.026 0.027	21 42	3300 3450 3330	2400 2380 2500
Ford 223085	0.191/0.348 0.263/0.348	0.080	40	3300	2100
Holtzer-Cabot RBT-4422	0.600/0.490	0.101	47	3160	2350

C. *Measurements on servo motors.*

Motor	Max output (watts)	Criteria of merit: T^2/I (watts/sec)	Criteria of merit: T/I (radians/sec²)	Criteria of merit: T/VA ph 2	Stalled VA ph 2
Brown 54 rpm M62SAY XI	1.4 2.1	170 373	9,100 13,000	0.2360 0.1770	2.5 4.8
Diehl CDA 211052	3.0 5.5 1.8	192 450 485	11,300 17,300 18,000	0.0021 0.0019 0.0028	7.2 13.9 9.6
Ford 223085	11.2	161	2,000	0.0020	40.0
Holtzer-Cabot RBT-4422	19.7	276	2,700	0.0037	27.5

9.3.1 Power Stage

Motor Considerations

There is a definite limit to the amount of power that can be dissipated by a given servo motor.

Any harmonic, off-frequency, out-of-phase, or direct currents sent into the motor diminish the amount of useful power that it can handle. Accordingly the amplifier should be designed to give an output as free as possible from such undesirable components.

Amplifier regulation may be adjusted to take advantage of the motor's ability to dissipate increased power as its speed increases. Circuits, components, output tubes, and load impedance are all factors which may be changed to alter regulation. If desired, the load impedance can be adjusted to the extent of a 20 per cent mismatch with the tubes, without appreciable power loss. However, if the impedance is made too large, screen dissipation is exceeded with full input; if it becomes too small, plate dissipation is exceeded at about half output. Regulation changes can also be effected by alterations in the network controlling the exciting phase. In general, marked differences in the performance curves of a given motor-amplifier combination result whenever regulation is made to vary.

Tube Considerations

There are six factors associated with the power tubes which impose restrictions on amplifier output. The first is the maximum plate power that the tube can dissipate; instantaneous peak power delivered to the load is proportional to this quantity. If tube impedance could go to zero, peak load power would reach a value equal to four times plate dissipation. The second restricting factor is the permissible plate voltage, and the third is the maximum cathode emission. If the product of these is less than the plate dissipation rating, they supplant the latter in restricting power output. The fourth factor is the power permissible for electron acceleration within the tube; ratings on screen dissipation and grid current must not be exceeded. The power supply is the fifth controlling factor. It is sometimes found that a supply of normal size cannot furnish full power to the tubes as they are used in these amplifiers.

Finally, the circuit itself determines the extent to which tube output is utilized. For example, a one-tube stage with half-wave output delivers only one-quarter of the power available from a two-tube circuit with full-wave output. Provision of both half-cycles by the second circuit allows each individual tube to deliver twice as much power.

Choice of Tubes

After deciding on tube and operating conditions to put maximum power into the load, the choice among specific tube types must be made on the basis of efficiency. Cathode heater requirements, grid circuit driving power, screen power dissipation, and plate impedance must be given consideration.

In general, pentodes (beam power tubes) are preferable to triodes. The smaller grid driving power needed by the former usually more than compensates for their higher output impedance. Where two small tubes can do the work of a single large one, the small ones should be chosen since some output is obtained even if one tube fails. However, the use of pentode output tubes in parallel ordinarily necessitates the installing of parasitic-suppression resistors.

9.3.2 Voltage Amplifier

The voltage amplifying section must be designed with the overall dynamic range of the complete amplifier in mind. In general, this should amount to approximately 40 db. A smaller range causes waste of output power at balance, and a larger one is usually unnecessary since static friction is generally greater than the torque produced with very small input signals. In order of importance, the requirements for a voltage amplifier are: gain, stability, low noise level, and proper phase response.

Gain

Obtaining sufficient gain at the 60-c carrier frequency is no problem. However because of the necessary phase-frequency characteristic, any amplifier of three or more stages operating from a single power supply with practical nonelectrolytic filtering tends to motorboat. Four class A stages in cascade seem to be the limit. Two additional stages can be cascaded if they are well-balanced push-pull.

Stability

Because the carrier bearing the error signal from a position servo has balanced modulation, the amplifier must be stable for all carrier levels from zero up to perhaps a hundredfold overload. Therefore the use of iron-cored inductors must be held to a

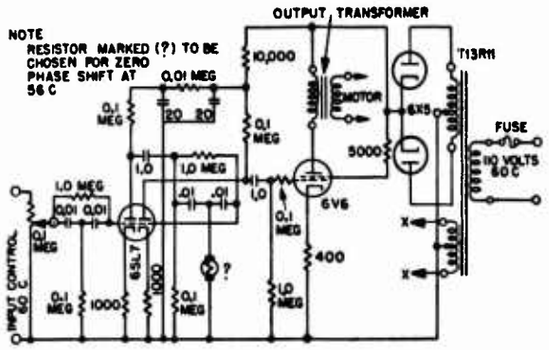

FIGURE 4. Circuit diagram of 4-w servo amplifier.

minimum because their impedance, and hence the overall phase shift, varies with the amplitude of the carrier. In practice, this limits the servo to one signal-carrying inductor, generally an output transformer. With inductors and electrolytic capacitors eliminated, resistance-coupled amplifiers seem to be sufficiently stable if large series grid resistors are used.

NOISE LEVEL

With at least 1 volt rms on the grid, almost any tube can be used without introducing spurious signal. Most tubes designed for audio use can be used provided the grid voltage is greater than 10 mv. The 6SL7 can be used down to 1 mv but for less than that value, the 6SJ7 or 6J7 must be used. With reasonable circuit isolation and shielding, resistors may be as much as 1 megohm for each 10 mv of signal across them.

PHASE-FREQUENCY RELATIONSHIP

For satisfactory response to transients, the output of a servo must be proportional not only to the input signal itself but also to its time derivative. This is equivalent to a requirement that the output phase should increase with frequency over the operating range. The use of bridged-T networks or parallel-T notching filters[2] as coupling elements between amplifier stages seems to be the best way to accomplish this (see Figure 4). Such circuits eliminate the carrier frequency and shift the phase of the sidebands by a suitable amount to give correspondence with the derivative of the error modulation. The necessary recombination of the carrier with this derivative signal then occurs in the succeeding stage.

In equipment for laboratory use or wherever it is permissible to require adjustment of the servo filter network to the power line frequency, any amount of modulation phase lead can be incorporated. Equipment for shipboard use is limited to a maximum of about 7 degrees per cycle because the equipment must operate satisfactorily over a frequency range of 50 to 62 c. This amount of phase lead is sufficient to stabilize a servo system with a well-designed mechanical system. Should the mechanical design be such as to require further phase lead, either a d-c phase-lead controller or a mechanical phase-lead controller[3] must be used. In any event, the phase-lead controller operates only over the range in which it receives undistorted signal.

9.3.3 Amplifier Ratings

Several general types of servo amplifiers are classified on the basis of input volts required, ease of manufacture, size, useful power output versus unusable power output, reliability, maintenance, performance, tube types needed, stand-by power input, and power input for 5-w power output. The same driver stage, with or without a phase inverter as

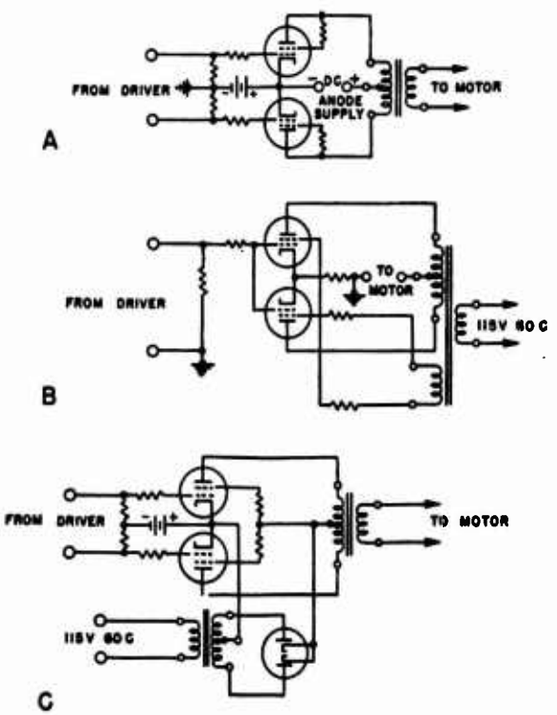

FIGURE 5. Preferred servo power amplifiers. A, pentode power amplifier with anode supply. B, pentode grid-controlled rectifier as power amplifier. C, push-pull pentode power amplifier with unfiltered, rectified a-c anode supply.

TABLE 2. Relative merit of various power amplifiers.*

Circuit	Input required (volts)	Ease of manufacture	Size	Motor eff.	Reliability	Maintenance	Performance	Tube types needed	Power input: Stand-by	Power input: For 5-w output	Total of scores†
D-C anode supply											
Single-sided											
Triode	1 (0.05)	1	2	1	2	2	2	3	5	5	24
Pentode	1 (0.02)	1	3	1	2	2	2	3	4	4	23
Push-pull											
Triode	3 (1.00)	1	3	1	1	2	1	3	5	6	26
Pentode	2 (0.25)	1	3	1	1	2	1	3	5	6	25
Grid-controlled rectifier											
Half-wave											
Triode	3 (1.00)	1	1	2	2	3	3	2	3	3	23
Pentode	2 (0.25)	2	1	2	2	3	3	2	3	3	23
Gas tube	3 (1.00)	2	1	2	2	3	5	1	2	3	24
Full-wave											
Triode	3 (1.00)	3	3	1	0	4	2	1	3	3	23
Pentode	2 (0.25)	3	3	1	0	4	2	2	3	4	24
Gas tube	3 (1.00)	4	2	1	0	4	5	1	2	3	25
Unfiltered-rectified a-c anode supply											
Push-pull											
Pentode	2 (0.25)	1	2	1	1	1	2	3	3	4	20

* Lowest number in column indicates highest rating.
† Underlined scores indicate preferred types.

TABLE 3. Relative merit of various power amplifiers.*

Tube type	Circuit	Output available (watts)	Scores for other output wattages† 2 w	15 w	40 w	100 w
	D-C anode supply					
	Single-sided					
6B4	Triode	5	21	28	32	.....
6V6	Pentode	6	19	25	30	.....
	Push-pull					
6V6	Triode	7	24	28	31	.....
6V6	Pentode	14	21	26	28	.....
	Grid-controlled rectifier					
	Half-wave					
6B4	Triode	5	19	25	33	.....
6V6	Pentode	10	21	25	30	.....
2050	Gas tube	25	25	27	30	.....
	Full-wave					
6SN7	Triode	5	22	25	28	31
6V6	Pentode	20	23	25	24	28
2050	Gas tube	100	24	26	25	28
	Unfiltered-rectified a-c anode supply					
	Push-pull					
6V6	Pentode	20	19	20	23	26

* Lowest scores indicate highest ratings; underlined scores indicate preferred types.
† With the necessary alterations in tubes and components.

necessary, is used for all the amplifiers to test the power output stages. It is found that the best power output stages are: (1) a pentode power amplifier using a d-c anode supply; (2) a pentode grid-controlled rectifier as a power amplifier; and (3) a push-pull pentode amplifier with unfiltered, rectified, a-c anode supply. The circuits for these three power stages are shown in Figure 5. The results of this classification are summarized in Table 2.

These various amplifiers are also evaluated in terms of available power output in addition to the factors mentioned above. The last amplifier of the three is most satisfactory for all wattages from 5 to about 100 w, although for the highest powers in

TABLE 4. Comparison of amplifiers tried.

Circuit		Rated output (watts)	Maximum output (watts)	Weight (lb)	Volume (in.^{3})	Power consumption Stand-by (watts)	Power consumption Max output (watts)	Servo rating: Max output Stand-by input
Unfiltered rectified a-c supplied to plates of 6V6	Push-pull AB_1	10	16	12	225	36	65	0.44
	Push-pull parallel	40	40	15	380	52	135	0.77
	Single-sided Class A_1	4	3½	10	156	29	33	0.12
Raw a-c supplied to plates of grid-controlled rectifiers	Parallel 6SN7	2	2	8	165	28	29	0.07
	6V6	5	6	8	190	53	54	0.11
	Full-wave 6V6	20	27	9	176	20	65	1.35
	Full-wave 2050	100	← estimates →		300	40	170	2.50

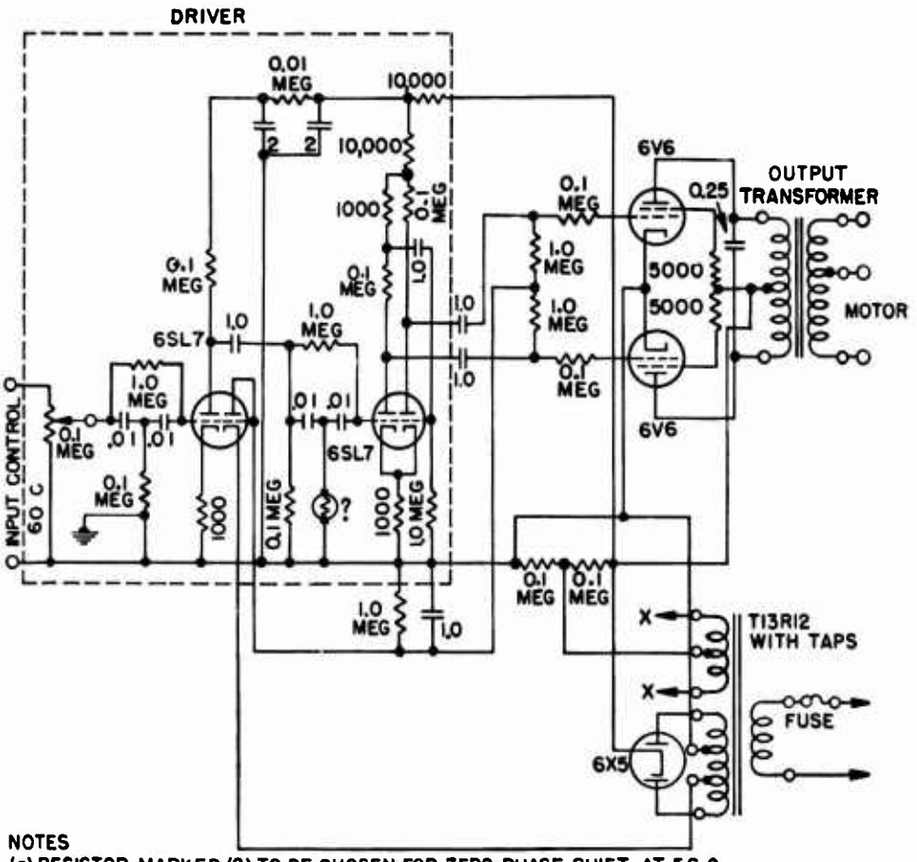

NOTES
(a) RESISTOR MARKED (?) TO BE CHOSEN FOR ZERO PHASE SHIFT AT 56 C
(b) 40 WATT SERVO AMPLIFIER IDENTICAL EXCEPT
ADD 2 MORE 6X5 TUBES IN PARALLEL WITH 6X5
ADD 1 MORE 6V6 TUBE IN PARALLEL WITH EACH 6V6
CHANGE TRANSFORMER TO TO T13R15

FIGURE 6. Circuit diagram of 10-w servo amplifier.

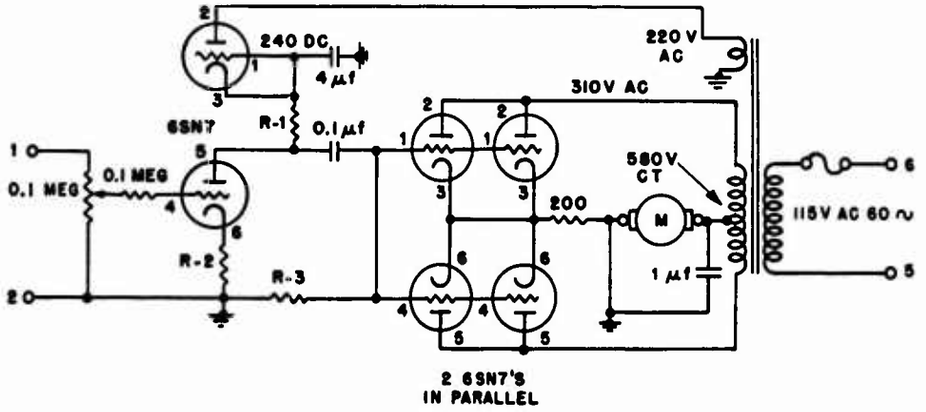

Unit	Center-tap transformer	No center tap
R-1	33,000 ohms	1.0 megohm
R-2	1,500 ohms	5,000 ohms
R-3	1.0 megohm	1.0 megohm

FIGURE 7. Circuit diagram of 2-w servo amplifier.

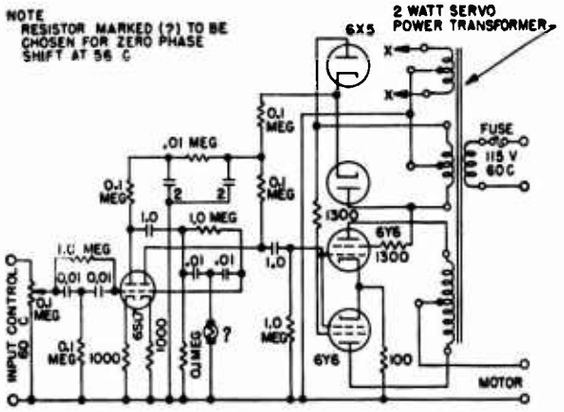

FIGURE 8. Circuit diagram of 5-w servo amplifier.

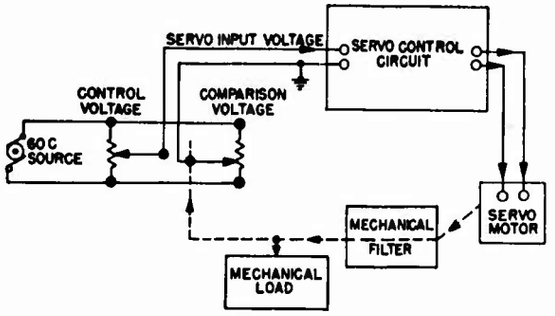

FIGURE 10. Servo using mechanical band-elimination filter.

this range, full-wave grid-controlled rectifiers using gas tubes are somewhat more suitable. The results of this evaluation are shown in Table 3.

The amplifiers built and tested included (1) a 10-w amplifier with unfiltered rectified a-c anode supply (Figure 6); (2) a 40-w amplifier similar to the 10-w, except for larger power amplifier components to handle the greater output power; (3) a 4-w amplifier using unfiltered rectified a-c anode supply (Figure 4); (4) a small 2-w amplifier (Figure 7); (5) a 5-w amplifier using a pair of pentodes in a grid-controlled rectifier circuit (Figure 8), similar in this respect to the 2-w amplifier, and (6) a 20-w amplifier using a full-wave grid-controlled rectifier circuit which proved more efficient than the others in the use of circuit components to produce a given amount of output power (Figure 9). It will be noted from the diagram for (6) that V-1 and V-3 operate alternately to give full-wave output when the input signal is in one phase, and that V-2 and V-4 join in supplying output when the input phase reverses. This circuit is noteworthy also both because it cannot motorboat and because the amount of phase lead which can be incorporated is not restricted by variations in power supply frequency. A 100-w amplifier was designed similar to (6), making use of thyratrons, but it was not built because a suitable phase controller was not designed for it. A summary of the data on these amplifiers is given in Table 4.

Satisfactory operation usually can be secured from any of these amplifiers provided that its power output is sufficient for the motor which it drives. Where peak performance is required, however, it may prove desirable to use an oversized amplifier but, in such

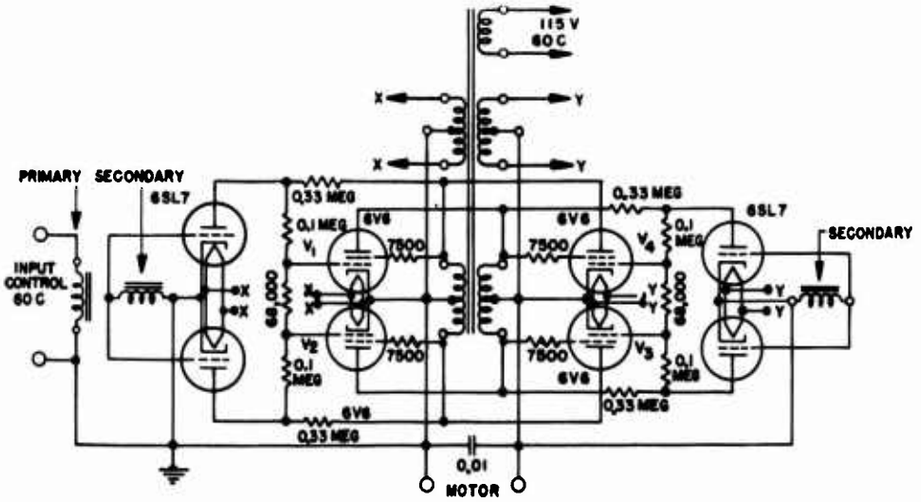

FIGURE 9. Circuit diagram of 20-w servo amplifier.

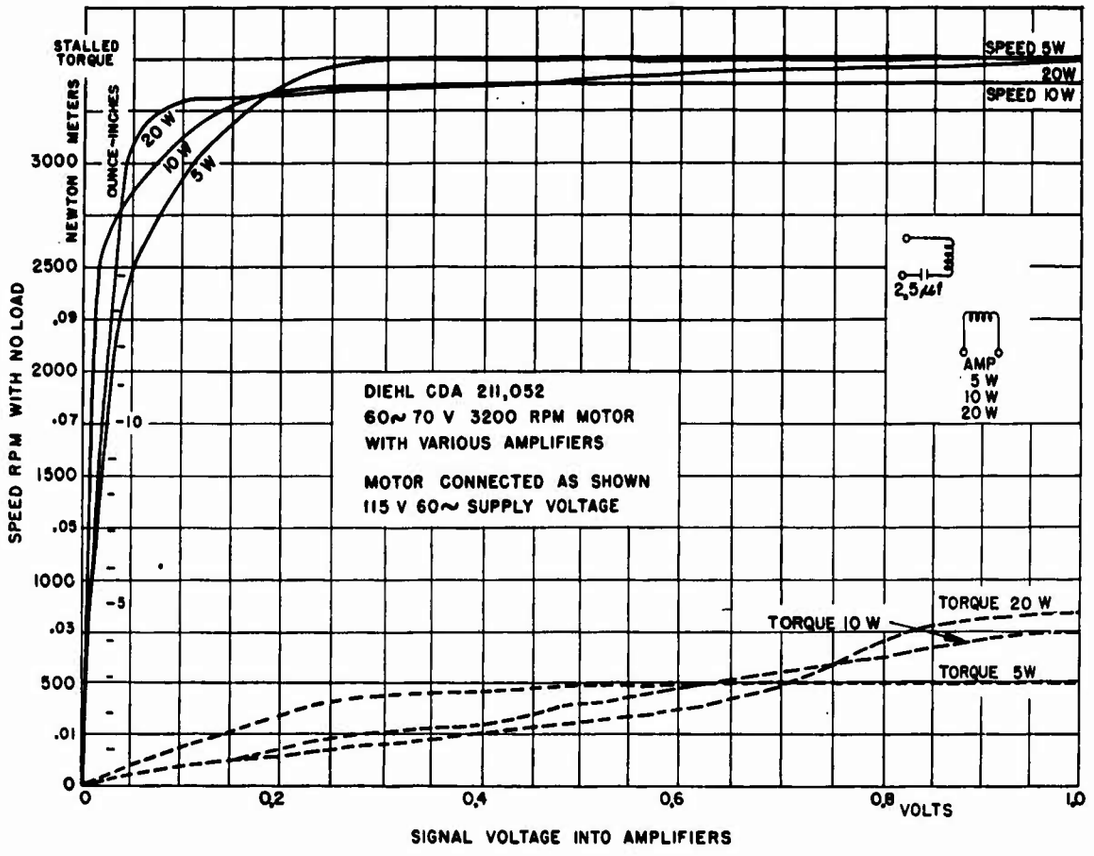

FIGURE 11. Speed-voltage and torque-voltage curves for motor-amplifier combinations.

cases, due care must be exercised to avoid overheating the motor. Where large values of phase lead are required, special consideration should be given to the 20-w amplifier (6). A mechanical band-elimination filter used as in Figure 10 may sometimes be found necessary, if sufficient phase lead cannot be incorporated in an amplifier.

Figures 11 and 12 show the operation of the Diehl motor combined with several different amplifiers. The high quality of the motor is clearly reflected in the excellent characteristics of the performance curves shown.

9.4 DETECTION AND MODULATION

The 60-c carrier servos which have been described can also be used when the error signal is a modulated carrier of different frequency. In such cases, a detector-differencer circuit (sometimes called a sense-detecting rectifier) can be used in combination with a modulator circuit to provide the required 60-c amplifier input. Figure 13 shows an arrangement of this type as incorporated in the *portable polar chart recorder* [PPCR]. A "derivative control" circuit, which eliminates the need for "phase-lead controller" networks in the following-amplifier, is added to this detector-modulator combination.

In operation, an error signal in the form of a modulated supersonic carrier is applied to the detector-differencer input. The rectified output is then compared with a standard d-c voltage from the power supply. The voltage difference thus obtained varies in magnitude and polarity in accordance with the amount of rectifier output.

This voltage difference is then applied to the grid of one tube (V-107A) of the modulator circuit. The grid of the second tube (V-107B) of the modulator may be considered for the moment to be at ground potential, so that it draws a steady current, making constant the amount of 60-c signal that appears on its plate. When the voltage from the differencer is zero, the first tube conducts the same amount of

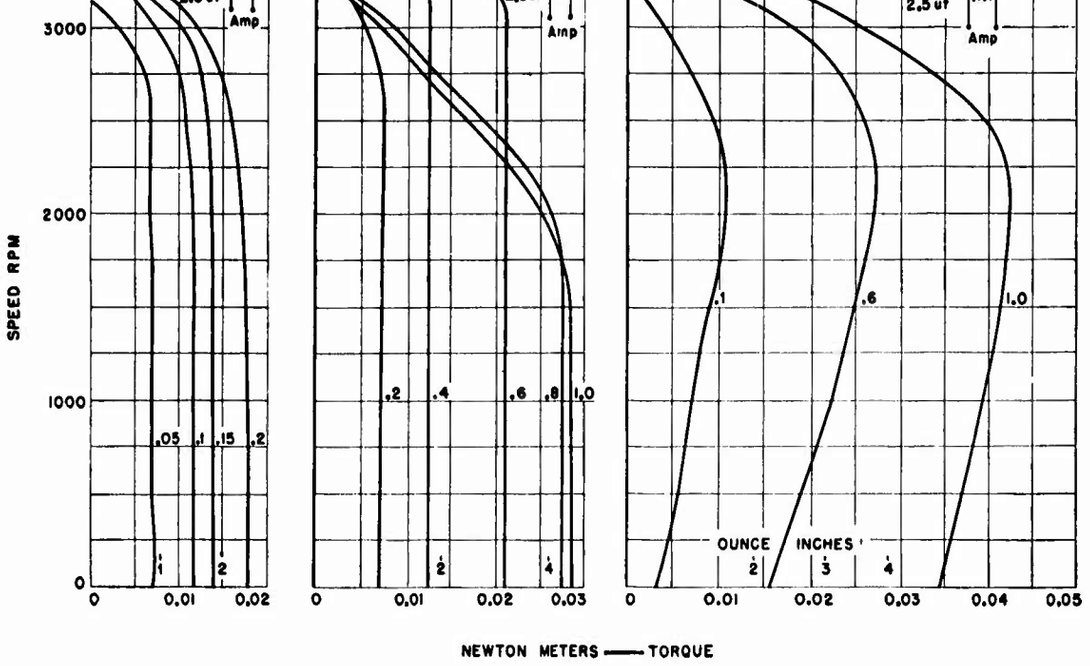

FIGURE 12. Speed-torque curves for motor-amplifier combinations. Diehl CDA 211052, 60-c, 70-v, 3,200-rpm motor; speed against torque for 115-v, 60-c supply voltage; motor connected as shown; signal voltages as shown on each curve.

current as the second tube, so that the combined output of the two tubes contains no 60-c component. When the difference voltage is other than zero, the first tube conducts more (or less) current than the second, and there is a 60-c component in the output whose phase depends on the sign of the difference voltage. This modulator output furnishes the driving voltage for the following-motor control-amplifier.

In the derivative control circuit the differencer

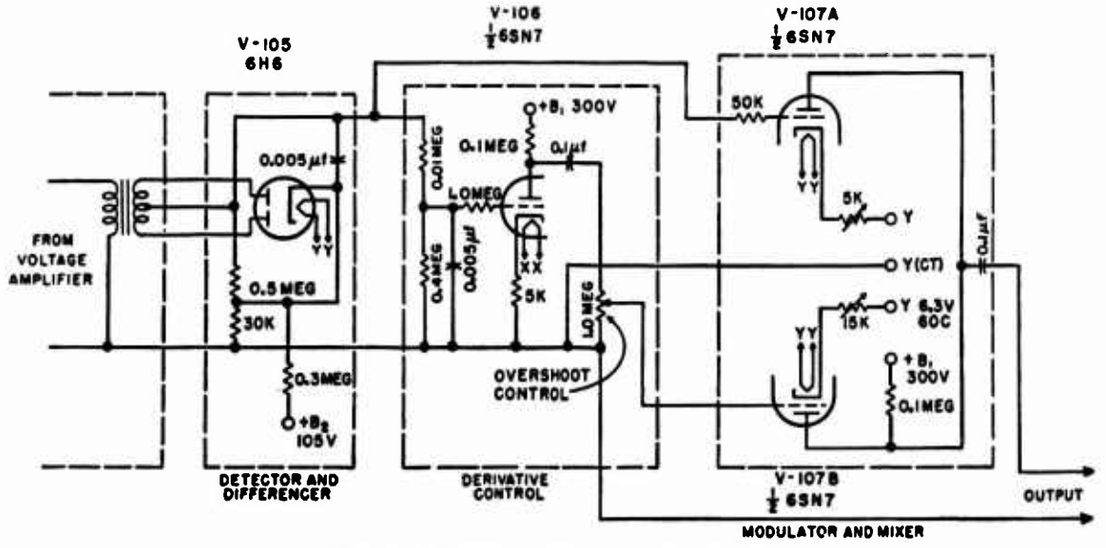

FIGURE 13. Carrier frequency conversion circuit.

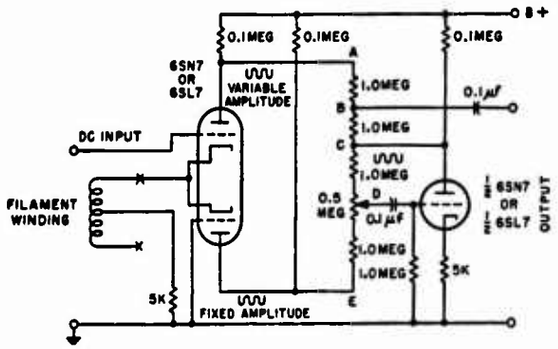

FIGURE 14. Improved servo modulator circuit.

output is applied to the grid of a tube (V-106) which acts as an amplifier for the low frequencies from the rectifier, that is, the modulation frequencies on the signal. Associated with this amplifier are resistor-capacitor combinations arranged so that the output signal from the circuit is shifted in phase approximately 90 degrees from the rectifier signal. The output from this derivative circuit is then approximately the derivative of the input signal to the circuit. This output signal is applied to the second tube (V-107B) of the modulator, so that the output of the modulator varies with the derivative of the difference voltage as well as with the difference voltage itself.

With the PPCR modulator a certain amount of 120-c hum caused by tube distortion is present in the output at all times. Figure 14 shows the diagram of an improved modulator which completely eliminates this 120-c output. In operation, the changing d-c input signals cause a varying 60-c a-c voltage at *A*, while an unvarying a-c comparison voltage appears at *E*. The tap at *D* is so adjusted that the instantaneous voltage at *C* is equal and opposite to the voltage at *E*. Therefore the voltage at *B*, which is the sum of the voltages at *A* and *C*, equals the difference between the voltages at *A* and *E*. Because of the exactness of the phase inversion which occurs, complete cancellation of 120-c hum is obtained.

9.5 CONCLUSION AND RECOMMENDATION

The information secured in the studies of these different motors, amplifiers, and combinations has

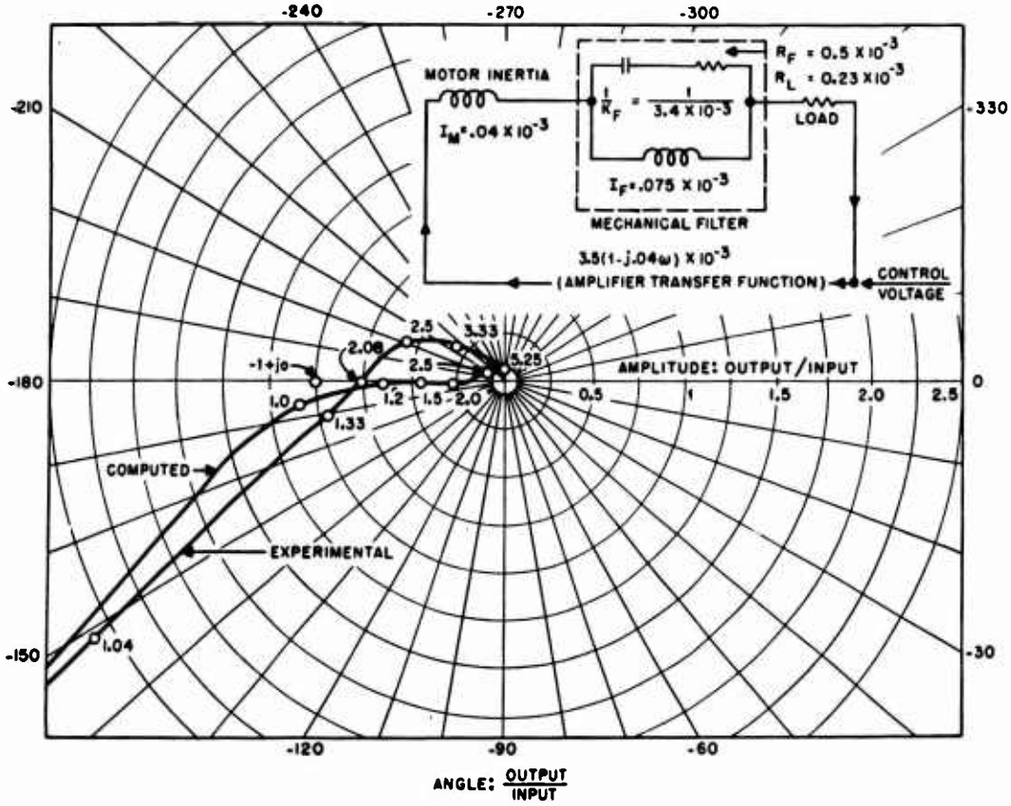

FIGURE 15. Transfer function for servo amplifier and load.

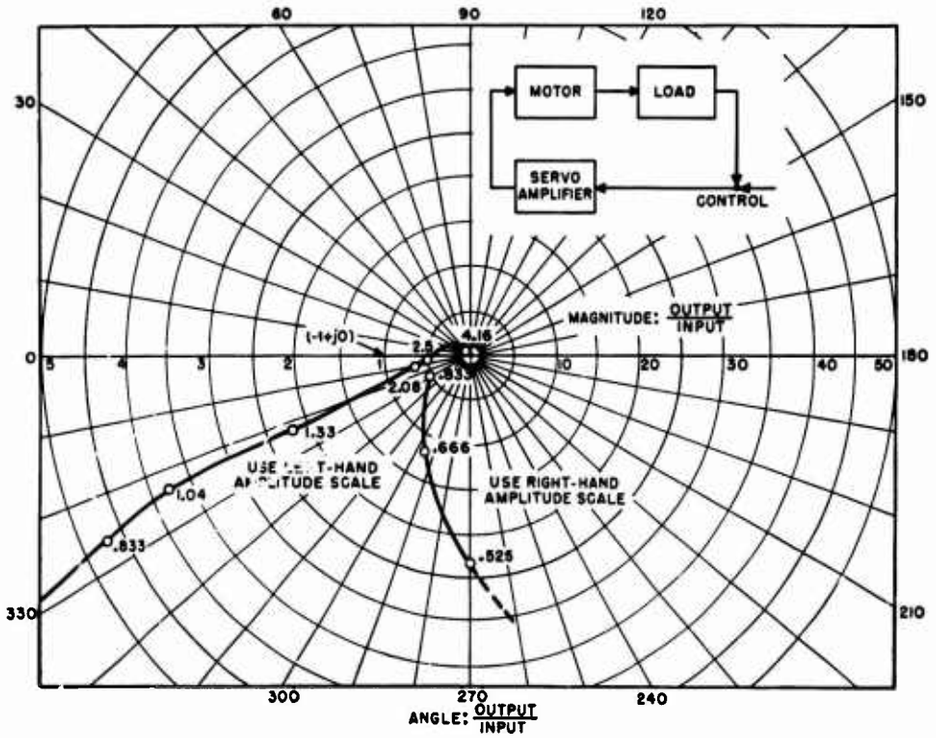

FIGURE 16. Transfer function for servo system with simple load.

proved very valuable in designing suitable servomechanisms for several projects. Application to specific problems always requires certain adjustments of the circuits because of the inevitable variation from one problem to another of the mechanical load on the servo. The specific changes in the circuits involve primarily the amount of derivative control compared with the amount of amplitude control required to make the servo operate stably, with the proper speed and overshoot values. A suitable overall criterion of the stability of the servo system is its transfer function, that is, the ratio of the output from the servo to the input to the servo. Such a transfer function is shown in Figure 15 for the circuit shown in block diagram form in Figure 10, together with the computed function using measured, and in part estimated, values of the various electrical and mechanical constants of the system. The transfer function for another servomechanism which made use of the same amplifier as the unit shown in Figure 10, but which had a simple load, is shown in Figure 16. It is to be noted that both of these functions indicate stable operation, since the curve does not enclose the point $(-1 + j0)$. It is known that a system is unstable if the transfer function curve does enclose that point.

In the cases in which it was used, the transfer function proved itself extremely useful in servomechanism analysis. A device for measuring the transfer function of the modulation in carrier frequency systems has already been suggested.[4] The use of small servos for fire control and similar equipment will probably increase. It is recommended, therefore, that this device, together with other instruments for experimental determination of transfer functions, be investigated and developed in the interest of obtaining high quality servomechanism performance.

Synchro System Test Unit

The synchro system test unit [SSTU], a device for determining the dynamic accuracy of synchro systems, is used for factory synchro inspection tests and for study of synchro performance on shipboard. The instrument includes an amplifier, a power supply, and an indicator section made up of synchros, a motor, and a 7-in. cathode-ray oscilloscope. Dynamic inaccuracy of a system is indicated on the cathode-ray oscilloscope screen. The unit was developed by CUDWR-NLL.

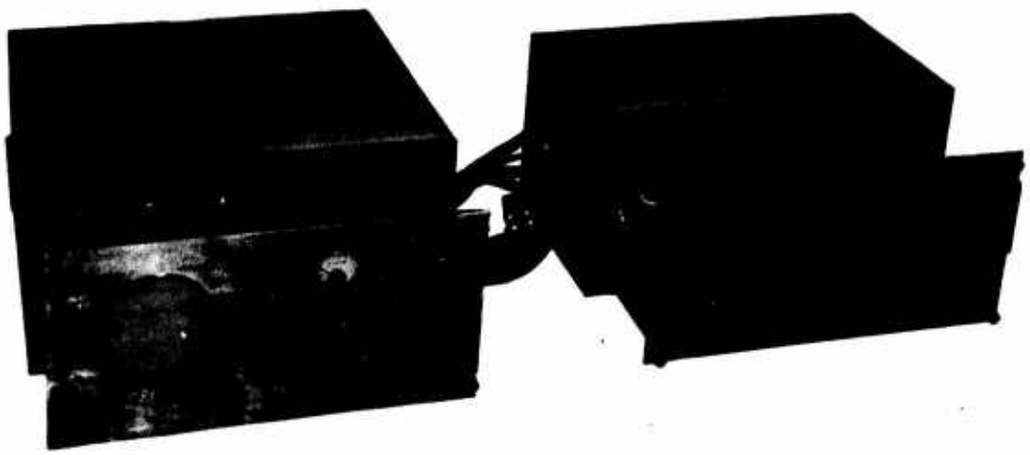

FIGURE 17. Indicator unit; amplifier and power supply.

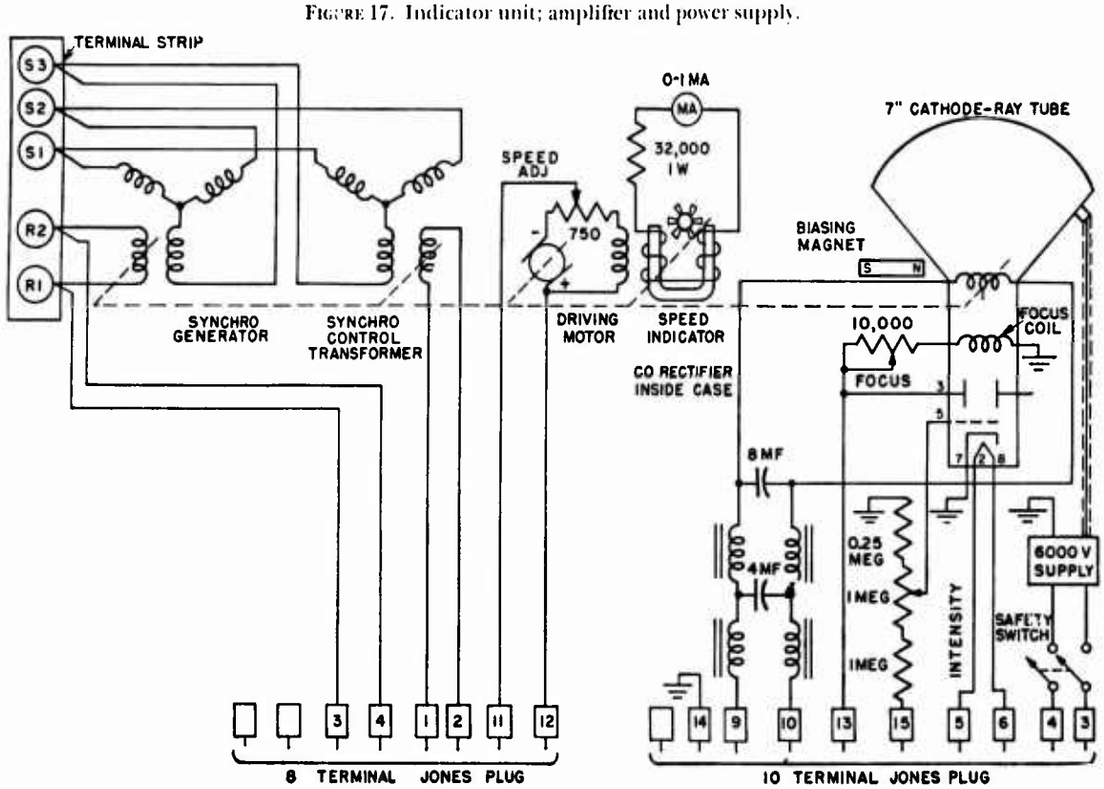

FIGURE 18. Wiring diagram of indicator unit.

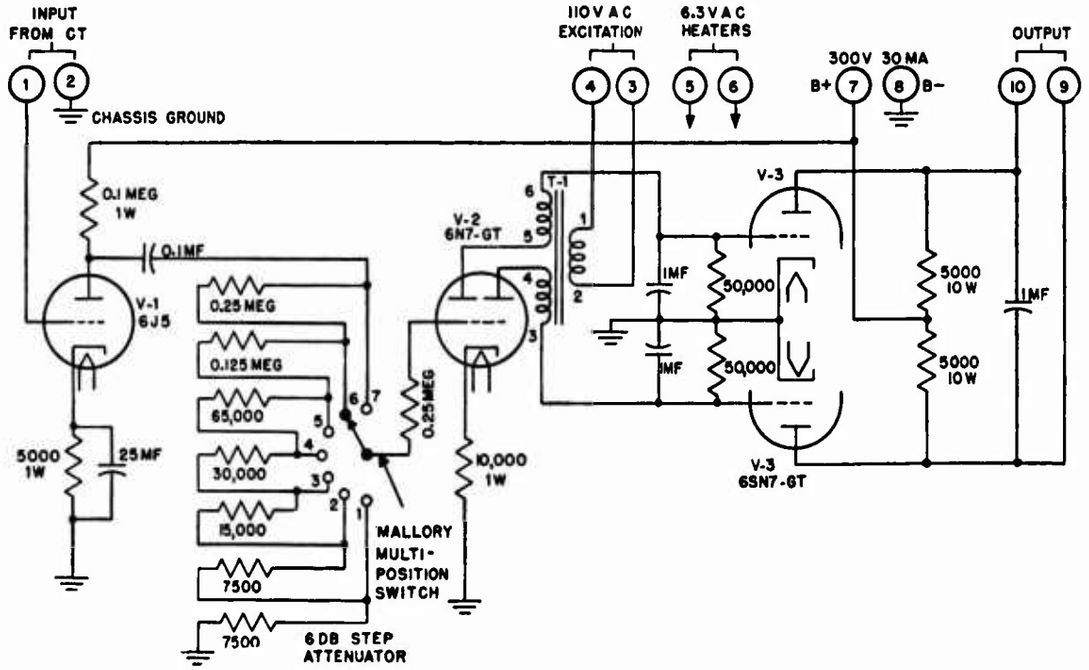

FIGURE 19. Wiring diagram of amplifier.

DESCRIPTION

At the time of this development, no simple device was available for determining the dynamic accuracy of synchros and synchro systems. As this information is useful in evaluating the performance of synchro systems on board ships, equipment was constructed capable of performing this function. The SSTU consists of two separate parts, one containing the amplifier and power supply, and the other containing the indicator unit, as shown in Figure 17.

The indicator unit, shown in Figure 18, contains a 5G synchro, a 5CT synchro, a 7-in. cathode-ray tube, and a motor and mechanical drive to swing the cathode-ray spot through a 90-degree arc on the cathode-ray screen. This spot is deflected from the center of the screen by a biasing magnet. The two synchros are mechanically interlocked through anti-backlash gears and are connected to the motor through a mechanical differential so that they have an oscillatory motion corresponding with the spot on the CRO screen. There is also a hand wheel for manually rotating the synchros through the mechanical differential. This enables the test to include all synchro positions through 360 degrees. The wiring diagrams of the amplifier and power supply are given in Figures 19 and 20.

METHOD OF OPERATION

A synchro to be tested for dynamic accuracy is connected as a follower to the synchro generator in the indicator unit (see Figure 21). It then oscillates in keeping with the motion of the generator. Any rotational lag shows up as a radial displacement of the cathode-ray tube spot from its normal arc of oscillation. This radial displacement is away from

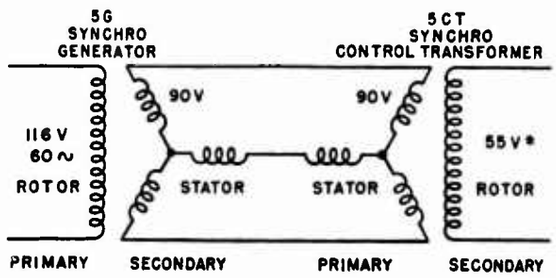

*MAGNITUDE OF OUTPUT IS PROPORTIONAL TO SINE OF ANGLE OF ROTATION OF GENERATOR MOTOR

FIGURE 21. Synchro generator and control transformer connections.

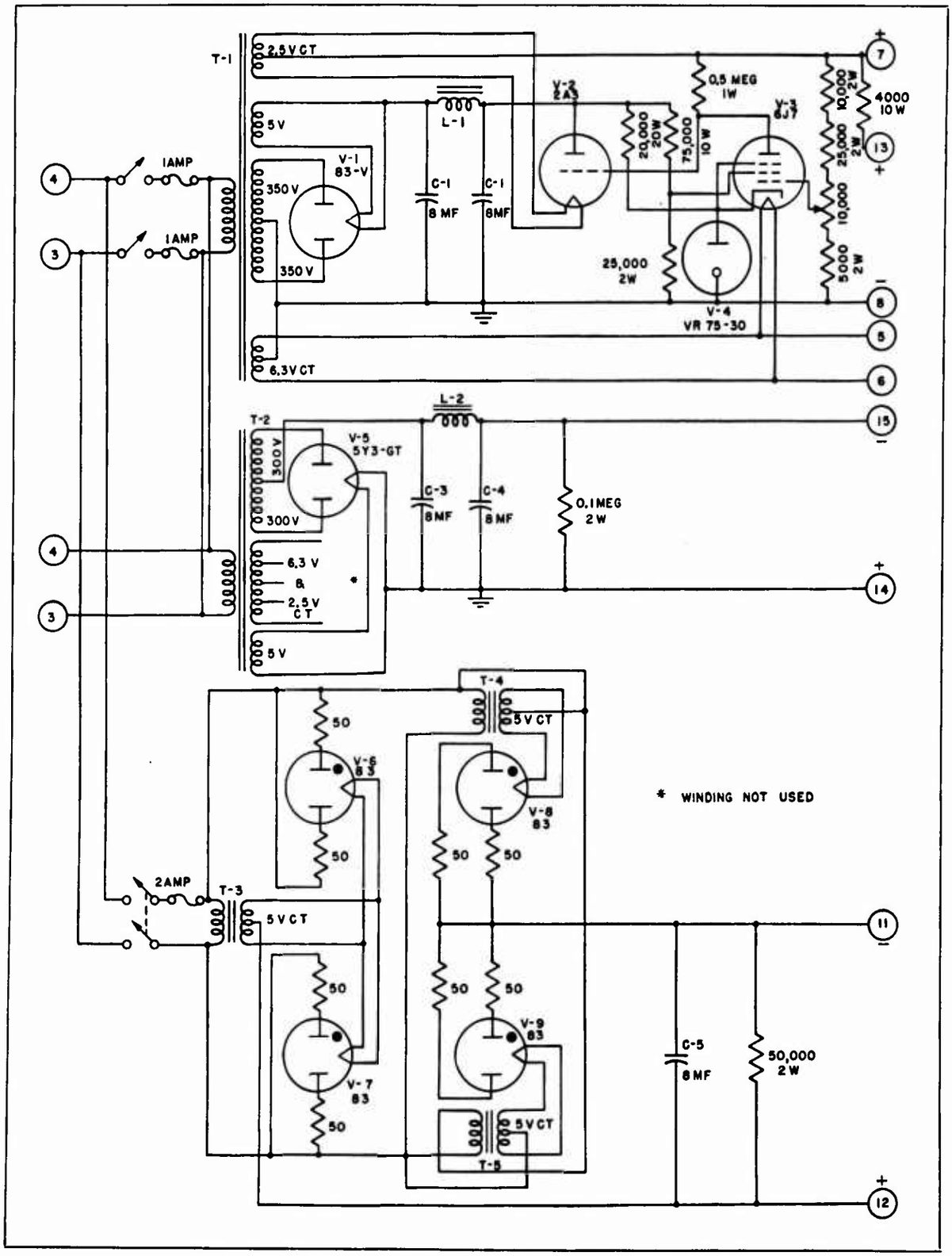

FIGURE 20. Wiring diagram of power supply.

the center of the tube for one-half of the cycle and toward the center for the return half. The result is a bounded area corresponding in size to the dynamic inaccuracy of the synchro being tested. This occurs since any angular difference between the driver and driven synchros is picked up, amplified by the amplifier, and used to actuate the moving coil whose action is reflected on the cathode-ray screen.

Performance

Tests of the SSTU gave results which showed the arrangement was basically sound but further mechanical refinement was desirable for the most satisfactory performance. However, because of a lack of interest in the device and pressure of other work, the project was terminated without practical application.

Chapter 10

ORDNANCE

Antisubmarine Scatter Bomb

The antisubmarine scatter bomb is a cluster of twelve small projectiles that can be launched from a standard airplane bomb rack. The projectiles scatter into an elliptical pattern, arm automatically, and either fire on impact, or disarm. The Armour Research Foundation, Division 8, and Division 3 participated in this development.

FIGURE 1. Antisubmarine scatter bomb.

10.1 INTRODUCTION

PRIOR TO THE DEVELOPMENT of the antisubmarine scatter bomb, successful antisubmarine bombing depended upon pin-point accuracy. To bring about detonation of an airborne projectile sufficiently close to a submarine to have a lethal effect, accuracy had to be maintained both *in* and *across* the line of flight. In addition, accuracy also had to be maintained in the vertical direction so that detonation would occur within lethal range whether the target was surfaced or submerged. The scatter bomb was developed to simplify the air crew's task in relation to all these considerations.

The first requirement was a design for a cluster of bombs with a charge to scatter them in a circular pattern in the air without detonating them. This end was achieved by strapping twelve bombs in groups of four around a central column containing scatter charges, as shown in Figure 1. Detonation of the scatter charges had to be timed so that it would not endanger the releasing aircraft yet would scatter the bombs well in advance of their hitting the water. This was accomplished by electrically connecting the scatter charge and also the blasting caps on the bomb-retaining bands to a charged condenser, with a delay system to time the bursting of the cluster 1 sec after release.

There was a further problem in that the individual bombs were to detonate only upon contact with a submarine whether surfaced or submerged. One solution was a system of electric contactors or horns on the nose of each bomb, strong enough to resist crushing on water entry, but designed to detonate the bomb when crushed against the target. The bombs used in this version incorporated the Munroe effect, or shaped-charge principle. A second solution was the use of larger individual bombs with standard Mark 140 fuzes which were armed on contact with the water. In this version, the shaped-charge principle was not used.

Following successful tests, the bomb cluster with the bomb and scatter mechanism described in this summary was put in production and effectively used in antisubmarine warfare.

10.2 NATURE OF THE PROBLEM

The main problem was to work out a means of scattering a cluster of bombs in air in a more or less controllable pattern without detonating them. This involved considerations of mechanical design, both for the individual bombs and for the cluster as a whole; the nature, quantity, and placing of the scatter charges; and a means of shearing the retaining straps around the bombs, if such were to be used, at the moment of bursting. A device which could be accurately timed for firing the scatter charges and blasting caps was also required. Finally, a bomb detonation mechanism was needed which would detonate the bomb only upon contact with a submarine whether surfaced or submerged. This made it necessary to determine the maximum water entry velocity permissible during an attack on submerged targets in order to avoid detonating the bombs on the water surface. To insure keeping the water entry velocity below the permissible maxi-

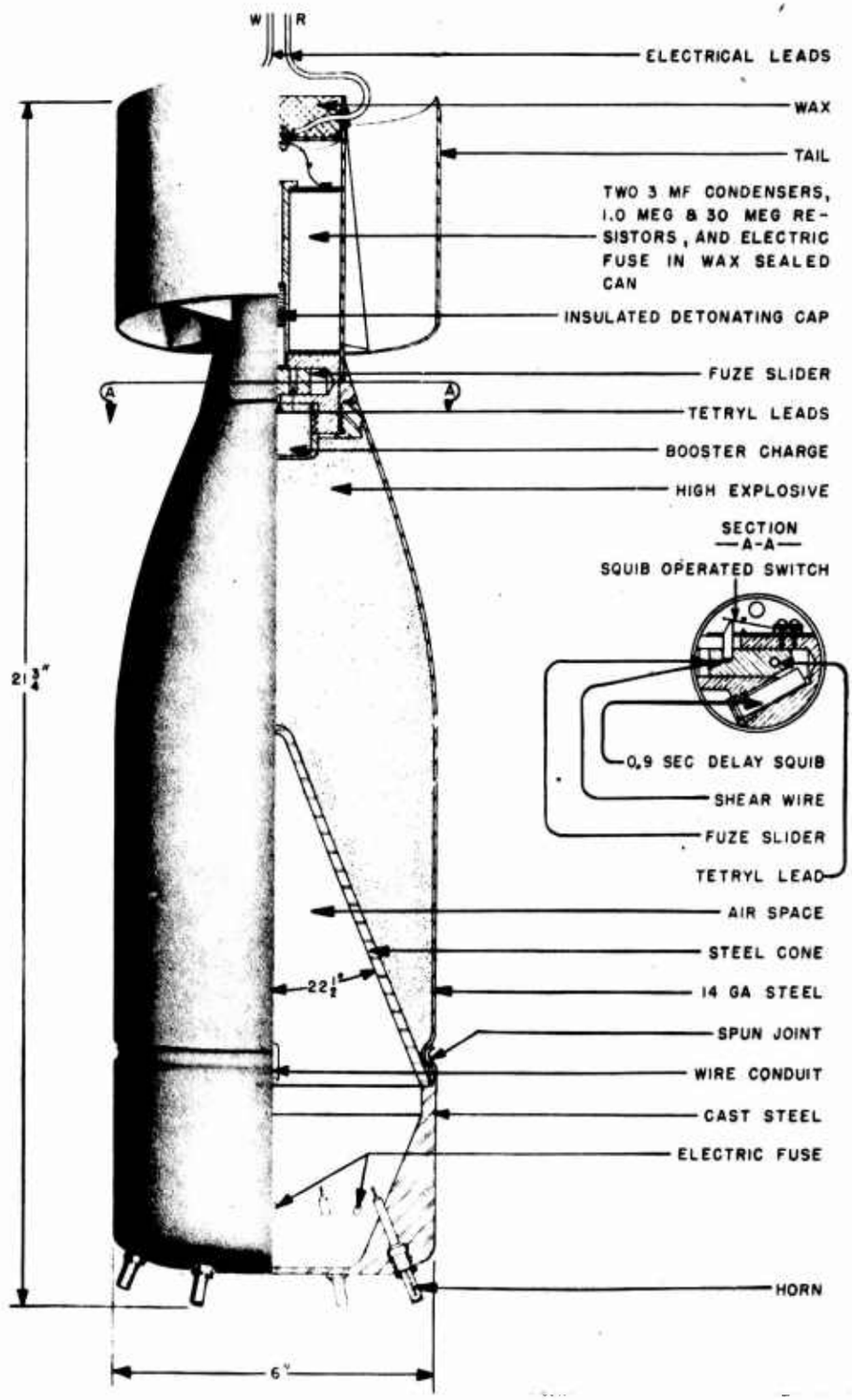

FIGURE 2. Cross section of individual bomb.

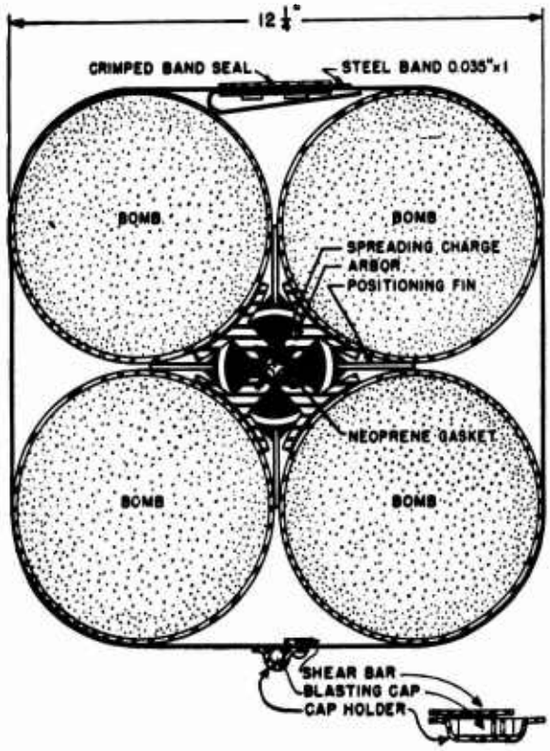

FIGURE 3. Section through four-bomb group.

mum, aircraft altitude and speed limits for attacking submerged targets also had to be determined.

10.3 TECHNICAL DEVELOPMENT

INDIVIDUAL BOMBS

The type of individual bomb used in the first version of the cluster is a small, shaped-charge projectile with a H.E. load of 12½ lb of Cyclotal (60-40 TNT-RDX), which is detonated from the tail end by an electrically energized detonating cap and tetryl booster (see Figure 2). The front end of the H.E. charge is shaped by a steel cone with a $\frac{3}{16}$-in. wall thickness and 45-degree included angle. In an early experimental construction a steel conduit for wiring was run through the bomb center, but it was found that this materially reduced the jet effect of the shaped charge. In the final model, therefore, the conduit runs through the cone and charge near the bomb periphery.

Although these bombs are somewhat smaller than the airborne antisubmarine ordnance previously in general use, the action of the shaped charge (Munroe effect), together with the contact-firing fuze, effectively offsets their smaller size. The shaped charge produces a jet through the nose of the bomb capable of penetrating 8 in. of armor plate. In addition, a considerable mining or general blast effect is produced.

SCATTER MECHANISM AND PATTERN

The individual bombs are strapped to the cluster frame in three groups of four bombs each, with 90-degree angular relation between the four bombs of each group, and 30-degree angular relation between the three groups. Thus there is a 30-degree angular separation of bombs along the entire cluster.

Figure 3 shows a section through the center of gravity of a four-bomb group, with the scatter charge in the central column or spreading gun on which the arbors holding the individual bombs are mounted. One second after release from an aircraft, the spreading charges and blasting caps (attached to the bomb-retaining bands) are simultaneously fired by being electrically connected to a charged condenser in the cluster frame. In each four-bomb group, the retaining band is sheared by the blasting cap, and the spreading charge pushes the arbors and bombs radially outward at a velocity of 19 fps. Because of the symmetry of construction, there is no net force acting on the frame.

Figure 4 illustrates the trajectories of one four-bomb group. In the actual cluster there are three such groups of bombs having a 30-degree angular relation between groups. The other two groups of bombs, not shown in the figure, fall in between those shown and produce an elliptical pattern of 12 bombs.

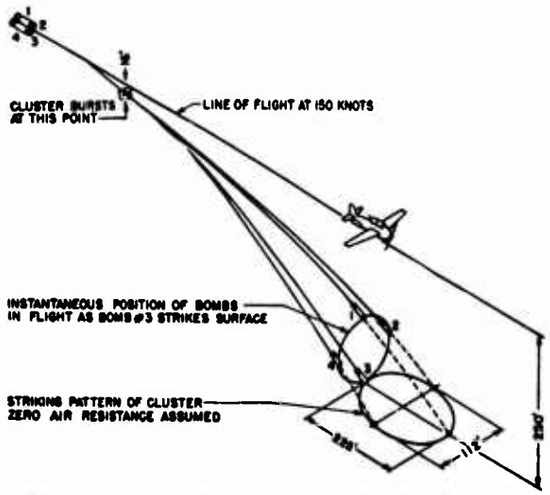

FIGURE 4. Theoretical trajectory of four-bomb group.

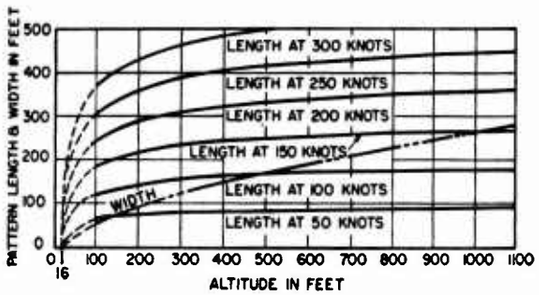

FIGURE 5. Axes of elliptical pattern.

The width of the elliptical pattern obtained is determined solely by the altitude of the aircraft; the pattern length is controlled by both altitude and speed. The scatter bomb is designed to be dropped from aircraft in level flight at altitudes of from 100 to 500 ft and at speeds up to approximately 240 knots. The pattern sizes for various altitudes and speeds are shown in Figure 5. For surfaced targets, the plane altitude should be at least 100 ft to insure adequate time for arming of the individual bombs. For submerged targets, drops from less than 100 ft may be made, but the pattern width will be small.

When attacking submerged targets, the cluster should be dropped from altitudes and at aircraft speeds which produce a water entry velocity of less than 450 fps in order to avoid detonating the bombs on the water surface. Since water entry without detonation is not required for attacks on surfaced targets, these drops may be made at greater speeds and altitudes.

If the aircraft is "drifting" (misaligned with its direction of flight), the cluster axis is also out of horizontal alignment with its trajectory. This distorts the pattern in such a way that its width is reduced. The width is then proportional to the cosine of the angle between the trajectory and the cluster axis. If for any reason the cluster is tilted nose up at the instant it bursts, the pattern is shortened. If it is tilted nose down, the pattern length is increased for slight tilt but is decreased for extreme tilt.

Timing Delay System

The delay system to time the bursting of the cluster 1 sec after release is positive in its action. Slightly more than ½ sec of delay is provided by 4½ ft of slack in the arming cord, so that no electric functions are initiated until the cluster has fallen 4½ ft. The remainder of the 1-sec delay is provided by delay squibs which operate electric switches to close the cluster-bursting circuit. As shown in the schematic wiring diagram in Figure 6, the d.p.s.t switch is closed by the pull-out cord when the cord becomes taut. This connects the aircraft's 24-v battery, through the cord, to two 4/10-sec delay squibs. As each squib fires, it closes one of the squib-operated switches. When both squib-operated switches are closed, the band shearing caps and the spreading charges are fired by current drawn from the charged 7-μf condenser.

If the probability of a squib's firing without delay is 1 in 12,000, the probability of a premature cluster burst from this cause with the double-squib switch (both squibs instantaneous) would be only 1 in 144,000,000, since the two squibs independently operate two switches, both of which must be closed to complete the cluster-bursting circuit.

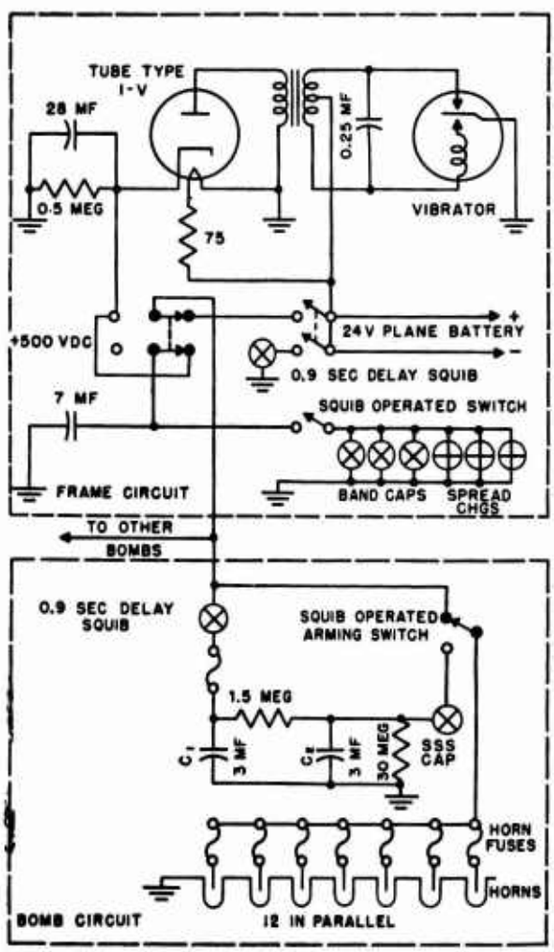

FIGURE 6. Scatter-bomb schematic wiring diagram.

Arming For Attack

In order to arm the cluster for attack, the switch in the line connecting the aircraft's 24-v battery to the cluster must be closed for at least 2 min before the cluster is dropped, and the switch must remain closed as the cluster is dropped. The 2-min period is required to allow the power pack within the cluster to warm up. This power pack is similar to the vibrator B supply in automobile radios.

Regardless of the position of the 24-v switch, a safe or "dud" drop results if the aircraft's standard arming control is in the "safe" position when the cluster is dropped, because the pull-out cord pulls clear of the shackle without operating the internal switches of the cluster. This is accomplished by the use of a shear wire in the fitting through which the pull-out cord enters the upper tube of the cluster.

If the 24-v switch has been off for 15 sec or longer when the cluster is released, the result is a safe or "dud" drop regardless of the position of the aircraft's standard arming control, because the power pack condensers within the cluster are discharged to less than minimum operating voltage. When a safe drop is desired, either or both of the above methods may be used. The 24-v battery may be connected to the cluster numerous times or left connected for long periods without harmful effect.

Horn Condenser Fuze

The electric circuit for the individual bomb fuzes in the condenser-fuzed cluster is shown in Figure 6, and the position of the fuze in the bomb appears in Figure 2.

When the fuze slider is in the position shown in Figure 2, the booster and H.E. load cannot be detonated by firing the detonating cap. If the slider is moved to the right, aligning the tetryl leads, an explosion of the detonating cap would detonate the tetryl leads, booster, and H.E. load. The slider is normally restrained in the safe position by a shear wire.

In actual operation the explosion of the 9/10-sec delay squib parts the shear wire and moves the slider to the armed position. The slider strikes the bomb-tail wall with sufficient energy to swage the end of the slider so that it cannot bounce back. This movement of the slider aligns the tetryl leads for detonation and also accomplishes an electric switching function. The bomb is still not fully armed when the slider is moved over, however, since at that instant there is not sufficient energy stored in condenser C-2 (Figure 6) to be capable of firing the detonating cap.

When the cluster is released from the plane, all switches are in the positions shown in Figure 6; the 28- and 7-μf condensers are charged to 500 v direct current; and the 3-μf condenser sections (C-1 and C-2) in the fuzes have no charge. When the cluster has fallen 4½ ft, the pull-out cord becomes taut, operating the d.p.s.t. switch. This energizes the 4/10-sec delay squibs for the cluster-bursting circuit, as previously described, and also applies the aircraft battery to the individual bomb tail wires. If any bomb horn has been shorted in shipment or handling, the electrical fuse associated with it is burned out by the aircraft battery at this time, thus disconnecting such pre-shorted horns from the circuit and leaving the bomb still operable with the remaining uncrushed horns.

After the cluster has fallen another 4 in., the pull-out cord operates the d.p.d.t. switch. This transfers the bomb tail wires from the 24-v aircraft battery to the charged 28-μf condenser, which sends a surge of current through the 9/10-sec delay squib, its associated electrical fuse, and the 3-μf condenser C-1, charging C-1 to approximately 220 v, burning out the electrical fuse, and igniting the 9/10-sec delay squib. (The 24-v battery previously applied to this circuit provides much too small a surge to ignite the squib.) Burning out the electrical fuse associated with the 9/10-sec delay squib isolates C-1 from the external bomb tail wires, so that the charge of C-1 is not lost through these wires when immersed in sea water.

The charge on C-1 causes a current through the 1-megohm resistor, charging C-2. In 1½ sec from the time that operation of the d.p.d.t. switch charges C-1, C-2 accumulates sufficient charge to be capable of firing the SSS detonating cap if the circuit through this cap is then closed by the crushing of one or more horns. While this transfer of charge from C-1 to C-2 is in progress, the 9/10-sec delay squib fires, moving the slider as previously described.

Movement of the slider operates the arming switch of the fuze, transferring the horns from the bomb tail wires to the SSS detonating cap. If a horn is crushed after operation of the d.p.s.t. switch and before C-2 has accumulated enough charge to be capable of firing the SSS detonating cap, the bomb becomes a dud, because continuous leakage through the SSS cap discharges C-2 without raising the cap filament to the detonating temperature. If

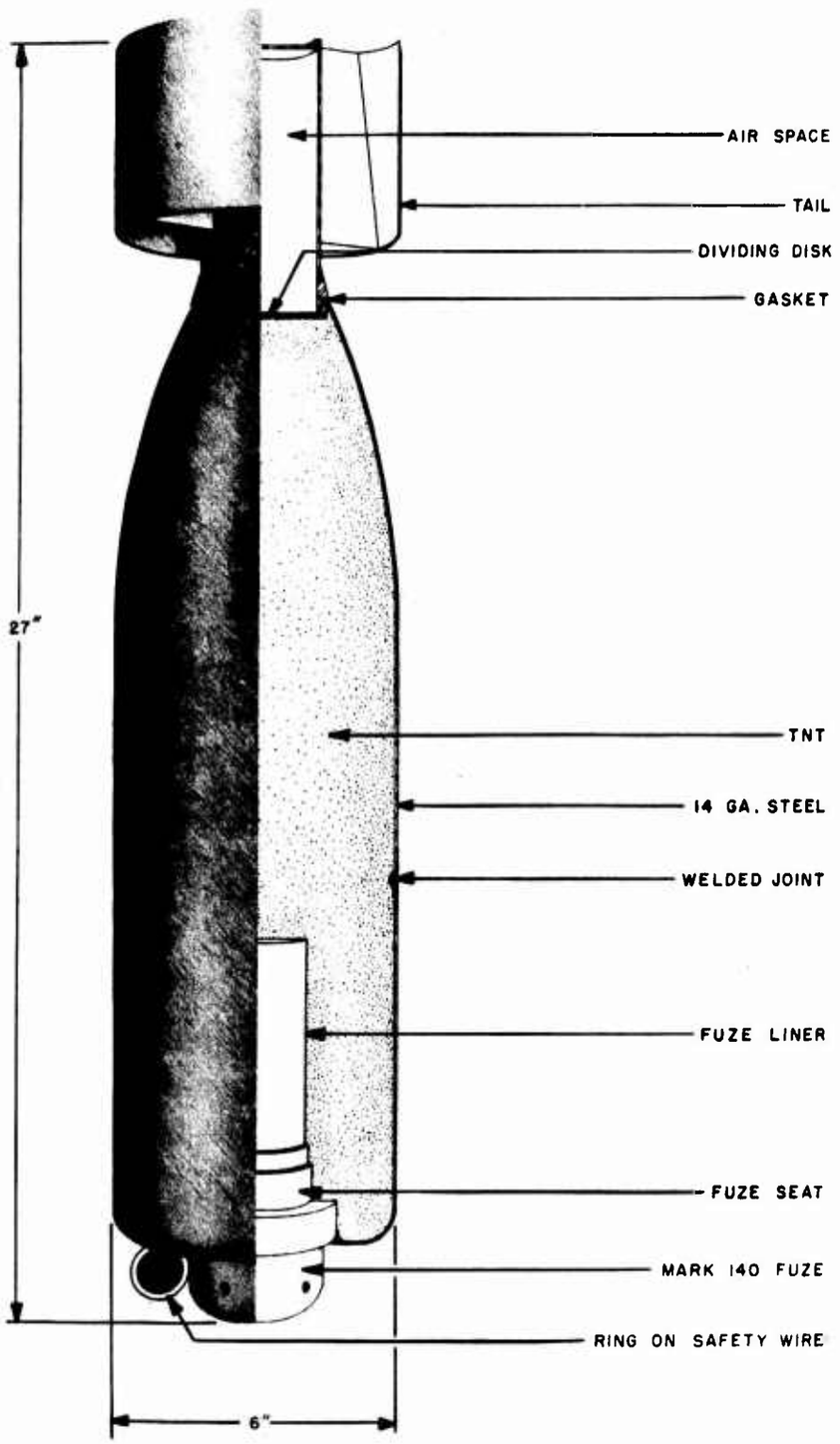

FIGURE 7. Individual Mark 140 fuzed bomb.

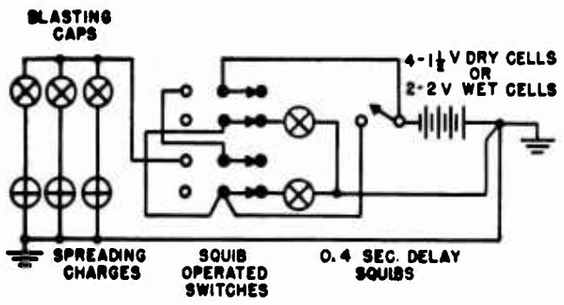

FIGURE 8. Wiring diagram Mark 140 fuzed cluster.

a horn is crushed after C-2 has accumulated sufficient charge, the bomb detonates. If the bomb misses the target, the charge on C-2 slowly leaks off through the 30-megohm resistor, so that after 2½ min the bomb becomes electrically disarmed.

Detonation is extremely rapid in this bomb, occurring approximately 0.0002 sec after the electric circuit is established by crushing a horn. This prevents appreciable distortion of the bomb against the target before detonation. Such distortion would reduce the effectiveness of the shaped charge.

HYDROSTATIC-FUZED CLUSTER

Because early tests of the condenser-fuzed cluster frequently resulted in premature detonations (later found to be due to high-voltage insulation failure), a second version of the weapon was concurrently designed to obviate this difficulty.

In this design the horn-condenser type of fuze is replaced by a standard hydrostatic (Mark 140) fuze. The individual bombs, shown in Figure 7, are "general blast" projectiles somewhat larger than those of the condenser-fuzed cluster. They incorporate some of the features of the previous design such as the tail assembly and drawn steel body, but they do not include the shaped charge.

Since this weapon is designed to be dropped from type K airships in level flight under conditions identical with those specified for the condenser-fuzed cluster, its scatter mechanism and pattern are essentially the same as in the earlier version. Although the framework is of slightly different design to accommodate the larger bombs and there are minor differences such as in the arming device, the angular relation of the bombs to one another is unchanged. The electric energy required for firing the spreading charges and band-shearing caps is supplied from batteries (two 2-v wet cells for use in all temperature ranges, or four 1½-v dry cells for use in temperatures above freezing) contained within the cluster frame. Figure 8 is a wiring diagram of the Mark 140 fuzed cluster as finally designed.

10.4 PERFORMANCE AND CONCLUSIONS

When manufactured in strict accordance with the blueprints developed for the purpose, the horn-condenser-fuzed cluster has performed satisfactorily in operational tests. When manufacturing errors are made, however, it is possible that the individual bombs may become armed even though the cluster has failed to scatter. When such a cluster strikes the water, the bombs may be broken loose from the frame, crushing one or more bomb horns in the process. This would result in a surface detonation dangerous to low-flying aircraft. It is suggested that experiments be conducted in which aircraft flying at standard attack elevation and speed would drop clusters as duds into water 10 to 20 ft deep with a sand bottom. The clusters could then be recovered and investigated for failure of the bomb-retaining bands and for crushing of bomb horns. If it is found that surface detonations could occur, the bomb-arming circuits should be redesigned so that the electric arming surge would be delivered to the bombs only after the spreading charges had fired. The necessary redesign would be fairly extensive and would require a considerable amount of testing.

In the case of the Mark 140 fuzed cluster, a production design has been achieved which could be put to service use. Since this cluster does not arm until it enters the water, there is no danger of premature detonation. From time to time, as new types of batteries become available, their application to this cluster might profitably be considered.

The scatter principle also should be useful in the design of other weapons, particularly antipersonnel and incendiary bombs.

Scatter Charge for Surface Vessels

The scatter charge was designed to permit surface vessels to attain greater effectiveness in placing depth charges. It consists of a cluster of six Mark 10 depth charges surrounding and bound to a bursting unit assembly. It is held by a nose stop and stabilizer plate in a modified Mark 7 depth-charge arbor and projected from a ship's modified K gun. The bursting unit assembly contains a charge which is fired mechanically, approximately 0.4 sec after the cluster leaves the K gun, dispersing the projectiles without detonating them or damaging their fuzes. Nine grams of 20 M/M smokeless powder is used for this bursting charge. The charges fall on the water surface in a circular pattern approximately 130 ft in diameter and centered about 50 yd from the K gun. Although Division 6 was not responsible for the design of the Mark 10 depth charges, work on the scatter mechanism was done by the division at CUDWR-NLL.

FIGURE 9. Scatter charge for surface vessels.

10.5 INTRODUCTION

The development of the scatter charge for surface vessels parallels the development of the antisubmarine scatter bomb for aircraft. As in the case of the scatter bomb, the idea was to eliminate the need for absolute accuracy in placing a depth charge so as to hit a submarine. It was thought that a group of depth charges fired from a single gun but dispersed in a circle would greatly increase the probability of striking the target. This requirement was met by binding six Mark 10 depth charges around a bursting unit, and modifying the standard Mark 7 depth-charge arbor and K gun so that the cluster could be projected from them. The firing mechanism provided was equipped with a delay squib to insure that the bursting unit would be fired approximately 4/10 sec after the cluster left the K gun.

Tests of the cluster as finally designed showed that the six depth charges strike the water surface spaced about the edge of an essentially circular pattern of the required size. Following sea tests the scatter charge was put in production and effectively used in antisubmarine warfare.

10.6 NATURE OF THE PROBLEM

The core of the problem was to devise a means of projecting a cluster of six Mark 10 depth charges from a ship's K gun so that the water surface pattern of the projectiles would be a circle 60 ft or more in diameter with a space of 30 ft or more between projectiles and the center of the pattern 50 yd from the base of the K gun. (Later the pattern requirement was increased to an optimum diameter of 120 ft with a minimum allowable diameter of 80 ft.) To this end various mechanical designs for the cluster, with appropriate modifications of the arbor and K gun to hold them, had to be evolved and tested. A bursting unit had to be devised to disperse the projectiles in mid-air without detonating them or damaging their fuzes. A firing mechanism for the bursting unit was needed, with a delay system to insure that the cluster would burst at an appropriate time after leaving the K gun, and with safety features to prevent premature firing. Finally, the various factors governing the size and shape of the water surface pattern of the projectiles had to be determined and brought under control in order to secure the pattern required.

10.7 TECHNICAL DEVELOPMENT

MECHANICAL DESIGN

In the first scatter-charge designs tested, the six Mark 10 depth charges were mounted on a cylindri-

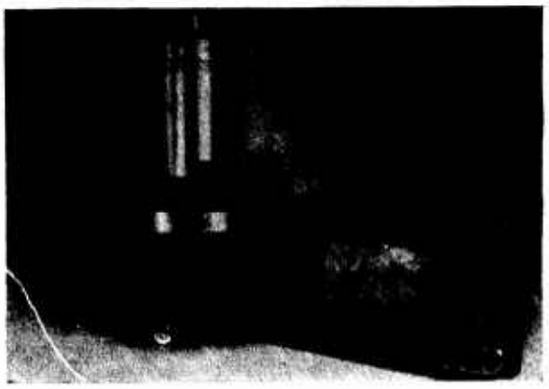

FIGURE 10. Bursting unit assembly with mechanical firing device.

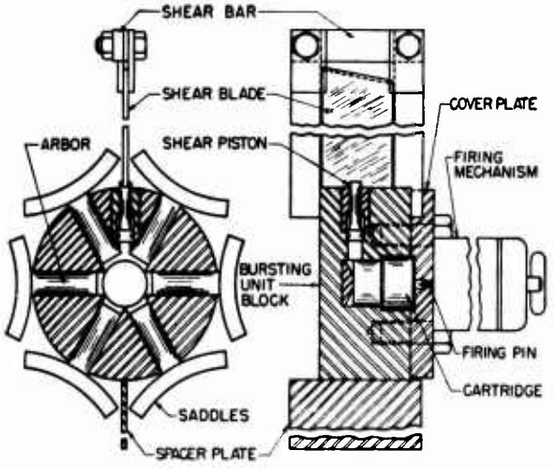

FIGURE 11. Details of bursting unit assembly.

cal central core the same length as the projectiles. Later designs incorporated a shorter cylindrical core, as shown in Figure 10. This core contains the bursting charge and its firing mechanism, six dispersing pistons associated with the arbors on which the projectiles are mounted, and a shear piston which, at the moment of firing, operates the shear blade in the flat extension of the core, thus cutting the binding strap around the projectiles (see Figure 11).

PATTERN CHARACTERISTICS

In the early stages of the development, experiments were conducted to determine whether clusters of sidewise-thrown projectiles or clusters of forward-thrown projectiles would produce the best pattern.

Studies of slow motion pictures of tests showed that, although the air flight characteristics of the sidewise-thrown cluster (see Figure 12) before bursting, and of the individual projectiles after dispersion, were eccentric, the water surface pattern was a reasonably regular circle, varying from 30 to 80 ft in diameter on different tests. The K-gun arbor, although released from the cluster, followed it closely in flight. At times this resulted in interference at dispersal, since the projectiles adjacent to the arbor struck it, and their normal trajectory was disturbed although all projectiles entered the water nose down or nearly so.

In an attempt to secure a more regular flight of the projectiles and to eliminate arbor interference, a new arbor was designed to project the cluster from the K gun with the projectiles nose first. Tests using this new arbor produced regular flight but an elliptical pattern which was no larger than that secured with the sidewise-thrown cluster. A time delay of 2/10 sec in the bursting charge was used with the idea that the projectile separations would be greater if given more time to spread. This was not the case. The use of heavier bursting charges, up to 33 g (the capacity of the cartridge chamber), likewise produced no better results. When the dispersal force was applied 4 in. above the center of gravity of

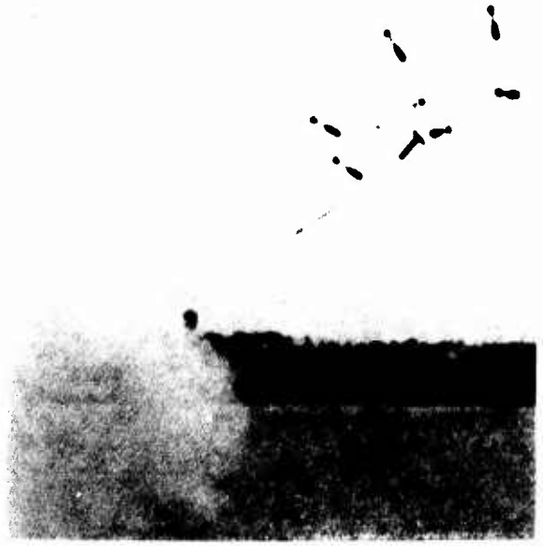

FIGURE 12. Sidewise-thrown scatter charge bursting (14-g bursting charge, 0.5-sec delay electrically ignited detonating squib, inertia-operated safety switch, No. 3 K-gun impulse charge).

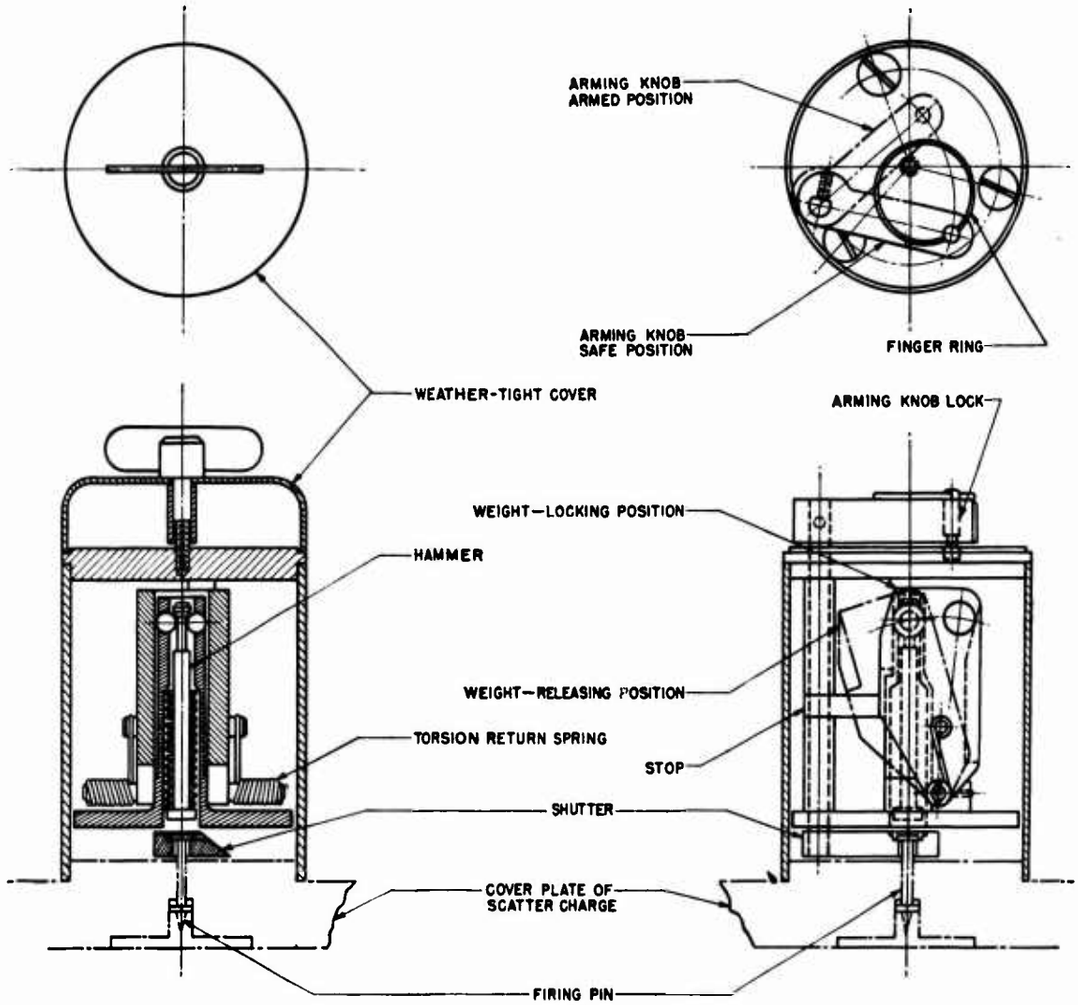

FIGURE 13. Diagram of mechanical firing device.

the projectiles, the air flight characteristics of the projectiles were destroyed and the pattern size was not increased.

From the slow motion pictures[a] made of these and other tests, and from plots made of each charge fired, it was determined that the factors governing the size and shape of the pattern are (1) the amount of powder used in the bursting charge, (2) the efficiency of the gas seals in the bursting unit, and (3) the position of the cluster in the air at the instant of bursting.

Nine grams of 20 M/M smokeless powder is used for the bursting charge. A cartridge of all plastic material was tested without success. Loss of the gas seal provided by the metal cartridge base resulted in small ground patterns, even with large increases in the weights of the bursting charges. The cartridge finally adopted is a standard Mark IV Hedgehog cartridge base into which is cemented a plastic powder container. This cartridge is inserted in the scatter charge when the K gun is readied for action.

It has been found that the cluster should burst about 0.35 to 0.4 sec after the charge leaves the K gun. Use of a percussion squib of this time delay in the bursting charge and a standard No. 1 (12½-oz) impulse charge in the K gun has resulted in the center of the pattern falling approximately 50 yd from the base of the K gun.

It has been found that the placement of the cluster

[a] Moving pictures of all tests are on file at the U. S. Navy Underwater Sound Laboratory, New London.

in the K-gun Mark 7 arbor tray materially affects the orientation of the cluster in flight. If the projectile noses are placed about 3 in. above the lower lip of the tray (which brings the center of gravity of the cluster directly on the axis of the K-gun barrel and the arbor stem), the nose of the cluster tends to rise in flight, resulting in bursting when the cluster is approaching the horizontal position with respect to the water. Dropping the nose end of the cluster to the lower lip of the tray results in a flight such that the bursting takes place with the bombs nose down in the most favorable position for water entry. This slight displacement of the center of gravity caused neither damage nor apparent strain on the Mark 7 arbor of the K gun.

Tests of the effect of the setback forces on the Mark 140 fuzes in the individual Mark 10 projectiles indicate that no damage results to the fuze when used in the scatter charge.

Bursting Charge Firing Mechanism

Because a mechanical firing system requires no connection to the K gun and is therefore independent of the ship's firing circuit, this type of firing mechanism was finally adopted. (An electric firing system[1] was used in early models of the scatter charge.)

Figure 13 shows how the mechanical firing device operates. Mounted on the cover plate of the bursting unit, it employs a spring-driven hammer held in cocked position by a ball latch. The latch is operated by a weight or pendulum which is moved to the releasing position by the acceleration of the cluster leaving the K gun. Tripping the latch releases the hammer which drives the firing pin in the cover plate into the percussion-initiated delay squib and fires the bursting charge.

Three safety features are built into the device: (1) the weight is maintained in the safe position by a cam or stop; (2) a shutter is held between the hammer and the firing pin to prevent premature movement of the firing pin toward the cartridge; and (3) even in the armed condition, a torsion return spring holds the weight in the locking position until the latter is moved to the releasing position by a force greater than 40 G's.

In arming the equipment, the weather-tight cover is removed and the arming knob is moved from the safe to the arm position. This removes the pendulum stop and moves the shutter to a position enabling the mechanism to arm when it is fired from the K gun. If the scatter charge is not fired, the arming knob can be returned to the safe position, thus replacing the safety stop and shutter and allowing replacement of the weather-tight cover.

Modification of Arbor and K Gun

The standard Mark 7 arbor was modified for use with the scatter charge by the addition of a nose stop and stabilizer plate to hold the cluster in place before firing and by the substitution of a longer retaining cable than that required for the Mark 6 depth charge.

The K gun was modified for use with the scatter charge by providing an additional positioning notch and a lashing loop on the side of the barrel opposite the breech, between the original notches and lashing loops. This makes it possible to use either Mark 6 depth charges or scatter charges in the same K gun.

10.8 PERFORMANCE AND CONCLUSIONS

Sea tests of the cluster showed that the six depth charges strike the water surface spaced about the edge of an essentially circular pattern approximately 130 ft in diameter, whose center is about 50 yd from the base of the K gun. The scatter charge is safe to handle and has proved efficient in operation, and it is considered that the objectives enumerated at the beginning of this summary have been met.

Roller Loader for Scatter Charge and Depth Charge

The roller loader is a dual-purpose L-shaped structure which facilitates the loading of a standard K gun with either the scatter charge or the Mark 6 depth charge. For this purpose it is equipped with a carriage running on a track level with the arbor of the K gun. This carriage has interchangeable cradles, one adapted to hold Mark 6 depth charges, the other to hold scatter charges. In addition to the ready charge in the K gun, three charges can be held in the roller loader: one in the loading carriage on the front leg of the L, and two in the ready-storage position on the side leg of the L. Development work was done by CUDWR-NLL.

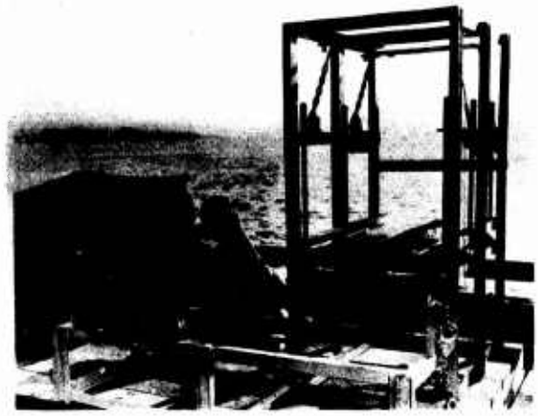

FIGURE 14. Roller loader.

10.9 INTRODUCTION

The roller loader was designed as part of the development of the scatter charge for surface vessels. The chief requirement was a carriage level with the arbor of the K gun and running on a track. This carriage had to have interchangeable cradles, one adapted to hold a Mark 6 depth charge, and the other to hold a scatter charge.

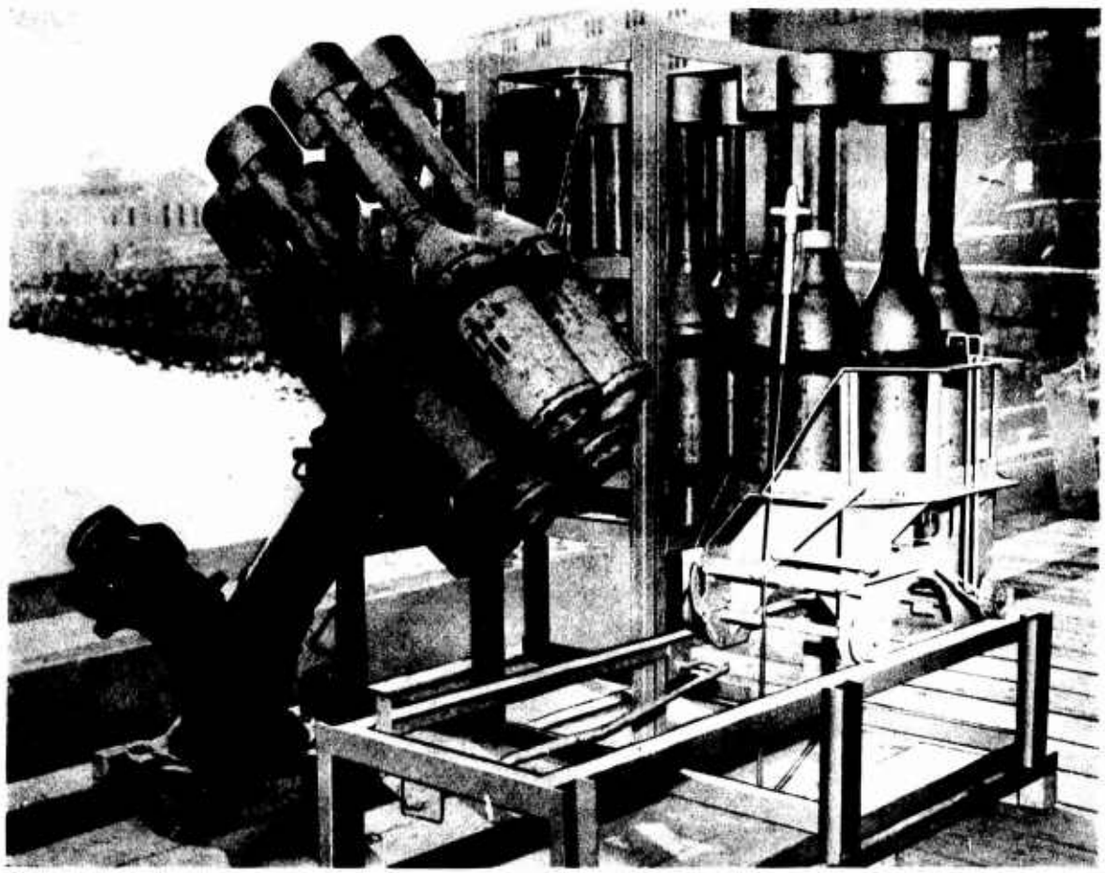

FIGURE 15. Roller loader with scatter charges.

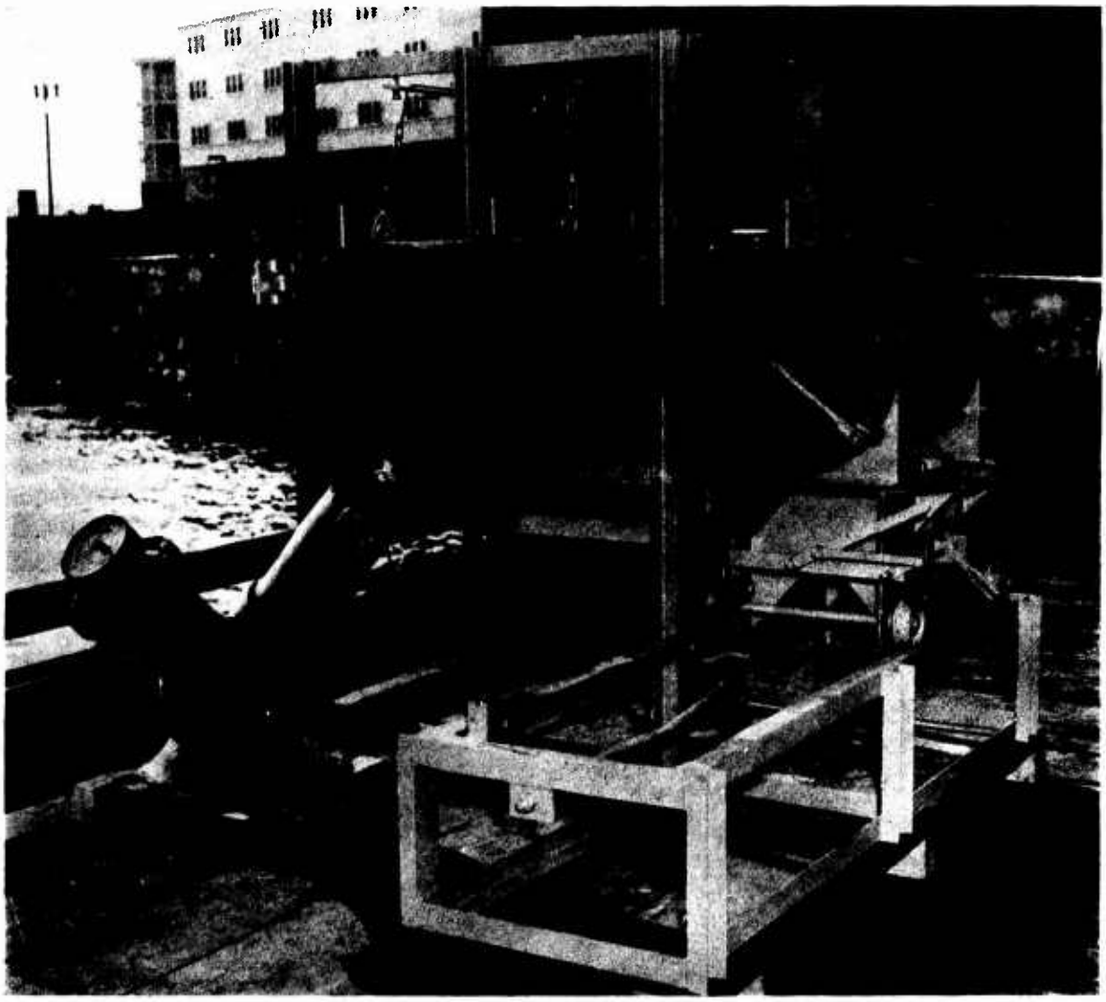

FIGURE 16. Roller loader with Mark 6 depth charges.

10.10 **DESCRIPTION**

In its final form, the roller loader is a welded framework of structural angles and channels. In plan it is L-shaped, extending down one side and across the muzzle of the K gun (see Figure 14). The front leg of the L is a track on which a carriage operates to transfer charges from the ready-storage section in the side leg of the L to the loading position in front of the gun. This carriage is provided with two interchangeable cradles, one for the scatter charge, the other for the depth charge.

In handling the scatter charge, the cluster, in its normal nose-down position, is moved on a roller track from the ready-storage section to the carriage (see Figure 15). The track in the ready-storage section consists of a double row of narrow 1-in. diameter rollers and a central guide fin projecting ½ in. above the rollers, which prevents the cluster from turning on the track while in motion. Outside the steel angles, carrying rollers, one located at each side of the cluster and placed slightly below the level of the center track, stabilize the cluster in an upright position. The carriage running on the track in the front leg of the L is permanently equipped with an extension of the storage section tracks to facilitate transfer of clusters to the carriage. The cradle for the scatter charge is provided with back railing to stabilize the cluster. A locking device prevents movement of the cluster during transport to the loading position. Figure 15 shows one scatter charge in the K gun, one in the loading carriage, and two in the ready-storage section.

In handling the Mark 6 depth charge, the charge is rolled on its own periphery from the ready-storage section to the carriage on steel angle tracks which serve also as bracing members of the structure. The cradle with which the carriage is fitted to receive the depth charge is in the form of a curved tray equipped with a locking device to prevent movement of the charge. Figure 16 shows the loader with one depth charge in the K gun, one in the loading carriage, and two in the ready-storage position.

Suitable clamps and stops are provided to prevent any movement of the charges in the storage rack and carriage when the equipment is secured. Charges of either type are fed into the loader from the deck by means of a davit installed at the inboard end of the storage section.

Fast-Sinking Depth Charge

FIGURE 17. Full-scale model of proposed Mark 12 fast-sinking depth charge.

The fast-sinking depth charge was designed to eliminate such shortcomings of the conventional depth charge as excessive handling, weight, low sinking speed, and deviation from the desired trajectory. The latest design of the fast-sinking depth charge (Mark 12) has the form of an elongated, streamlined cylinder with a blunt nose and a tapering afterbody. A tail-mounted shroud ring and set of fins improve the dynamic characteristics of the projectile. This unit, designed for individual or multiple barrage launching from surface craft, is 6 in. in diameter, 36 in. long, and carries a charge of 36 lb of Torpex 2. It weighs 91 lb and has a sinking speed of 45 fps. The shape of an earlier model (7-40-M) of the fast-sinking depth charge was utilized in the Mark 52 depth bomb designed for projection from blimps. This missile is 7 in. in diameter and 44 in. long. It contains 52 lb of Torpex 2 and weighs approximately 100 lb. The development of the fast-sinking depth charge was conducted by GUDWR-NLL. Certain related investigations were carried out at MIT-USL and at CIT.

10.11 INTRODUCTION

The development of the fast-sinking depth charge was initiated to overcome many of the objectionable features of the conventional depth charge, such as slow sinking rate, uncertain trajectory, and excessive handling weight. At the time, little information was available concerning the factors which affect the resistance and stability of a body in free underwater travel. There was also little understanding of the phenomena associated with passing a body through an air-water interface at velocities of 30 fps or more. Neither the minimum acceptable explosive charge nor the size and shape of the fuze mechanism had yet been determined quantitatively.

From this starting point, an intensive investiga-

tion and development program was undertaken on scale model projectiles to obtain basic information on the resistance and the stability requirements of certain underwater depth-charge shapes. Measurements of the time required to reach different depths were recorded electrically. The velocities and resistance coefficients were calculated from the oscillograph records. The tests showed the effects on stability of changes in the position of the center of gravity and of certain variations in nose and tail design. In particular, this work had an important bearing on development of the value of projectile spin accomplished through oblique tail fins. In experiments to gain knowledge of entry phenomena, models were projected from an air gun, and high-speed moving pictures recorded the underwater travel. Several hundred tests of approximately full-size models verified the results obtained with smaller-scale ratios. The project was carried to a point where preproduction samples of a charge designated the Mark 12 depth charge were built and tested, achieving a sinking rate of 45 fps in 170 ft of water.

Conflicting opinions persisted, however, on such matters as terminal velocity versus deep water dispersion and explosive content versus size and weight. A coincidental project devoted to the development of fuzes suitable for use in fast-sinking depth charges (discussed in a later section of this chapter) did not succeed in evolving a fuze which was both safe and efficient, since requirements for safety and for certainty of operation, particularly in proximity fuzes, tend to conflict. Service acceptance and use of the Mark 12 depth charge were therefore hampered by lack of adequate fuzes.

It was felt, however, that the experiments and investigations undertaken in the development of the Mark 12 added considerably to the existing knowledge of depth-charge behavior and should be of value in any future work of this nature.

10.12 DESIGN REQUIREMENTS

In addition to the general requirements that the underwater depth charge be of a faster-sinking type, that it be more certain in trajectory, and that it be lighter in weight than the 1941 standard depth charge, the Bureau of Ordnance required that it be capable of being dropped individually or in a multiple barrage from surface craft. Later, the desire to use such charges from aircraft was indicated. The depth charge was to have safety features adequate to protect operating personnel from the hazards of accidental explosion. It was to be provided with a fuze that would not become armed until it reached a water depth of approximately 30 ft. The firing mechanism was to be either of a type energized by impact with a rigid body or of a type actuated by close proximity to a ferromagnetic body.

10.13 HYDRODYNAMIC CONSIDERATIONS

Preliminary investigations embracing some 400 experiments with spheres, cylinders, darts, and various other shaped bodies moving through water provided a background of data for the design of a stable and fast-sinking projectile.[b] The final design and its various modifications were subjected to exhaustive dynamic tests. Some of the significant observations and conclusions resulting from these experiments are described below.

A sphere falling freely in water does not descend in a straight line but follows a helical path. Cylinders falling end-on have maximum stability when they possess a length-diameter ratio of about five. By "stability" in the case of a projectile is meant the tendency of the projectile to assume and maintain an orientation such that its major axis is tangent to its trajectory.

Streamlined bodies are inherently unstable. The shape of the nose and the afterbody of a projectile can be modified to increase stability but at the expense of increasing the drag correspondingly. The shape of the nose is most important in the transitional section where the nose meets the cylindrical body. The central 60 per cent of the projected nose area may be made flat with little effect on stability and with an increase in drag of only about 10 per cent. An otherwise streamlined afterbody may be terminated abruptly without serious increase in drag. Increasing the diameter of the flat end of such a terminated afterbody from 14 to 25 per cent of the cylinder diameter increases the drag by only 6 per cent.

The stability of a streamlined projectile can be

[b] This program was carried out at the Training Tank, U. S. Submarine Base, New London, Conn.; at Morris Dam near Pasadena, Calif.; at the Alden Hydraulics Laboratory, Worcester, Mass.; at the Massachusetts Institute of Technology, Cambridge, Mass.; and at the U. S. Navy Underwater Sound Laboratory, New London, Conn.[2]

increased with very little increase in drag by the addition of a shroud ring and set of fins to the tail structure. The shroud ring is particularly effective. For maximum stability the length of the ring should be between 40 and 50 per cent of the projectile diameter. Alignment should be such that angular tilt does not exceed about 30 min of arc. Radial displacement up to about 1½ per cent of diameter produces no noticeable effect on stability. There appears to be a best location for the leading edge of the shroud ring relative to the curved afterbody. An airfoil cross section is desirable but a bevelled profile is a satisfactory compromise for ease of fabrication.

Stability is greatly increased by causing the projectile to spin around its longitudinal axis. To accomplish this, spiral (helicoidal) fins having a pitch angle of from 10 to 15 degrees are most effective. However plane fins inclined to the axis of the projectile yield essentially the same stability and produce an increase of only a few per cent in drag above the corresponding spiral fins. With spin, minor irregularities in body dimension are less significant and hence manufacturing tolerances may be less stringent.

Stability is measured in terms of the Loring factor. The Loring factor of a projectile is the distance between its center of gravity and center of longitudinally projected area divided by its overall length. It is a measure of the moment arm on which the hydrodynamic turning forces act. In general, the larger its value, the more stable the projectile.

Not only should a fast-sinking depth charge be stable but it should also describe a trajectory which rapidly approaches the vertical so that its horizontal position may be known more accurately. The force of buoyancy acts at the center of volume of the projectile and is responsible for producing the desired vertical motion. The eccentricity of a projectile is defined as the ratio of the distance between the center of gravity and center of volume to the overall length. It is thus a measure of the moment arm on which the buoyant force acts, and the larger its value, the more rapidly the trajectory approaches the vertical. The eccentricity of a projectile can, of course, be increased by adding weight to the nose or by removing weight from the tail. Increasing the eccentricity also increases the Loring factor and, hence, improves the stability as well.

A large number of moving pictures were taken to determine the behavior of a recommended projectile, both at water entry and also during its subsequent descent into the water. The recommended projectile had a diameter of 6 in., a length of 49 in., a hemispherical nose, and an approximately streamlined afterbody fitted with fins and a shroud ring. Plane fins inclined at 10 degrees to the axis were used. The shroud ring was about 3 in. long. The 41-lb load was so adjusted that the eccentricity was about 0.12.

When launched underwater, such a projectile duplicated quite accurately its entire trajectory. The rms dispersion on a large number of trials was only about 4½ in. at a depth of 180 ft.

When launched from air into water, however, dispersion was considerably greater. A variable amount of air is carried along with the projectile as it splashes into the water. This entrapped air reduces the ability of the tail fins and shroud ring to stabilize the motion. Even for vertical axis entry the rms dispersion was 70 in. at 180 ft. When the projectile is thrown into the water with a velocity of from 35 to 45 fps along a trajectory making an angle of from 45 to 55 degrees from the vertical and with a body orientation of between 45 and 90 degrees from the trajectory (but in the same plane), the rms dispersion is about 12 ft at 180 ft. When the projectile axis is skewed out of the plane of the trajectory by as much as 20 degrees, little increase in deviation is observed. However, increasing the skew to 45 degrees approximately doubles the dispersion.

Out of this work came the conclusion that the range of 6- to 7-in. diameters seems fairly close to optimum and, considering fuze sizes, explosive charge sizes, and gross projectile weights, this range permits choice of projectile diameter in accordance with practical design consideration. For the depth charge using the inertia-type fuze, it seemed desirable to maintain the 6-in. diameter, but the magnetic fuze required a 7-in. diameter projectile. The explosive charge originally set at 30 lb of TNT was later increased to 40.

The K gun was at first indicated as the probable dispenser for the proposed fast-sinking depth charge. Model tests of simulated K gun launching, however, indicated that better methods could be found for the purpose. Parallel projects, discussed later in this chapter, were therefore undertaken to develop (1) two types of surface craft dispensers, and (2) the Mark 53 bomb rack for launching the projectiles from blimps.

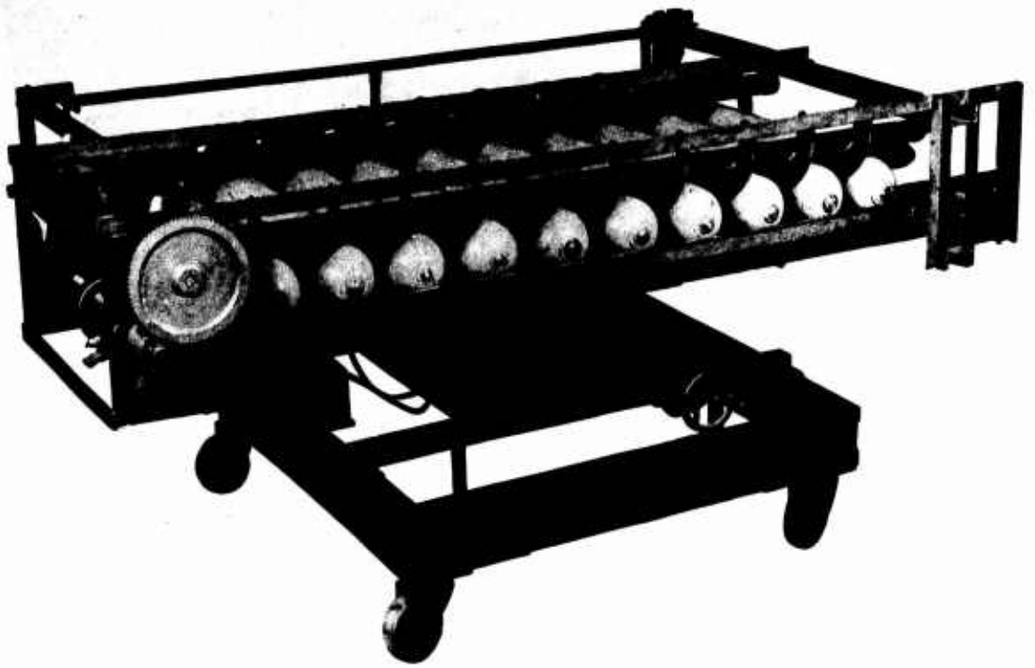

FIGURE 18. Screw-type power-operated dispenser (preliminary assembly without gear and motor enclosure).

10.14 DESCRIPTION OF FINAL MODEL

The latest and most effective model of the fast-sinking depth charge designed before the project was discontinued was designated the Mark 12 depth charge (see Figure 17). It is 6 in. in diameter and 36 in. long, exclusive of the Mark 140 fuze protective cap. The charge has a capacity of 36 lb of Torpex 2 with a gross weight in air of 91 lb including fuze and boosters. The sinking rate is 45 fps as determined by tests of preproduction samples in 170 ft of water.

The Bureau of Ordnance also produced the Mark 52 bomb for use from blimps. It conforms in shape to one of the earlier models of the fast-sinking depth charge, known as the 7-40-M depth charge.[3] The dimensions are 7 in. in diameter and 42 in. in length exclusive of the Mark 140 fuze protective cap. The explosive cavity holds about 52 lb of Torpex 2. The gross weight in air is about 100 lb.

10.15 CONCLUSIONS

Conflicting opinions on questions of terminal velocity versus deep water dispersion, and explosive content versus size and weight, together with the lack of adequate fuzes delayed actual production and use of the fast-sinking depth charge. Nevertheless, a model was developed, the Mark 12, which gave promise in preproduction tests of greater efficiency than the then standard depth charges, particularly in sinking rate. The investigations undertaken on this project added considerably to knowledge of depth-charge behavior and should be of value in any future work of this nature.

10.16 SURFACE CRAFT DISPENSERS FOR FAST-SINKING DEPTH CHARGES

In the early stages of development of the fast-sinking depth charge, simulated K-gun launching tests revealed that the K gun did not provide an ideal method of launching. As a corollary to the fast-sinking depth-charge project, therefore, a project was initiated to develop a device for launching or projecting fast-sinking depth charges from destroyers and similar surface craft.

FIGURE 19. Mark 12 depth charge in gravity-type dispenser.

The mechanism was to be capable of launching in multiple barrages depth charges of the type which had been under development at the New London Laboratory up to that time. One of these charges was 6 in. in diameter and 49 in. long; the other was 7 in. in diameter and 44 in. long. A power-operated, twin-screw dispenser (see Figure 18) was built for test purposes only and had a capacity of ten 6-in. diameter charges. A gravity-operated type (see Figure 19) intended for Service was developed for launching three 6- or 7-in. diameter units at one time.

Both types of fast-sinking depth-charge dispenser were tested under operating conditions and satisfactorily met the requirements laid down for their design. As the screw-type dispenser had been designed for test purposes only, its development did not extend beyond the model stage. Fifty units of the gravity-type dispenser were put into production, but, since use of the Mark 12 fast-sinking depth charge was postponed, the dispenser project was likewise halted.

Fuzes for Fast-Sinking Depth Charges

Fuzes for fast-sinking depth charges are detonating devices mounted inside the nose of the projectile. The two types developed by the Bell Telephone Laboratories, Inc. and the New London Laboratory are inertia-actuated and magnetically actuated fuzes. The former type includes a mercury jiggle switch which, upon impact of the projectile, starts a detonating current flowing. This sets off the booster charge which in turn causes explosion of the principal charge. The latter type differs from the inertia-actuated fuze in that the detonating current is obtained by a change or a distortion of a magnetic field. In the magnetic flux-change fuze, a current is induced in a coil surrounding a permanent magnet when the magnetic field changes; in the balanced-bridge magnetic fuze, two Permalloy strips are mounted at right angles to a strong balanced field and become magnetized and come together, thereby actuating a battery, when a ferro-magnetic body distorts the existing field balance.

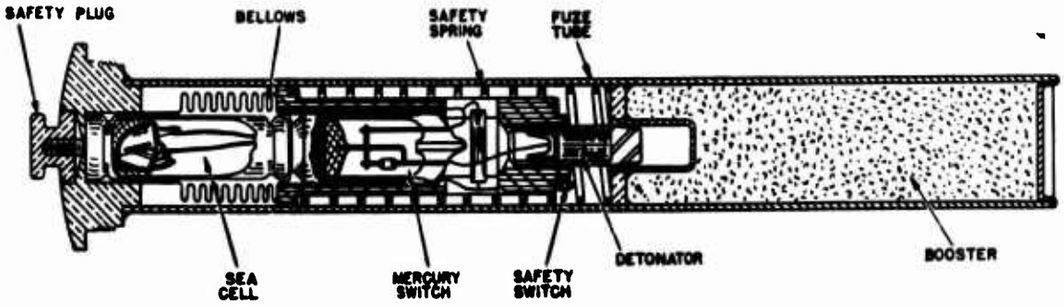

FIGURE 20. Inertia-actuated fuze, bellows armed.

10.17 INTRODUCTION

The development of a suitable fuze for the fast-sinking depth charge paralleled the development of the depth charge itself which was discussed earlier in this chapter, page 202. The design of an efficient underwater projectile, as well as its effective use, depends in considerable measure on the fuze employed.

An acceptable fuze must be designed so that it can be accommodated in the 6- or the 7-in. diameter depth-charge shell. It should not fire on impact with the surface of the water whether launched from surface craft or from aircraft. Furthermore, it should remain unarmed until a depth of about 40 ft is reached at which level it should become fully armed. The mechanism should provide safety protection for all personnel during assembly and shipment, in operations, and in case of own-ship's sinking. It must also be weatherproof.

Two types of firing mechanisms were developed, one actuated on impact as a result of inertia effects and the other actuated as a result of magnetic effects when in close proximity to a ferromagnetic body. In each case the fuze is mounted in the nose of the projectile. To arm the mechanism certain mechanical and electrical steps must be completed. Final explosion of the principal charge is initiated by the explosion of a booster charge which in turn is set off by the electric detonation of a blasting cap. In the case of the inertia-actuated mechanism, the electric detonator is initiated when its electric circuit is completed through a mercury "jiggle switch." Two types of magnetically actuated fuzes were developed. In one, when the system moves close to a ferromagnetic body, the change in magnetic flux through a coil associated with a permanent magnet produces the electric current for the detonator. In the other, a balanced magnetic bridge becomes unbalanced when brought near a ferromagnetic body and hence magnetizes two metallic strips so that they move together and close the necessary electric circuit.

None of these fuzes was developed to the point where it was considered entirely safe and reliable for operation, and further work was discontinued with the termination of the fast-sinking depth-charge project. However, it is felt that the experimental results may be valuable in future similar investigation.

10.18 INERTIA-ACTUATED FUZES

Two inertia-actuated fuzes were developed, differing from each other primarily in the method of arming. In both cases an electric current initiates the detonator when a mercury jiggle switch closes as the result of a collision with a rigid body. Arming is initiated by the removal of a safety plug in the nose cap of the projectile when it is released. The arming process is completed when hydraulic pressure is sufficient to cause the detonator to engage the booster and close a safety arming switch in the detonator circuit. One of the fuzes employs a plunger to accomplish this step; the others, a bellows. The bellows-armed type appeared more promising than the other.

10.18.1 Bellows-Armed Fuze

General Description

The mechanism of the bellows-armed fuze is shown in cross section in Figure 20. The safety plug is removed as a part of the operation of launching, thereby tearing out the threaded stem of the sea cell. This permits activation of the sea cell and admits water pressure to the metal bellows. The bellows and the safety spring hold the detonator in the safe position until water pressure acting on the bellows compresses the spring, causing the detonator jacket and detonator to engage the booster and the safety switch to close. Arming is then complete and the detonator is fired when the mercury switch is closed as the result of impact against a target.

Tests and Results

Very few tests were made on this fuze. One unit was dropped through air twice from a height of 40 ft onto a steel target. On neither occasion did it explode. When dropped 40 ft through water onto a steel target the fuze exploded as expected. Statistical tests were never carried out. The limited number of tests nevertheless indicated that this mechanism could probably be made to fulfill all the requirements of an inertia-actuated fuze.

10.18.2 Type HIR Fuze

In an effort to hasten Service trials of the fast-sinking depth charge, the HIR fuze which had al-

ready been approved by the Bureau of Ordnance was installed in a number of projectiles. This required certain modification in the design of the nose to receive the fuze and booster.

A number of the modified depth charges (loaded with 40 lb of TNT) were drop-tested from a blimp at an altitude of 600 ft. The first was dropped on land and, properly, did not explode. Four others did not explode when dropped in 40 ft of water over a hard bottom. Ten others were dropped in 70 ft of water over a soft bottom and all exploded upon hitting the bottom. The number of tests was insufficient to give more than a rough indication of the range of performance of the HIR fuze.

10.19 MAGNETICALLY ACTUATED FUZES

A magnetically actuated fuze should fire as the result of a glancing blow or a near miss and hence should have a somewhat larger range of actuation than an inertia-actuated fuze. Furthermore the magnetic fuze should not fire on impact with the bottom.

Two types of magnetically actuated fuzes were developed and tested. Each has a plunger arming mechanism similar to that described above. The two fuzes differ primarily in the method of initiating the electric current to the detonator. In one, a flux-change type of fuze, the detonating current is induced in a coil associated with a permanent magnet when the unit is moved close to a ferromagnetic body. In the other, a balanced-bridge type of fuze, the current is obtained from a battery as the result of contact between two ferromagnetic strips. The strips are mounted at right angles to a strong local magnetic field such that when the field is distorted by the presence of a nearby ferromagnetic body, they become magnetized and attract each other.

Development work on the flux-change fuze was not completed in view of the apparently greater promise offered by the balanced-bridge fuze. The results obtained with the latter are discussed below.

10.19.1 The Balanced-Bridge Magnetic Fuzes

Theory

Figure 21 illustrates the principle of operation of the balanced-bridge mechanism. Two ferromagnetic tubes *T*, with an air gap between them, are placed at one side of an electromagnet as shown. In the space between the tubes two flexible ferromagnetic strips *S* are mounted with adjacent ends overlapping, and oriented to lie at right angles to the lines of flux of the magnetic field (i.e., parallel to the equipotential lines shown in the figure). The strips are supported at their far ends so that on bending toward each other the near ends can make contact. In the normal balanced condition the strips do not touch. When a ferromagnetic body is brought near the system, as in Figure 21B, the magnetic field is distorted, thereby magnetizing the strips longitudinally so that they attract each other. Contact between the strips is used to complete the circuit to an electric detonator.

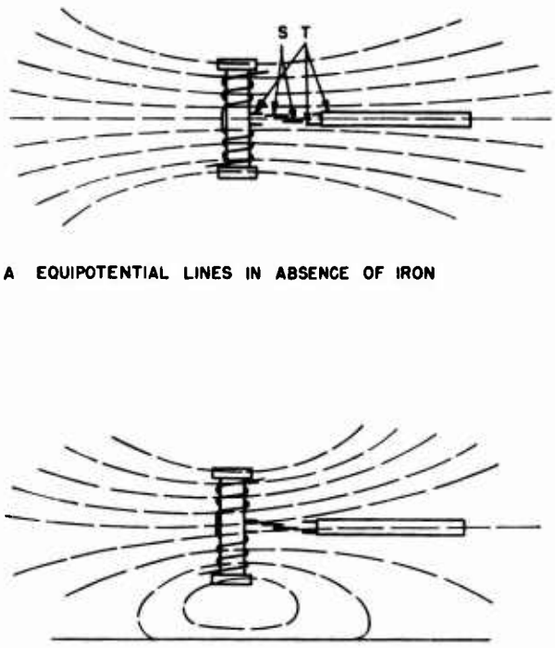

Figure 21. Magnetic field in vicinity of magnetic bridge.

Development

The specifications established for the balanced-bridge fuze required that it function when the nose of the projectile comes within about 4 in. of an iron body. Deck planking and other barriers to intimate contact should not prevent explosion. To obtain the required sensitivity it is necessary to maintain a high degree of balance in the magnetic circuit, and yet the mechanism must be sufficiently

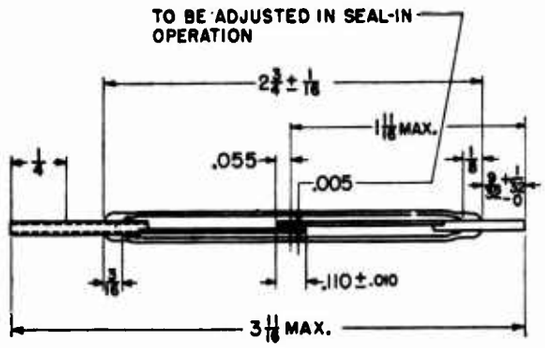

FIGURE 22. Magnetic switch for balanced-bridge fuze.

rugged to be unaffected by shock experienced in handling, launching, and entering the water.

The original design called for permanent magnets to produce the magnetic field and for dry cells to actuate the electric detonator. These were soon discarded in favor of an electromagnet powered by a sea-activated battery. (See Chapter 12.) This provided a more reliable magnetic field and was easier to construct than a balanced permanent-magnet bridge. The sea cell also served to ignite the detonator and thus provided an additional safety measure in that the detonator could not be fired by accidental closing of the magnetic switch before salt water reached the cell. The problem of dry-cell shelf life was also thereby avoided.

To determine the optimum design for the various components of the system, it was necessary first to develop a magnetic switch having the greatest possible sensitivity consistent with reliable operation. The switch finally adopted is shown in Figure 22. The two ferromagnetic strips, gold-tipped for good electric contact, are sealed in a hydrogen-filled glass tube. The application of a magnetic field equivalent to about 15 ampere-turns along the axis of the tube is sufficient to magnetize the strips so that their free ends make contact.

A number of sea cells which would furnish the power required and also become activated quickly on entry of salt water were designed and tested. The cell finally adopted to power the electromagnet employed 17 alternate silver and magnesium plates, with phenol fiber separators. The cell for firing the detonator employed only 3 plates.[4]

FINAL MODEL

Description. A cross-sectional drawing of the balanced-bridge fuze appears in Figure 23. The arming mechanism is housed inside the Permalloy tube which lies along the axis of the projectile. Between this "collector tube" and the electromagnet assembly is the glass-sealed magnetic switch. The sea cell is mounted next to the coils of the electromagnet in the nose of the projectile. Between this "collector tube" and the electromagnet assembly is the glass-sealed magnetic switch. The sea cell is mounted next to the coils of the electromagnet in the nose of the projectile. In order that the magnetic flux extend into the region surrounding the projectile, it is

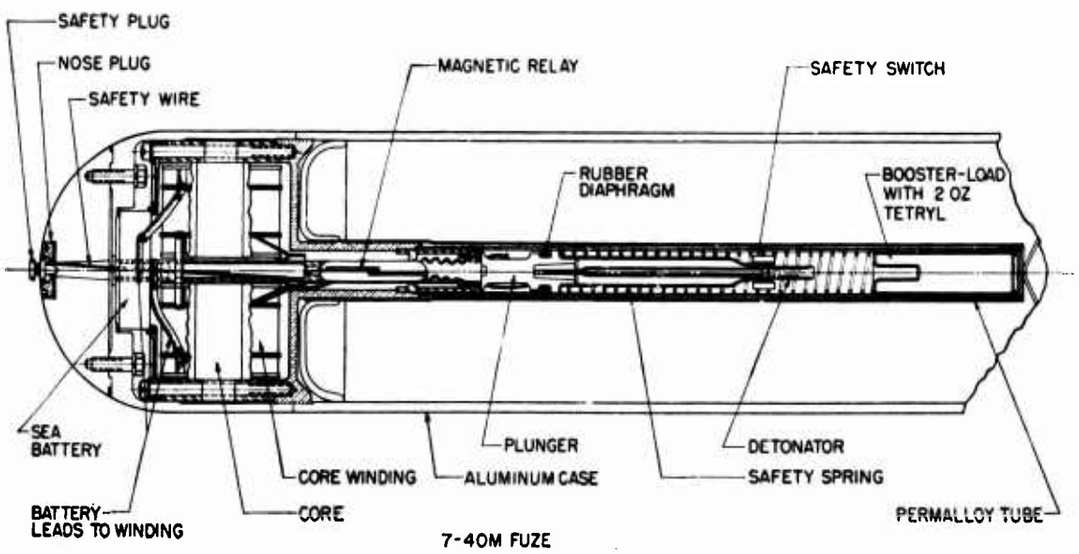

FIGURE 23. Balanced-bridge magnetic fuze.

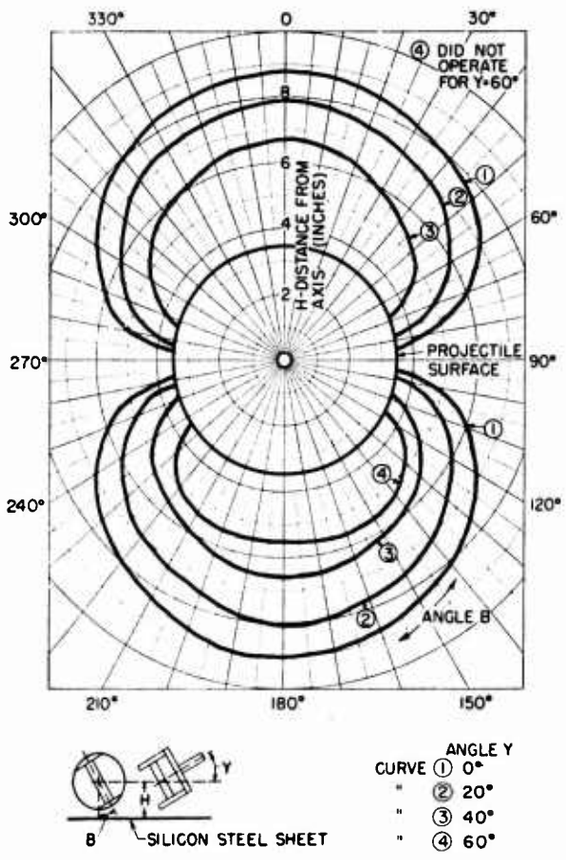

FIGURE 24. Operating range of magnetic-bridge fuze.

necessary that the housing be of nonmagnetic material.

Operation. There are three phases to the operation of the balanced-bridge magnetic fuze: (1) mechanical arming, (2) electric arming, and (3) magnetic firing.

A safety wire which locks the arming piston in the safe position is withdrawn when the safety plug is removed at the time when the depth charge is launched. This admits water to the sea cell and also through a hole in the electromagnet to the arming piston. As the pressure increases, the piston moves back and compresses the safety spring. At a depth of about 35 ft the detonator engages the booster and the safety switch is closed. This requires about 2 sec with overside launching. Electric arming is completed when the cell becomes activated and energizes the electromagnet. This is well under way in about 1/3 sec, although the current to the coils continues to rise for several seconds.

When the presence of a target distorts the magnetic field sufficiently, the magnetic switch closes and thereby completes the circuit to the detonator. Firing of the detonator explodes the booster and hence the main charge.

It should be noted that there are "dead" regions in the vicinity of the nose of the projectile — regions in which a target will not operate the magnetic switch. This is because the distortion which actuates the switch must be one which creates a difference between the magnetic paths from the collector tube to the two poles. In general, if the direction of the target (the line from the center of the electromagnet to the target and perpendicular thereto) lies in the plane which is at right angles to the axis of the electromagnet, the switch will not close. Figure 24 shows the range within which the mechanism does function for various orientations of the projectile with respect to the target. To increase the probability of firing, the projectile is given spin as it descends through the water. This is accomplished by the use of spiral tail fins.

10.19.2 Results

Laboratory tests on the magnetic bridge mechanism and on the other components of the fuze demonstrated that reliable field performance of the final model might be expected. However, such a result was not realized. The sea trials of the magnetic bridge fuze showed quite conclusively that the mechanism was unreliable and also unsafe for use by surface craft. Furthermore, the fuze would be costly and complicated to manufacture. Consequently, further development was discontinued.

10.20 CONCLUSIONS

The entire fuze program for the fast-sinking depth charge was terminated along with the depth-charge program itself. No satisfactory fuzes were developed. However, it is believed that a considerable amount of design art evolved and this should be of value in any future fuze work.

Mark 53 Bomb Rack

The Mark 53 bomb rack was developed by CUDWR-NLL to permit launching of fast-sinking depth charges from lighter-than-air craft. Its design (1) provides for dispensing projectiles either individually or in a "stick" barrage, and (2) obviates any necessity for protuberances or indentations on a projectile's surface which might impair its hydrodynamic performance. Automatic release for normal operation and manual release for emergency conditions are available. The equipment, weighing about 95 lb, includes: bomb release mechanism and support, arming and forward spacer assembly, aft spacer, release spring assembly, and bomb release handle. Sixteen projectiles constitute a full load for the rack; eight is the maximum number that can be dispensed in a single "stick."

FIGURE 25. Lower section of bomb rack.

10.21 INTRODUCTION

Though fast-sinking depth charges were originally intended to be launched from surface craft, it soon appeared desirable to launch them from lighter-than-air craft as well. Accordingly it became necessary to develop a special rack for carrying and automatically dispensing them.

The requirements established for the rack were (1) that it be suitable for "stick" bombing, (2) that its design not impose the necessity of any protuberances on, or indentations in, the projectile which might disturb its hydrodynamic characteristics, and (3) that it carry up to 16 of the 6-40 projectiles (6 in. in diameter, 49 in. long, 40 lb of TNT) to be dispensed either individually or in sticks. This requirement was later expanded to include the 7-40 projectile (7 in. in diameter, 44 in. long, 40 lb of TNT).

10.22 DEVELOPMENT

Since the 6-40 and 7-40 bombs were originally designed for launching from surface craft, air flight tests were first made on one-third scale models launched from a K-type ship. The projectiles were found to have satisfactory air flight characteristics when launched horizontally with nose forward.

Design of a suitable rack and dispensing mechanism commenced with a wood mockup model. After testing in the laboratory this rack was installed in a K-type airship for further tests. These indicated the need for an automatic release mechanism to space the projectiles more uniformly in a "stick" barrage. The final model, the Mark 53 bomb rack, incorporated automatic release and provision for dispensing either the 6-40 or the 7-40 bomb. After further tests, manufacture of 20 units of the final design was undertaken at the Naval Gun Factory, Washington, D. C.

10.23 FINAL DESIGN

10.23.1 General Description

Figure 25 shows how two rows of four depth charges each are mounted in the Mark 53 bomb rack. Two additional rows of projectiles may be supported so that 16 depth charges can be dispensed from a single rack. Each projectile is supported by a cable, one end of which can be released. The two layers are separated by a pair of spacers; one end of the forward spacer appears in the figure. These spacers swing down out of the way when the lower row of projectiles has been released. Spacers are available for both the 6- and the 7-in. diameter depth charges.

10.23.2 Bomb Release Mechanism

The section of the bomb rack shown in Figure 25 is supported by the truss framework of Figure 26. The release hooks for the support cables and their associated trigger mechanisms are mounted in the V-shaped member of this truss. This member also houses the cable take-up units for the fixed ends of the support cables. The release mechanisms are triggered in sequence by the escapement wheel which

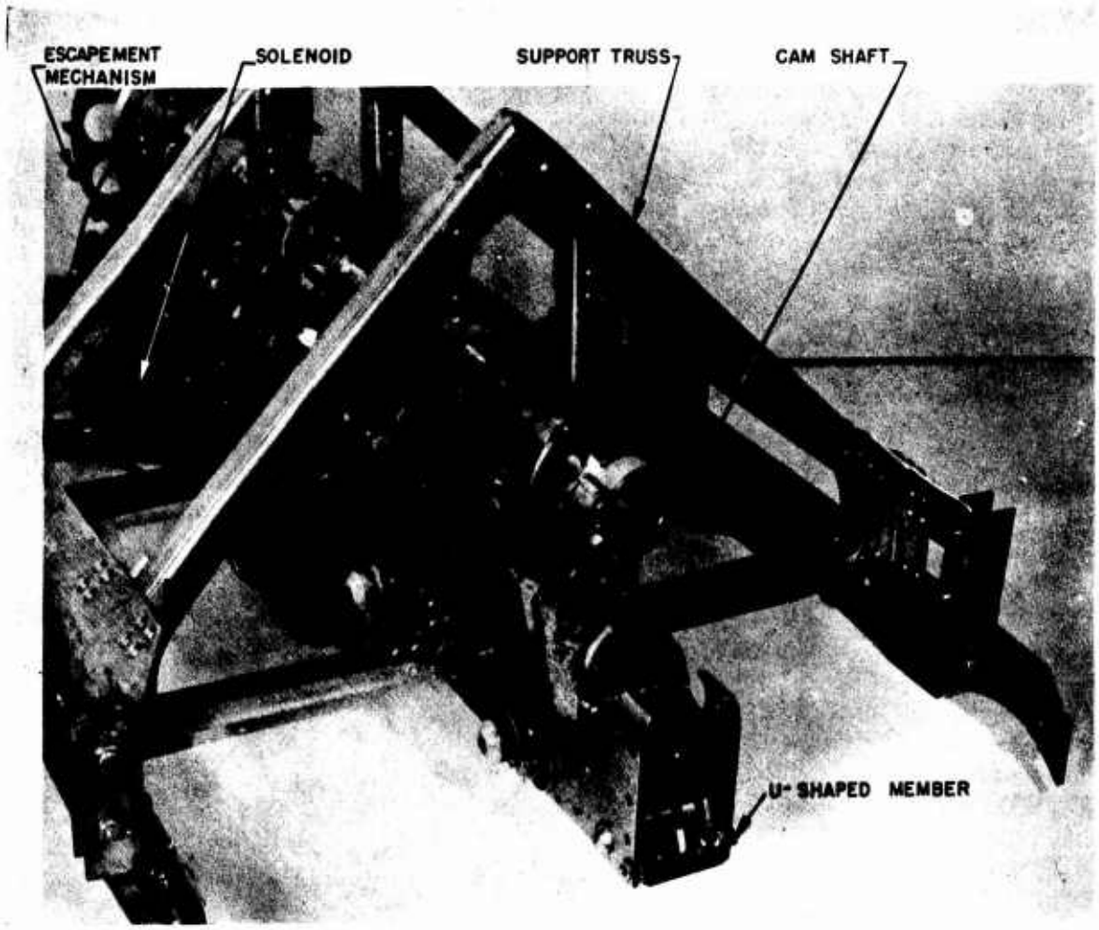

FIGURE 26. Upper section of bomb rack.

in turn is actuated by the solenoid. Electric impulses from an external interval-timing circuit (the Navy K-2 intervalometer powered by the ship's battery) operate the solenoid and thus determine the pattern of the barrage.

Manual control of bomb releases is also available. A lever installed in the front of the ship can be used to trip the escapement mechanism by way of an interconnecting cable.

10.23.3 Arming Mechanism

Arming is initiated in some of the fast-sinking depth charges by removing a small plug soldered into the fuze in the nose of the projectile. A plug-removing wrench is attached to each of these plugs when the projectile is mounted in the bomb rack (see Figure 25). A cable connects the arm of each wrench to a cam-actuated lever. The associated cams and cam shaft are controlled by the escapement mechanism (see Figure 26). Timing is so adjusted that just prior to the release of a particular projectile the arm of the appropriate wrench is jerked upwards. This action tears out the soldered plug.

Some of the fast-sinking depth charges require the removal of an arming wire to effect arming. This is readily accomplished by connecting the loop in the arming wire to the arming cable.

Depth-Charge Intervalometer

The depth-charge intervalometer is an electronically operated timing mechanism for surface craft use in releasing depth charges and firing depth-charge projectors. It may also be used to actuate the discharge of signals for manually operated depth-charge tracks or projectors. The instrument automatically lays a complete depth-charge pattern properly adjusted for the range rate, which is manually inserted in the intervalometer up to the time of firing. The available sizes and types of pattern depend upon the kind and number of tracks and projectors connected to the control circuits. These circuits are governed by a multichannel rotary selector switch which is the essential feature of the intervalometer. The operation of this unit is controlled by the action of a gaseous discharge tube associated with a resistor-capacitor circuit, whose time constant is controlled by the inserted value of range rate. The device was developed by CUDWR-NLL.

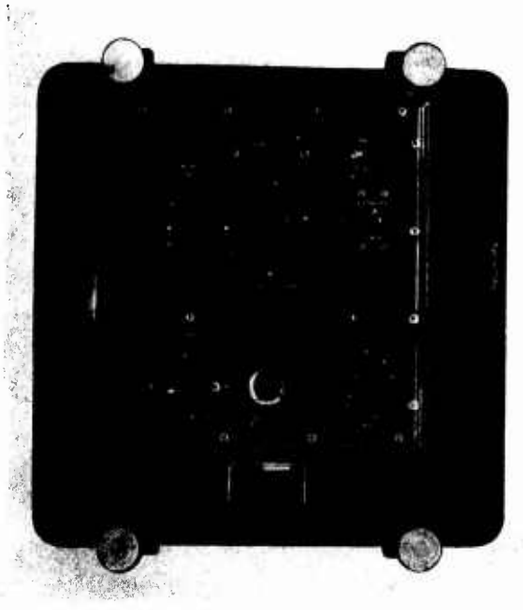

FIGURE 27. Front view of intervalometer.

10.24 INTRODUCTION

The use of closely spaced patterns of fast-sinking depth charges from surface craft imposes demands on the release gear not likely to be fulfilled by manual operation. Automatic release of charges from conventional tracks and projectors improves the shape of the pattern and the probability of success in the attack. As existing interval timers of the aircraft type were not suitable for surface craft use, the electronic timer called the depth-charge intervalometer was developed.

10.25 DEVELOPMENT

The first model was battery-operated and limited to an 18-charge pattern. It was used successfully to demonstrate the accuracy and flexibility of an intervalometer for laying depth-charge patterns. Time of release was determined by a multiple-position rotary switch of the type used in automatic telephone circuits with its stepping magnet actuated by a pair of interlocked relays. The timing pulse to the relays was provided by a variable resistor-capacitor network together with a cold cathode discharge tube.

A second model was constructed to operate on 115 v direct current which eliminated the need for batteries. It provided 31 external firing circuits in a manner similar to the first model.

Since d-c regulation aboard ship is poor and since the trend in new ship construction is toward alternating current, it was decided to design the final model for a-c operation. Furthermore, it was decided to base the timing cycle on range rate instead of ship's speed, so that the projectile discharge rate would be independent of own-ship's motion.

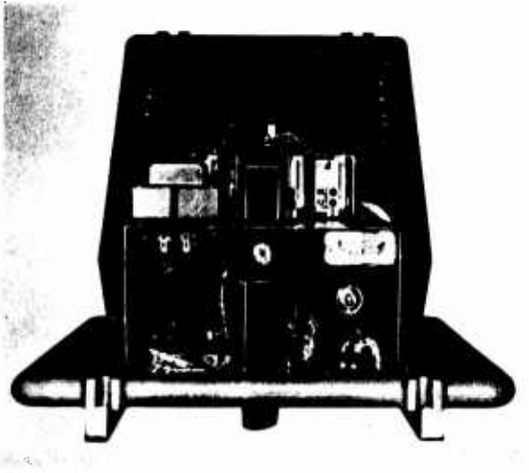

FIGURE 28. Interior view of intervalometer.

10.26 FINAL DESIGN

Views of the final model of the depth-charge intervalometer are shown in Figures 27 and 28. The heart of the unit is the 25-position six-bank rotary selector switch which can be seen in Figure 28. This switch connects the electric firing circuits to the various tracks and projectors at the correct time and in proper sequence. The other elements control the operation of the selector switch and provide certain safety features.

Pushing the firing button causes the contact arms of the selector switch to move at once to the first contact and then advance at regular intervals to subsequent contacts. The time interval between contacts is determined by a resistor-capacitor combination in conjunction with a gaseous discharge tube. The operator selects the combination appropriate to the range rate at the moment so that the resulting spacing with respect to the submarine is 10 yd for side-track launched depth charges and 40 yd for those launched from stern tracks and from projectors.

Other switches are available to enable the operator to select the bank of projectiles to be discharged and the number of charges to be used in a particular barrage.

An electric circuit drawing of the intervalometer and a detailed explanation of its operation may be found in the completion report on the device.[5]

10.27 CONCLUSION

Two units of the depth-charge intervalometer were constructed and delivered to the Bureau of Ordnance. One of these was installed under NDRC supervision aboard the USS *Asheville* for use in sea trials under the direction of ASDevLant.

Hydrostatically Detonated Exploder

The hydrostatically detonated exploder developed by CUDWR-NLL is a device which explodes with hydrostatic pressure at an approximate depth of 4,000 ft about 6½ min after entering the water. It comprises a cylinder loaded with TNT, a hydrostatically armed and fired fuze, a sea-water battery, and a tail. It can be launched from airships, aircraft, surface vessels, or underwater craft.

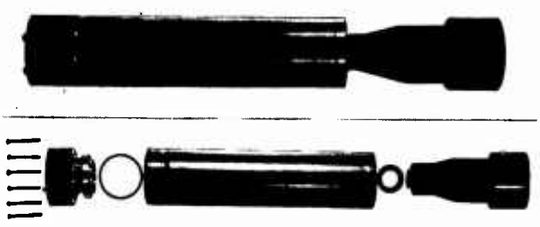

FIGURE 29. Hydrostatically detonated exploder.

10.28 INTRODUCTION

In connection with the experimental investigations of the Woods Hole Oceanographic Institution in long-distance underwater sound transmission, a need arose for devices to generate explosions at depths of several thousand feet beneath the surface of the ocean. The *hydrostatically detonated exploder* [HDE] described below is the first design in a program undertaken to develop a special type of ordnance for such work.

Satisfactory performance was obtained from the first group of 15 HDE test units constructed. Arrangements were then made with a manufacturer for the construction of 110 additional units to be used for further test and experimental work by the Bureau of Ships and the Bureau of Ordnance. Future plans for the laboratory program call for development of a multiple-unit type of exploder with controllable time intervals between successive explosions.

10.29 DESCRIPTION OF DESIGN

The present design of the HDE consists of a body, fuze, and tail. These parts are shown in the assembled and exploded views of Figure 29. The fuze is attached to the body of the exploder by engaging six 10/32-in. socket-headed Allen screws. The fact that the fuze is detachable facilitates shipping and permits insertion of the booster at the final point of assembly. The tail section is fastened to the opposite end of the body by a coarse-threaded plug which forms a part of the tail section. The en-

tire unit, when assembled, is 21½ in. long, weighs approximately 12½ lb, and withstands pressures of 3,000 psi without damage.

Body

The body of the exploder is 11½ in. long and filled with 4 lb of TNT. One end, recessed to accommodate the booster end of the fuze, also incorporates a watertight cell between fuze and body. The other end of the body has a threaded hole to accommodate the tail section and to permit loading of the body with molten explosive.

Tail Assembly

The tail assembly is a split-vein construction with a spoiler ring on its upper end. This assembly is fastened to a hexagon-shaped plug which is threaded into the filler hole of the exploder.

Fuze

The fuze is armed and fired by hydrostatic pressure. Removal of a safety wire permits operation of the arming mechanism when external pressure is applied to a copper bellows. This bellows is attached to a yoke supported by two helical coil springs. The springs are brought under compression as the bellows is elongated by increasing pressures. Compression of the two springs and elongation of the bellows require approximately 1,000 psi to permit sufficient motion of the combination to release the safety shutter. This shutter contains the detonating cap, electric closing contact, and locking detent for the armed position. The travel of the shutter is approximately ½ in. When locked in the armed position, the detonating cap is in line with the detonating train.

The detonating sequence is performed at a pressure of approximately 2,000 psi (±10 per cent). This pressure shears one of the two special alloy diaphragms which are placed over the metering orifices entering the sea-cell cavity. Two diaphragms and two separate metering orifices are used to insure more accurate control of the detonating depth, since any damage to the shearing surface of a metering orifice increases its detonating depth an appreciable amount. (Similar applications of this type of diaphragm and metering orifice can be found in the safety control mechanisms of all commercial gas cylinders and fire extinguishers.)

Battery

The sea water-activated battery is sealed in a pressure-proof chamber. When the exploder has reached sufficient depth, hydrostatic pressure shears the special diaphragms and admits water to the sea-cell cavity. Thus activated, the sea cell fires the electric cap and detonates the main charge of the exploder.

Chapter 11

SEA MARKERS

Mark V Float Light

The Mark V float light for use with the magnetic airborne detector is a cylindrical projectile which may be dropped from a blimp to mark suspected target location. Enclosed in the body, which is 3 in. in diameter and 19 in. long, is a single pyrotechnic column which has a burning time of approximately 15 min. The light has an impact-type firing mechanism and, while burning, floats vertically in the water, tipping as the flare material is consumed, but remaining sufficiently vertical to complete the burning period. It was developed by the Columbia University Division of War Research at New London.

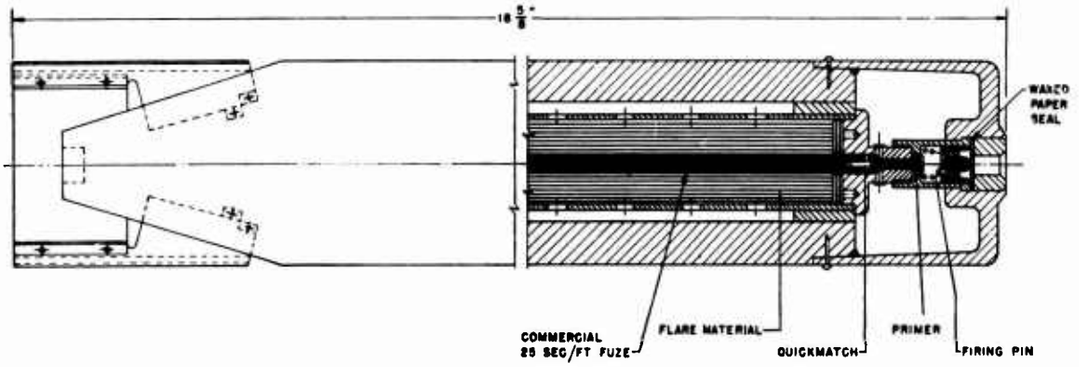

FIGURE 1. Cross section of Mark V float light as finally designed.

11.1 INTRODUCTION

DEVELOPMENT OF the *magnetic airborne detector* [MAD][a] and later the *expendable radio sono buoy* [ERSB][b] created a need by the Navy for two new types of float lights to supplement the Mark IV then in service. One of these was needed for use with MAD for marking the location of a suspected target during brief tactical maneuvers of the searching aircraft. The other, required for ERSB, was for use as a marker during the buoy's operating life of approximately 2 hours.

The Mark IV was being used with MAD at the time but its burning time was not sufficient for a blimp to circle and return to the target area after dropping a flare. However, its performance in other respects, namely launching, flight, ignition, and visibility, were satisfactory. There was no float light available which was considered usable with ERSB.

As a result of these requirements, the Mark V and Mark VI float lights were developed for use with MAD and ERSB respectively. To facilitate presentation of the material in this report each model will be covered separately. This section describes the Mark V light.

11.2 DEVELOPMENT

In developing the first Mark V float lights, the original Mark IV was employed as a basic design. The 3-in. diameter of the Mark IV was retained; however its length was increased from 13 to 19 in. to accommodate additional flare material which it was believed would give the desired 15-min burning time. This also raised the weight from 2 to 4 lb.

The first Mark V lights produced a large percentage of duds due to inconsistent ignition. At the time, it was felt that this was due entirely to faulty ignition mechanism and a method of electric ignition was designed.[1] However, later experiments indicated that poor flight characteristics were the real source of the trouble. The water-impact type of ignition used in the Mark V lights depends entirely upon almost head-on contact between the nose of

[a] Described in Division 6, Volume 5.
[b] Described in Division 6, Volume 14.

the light and the water surface, so that water at high-impact pressure can enter the opening in the nose and drive the ignition piston against the priming cap. As the original Mark V was striking the water at all angles, it was impossible to expect consistent ignition.

After the flight characteristics had been improved by installing a flat nose on the light in place of the original pointed type, more tests were made with the impact-type ignition and satisfactory results were obtained immediately. Accordingly, this type of ignition was incorporated in the final design which is shown in Figure 1.

Tools were then made for die-casting the flat nose, and a production run of Mark V float lights for further testing was supplied by a commercial manufacturer. The lights were tested by several different groups, all of whom arrived at similar findings. Performance efficiency was approximately 85 per cent, average ignition time was 44 sec, average burning time was 12 min, and the flight characteristics were excellent.

It was noticed in these tests that a few of the lights exploded on the surface of the water after they had ignited. This and the fact that they were floating quite low in the water was discussed with the manufacturer, who analyzed the difficulty and furnished the New London Laboratory with another test quantity which had been modified slightly in internal construction, and in which the nose weight had been decreased slightly.

11.3 RESULTS

The lights thus modified were tested immediately with the following results: 100 per cent successful ignition; 95 per cent successful burning; average ignition time, 20 sec; average burning time, 14.7 min; air flight excellent; and floating position satisfactory. These tests were made from a plane traveling 125 mph at altitudes ranging from 250 to 4,000 ft.

Evidence produced by tests, together with demonstrations before interested naval personnel, resulted in Navy acceptance of the Mark V. Acceptance, however, was accompanied with a request that the ignition time be reduced from 20 sec, if possible. It has since been cut to 15 sec.

Mark VI Float Light

The Mark VI float light is an aircraft-launched float light used to mark the position of expendable radio sono buoys. Essentially, it is a group of Mark V float lights mounted in a single, square, oblong unit, pull-match ignited, and arranged to burn consecutively. The Mark VI burns for 40 to 50 min but otherwise has the same burning characteristics as the Mark V. It was developed by the CUDWR at New London.

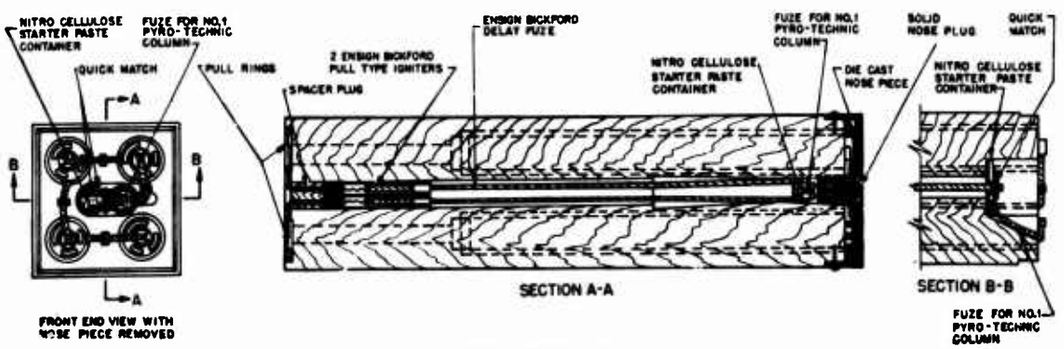

FIGURE 2. Cross section of Mark VI float light as finally designed.

11.4 DEVELOPMENT

Since the Mark V was the only float light in production with acceptable smoke and light properties, it was employed as the basic design unit in producing the Mark VI. In the initial trials, four 15-min candles such as are used in the Mark V were incorporated in both dummy and live wood models which were suitable for launching from an aircraft.

These models, in various body shapes with and without tail assemblies, and several with parachutes, were given extensive static dropping tests from New London Bridge into the Thames River. These tests resulted in the further developments of two

models, one a square, oblong body without a tail assembly, the other a round body with a tail assembly similar to that of the Mark V. Although the latter model had somewhat better flight characteristics, it was decided that the advantage did not justify the more complicated structure.

A subsequent design, supplied by a commercial manufacturer, consisted of a square oblong wood body built up of three thicknesses, with suitable holes for the four candles and a metal nose for the impact ignitors. Tests of these units showed burning periods up to 66 min but indicated that the unit was subject to "crossover" trouble, i.e., the candle which was burning ignited an adjacent one prematurely through the glued joint between the wood sections of the body.

The design was modified to incorporate four wood sections glued together with a candle hole drilled in each. Tests of samples of this design showed that the crossover difficulty had been remedied but that some failures resulted because of inadequate sealing of the nose to the body. Another fault was the failure in transfer of ignition from the starter mixture to the pellet at the top of each candle. These difficulties were remedied in subsequent units.

In all the original Mark VI float lights, impact ignitors were used to fire the fuze to the first candle. The four candles have interconnecting fuzes at the nose end of the body. Upon ignition the internal pressure in the candle chamber expels a perforated metal cap which is held in place by wax at the tail end of the body. The flame of the burning candle melts the wax holding the metal caps of the remaining candles which are burned successively. Tests with the marker thus equipped indicated that under normal floating conditions water was apt to dislodge these caps, enter the chamber, and impair operation of the light. It was found that a piece of adhesive tape somewhat larger than the metal cap and placed over the cap held it in position and prevented access of water to the unburned candles.

Further laboratory tests of the light, thus altered, led to the belief that the Mark VI would give satisfaction under normal conditions of usage.

11.5 PULL-MATCH IGNITION FOR THE MARK VI

However, when quantities of the Mark VI lights began to reach various operating units of the Atlantic Fleet, they were used for various purposes in addition to the one for which they were originally designed, and were launched from many types of air and surface craft. Launching speeds and heights varied widely and, since the light depended for ignition upon hitting the water nose first, a large percentage of them failed to function.

To correct this situation, a pull-match type of ignition[2] was tested and adapted to the Mark VI float light by the New London Laboratory.

Design

In the Mark VI thus converted, two standard Ensign Bickford pull matches are used to ignite the fuze to the first candle as shown in Figure 2. The metal nose cap containing the impact-fired caps is replaced by a blank nose cap which is made watertight with hot pitch and fastened to the body of the light with four small nails. This precludes any possibility of water leaking in at the bottom. A hole is drilled through the full length of the body at the center to accommodate the pull matches and pull wires. Into the top of this hole is fitted a plug having two openings just large enough to allow the pull wires to pass through. Pull rings are fastened to the wires and left in position to be readily available during launching operations. These rings are covered with tape to prevent accidental ignition during handling and shipping. Burning characteristics duplicate those of the Mark VI with impact ignition.

Launching

When launching Mark VI float lights from aircraft, the adhesive tape over the pull rings is removed and the rings are attached to one end of a light static line. The other end of the static line is fastened to some secure point inside the aircraft. The line must be of sufficient length to permit the light to clear the ship before the rings are pulled.

To launch a Mark VI light from surface craft it is necessary only to pull the rings manually and throw the light overside. This method also may be used in aircraft where extreme haste is required.

Conclusion

Pull-match ignition has proven applicable to the Mark VI float light because its operation is not affected by the altitude and speed of aircraft, the position of launching, the stability of air flight, or the angle of entry into the water. The same unit

can be used successfully from surface craft as well as from aircraft.

11.6 MODIFIED MARK VI FLOAT LIGHT

Although the square, pull-match type Mark VI gave acceptable performance, efforts were made later toward design of a float light with a round body, capable of being projected from launching tubes in naval aircraft.[3] Specific requirements also called for longer burning time and less weight. Development consisted largely of modifying the square Mark VI so that it would conform to these requirements.

Although results of first tests were satisfactory so far as launching and initial ignition were concerned, the average burning time was not up to expectations. The flare was so limited in size by having to fit inside a standard launching tube that the intense heat generated by the first and second pyrotechnic columns could not be dissipated readily. This resulted in pre-ignition of the third and fourth columns. All attempts to insulate the columns from each other met with failure. However, the situation was corrected by changing to a starting compound having a higher ignition temperature.

Although indications during development pointed to achievement of the specified requirements, work was not completed by the laboratory because of a decision of the Navy to eliminate launching tubes in naval aircraft, thus removing any need for the modified Mark VI float light.

Pneumatic Projectors

The pneumatic projectors are devices designed to fire float lights from blimps and from airplanes by means of the release of compressed air. Each type of projector consists of a pressure regulating system, a charge valve and chamber, and a firing trigger which releases the air. The projectors may be azimuth-trained about the gun pivot bolt. Both projectors were developed by CUDWR-NLL.

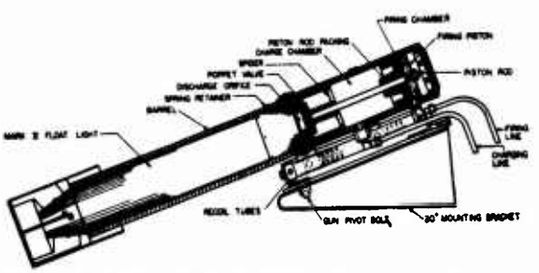

FIGURE 3. Cross section of pneumatic projector for the Mark V float light (for use on blimps).

11.7 INTRODUCTION

During one phase of antisubmarine activity, desire was expressed by the Navy for a means of achieving vertical descent for float lights to mark as nearly as possible the exact point of maximum indication on the *magnetic airborne detector* [MAD]. This end was met with the development of two types of pneumatic launching tubes for use with lighter-than-air craft and heavier-than-air craft respectively. Although launching tubes were finally removed from naval aircraft, they are reported to have given valued assistance in the field prior to their elimination.

Both types developed by the laboratory were capable of ejecting Mark V float lights at relative velocities equal to, and opposite in direction to, the velocity of the launching craft. In this manner reasonably vertical flight was achieved by canceling the forward velocity of the lights relative to the water, thus making possible their initial water contact at the point indicated by the MAD response.

11.8 DEVELOPMENT

In designing pneumatic launching tubes for float lights, the basic problem faced was that of overcoming and canceling out variable projectile velocities ranging as high as 85 mph with blimps and 230 mph with airplanes. Even though fulfilment of these specifications would theoretically make possible a practically vertical drop, other limitations interfere with complete nullification of the velocity and motion of the launching craft. Rolling, pitching, and yawing of the craft caused by wind at the moment of firing affect accuracy of placement to a much greater extent than any of the other limitations. The operator's skill in aiming so as to compensate for the motion of the craft is another variable factor. Similarly, the experience of the MAD operator in anticipating the duration and strength of the signal before firing the projector limits the degree of success in placement.

Launching Devices. The first projector designed for use with the Mark V float light, a spring-oper-

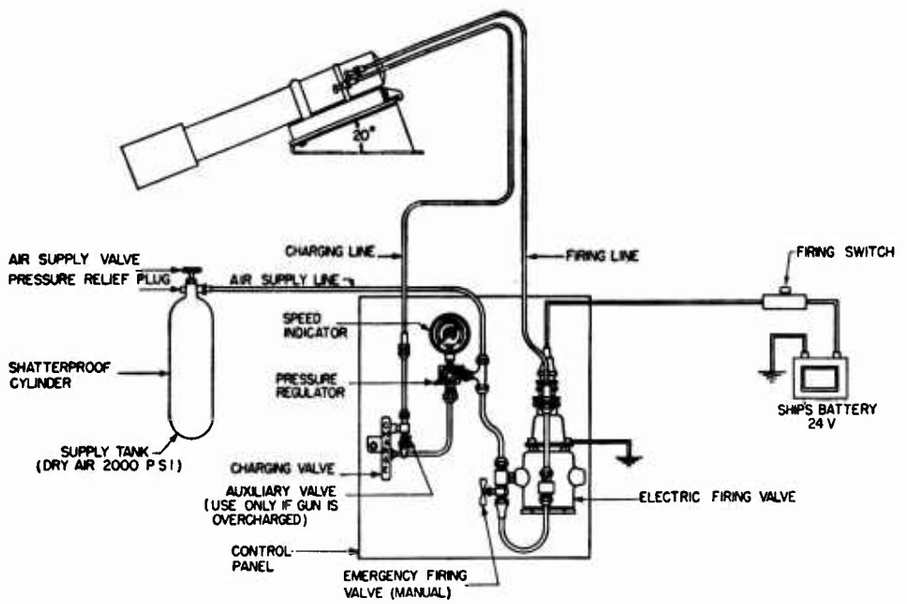

FIGURE 1. Schematic diagram of pneumatic projector assembly for blimps.

ated gun, proved dangerous to handle and too low-powered for speeds above 40 mph. These and other mechanical design problems involved suggested the alternative investigation of a pneumatic-type projector. Carbon dioxide, nitrogen and air, and compressed air were tried as propellants, the latter being found most satisfactory. Initial calibration of the speed indicator was made by firing projectiles from the projector mounted on the ground, with the result that the projectile was affected by air resistance. In actual use the projectile velocity at a given charge-chamber pressure is higher, because not only is there no decrease in projectile velocity due to air resistance, but there is an increase due to the slip stream of the ship. Calibration of the equipment could be corrected, it was believed, under conditions of actual use. To reduce placement errors due to wind effect on the initial stage of flight of a free-falling projectile, provision was made for a 20-degree declination of the gun. Remote firing control was also installed to enable the MAD operator to fire the gun at the exact moment of maximum MAD detection.

Design for Blimps. The final design of the pneumatic flare gun for blimps[4] is shown in cross section in Figure 3. Figure 4 is a schematic diagram of the complete assembly. Rotation of the projector and its mounting plate about the gun pivot bolt provides azimuth training. A spring-loaded ball system holds the float light in position until it is fired. The pressure regulator is adjusted until the speed indicator needle points to the figure equal to the ship's ground speed, thus insuring that the pressure is sufficient to impart to the flare an initial velocity equal to that speed. The charge valve when opened admits air at the proper pressure to the charge chamber. Then, when the firing trigger is depressed, air is admitted into a large-diameter, small-volume firing chamber. The firing chamber actuates a poppet valve in the charging chamber to release the air, which expels the flare. If the air supply tank is filled with dry air at a maximum allowable pressure of 2,000 psi, about 25 projectiles can be discharged at 45 mph.

Design for Airplanes. The design of the pneumatic projector for use by heavier-than-air craft[5] is similar to that of the flare gun for blimps, except that the greater energy called for necessitates an increase in length of barrel, volume of charge chamber, air pressure, and capacity of recoil mechanism. Preliminary experiments were largely concerned with the problem of obtaining a satisfactory air seal between the barrel wall and the float light at the time when the air propulsion charge is released. Several materials were tried for air sealing. The best combination found was a ½-in. thickness of Celotex and a ¼-in. thickness of plywood, placed with the plywood against the nose of the float light, which

faces aft when loaded in the gun. When a solid air seal is used with an impact ignition device, the float light ignites in the usual manner upon impact with the water surface. Another type of air seal, which has a ½-in. diameter hole in the center, is used to cause ignition within the gun barrel. In this case, air upon sudden release from the charge chamber is forced through the hole immediately before the float light is discharged, and operates the ignition device.

In preliminary tests it was found necessary when operating at altitudes of 50 to 75 ft to ignite the float light inside the gun, because these altitudes did not allow time for it to reach a velocity high enough to set off the impact ignition device when it hit the water. Igniting the float light inside the gun possesses the added advantage of eliminating the falling time delay in starting the float light fuze.

The flare gun assembly for airplanes operates in a similar way to the blimp flare gun. When the tank is filled with dry air at a maximum allowable pressure of 1,800 psi, about 38 float lights can be discharged at ground speeds of 150 mph, or 24 at 200 mph.

11.9 PERFORMANCE AND CONCLUSIONS

In the case of the pneumatic projectors developed for discharging Mark V float lights from blimps and airplanes, only approximately satisfactory results have been obtained. Extreme placement accuracy can be obtained principally by a greater degree of control of the overall motion of the ship. An additional degree of accuracy may be achieved by a more accurate calibration of the speed indicator under conditions of actual use and by more experience on the part of personnel in the operation of both the flare gun and the MAD equipment.

Underwater Flares for Antisubmarine Operations

The underwater flares for nighttime antisubmarine operations may be launched from aircraft or surface craft to burn under water for 2½ min, thus silhouetting enemy submarines submerged in shallow water. The flares comprise essentially an ignitor and a flare mixture encased in a water-resistant material. Development work was carried out by CUDWR-NLL, UCDWR, and NDRC at Wesleyan University.

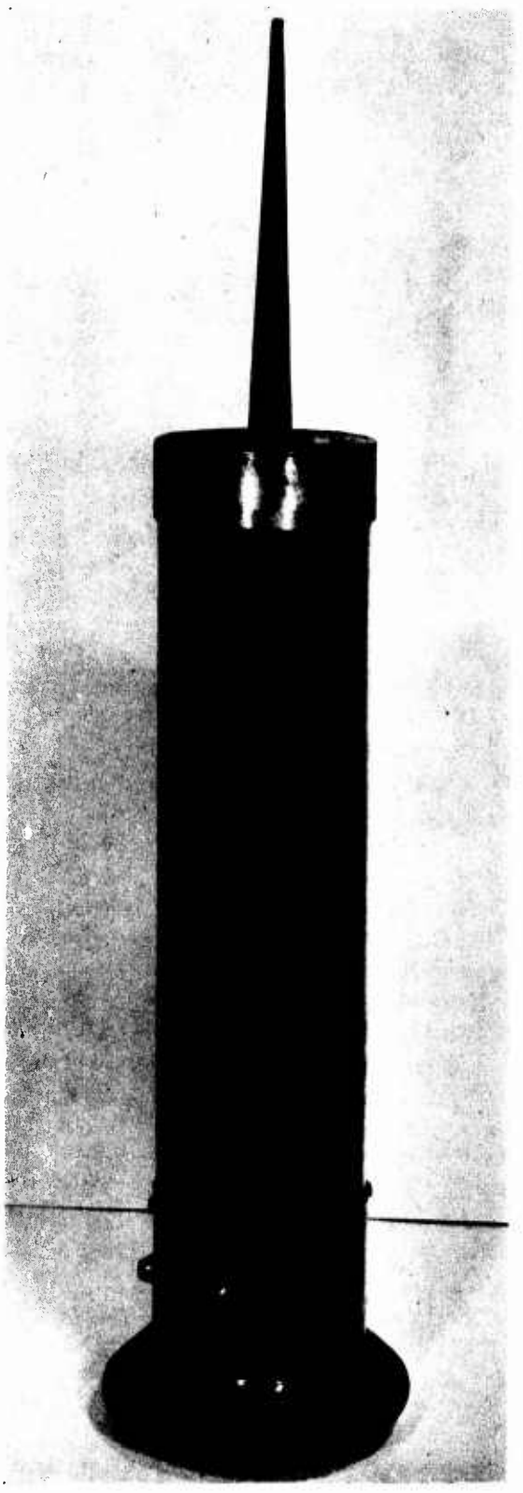

FIGURE 5. Underwater flare.

11.10 INTRODUCTION

During a period when enemy submarines were operating off the Atlantic Coast of the United States, the development of underwater flares was undertaken as an aid to the detection of submarines at night. Thus, in relatively shallow coastal waters, the submarine might be located by its silhouette. Later, when enemy submarines had withdrawn to deep waters where underwater flares would have been useless, the project was discontinued. The work had progressed far enough, however, to indicate that the flare composition developed was satisfactory for the specified application and that the proposed mechanical design was operable. Slight modification in the mechanical design might be found desirable during final testing.

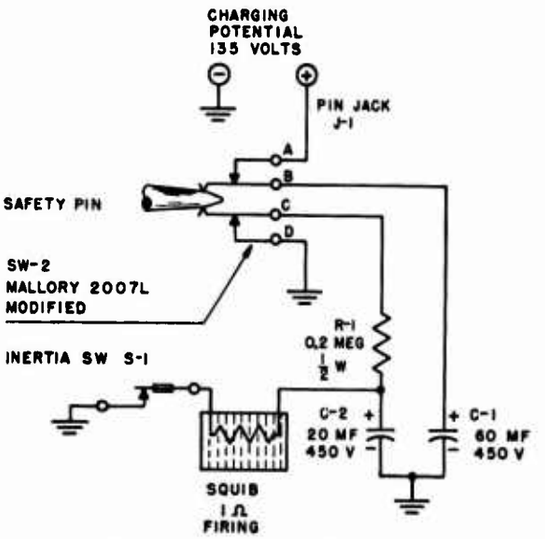

FIGURE 6. Schematic diagram of impact-type capacity ignitor for underwater flare.

11.11 PRELIMINARY INVESTIGATION

COMMERCIAL AND AIRCRAFT PARACHUTE FLARES

In the first experiments, tests were made on small commercial movie flares having a burning time in air of 1 min and on large aircraft parachute flares with a burning time in air of 3 min. Both types burned irregularly under water, with a flickering light. The light intensity and burning time decreased markedly at the lower depths.[6]

B-1 STAR SHELL FLARES

Flares made up by the Bureau of Ordnance with B-1 star shell formula were given preliminary tests. Some were clamped in frames which were supported at predetermined depths by floats, so that the light intensity of the flares could be observed at different depths. A horizontal "flag" simulating a submarine was towed at various depths over the area illuminated by the flares. Its silhouette was visible from immediately above and out to angles of 55 degrees from the vertical and from altitudes varying between 400 and 700 ft. Clearest silhouettes were obtained when the flag was near the surface, but even with the flag at a depth of 60 ft and the flare at 90 ft, the silhouette was visible.[7] However, the fact that half the flares failed to ignite or to burn underwater satisfactorily indicated the need for a better ignition device and an improved flare mixture.

CAPACITY-TYPE IGNITORS

The capacity ignitors with which experiments were performed[8] were of two different types: one which fires upon impact, and the other which fires after a definite time interval following release.

The mechanism of the impact-type capacity ignitor, shown schematically in Figure 6, consists of a main capacitor C-1, a firing capacitor C-2, a resistor R-1, a charging jack J-1, an inertia switch S-1, and a safety jack switch S-2, modified so that the plunger can be completely withdrawn. A 135-v potential is applied to C-1 through J-1 shortly before the flare is dropped. As the flare is released, it pulls the plunger of S-2 and the charging leads by means of its own weight. Switch S-2 then operates to open contacts *A* and *B*, and *C* and *D*, and to close contacts *B* and *C*. This allows C-2 to become charged through *B* and *C* from C-1, R-1 providing a "safe time" of about 2 sec before the potential is built up sufficiently to fire the squib. As the flare hits the water, S-1 operates, and the squib is fired by discharge of the firing capacitor.

Other designs evolved and tested were a lanyard-pulled, multiple-friction ignitor and a time-delay type of capacity ignitor (Figure 7), which was essentially the same as the contact type except that the inertia switch is replaced by a neon lamp serving as a potential relay. In trials of Baldwin B-1 flares with capacity ignitors, only 66 per cent successful ignition was achieved. It was believed that relatively high humidity conditions might have affected the primer elements to such an extent that they would not burn after ignition of the fuze. Tests of Baldwin B-1 flares with lanyard-pull ignitors gave

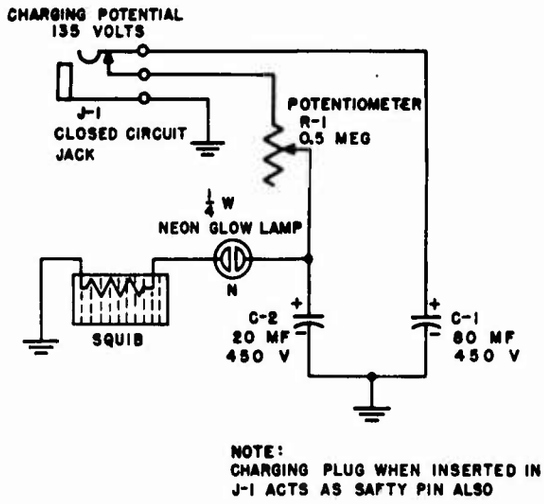

FIGURE 7. Schematic diagram of time-delay type capacity ignitor for underwater flare.

consistently successful ignition, but the flares were all extinguished shortly after they submerged, suggesting some fault in the flare material.

11.12 FLARE DEVELOPMENT AT WESLEYAN UNIVERSITY

FLARE MIXTURES

The Wesleyan group, after testing 93 flare mixtures, developed a combination known as the Wesleyan No. 47 mixture.[9,10] The reliability and relative effectiveness of the B-1 star shell mixture and the Wesleyan mixture were investigated exhaustively. It was found that the B-1 flare must burn at least 15 sec in air before it can be successfully submerged. Otherwise it is extinguished in water. Based on an average of 20 flares the B-1 apparently produced about 65,000 cp when submerged. The Wesleyan No. 47 flare is rated at only 60,000 cp in water, but it can be submerged with little or no likelihood of failure as soon as it is ignited.

Two formulas of the No. 47 mixture are given:

I

Magnesium (200 mesh)	16%
Aluminum (100 mesh or finer; paint flake or scrap)	12%
Barium sulfate (USP "For X-ray diagnosis")	40%
Barium nitrate (CP; ground to 200 mesh; dried at 110 C before use)	31%
Manganese dioxide (native pyrolusite ground to 200 mesh)	1%

II

Magnesium-aluminum alloy (50% each metal; ground to 200 mesh)	27%
Barium sulfate (specifications as above)	40%
Barium nitrate (specifications as above)	32%
Manganese dioxide (specifications as above)	1%

The No. 47 formula has the advantages of safety from accidental ignition, positive ignition by primer, great water resistance, and slow, sure burning when submerged. Although its light output is somewhat lower than that of the B-1 mixture, its efficiency in water is high. It does not seem to deteriorate with age and is not quenched in water when the flare mass is cold (lowest temperature tested —40 C).

A disadvantage of the No. 47 mixture, on the other hand, is its tendency to form a solid ash cake, which interferes with smooth burning in water. This fault may be mitigated to some extent by a suitable type of flare casing. A casing which disintegrates completely as the flare burns offers no protection to the ash cake, which consequently is dissipated as soon as it is formed.

PRIMING COMPOSITIONS

From previous experience with the use of magnesium-sodium nitrate mixtures as flash powders, the Wesleyan group believed that such mixtures, if slowed by a binder, might be effective primers with match ignition. They therefore prepared and tested the following mixture:

Magnesium (200 mesh)	38%
Sodium nitrate (CP 200 mesh *dried*)	57%
Boiled linseed oil	5%

Such a mixture packed to 6,000 psi burns at approximately 0.2 in. per second, and hence if a ¼-in. cake can be used, it will burn well within the set time limit (the flare mass to be ignited 2.7 sec after firing). It was thought advisable to use a first and second fire primer, the first fire mixture to be "spiked" with meal powder to insure match ignition, and the second to produce a hotter fire to ignite the flare cake. The above mixture was therefore used as second fire and was mixed with meal powder to form the first fire, as follows:

Meal powder	25%
Second fire	75%

The Problem of Aging

With the use of heavy paperboard cases and high packing pressures, it was found that the oil-bound flare cakes remain rather soft for a month or two. With fairly porous cases and light packing, hardening is much more rapid. As a result of tests made on samples aged for 1 month, it was concluded that age does not produce any significant change in burning speed or efficiency of the No. 47 composition, and hence fresh flares can be used for test purposes with the expectation of valid results. Mechanical strength varies greatly with age, however, and tactical tests require aged and hardened flare masses.

11.13 PERFORMANCE AND CONCLUSIONS

Sea tests of the underwater flares designed by the New London Laboratory indicated that the mechanical design performed satisfactorily, and that electric ignition of the impact or time-delay type, or lanyard-pulled multiple-friction-match ignition served to ignite the flare. Burning of the B-1 flare mixture used was unsatisfactory, however.

Laboratory and quarry tests conducted by the Wesleyan group indicated that the Wesleyan No. 47 flare mixture, used with the Wesleyan primer cake, burns well under water for the required minimum 2½ min. These materials, however, were never incorporated in a mechanical design for tactical use and tested operationally.

As a recommendation in the event of further work, the Wesleyan group advises the use of a destructible casing to insure steady burning of the flare, e.g., a light canvas casing coated with water- and air-impervious lacquer. For flight stability, uncoated canvas flaps may be allowed to hang from the trailing end of the flare. To give strength to the flare body, a central paperboard tube is also recommended. With the impact type of ignition, the fuze from igniter to primer would follow the channel in this central tube.

Navigational Marker Buoy

The navigational marker buoy [NMB] was an experimental beacon for night operation off enemy shorelines. After being launched from an airplane, the unit was to submerge, descend to the ocean bottom, remain anchored until the predetermined time for action, then rise to the surface and display its signal light to offshore observers. Through proper shielding and automatic orientation, the light was to be concealed from enemy sentinels inshore. The latest version of the NMB had a large, cylindrical main section resembling a standard 300-lb aerial bomb. Attached to the lower end of this main section was a short, heavy, detachable anchor cap. An extensible supporting mast in the main section was designed to erect the beacon light several feet above the surface of the sea during the period of operation. Located within the main section were (1) a pressure-actuated switch, to provide for detachment of the anchor cap upon submergence of the buoy, (2) a clock-operated timing mechanism, to provide for surfacing and illumination at the proper time, and (3) the necessary batteries to provide power for the light and detonating currents for two blasting caps used during anchoring and surfacing operations. Experiments on the NMB were conducted by the Armour Research Foundation.

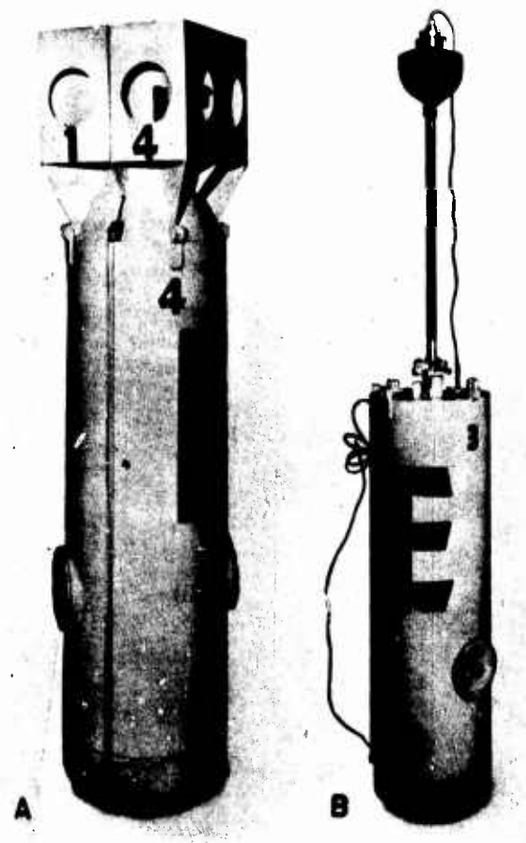

Figure 8. *A*. Completed buoy. *B*. Unit with mast raised.

11.14 INTRODUCTION

In November 1943, it appeared evident that there would be a need for a marker buoy which could be established on an enemy coast line to give a visible, offshore, nighttime signal without disclosing its presence to inshore observers. Since existing equipment could not fill this need, the *navigational marker buoy* [NMB] was designed and several experimental models were constructed.

In its final form, as shown in Figure 8, the NMB was a bomb-shaped, airplane-launched buoy, designed to emit a unidirectional light beam with any desired orientation over a predetermined time interval. Its major components were a light-orienting unit supported on a collapsible mast, a large, cylindrical, buoyant section containing the timing mechanism and batteries, and a small, detachable nose section utilized as an anchor after the buoy's entry into the water.

The intended operating sequence was as follows: the stabilizing fins, which guide the buoy's aerial flight, were discarded as the buoy submerged. Simultaneously, the extending mast raised the light-orienting unit above the main section of the buoy, while the detachable anchor fell away beneath it. After being moored near the ocean bottom until the time selected, the buoyant section rose to the surface and the light beam came into action (see Figure 9). A compass-controlled light shield restricted the beam to the desired direction, regardless of the buoy's orientation.

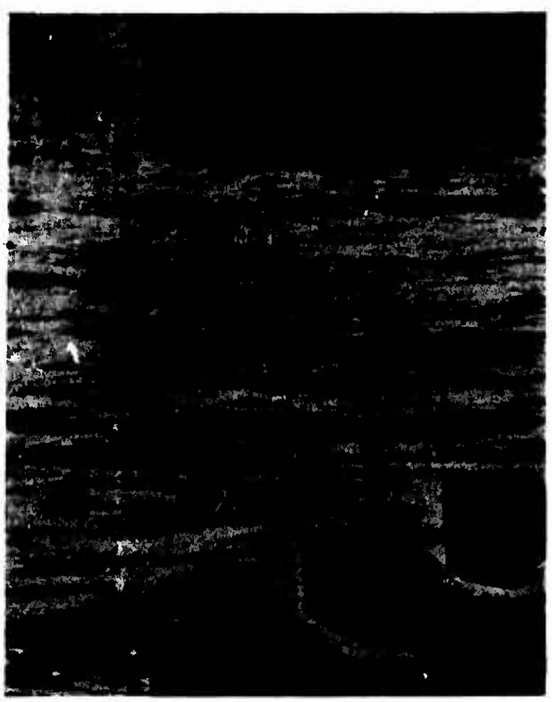

FIGURE 9. Buoy heeling in calm sea, light on.

The very high percentage of failures encountered in performance tests make it evident that further developments are required before the NMB can be of value in tactical operations. The most frequently encountered source of trouble was stoppage of the timer. Increased power for this component and improved protection against corrosive battery fumes would be primary objectives if tactical considerations should demand resumption of development work.

11.15 EARLY DEVELOPMENT

The original design requirements called for an airplane-launched buoy, capable of emitting a unidirectional light beam with good orientation, over a maximum period of 12 hr. Allowance was to be made for a maximum launching altitude of 500 ft and for a maximum water pressure of 150 psi.

The major problems encountered were the incorporation of sufficient shock resistance in the various components and the design of a satisfactory light-orienting device.

A shock-resistance development program was carried out until each component could pass a 1,000 G test. Although a large share of this program was devoted to the timing mechanism, the final result with that unit was still not completely satisfactory.

Early work on the light-orienting device centered around a compass-governed, selector switch controlling a group of lamps spaced around a horizontal circle. Because of operating difficulties and the weight of the batteries needed for relays in this arrangement, it was eventually discarded. In its stead, direct compass control of the light beam from a single bulb was adopted.

To secure orientation, a shielded mirror was so fastened to the compass card as to rotate around a centrally located bulb, suspended from above. In the final model, the mirror was replaced by an enclosing cylinder or light shield containing an aperture for directing the outgoing beam. For the guiding compass, a type utilizing a jewel-bearing sup-

port was chosen. A float type was also considered but the danger of short circuits arising from spilled liquid caused its rejection.

11.16 FINAL MODEL

The external appearance of the NMB is shown in Figure 8. It resembled in general configuration a standard 300-lb bomb, with a flat, blunt nose instead of the usual type.

The main section, 56 in. long and 15 in. in diameter, was a steel cylinder, tightly sealed at both ends. In addition to providing buoyancy, it served as a housing for the batteries and the timing mechanism. Down its center ran a steel tubing or well which contained the collapsible mast before erection occurred. To the lower end of the main section was fastened a detachable anchor section. This had the form of a short, heavy, cylindrical cap and it enclosed the mooring cable and the anchor chain (see Figure 10). It was clamped in place initially by an extension on the "mast bolt," a special bolt which locked both mast and anchor in position. This bolt contained a blasting cap which exploded on submergence of the buoy, thereby permitting detachment of the anchor section and erection of the mast.

FIGURE 10. Partial assembly of lower end of buoy.

The collapsible mast is shown in Figure 11. It was a stainless steel tube with the light-support casting fastened on its upper end. From a terminal block on its lower portion, a bronze lift cable ran up the center well and down the outside of the buoy to the anchor section. When the anchor left the main section, this cable pulled the mast erect and then disengaged as a mast lock clamped into place.

While mast erection proceeded, the stabilizing fins, which are visible in Figure 8A, were being discarded. Initially they were clamped in place by projections on the light-support casting. The upward motion of the mast released them and a spring threw them clear of the buoy.

Mounted on gimbal rings within the light-support casting, was the light-orienter unit. In this device, a magnetic compass, utilizing two Alnico magnets and mounted upon a "V" jewel bearing, was used. It oriented a phosphor bronze, cylindrical light shield which had an aperture for the emerging beam (Figure 12). The light source was a special 12-v, 2-amp bulb suspended in the center of the light shield. A Lucite cylinder served as a transparent and watertight housing for this assembly and carried external, vertical louvers to reduce stray light (see Figure 13).

11.16.1 Timing Circuits

There were three electric circuits controlling the automatic operation of the buoy. They are discussed in the order of their operational sequence.

The pressure-switch circuit shown in Figure 14 was arranged to detonate the mast-bolt blasting cap when the buoy submerged. As a special safety measure it contained an arming switch. This switch was a spring-operated, plunger type (see Figure 10), normally held open by the arming wire. When this wire was withdrawn as the buoy left the plane, the arming switch closed and full control of the circuit was assumed by the pressure-operated switch. The latter was designed for actuation by a metal bellows-driving element which closed the circuit when external water pressure reached 5 psi.

The cable-release circuit is drawn in Figure 15.

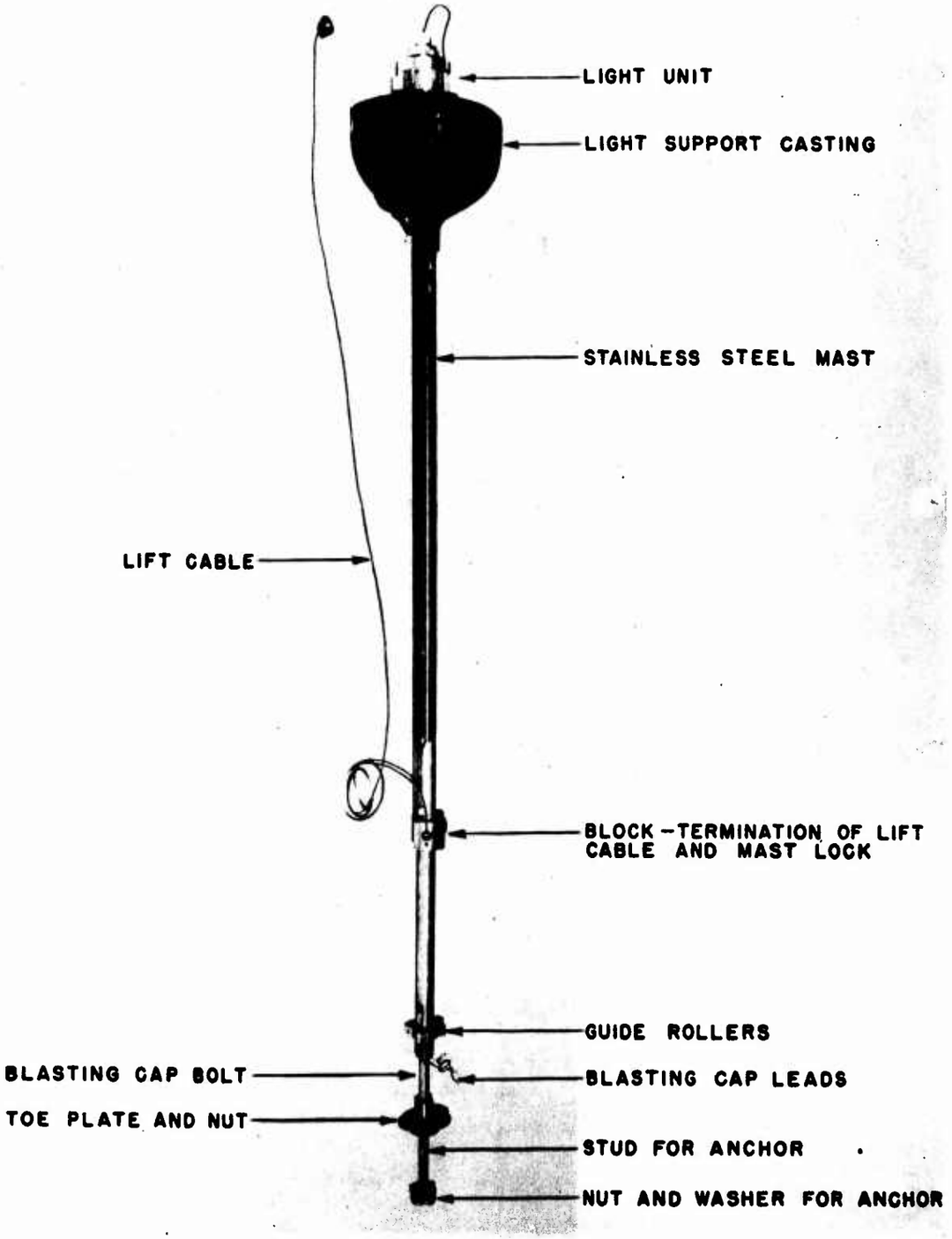

FIGURE 11. Mast assembly.

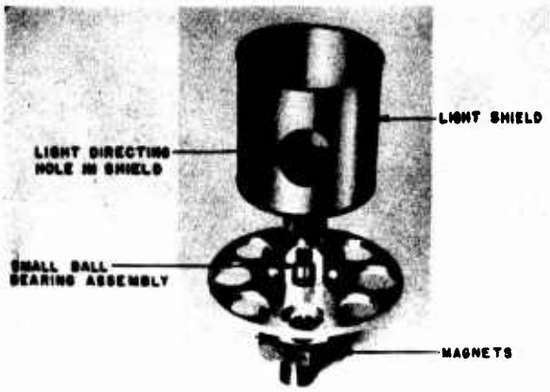

FIGURE 12. Cutaway view of orienting unit.

The blasting cap shown was embedded in a bolt clamping the outer end of the mooring cable near its junction with the anchor chain. While this cable bolt held, the buoyant section could rise above the anchor only to the extent permitted by the 10-ft chain. When the clock-operated switch closed and the bolt was shattered, the mooring cable paid out and the buoy ascended to the surface.

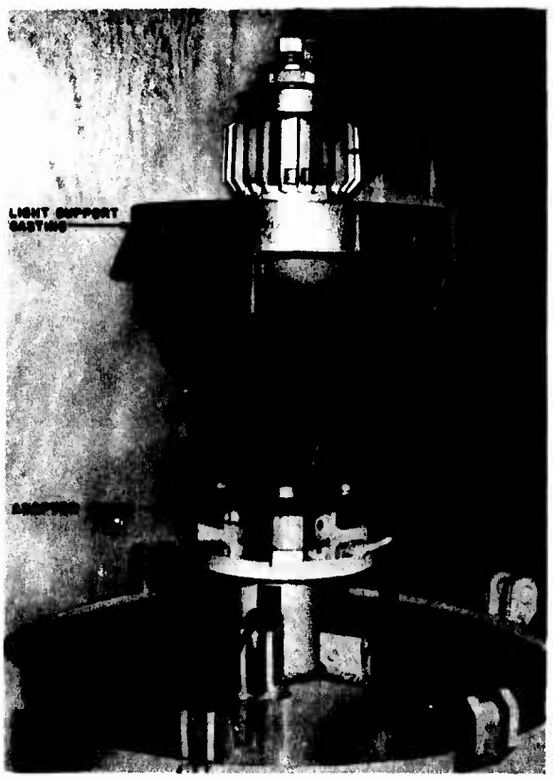

FIGURE 13. Light unit and upper end of buoy.

The light circuit (Figure 16) was also controlled by the timing mechanism. The main switch shown was closed by hand when the buoy was being prepared for use. Shortly after the buoy surfaced, the clock-operated switch closed and turned on the light beam.

The timing mechanism used for controlling these circuits was built with a Seth Thomas, double-spring engine lever clock as a basis. Switch contacts were closed at the desired times by pawls which rode on the surface of a slotted cylindrical cam.

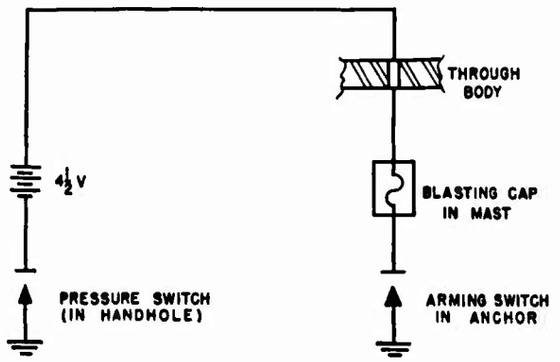

FIGURE 14. Pressure switch circuit.

11.16.2

Operation

The designed sequence of operations follows.

In preparation for launching, the buoy was suspended on the bomb rack of a plane and its arming wire was attached to the appropriate fitting. As launching took place, this wire pulled out of the arming switch and permitted its contacts to close.

When the buoy had submerged to a depth of 10 ft, the pressure-operated switch closed and the mast bolt was shattered. The anchor separated from the buoyant section and dropped to the end of the anchor chain. Simultaneously the mast rose into position under the pull of the lift cable and the detachable fins were discarded. The entire buoy then descended to the bottom where it remained until the time set for surfacing. During the waiting interval, the 10-ft length of the anchor chain permitted the buoyant section to remain clear of entangling obstructions on the ocean floor.

At the appointed time the cable release circuit was closed by its clock-operated switch and, as the cable unreeled, the buoyant section rose to the surface. After a short delay to allow attainment of

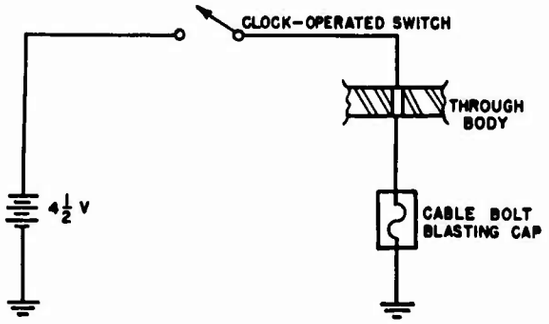

FIGURE 15. Cable release circuit.

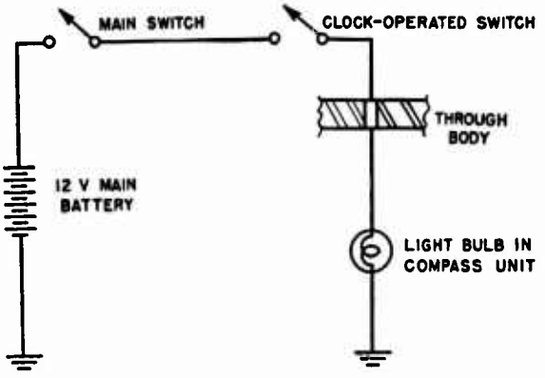

FIGURE 16. Light circuit.

equilibrium, the clock mechanism closed the lamp circuit and turned on the light beam. Proper orientation was effected by the compass-controlled light shield, and continuous operation over a 12-hr period was possible with the size of battery installed.

11.16.3 Performance

Performance tests, including both shipboard and airplane launchings, were carried out on a pilot model and on a group of six additional units. Of the 13 trials attempted, only two shipboard launchings were successful.

Since several buoys were not retrieved, investigation of all failures was not possible. In most of the observed cases, however, stoppage of the clock was the source of the trouble. Leakage, battery fume corrosion, blasting cap failure, and jamming of the detachable fins were other causes of failure.

On the favorable side, orientation and visibility of the light beam were good in cases where the operating sequence was completed. On plane launchings, moreover, good aerial performance indicated that the buoy was properly balanced.

11.17 CONCLUSIONS

The test results indicate that, although the general design was sound in principle, further development would be needed before the buoy could be of service in tactical operations. If conditions should necessitate such development, the timing mechanism should be improved by increasing its power and by protecting it from corrosive battery fumes. Also, increased simplicity and reliability in operation could be achieved by elimination of both the collapsible type of mast and the detachable type of fin.

Submarine Marker Buoy

The submarine marker buoy designed by CUDWR-NLL is an 8-ft long buoy used to mark the position of submerged submarines in training and testing exercises. It is attached to a submarine's conning tower by a cable so that it can be made to float on the water surface just over the stern of the vessel. With a 100-ft cable attached to a USS S48 type submarine traveling at 7 knots, the buoy will remain on the surface with the submarine submerged to 97 ft. To increase the perception distance, a 4-ft steel flagstaff with a large colored pennant was attached to the buoy. Later, the FS smoke agent and the British marine marker were tested; visual ranges up to 4,000 yd were attained in clear weather.

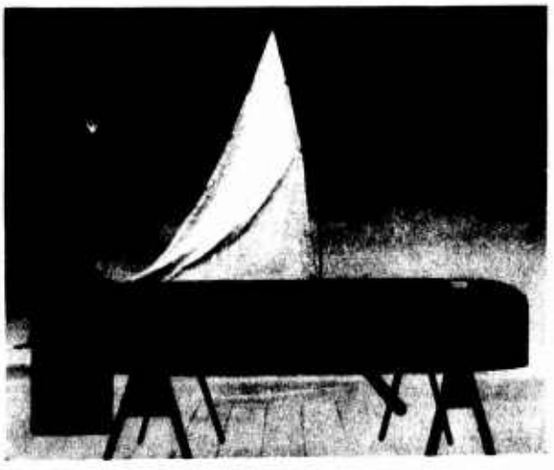

FIGURE 17. Submarine marker buoy.

11.18

INTRODUCTION

Early in 1942, engineers concerned with the testing of antisubmarine attack aids reported the need for a towed marker buoy to mark continuously a submerged submarine's position while under way during training exercises. To satisfy this need, the design of a *submarine marker buoy* [SMB] primarily for use by the laboratory in antisubmarine attack aid tests was undertaken. Upon completion of successful trials of the first models, the Navy became interested in the buoy for use in other submarine exercises as well. Plans were made to construct additional units for transfer to the Navy.

Description of Buoy

A design of the buoy is shown in the photograph of Figure 17. The fins give towing stability and the tow point is located so that the cable pull passes through the approximate center of buoyancy in order that the pull may have a minimum effect on the fore and aft trim. The cable recommended for strength and availability was 1/8-in. tinned aircraft strand (American Steel and Wire Company).

Observations of the submarine marker buoy with its pennant mounted on a 4-ft rod have been made from surface craft at distances up to 4,000 yd on days when good visibility conditions prevailed.

Operation

In order to mark a submarine's position while submerged and underway, the buoy should be fastened to the submarine at the farthest forward point possible so that the trail of the buoy places it over the submarine.

To operate successfully, a submarine marker buoy must have a high ratio of reserve buoyancy to drag, since the lower limit on its trail distance behind the submarine is the point at which the buoy is pulled under the water by the cable. The force diagram for the buoy operating at this limit point of submergence is shown in Figure 18. The tangent of θ at submergence is the drag divided by the difference between maximum displacement and weight.

A desirable characteristic of the buoy is that the drag of the cable be sufficiently low to allow the cable to operate with little curvature so that the trail distance, depth of submergence, and cable length are approximately related by the square law. If the buoy is small the cable may be small, but the

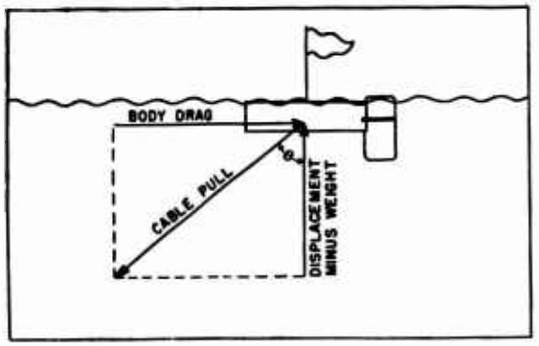

Figure 18. Force diagram.

drag of the cable is a large percentage of the buoy drag for great depths. By increasing the buoy displacement, the diameter of the cable necessary to submerge the buoy without breaking increases only as the square root of the displacement, and hence the ratio of cable drag to buoy drag varies inversely as the square root of the buoy displacement. Therefore, the buoy as designed is large (94 in. long) and the cable is the smallest possible to carry the load.

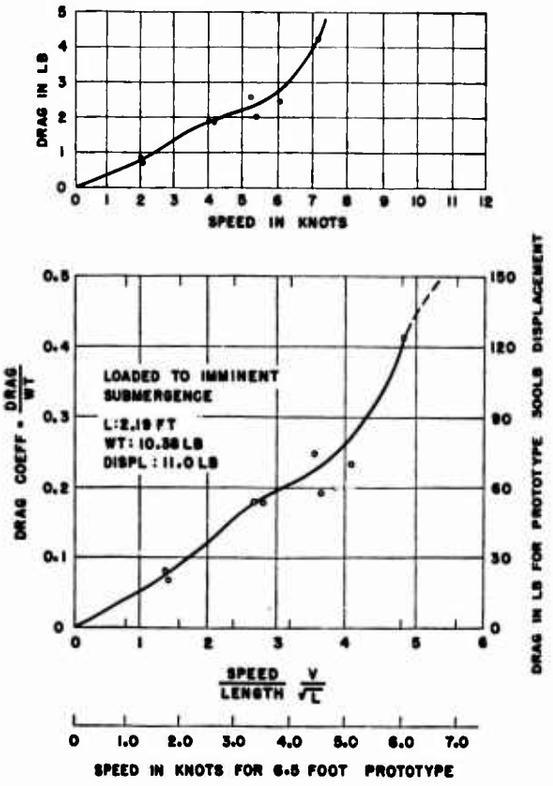

Figure 19. Curves of drag tests on one-third scale model.

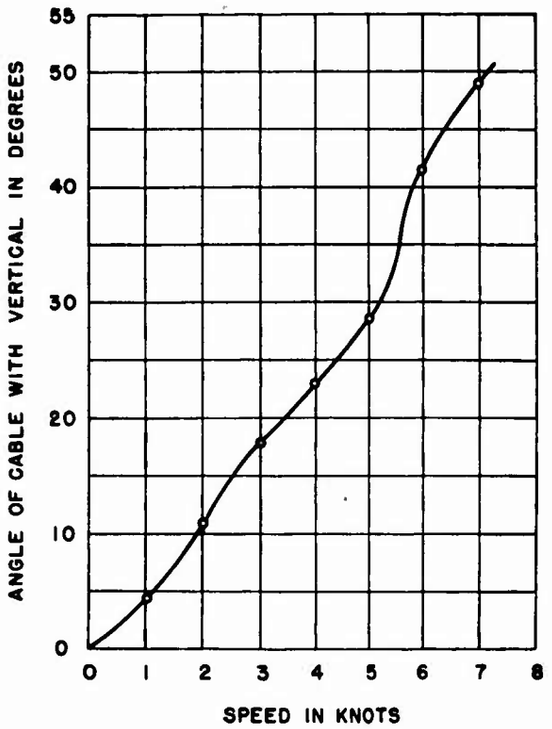

FIGURE 20. Curve showing tow conditions of buoy.

PERFORMANCE TESTS

With reference to the force diagram of Figure 18, the performance of the buoy can be predicted from the drag and buoyancy if the cable drag can be disregarded. Following are test results which indicate that the cable drag is small. The buoy drag was measured by towing a one-third scale model loaded to imminent submergence and stepping up the drag to full size by similarity laws. Data from these tests are plotted in Figure 19 where model test results are shown above and the prototype prediction indicated below.

The prototype buoy was towed from a submarine at given speeds while the submarine slowly submerged. The depth at which the buoy was pulled under was determined from a time record of depth kept by an observer in a surface boat. The two watches were accurately synchronized and calibrated.

At a speed of 6 knots and with a 76-ft cable, the float just pulled under at a submergence of the anchorage point of 52.5 ft. Therefore the angle θ from Figure 18 at which the buoy submerged, assuming no appreciable cable curvature was

$$\cos^{-1} = 52.5/76 = 46.2°.$$

At this speed the drag for each pound of displacement was 0.41 as seen in Figure 19. Since the float had a displacement of 300 lb, the drag was 123 lb. The weight of the float was 157.5 lb; hence the vertical cable component was 300 − 157.5, which equals 142.5 lb. Therefore, the value of θ at the buoy was

$$\tan^{-1} = 123/142.5 = 40.8°.$$

This shows that the actual cable angle departs only about 5 degrees from that formed by a straight line.

From the data obtained, it is evident that the curvature of the cable can be neglected without prohibitive error and that the buoy trails the point of attachment by a distance corresponding to a straight cable even up to 6 knots. Thus the problem of trail distance versus depth for a given cable length can be computed by the solving of a right triangle with two known sides.

From the resistance curve shown in Figure 19, the limiting approach of the buoy to the vertical position above the attachment point can be computed for various speeds with the force diagram method used in the preceding paragraphs. These results are plotted in Figure 20.

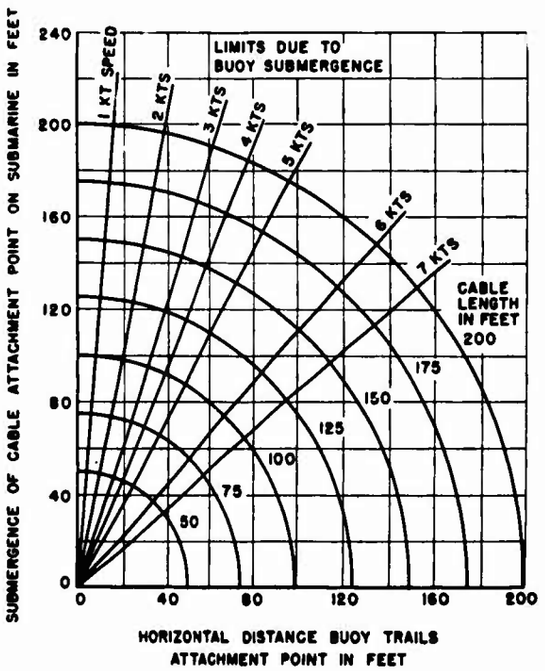

FIGURE 21. Curves showing submarine submergence versus trail distance.

By use of the data in Figure 20 and through consideration of the fact that the cable is practically straight, the performance curves of Figure 21 were prepared. The circle arcs indicate buoy trail distance versus submarine anchor point submergence for a given length of cable. The radial lines are the limits to which the vertical is approached by the cable at the point of buoy submergence. For any particular speed and cable length, the part of the circle arc to the right of the radial line for that speed corresponds to a floating buoy; the part to the left of the line corresponds to a submerged buoy.

For example, if the buoy is used with a submarine of the USS S48 type (approximately 260 ft long), and is towed from a point just aft of the conning tower, the buoy is well ahead of the propellers when a 100-ft cable is used. This length of cable permits operation to a keel depth of 97 ft at a maximum speed of 7 knots. The distance from the keel to the top of the conning tower, where the cable would be attached, is 32.5 ft and this distance is added to the submergence depth of the attachment point to obtain the operating keel depth of Figure 21. At this depth the trail of the buoy behind the attachment point is 76 ft.

Thirteen units of this buoy were built by CUDWR. Four were expended in tests incident to development; seven were transferred to the Navy; and two were retained for laboratory tests involving the use of submarines.

11.19 SMOKE SIGNAL FOR PRACTICE SUBMARINE MARKER BUOY

To increase the distance from which the submarine marker buoy could be seen, steps were taken to replace the pennant with a device for producing a smoke signal. The development of such a device was undertaken at the New London Laboratory in June 1943.

Preliminary tests were made at the laboratory pier using (1) individual candles such as were used in the Mark IV and Mark V float lights, and (2) a container of titanium tetrachloride equipped with a nozzle for spraying. These materials were found unsuitable. Tests on the FS smoke mixture and the British marine marker showed promise and these were more thoroughly investigated.

FIGURE 22. Modified M1A2 cylinder attached to submarine marker buoy.

FS Smoke Agent

The FS smoke agent (described in War Department Technical Manual TM 3-315) is an anhydrous liquid mixture of chlorosulfonic acid and sulfur trioxide. Carbon dioxide was dissolved in the FS mixture which was contained in a standard M1A2 steel cylinder equipped with an atomizing nozzle (see Figure 22). A distinct disadvantage in the use of this mixture is the extreme danger in handling. Under operating conditions, pressure from the dissolved carbon dioxide caused a dense white smoke to spray through the nozzle into the air.

British Marine Marker

The British "Marker, Marine, Aircraft, T2" is shown in Figure 23 attached to a submarine marker buoy. A material very much like calcium carbide and an igniting chemical are stored dry in the lower end of the metal container, the upper end of which serves as a buoyancy tank. To prepare the marker for operation, the nozzle is exposed by removal of a cap and nipple from the top, and a plastic seal at the bottom is broken so that the marker is activated by entrance of water into the container when it is placed

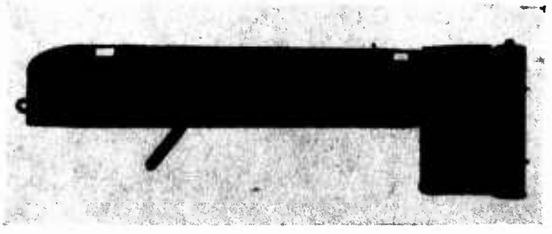

FIGURE 23. Submarine marker buoy with British "Marker, Marine, Aircraft T2" attached.

in operation. The water reacts with the material in the container to produce gas which ignites spontaneously at the nozzle. When floating freely this marker sinks after 1½ to 2 hr, but when attached to a buoy it provides a good signal for over 2½ hr.

Comparative Performance

The FS mixture in a container with a suitably designed nozzle provided a satisfactory signal. Its disadvantages were the possibility of clogging at the pin-size orifice in the nozzle and the extreme danger in handling.

The British marker as designed supplies a satisfactory signal for approximately 2½ hr. It is much more reliable, simpler to use, and much safer to handle than the FS mixture.

The two markers provide signals which are approximately equally visible at ranges greatly in excess of those possible when using an orange-colored pennant with the buoy.

Chapter 12

SEA-WATER BATTERIES

Sea-Water Batteries

The sea-water battery is a primary battery which utilizes magnesium alloy and silver chloride electrodes functioning in a sea-water electrolyte. It is much smaller and lighter than conventional batteries of similar output capacity. Altogether 20 to 25 different types of sea-water batteries have been produced. They range from a small detonator battery weighing 1 oz and delivering 1 w for 1 min to torpedo propulsion batteries weighing 575 lb and delivering approximately 220 kw for 5 min. In addition to the detonator batteries and the torpedo batteries, the types developed include low-power, long-time batteries; AB type high-voltage, low-current, intermediate-time batteries; and the battery designed for the 7–40–M proximity fuze. Development was directed primarily, however, toward the attainment of a suitable unit for torpedo propulsion. Successful construction of such units, and further experimental work on the improved "duplex" type, was carried out by the Bell Telephone Laboratories.

12.1 INTRODUCTION

12.1.1 General Description of Sea-Water Batteries

THE SEA-WATER BATTERIES described in this chapter employ a magnesium alloy as the anode, silver chloride as the cathode, and sea water as the electrolyte. Their chief advantage lies in the fact that they are capable of delivering larger amounts of power per unit weight and per unit volume than any other type of battery. They were developed principally for torpedo propulsion, but many other applications have been found for them in marine signaling devices, detonator actuators, and various underwater ordnance devices. This report describes the research, development, and construction work done on all types of magnesium-silver chloride sea-water batteries developed to date (January 1, 1946).[1]

In sea-water batteries, just as in other primary batteries, materials are consumed in chemical reactions which yield electric energy. In the case of these batteries, magnesium was chosen as the most satisfactory material for the negative electrode, the anode, and silver chloride was chosen as the best material for the positive electrode, the cathode. At the anode, the magnesium goes into solution as magnesium chloride, and at the cathode, the silver chloride is reduced to elementary silver. Hydrogen

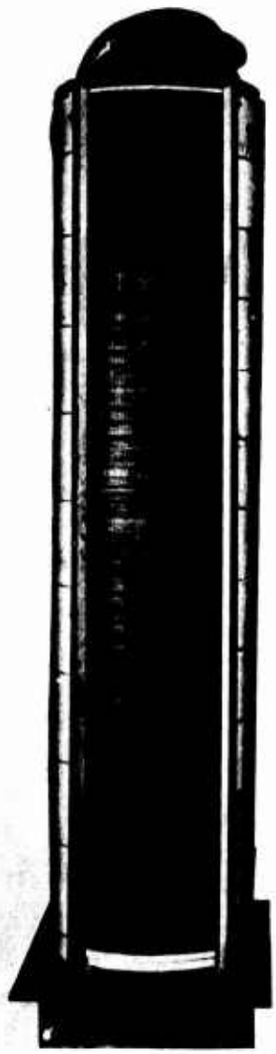

FIGURE 1. Multiplate battery showing complete plate pile-up.

is evolved, which, along with certain insoluble corrosion products, must be removed in order to keep the battery from poisoning itself.

On open circuit the voltage of a single cell is about 1.55 v. Batteries of this type are capable of delivering current at rates as high as 7.5 amp per square inch of plate surface without becoming passive. Satisfactory efficiencies can be developed at any current density up to the maximum. However, for most applications where considerable amounts of power are required for periods of several minutes, current densities of from 1 to 2.5 amp per square inch are in the range of maximum efficiency. The optimum rates for batteries with long periods of discharge are much lower.

Since the magnesium anode of these batteries reacts with the moisture of the atmosphere, it was found desirable to seal the batteries as soon as they were assembled. When the battery is put into use, the seal is broken, sea water is admitted to the plates and continuously flushes them as long as the battery is in operation. This irrigating action not only furnishes the electrolyte, but also removes the corrosion products and dissipates the heat generated by the chemical reaction.

12.1.2 Advantages of Sea-Water Batteries

One of the chief advantages of sea-water batteries over the conventional battery is that they are much lighter in weight and much more compact per unit of power delivered. For example, one of the torpedo batteries developed has a volume advantage of 4 to 1, and a weight advantage of 5 to 1, over the best types of primary or secondary batteries previously used. Other sea-water battery advantages which might be mentioned are as follows: (1) they require no maintenance, (2) they do not deteriorate during storage provided they are kept in a completely dry atmosphere, (3) the sea-water electrolyte is drawn from their operating environment and hence need not be separately stored or transported, (4) the discharge curve is very flat throughout the useful range of the battery, and (5) in most applications it is possible to simplify the design of the batteries because all the cells can be operated in a common electrolyte chamber without excessive internal electrical leakage. The reason for this is that the conductivity of sea water is less than that of other commonly used electrolytes.

12.1.3 Research and Development

After sea water was decided upon as the electrolyte to be used with these batteries, a program of research work was started to find the most satisfactory materials to be used in the cell elements. Suitable materials were selected for the anodes, cathodes, and separators, some early batteries were constructed, and an investigation was made of the electrochemical and physical principles on which they operated. With a knowledge of these principles, more suitable physical forms and arrangements of the elements were designed, which gave the batteries improved performance. This process continued through many stages of development before satisfactory anodes, cathodes, and separators were produced.

In the case of anodes and cathodes, the development process involved an investigation to find the best chemical and metallurgical forms; the most satisfactory size, shape, and thickness; and the proper surface finish. In the case of the separators it involved an investigation to find materials which had the correct insulating properties, which would permit adequate circulation of the electrolyte, and which could be embedded in the plates or mounted firmly on them.

After satisfactory anodes, cathodes, and separators were developed, considerable work was done on the features of mechanical design. The mechanical design must be such that the battery has (1) low weight and small size per kilowatt delivered, (2) small leakage current losses, (3) proper circulation of the electrolyte, (4) long shelf life, (5) quick come-up to full power, and (6) the proper voltage-current-time characteristics. These requirements demanded an investigation of the principles which control leakage currents, internal resistance, and rates of circulation of the electrolyte. In addition to the development work, an extensive program of electrical, mechanical, and hydraulic testing was carried out in order to evaluate the performance of each type of battery under varying operating conditions.

Before the batteries could be produced on a large scale, it was necessary to develop special tools, machines, and techniques in order to manufacture and assemble the parts. This was especially true of the elementary parts of the batteries since most of the materials had never been produced before in the forms needed and were not available commercially.

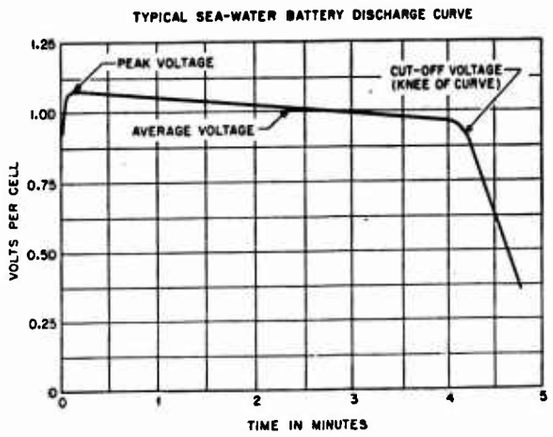

FIGURE 2. Typical sea-water battery discharge curve.

Also, in order to produce specific types of batteries, it was necessary to develop satisfactory production and manufacturing methods. As an aid in this work a small pilot plant was established which not only assured an adequate supply of sea-water batteries for test purposes but also allowed changes to be made in the manufacturing methods before the final production procedure was adopted.

12.1.4 Specific Types of Batteries

Altogether, between 20 and 25 different designs of sea-water batteries have been produced. Principal emphasis was placed on batteries for torpedo propulsion in which large amounts of power are required for short periods of time. However, the types produced have ranged in size from a small detonator battery weighing about 1 oz and delivering approximately 1 w for 1 min, to the large torpedo propulsion battery weighing 575 lb and delivering approximately 220 kw for about 5 min. In addition to the detonator battery and the torpedo propulsion battery, sea-water batteries have been made to operate various marine signaling devices and to actuate an underwater proximity fuze.

Sea-water batteries can be designed to furnish large currents for short periods of time, as in the 139-6-0 battery which furnishes 2,000 amp for 5 min in the Mark 26 torpedo, or they can be designed to furnish a steady voltage for long periods of time as in the Pentagon battery (5-3-BP) which supplies the energy to operate the vacuum tubes of a marine signaling device for 60 hr.

12.2 PRINCIPLES OF ELECTROCHEMICAL DESIGN

12.2.1 Electrochemical Reactions

The sea-water batteries which are treated below employ a magnesium alloy (usually ASTM B90-44T alloy AZ61X) as an anode material, silver chloride in one form or another as the cathode material, and sea water as the electrolyte. At the anode, magnesium goes into solution as magnesium chloride, and at the cathode, silver chloride is reduced to elementary silver. The action is not practically reversible, i.e., sea-water batteries cannot be recharged, and the useful action ceases as soon as either the magnesium or the silver chloride is consumed. The chemical reaction involved is

$$Mg + 2AgCl \rightarrow MgCl_2 + 2Ag$$

and the open circuit voltage of each cell at 20 C is 1.55 v. In addition to this primary reaction, a secondary reaction also occurs but does not contribute to the voltage of the cell. The equation is

$$Mg + 2H_2O \rightarrow Mg(OH)_2 + H_2.$$

This reaction occurs at a rate proportional to the primary reaction and results in the formation of insoluble corrosion products which must be removed.

A typical discharge curve of a sea-water battery is given in Figure 2. The peak voltage, the average voltage, and the cutoff voltage at the knee of the curve are all labeled. This battery was discharged at approximately 2 amp per square inch through a fixed resistance so that the current and voltage are directly proportional. The cutoff voltage is set by the particular requirements of the load and need not be at the knee of the curve. However, the active material is not efficiently used with a higher cutoff and little extra capacity can be obtained with a lower one. Discharge curves of other batteries, of different construction and operating under different conditions of load and temperature, differ from this one only in detail.

The fundamentals of sea-water battery design and operation can be understood best by considering a unit cell. A unit cell is defined as a cell formed by 1 sq in. of cathode surface, a corresponding anode area, and the intervening electrolyte. Electrochem-

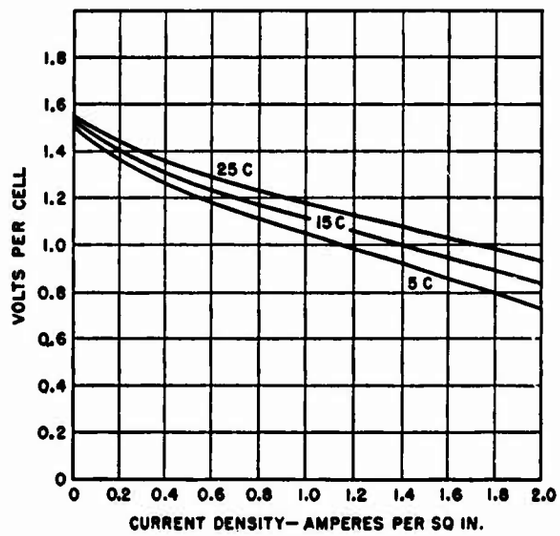

FIGURE 3. Typical voltage-current density curves.

ically the full battery consists merely of a suitable number of unit cells in parallel to give the required current, and a sufficient number in series to provide the required voltage.

The potential available from a unit cell depends chiefly on the following factors, (1) the current density, i.e., the amount of current being drawn per unit area, usually expressed in amperes per square inch, (2) the spacing between the anode and the cathode, and (3) the temperature and the concentration of the electrolyte. Figure 3 shows a typical set of curves for a unit cell showing the relation of cell potential to current density for three different temperatures.

The difference between the open-circuit voltage of a cell and the terminal potential difference when the cell is furnishing a current is due to polarization and to the IR drop in the electrolyte. For a given current, the value of the terminal potential difference depends on the internal resistance; thus anything which affects the internal resistance alters the terminal potential difference.

12.2.2 Factors Affecting Electrochemical Design

Variables beyond control which affect the electrochemical design of sea-water batteries are the salinity and the temperature of the sea water. Controllable variables which affect the electrochemical design are: (1) electrode spacing, (2) circulation of the electrolyte, (3) leakage currents, and (4) electrode thickness. Items (1) and (2) are discussed in the sections immediately following, while item (3) is discussed in Section 12.2.3 and item (4) is covered in Sections 12.3.1 and 12.3.2.

Electrode Spacing

Electrode spacing directly affects the internal resistance of a cell. If the internal resistance of a cell required to furnish large current densities is high, the terminal potential difference drops to a value so low that the cell becomes inefficient as a source of power. In addition, the large amounts of heat generated may cause internal damage. For these reasons, internal resistance must be minimized. Close spacing of the electrodes is the best way to accomplish this.

There is an additional spacing effect which is of importance in high current density cells. During discharge, the effective spacing between electrodes grows because of the dissolving action at the magnesium anode and the reduction of the silver chloride cathode to silver. The effect of the change in the cathode is less than one would expect because the pores of the electrode become filled with a strong NaCl solution which is more conducting than the sea water. However, the magnesium electrode is eaten away to the extent of about 0.001 in. for every 3 amp-min per square inch. Thus, if the original spacing is 0.015 in., after a discharge of 12 amp-min per square inch the spacing has become 0.019 in. The resultant increase in internal resistance accounts for part of the slope of the voltage-time discharge curve.

The method of obtaining and maintaining the desired spacing between the electrodes is one of the major differences between sea-water batteries and conventional batteries. After very little research it was realized that discontinuous separators are required if appreciable capacity per square inch is to be realized. Standard storage battery separators were found to impose too high an internal resistance and clogged the battery badly with corrosion products. Filter paper can be used for a very short period of time but eventually it also clogs with corrosion products, both solid and gaseous.

The only completely satisfactory separators for sea-water batteries are discontinuous ones such as filaments running parallel to the sea-water flow between the plates, or small pieces of insulation applied to one electrode and spaced closely enough

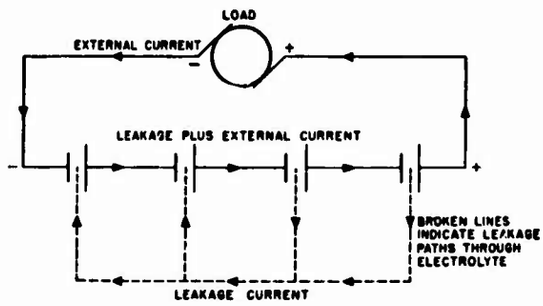

FIGURE 4. Schematic circuit of leakage paths in four-cell battery.

so that the electrodes cannot short-circuit between them. Nylon filament separators and glass bead separators were found to be the two most satisfactory insulators (see Section 12.3.3). With heavy electrodes and wide spacing, insulators can be few and far between, but with thin electrodes and close spacing, the insulators must be close together in order to support the electrodes and to prevent short circuits.

CIRCULATION OF ELECTROLYTE

Even though discontinuous separators are employed, it is usually necessary to provide for forced irrigation in order to remove the corrosion products formed and the heat generated. In those cases where the current density is low, the pumping action of the hydrogen bubbles causes sufficient circulation of the electrolyte to carry away the major part of the precipitates. This self-circulation requires a larger spacing between the electrodes than when forced circulation is used, since it is not so efficient and does not remove all the corrosion products. Self-circulating batteries normally use spacing of from 0.020 to 0.064 in., depending on the ampere-hour capacity per square inch. The greater the capacity per square inch, the greater the amount of corrosion products formed and the more space required between plates to prevent the battery from clogging.

In high current density batteries where the electrode spacing is necessarily close, forced circulation of the electrolyte is imperative to secure satisfactory battery performance. Not less than 20 changes of electrolyte per minute are usually required but renewal rates as high as 100 per minute are found to have no adverse effects on battery performance. The forced circulation battery has a good linear power-time curve which is independent of the rate of circulation, provided it is maintained above 20 changes per minute.

In certain cases also where great steadiness of voltage is required at a comparatively low current drain, such as in some B battery applications, forced circulation is required. It prevents gas accumulation and the resulting variable internal resistance and also prevents nonuniform anode corrosion, both of which cause voltage fluctuations.

12.2.3 Principles for Controlling Leakage Currents

Since a battery must furnish the energy to supply all leakage currents as well as the working current, careful design is essential to produce an efficient battery. Obviously it is desirable to keep leakage currents at a minimum whether the battery is to furnish large or small working currents. Since sea water must be introduced to and circulated through each cell of the battery, there will be a multiplicity of leakage paths from each cell to every other cell through the water channels. These water channels therefore should be so designed as to limit the leakage currents within them as far as consistent with adequate circulation. A theoretical investigation of the factors affecting leakage currents was undertaken. Only a summary of the essential points is included here.

Figure 4 shows a schematic circuit diagram for a four-cell battery. The dotted lines show the possible leakage paths through the electrolyte which is common to all the cells. Figure 5 shows a generalized schematic circuit of a battery composed of two N cells in a common electrolyte. The chief method of controlling the amount of the leakage currents which flow in any particular battery design is to control the two resistances a and b, which are shown in Figure 5. By carefully designing the battery in accordance with the information outlined below, leakage currents can be kept to a minimum.

The results of the investigation may be summarized as follows:

1. In general the maximum leakage current flows through the center cells of a given series assembly of cells in a common electrolyte.

2. The magnitude of the maximum leakage current is given by the following equation:

$$I_{\max} = \frac{E(1 - B^N)^2}{a(1 + B^{2N})},$$

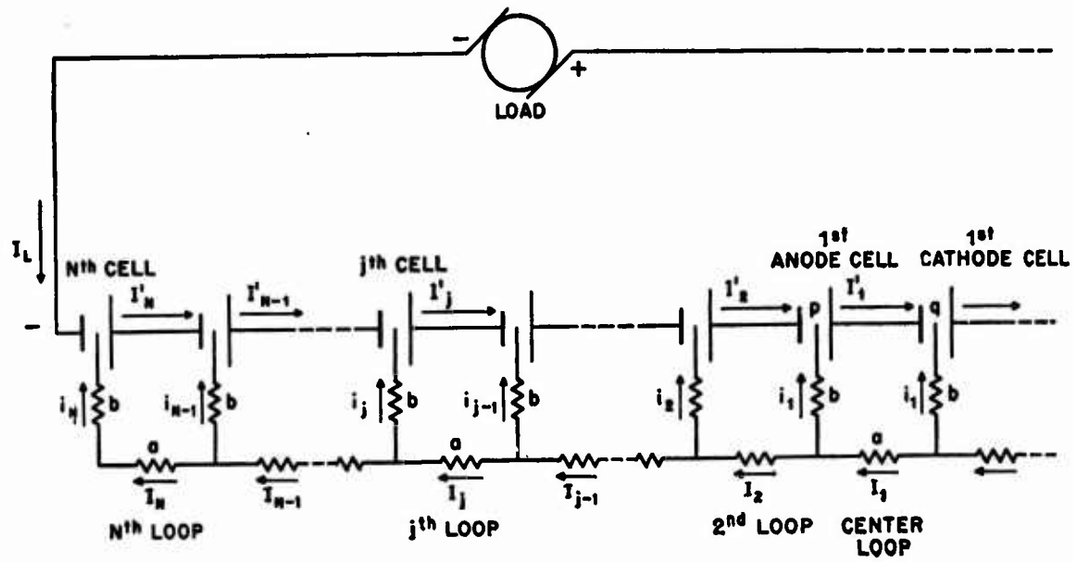

FIGURE 5. Generalized schematic circuit of battery composed of two N cells in common electrolyte.

where E is the operating voltage per cell,

a is the resistance of the path external to the cell between adjacent cell assemblies,

b is the resistance of the electrolyte path from any given cell to the general body of the electrolyte surrounding the series assembly,

$2N$ is the total number of cells connected in series, and

$$B = \frac{a + 2b}{2b} - \sqrt{\frac{(a + 2b)^2}{2b} - 1}.$$

3. For the case where a is very small compared to b, the maximum leakage current is given by the equation

$$I_{max} = \frac{EN^2}{2b}.$$

4. For the case where b is very small compared to a or when N is large, the maximum leakage current is given by the equation

$$I_{max} = \frac{E}{a}.$$

For a small number of cells in series, it is possible to reduce leakage currents by increasing the resistance either of the path leading from a single cell to the common electrolyte or of the portion of the common electrolyte connecting two adjacent cells. For a large number of cells in series, however, in general it is practicable to reduce leakage currents only by increasing the resistance in the portion of the electrolyte external to the individual cells.

12.3 RESEARCH ON THE MATERIALS FOR THE ELEMENTS OF A CELL

12.3.1 Anode Research

The anode material must be able to generate a satisfactory voltage as soon as it is brought into contact with sea water. It must be sufficiently stable, when exposed to the atmosphere, to permit practical handling in battery construction.

Two materials which were seriously considered were zinc and magnesium. Magnesium was selected rather than zinc because of its higher electrode potential and low density. Although various magnesium alloys were tried, the material used in nearly all types of batteries was ASTM Specifications B90-44T, alloy AZ61X. This alloy produces a minimum of corrosion products under conditions of battery operation, but it presented some production problems which had to be overcome before it could be manufactured in a usable form.

The procurement of alloy AZ61X in sheet form of the necessary thinness, flatness, and surface cleanliness posed a problem of considerable proportions. Several battery designs required that the anode

sheets be between 0.010 and 0.014 in. in thickness, with very close limits on specific thicknesses within this range. The alloy was difficult to roll to this thinness, and the magnesium industry did not have the facilities for supplying it in the form needed. Production was undertaken by a steel company which had potentially usable rolling equipment but no experience with magnesium. Months of cooperative work with the steel company were required to work out a satisfactory method of rolling these plates to the desired thinness. Included in this work was the development of a roller-leveler for flattening the sheets. Later this device also proved effective in rolling and flattening the silver chloride sheets.

Another problem which the use of a magnesium alloy presented was the development of a suitable surface finish. The finish needs to be one which permits the anode to come up to its full voltage quickly on admission of sea water. It must also have the ability to withstand the necessary exposure to the atmosphere during manufacture and assembly without losing this quick come-up property.

Two types of surface finish which gave the magnesium satisfactory properties as an anode material were the chromate finish and the scratch-brush finish.

Chromate Finish

This type of finish was evolved through a series of developments which started with a commercial magnesium sheet having a chromate protective finish applied at the mill. The come-up of an anode with this surface finish was neither fast nor consistent. Removal of the chromate film by dipping the anode in a caustic solution produced a satisfactory reactive surface, but the beneficial effect was lost upon drying. Further work disclosed that the benefits of caustic cleaning could be preserved by acid-etching the freshly cleaned plates and then applying a controlled layer of chromate in an acid-chromate bath. Following early success with this treatment, arrangements were made with the magnesium suppliers to obtain sheets without the mill-applied protective finish, and thus the need for the caustic cleaning was eliminated. Altogether about 72,000 anodes were made with a chromate finish.

Scratch-Brush Finish

In the course of experimental work on the development of a suitable reactive surface, it was found that wet processes in general, such as dipping in solvents or cleaning solutions, had deleterious effects. This led to the investigation of dry processes of surface preparation and it was found that scratch-brushing with clean brushes was very satisfactory.

Experience with the resulting type of finish has shown that it is superior to the chromate finish in its ability to withstand shelf aging in the factory atmosphere without appreciable loss of reactivity. However it has been found that the burnishing brushes must be kept free from oils, greases, waxes, or other materials which would tend to leave a surface film. Any surface film prevents the free wetting of the anode surface by the salt water. For this reason, it has been judged advisable to provide for the final scratch-brushing in the factory just before processing for assembly.

12.3.2 Cathode Research

Many possible cathode materials were investigated. The study included most of the common oxidation-reduction reactions for which half-cell electromotive force values are published. Most of the cathode materials investigated polarized too badly or were not readily applicable for use in a sea-water electrolyte. The most effective type of reaction was that of reduction of a metallic oxide or salt to the metal. From the position of silver in the electromotive force table, silver salts were the best practical choice. Copper salts were also studied but their lower voltage and lesser stability prevented their use in a battery in which maximum power and reproducibility were required.

After careful investigation of the various available silver salts, silver chloride was chosen as the most practical cathode material. Silver salts less soluble than silver chloride, such as the bromide, iodide, and sulfide, give lower voltages per cell. Silver salts more soluble than silver chloride, such as chromate, phosphate, carbonate, and nitrate, give initially higher voltages, but since these salts change to chloride during the time the battery operates, the voltage drops to the chloride value and thus produces an unsatisfactory discharge curve. Also, the more soluble salts are not so readily prepared in suitable form for cathodes.

Three general types of silver chloride cathodes have been developed: the anodized, the rolled, and the cast. By far the largest number of cathodes pro-

duced have been made of the anodized silver screen type.

Type	Number made
Anodized silver screen	65,800
Rolled	8,900
Cast	1,450

Anodized Cathodes

The method first developed, and subsequently most used, for applying silver chloride to silver is an electrochemical one, and the product is known as an anodized cathode. In it the plate to be coated is made to function as an anode in a chloride solution so that the chloride ions which arrive at the surface convert the outer layers to silver chloride. By this method the amount of silver transformed into silver chloride can be controlled by controlling the number of ampere-minutes per unit area.

The cathode base is a woven wire screen made from silver wire 0.012 in. in diameter, woven to a mesh of 40 wires per inch in each direction. This choice was made because thick layers of chloride adhere better to a screen than to a sheet, and because the ratio of exposed surface to total mass of silver is relatively high, thus providing conditions favorable to the anodizing process.

Some early efforts were directed toward using cathodes with a copper screen base, silver plating them, and then anodizing them. Although this seemed to offer potential silver savings, it was abandoned because of its shortcomings in making batteries required to deliver power for more than a very few minutes. Since the silver plating was not uniform, especially at the crossover points, some copper became exposed early in the anodizing process and the discharge of copper into the solution prevented further formation of silver chloride.

Anodized silver-screen cathodes, unless further processed, proved to be undesirably slow in come-up, principally because silver chloride is a poor conductor of electricity and thus acts as an insulating layer over the metallic silver core. This was remedied by research which led to two subsequent treatments referred to as *activation* and *development*.

Activation is an operation in which a little of the silver chloride coating is converted back to metallic silver. The first step is taken by placing the chloride-coated plate in a salt solution and causing it to act as a cathode at a high current density for a short period of time. In this process the cathodic action concentrates at the points where the resistance of the chloride layer is lowest and small snowflake-shaped areas of metallic silver develop on the surface of the plate. Moreover, small filaments of metallic silver are formed leading from the surface areas through the chloride to the underlying silver. If such low-resistance paths are not formed when the cathodes are made, the discharging battery must form them, thereby delaying full power delivery until the conducting paths have been created.

The second step in the process consists of treatment of the activated plates in a solution of photographic developer. Such treatment puts a thin film of porous metallic silver over the entire cathode surface. This film interconnects the entire plate surface with the underlying silver through the filament linkages of the activated areas.

The third and final step in preparing anodized cathodes consisted of compressing them in a hydraulic press with a pressure of about 2 tons per square inch. This reduces the thickness from about 0.038 to 0.022 in. and, in so doing, substantially improves physical properties such as flatness, surface finish, and homogeneity. Figure 6 shows schematically the various steps described above in the preparation of an anodized cathode.

An anodized silver-screen cathode made as described above has a capacity of approximately 7.5 amp-min per square inch on each side. At most rates of discharge, about 85 to 95 per cent of the available chloride is utilized in the useful voltage-current range of operation. For this reason a design figure of 6.4 amp-min per square inch of cathode surface has been selected for general use.

Anodized cathodes are used in multiplate cell construction which employs in the same cell as many anodes in parallel and as many cathodes in parallel as are needed to furnish the required current. Since most applications call for a discharge time of from 3 to 6 min, the available capacity of 6.4 amp-min per square inch causes the usual current density to be in the range of 1.0 to 2.0 amp per square inch. These batteries can be operated at considerably higher current densities, but generally this is not desirable because the voltage output drops appreciably as the current density is increased beyond 2 amp per square inch. The time of operation, which is the time it takes for the silver chloride to become changed to silver, is very nearly inversely proportional to the current density.

ROLLED SILVER CHLORIDE CATHODES

The fact that silver chloride can be rolled to sheet form either from a billet or from the molten state permitted it to be used in the development of a second type of silver chloride cathode. The resultant product has physical properties not usually associated with metallic salts. In appearance the rolled sheet resembles a transparent organic plastic, while its physical behavior is very similar to that of a soft heavy metal, such as lead.

Advantage was taken of the soft metallic properties of the silver chloride to embed in it discrete glass beads which acted as insulating separators. The unit developed for use with this type of cathode

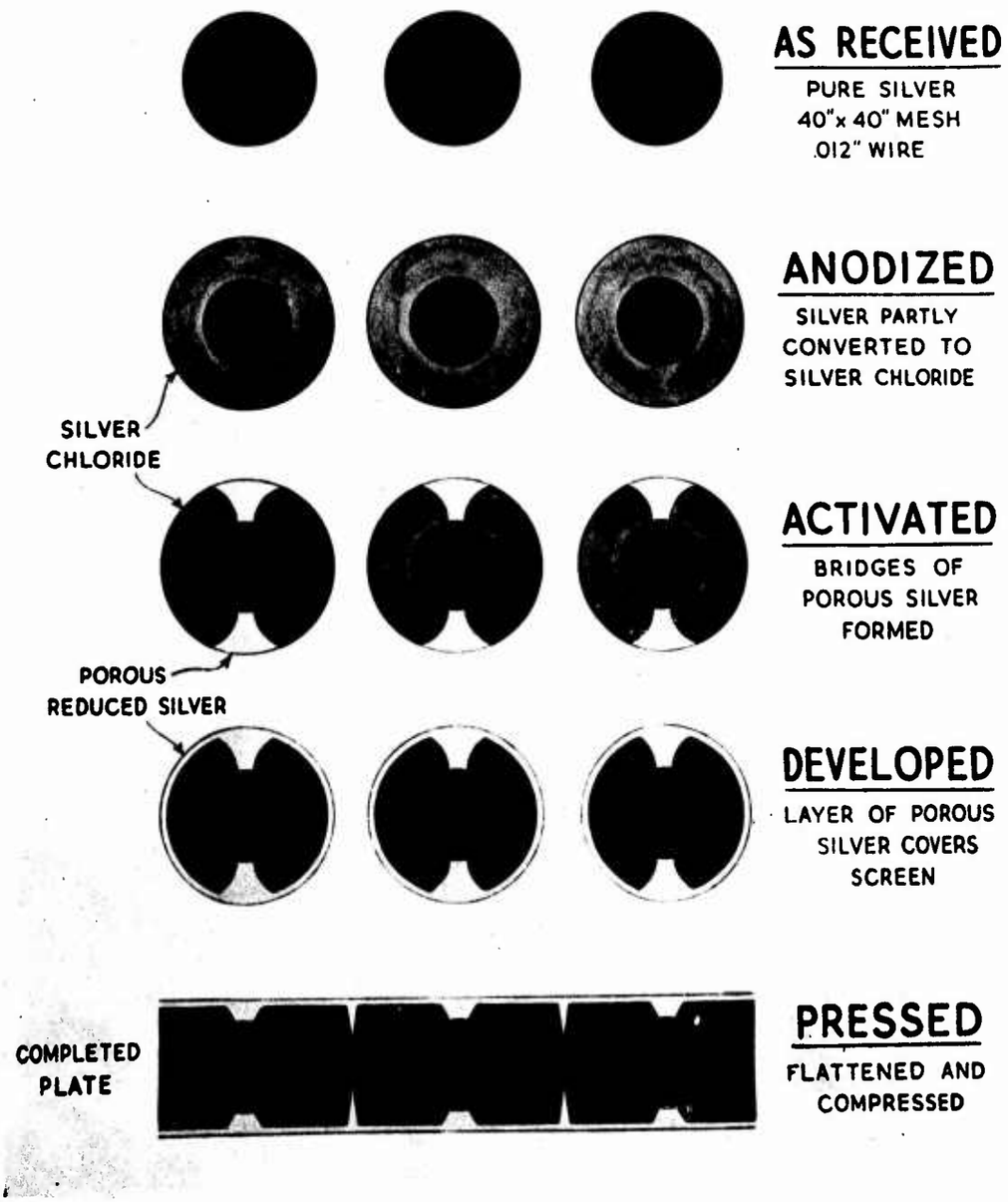

FIGURE 6. Schematic cross-sectional view of three silver wires; successive stages in electrochemical processing of silverware cloth in cathodes.

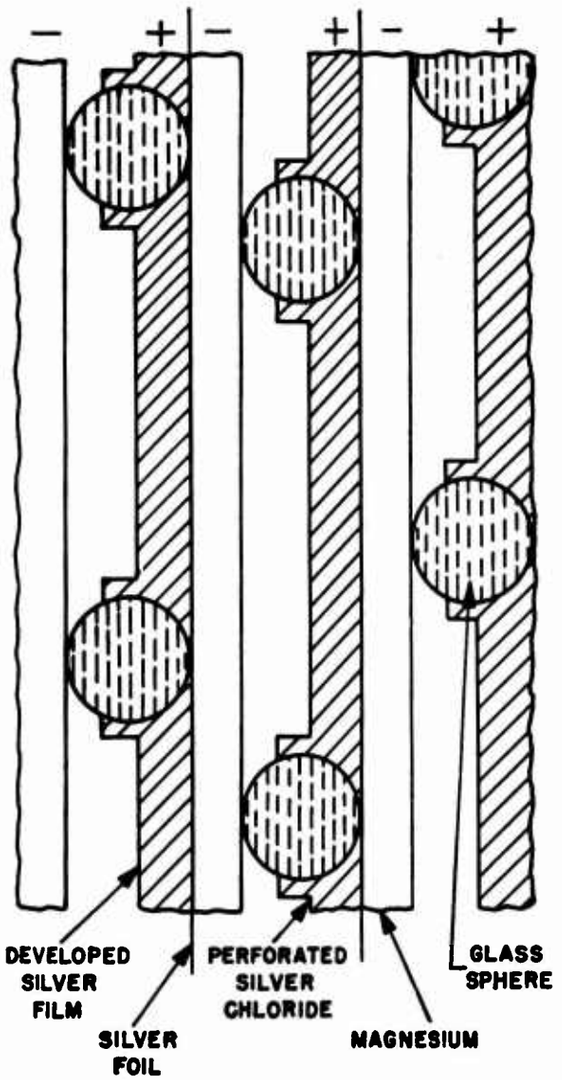

FIGURE 7. Cross section of duplex battery assembly.

consists of a sheet of rolled silver chloride with the embedded glass bead insulators, a thin foil of fine silver, and a magnesium sheet anode. These are assembled in the correct order and held together by cement applied to the edges to form a compound unit referred to as a duplex electrode. The duplex-type battery assembly of Figure 7 shows the glass beads embedded in the soft silver chloride, the position of the silver foil, and the magnesium anode.

Since the glass beads are embedded to full depth in the soft silver chloride, they serve to press the chloride firmly against the silver foil at frequently spaced points and also to hold the silver foil against the magnesium. This provides a low-resistance path from the cathode of a cell to the anode of the adjoining cell, and thus assures good series connection of the cells.

The use of rolled silver chloride as a cathode material also involved the development of a new method to make the cathode respond quickly upon the admission of the sea water to the battery. Low-resistance current paths had to be provided to conduct the current generated on the face of the cathode back through it to the silver foil. This was accomplished by perforating the sheet silver chloride with holes about 0.020 in. in diameter and 0.25 in. apart and then treating the perforated sheet with a photographic developer. This process produced a silver coating on both sides of the sheet and on the walls of the perforations. It performed the same function as the activation and development of the anodized screen described above.

Cast Cathodes

Certain batteries which are required to furnish power for long periods of time (up to 60 hours) need cathodes carrying large amounts of silver chloride. It was found that a heavy layer of this material could be cast on both sides of a special silver insert. This insert, which may be either a screen or a sheet structure, is corrugated so that it comes to the surface on both sides of the cast slab at the crests of the corrugations. The cast slab is given a porous silver surface by treatment in a photographic developer similar to that used with the anodized cathodes and with the rolled silver chloride cathodes.

12.3.3 Separator Research

One feature common to the design of all seawater batteries is that insulating spacers must be provided to separate the electrodes mechanically and electrically and, at the same time, to provide interelectrode channels for the free circulation of sea water. The design of the spacers must be such that the electrode surface exposed to the electrolyte is the maximum compatible with mechanical rigidity. For power types of batteries the separation distance between plates is of the order of 0.015 to 0.020 in.

Considerable exploratory and development work was undertaken to find suitable materials for insulating spacers and methods of applying them. Among early schemes tried and rejected were (1) cementing phenolic strips to anodes, (2) setting polystyrene rivets into cathodes at predetermined points,

and (3) using a sewing machine to apply stitched rows of nylon thread on the cathodes.

The two most successful methods of providing separators consisted of (1) cementing 0.015-in. nylon filaments on the magnesium anode plates, and (2) embedding glass beads in the silver chloride of the cathode plates.

Nylon Filament Separators

Considerable development work was done before a satisfactory method of cementing nylon filaments to the magnesium anode was evolved. The filaments must be positioned precisely on the anodes; otherwise, when alternate cathodes and anodes are pressed together in the assembled battery, the cathodes become corrugated. In order to insure accurate alignment, a special fixture was developed to hold the filaments firmly while they were being cemented to the anode. The filaments are strung in parallel rows on the fixture, dipped in cement, accurately lined up with the magnesium anode plate, and brought in contact with it. Anode and fixture are then passed through an oven where the cement-covered filaments are baked in place.

Glass Bead Separators

Research showed that spherical glass beads, when embedded in the soft silver chloride of the cathode, act as very satisfactory separators. In order to give a spacing of 0.015 in. between electrodes, it is necessary that the beads have a diameter 0.015 in. greater than the cathode thickness. It was found necessary to use nearly spherical beads in order to give uniform spacing of electrodes and to make possible machine methods of beading. It was also found that a pressure of about 25 lb was sufficient to push the beads to the desired depth in the silver chloride sheet without crushing them, and that the beads provided satisfactory insulation when they were spaced about 0.125 in. apart laterally and longitudinally in the cathode.

Special machinery had to be developed to sort and embed the beads. The small glass pellets used were supplied from a material known commercially by the trade name of Ballotini, but they were not uniform in size or spherical in shape. Therefore special apparatus had to be used to select reasonably spherical beads of the proper diameter.

Originally the beads were sorted for size by passing them through a series of grading sieves of the type used in particle separation analysis. Subsequently a machine was developed which consists of a pair of inclined parallel cylindrical rollers, driven at slow speeds in opposite directions. The spacing of the cylinders can be adjusted so that when the beads are fed into the rolls at the upper end, beads of a given size or smaller fall through the slot between the rolls; the larger beads roll down the incline and off at the end of the rolls. By adjustment of the roll spacing, selective sorting can be used to produce any desired size. Figure 8 shows a picture of this machine.

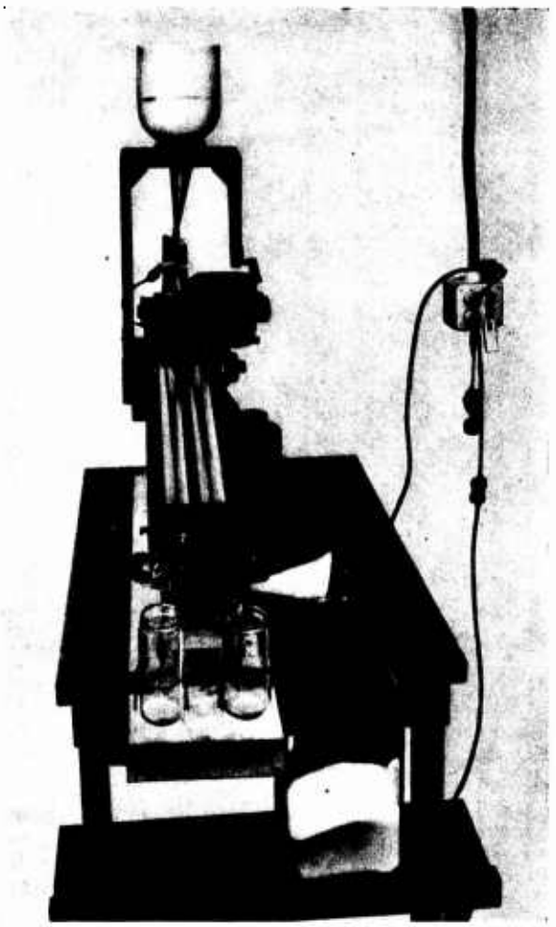

Figure 8. Roller machine, sorting beads for diameter.

Since a large percentage of the glass pellets furnished in commercial Ballotini are not spherical, it was necessary to develop a special vibrating plate machine which sorts beads for sphericity. The beads are fed to one corner of a specially baffled, slightly inclined, vibrating plate. Nonspherical beads follow a course to one side of the plate, and round ones roll off the lower edge. A number of different baffle

FIGURE 9. Vibrating-plate machine, sorting beads for sphericity.

patterns had to be tried before a satisfactory one was found. Figure 9 shows this machine with the baffle plate which proved most effective. An interesting feature of this machine is that the surface of the plate must be treated with graphite and the machine grounded to drain off static electricity generated by the rolling beads. Unless this is done, the static charges cause the beads to be drawn into clusters and effective operation of the device ceases.

Early experimental work showed that it was possible to embed glass beads in the silver chloride sheet by applying a pressure of about 25 lb per head. At first an hydraulic press was used, but the beads were so insecurely fastened that many of them fell out and had to be replaced by hand. Later two machines were developed which formed the silver chloride into a close-fitting collar, or bezel, around each embedded bead just above its equator. The first type (see Figure 10) embedded beads in a continuous strip of silver chloride about 1.25 in. wide. Successful practical service was obtained from this device.

The second type of bead-setting machine is known as the corn planter and is designed to set beads 0.125 in. apart and at 0.125-in. intervals in sheets 12 in. wide and from 2 to 6 ft long. This machine operates by planting row after row with a plunger-like action. It was used for experimental beading only and would require some additional development work to bring it to a state suitable for production use.

OTHER SEPARATORS

For certain designs in which the spacing between electrodes is greater than 0.020 in., separators need not be so closely spaced and materials other than nylon filaments or glass beads have been used. Insulating washers were used with cast cathodes and with certain other designs while phenolic strips cemented to the anodes were utilized in certain "beacon" batteries.

12.4 PRINCIPLES OF MECHANICAL DESIGN

Mechanical design must provide for making plate and cell connections, supporting the battery plates, establishing and maintaining plate separation, encasing the battery in an insulating container, and insuring adequate flow of sea water through the battery. Also the design should be such that (1) weight and size are kept small, (2) leakage currents are held to a minimum, (3) correct valving and irrigation is secured, (4) the battery has a long shelf life

FIGURE 10. Model 1 beadsetting machine.

and quick come-up, and (5) satisfactory voltage-current-time characteristics are secured. These items are discussed, in order, in the following paragraphs.

Design for Low Weight and Reduced Size

The mechanical design of the sea-water battery must be such that its weight and size are a minimum for the required energy output. This is accomplished by employing (1) the minimum feasible plate spacing, (2) the lightest case which will support the battery pile-up, (3) the smallest feasible water passages, and (4) the optimum thickness and weight of battery plates to give the required voltage-current-time characteristics. The final shape should permit efficiency in production and ease of installation.

To show how a typical sea-water battery compares with a conventional battery in weight and size, the 80-kw power supply for a Mark 18 torpedo may be cited. The conventional storage battery unit weighs 272 lb per kilowatt-hour and occupies 8.8 cu ft of space, whereas a sea-water battery unit designed for the same purpose weighs 54 lb per kilowatt-hour and occupies 2.1 cu ft of space. The sea-water battery has a weight advantage of about 5 to 1 and a volume advantage of about 4 to 1.

Design to Minimize Current Leakage Losses

As pointed out above, it is essential that leakage currents be kept at a minimum. Except for a few batteries designed for long-time use, sea-water batteries are operated in a common electrolyte, without any means of intercell separation except that required to prevent simple metallic contact between adjacent cells. This use of a common electrolyte imposes the strict design requirement that water passages be as small as possible so that there may be a minimum of conducting path between water inside the battery and any external conductors. In general, the practice followed in this respect has been to encase the battery plate pile-up in an insulating container, usually made of phenolic material. The joints of this container are made as waterproof as possible, by cementing or by other means, and water entrance and exit holes are kept as small as is compatible with proper irrigation for the battery.

In many battery designs it has been possible to place the entrance and exit holes of the battery at points of equal potential. For instance, in the case of torpedo batteries both holes are at the forward end of the battery. In the design of batteries intended for discharge over long periods of time, the cells are individually housed in insulating containers and the water holes communicating with the common electrolyte are made quite small to give a high-resistance water path between cells. An example of this type of construction is the Pentagon (5-3-BP) battery which is one of the low-power, long-time batteries described in subsequent text.

In addition to the limitation of current losses by means of the methods discussed above, it is the general practice to insulate all metal parts where local current leakage would result in loss of capacity and would corrode terminals, electrode edges, or other important battery elements. This type of protection is sometimes accomplished by painting the surfaces involved with an insulating material.

Design of Valving and Irrigation Instrumentalities

Proper means must be furnished for admitting sea water when it is desired to start operation of the battery. This is ordinarily accomplished by means of a valve or valves in the metal battery housing. The simplest battery design, however, requires only tab-covered holes in the housing. The tabs are removed manually before the unit is put into operation. In such simply designed batteries, pumping action of the evolved hydrogen maintains the irrigation required to remove the products of corrosion.

In the case of torpedo batteries, the design of the valving and irrigating system is considerably more complicated. Sea water must fill the spaces between battery plates within a very short time after firing of the torpedo so that power may be quickly available for propulsion. A uniform and rapid flow must then be maintained to remove the swiftly formed corrosion products and the heat generated in the battery. To obtain such effects, the electrolyte must be forced through the battery by positive means, since the action of evolved hydrogen alone is inadequate. Special scoops have been designed to force water into the battery, and the internal water passages have been proportioned so that the electrolyte may be uniformly distributed. Since small quantities of moisture adversely affect the battery's shelf life, the valves used must be designed so that they remain tight until the battery is put into use. They must be strong enough to withstand the hydrostatic pressures to which they may be exposed, and they must be protected against corrosion.

Design for Long Shelf Life and Quick Come-up

One of the advantages of the sea-water battery is the long shelf life which can be realized if proper precautions are taken in the design, manufacture, and storage of the battery. Battery elements, particularly the magnesium anodes, must be kept free of moisture during the manufacturing process and must be maintained in a dry atmosphere until the instant of use. Moisture corrodes the magnesium surface and thereby increases the come-up time, i.e., the time required to reach substantially 75 per cent of full power. Batteries are usually stored or installed in dry air, dry nitrogen, or a vacuum.

It is also of considerable importance that certain organic contaminants be kept away from the battery plates both in manufacture and in storage. Such materials prevent proper wetting and thus delay the come-up time of the battery. Their presence is avoided by selecting only those insulating materials which have been found free from substances which affect the surface of the magnesium plates. Unplasticized phenolic molding, polystyrene, and nylon have been found satisfactory as insulating materials. The use of sulphur-bearing substances is avoided to prevent tarnishing of the silver film on the cathode surfaces.

Design to Give Satisfactory Voltage-Current-Time Characteristics

The voltage-current-time characteristics of any particular battery are determined by the requirements of the device which the battery is to operate, and, in general, can be met by connecting the proper number of suitable cells in series and parallel. The length of time that the battery is to operate determines the type and thickness of the cathode to be used, and the thickness of the anode must then be compatible with the thickness of the cathode chosen. The thickness of the cathode determines the capacity of the battery in ampere-minutes per square inch. If this capacity is divided by the time of discharge, the operating current density in amperes per square inch is secured. Once the operating current density is known, the operating voltage per cell, for any specified temperature, can be obtained from curves similar to those shown in Figure 3.

These curves show that on open circuit a cell furnishes an electromotive force of approximately 1.55 v, but that this value rapidly decreases as the current density is increased. For example, if it is necessary to maintain a current density of 1.4 amp per square inch at 15 C, the operating voltage of a cell would be 1 v. Once a battery is put into operation and is furnishing a constant current, the voltage-time discharge curve remains fairly flat as shown in Figure 2. The voltage does not begin to drop off until the knee of the curve or the end of the discharge time is reached.

Internal resistance also affects the operating voltage of a cell. Operating voltage is the difference between the cell's electromotive force and the internal resistance multiplied by the current flowing. For cells which must furnish large currents, internal resistance must be reduced to a minimum by making the space between the plates as short as possible. By proper design the desired currents can be secured but certain mechanical features and manufacturing limitations must be provided for at the same time.

The voltage requirements for sea-water batteries vary widely. The small detonator battery requires only 1 v, whereas a big torpedo battery may require as much as 140 v. Any required voltage may be secured by connecting the proper number of cells in series.

The area which the plates of a cell must have is determined by dividing the operating current density into the total current which the battery must furnish. Thus the battery which is used to drive the Mark 26 torpedo requires a current of 2,100 amp. If its operating current density is 1.4 amp per square inch, the area necessary for the plates of this battery is 1,500 sq in. This area can be secured either by connecting a number of cells in parallel or by employing a single set of electrodes with sufficient area.

12.5 DEVELOPMENT, CONSTRUCTION, AND TESTING OF SPECIFIC BATTERIES

12.5.1 Torpedo Batteries

General Survey

The major part of the work on sea-water batteries was concerned with the development of batteries for torpedo propulsion. The original request that the possibility of sea-water propulsion batteries be investigated was a result of the successful performance of the 7-40-M proximity fuze battery. Work on small propulsion units which were developed and bench-tested in the laboratory progressed to

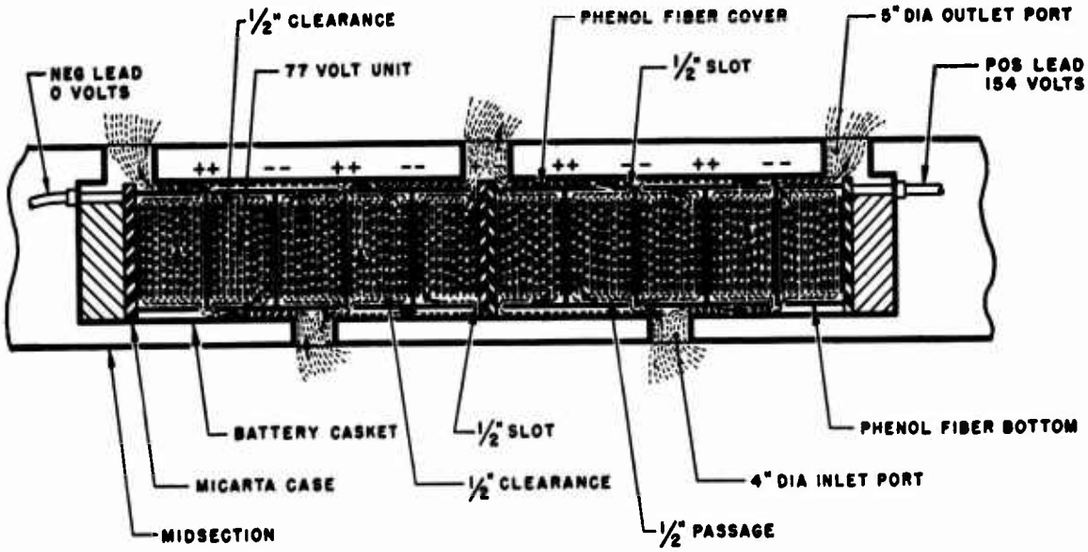

NOTE: CASKET & MIDSECTION SURFACES FINISHED WITH .006 IN. COAT OF BAKED BAKELITE VARNISH

LONGITUDINAL SECTION OF MARK 18 MIDSECTION

FIGURE 11. Sea-water power battery functional schematic.

large units as questions about design, materials, and manufacturing methods were explored and answered. When it was found that satisfactory current densities and ampere-minute capacities could be attained, work was undertaken on a small 8-kw, 50-v, 160-amp, book-type sea-water battery with a 5-min rating. Several models of this battery were bench-tested in the laboratory, and then range-tested in a small torpedo-like device. From these tests information was secured which served to guide the design of models with larger capacity.

The next step was taken when four 120-kw, 150-v, 800-amp batteries were made by suitable series-parallel combinations of component assemblies, each having 75 book-type cells. Two of these batteries were range-tested in a full-size Mark 18 torpedo. The tests yielded the following important information: (1) the batteries showed the expected power-time characteristics, (2) the batteries were able to drive the torpedoes at speeds of 31 and 32 knots, (3) the torpedoes showed no visible wake in spite of the fact that hydrogen evolution is a characteristic of sea-water batteries, (4) the rise to full voltage occurred within a few seconds after firing, and (5) it was found possible to irrigate a large-size battery effectively during the torpedo run, provided proper ports for entry and exit of sea water are included in the design. The battery housing and irrigating system used in these tests is shown schematically in Figure 11.

Successful bench and range tests of the 120-kw book-type battery hastened completion of the more efficient multiplate type of design. Work was begun on batteries with the capacities needed to operate the Mark 20 (175-kw) and the Mark 26 (250-kw) torpedoes. In early models no irrigation problems were considered beyond the use of ample openings in the torpedo shell to allow large amounts of sea water to enter and leave the battery. In later models, forced irrigation was found necessary, quick opening valves were adopted, and the battery was evacuated in order to insure quick filling.

In order to perform bench tests on the various models during their development, the discharge tests were run in torpedo-like housings known as the "iron pony" and the "iron horse." Inlet and outlet ports were provided, instantaneously acting water valves were installed, and salt water was pumped through the assembly to simulate an actual torpedo run. Precise controls were maintained over water salinity, temperature, and circulation rate, and over the resistance load into which the battery discharged

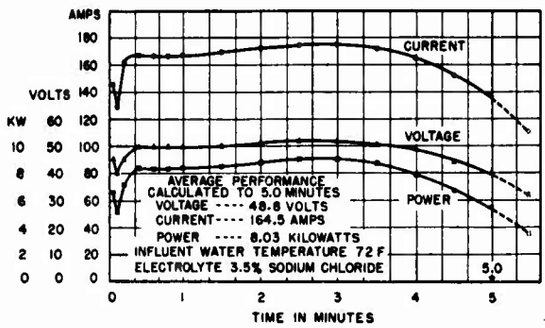

FIGURE 12. Sea-water battery 48-1-P; bench test.

current. Provision was made for obtaining data as follows: (1) a motion-picture photographic record of all panel meter readings was made, (2) a six-element permanent-magnet oscillograph was used to record the voltage of each section of the battery, and (3) precision-type laboratory meters were read at specified intervals.

Bench tests with the iron horse resulted in the perfection of numerous improvements before actual range tests were performed. In this way time and energy were conserved, for it was found that the range method of testing performances during development was very inefficient.

CONSTRUCTION AND TESTS OF BOOK-TYPE BATTERIES

General Description. Preliminary models of torpedo batteries were of the book-type construction. Essentially each "book," which is in the form of the letter Z, contains two magnesium anodes, one anodized silver cathode, and an insulating separator of phenolized nylon. One side of each magnesium anode has cemented to it nylon filaments which act as separators when the books are stacked together to make a battery. The books are stacked together by inserting the silver cathode of one cell between the two magnesium anodes of the next one. The interleaving of the books results in a somewhat loosely packed, accordion-like assembly, in which the spacing between electrodes is variable and, in general, greater than required for efficient performance. After being interleaved, the cell groups are therefore compressed until the overall thickness closely approaches the sum of the thicknesses of the individual books.

The 8-kw Battery. Among the first batteries of this type constructed was the 8-kw unit designed to deliver 160 amp at 50 v for 5 min. It was bench-tested in the laboratory by discharging it in a tank of salt water and making measurements of its various characteristics. Figure 12 shows the results of the tests on one of these batteries. It will be noted how closely the performance followed the desired characteristics. The battery has a quick come-up and tends to maintain a uniform voltage throughout the run. At the end of 5 min, the voltage is still 85 per cent of its nominal value.

Following the bench tests, some 30 range tests were made with 8-kw batteries. In order to compensate for the low salinity experienced at Solomons Island, Maryland, where the range tests were carried on, variations in the number of cells per battery were made. Figure 13 shows a typical discharge curve for one of these range runs. The results of these tests were deemed satisfactory, so that development work on larger capacity batteries for high-speed torpedoes was given added emphasis.

120-kw Battery. The next book-type battery to be tested was the 120-kw model, designed to deliver 760 amp at 154 v, for 5 min. One of these batteries was bench-tested by inserting it in a specially built Mark 18 battery compartment and immersing it in a tank of artificial sea water. No attempt was made to gain forced circulation of the electrolyte, but irrigation was provided by the self-pumping action of the evolved hydrogen. A direct-connected d-c generator working into a resistance load was employed to simulate the normal Mark 18 motor. The results of these bench tests are shown in Figure 14. Two similar batteries were placed in modified Mark 18 torpedoes and range tested at Newport, R. I., in near-freezing water. The results showed (1) that the battery could develop the required power even in cold water, (2) that it could drive the torpedo at a speed of 30 knots or greater over a 5,000 yd range, (3) that it had a sufficiently rapid come-up

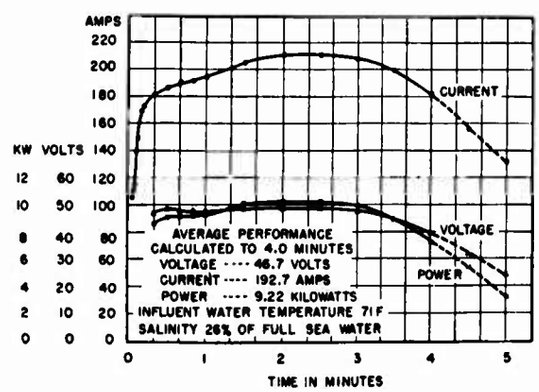

FIGURE 13. Sea-water battery 54-1-P; range test.

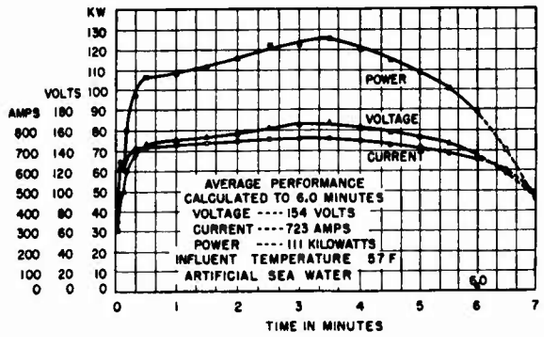

FIGURE 14. Sea-water battery constructed from ten 75-1-P units; bench test.

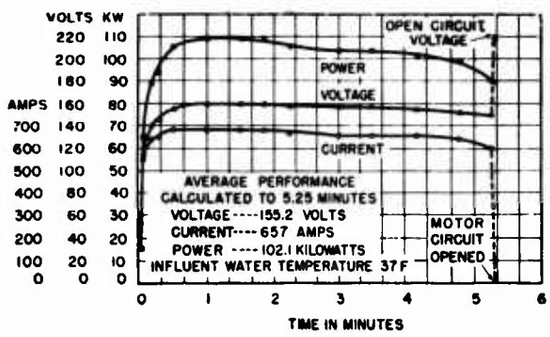

FIGURE 15. Sea-water battery constructed from ten 75-1-P units; range test at Newport, R. I.

to permit good control of the torpedo during the initial stages of the run, and (4) that it left no visible wake. Figure 15 shows the discharge curves for one of these runs.

CONSTRUCTION AND TESTS OF MULTIPLATE-TYPE BATTERIES

General Description. Although the book type of battery construction proved satisfactory, it was not economical of weight and space chiefly because each cell was composed of two anodes and one cathode. The multiplate-type cell is superior to the book type, not only as far as weight and space are concerned, but also in its electrical characteristics. The multiplate-type of construction was employed in all batteries for torpedoes which required large amounts of power such as the Mark 20 (175-kw) and the Mark 26 (250-kw).

A description of the research and development on anodes, cathodes, and separators for the multiplate-type cell is given in Section 12.3. Some of the features developed for the book-type cell, such as the anodized screen method of making cathodes, the cementing of nylon filaments on anodes, and the development of phenolized nylon cloth to provide a very thin but pore-free insulating separator were also used in the multiplate-type cells. However other features had to be developed specifically for the multiplate batteries.

In order to build up batteries of large capacity, such as those needed for the Mark 20 and the Mark 26 torpedoes, subassemblies, each composed of ten multiplate cells, were utilized. In each subassembly cathodes were parallel-connected by riveting together tabs located at the edges of the plates. The anodes were similarly parallel-connected. Series connections were made by riveting the anodes of one cell to the cathodes of an adjoining cell. Phenolized nylon-sheet insulators were placed between plates and between cells. The battery was built up to the desired capacity by bolting together as many subassemblies as needed. The finished battery was encased in a phenol-fabric tube in which it was supported by six phenol-fabric rails attached to the tube by screws. The forward end of the battery casing was sealed off by a heavy phenolic plate having suitable cutouts at top and bottom for water entry to and exit from the battery. One of the finished batteries with rail supports and end plates is shown in Figure 1.

A series of battery filling tests were made on the multiplate-type battery with simulated battery structures. The tests showed that, in the absence of positive scooping action, complete quick filling of the battery case could be achieved only by evacuating it. They also resulted in the development of types of quick-opening valves and demonstrated the feasibility of having both entrance and exit ports for the sea water at the same end of the battery.

After batteries had been constructed for the Mark 20 and the Mark 26 torpedoes, they were range-tested. It was felt that such things as battery come-up, admission and circulation of the electrolyte, and the electrical characteristics should be studied under actual operating conditions.

The first range trials were unsuccessful because of an inadequate hydraulic system. Therefore the "iron horse" was set up to study the internal and external hydraulic action of the batteries. As a result of these studies, a new system of valves and water passages was designed to insure positive circulation of the electrolyte, and the case of the battery was enlarged to provide internal water passages of greater cross section. Bench tests showed that the

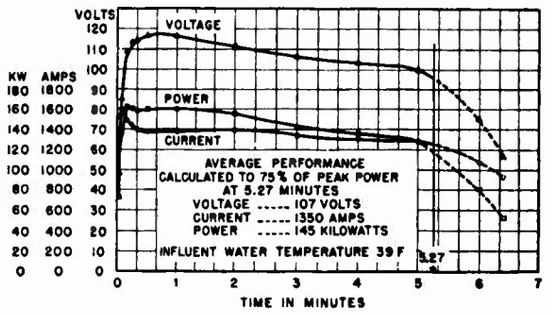

FIGURE 16. Sea-water battery 119-6-0; Newport range test in Mark 20 torpedo.

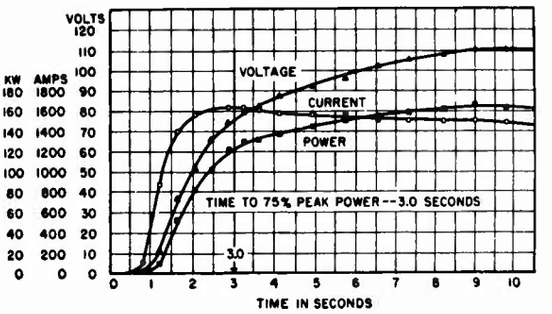

FIGURE 17. Sea-water battery 119-6-0; initial portion of Newport range test in Mark 20 torpedo.

redesigned internal hydraulic system was satisfactory. Subsequent range tests of batteries with the new irrigation system showed adequate flow of the electrolyte and delivery of full power, but the rate of come-up was slow.

Tests to determine the cause of the slow come-up followed three lines of attack: (1) tests at Newport, R. I., to see if the sequence of valve openings or the interference of impulse air caused slow come-up, (2) further tests with the "iron horse" on hydraulic conditions, to determine the effects of turbulence and flow, and (3) tests with the "pony" facilities, to study the effects of contamination on the surface plates of the assembled batteries. In the course of the tests, the cause of the slow come-up was found to be surface contamination, caused by the effects of moisture on the chromate-finished anode plates of the assembled batteries. Later tests with batteries processed by scratch-brushing unchromated anodes or made up from freshly chromated anodes gave very satisfactory performance as far as quick come-up was concerned.

Altogether, 43 range test runs were completed at Newport, R. I., on Mark 20 and Mark 26 torpedoes driven by multiplate batteries. It was not possible in all cases to control the variables which affected battery performance only, since the tests also involved the study of conditions which affected the operation of the torpedo as well. As a result, in some runs, torpedo performance was normal and a complete record relating voltage, current, battery come-up et cetera was made. In some runs, however, complete data is lacking due to erratic torpedo behavior, mechanical failures, accidental water leakage, failure to obtain complete oscillograph records of voltage, current, and time, or clogging of the battery with mud as the result of too deep a dive.

Battery for Mark 20 Torpedo. Figures 16 and 17 show typical performance data for the Mark 20 torpedo battery in cold water. The data for Figure 16 were obtained from a chromated 119-6-0 battery used to drive a Mark 20 torpedo on the range at Newport, R. I. In order that the battery casket might fill quickly with sea water, it was evacuated before the torpedo was fired, and both top and bottom valves were opened simultaneously at the instant of firing. The voltage-current-power-time relationships are of the order predicted from laboratory control tests. The power remained at or above 75 per cent of the peak value for 5.27 min, which was sufficient to drive the torpedo over the 6,800-yd range at the desired speed.

Figure 17 shows in detail the data for the first 10-sec part of the range run. The battery come-up was satisfactorily rapid since it reached 75 per cent of peak power in 3 sec. This means that the torpedo with its compound motor, with this battery, is able to attain a speed of 34 knots within the first 500 yd. Such performance is considered entirely satisfactory.

Battery for Mark 26 Torpedo. Figures 18 and 19 show typical performance data for the Mark 26 torpedo when driven by a multiplate-type battery. The battery, which must drive this torpedo over the 6,000-yd range at an average speed of 40.6 knots, is a 232-kw one, one of the largest capacity batteries made. The data for Figure 18 were obtained from a chromated 121-7-0 battery, fired in a Mark 26 torpedo at the Newport, R. I., range. In this case, the battery casket was filled, until firing, with nitrogen at atmospheric pressure in order to avoid moisture contamination of the battery plates and to aid the battery come-up; both top and bottom valves were opened simultaneously at the instant of firing the torpedo.

The voltage-current-power-time relationships shown in Figure 18 are in good agreement with those

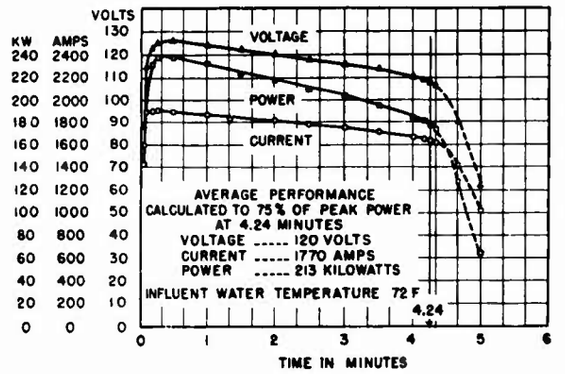

FIGURE 18. Sea-water battery 121-7-0; Newport range test in Mark 26 torpedo.

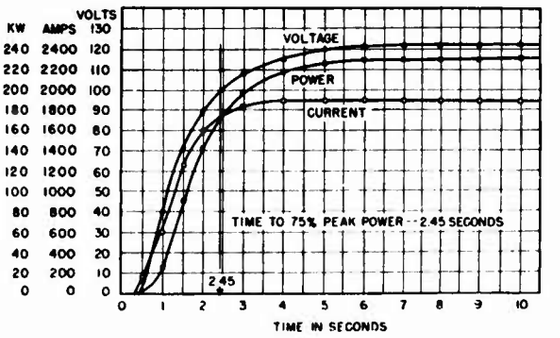

FIGURE 19. Sea-water battery 121-7-0; initial portion of Newport range test in Mark 26 torpedo.

predicted from laboratory control tests of seven-cathode cell subassemblies. It will be noted that, with the series motors used in the Mark 26 torpedo, the voltage and current increase more nearly at the same rate than is the case with the compound motor used in the Mark 20 torpedo. The power did not drop below 75 per cent of the peak value until the battery had driven the torpedo for 4.24 min, over a 6,000-yd range.

Figure 19 shows in detail the data for the first 10 sec of the run. The come-up of the battery is satisfactory as it reached 75 per cent of the peak power in 2.4 sec. This come-up was sufficient to accelerate the torpedo so that it attained an average speed of 38 knots over the first 500 yd of the run.

CONSTRUCTION AND TESTS OF DUPLEX-TYPE BATTERY

Each duplex-type electrode consists of an anode of magnesium (for one cell) and a cathode of silver chloride (for the adjacent cell) connected through a thin sheet of silver foil. The electrodes within a cell are insulated from one another by glass beads which are firmly embedded in the silver chloride. Figure 7 shows a duplex-type battery assembly. The duplex type of construction has the advantage that it weighs less and occupies less space per unit of power output than any other type of construction. Figure 20 shows a comparison of weights per kilowatt for the duplex type and the multiplate type of battery.

Since effort was concentrated on the development and production of satisfactory multiplate-type batteries, rapid development of the duplex type was hindered. The multiplate type was started first and was well on its way to completion when the first practical duplex type was evolved. However, successful methods of making small-capacity duplex batteries such as the 8-kw were fully developed, and an 80-kw battery was designed. Its components were, to a large extent, completed at the time when the project terminated.

The 8-kw duplex-type battery, which may be regarded as the forerunner of the large-capacity torpedo battery of the future, was constructed and bench-tested in the laboratory. Some of the pertinent data are as follows:

Average current	163 amp (2 amp per square inch)
Average voltage	50.7 v (1.01 v per cell)
Average power	8.27 kw
Peak power (12 sec)	9.08 kw
Power at cutoff (4 min, 8 sec)	7.70 kw
Efficiency of silver chloride utilization	81.5 %
Loss of efficiency due to leakage currents	7 %

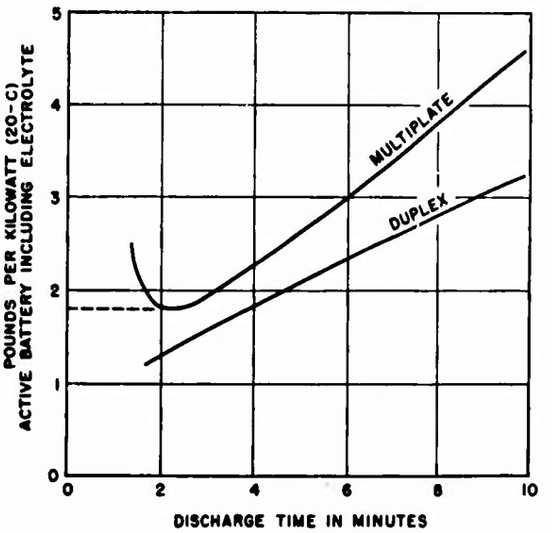

FIGURE 20. Comparison of "wet" weights of duplex and multiplate batteries.

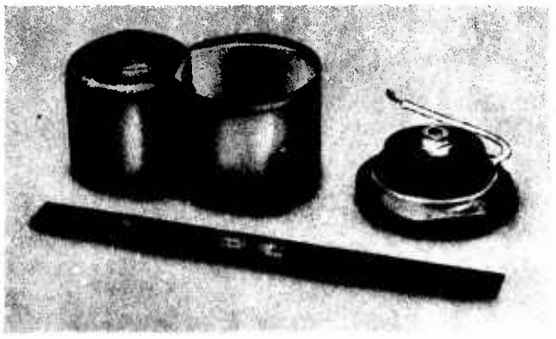

FIGURE 21. XDCA battery showing cell pile-up.

As a result of the tests on the 8-kw duplex type of battery, the following conclusions are drawn:

1. Duplex-type batteries that have been constructed and tested in the laboratory are suitable for range trials for torpedo propulsion.

2. All the advantages found in the small-capacity duplex-type battery appear capable of realization in large-capacity batteries for torpedo propulsion.

Many of the manufacturing methods have been developed for making duplex-type batteries on a production basis.

CONCLUSIONS ON SEA-WATER TORPEDO BATTERIES

1. Sea-water batteries have been developed that are able to furnish smooth driving power for torpedoes requiring as much as 280 kw (140 v and 2,000 amp) for a period of 3.4 min.

2. Torpedoes powered by sea-water batteries have attained speeds of 44 knots and have been driven over useful ranges (speed constant to within ±1 knot) in excess of 7,000 yd.

3. Batteries have performed satisfactorily in sea water under temperature conditions varying from 30 to 72 F.

4. Batteries have been constructed in which the come-up time, (the time required to reach 75 per cent of peak power) has been as small as 1.1 sec. In most batteries it is under 3 sec. The come-up time depends on the condition of the surface of the plates, on the removal of corrosion products, and on such variables as scoop size, impulse pressure, motor characteristics, and the initial pressure existing within the housing.

5. Even though hydrogen is evolved from the batteries, the bubbles of this gas are so small and widely diffused as to produce no visible wake. Any initial wake which occurs is caused by nitrogen or air being expelled from nonevacuated batteries; however, torpedoes running as shallow as 5 ft left no visible wake after the first 50 yd of the run.

6. An essential part of the design of the battery is a suitable irrigation system. This is necessary not only to get the sea water in contact with the plates and to remove the heat generated, but also to remove the corrosion products. For the large-capacity batteries it was considered wise to design the irrigation system so that at least 50 complete changes of the sea-water electrolyte occurred per minute.

12.5.2 Detonator Batteries

General Description. Detonator batteries are designed for use in various devices such as the XDCA depth-charge pistol and are characterized by small-size, rapid-voltage build-up and short discharge periods. While the design of the detonator batteries follows the same basic electrochemical principles as other types of sea-water batteries, their constructional features represent a complete departure from these types. The construction and test results of the XDCA battery, which is now in manufacture, is described as a typical example.

CONSTRUCTION OF XDCA BATTERY

A photograph of the XDCA battery is shown in Figure 21 and an assembly drawing of it in Figure 22. It is designed to meet the following requirements:

1. Power-time performance: 2 amp, 1 v for 0.25 sec; followed by 0.3 amp, 2.8 v for 1 min.

2. Size and shape: to fit into 1.9-in. diam cylindrical container about 1.125 in. deep.

3. Voltage come-up requirements: 1 v at 2 amp within 0.2 sec at 0 C.

4. Valving system: inlet and outlet ports hermetically sealed with thin lead foil designed to rupture at a given water pressure.

The battery consists of four disk-shaped cells, centrally mounted on a common screw, connected to provide two two-cell batteries in parallel. The parallel construction provides an added factor of reliability, for, should one of the two sections be rendered inoperative, the other carries the load.

No attempt is made to control intercell leakage currents in this type of battery, although it is possible to do so and still obtain rapid come-up by a special design of the container and the water ports. The speed of the voltage build-up, which must be very rapid, is adversely affected by exposure of the plates to high humidity or contaminants such as oil,

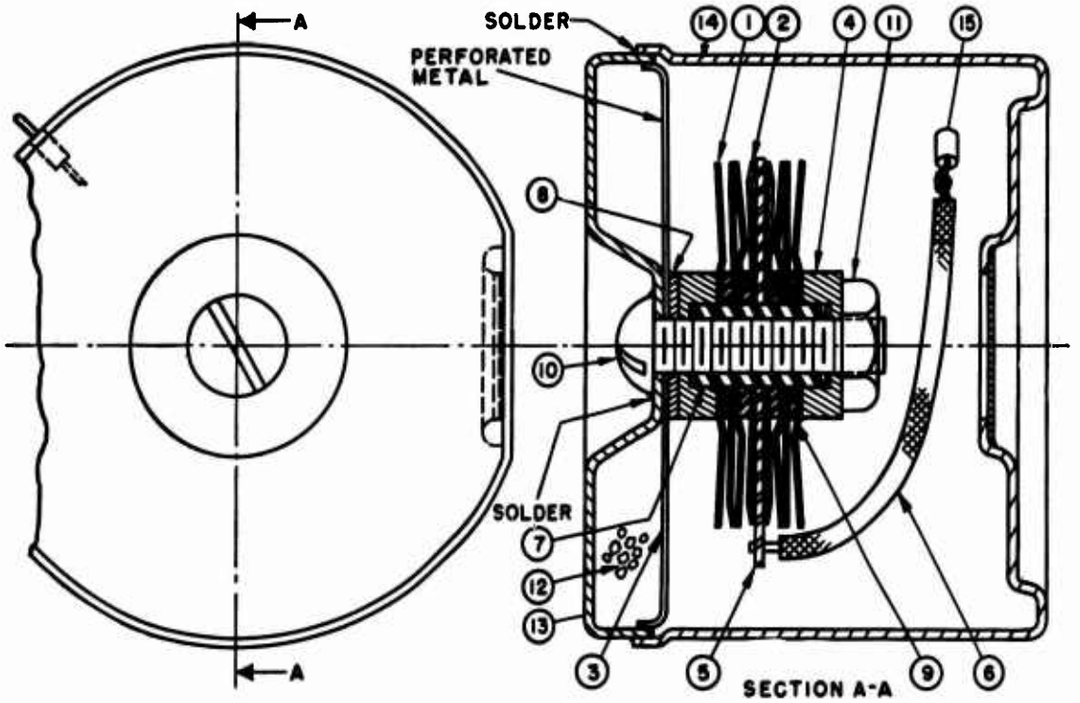

1. Anode plate
2. Cathode plate
3. Desiccant container
4. Brass bushing
5. Terminal lug
6. Wire
7. Ceramic bushing
8. Guard
9. Mica washer
10. Mounting screw
11. Brass nut
12. Desiccant
13. Cover
14. Casing
15. Metal-to-glass bushing

FIGURE 22. Assembly of XDCA battery.

sulphur, wax, or other substances which prevent the plates from being wet by the sea water. During manufacture all parts of the battery are kept in a desiccator except when being worked on and a desiccant is placed within the assembled cell before it is sealed. The battery come-up would be aided somewhat by forced circulation, but it was found that this was not necessary. Sufficient circulation is attained by the bubbling of the evolved hydrogen between the battery plates.

TEST RESULTS

A typical discharge curve is shown in Figure 23 for a load resistance of 9 ohms. It will be noticed on the expanded time scale that the build-up of the battery is very rapid. Full voltage is reached in about 0.09 sec. This curve shows the battery performance for a current drain of about 0.33 amp. If larger currents are drawn, the voltage is correspondingly smaller, but otherwise the performance is approximately the same. These batteries can furnish currents up to 7 amp.

12.5.3 Intermediate-Power and -Time Batteries

GENERAL DESCRIPTION

Batteries to deliver moderate amounts of power, 300 to 1,000 w, for periods of from 30 to 90 min, differ from torpedo batteries only in size and details of construction. The lower power delivery makes low internal resistance less important and the longer time of discharge requires that more attention be paid to leakage currents and local corrosion. A number of batteries of this general type have been designed, built, and tested. A typical example of this class is No. 17-3-E. At the present time it is being manufactured to propel underwater mechanisms.

CONSTRUCTION OF 17-3-E BATTERY

A photograph of the 17-3-E battery is shown in Figure 24. It is designed to meet the following requirements:

1. Power-time performance: 15 amp, 24 v for 30 min.

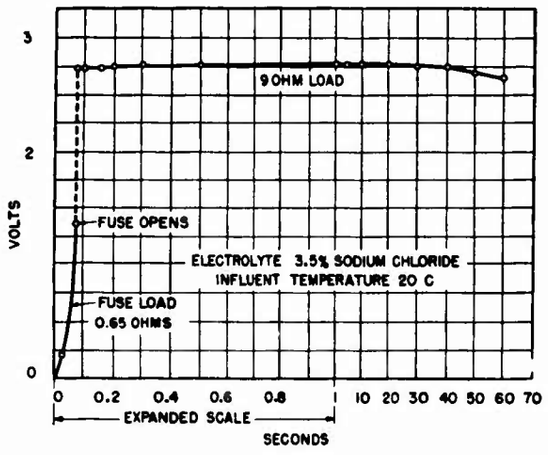

FIGURE 23. Typical discharge curves for XDCA battery consisting of two 2-SA units in parallel, illustrating use of fuse to promote very rapid come-up.

2. Size and shape: to be fitted into 5.75-in. diameter cylinder.

3. Come-up performance: not exceptionally rapid.

The design best meeting the above requirements was one using multiplate cells made with nyloned anodes and anodized screen cathodes. It is essentially like that of a torpedo propulsion battery, except that it is in miniature and is mechanically simplified. However, the following changes are noteworthy:

1. Water admission and venting ports are merely holes in the battery case aligned with holes in the shell of the housing. Sea water entering and discharging through these holes circulates through the battery and enables it to perform satisfactorily in regard to come-up, and also affords sufficient flushing of the corrosion products from the battery. The evolution of hydrogen in this battery is at a rate sufficient to cause a complete change of electrolyte every 20 sec.

FIGURE 24. 17-3-E battery; two views showing complete assembly and battery with case partially removed.

2. In order to compensate for the estimated leakage current of 1.4 amp, an excess capacity of approximately 10 per cent has been provided. Although this adds to the weight and volume of the battery, any other method would add to the complexity of the design.

3. Since this battery does not have forced irrigation, the nylon filament spacers used were of larger diameter (0.020 in.) than those employed in torpedo batteries. The extra space between the plates permits corrosion products to be swept away rapidly and prevents any possible clogging. The increased internal resistance resulting from wider spacing has only a slight effect on the battery voltage at the low current density employed.

TEST RESULTS

A typical discharge curve for a type 17-3-E battery is shown in Figure 25. The gradual rise in power during the first several minutes is typical of self-circulated batteries and is probably due to the gradual rise in temperature and salinity which occurs when the passage of the electrolyte over the plates takes place at a slow rate. A quick come-up is not essential for this battery; therefore, this effect is not an important one. In fact, these batteries have operated satisfactorily in fresh water, although at a somewhat lower voltage than normal. Under such conditions the come-up is very slow, since the electrolyte must be made from the magnesium chloride which is a product of the battery discharge.

12.5.4 Low-Power, Long-Time Batteries

GENERAL DESCRIPTION

Many requests for a long-time battery to supply A and B power for vacuum-tube operation have been satisfied by the development of a low-voltage sea-water battery using a vibrator pack to give the necessary high voltage. The requirements called for a battery without forced circulation to operate for periods up to 60 hr, and to supply 40-150 amp-hr of discharge capacity at 6 to 24 v. This low-power, long-time battery demanded a type of construction different from the higher powered batteries used for torpedo propulsion. Thick magnesium anodes and thick cast silver chloride cathodes were required for the most compact design.

Batteries of this general type have been called beacon batteries. Several, of different sizes and shapes, have been developed and built for the

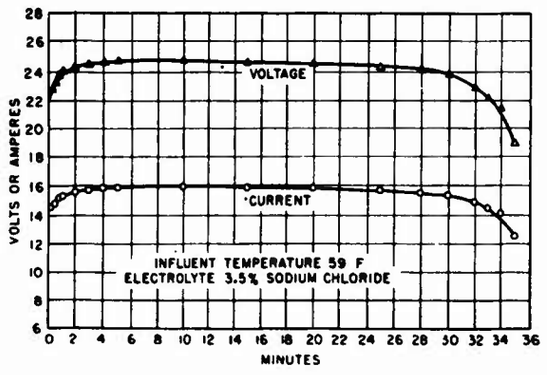

FIGURE 25. Sea-water battery 17-3-E; bench test.

Bureau of Ships, and one was designed for the Army Air Forces and Signal Corps. The latter battery, although different in construction from those designed for the Bureau of Ships, is the same in principle and is described here. This battery, which is shown in Figure 26, is called the Pentagon (5-3-BP) battery because it consists of an arrangement of five cells in a regular pentagonal formation. Normally, it furnishes 7.5 v.

CONSTRUCTION OF PENTAGON (5-3-BP) BATTERY

The five cells are connected in series and placed in pentagonal formation within a phenol-fiber case of annular cross section. Wood filler pieces are used in the spaces not occupied by cell boxes. The whole assembly is encased in a cylindrical container which has two holes in it, one near the bottom to provide for the entrance of the sea water, and one near the top to provide for the exit of the sea water and the corrosion products. Through these two holes, the electrolyte is supplied to each individual cell by means of a top and bottom manifold.

Because of the long time of operation and slow self-circulation of this type of battery, a wide electrode spacing (0.064 in. as compared with 0.015 in. for the high-power, short-time torpedo battery) is required. This wider spacing between plates insures that no clogging takes place, and that corrosion products may be promptly removed. Cathodes having sufficient silver chloride to provide high capacity were made by casting silver chloride onto a coarse silver screen. These cast cathodes are approximately 0.150 in. thick and have about 1 amp-hr of capacity psi of cathode surface.

An operating life of 24 hr or more in sea water necessitates severely limiting leakage currents. They are minimized by making the electrolytic resistance as large as possible. This is effected by building each cell as an almost completely enclosed unit and by making the holes in each individual cell box as small as possible consistent with adequate irrigation.

TEST RESULTS

Figure 27 shows typical discharge curves, one at 0 C and the other at 20 C for a Pentagon 5-3-BP battery. The voltage drops slightly during the first 12-hr period when the 92.5-ohm load is in the circuit, especially at the lower temperature. However, it remains fairly constant when the 3.80-ohm load and the 1.55-ohm load are inserted in the circuit. The voltage drops off slightly only for the 1.55-ohm

FIGURE 26. 5-3-BP battery; five cells in series; blocks used to position cells are shown.

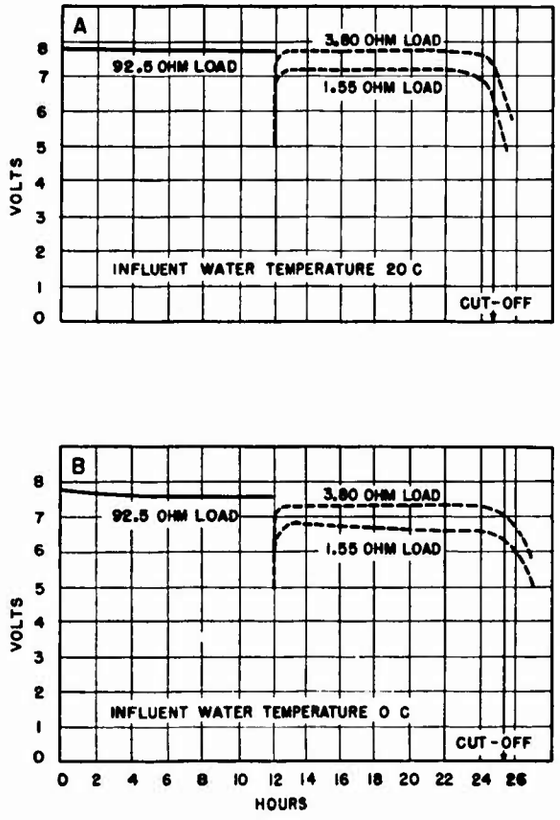

FIGURE 27. Pentagon batteries, discharged at low drain for first 12 hr, and then for alternate 1-min periods at two higher drains.

load at the 0 C temperature. This is quite remarkable because current is increased about 25-fold in one case and about 60-fold in the other case.

12.5.5 AB Type, High-Voltage, Low-Current, Intermediate-Time Batteries

A sea-water battery to supply both A and B power for a torpedo exploder was requested by the Naval Ordnance Laboratory. It was not possible to use a low-voltage battery with a vibrator pack to get the high B-battery voltage needed in this case. Therefore it was necessary to design a sea-water B battery with a large number of cells, so constructed that leakage currents were at a minimum and yet electrolyte circulation was adequate.

After a careful survey of the proposed torpedo exploders, the following requirements were set up for a sea-water AB battery which would power any of them:

1. Power time: A section: 6 v, 2 amp for 15 min; B section: 110 v, 2 amp for 15 min.

2. Size: as small as possible. Final size of the battery is 3.5x3.25x1.875 in.

3. Come-up performance: 90 per cent of full voltage in 3 sec.

4. Housing: a specially designed, hermetically sealed battery housing is required.

5. Irrigation: a rate of flow of from 2 to 4 liters per minute is required. This amounts to 36 to 72 changes of electrolyte per minute.

The irrigation is provided by a water-driven impeller in the side of the torpedo war head which starts turning as soon as the torpedo is launched. This actuates an opening mechanism which provides water inlet and outlet holes either by pulling soldered sealing tabs off the water ports or by piercing the case. The water intake and discharge holes are located on the side of the torpedo in such a fashion that ample hydraulic pressure is developed by the forward motion of the torpedo, and thus a high rate of circulation is provided.

The A and B batteries, both of which are of the duplex type of construction, are connected in series and housed in a battery case made from sheet phenolic stock. The case members are all rigidly held in place with screws, and four setscrews pass through the end plates and bear against the pressure plates of the battery inside the case. This provides means of compressing the cell pile-up to get the intimate contact between electrode elements necessary for the proper operation of this type of battery. The setscrews are turned up to a constant torque and thus provide constant and reproducible pressure on the cell pile-up. The AB battery assembly in a special transparent case (showing the setscrews) is shown in Figure 28.

The sea-water B battery is unique among all sea-water batteries, and probably among all batteries, in that the nonuseful leakage current is from 3 to 100 times the useful current. The reason for this is that the battery is essentially a source of potential rather than of power. The voltage must not only remain steady and constant, but for certain applications must not show more than a 1 per cent ripple for the frequency range from 0.5 to 50 c. In order to hold the voltage constant, the leakage currents, which may be as much as 99 per cent of the total current, must be kept very steady. In the final design, the B battery voltage ripple was kept below 0.3 v at a temperature of 30 C and below 0.05 v at a temperature of 2 C. Figure 29 shows typical dis-

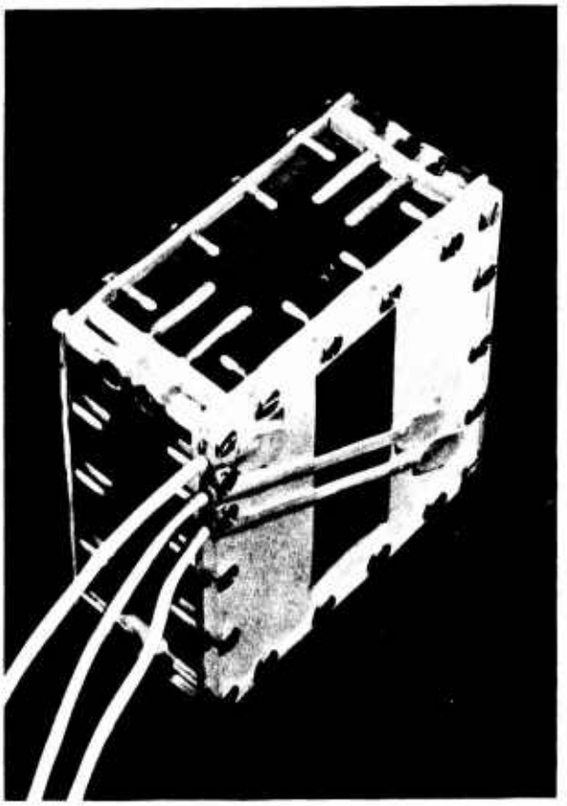

FIGURE 28. AB battery; top water channel and terminal wires.

charge curves for the torpedo exploder battery at two temperatures and for both the A and the B units. It will be noted that all voltages remain fairly constant for the first 13 min and then drop off without fluctuations.

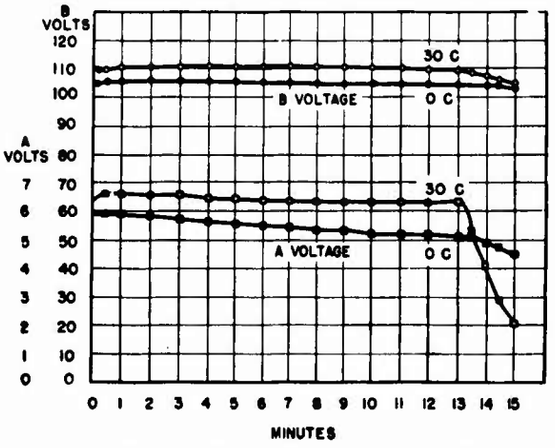

FIGURE 29. Sea-water battery 75-dc; bench tests; discharge curves for AB batteries; approximate current drain: A load, 2 amperes; B load, 6.7 milliamperes.

12.5.6 Battery Designed for 7-40-M Proximity Fuze

A request was forwarded by the National Defense Research Committee in September of 1942 that a sea-water battery be developed for the 7-40-M underwater proximity fuze. This was the first sea-water battery undertaken and represents the starting point of the entire sea-water battery development program. Many of the features incorporated in the design of this early type of battery have been greatly improved as a more comprehensive knowledge of the art of sea-water battery-making has been gained.

One of the features of a battery for this fuze is that it must remain inactive until the proper time, and then must go into action with its full power available. The sea-water battery lends itself to these requirements very nicely, since the electrolyte does not enter the battery until the underwater proximity fuze is in its operating medium, i.e., sea water.

12.6 CONCLUSIONS AND RECOMMENDATIONS

CONCLUSIONS

1. It is possible to produce primary batteries of the magnesium-silver chloride type which use sea water as the electrolyte and which have considerable weight and volume advantages over the conventional types of primary and secondary batteries. Sea-water batteries have been produced for torpedo propulsion which have a weight advantage of 5 to 1 and a volume advantage of 4 to 1 over the best secondary batteries used for this purpose.

2. Three successful types of silver chloride cathodes have been developed for sea-water batteries. They are the anodized, the rolled, and the cast. Two satisfactory methods of finishing the magnesium anodes have been developed, namely the chromate finish, and the scratch-brush finish. Two types of separators have been devised which have stood up through rigorous bench and range tests. They are known as the nylon filament separator and the glass bead separator.

3. Sea-water batteries have been developed which have ranged in size from a small detonator battery weighing about 1 oz and delivering approximately 1 w for 1 min, to the large capacity torpedo propulsion battery weighing 575 lb and delivering approximately 220 kw for about 5 min.

4. Sea-water batteries have been developed which supply energy sufficient to drive large torpedoes like the Mark 26 at speeds up to 44 knots and over ranges in excess of 7,000 yd.

5. Most of the sea-water batteries built have a come-up time of less than 3 sec. Batteries for torpedo propulsion have been constructed whose come-up time has been as short as 1.1 sec.

6. Sea-water batteries have been developed for a wide variety of applications. Among them may be mentioned batteries for detonator actuators, for A and B power supplies in marine signaling devices, for torpedo exploders, for depth-charge exploders and mechanisms, for an underwater proximity fuze, and for torpedo propulsion.

Recommendations

1. Since the duplex type of construction has proven to be the best developed so far, it is recommended that further experimental and developmental work be done on batteries of this type in an effort to produce large capacity batteries such as those needed for torpedo propulsion. So far, duplex-type batteries of low capacity, such as the 8-kw torpedo propulsion battery, have been constructed and successfully tested. Also an 80-kw battery of this type was planned and the component parts were nearly completed when the project terminated. Since the fundamental research and development work on component parts has been completed, it should not take much additional work to construct and test large-capacity batteries of this type.

2. It is recommended that further research work be done in an effort to develop better methods of setting the glass bead insulators in the silver chloride cathodes of duplex batteries. Two machines have been used for experimentally setting these beads, the "continuous strip" one and the "corn planter" one but considerable further development work needs to be done before large quantities of beaded cathodes can be produced. The production of large quantities of beaded cathodes on a commercial scale is necessary before large-capacity duplex-type batteries can be made in quantity lots.

3. Considerable additional developmental work could be done on the hydraulic and mechanical designs for particular applications. Improvement in battery performance may be expected as the hydraulic and mechanical designs are perfected.

4. So far most of the emphasis has been on the development of batteries for torpedo propulsion, although a few other applications have been found. An investigation should be made to find new applications for sea-water batteries and to adapt the existing developments to uses other than their present ones.

GLOSSARY

ACTIVATION. An electrochemical process in the preparation of a sea-water cell cathode in which some of its silver chloride coating is reduced to metallic silver, forming bridges between the underlying conductor and the cathode surface.

AD III. Attack director III.

AD B. Attack director B.

AMPS. Acoustic marine pinging speedometer.

AMS. Acoustic marine speedometer.

ANODE, SEA-WATER CELL. The *negative* electrode, made of a magnesium alloy.

ANODIZED CATHODE. The metallic silver cathode, in a sea-water cell, which has been coated electrochemically with silver choloride.

A S. Antisubmarine.

ASAP. Antisubmarine attack plotter.

A SCOPE. A CRO indicator depicting echo intensities by vertical deflections, and ranges by the positions of these deflections on the horizontal trace.

ASDEVLANT. Antisubmarine Development, Atlantic.

ASDIC. British echo-ranging equipment; letters are derived from "Anti-Submarine Development Investigating Committee."

ATP. Automatic target positioner.

ATT. Automatic target training.

ATTACK TEACHER. A training device which provides simulation of an antisubmarine attack.

BALANCED MODULATION, SERVO. A modulation process in which the carrier frequency output drops to zero in the absence of any error signal.

BALLOTINI. Small glass beads used in certain sea-water batteries as separators between electrodes.

BDI. Bearing deviation indicator.

BEARING TIME. Bearing rate, the change in bearing per unit of time.

BLIND TIME. In an antisubmarine attack, the elapsed time between the last echo-ranging contact with the submarine and the explosion of the charges.

CATHODE, SEA-WATER CELL. The *positive* electrode, made of silver and silver chloride.

CAVITATION. The formation of gas or vapor cavities in water, caused by sharp reduction in local pressure.

CHEMICAL RECORDER. An indicator which records range on chemically treated paper.

CHLORINITY. The number of grams of chlorine per kilogram of sea water, assuming all bromine and iodine are replaced with chlorine. Expressed in parts per thousand.

CHROMATE FINISH. A protective surface for the magnesium anodes in sea-water cells, obtained through immersion in an acid chromate bath.

COME-UP TIME. The time necessary for a sea-water battery to reach 75 per cent of peak power output.

CUDWR. Columbia University Division of War Research.

CUT-ONS. Method of bearing determination from initial and final echoes obtained as the echo-ranging beam is swept across the target.

DCDI. Depth charge direction indicator.

DCRE. Depth charge range estimator.

DEAD TIME. The elapsed time between the will to fire and the instant the charges strike the water.

DEVELOPMENT. A chemical process in the preparation of a sea-water cell cathode, in which the surface of the silver chloride is reduced to metallic silver.

DIFFERENTIAL SYNCHRO. A synchro unit which responds to the sum or difference of two rotation orders.

DIRECTIVITY INDEX. A measure of the directional properties of a transducer. It is the ratio, in decibels, of the intensity, or response, on the acoustic axis to the average intensity, or response, over the whole sphere surrounding the projector or hydrophone.

DOME. A transducer enclosure, usually streamlined, used with echo-ranging or listening devices to minimize turbulence and cavitation noises arising from the transducer's passage through the water.

DOW NO. 11 FINISH. A commercial protective surface for magnesium, similar to the chromate finish.

DRA. Dead reckoning analyzer.

DRT. Dead reckoning tracer.

ER. Echo repeater.

ERC. Echo repeater calibrator.

ERSB. Expendable radio sono buoy.

EXPENDABLE RADIO SONO BUOY. A buoy listening device that contains a hydrophone for receiving target signals, and a radio transmitter for relaying the signals to patrolling air or surface craft.

FOLLOWER. A device used with attack directors to supply range and bearing information corresponding to the position of a virtual target.

HDE. Hydrostatically detonated exploder.

HEDGEHOG. A forward-throwing projector used by antisubmarine vessels.

HUSL. Harvard Underwater Sound Laboratory.

HYDROPHONE. An underwater microphone.

IRON HORSE, IRON PONY. Housings used for bench-testing torpedo sea-water batteries.

ISGM. Installed sound gear monitor.

K GUN. A device which throws antisubmarine charges by projecting the charge-holding arbor.

LAC. Lead angle computer.

MAD. Magnetic airborne detector.

MGAP. Mechanical geographic attack plotter.

MUNROE EFFECT. Concentration of an explosive force, achieved by special shaping of the charge.

MOUSETRAP. An antisubmarine weapon which projects rocket-type depth charges.

MTB. Maintenance of true bearing.

NLM. Noise level monitor.

NMB. Navigational marker buoy.

NRL. Naval Research Laboratory.

PAMS. Phase acoustic marine speedometer.

PING. Acoustic pulse signal projected by an echo-ranging transducer.

PPCR. Portable polar chart recorder.

PPI. Plan position indicator.

PROJECTOR. An underwater acoustic transmitter.

QBE. Small echo-ranging equipment, made by the Submarine Signal Company, using a JK crystal hydrophone for listening.

QC. Standard Navy echo-ranging equipment using magnetostriction transducers.

QCS. 24-kc echo-ranging and listening equipment.

QFA. A standard model of attack teacher which provides visual presentation of attack problems.

QH. Navy designation for CR scanning sonar, originally applied to Harvard designs.

RANGE RATE. Rate of change of range between own ship and target.

RELATIVE BEARING. Target bearing relative to own-ship's heading.

RELATIVE CENTER BEARING. Average of initial and final relative bearings obtained as the echo-ranging beam is swept across the target.

REVERBERATION. Sound scattered diffusely back toward the source, principally from the surface or bottom and from scattering sources in the medium such as bubbles of air and suspended solid matter.

ρc RUBBER. A rubber compound with the same ρc (density times velocity of sound) product as water.

RLBI. Right-left bearing indicator.

SALINITY. The number of grams of solid material per kilogram of sea water when all carbonates are converted to oxides, the bromine and iodine are replaced by chlorine, and all organic matter is completely oxidized. Expressed in parts per thousand.

SAMS. Steady-state acoustic marine speedometer.

SCRATCH-BRUSH FINISH. A surface for the magnesium anodes in a sea-water cell, obtained by burnishing with a clean, dry, steel wire brush.

SEA-WATER CELL. As discussed in this volume, a primary cell using sea water as its electrolyte, and having a magnesium alloy anode and a silver and silver chloride cathode.

SGM. Sound gear monitor.

SONAR. Generic term applied to methods or apparatus that use SOund for NAvigation and Ranging.

SPTU. Split projector test unit.

SSTU. Synchro system test unit.

STACK, TRANSDUCER. Pile of consolidated laminations.

TARGET ASPECT. Orientation of the target as seen from own ship.

TRANSDUCER. Any device for converting energy from one form to another (electrical, mechanical, or acoustic). In sonar, usually combines the functions of a hydrophone and a projector.

TRANSFER FUNCTION. In a servomechanism, the ratio of output to input.

UCDWR. University of California Division of War Research.

USRL. Underwater Sound Reference Laboratories.

BIBLIOGRAPHY

Numbers such as Div. 6-641.1-M3 indicate that the document listed has been microfilmed and that its title appears in the microfilm index printed in a separate volume. For access to the index volume and to the microfilm, consult the Army or Navy agency listed on the reverse of the half-title page.

Chapter 1

1. *Sound Material Handbook,* West Coast Sound School, West Coast Sound Training Squadron, San Diego, Calif., pp. 354-374.
2. *QC Driver Tuning. Comparison of Several Methods,* W. F. Arndt, Report No. P29/R474-NS-124, CUDWR-NLL, Aug. 11, 1943. Div. 6-641.1-M3
3. *Instruction Book for OBY,* David Bogen Company, New York, N. Y.
4. *Instruction Book for OCH,* Harvey Radio Laboratories, Cambridge, Mass.
5. *Sound Gear Monitor,* NDRC 6.1-sr287-2086, HUSL, Nov. 1, 1945, pp. 106, 107. Div. 6-641.1-M9
6. *Extended Range Monitor. Instructions for Converting Frequency Range of Sound Gear Monitor, Model 5C or 5E (Underwater Sound Portable Testing Equipment, Model OAX) from 17 kc-26 kc to 17 kc-71 kc,* NDRC 6.1-sr287-1550, HUSL, May 20, 1944. Div. 6-641.12-M1
7. *Operator's Manual for Sonar Portable Testing Equipment, Model X-OCP (Wide Range Monitor),* Lab. Report H-383, HUSL, Mar. 1, 1945. Div. 6-641.12-M3
8. *QC Monitor,* O. Hugo Schuck and I. P. Rodman, OEMsr-287, NDRC 6.1-sr287-388, HUSL, Jan. 12, 1943. Div. 6-641.1-M1
9. *Methods Suitable for the Calibration and Use of an Octave-Band Sound Level Meter,* R. W. Young, Lab. Report M-32, UCDWR, Feb. 10, 1943. Div. 6-641.1-M2
10. *Effect of Measuring Distance on Directivity Patterns and on Maximum Intensity,* M. J. Foral, Lab. Report M-01.72-45, HUSL, Nov. 16, 1943. Div. 6-641.1-M4
11. *Installed SGM Transducer B-19D #4 VIR Teardrop Shell,* Francis P. Bundy and Jack C. Cotton, Lab. Report M-02.331-105, HUSL, Jan. 28, 1944. Div. 6-612.612-M2
12. *ISGM, Recommendations On,* O. Hugo Schuck, Lab. Report M-02.331-140, HUSL, Mar. 20, 1944. Div. 6-641.11-M1
13. *The B-19H Expanded Range Monitor,* J. R. Reitz, Lab. Report M-02.331-168, HUSL, May 12, 1944. Div. 6-612.613-M5
14. *The Monitor as a Vacuum Tube Voltmeter,* C. E. Houston, B. A. Wooten, and Dwight E. Gray, OEMsr-287, NDRC 6.1-sr287-1708, HUSL, July 10, 1944. Div. 6-641.1-M5
15. *Characteristics of B-19H Hydrophone Used as a Projector,* Paul E. Sabine and Paul Ebaugh, Lab. Report M-02.331.7-85, HUSL, Aug. 7, 1944. Div. 6-612.613-M9
16. *Driving Data on B-19H at Low Frequency,* Paul E. Sabine and Paul Ebaugh, Lab. Report M-02.331.7-92, HUSL, Aug. 18, 1944. Div. 6-641.1-M6
17. *Characteristics of B-19B Hydrophone from 10 to 40 kc,* Paul E. Sabine, Lab. Report M-02.331.7-95, HUSL, Aug. 30, 1944. Div. 6-641.1-M7
18. *Response of B-19B and B-19H Hydrophones in a Strong Sound Field,* Charles R. Rutherford, Lab. Report M-01.213-224, HUSL, Sept. 7, 1944. Div. 6-641.1-M8
19. *Artificial Projector,* O. Hugo Schuck, John O. Hancock, and B. A. Wooten, NDRC 6.1-sr287-1786, HUSL, Nov. 1, 1944. Div. 6-321.5-M9
20. *Projector Test Gear,* NDRC 6.1-sr287-2050, HUSL, Dec. 1, 1944. Div. 6-641.14-M1
21. *Split Projector Test Unit,* NDRC 6.1-sr287-2051, HUSL, Dec. 1, 1944. Div. 6-641.13-M1
22. *Hydrophone Specifications for X-OCP Monitors,* J. R. Reitz, Lab. Report M-02.331.7-118, HUSL, Dec. 18, 1944. Div. 6-641.12-M2
23. *Field Studies of Sonar Domes,* NDRC 6.1-sr287-2073, HUSL, Oct. 1, 1945. Div. 6-631.43-M8
24. *Instruction Manual for Underwater Sound Portable Testing Equipment — Model OAX,* Harvey Radio Laboratories, Cambridge, Mass.
25. *Instruction Manual for Underwater Sound Portable Testing Equipment — Model OAX-1,* Presto Recording Corporation, New York, N. Y.

Chapter 2

1. *Sound Gear Monitor,* NDRC 6.1-sr287-2086, HUSL, Nov. 1, 1945. Div. 6-641.1-M9
2. *The Dynamic Monitor,* NDRC, 6.1-sr287-2058, HUSL, Apr. 10, 1945. Div. 6-641.2-M6
3. *A Survey of the Problem of Maximum Echo Ranges,* Carl Eckhart, NDRC 6.1-sr30-1315, UCDWR, Nov. 20, 1943.
4. *Minutes of a Conference on Maximum Echo Ranges,* CUDWR, Lab. Report 01.921-DC-11, Dec. 14, 1943.
5. *Dynamic Monitor,* Roderic M. Scott, Lab. Report M-02.33-12, HUSL, Dec. 20, 1943. Div. 6-641.2-M1
6. *Figure of Merit of QH Sonar, WEA-1 and QBF,* Charles A. Ewaskio, Lab. Report M-02.07-58, HUSL, July 24, 1944. Div. 6-641.2-M2
7. *Dynamic Monitor,* Charles A. Ewaskio, Lab. Report M-02.33-43, HUSL, Oct. 5, 1944. Div. 6-641.2-M3
8. *Operating Instructions for Dynamic Monitor,* Lab. Report H-343, HUSL, Oct. 18, 1944. Div. 6-641.2-M4
9. *Figure of Merit of QH Gear,* Charles A. Ewaskio, Lab. Report M-02.45.7-123, HUSL, Nov. 1, 1944. Div. 6-632.0-M20

10. *I. Figure of Merit of QCL on Galaxy. II. Electrical Noise Level of QH Model II*, Charles A. Ewaskio, Lab. Report M-02.07-65, HUSL, Nov. 13, 1944. Div. 6-641.2-M5

11. *I. Figure of Merit vs. Ship's Speed. II. Figure of Merit of QH Model II on November 19, 1944*, Charles A. Ewaskio, Lab. Report M-02.45-7-138, HUSL, Nov. 22, 1944. Div. 6-632.212-M19

Chapter 3

1. *Measurement of AX-58 Hydrophones*, Edward Gerjuoy, Lab. Report G27/R353, CUDWR-NLL, May 21, 1943. Div. 6-554.3-M22

2. *Calibration of OAY Sound Measuring Equipment No. 1 and General Radio Sound Level Meter, Type 759, Model OR-1, Serial Number 9*, Wilbur T. Harris, Lab. Report G7/R478, CUDWR-NLL, Aug. 12, 1943. Div. 6-641.3-M1

3. *Modification of OAY Sound Meter*, Frank P. Herrnfeld, Lab. Report D-53, CUDWR-NLL, Dec. 15, 1943. Div. 6-641.3-M2

4. *Improved Preamplifier Mounting for OAY S. L. Meter Hydrophone*, Garland W. Archer, Lab. Report P35/R679, CUDWR-NLL, Jan. 11, 1944. Div. 6-612.62-M20

5. *Modification of Type OAY Sound Measuring Equipment*, Frank P. Herrnfeld, Lab. Report D53/R714, CUDWR-NLL, Mar. 30, 1944. Div. 6-641.3-M3

6. *Dockside Noise Measurements of New-Construction Submarines*, Donald P. Loye, Robert A. Wagner, Robert W. Pratt, OEMsr-1128, NDRC 6.1-sr1128-1572, CUDWR-NLL, May 10, 1944. Div. 6-641.31-M2

7. *Manitowoc Dockside Auxiliary Noise Measurements — USS Hardhead (SS-365)*, Donald P. Loye and Robert A. Wagner, Lab. Report D53/R926, CUDWR-NLL, May 13, 1944. Div. 6-641.31-M3

8. *Submarine Noise Measurements at the Canal Zone, Pearl Harbor, Midway, and Mare Island*, Donald P. Loye and Robert A. Wagner, Lab. Report D53/R1034, CUDWR-NLL, July 18, 1944. Div. 6-641.31-M4

9. *Overside Noise Measurements of Submarines*, Donald P. Loye, Robert A. Wagner and Robert W. Pratt, NDRC 6.1-sr1128-1584, CUDWR-NLL, Sept. 12, 1944. Div. 6-641.31-M5

10. *Methods for Calculating Correction Factor for the RQ-51055 Hydrophone*, William B. Snow, Lab. Report D53/R1155, CUDWR-NLL, Oct. 21, 1944. Div. 6-641.3-M5

11. *Calibration of RQ-51055 (AX-58-A) Hydrophones to be Employed with OAY Sound Meters — Comparison of Two Methods*, David W. Van Lennep, Lab. Report D53/R1271, CUDWR-NLL, Dec. 7, 1944. Div. 6-554.3-M45

12. *Model OAY Sound Measuring Equipment*, William B. Snow and Frank P. Herrnfeld, NDRC 6.1-sr1128-1922, CUDWR-NLL, May 3, 1945. Div. 6-641.3-M6

13. *Preliminary Installation, Operation, and Maintenance Instructions for Model OAY Sound Measuring Equipment*, CUDWR-NLL, June 26, 1944. Div. 6-641.3-M4

Chapter 4

1. *Noise Level Monitor and Cavitation Indicator*, William B. Snow, OSRD 4685, NDRC 6.1-sr1128-1930, Lab. Report P55/R1281, CUDWR-NLL, Jan. 31, 1945. Div. 6-642.1-M3

2. *Effect of Thermal Gradient on DCDI Above-Below Indication*, Jordan J. Markham, Lab. Report D50/R1049, CUDWR-NLL, Aug. 8, 1944. Div. 6-642.21-M4

3. *Effect of Temperature Gradients on DCDI Above-Below Indications*, CUDWR-NLL Nov. 25, 1944. Div. 6-642.21-M5

4. *The Influence of Thermal Gradients on Relative Sound Intensities with Special Reference to the Depth Charge Range Estimator*, George R. Perry, Lab. Report P28/1398, CUDWR-NLL, Feb. 28, 1945. Div. 6-642.31-M3

5. *Depth Charge Range Estimator*, William B. Snow, Gaynor O. Rockwell, and James R. Ording, OSRD 5249, NDRC 6.1-sr1128-1948, CUDWR-NLL, May 21, 1945. Div. 6-642.3-M2

6. *Summary of Sea Trials of Depth Charge Range Estimator*, James R. Ording, Lab. Report NP24/D50, CUDWR-NLL, July 4, 1945. Div. 6-642.31-M1

7. *Effect of Submarine Roll on Operation of DCI*, James W. Follin, Jr., Lab. Report G12/R570, CUDWR-NLL, Oct. 26, 1943. Div. 6-642.21-M1

8. *Preliminary Installation, Operation, and Maintenance Instructions for Preproduction Model of Depth Charge Direction Indicator*, NDRC 6.1-sr1128-1240, Lab. Report D50/R665A, CUDWR-NLL, Jan. 25, 1944. Div. 6-642.2-M1

9. *Water-Tight Cable Entrance Fitting for Underwater Service*, Gaynor O. Rockwell, NDRC 6.1-sr1128-1036, Lab. Report D50/R730, CUDWR-NLL, Feb. 24, 1944. Div. 6-642.2-M2

10. *Auxiliary and Underway Tests on USS Gabilan (SS-252)*, Donald P. Loye and Malcolm T. Rodger, Lab. Report D52/R866, CUDWR-NLL, Apr. 10, 1944. Div. 6-641.31-M1

11. *Cavitation Speeds of Fleet-Type Submarines*, William B. Snow and Henry B. Hoff, Lab. Report P32/R876, CUDWR-NLL, Apr. 19, 1944. Div. 6-642.11-M1

12. *Recommendation for Range Measurement for the DCDI*, James W. Follin, Jr., Lab. Report D50/R868, CUDWR-NLL, Apr. 28, 1944. Div. 6-642.21-M2

13. *Recommendations for Monitoring and Measuring Sonic Output of Submarines*, L. W. Sepmeyer and R. S. Gales, Lab. Report A13, UCDWR, May 13, 1944.

14. *Permanent Magnet Blastphones*, James W. Follin, Jr., Lab. Report D50/R930, CUDWR-NLL, May 15, 1944. Div. 6-642.2-M3

15. *Effect of Temperature Gradients on the Above-Below Indications of the Depth Charge Direction Indicator*, Lab. Report D55/R987, CUDWR-NLL, July 4, 1944. Div. 6-642.21-M3

16. *Comparative NLM and Standard Range Noise Tests on USS Besugo*, Robert A. Wagner, Lab. Report P55/R1052, CUDWR-NLL, July 31, 1944. Div. 6-642.11-M2

17. *Masking Attachment for the Noise Level Monitor*, William B. Snow, Lab. Report P55/R1062, CUDWR-NLL, Aug. 10, 1944. Div. 6-642.1-M1

18. *JP-1 vs QB/JK for Cavitation Indication*, William B. Snow, Lab. Report P55/R1115, CUDWR-NLL, Oct. 4, 1944. Div. 6-642.11-M3

19. *Some Tests of the Cavitation Indicator on the USS Boarfish*, Mark Harrison, Lab. Report P55/R1203, CUDWR-NLL, Oct. 23, 1944. Div. 6-642.11-M4

20. *Depth Charge Direction Indicator*, Gaynor O. Rockwell, NDRC 6.1-sr1128-1251, Lab. Report D50/R668, CUDWR-NLL, Oct. 31, 1944. Div. 6-642.2-M4

21. *Depth Charge Range Meter Tests*, Henry B. Hoff, George R. Perry, and others, CUDWR-NLL, Nov. 20, 1944. Div. 6-642.31-M1

22. *Depth Charge Meter Model IV*, Sylvester J. Haefner, Lab. Report D50/R1252, CUDWR-NLL, Nov. 24, 1944. Div. 6-642.3-M1

23. *Supplement to "Depth Charge Range Meter Tests,"* Gaynor O. Rockwell, Henry B. Hoff, and James R. Ording, CUDWR-NLL, Dec. 16, 1944. Div. 6-642.31-M2

24. *Noise Level Monitor Meter Circuit*, Frank P. Herrnfeld Lab. Report P55/1323, CUDWR-NLL, Jan. 22, 1945. Div. 6-642.1-M2

Chapter 5

1. a. *Marine Speedometer*, John D. Lane, Lab. Report M-93-10, HUSL, May 20, 1943. Div. 6-642.1-M1

b. *Marine Speedometer*, Robert B. Watson, Lab. Report M-93-11, HUSL, May 21, 1943. Div. 6-642.4-M2

c. *Marine Speedometer*, Fred H. Smith, Lab. Report M-93-13, HUSL, May 25, 1943. Div. 6-642.4-M3

2. a. *Probe Microphone*, Robert B. Watson, Lab. Report M-01.223-16, HUSL, Feb. 17, 1943. Div. 6-642.44-M1

b. *Probe Microphone*, Frederick V. Hunt, Lab. Report M-01.223-17, HUSL, Feb. 23, 1943. Div. 6-642.44-M2

3. *Reciprocity Calibration of the 9k-h Speedometer Cone Hydrophone*, Robert E. Payne, Lab. Report M-01.10-29, HUSL, Feb. 23, 1943. Div. 6-642.44-M3

4. *Acoustic Marine Speedometer, Transducer for*, Robert B. Watson, Lab. Report M-09.10-53, HUSL, Dec. 18, 1943. Div. 6-642.44-M5

5. *Test of Acoustic Marine Speedometer*, Robert B. Watson, Lab. Report M-09.10-9, HUSL, Dec. 21, 1942. Div. 6-642.41-M1

6. a. *Test of Acoustic Marine Speedometer*, Robert B. Watson, Lab. Report M-09.10-13, HUSL, Feb. 1, 1943. Div. 6-642.41-M2

b. *Acoustic Marine Speedometer*, Frederick V. Hunt, Lab. Report M-09.10-14, HUSL, Feb. 4, 1943. Div. 6-642.41-M3

c. *AMS*, Robert B. Watson, Lab. Report M-09.10-16, HUSL, Feb. 6, 1943. Div. 6-642.41-M4

7. a. *AMS*, Robert B. Watson, Lab. Report M-09.10-18, HUSL, Feb. 10, 1943. Div. 6-642.41-M5

b. *AMS*, Frederick V. Hunt, Lab. Report M-09.10-20, HUSL, Feb. 13, 1943. Div. 6-642.41-M6

8. *Acoustic Marine Speedometer*, NDRC 6.1-sr287-2074, HUSL, Aug. 15, 1945. Div. 6-642.4-M6

9. *Frequency Measurement, Influence of Uncertainty Principle on Measurement of*, Frederick V. Hunt, Lab. Report M-66.1-7, HUSL, Aug. 13, 1943. Div. 6-642.41-M7

10. a. *Acoustic Marine Phase Speedometer*, Robert B. Watson, Lab. Report M-09.10-50, HUSL, Dec. 9, 1943. Div. 6-642.43-M5

b. *Dopplerized Brainstorms*, Frederick V. Hunt, Lab. Report M-09.60, HUSL, June 26, 1944. Div. 6-642.41-M8

11. *Report on Observations Using the QC Echo-Ranging Device Aboard the Galaxy, May 4 to May 10 Inclusive, 1942, in re Doppler, Acoustic Speedometer, Reverberations, Etc.*, Leon G. S. Wood, Lab. Report M-02.301-36, HUSL, Mar. 15, 1943. Div. 6-642.42-M1

12. a. *Measurements of Reverberation Frequency with QC Equipment*, Robert B. Watson, Lab. Report M-01.40-50, HUSL, July 23, 1943. Div. 6-642.42-M2

b. *Measurements of Reverberation Frequency with QC Equipment*, Robert B. Watson, Lab. Report M-01.40-53, HUSL, July 29, 1943. Div. 6-642.42-M3

13. *Analysis of the Pinging Speedometer Problems*, Robert B. Watson, Lab. Report M-09.10-35, HUSL, Aug. 5, 1943. Div. 6-642.42-M4

14. *Acoustic Speedometer, New Type Using Phase Indication*, Malcolm H. Hebb, Lab. Report M-09.10-5, HUSL, Nov. 26, 1942. Div. 6-642.43-M1

15. *Sound Gear Monitor*, NDRC 6.1-sr287-2086, HUSL, Nov. 1, 1945. Div. 6-641.1-M9

16. *Acoustic Phase Speedometer*, Malcolm H. Hebb, Lab. Report M-09.10-26, HUSL, Apr. 28, 1943. Div. 6-642.43-M3

17. *Acoustic Marine Speedometer Proposal*, Harold P. Knauss, Lab. Report M-09.10-12, HUSL, Jan. 26, 1943. Div. 6-642.43-M2

18. *Acoustic Marine Phase Speedometer*, Robert B. Watson, HUSL, Apr. 29, 1943. Div. 6-642.43-M1

19. *Visit of Mr. Primakoff of the Underwater Sound Reference Laboratory*, Robert B. Watson, Lab. Report M-09.10-40, HUSL, Sept. 17, 1943. Div. 6-642.44-M4

20. *Acoustic Marine Speedometer*, Robert B. Watson, Dwight E. Gray, and M. Kathleen Ahern, NDRC 6.1-sr287-1541, HUSL, Apr. 28, 1944. Div. 6-642.4-M1

21. *Acoustic Marine Speedometer*, Robert B. Watson, HUSL, June 30, 1944. Div. 6-642.41-M9

22. *Check of the Reactance Tube Voltage of the ODN as a Speed Indicator*, Allen A. Chernosky, Lab. Report M-09.10-60, HUSL, Sept. 2, 1944. Div. 6-642.4-M5

Chapter 6

1. *Echo Repeater Experiments with a Submarine at San Diego,* Robert B. Bowersox, Lab. Report M-91.236-23, HUSL, Feb. 11, 1943. Div. 6-643.3-M2

2. *Proposal for Method of Measuring the Signal Reflecting Strength of a Submarine,* I. P. Rodman, Lab. Report M-01.80-5, HUSL, Oct. 9, 1944. Div. 6-643.4-M3

3. *Experimental Surface Model Echo Repeater,* Wm. A. Myers and Edwin M. McMillan, UCDWR, June 20, 1942. Div. 6-643.27-M1

4. *Preliminary Study of the Stability of a Towed Underwater Body with Diving Wing,* Calvin A. Gongwer, NDRC C4-sr20-240, CUDWR-NLL, Aug. 26, 1942. Div. 6-643.12-M1

5. *Proposed Sonic Target,* L. C. Gibson, Lab. Report M-91.236-5, HUSL, Sept. 9, 1942. Div. 6-643-M1

6. *Echo Repeater Delevoped by NDRC Laboratory at San Diego, California,* A. Nelson Butz, Jr., Lab. Report M-91.236-7, HUSL, Sept. 29, 1942. Div. 6-643.3-M1

7. *Towable Targets,* Carl M. Herget, Lab. Report M-91.236-15, HUSL, Nov. 2, 1942. Div. 6-643.21-M1

8. *The Triplane,* Donald E. Ross and F. N. D. Kurie, NDRC C4-sr30-402, Lab. Report U-4, Nov. 23, 1942. Div. 6-643.21-M2

9. *Reverberation Studies at 24 kc,* OSRD 1098, NDRC 6.1-sr30-401, Lab. Report U-7, UCDWR, Nov. 23, 1942. Div. 6-520-M2

10. *The Shape of a Flexible Rope Towing a Submerged Body,* Glen D. Camp, Lab. Report M-5, UCDWR, Nov. 30, 1942. Div. 6-643.12-M2

11. *The Echo Repeater. Sonar Question,* Carl M. Herget, Lab. Report M-91.236-25, HUSL, Feb. 25, 1943. Div. 6-643.11-M1

12. *Trials and Tribulations of Rotoscope and Echo Repeater,* Harold P. Knauss and Carl M. Herget, Lab. Report M-91.236-29, HUSL, Apr. 10, 1943. Div. 6-643.3-M3

13. *Artificial Echo Repeater,* Russell O. Hanson and Frank P. Herrnfeld, Lab. Report G29/R355, CUDWR-NLL, May 24, 1943. Div. 6-643.26-M1

14. *A Streamlined Cable Depressor,* Albert R. Champion, Lab. Report M-68, UCDWR, May 25, 1943. Div. 6-643.12-M3

15. *Smecho,* Frederick V. Hunt, Lab. Report M-91.236-38, HUSL, June 12, 1943. Div. 6-643.22-M1

16. *Depth of Towed Fish and the General Curve of a Towing Cable in Water or Air,* Calvin A. Gongwer, NDRC 6.1-sr20-659, Lab. Report G2/R238, CUDWR-NLL, June 14, 1943. Div. 6-624.3-M7

17. *Cross Talk Reducer for Smecho,* Harold P. Knauss and C. W. Horton, Lab. Report M-91.236-40, HUSL, June 18, 1943. Div. 6-643.22-M2

18. *Present State of Smecho Towing,* Carl M. Herget, K. L. Zapf, and C. W. Horton, Lab. Report M-91.236-42, HUSL, June 28, 1943. Div. 6-643.22-M3

19. *Supplement to the Triplane,* Donald E. Ross and F. N. D. Kurie, Lab. Report U-4a, UCDWR, June 29, 1943. Div. 6-643.21-M3

20. *The Fundamental Electronic Problem of the Echo Repeater,* Roderic M. Scott, Lab. Report M-91.236-43, HUSL, July 13, 1943. Div. 6-643.11-M2

21. *Echo Repeaters Reference: Scott Memo on "The Fundamental Electronic Problem of the Echo Repeater" Dated 7-13,* Frederick V. Hunt, Lab. Report M-91.236-46, HUSL, Aug. 3, 1943. Div. 6-643.11-M2

22. *Echo Repeaters,* Robert B. Watson, Lab. Report M-91.236-47, HUSL, Aug. 4, 1943. Div. 6-643.11-M4

23. *Clarification of the Echo Repeater Problem,* Roderic M. Scott, Lab. Report M-91.236-48, HUSL, Aug. 6, 1943. Div. 6-643.11-M5

24. *Echo Repeater Problem,* Roderic M. Scott, Lab. Report M-91.236-50, HUSL, Aug. 13, 1943. Div. 6-643.11-M6

25. *Triplane Echo Repeaters,* Fred H. Smith, Lab. Report M-91.236-51, HUSL, Aug. 16, 1943. Div. 6-643.21-M4

26. *B-19F 15" Tubular Sonar Echo Repeater Hydrophone,* Francis P. Bundy, Lab. Report M-91.236-55, HUSL, Sept. 6, 1943. Div. 6-643.11-M7

27. *The Effect of Bottom Reflections on Echo Repeaters,* Harold P. Knauss, Lab. Report M-91.236-64, HUSL, Oct. 2, 1943. Div. 6-643.3-M4

28. *Echo Repeater, Compression Amplifier for,* Frederick V. Hunt, Lab. Report M-91.236-66, HUSL, Oct. 12, 1943. Div. 6-643.11-M8

29. *Echo Repeaters with Reference to F. V. Hunt's Memorandum of October 12, Concerning the Application of AVC,* A. Nelson Butz, Jr., Lab. Report M-91.236-67, HUSL, Oct. 19, 1943. Div. 6-643.11-M9

30. *Tests of the Large 4-Segment 20 kc Ring Stack,* Francis P. Bundy, Lab. Report M-01.213-98, HUSL, Oct. 21, 1943. Div. 6-612.61-M3

31. *Preliminary Triplane Tests,* Wm. Fred Arndt, Lab. Report G37/A24A/R577, CUDWR-NLL, Oct. 28, 1943. Div. 6-643.21-M5

32. *Performance of the 5" 20 kc Oxide Annealed Ring Stacks 20 ARS-2,* Francis P. Bundy, Lab. Report M-01.213-110, HUSL, Nov. 8, 1943. Div. 6-612.41-M10

33. *Performance of the 60 kc ARS-1 and ARS-2 Ring Stacks,* Jack C. Cotton and Francis P. Bundy, Lab. Report M-01.213-121, HUSL, Dec. 1, 1943. Div. 6-612.61-M7

34. *Construction and Performance of Echo-Repeater Pair (1" Hard Nickel and 2" Annealed Nickel Ring Stacks),* Jack C. Cotton, Francis P. Bundy, Lab. Report M-91.236-81, HUSL, Feb. 17, 1944. Div. 6-612.41-M14

35. *Tests on Lucite-Impregnated 60 kc Ring Stacks,* Jack C. Cotton and Francis P. Bundy, Lab. Report M-01.213-174, HUSL, Mar. 11, 1944. Div. 6-612.61-M8

36. *Modification of the Triplane Target,* A. Kenneth Tatum and Vernon M. Setterholm, Lab. Report G37/R884, CUDWR-NLL, Apr. 20, 1944. Div. 6-643.21-M6

37. *Project Whale,* I. P. Rodman, Lab. Report M-91.236-88, HUSL, Apr. 21, 1944. Div. 6-643.24-M1

38. *Construction and Performance of 60 kc Echo Repeater Transducer Pair #3*, Francis P. Bundy and Milton R. Carlson, Lab. Report M-91.236-106, HUSL, May 24, 1944. Div. 6-612.61-M10

39. *Safety Devices for Towed Targets*, Leon G. S. Wood, Lab. Report M-91.236-107, HUSL, May 29, 1944. Div. 6-643.12-M4

40. *Modifications and Tests Made on Taylor Model Basin Self-Propelled Practice Target*, David J. Evans, NDRC 6.1-sr30-1689, Lab. Report M-225, UCDWR, June 14, 1944. Div. 6-651.4-M1

41. *Log of the Trip to Fort Lauderdale, June 5 to June 15, Experiences with the 60 kc Harvard Echo Repeater*, Leon G. S. Wood, Lab. Report M-91.236-119, HUSL, June 23, 1944. Div. 6-643.25-M1

42. *60 kc Repeaters*, I. P. Rodman, Lab. Report M-91.236-125, HUSL, July 10, 1944. Div. 6-643.25-M2

43. *The Construction and Performance of the "Whale" Transducer*, Milton R. Carlson and Francis P. Bundy, Lab. Report M-91.236-129, HUSL, July 16, 1944. Div. 6-643.24-M2

44. *Echo Repeater Calibrators*, I. P. Rodman, Lab. Report M-91.236-137, HUSL, July 22, 1944. Div. 6-643.4-M1

45. *Instructions for Whale Echo Repeater*, Lab. Report H-305, HUSL, Aug. 1, 1944. Div. 6-643.24-M3

46. *The Calibration of the "Whale" Echo Repeater*, Leon G. S. Wood, Lab. Report M-91.236-149, HUSL, Aug. 12, 1944. Div. 6-643.24-M4

47. *Sea Test on Whale Echo Repeater*, Robert H. Hughes, Lab. Report M-91.236-151, HUSL, Aug. 14, 1944. Div. 6-643.24-M5

48. *The Calibration of the 60-kc Repeater on the QUESTOR*, Robert H. Hughes, Lab. Report M-91.236-153, HUSL, Aug. 17, 1944. Div. 6-643.25-M3

49. *Influence of Transducer on Howl Point in Echo Repeaters*, Malcolm H. Hebb, Lab. Report M-91.236-158, HUSL, Sept. 6, 1944. Div. 6-643.25-M4

50. *Echo Repeater Design*, R. D. Whitmore, Lab. Report M-91.236-169, HUSL, Sept. 22, 1944. Div. 6-643.12-M5

51. *Equations of Depth, Cable Resistance, etc., of Towed Underwater Body and Depressor*, W. Starling Burgess, Lab. Report M-91.236-176, HUSL, Sept. 28, 1944. Div. 6-643.12-M6

52. *Notations Concerning Echo Repeater Calibration Gear*, Edward R. Myrbeck, Lab. Report M-91.236-180, HUSL, Sept. 30, 1944. Div. 6-643.4-M2

53. *3-Foot Sphere Echo-Ranging Data*, Thomas P. Merritt, David C. Whitmarsh, and Roderic M. Scott, Lab. Report M-02.453.4-60, HUSL, Nov. 10, 1944. Div. 6-632.312-M7

54. *60 kc 2 VP-1 #1*, G. W. Renner, Lab. Report M-01.213-263, HUSL, Oct. 24, 1944. Div. 6-612.61-M15

55. *Target Strength Determination with the Echo Repeater Calibrator*, Frederick V. Hunt, Lab. Report M-01.80-8, HUSL, Nov. 21, 1944. Div. 6-643.4-M4

56. *Low Frequency Thin-Walled 2 VP Ring Stacks*, G. W. Renner, Lab. Report M-01.213-298, HUSL, Jan. 18, 1945. Div. 6-612.61-M22

57. *24.5 kc 2VP Spherical Source Nos. 9 and 10*, G. W. Renner, Lab. Report M-01.213-326, HUSL, Apr. 16, 1945. Div. 6-612.61-M28

58. *First Sea Test of the Self-Contained Echo Repeater Model II*, Edward R. Myrbeck, Lab. Report M-91.236-233, HUSL, Apr. 20, 1945. Div. 6-643.23-M1

59. *The Calibration of the Low Frequency Self-Contained Echo Repeater Model II*, Edward R. Myrbeck, Lab. Report M-91.236-237, HUSL, May 1, 1945. Div. 6-643.23-M2

60. *Transducer Construction in the Low Frequency Self-Contained Echo Repeater, Model II*, Milton R. Carlson, Lab. Report M-91.236-238, HUSL, May 5, 1945. Div. 6-612.61-M29

61. *Dual Frequency Driver*, NDRC 6.1-sr287-2083, HUSL, May 25, 1945. Div. 6-631.45-M17

62. *Preliminary Analysis of Hit Performance on Echo Repeater Runs*, R. H. Bolt and W. H. Wilson, CUDWR, May 28, 1945. Div. 6-645.3-M5

63. *Echo Repeater Calibrator*, NDRC 6.1-sr287-2068, HUSL, Aug. 1, 1945. Div. 6-643.4-M5

64. *Echo Repeaters*, NDRC 6.1-sr-287-2070, HUSL, Sept. 1, 1945. Div. 6-643-M2

Chapter 8

1. *The Automatic Target Positioner for the Dead Reckoning Tracer, Model 1*, Lab. Report U-353, UCDWR, Sept. 20, 1945. Div. 6-644.11-M3

2. *Sine Potentiometers*, H. R. Davidson, NDRC 6.1-sr1131-1147, CUDWR-NLL, Nov. 1943. Div. 6-644.21-M6

3. *Slant Range Correction Recorder*, Hugh E. Harlow, B. A. Wooten, and Dwight E. Gray, NDRC 6.1-sr287-1707, HUSL, July 15, 1944. Div. 6-644.21-M12

4. *A. S. DevLant Conf. Report "Depth Charge Trials of Attack Directors and Attack Aids,"* T. A. Turner, ASDD/S 68, Jan. 3, 1945 (N354).

5. *Recorder and Predictor*, Frank C. Gilbert, Lab. Report P9/1422, CUDWR-NLL, Oct. 16, 1941. Div. 6-644-M1

6. *Graphical Triangle Solver for Anti-Submarine Attack Prediction*, Leonard I. Schiff, University of Pennsylvania, Apr. 10, 1942. Div. 6-644.22-M1

7. *Graphical Attack Predictor for Forward Thrower*, Leonard I. Schiff, University of Pennsylvania, Apr. 15, 1942. Div. 6-644.22-M2

8. *Plotting Devices*, O. Hugo Schuck, Lab. Report M-30-6, HUSL, Aug. 7, 1942. Div. 6-644.13-M1

9. *A/S Attack Directors*, W. Congers Herring, Harold H. Baker, and others, NDRC C4-sr20-345, Lab. Report D26.2/3947, CUDWR-NLL, Oct. 5, 1942. Div. 6-644.21-M1

10. *An Electrical Triangle Solver*, Frank P. Herrnfeld, Lab. Repor. D26.2/4396, CUDWR-NLL, Oct. 30, 1942. Div. 6-644.23-M1

11. *Anti-Submarine Attack Plotter*, Kenneth H. Kingdon and H. C. Pollock, NDRC C4-sr323-621, GE., Nov. 18, 1942. Div. 6-644.12-M1

12. *Geographical Plotter Design Considerations*, O. Hugo Shuck, Lab. Report M-84-20.5, HUSL, Jan. 13, 1943. Div. 6-644.13-M2

13. *Cogitations and Ruminations During Trip*, O. Hugo Shuck, Lab. Report M-80.20-15, HUSL., Jan. 20, 1943. Div. 6-644.21-M2

14. *Lead Angle Calculator for Bearing Recorder*, O. Hugo Shuck, Lab. Report M-80.20-14, HUSL., Jan. 20, 1943. Div. 6-644.21-M3

15. *Plotters and Directors*, O. Hugo Schuck, Lab. Report M-80-28, HUSL., Jan. 21, 1943. Div. 6-644-M2

16. *Theoretical Principles Involved in Lead Prediction*, Harvey A. Brooks, Lab. Report M-80.10-10, HUSL., Feb. 3, 1943. Div. 6-644.21-M4

17. *Simplified Bearing Recorder Lead Angle Calculator*, O. Hugo Shuck, Lab. Report M-80.20-17, HUSL., Feb. 10, 1943. Div. 6-644.21-M5

18. *Sonar Attack Plotter*, Harold P. Knauss, Lab. Report M-80-35, HUSL., Mar. 6, 1943. Div. 6-644.22-M3

19. *Sonar Attack Plotter*, Frederick V. Hunt, Lab. Report M-80-39, HUSL., Mar. 16, 1943. Div. 6-644.22-M4

20. *The Development and Testing of Anti-Submarine Attack Director*, ARF, Mar. 31, 1943. Div. 6-644.23-M2

21. *Course Plotter, Methods of Marking Plotting Surface*, L. K. Davis, Lab. Report M-80.20-24, HUSL., Apr. 7, 1943. Div. 6-644.13-M3

22. *Inspection of Odograph Plotter*, Fred H. Smith, Lab. Report 84-5, HUSL., Apr. 26, 1943. Div. 6-644.13-M4

23. *Wellings Attack Computator*, J. Warren Horton, Lab. Report D26/R309, CUDWR-NLL., Apr. 26, 1943. Div. 6-644.23-M3

24. *Asdic Attacks, Part II — Attack Instruments*, W. E. Dawson, Lab. Report WA-897-23, Internal Report No. 83, Fairlie Lab., June 30, 1943. Div. 6-644-M3

25. *Aid for Solving the Attack Course Problem*, William T. Bartholomew, Lab. Report M-80-74, HUSL., Aug. 13, 1943. Div. 6-644.22-M5

26. *The Dynamic Characteristics of the ATT Gate as They Affect the Plotter*, Fred H. Smith, Lab. Report M-84.40-5, HUSL., Aug. 27, 1943. Div. 6-644.13-M5

27. *Course Plotter Using Light Beam Instead of Cathode Ray Tube*, W. K. Kearsley, NDRC 6.1-sr323-1203, GE., Sept. 3, 1943. Div. 6-644.12-M2

28. *Mathematical Prediction of Attack Course*, William T. Bartholomew, Lab. Report M-80-89, HUSL., Dec. 1, 1943. Div. 6-644.22-M6

29. *Installation, Operation, and Maintenance of the Attack Plotter, Mark I, Model 2*, CUDWR-NLL, Jan. 3, 1944. Div. 6-644.12-M3

30. *Description of a Proposed Optical DRT Tabl* , Firth Pierce, UCDWR, Jan. 24, 1944. Div. 6-644.11-M1

31. *A Mechanical Attack Director*, Hugh E. Harlow, Lab. Report M-80-109, HUSL., Feb. 2, 1944. Div. 6-644.21-M9

32. *Attack Director, Mark III*, Robert B. Watson, Lab. Report M-86-13, HUSL., Feb. 17, 1944. Div. 6-644.21-M7

33. *Proposed Method of Solving Attack Problem for Forward-Thrown Weapons*, Robert B. Watson, Lab. Report M-80-108, HUSL, Feb. 22, 1944. Div. 6-644.21-M8

34. *Attack Director B*, William T. Bartholomew, Lab. Report M-80-112, HUSL., Feb. 28, 1944. Div. 6-644.22-M7

35. *A Synopsis of Mechanical and Electronic Functions Incorporated in Indicating Range Recorder CAN 55134 Serial 3438 as Revised for Operation with AD III*, Lab. Report M-86-30, HUSL., May 8, 1944. Div. 6-644.21-M10

36. *AD III, A Combination Range Keeper, Depth Compensator, Own-Ship Motor Compensator and Range Rate Determination*, Hugh E. Harlow, Lab. Report M-83-35, HUSL., May 25, 1944. Div. 6-644.21-M11

37. *Attack Aids for Relative Plot PPI's*, William T. Bartholomew and Harold P. Knauss, Lab. Report M-80-140, HUSL., June 6, 1944. Div. 6-644.22-M8

38. *Electro-Mechanical Attack Director for QH Sonar*, William T. Bartholomew, Lab. Report M-80-142, HUSL., June 8, 1944. Div. 6-644.22-M9

39. *Ad III Servos*, Norman B. Saunders, Lab. Report M-86-39, HUSL., June 15, 1944.

40. *An Electro-Mechanical Solution for Attack Director B*, William T. Bartholomew, Lab. Report M-80-147, HUSL., June 16, 1944. Div. 6-644.22-M10

41. *Attack Aid, Marriage of IP and AD*, O. Hugo Shuck, Lab. Report M-80-157, HUSL., July 20, 1944. Div. 6-644-M4

42. *Dynamic Character of the ATT Gate — Part II*, Fred H. Smith, Lab. Report M-84.40-8, HUSL., Sept. 13, 1943. Div. 6-631.21-M4

43. *Automatic Target Positioner for DRT*, H. E. Hartig and Firth Pierce, NS-329, UCDWR, Dec. 4, 1944. Div. 6-644.11-M2

44. *Path Integrator*, Elmer J. Wade, GE, Dec. 14, 1944. Div. 6-644.14-M1

45. *Lead Angle Computer*, OSRD 3201, NDRC 6.1-sr1131-1313, CUDWR, 1944. Div. 6-644.21-M15

46. *Mechanical Geographic Attack Plotter*, NDRC 6.1-sr287-2061, HUSL., Jan. 15, 1945. Div. 6-644.13-M6

47. *Attack Directors*, Woodman Perine, NDRC 6.1-sr1128-1934, Lab. Report D26/R1350, CUDWR-NLL., Feb. 28, 1945. Div. 6-644.2-M1

48. *Operational Bearing Recorder*, NDRC 6.1-sr287-2065, HUSL., Mar. 1, 1945. Div. 6-326.1-M2

49. *Changes Made in the General Electric Attack Plotter (known as the ASAP)*, R. B. Bowersox, Lab. Report M-80-165, HUSL, Mar. 19, 1945. Div. 6-632.05-M1

50. *Attack Director B*, NDRC 6.1-sr287-2071, HUSL, July 30, 1945. Div. 6-644.22-M11

51. *Attack Director III and Related Developments*, NDRC 6.1-sr287-2082, HUSL, Sept. 1, 1945. Div. 6-644.21-M13

52. *Attack Director III*, H. R. Davidson and W. Conyers Herring, NDRC 6.1-sr1131-1890, CUDWR, Sept. 17, 1945. Div. 6-644.21-M14

Chapter 9

1. *General Properties of Low Inertia Motors*, No. X-63649, BTL, Feb. 16, 1943. Div. 6-645.32-M1

2. *Servo, RC Notching Filters*, Norman B. Saunders, Lab. Report M-02.311.4-34, HUSL, Jan. 4, 1944. Div. 6-645.31-M1

3. *Ad-III Servos*, Norman B. Saunders, Lab. Report N-86-39, HUSL, June 15, 1944. Div. 6-645.3-M1

4. *A Device for Measuring the Transfer Function of the Modulation for Carrier Frequency Servo Systems*, Norman B. Saunders, Lab. Report M-110-370, HUSL, Feb. 21, 1945. Div. 6-645.31-M6

5. *The Analysis and Synthesis of Linear Servo Mechanisms*, Albert C. Hall, Servo Mechanisms Laboratory, MIT, May, 1943. Div. 7-321.1-M3

6. *Performance Curves of Brown Two-Phase Motor in Controlled Rectifier Circuit*, M. O. Marquardt, Lab. Report M-110.50-45, HUSL, Nov. 23, 1943. Div. 6-645.32-M2

7. *Servo Motor, Amplifier Investigation*, O. Hugo Schuck, Lab. Report M-110-245, HUSL, Jan. 28, 1944. Div. 6-645.32-M3

8. *A Graphical Method for Computing the Transfer Function of the Modulation upon a Carrier When the Modulated Carrier is Passed Through a Filter Whose Transfer Function is Known*, Norman B. Saunders, Lab. Report M-110.3-74, HUSL, May 9, 1944. Div. 6-645.31-M2

9. *Two-Phase Servo Motor Properties*, M. O. Marquardt and Norman B. Saunders, Lab. Report M-110-283, HUSL, May 18, 1944. Div. 6-645.32-M4

10. *A New Servo Modulator for PPCR, AD-III, and Proportional Training*, Norman B. Saunders, Lab. Report M-110-287, HUSL, May 30, 1944. Div. 6-645.31-M3

11. *Servo Motor Power and Voltage Amplifiers*, M. O. Marquardt and Norman B. Saunders, Lab. Report M-110-301, HUSL, June 30, 1944. Div. 6-645.32-M5

12. *Synchro Test Unit*, Francis W. Ferri, Lab. Report A30/R1112, CUDWR-NLL, Oct. 25, 1944. Div. 6-645.33-M1

13. *Synchro System Test Unit*, Glen D. Gillett and Wayne G. Shaffer, NDRC 6.1-sr1128-1926, UCDWR-NLL, Jan. 17, 1945. Div. 6-645.33-M2

14. *Reducing the Output Impedance of Power Amplifiers with Specific Application to Servos and the DPT and PPCR*, Norman B. Saunders, Lab. Report M-110-366, HUSL, Feb. 12, 1945. Div. 6-645.31-M4

15. *Reducing the Output Impedance of Power Amplifiers with Specific Application to Servos and the DPT and PPCR, Correction*, Norman B. Saunders, Lab. Report M-110-368, HUSL, Feb. 14, 1945. Div. 6-645.31-M5

16. *Portable Polar Chart Recorder*, NDRC 6.1-sr287-2060, HUSL, Sept. 15, 1945. Div. 6-553.5-M2

Chapter 10

1. *Scatter Charge for Surface Vessels*, George M. Gourley and Gaynor O. Rockwell, NDRC 6.1-sr1128-1248, CUDWR-NLL, Dec. 13, 1943. Div. 6-646.12-M6

2. *An Investigation of the Hydrodynamics of Underwater Projectile Forms*, L. J. Hooper, Clifford P. Kittredge, Calvin A. Gongwer, and John F. Ripkin, Lab. Report P16/3023, CUDWR-NLL, Jan. 1, 1943. AMP-102-M1

3. *Fast-Sinking Depth Charges*, Clifford P. Kittredge, NDRC 6.1-sr1128-1935, CUDWR-NLL, May 21, 1945. Div. 6-646.11-M6

4. *Bridge-Type Magnetic Fuze for A/S Projectile*, NDRC 6.1-sr346-831, BTL, Apr. 1, 1943. Div. 6-646.21-M11

5. *Depth Charge Intervalometer*, Clifford P. Kittredge, NDRC 6.1-sr1128-1939, Lab. Report D28/R1364, CUDWR-NLL, May 17, 1945. Div. 6-646.22-M3

6. *Effect of Nose Shape on the Performance at Entrance of Model Underwater Projectiles*, Leslie J. Hooper, Lab. Report D10/3075, CUDWR-NLL, June 10, 1942. Div. 6-646.11-M1

7. *The Use of Spin in Underwater Projectiles*, Leslie J. Hooper, Lab. Report D10/3099, CUDWR-NLL, June 11, 1942. Div. 6-646.11-M2

8. *A New Type of Bomb Fuse*, Raymond D. Atchley, UCDWR, June 13, 1942. Div. 6-646.21-M1

9. *Relative Effectiveness of Different Barrage Patterns for Aircraft Retro-Contact Rocket Bombs, Fired On MAD Contract*, Leonard I. Schiff and W. H. Wilson, NDRC C4-sr20-207 CUDWR-NLL Aug 4 1942 Div 6-415-M1

10. *Magnetic Signal Device*, John H. Payne, Kenneth H. Kingdom, and others, OSRD 917, NDRC C4-sr42-516, GE, Aug. 11, 1942. Div. 6-646.4-M1

11. *Notes on Dispenser Tests on USS Semmes, August 13, 1942*, Leslie J. Hooper, Lab. Report D28.2/3702, CUDWR-NLL, Sept. 3, 1942. Div. 6-646.23-M1

12. *Safety Tests Made on Model 6-40-C Fuzes and Projectiles, Groton Quarry, June 13, 1942*, George E. Breeze, Lab. Report D10.2/4022, CUDWR-NLL, Sept. 18, 1942. Div. 6-646.21-M2

13. *6-40-M Magnetic Flux-Change Fuze*, Edward E. Noyes, Lab. Report D37.2/4420, CUDWR-NLL, Nov. 4, 1942. Div. 6-646.21-M3

14. *Comparison Between Statham Fuze and New London 6-40-FCF Fuze (6-40-M)*, Dick P. Fullerton, Jr., Lab. Report D37/P17, CUDWR-NLL, Nov. 23, 1942. Div. 6-646.21-M4

15. *Comments of the Royal Aircraft Establishment, October 16, 1942 on OSRD Report No. 737. Effect of Nose Shape*

on the Performance at Entrance of Model Underwater Projectiles, Leslie J. Hooper, Lab. Report D10/R133, CUDWR-NLL, Dec. 15, 1942. Div. 6-646.11-M3

16. *The Magnetic Close Proximity Fuze,* S. C. Baden, NDRC 6.1-sr30-405, UCDWR, Dec. 19, 1942. Div. 6-646.21-M5

17. *Variable Electronic Interval Timer,* Wayne G. Shaffer, NDRC 6.1-sr20-557, Lab. Report D23/R132, CUDWR-NLL, Dec. 23, 1942. Div. 6-646.21-M6

18. *Electric Squib Actuated Bomb Release Latch,* Gaynor O. Rockwell and Edward E. Noyes, Lab. Report D23/R135, CUDWR-NLL, Dec. 23, 1942. Div. 6-646.23-M2

19. *Projectile Fuzes,* George E. Breeze, George W. Martin, and Edward E. Noyes, Lab. Report D10/R108, CUDWR-NLL, Dec. 28, 1942. Div. 6-646.21-M7

20. *Projectile Rack for Blimps,* Joseph A. Cerny, Lab. Report D23/R110, CUDWR-NLL, Dec. 28, 1942. Div. 6-646.23-M3

21. *The Magnetic Flux-Change Fuze,* L. D. Statham, OSRD 1332, NDRC 6.1-sr30-407, Lab. Report S-11, UCDWR, Dec. 30, 1942. Div. 6-646.21-M8

22. *Flux-Change Fuze for A/S Projectile,* NDRC 6.1-sr346-726, BTL, Feb. 25, 1943. Div. 6-646.21-M9

23. *Special Electric Detonators for Condenser Firing Circuits,* Gaynor O. Rockwell, Lab. Report P17/R194, CUDWR-NLL, Mar. 5, 1943. Div. 6-646.21-M10

24. *Towed Projectile,* Joseph A. Cerny, Lab. Report D27/R227, CUDWR-NLL, Mar. 24, 1943. Div. 6-646.4-M2

25. *Squib Latch Tests,* George W. Martin, Lab. Report D23/R245, CUDWR-NLL, Mar. 30, 1943. Div. 6-646.23-M4

26. *Sea Trials of 7-40-M Projectiles in Combination with the Chute and Screw Type Dispensers,* George W. Martin, Lab. Report D29/D28/R319, CUDWR-NLL, May 10, 1943. Div. 6-646-M1

27. *7-40-M Blimp Tests, Lakehurst, New Jersey,* George M. Gourley, Lab. Report D29/D23/R327, CUDWR-NLL, May 11, 1943. Div. 6-646-M2

28. *Intervalometer,* Clifford P. Kittredge, Lab. Report D28/R383, CUDWR-NLL, June 7, 1943. Div. 6-646.22-M1

29. *Tests on A. S. Scatter Bomb Clusters with Live Fuzes in Inert Bombs,* R. J. Tinkham, H. A. Leedy, and T. C. Poulter, ARF, July 26, 1943. Div. 6-646.12-M1

30. *Laboratory Tests on Severing and Strength of the Steel Banding Strap for the A. S. Scatter Bomb Cluster,* R. J. Tinkham, H. A. Leedy, and T. C. Poulter, ARF, July 28, 1943. Div. 6-646.12-M2

31. *A. S. Scatter Bomb Horn Tests,* Irwin Fieldhouse, H. A. Leedy, and T. C. Poulter, ARF, July 29, 1943. Div. 6-646.12-M3

32. *Submersion Tests for Watertightness of A. S. Scatter Bombs,* R. H. Esling, H. A. Leedy, and T. C. Poulter, ARF, July 30, 1943. Div. 6-646.12-M4

33. *Gun Train Indicator, Mark 53, [For Temporary Installation on Projector, Mark 10 (Hedgehog)],* Clifford P. Kittredge, NDRC 6.1-sr20-799, Lab. Report D42/R200, CUDWR-NLL, Sept. 10, 1943. Div. 646.26-M1

34. *The Scatterbomb,* Gaynor O. Rockwell and George M. Gourley, NDRC 6.1-S3279-1024, CUDWR-NLL, Sept. 13, 1943. Div. 6-646.12-M5

35. *Release Latches Actuated by Electric Squibs,* Clifford P. Kittredge, Lab. Report D28/R511, CUDWR-NLL, Sept. 15, 1943. Div. 6-646.23-M5

36. *Velocity Characteristics of a 6" by 32" Fast Sinking Projectile,* John F. Ripken, NDRC 6.1-sr20-1026, Lab. Report D10/R508, CUDWR-NLL, Sept. 18, 1943. Div. 6-646.11-M4

37. *Mark 53 Bomb Rack,* Vernon M. Setterholm, NDRC 6.1-sr20-1029, CUDWR-NLL, Sept. 29, 1943. Div. 6-646.23-M6

38. *The Scatter Charge for Surface Vessels,* Gaynor O. Rockwell and George M. Gourley, NDRC 6.1-sr1128-1252, CUDWR-NLL, Feb. 2, 1944. Div. 6-646.12-M7

39. *The Roller Loader for the Scatter Charge and the Mark 6 Depth Charge,* Gaynor O. Rockwell, NDRC 6.1-sr1128-1037, Lab. Report D49/R684, CUDWR-NLL, Feb. 11, 1944. Div. 6-646.23-M7

40. Letter to Dr. E. H. Colpitts, Subject: *Hydrostatically Detonated Exploder,* Roger Revelle, BuShips, Feb. 18, 1944. Div. 6-646.24-M1

41. *Tests of Mark 12 Depth Charges, Mine Tank, NOL, Washington, D. C.,* Clifford P. Kittredge, Lab. Report D10/R740, CUDWR-NLL, Apr. 4, 1944. Div. 6-646.11-M5

42. *The Anti-Submarine Scatter Bomb,* NDRC 6.1-sr673-1014, ARF, Apr. 28, 1944. Div. 6-646.12-M8

43. Letter to Chief of Naval Operations, Subject: *Sonar—Submarines—Long Range Ship-to-Shore Communication,* J. B. Don, BuShips, June 19, 1944. Div. 6-646.24-M2

44. *Depth Charge Intervalometer, Description and Instructions for Use,* Lab. Report D28/R981, CUDWR-NLL, June 29, 1944. Div. 6-646.22-M2

45. *Description and Instructions for Use of the Anti-Submarine Scatter Bomb,* NDRC 6.1-sr673-1618, ARF, July 17, 1944. Div. 6-646.12-M9

46. Letter to Dr. E. H. Colpitts, Subject: *Hydrostatically Detonated Exploder,* Roger Revelle, BuShips, Sept. 14, 1944. Div. 6-646.24-M3

47. *Specification for NL-143 Detonating Device,* Lab. Report P62/R1190, CUDWR-NLL, Oct. 21, 1944. Div. 6-646.24-M4

48. *Development of Recoverable Bomb,* NDRC 6.1-sr20-1587, Lab. Report D27/R1098, CUDWR-NLL, Oct. 25, 1944. Div. 6-646.4-M3

49. *Subcaliber Practice Projectile and Subcaliber Spigot Unit for the Mark X Projector,* Gaynor O. Rockwell, NDRC 6.1-sr1128-1923, Lab. Report D25/R1250, CUDWR-NLL, Dec. 11, 1944. Div. 6-646-M3

50. *Hydrostatically Detonated Exploder,* Gaynor O. Rockwell, NDRC 6.1-sr1128-1937, CUDWR-NLL, Mar. 6, 1945. Div. 6-646.24-M5

51. *Anti-Submarine Scatter Bomb Hydrostatic Arming Fuze,* ARF, Mar. 14, 1945. Div. 6-646.12-M10

52. *Surface Craft Dispensers for Fast-Sinking Depth Charges,* Clifford P. Kittredge, NDRC 6.1-sr1128-1938, Lab. Report D28/R1363, CUDWR-NLL, Apr. 30, 1945. Div. 6-646.23-M8

53. *Fuzes for Fast-Sinking Depth Charges,* Clifford P. Kittredge, George M. Gourley, and George E. Breeze, NDRC 6.1-sr1128-1940, Lab. Report P17/R1328, CUDWR-NLL, May 24, 1945. Div. 6-646.21-M12

54. *Tests of the AN-Mark 53 Aircraft Depth Bomb,* Robert T. Knapp, Harold L. Doolittle, OSRD 6091, NDRC 6.1-sr207-2350, Lab. Report ND-44, CIT, Aug. 31, 1945. Div. 6-723-M6

Chapter 11

1. *Electric Ignition Applied to Mark V Aircraft Float Light,* Joseph A. Cerny, NDRC C4-sr20-145, Lab. Report D21/3364, CUDWR, July 6, 1942. Div. 6-646.31-M1

2. *Pull-Match Ignition for Mark VI Float Light,* David O. Rhea, NDRC 6.1-sr1128-1585, CUDWR-NLL, Nov. 20, 1944. Div. 6-646.31-M10

3. *Modified Mark VI Aircraft Float Light,* NDRC 6.1-sr1128-1586, CUDWR-NLL, Sept. 1, 1944. Div. 6-646.31-M9

4. *Pneumatic Projector for the Mark V Float Light (For Use by Lighter-than-Air Craft),* Joseph A. Cerny, NDRC 6.1-sr20-641, CUDWR-NLL, May 10, 1943. Div. 6-646.31-M4

5. *Completion Report — Pneumatic Projector for the Mark V Float Light (For Use by Heavier-than-Air Craft),* Joseph A. Cerny, NDRC 6.1-sr20-796, CUDWR-NLL Sept. 3, 1943. Div. 6-646.31-M7

6. *Use of Commercial Flares Under Water,* F. A. Jenkins, UCDWR, Dec. 9, 1941. Div. 6-646.32-M1

7. *Underwater Flares for Anti-Submarine Operations, Report On Tests of July 7, 1942,* F. M. Varney, NDRC C4-sr20-162, UCDWR, July 20, 1942. Div. 6-646.32-M3

8. *Capacity Type Ignitors for Underwater Flares,* Wayne G. Shaffer, Lab. Report D31.2/3998, CUDWR-NLL, Sept. 17, 1942. Div. 6-646.32-M5

9. *Underwater Flares,* G. Albert Hill and R. G. Clarke, OSRD 1522, Wesleyan University, June 17, 1943. Div. 11-202.11-M2

10. *Underwater Flares,* G. Albert Hill and R. G. Clarke, OSRD 4030, Wesleyan University, Aug. 15, 1944. Div. 11-202.11-M3

11. *Test of Underwater Flares, Lakehurst, New Jersey, July 7, 1942. Report on Electric Ignition.* G. R. F. Gay, Lab. Report D21/R3423, CUDWR-NLL, July 9, 1942. Div. 6-646.32-M2

12. *Aircraft Marker Flares. Test at Lakehurst, New Jersey, August 18, 1942,* Joseph A. Cerny, Lab. Report D21.2/3802, CUDWR-NLL, Aug. 22, 1942. Div. 6-646.32-M4

13. *Underwater Flare Test, September 30, 1942,* Wayne G. Shaffer, Lab. Report D31.2/4153, CUDWR-NLL, Oct. 6, 1942. Div. 6-646.32-M6

14. *The Mark V Float Light,* Joseph A. Cerny and Dick P. Fullerton, Jr., NDRC C-4-sr20-542, CUDWR-NLL, Nov. 9, 1942. Div. 6-646.31-M2

15. *Trials of Pneumatic Flare Gun for Blimps at Lakehurst, New Jersey, December 22 and 23, 1942,* Edward E. Noyes and Vernon M. Setterholm, NDRC 6.1-sr20-567, Lab. Report D36/R146, CUDWR-NLL, Jan. 11, 1943. Div. 6-646.32-M7

16. *Velocity Traverses and Stability Test of Mark V Flare, Aeronautic Laboratory, Worcester Polytechnic Institute, March, 1943,* Lab. Report D21/R285, CUDWR-NLL, Apr. 22, 1943. Div. 6-646.31-M3

17. *Noise Produced by Burning Aircraft Flares,* Edward Gerjuoy, Lab. Report D21/R463, CUDWR-NLL, July 31, 1943. Div. 6-646.31-M5

18. *The Smoke-Light Marker,* Joseph A. Cerny, NDRC 6.1-sr20-797, CUDWR-NLL, Aug. 26, 1943. Div. 6-646.31-M6

19. *Drop Tests of Mark VI Aircraft Float Lights, December 7, 1943,* David O. Rhea, Lab. Report D21/R649, CUDWR-NLL, Dec. 15, 1943. Div. 6-646.31-M8

20. *Test of British Markers, Marine Aircraft,* David O. Rhea, Lab. Report D21/R951, CUDWR-NLL, June 5, 1944. Div. 6-646.33-M2

21. *Submarine Marker Buoy,* Lab. Report D19/R1205, NDRC 6.1-sr1128-1599, CUDWR-NLL, Nov. 30, 1944. Div. 6.646.33-M3

22. *Smoke Signal for Practice Submarine Marker Buoy,* David O. Rhea and Vernon M. Setterholm, Lab. Report D21/R719, NDRC 6.1-sr1128-1039, CUDWR-NLL, Mar. 24, 1944. Div. 6-646.33-M1

23. *The Development of a Navigational Marker Buoy,* OSRD 5658, NDRC 6.1-sr1224-2347, ARF, June 1945. Div. 6-646.33-M4

Chapter 12

1. *Sea-Water Batteries,* W. H. Martin, OSRD 6420, NDRC 6.1-sr1069-2128, BTL, Nov. 30, 1945. Div. 6-647-M1

SPECIAL BIBLIOGRAPHY

The following list includes (1) reports on certain projects not covered in the preceding chapters and (2) reports of general interest to the designer.

1. *Electronic Design and Measurements at the New London Laboratory*, Frank B. Herrnfeld and William B. Snow, NDRC 6.1-sr1128-2217, Lab. Report P35/R1428, CUDWR-NLL, May 28, 1945. Div. 6-645-M2
2. *Sound Recording at the New London Laboratory*, Russell O. Hanson, OSRD 5248, NDRC 6.1-sr1128-1945, Lab. Report P37/R1365, CUDWR-NLL, May 23, 1945. Div. 6-645.2-M3
3. *Lateral Disc Recording at the New London Laboratory*, Russell O. Hanson, Lab. Report P37/R1312, CUDWR-NLL, Jan. 24, 1945. Div. 6-645.2-M2
4. *Equalizer Design*, Russell O. Hanson and William B. Watkins, Lab. Report P37/R1278, CUDWR-NLL, Jan. 8, 1945. Div. 6-645.2-M1
5. *Miscellaneous Studies in Electrical Transmission Networks*, NDRC 6.1-sr287-2088, HUSL, Nov. 15, 1945. Div. 6-632.62-M16
6. *An R-C Band Pass Filter*, Report Series A 4, No. 9, Lab. Report DIC 5985, MIT, June 10, 1943. Div. 6-645.13-M1
7. *Chart Computation Methods for Filters*, BTL, Sept. 10, 1943. Div. 6-645.13-M2
8. *Filter Design Formulas and Charts — Part I*, Sylvester J. Haefner, Lab. Report P35/R984, CUDWR-NLL, July 11, 1944. Div. 6-645.13-M3
9. *A Graphical Chart for Combining Single-Frequency Signals with Continuous Spectra*, Henry B. Hoff, Lab. Report P34, R860, CUDWR-NLL, Apr. 7, 1944. Div. 6-645-M1
10. *An Introduction to Amplitude Modulation*, Paul K. Hudson, CUDWR-NLL. Div. 6-645-M3
11. *Test Procedure for Audio Transformers (35-16000 cps)*, Frank P. Herrnfeld, Lab. Report P34/R1020, CUDWR-NLL, July 13, 1944. Div. 6-645.15-M7
12. *Gain Measurements*, Frank P. Herrnfeld, Lab. Report P35/R669, CUDWR-NLL, Dec. 30, 1943. Div. 6-645.15-M3
13. *Distortion Tests by Intermodulation Method*, Frank P. Herrnfeld, Lab. Report P35/R712, CUDWR-NLL, Mar. 28, 1944. Div. 6-645.15-M5
14. *Cathode Coupled Amplifiers*, Lab. Report 218, CUDWR-NLL, June 9, 1942. Div. 6-645.12-M1
15. *High Impedance Preamplifier*, David C. Kalbfell, Lab. Report M-55, UCDWR, Apr. 29, 1943. Div. 6-645.12-M2
16. *A Power Amplifier and Bridge for the Measurement of Impedance at High Power Level*, Sylvester J. Haefner, Lab. Report P35/R653, CUDWR-NLL, Feb. 15, 1944. Div. 16-612.53-M11
17. *Amplifier and Bridge Measurements*, Sylvester J. Haefner, Lab. Report P35/R870, CUDWR-NLL, Apr. 28, 1944. Div. 6-645.15-M6
18. *An Impedance Bridge for the Measurement of Balanced and Unbalanced to Ground Circuits*, Sylvester J. Haefner, Lab. Report G30/535, CUDWR-NLL, Sept. 30, 1943. Div. 6-645.15-M2
19. *The Direct Measurement of Impedance*, O. Hugo Schuck and W. A. Felsing, NDRC 6.1-sr287-891, HUSL, June 4, 1943. Div. 6-645.15-M1
20. *Data for the Design of Inductances Wound on Molybdenum Permalloy Cores*, R. S. Gales, Lab. Report M-37, UCDWR, Feb. 25, 1943. Div. 6-645.14-M1
21. *Hipersil Cores*, Arthur S. Westneat, Lab. Report P35/R871, CUDWR-NLL, Apr. 12, 1944. Div. 6-645.14-M2
22. *Hipersil Core Characteristics*, Sylvester J. Haefner and Arthur S. Westneat, Lab. Report P35/R1012, CUDWR-NLL, July 11, 1944. Div. 6-645.14-M3
23. *Motional Impedance Analysis of Underwater Sound Devices*, Frank H. Graham and Eginhard Dietze, NDRC C4-sr20-591, USRL, Dec. 5, 1942. Div. 6-551-M7
24. *Vector Impedance Locus Plotter*, NDRC 6.1-sr287-2175, HUSL, Mar. 15, 1945. Div. 6-612.53-M22
25. *Receiving Tube Characteristics*, Frank P. Herrnfeld, Lab. Report G21/R371, CUDWR-NLL, May 31, 1943. Div. 6-645.11-M1
26. *Dynamic Characteristics of Pentodes and Grid Current Effects in Triodes and Pentodes*, Sylvester J. Haefner and L. Eugene Chipman, Lab. Report P35/R1179, CUDWR-NLL, Oct. 23, 1944. Div. 6-645.11-M4
27. *Conversion Gain of Various Tubes Operating as Mixers*, L. Eugene Chipman, Lab. Report P35/R980, CUDWR-NLL, June 22, 1944. Div. 6-645.11-M3
28. *Triode Phase Detectors*, Douglas E. Mode, Lab. Report P35/R1255, CUDWR-NLL, Nov. 14, 1944. Div. 6-645.12-M4
29. *Reactance Tube Frequency Control*, NDRC 6.1-sr287-1344, HUSL, Jan. 5, 1944. Div. 6-631.31-M7
30. *The Magnitude of Tube Noise in the Sonic and Super Sonic Range*, Roland C. Quest, Lab. Report G30/R454, CUDWR-NLL, July 27, 1943. Div. 6-645.11-M2
31. *Elimination of Electrical Noise in Sonic Listening Equipment*, Edwin E. Teal, Lab. Report D24/D38/R726, CUDWR-NLL, Jan. 31, 1944. Div. 6-645.12-M3
32. *Peak Reading Vacuum Tube Voltmeter*, Albert T. Reynolds, Lab. Report D50/R721, CUDWR-NLL, Feb. 1, 1944. Div. 6-645.15-M4
33. *The MIT Oscillograph Recorder*, NDRC 6.1-sr1046-1671 MIT, Aug. 17, 1944. Div. 6-651.2-M3
34. *Description of the Fluid Gyroscope*, Calvin A. Gongwer, Lab. Report D42/R651, CUDWR-NLL, Dec. 22, 1943. Div. 6-646.25-M1
35. *Analysis of the Fluid Gyro*, Ralph E. Byrne, Jr., May 11, 1944. Div. 6-646.25-M2
36. *Range Keeper J*, Warren Horton, NDRC 6.1-sr279-1085, Lab. Report D49/R505, CUDWR-NLL, Sept. 14, 1943. Div. 6-646.26-M2

CONTRACT NUMBERS, CONTRACTORS, AND SUBJECT OF CONTRACTS

Contract Number	*Name and Address of Contractor*	*Subject*
OEMsr-20	The Trustees of Columbia University in the City of New York New York, New York	Studies and experimental investigations in connection with and for the development of equipment and methods pertaining to submarine warfare.
OEMsr-1128	The Trustees of Columbia University in the City of New York New York, New York	Conduct studies and experimental investigations in connection with and for the development of equipment and methods involved in submarine and subsurface warfare.
OEMsr-30	The Regents of the University of California Berkeley, California	Maintain and operate certain laboratories and conduct studies and experimental investigations in connection with submarine and subsurface warfare.
OEMsr-287	President and Fellows of Harvard College Cambridge, Massachusetts	Studies and experimental investigations in connection with (i) the development of equipment and devices relating to subsurface warfare.
OEMsr-323	General Electric Company Schenectady, New York	Studies, experimental investigations, and development work in connection with submarine and subsurface warfare.
OEMsr-346	Western Electric Company, Inc. New York, New York	Studies and experimental investigations in connection with submarine and subsurface warfare.
OEMsr-673	Armour Research Foundation Chicago, Illinois	Conduct studies and experimental investigations in connection with (i) the development and design of a satisfactory fuse for an armor-piercing "Scatter Bomb" and the development of one or more operating models as directed . . . . (ii) such development work on the application of this fuse for use with the vertical bomb as appears to be necessary, and (iii) the design, development, and testing of special types of antisubmarine bombs and of their components and accessories.
OEMsr-1224	Armour Research Foundation Chicago, Illinois	Conduct studies and experimental investigations in connection with the development of navigational marker buoy.
OEMsr-1069	Western Electric Company, Inc. New York, New York	Conduct studies and experimental investigations in connection with the development of primary batteries having high power output per unit of weight and volume; such mechanical design as to permit, in addition to other incidental uses, their use in bombs or torpedoes launched from an airplane from a ship's deck, or from a submarine, etc.
OEMsr-1131	The Trustees of Columbia University in the City of New York New York, New York	Conduct studies and investigations in connection with the evaluation of the applicability of data, methods, devices, and systems pertaining to submarine and subsurface warfare.

SERVICE PROJECT NUMBERS

The projects listed below were transmitted to the Executive Secretary, NDRC, from the War or Navy Department through either the War Department Liaison Officer for NDRC or the Office of Research and Inventions (formerly the Coordinator of Research and Development), Navy Department.

Service Project Number	*Subject*
NO-116	Scatter bomb for submarine attack by heavier-than-air craft.
NO-125	Oscilloscope course plotter – ASAP.
NO-141	Hydrodynamic characteristics of projectile forms.
NO-142	Attack predictors.
NO-147	A/S projector Mark 10 – fire control equipment temporary installation.
NO-175	Projected scatter charges for surface vessels.
NO-195	Depth-charge pattern recorder.
NO-200	Development of a sea-water primary battery.
NO-209	Stabilized roll indicator.
NS-142 (Ext.)	Development of a sturdy design of shipboard hoist equipment for model OAX (modified) portable testing equipment.
NS-143	Acoustic marine speedometer.
NS-212	Noise reduction of submarines.
NS-231	Development of navigational marker buoy.
NS-238	Depth-charge direction indicator.
NS-301	Consulting services on underwater sound portable testing equipment.
NS-321	Twenty-five models of the extended-range underwater sound portable testing equipment (7- to 70-kc monitor).
NS-326	Artificial projector for operator training on shipboard monitor equipment model OAX, 10 units of.
NS-329	Development of a device which provides automatic target positioning on dead reckoning tracers from an input of target range and bearing.
NS-355	Consulting service on production of 21-volt sea-water battery.

INDEX

The subject indexes of all STR volumes are combined in a master index printed in a separate volume. For access to the index volume consult the Army or Navy Agency listed on the reverse of the half-title page.